NASA TT F-11, 530

ROTORCRAFT

F. Legrand

Translation of "Giravions". Ecole Nationale Supérieure de l'Aéronautique, France, 1964, 458 p.

Text and Figures

GPO PRICE $ _____

CFSTI PRICE(S) $ _____

Hard copy (HC) 3.00

Microfiche (MF) .65

ff 653 July 65

N68-21441

FACILITY FORM 602

(ACCESSION NUMBER) 467 (PAGES) / (NASA CR OR TMX OR AD NUMBER)

(THRU) 1 (CODE) 02 (CATEGORY)

NATIONAL AERONAUTICS AND SPACE ADMINISTRATION
WASHINGTON, D. C. 20546 APRIL 1968

APR 1968
RECEIVED
NASA STI FACILITY
INPUT BRANCH

HIGHER NATIONAL SCHOOL OF AERONAUTICS

ROTORCRAFT

by

F. Legrand
Chief Air Engineer
Director of Helicopter Studies at "Sud-Aviation"

Text

1964

FOREWORD

In the absence of a French-language work that can be used by the student engineer to deal with the set of problems relating to rotorcraft aviation, we thought it would be useful, by this course, to attempt a synthesis, necessarily concise, of the present state of the art. Of course, this is not to be an encyclopedia, but rather a guide, making it easy to advance to specialized work. /1*

Composition of the Course

We know of no better way of explaining how to approach the study of rotating airfoils except by relying on a comparison made by one of the most brilliant personalities of rotorcraft aviation, Mr. R. Hafner, who said: "Aviation, with its numerous techniques, is like modern medicine, which has specialists in cardiology, neurology, etc. Unfortunately, when it is a dog that must be treated, these specialists are not very qualified. We must go to a veterinary... Well, the helicopter is to the airplane what the dog is to man, which is as much as saying that even while benefitting from airplane progress and using it to the best advantage, the rotorcraft engineer must look at all the disciplines from a particular viewpoint: aerodynamics, flight mechanics, strength of materials, etc. (without counting, obviously, the specific maladies of the "dog")".

Therefore, this course studies, from the rotating-wing angle, subjects which have already been dealt with at the Higher National School of Aeronautics insofar as their general aspects are concerned.

Since these questions are intimately overlapping, it is impossible to avoid repetition, some subjects being raised several times.

We have not tried to eliminate this drawback, because, even though the text becomes somewhat heavy, only one goal is intended, in our opinion, that is, to study and resolve the problems from several sides at the same time; this is the modus operandi of the engineer himself.

Spirit in Which the Course was Prepared

Mathematical developments, as disagreeable as they may be, have been reduced as much as possible, or relegated to appendices. We have endeavored above all, without doing injustice to scientific rigor, to throw light on the nature of the phenomena involved and on the way in which they can be studied. However, the formulas, graphs and diagrams given in the appendix allow solution of the

*Numbers in the margin indicate pagination in the foreign text.

majority of the problems confronting the helicopter student engineer. An effort has been made, besides, to illustrate the presentation with ample numerical data, drawn from actual practice insofar as possible.

How to Study the Course /2

Given the special nature of the questions treated in each chapter, it seemed useful to begin with an introductory chapter. This first acquaintance with the subject as a whole will subsequently prevent the reader from "not seeing the forest because of the trees." Moreover, each chapter begins with simple considerations, making it possible to understand what is being discussed; the more rigorous developments unfold progressively. The most important parts are emphasized by placing one or two vertical bars in the margin.

The course takes in three major sections: aerodynamics (Chapter 2), rotor mechanics (Chapter 3), performance (Chapter 4), which hold the key to the helicopter field. Although they are somewhat "undigested," especially the first two, they must be assimilated, at least along the main lines.

The chapters dovetail, one into the other, and it is therefore recommended that they be read in order. However, Chapters 5, 6, 7, 8, and 9 are relatively self-contained and thorough study of the preceding ones is not necessary to understand them.

To facilitate use of the formulas and graphs, all the important notation has been recapitulated in a table given in Appendix 2.

A brief glossary has been given in Appendix 4 to facilitate comprehension by the Anglo-Saxon reader.

Finally, a bibiography has been added at the end of the course for those readers who intend to specialize.

TABLE OF CONTENTS

	Page
Foreword	
Chapter 1	
Introduction	1
1.1 The Different Types of Rotorcraft	1
1.2 A Brief History	2
1.3 Some Ideas of a Helicopter	5
1.4 Performance of Modern Helicopters	10
1.5 Uses of a Helicopter	10
Chapter 2	
Aerodynamics	13
2.1 Aerodynamics of the Rotor	13
2.2 Aerodynamics of the Anti-Torque Rotor	51
2.3 Aerodynamics of the Fuselage	52
Chapter 3	
Rotor Mechanics	54
3.1 The Origin of Flapping Hinges	54
3.2 Properties of an Articulated Rotor	56
3.3 The Forces Transmitted by the Rotor	80
Chapter 4	
Performance	91
4.1 General	91
4.2 Vertical Flight Performance	93
4.3 Level Flight	114
4.4 Optimum Climbing Conditions	119
4.5 Influence of Various Factors on Performance	120
4.6 Autorotation	123
4.7 Numerical Data	125
Chapter 5	
Stability and Flight Properties	128
5.1 Hovering Flight	128
5.2 Forward Flight	141
5.3 Maneuverability	145
5.4 Improvement of Flight Characteristics by Auxiliary Arrangements	146
5.5 Safety Limits	146
Chapter 6	
Some "Pitfalls" of the Helicopter	148
6.1 Vibrations	
6.2 Ground Resonance	154
6.3 Rotor Instability	164

Chapter 7
Strength of Materials 168
7.1 Static Forces 168
7.2 Alternating Forces 169

Chapter 8
Rotor Drive Assemblies 177
8.1 Jet and Mechanical Drive 177

Chapter 9
Technology 188
9.1 Airframe 188
9.2 Rotor Hubs 189
9.3 Blade Attachment 191
9.4 Hub Accessories 191
9.5 Blades 192
9.6 Flight Controls 196
9.7 Transmission 197
9.8 Operational Equipment 197
9.9 Integrated Design 198

Chapter 10
Synthesis 199
10.1 The Various Types of Helicopters 199
10.2 Choice of Structural Characteristics of the Rotor 202
10.3 Adaptation of the Helicopter to Rapid Flight 205
10.4 Disadvantages of the Modern Helicopter 207
10.5 Main Modern Trends in Helicopter Design 208

Chapter 11
New Types of Rotorcraft Competitors of the Helicopter 213
11.1 New Types of Rotorcraft 213
11.2 Rivals of the Helicopter 216

Appendix I 220

Appendix II 238

Appendix III 243

Appendix IV 269

Figures 281

Chapter 1

Introduction /3

As mentioned in the foreword, this chapter gives a rapid survey of the field, without any pretension to being complete or rigorous. Presented are definitions, vocabulary, history, make-up and operation, and use.

1.1. THE DIFFERENT TYPES OF ROTORCRAFT

Any heavier-than-air craft deriving its lift entirely or partially from one (or several) large-diameter propellors with a vertical axis, called rotors, is designated as a rotorcraft.

We distinguish between the following types:

1) The helicopter with an engine-driven rotor providing lift and propulsion simultaneously (Fig. 1.1). This is the only type of rotorcraft presently in service.

2) The gyrodyne, close relative of the preceding, but having a propellor with a horizontal axis for forward propulsion (Fig. 1.2) and sometimes with an auxiliary wing which bears some of the load while in motion (the exact terminology in this case is airplane-gyrodyne; see below). Such machines exist only as prototypes (Fairey Gyrodyne, for example).

3) Autogiro. It has, as the preceding, a propellor and sometimes an auxiliary wing, but its rotor is not powered; it rotates automatically (auto-rotation) due to the effect of speed of motion (Fig. 1.3). Thus this machine cannot hover, as do the preceding ones, but can only rise or descend at very steep angles: it is an aircraft with a broad range of speed, not affected by loss in speed, and can use very confined areas.

After having enjoyed great popularity between 1930 and 1940, the auto-giro has not disappeared, having been replaced by the helicopter. Attempts have been made for several years to reintroduce it for some specilized uses.

4) The compound. It offers a small advantage over the autogiro. It takes /4
off and lands in the same way as a helicopter, and cruises like an autogiro (automatically rotating rotor, tractor propellors). Auxiliary wings provide some of the lift, and therefore it can reach higher crusing speeds than the helicopter (Fig. 1.4). This type has not advanced beyond the experimental stage.

5) The convertibles. This designation covers all the rotorcraft which

change configuration during flight, that is, it takes off and lands in the helicopter configuration and cruises in the airplane configuration (since the rotor is retracted, tilted 90° to serve as a propellor and arrested to serve as an airfoil, etc.) (Fig. 1.5).

This type of machine, which existed for a long time only in the fertile mind of the inventor, is now reaching the experimental stage: prototypes are presently being built and tested in the USA.

1.2. A BRIEF HISTORY

The first trace of the use of a propellor on a vertical axis can be found in Chinese toys, prior to the Christian era*.

In the 15th century Leonardo da Vinci left sketches and notes relating to machines with rotating wings; because of this, he is considered to be the ancestor of rotorcraft afficionados.

In 1784 Launoy and Bienvenu flew a small-scale model before the Academy of Sciences. It was made of two counter-rotating rotors moved by a pre-flexed bow (Fig. 1.6).

In 1836 Nadar passionately backed the helicopter versus the balloon in his ringing mainfesto entitled "Aerial Auto-Locomotion": "It is the propellor, St. Airscrew, as an illustrious mathematician said one day, which will carry us off into the air like a drill enters wood."

But the drill had to be made to rotate, and so it was not until the beginning of the 20th century that the first machines of a size "almost able to fly" appeared, owing to the internal-combustion engine. We have time to cite only a few stages.

1900-1907. Aerodynamic study and theory of the lifting propellor by Colonel Renard, followed by Louis Breguet (who even at this time anticipated the importance of cyclic pitch variation). /5

1907. Paul Cornu's helicopter takes off with the inventor on board: this is without doubt the first free flight with a pilot. Later, in a second test, the assistant charged with holding it down was lifted from the ground: this is certainly the first flight with a "passenger" (Fig. 1.7).

---

*Note the existence of the "Virgin with the helicopter" by the Master of Vivion at the Museum in Mans, which shows that this investion had reached Europe by the Middle Ages.

1907. Louis Breguet, in collaboration with Prof. Richet, constructs his first gyroplane, which succeeds in leaving the ground; then the second one, a sort of combined helicopter-airplane, also leaves the ground.

1915. Tests on Lake Cercy of Papin and Rouilly's gyropter (Fig. 1.8), the the first full-scale jet-propelled helicopter; this machine was remarkable in principle but, because of bad balance and extremely low power, it did not succeed, during its tests, in anything but giving its pilot a good shower.

1916. The austrian army studies a tethered observation helicopter (Petroczy-Karman) which rises to 50 meters with surprisingly high payloads. The end of the war terminates development.

After 1919. Many devices succeed in leaving the ground (and in returning, in a more or less good condition). Among them let us cite the following.

1920-1930. Pescara helicopters.

Oehmichen helicopter (first closed-circuit kilometer in 1924).

1936. The Breguet-Dorand gyroplane, piloted by Claisse, makes a one-hour flight, exceeds 100 meters in altitude and performs the classical evolutions of a helicopter (including autorotation). This is the first helicopter to exhibit all the characteristics of a modern helicopter (Fig. 1.9).

1937. The German Focke-Anghelis helicopter tops all the existing records in succession (Flight duration: 1 hr 20 min; altitude: 3,400 m; speed: 120km/h). Piloted by Hanna Reitsch inside the Deutschlandhalle in Berlin, it also demonstrates its maneuverability.

Between 1930 and 1940. Invention of the autogiro by La Cierva, followed by successive improvements enabling these machines to be put into actual service. The experience gained with autogiro rotors is to become a great help in the ultimate development of helicopters. In particular, La Cierva is the first to have used articulated blades.

1940-1945. Helicopter studies are pursued in Germany with the Focke-Anghelis and the Flettners, but the engineering progress made in America becomes decisive. /6

The Sikorsky R-4 (Fig. 1.10) is put into service in the U. S. Air Force, becoming the first truly operational helicopter. At the same time, numerous constructors develop and mass-produce helicopters: namely, Piasecki, Bell, Hiller, etc.

Because of this fact, the United States after the war acquires a near monopoly in rotorcraft technology.

The Korean war was the occasion for systematic use of the helicopter and, in addition to a considerable inflation in the number of units, brought about the accumulation of valuable experience from the viewpoint of maintenance, endurance, employment, etc.

Although to our knowledge there are not exact statistics on this subject, it can be estimated that about 12,000 helicopters have been produced in the world to date*, the majority of American origin.

However, studies have been resumed in Europe, primarily in Great Britain (Bristol, Fairey, Percival, Saunders Roe, Westland) and in France (S.N.C.A.S.O., S.N.C.A.S.E., S.N.C.A. Nord, Dorand Rotorcraft Company, Breguet Company).

These two nations have recaptured a position in the world market in this field**.

The USSR, aside from copies pure and simple of Anglo-Saxon helicopters, is developing original machines on the basis of German technology.

Before closing this history, it would not be idle to ask why the helicopter, although older in principle than the airplane, has taken more time to arrive at maturity; the answer is contained in the following three points:

Power. Vertical flight requires at least 1/6 more horsepower to be transmitted to the rotor in the form of high torque (per kg weight lifted). We can get an idea of the difficulties involved if we know that a torque of 1000 kg transmitted to a helicopter rotor is of the order of magnitude of the torque transmitted to the driver wheel of a locomotive.

Much time was required to get engines, transmission systems and frames of sufficient rigidity and lightness in weight to be satisfactory. /7

Control. In contrast with the airplane, the helicopter does not fly "by itself", expecially not in vertical flight; it must be continuously piloted. Such control is possible only when the pilot has had special training and the machine has minimum qualities. This problem, long unsuspected, was revealed to its full extent when

---

*Beginning of 1964.

**At the present time helicopter construction has been concentrated at the Sub-Aviation Company in France and at the Westland Company in Great Britain.

piloted machines made their first landings. It is only quite recently that such problems have been solved in an acceptable manner.

Complexity. This is a consequence of the above-mentioned difficulties; the transmission of high torque and the achievement of satisfactory flight qualities have made it necessary to produce complicated and delicate parts which were often laborious to develop, namely transmission systems, rotors, control units, etc..

1.3. SOME IDEAS OF A HELICOPTER

As has been mentioned previously, the helicopter is the only rotorcraft in service today, and therefore this course will be concentrated almost entirely on studying it.

In what follows we will present a broad sketch if its makeup and of its operational peculiarities.

1.31. Makeup

The design of a helicopter is governed by the methods used to move and control the rotor or rotors.

1.311. Rotor Drive Systems

Two broad classes of methods exist:

Mechanical drive. The rotor is attached to an engine-driven shaft by some suitable mechanical system.

Jet drive. The rotor is mounted loosely on the fuselage and the blades are driven by jet units at the tips of the blades, eg., by ramjets, pulsejets, nozzles ejecting air of gas, etc.. These systems have the advantage of lightness and simplicity, but are poor in efficiency and are often very hot. They are not often used. /8

1.312. Integrated Design

Mechanical rotor drive, by far the most widely used method, presents a problem: application of a rather high drive torque to the rotor produces a yawing torque in the opposite direction on the fuselage, and this must be counterbalanced.

Depending on the solution chosen, the main lines to be applied in integrated design of the machine are defined. We will present the most current arrangements (among a mass of others).

1) Single rotor with antitorque tail rotor (Figs. 1, 11, 1.12, 1.13, 1.14, 1.15). This is the most frequent arrangement.

2) Two counter-rotating coaxial rotors (Fig. 1.16); this system is tending to disappear.

3) Two counter-rotating rotors, side-by-side, intermeshing (Fig. 1.17) or non-intermeshing (Fig. 1.18).

4) Two counter-rotating rotors in tandem (Fig. 1.19); this is the system most prevalent in large machines.

Jet-driven rotors do not induce a yawing torque on the fuselage; besides, since one of the principal advantages of a jet helicopter is that mechanical transmission is eliminated, no multirotor solutions have been planned up to the present time which would require synchronized rotor transmission.

Thus the problem that still remains is one of yaw control, which cannot be guaranteed by counter-torque. Relatively successful solutions have been reached, depending on the case: rudders in the rotor wake, flow deflection in turbines and even a small auxiliary rotor driven by the main rotor (see the two examples in Figs. 1.20 and 1.21).

1.313. Power Plants

A short time ago all operational helicopters were single-engined; the engine was a specially adapted reciprocal aviation engine.

We are presently witnessing two tendencies, a multi-engine design for high loads, and replacement of the reciprocal engine by a gas turbine. The latter presents many advantages which will be discussed in detailed in Chapter 8.

The helicopter SE 3130, Alouette II (Fig. 1.22), and SO 1221, Djinn (Fig. 1.21), are the first two turbine helicopters to be mass-produced (the second is also the first mass-produced jet helicopter). /9

1.314. Power Transmission

Just to give an example, we will consider only a single-rotor craft driven by

a reciprocal engine. It consists of the following parts, in succession: engine, flywheel, clutch (usually centrifugal), reduction gear, and rotor. A free-wheel, which permits the rotor to rotate while the engine is dead or idling, is mounted someplace in the transmission system. A powerful fan, designed to cool the motor in hovering flight, completes the plant.

1.315. The Rotor

Despite great diversity in production, all present-day rotors have the common property of permitting the blades, by suitable articulation, to describe a variable plane of orientation with respect to the fuselage. The orientation of this plane is controlled by appropriate devices ("swash-plate", or "spiders") linked to the flight controls.

This arrangement also permits simultaneous variation of blade pitch in order to regulate the lift.

1.316. Flight Control

Let us take a seat in the command post of a helicopter (Fig. 1.27), in the pilot's seat.

The right hand holds the control stick (1) (or feathering stick) which gives the rotor its orientation. For example, when it is pushed forward, the rotor tilts forward, and the helicopter will tend to move ahead and to pitch downward; when it is shoved to the left, the helicopter begins to move and to tilt to the left.

The left hand constantly holds a grip (3) attached to the end of a small stick, called the collective pitch (or mean pitch) stick.

Lifting and depressing this stick affects the collective pitch, that is, the lift of the rotor; lifting it augments the lift, the helicopter tends to rise, and vice versa.

The grip located at the end of this stick controls the gas feed; when it is turned in the direction indicated in the figure, the power increases. These two controls are lumped together in the same part because their action must be joint: augmentation of lift results in an increase in opposing torque (in constant flight) /10
and therefore more gas must be supplied. This coordinated effort is often facilitated by synchronizing pitch control and gas feed in such a way that an increase in the collective pitch results in an automatic increase in gas supply. The pilot need do no more than make corrections.

The feet actuate the rudder bar, which controls the yaw by acting on the

pitch of the anti-torque rotor, in the case of a single rotor. In multi-rotor configurations, the rudder bar acts as a differential on the rotors.

1.317. On-Board Instrumentation

In Fig. 1.29 can be seen one example of the instruments installed in a light helicopter; without dwelling on those instruments which are the same as in an airplane, let us mention only the essential one.

The Tachometer. In the case being considered, it has two needles, one indicating the rotor speed, the other the engine speed. The scales are such that in the normal mode (engine-driven rotor) these two needles are superposed. This instrument, which makes it possible to control the speed of the blades, is of the same importance as an anemometer in an airplane.

1.32. Piloting

Given below are some of the operations which must be performed by a helicopter pilot.

Starting the engine. (If the rotor is disengaged, it will not rotate.)

Shifting gears by gradually accelerating the engine and synchronizing; increase to normal rotor speed. Since the rotor pitch is small, it will not give much lift.

Takeoff. Pitch and gas-feed are gradually increased until the machine rises.

Vertical flight. A helicopter is by nature unstable, that is, if the pilot does not manipulate the control stick, the machine undergoes oscillating displacement and rapid loss of trim. Therefore, this tendency must be constantly corrected, and this is one of the main difficulties in handling the machine.

Another difficulty is that of controlling the rotor conditions. During all phase of flight, the pilot must make an effort to keep the operating conditions as constant as possible; he must absolutely remain within the following two limits:

Maximum mode: racing the motor and resisting the centrifugal force of the rotor.

Minimum mode: insufficient engine power ("excess torque"), loss of lift and control, which is analogous to a loss in speed in an airplane.

Example: /11

Powered: minimum mode - 320 rpm, maximum mode - 350 rpm.
Unpowered: minimum mode - 290 rpm, maximum mode - 360 rpm.

Climb and forward motion. Once the machine has reached speed by tilting the rotor forward, it is handled in much the same way as an airplane, despite its pitch stability, which is often rather poor.

Descent. Powered or unpowered descent. In the second case the rotor rotates automatically (autorotation) at a rate higher than that of the motor, owing to the flywheel. This operating mode implies that the rotor is set at a low pitch. In both cases descent is not vertical, but an an angle of 30 to 60° (lower descent speed and better control).

Autorotation is also the maneuver which permits safe landing in case of power failure. The important thing is to reduce the pitch fast enough to prevent losing rotation (which must usually be done within two seconds following failure). The machine lands by flattening out and keeping the machine on collective pitch (using the kenetic energy of the rotor).

1.33. Special Designs

What has been said so far applies to "conventional" helicopters. Many new designs have been the object of more or less urgent research. We will give only a few examples here.

One-Man Helicopters.

They have been conceived either as a small-scale conventional helicopter (Fig. 1.25) or have followed the "flying platform" configuration (Fig. 1.26). In the latter case the rotor is located beneath the pilot, who controls his machine by moving his body. The basic idea is to have a simple machine, which can be maneuvered by relying on the natural reflexes of a human in the standing position. However, this configuration has not yet been put in mass production.

Compound

By way of example, Fig. 1.27 shows the experimental compound SO 1310, Farfadet. The rotor is jet-propelled in the takeoff and landing configuration, and rotates automatically in the cruising configuration, when the machine is propellor-driven. The vechile is provided with two separate turbines, one for actuating the rotor, one for the propellor.

Convertibles. /12

As an example, Fig. 1.28 shows a photo of the Bell XV-3 prototype. Its two side-by-side rotors have vertical axes in the takeoff and landing configuration and tilt 90° in the cruising configuration, so as to act as propellors. The rotors are mechanically driven.

1.4. PERFORMANCE OF MODERN HELICOPTERS

We can get some idea of this by examining the table in Appendix I, which gives the principal characteristics of some particularly representative machines. A distinction is made between machines in service (mass-produced or in the process of being so) and those which are in the prototype development stage. Figure 1.30 gives an overall classification of the various types on the basis of the system used in the U.S. Army.

1.5. USES OF A HELICOPTER

We have no intention in this course of dealing with the diverse uses of rotorcraft. Everyone knows that they are manifold, and we will restrict ourselves here to classifying them in three groups, as follows.

1) "Crane" type mission

Vertical flight makes it possible to lift and transport loads to points which are often not widely separated, but otherwise difficult of access.

In this case the helicopter is a supplement to the surface means, namely, trucks, cranes, boats, mules, etc., but it outclasses them by its facility and speed of execution. Examples are the supply of depots in the mountains, unloading of ships, rescue work, etc.

2) Slow-flight missions

The safety inherent in using low-speed helicopters enables it to compete successfully with light aircraft in carrying out work that requires slow flight near the ground or obstacles; for instance, crop management, inspection of high-voltage lines, observation, etc.

3) Transport missions

This time it is the transport aircraft which are replaced by the helicopter

when it is necessary to use very confined or unprepared ground sites. Let us mention the following:

- Civil and military medical evacuation. /13

- Relief transport in case of a disaster (floods, earthquakes, etc.).

- Civil interurban cummunication transportion.

It should be stated that whatever the mission to be accomplished, the opportunity to use it, so tempting from the very start, depends on several rules based on the most elementary common sense. First of all, not just any helicopter can do what is wanted. Most of all, the cost of a helicopter is very high; for example, the cost per hour of flight of a light helicopter, all expenses included, fluctuates in France between 600 and 850 francs. Besides, its use requires highly skilled personnel and a large organization.

Therefore it will be rewarding to use a helicopter only when it is irreplaceable or when speed of execution is the decisive factor.

In concluding this section, let us cite a few of the normal expedient uses or rotorcraft.

Military use

Land. Organic complement of units as an aerial vehicle supplementing and reinforcing the ground vehicles. Communication, medical, flying CP, logistic or assult transport. Firing platforms for wire-guided missiles and light weapons.

Navy. Anti-submarine warfare (detection and attack). Rescue work on aircraft carriers, sounding, towing.

Civil Use

Agriculture. For some years the tendency here has been toward serious expansion. The preferred application is to small plots and crops requiring efficient, precise work.

Transportion. The use of helicopters for regular passenger transportation, from city to city or within large urban complexes, has been the subject of numerous studies and of commerical trials for some years now. In the USA we can mention the New York, Los Angles and Chicago Airways (airport service).

In Europe, Sabena serves an international network centered on Brussels; the BEA is intending to undertake experimental operation. /14

These types of transportation are much more costly per passenger seat than airplanes, and the problem now is that of return. It seems that the new generations of helicopters should bring strong improvements in this regard.

Civil Protection. In particular, mountain rescue work and at sea.

Advice
for reading Chapters 2, 3, 4

As these chapters unfold, numerous symbols will be used, and they will be defined as the occasion arises. However, the reader will do well to peruse beforehand the list of principal symbols given in Appendix 2.

Chapter 2

AERODYNAMICS /17

Helicopter theory, although of course calling upon the fundamental laws of aerodynamics, introduces notions that are appropriate to it.

The rotor is not a bearing wing, nor is it the propellor as conventionally studied. The operating conditions of a rotor are in fact quite different from those of the propellor in that (1) the (rotor) disc loading is very much lower, (2) the axial velocities are low, and (3) it can move with respect to the air in any direction — up, down, horizontally or obliquely.

In the most general case the analysis is quiet difficult and has not yet been accomplished in a manner that is completely satisfactory. Although large quantities of experimental data and a spate of theories are available, the sum total is still fragmentary and somewhat confused. Contradictions exist between authors, if not from page to page by the same author, and they will doubtless turn up in the reading of this chapter, although we shall attempt to present matters as coherently as possible.

In what follows we shall concentrate on rotor aerodynamics and then tough on the aerodynamics of the airframe.

2.1. AERODYNAMICS OF THE ROTOR

A first theoretical approach consists of comparing the rotor to a permeable disc that produces a pressure differential between its two faces (the "actuator disc" in the Anglo-Saxon literature, which we shall translate as "lifting disc").

This method yields results that are on the whole satisfactory as related to the calculation of performance, but if a more penetrating analysis is desired one must — as with the propellor — resort to vortex theory.

Hovering and vertical ascent can be handled by classical propellor theory /18
(Froude's method, vortex theory).

Vertical descent, on the other hand, introduces special phenomena that to date have not been amenable to other than empirical or semi-empirical investigation.

Rectilinear motion in any direction is the most difficult case to handle. Froude's theory no longer applies and one must resort to vortex theory, which is complicated and still inadequate in many points.

2.11. SIMPLIFIED ANALYSIS OF THE VARIOUS OPERATING MODES OF THE ROTOR

This analysis, quite brief from the standpoint of theory, is intended to give a basic appreciation of how the rotor acts on the air and to introduce the pertinent fundamental laws. Its oversimplified presentation will engender a sense of dissatisfaction in the critical reader which the subsequent sections will seek to allay.

The air will be assumed to be perfect.

Let us consider the arrangement of Fig. 2.1, which compares the rotor to a disc that creates a pressure differential between its two faces. The resultant lift, $\vec{F_N}$, normal to the disc, has its counterpart in an acceleration of the air. Along the flow line traversing the center of the rotor, the velocity goes from $\vec{V_0}$ at infinity upstream to $\vec{V_1}$ on crossing the disc and to $\vec{V_2}$ at infinity downstream.

More detailed analyses to be made later will show that results satisfactory to a first approximation are obtained if the following set of assumptions is adopted:

- the pressures at infinity are unvarying.

- everything happens as if the rotor had "teamed up" with a finite airflow Q moving with constant velocity, $\vec{V_1}$ to the right of the rotor and $\vec{V_2}$ at infinity downstream.

The flow Q is given by the relationship

$$Q = \rho S |\vec{V_1}| \tag{2.1}$$

where S is the rotor area. Note that it is not a question of the flow traversing the rotor (equal to $\rho S |\vec{V_1}| \sin \alpha$, see Fig. 2.1) but a flow that takes into account that even air that does not pass through the rotor can be deflected. The use of such an equivalent flow may be better understood if it is recalled that Prandtl's theory of the finite-span wing leads to considering the lift of the wing as resulting from the deflection of a stream of air of finite dimensions surrounding the airfoil.

We shall also see later that it is possible to give a physical explanation for this flow Q, whose sole justification for the moment is to allow us to make simple computations in keeping with a theory often advanced and with experience. /19

Under these conditions, the momentum theorem* applied to a large-diameter sphere surrounding the rotor yields:

$$\vec{F_N} = -\rho\,(\vec{V_2} - \vec{V_0}) \tag{2.2}$$

This demonstrates that the "induced" velocity at infinity downstream opposes the lift.

Let us now compute the power expended on the rotor, which exerts, by reaction, a force $-\vec{F_N}$ on the air passing through it. The relative velocity of the air being $\vec{V_1}$, the power expended on the rotor and communicated to the air is thus:

$$P = -\vec{F_N} \times \vec{V_1} \tag{2.3}$$

By definition we shall designate the "induced velocity" to the right of the rotor (or simply "induced velocity" when it will not cause confusion) as the vector $\vec{V_i} = \vec{V_1} - \vec{V_0}$.

As has been shown for the vector $\vec{V_2} - \vec{V_0}$, experiment and theory prove that the vector $\vec{V_i}$ is essentially perpendicular to the rotor disc. We shall assume it to be so in what follows.

Equation (2.3) can be written as

$$P = -\vec{F_N} \times (\vec{V_0} + \vec{V_i}) \tag{2-3'}$$

Formulas (2-3) and (2-3') lead to two important observations:

(1). The power to be furnished the rotor is positive when the air passes downward through the rotor from above $(-\vec{F_N} \times \vec{V_1} > 0)$. On the other hand, when the air passes upward from below the air furnishes power to the rotor.

*In the form of Euler's theorem. In setting up the equation it is assumed that the resultant of the pressures on the sphere is zero. This can be shown as the radius of the sphere tends toward infinity.

(2) The power P is composed of two terms: /20

- a thrust power $-\vec{F}_N \times \vec{V}_o$ which corresponds to the work done by the resultant $\vec{F}_N$ moving with velocity $-\vec{V}_o$ in air.

- an "induced" power $P_i = -\vec{F}_N \times \vec{V}_i$, which is the price that must be paid to obtain the force $\vec{F}_N$.

Another way of calculating the power is to write the total energy change communicated to the air between infinity upstream and infinity downstream (referred to axes tied to the rotor disc).

It suffices to write the change in kinetic energy of the air, taking into account the hypothesis $P_2 = P_0$:

$$P = \frac{1}{2} Q \left(\vec{V}_2^2 - \vec{V}_o^2\right) \overset{(*)}{=} \frac{1}{2} Q \left(\vec{V}_2 - \vec{V}_o\right)\left(\vec{V}_2 + \vec{V}_o\right) \qquad (2\text{-}4)$$

which, considering (2-2), becomes

$$P = -\vec{F}_N \times \frac{\vec{V}_o + \vec{V}_2}{2} \qquad (2\text{-}4')$$

Comparing (2-3') and (2-4'), we obtain

$$\vec{F}_N \times \left(\vec{V}_o + \vec{V}_i\right) = \vec{F}_N \times \left(\frac{\vec{V}_o + \vec{V}_2}{2}\right)$$

---

*Actually Bernouilli's theorem shows that in a perfect atmosphere only the air passing through the rotor can undergo a variation in total energy. The exact equation should be

$$P = Q \sin\alpha \left[\frac{p_2 - p_o}{\rho} + \frac{1}{2}\left(\vec{V}_2^2 - \vec{V}_o^2\right)\right]$$

The method of calculation used above is valid with the set of hypothesis made at the beginning of the section (in particular, uniform velocities in the stream $p_2 = p_0$).

or

$$\vec{F_N} \times \vec{V_i} = \vec{F_N} \times \frac{\vec{V_2} - \vec{V_o}}{2}$$

Since $\vec{V_i}$ and $\vec{V_2} - \vec{V_o}$ are both parallel to $\vec{F_N}$, we deduce that the velocity induced at infinity downstream is twice the velocity induced to the right of the rotor.

With which we can again write /21

$$\vec{V_1} = \frac{\vec{V_o} + \vec{V_2}}{2} \qquad (2\text{-}5)$$

The velocity on traversing the rotor is the arithmetic mean of the velocities at infinity downstream and infinity upstream*.

In view of (2-5), Eq. (2-2) can be written as

$$\vec{F_N} = -2\rho S \left| \vec{V_o} + \vec{V_i} \right| \vec{V_i} \qquad (2\text{-}2')$$

which is the fundamental equation of rotor theory.

Knowing the relationships relating $\vec{V_o}$, $\vec{V_1}$, $\vec{V_2}$, and $\vec{F_N}$, we can now describe the various operating modes of the rotor. $\vec{F_N}$ may be defined by its two components, with F_x in the direction of the velocity $\vec{V_o}$ and F_z perpendicular to $\vec{V_o}$. If F_x is positive the rotor pulls, otherwise it pushes.

Figure 2.2 describes the "helicopter" (or propellor) mode: With $P > 0$, it is necessary to supply power to the rotor. The air flow traverses the rotor downward from above and the energy expended on the rotor is recovered as kinetic energy communicated to the air. With $F_x < 0$, the lift has a thrust component (used in practice to make the helicopter rise or to compensate for parasitic drags).

*This property can also be demonstrated by considerations based on vortex theory (see 2.122).

Figure 2.3 corresponds to the "gyrodyne" mode. The rotor is bearing due to the power furnished it ($P > 0$) but does not provide thrust ($F_x = 0$) (Fig. 2.3 (a)). It can even pull slightly ($F_x > 0$, Fig. 2.3(b)). Examples are the gyrodyne proper, the helicopter in powered descent and the anti-torque rotor.

Figure 2.4 corresponds to "ideal autorotation" with $\left\{ \begin{matrix} P = 0 \\ F_x > 0 \end{matrix} \right\}$. The power /22

on the rotor is zero and the lift F_z has an "induced" drag F_x, as its counterpart, in the manner of a finite-span wing. The air does not traverse the rotor disc. Examples are maple leaves, seeds of the lime tree in free fall, the autogiro and the helicopter in autorotation.

Figure 2.5, finally, corresponds to the regime of "windmill-braking". The rotor receives energy from the air ($P < 0$) and pulls ($F_x \geq 0$). The air traverses the rotor upward from below and loses kinetic energy. Examples are windmills, air motors and true autorotation.

The operating modes we have just examined are much simplified theoretical pictures.

As pointed out at the beginning of this analysis, the velocities $\vec{V}_1$ and $\vec{V}_2$ are only average values permitting the calculation of lift and power, and are inadequate to handle the actual local velocities, which vary from point to point.

Moreover, an actual rotor differs from the ideal picture we have considered in that (1) it is necessary to add the power dissipated by the drag of the blade airfoil to the powers calculated above, and (2) it is also necessary to account for the "induced losses", whose origin we shall later make explicit, and, finally (3) the air is not "perfect".

Although formulas (2-1), (2-2) and (2-3) yield generally acceptable numerical values — at least to a first approximation — we will see that there are certain cases where, by reason of viscosity, the air does not "follow the arrows". The actual flow differs considerably from that suggested by the theory and the above formulas give results that are grossly in error. These are the "vortex-ring" regimes that occur at low speeds of descent.

2.12. JUSTIFICATION FOR THE CONCEPT OF THE LIFTING DISC

Before beginning the detailed study of the different flight modes, it is pertinent to see to what extent the comparison we have made (and shall continue to make) between the rotor and a lifting disc is justified.

The lift, rather than being applied uniformly over the disc swept out by the rotor, is actually concentrated on the blades.

The pressures and velocities induced at some point in space are not constant but vary periodically at the frequency of passage of the blades.

Two important observations can be made on this subject:

(1) The periodic nature of the flow is closedly tied to the total pressure variation (equal to F_N/S) to which the fluid is subjected in traversing the rotor. /23

(2) The theory of the lifting disc permits replacing the periodically varying quantities of the actual flow by an average value. There is here a source of uncertainty as regards the exact values of the physical quantities involved. As a matter of fact, with regard to the velocities we shall have to consider mean values that differ according to circumstances:

- the mean velocity defined by $\frac{\int_0^T \vec{V}\,dt}{T}$ which enters into the calculation of lift (momentum)

- the mean-square velocity $\sqrt{\frac{\int_0^T \vec{V}^2\,dt}{T}}$ which enters into the calculation of power (kinetic energy).

These two values are not the same, and the difference depends on the rate of modulation of the velocity*.

The theory of the lifting disc derives its value from the fact that the velocity modulation is small in practical cases, where the rotors turn rapidly compared to the induced velocities.

---

*A simple example makes this clear:

Assume: $\vec{V} = \vec{V}_m + \vec{V}_a \sin \omega t$

$$\frac{1}{T}\int_0^T \vec{V}\,dt = \vec{V}_m$$

$$\sqrt{\frac{1}{T}\int_0^T \vec{V}^2\,dt} = \sqrt{\vec{V}_m^2 + \frac{\vec{V}_a^2}{2}} > \left|\vec{V}_m\right|$$

In conclusion, we shall show how the fundamental law

$$P = -\vec{F}_N \times \vec{V}_1 \qquad (2\text{-}3)$$

is justified for the real rotor.

Consider a rotor in vertical flight (Fig. 2.6). A blade element is subjected to a total velocity $\vec{V}_t$ the sum of the velocity $\vec{V}_1$ and the drag velocity $-\vec{\omega r}$. If we assume ideal air, the lift dF_Z exerted on a blade element is perpendicular /24 to $\vec{V}_t$. The components of dF_Z on the vertical and along the tangent to the circle described by the element are

$$\begin{cases} dF_N = dF_Z \cos\phi \\ dF_T = dF_Z \sin\phi \end{cases} \qquad \left(\operatorname{tg}\phi = \frac{V_1}{\omega r}\right)$$

From this we get

$$\frac{dF_T}{dF_N} = \operatorname{tg}\phi$$

and

$$dP = -dF_T \times \omega r = -dF_N \times \omega r \operatorname{tg}\phi = -dF_N V_1$$

which, on integration, reverts to formula (2-3).

In particular, the mechanism of autorotation (P = 0) is explained by this process: The sum of the torques applied to a blade is zero, i.e. $\int_S dF_N V_1 = \frac{F_N}{S}\int_S V_1 d\sigma = 0$, and the flux of air traversing the rotor is zero, although locally it can have velocities of traverse in one sense or other. We shall have occasion to come back to this question in more detail.

Matters are a little more complicated in the general case, when there is a component V_x of air velocity in the tip-path plane. Figure 2.7 shows that the drags on two symmetrical blade elements are not equal; they form a couple and a force directed in the sense of the displacement. Therefore, an induced thrust force is present in the tip-path plane that is not predicted by the theory of the lifting disc. Calculation demonstrated readily that the power taken up by the rotor is in this case still equal to $\vec{V_0}$, $\vec{V_1}$ where $\vec{V_2}$ is the sum of $\vec{F_N}$ and the induced horizontal component. This induced component, moreover, is very small and can usually be neglected.

2.13. DETAILED STUDY OF THE VARIOUS MODES

2.131. Vertical Flight

This is the case when the rotor is displaced parallel to its axis of rotation. We shall analyze it using Froude's theory, in analogy with the propellor. /25

In the next section we shall give some elements of vortex theory designed to bring out the modifications it permits us to introduce.

Apart from exceptions that will be pointed out at the appropriate point, the flow is characterized by the existence of a stream of air which, after traversing the rotor disc, exhibits a velocity discontinuity with respect to the rest of the atmosphere (Fig. 2.8). The velocity and energy variations of this stream of air allow calculation of lift and power on the rotor.

The theory assumes that: (1) the rotor has an infinite number of blades, (2) the rotor disc is infinitely thin, (3) setting air into rotation is negligible, (4) the fluid is ideal, and (5) the thrust and velocities are uniform over the disc.

Let p_0, V_z, S_0 be the pressure, velocity and stream cross-section at infinity upstream, p_1, V_1, S these same elements at the upstream face of the disc, p_1, V_1', S these elements at the downstream face of the disc, and p_2, V_2, S_2 these elements at infinity downstream.

On taking the velocities to be positive downward and the lift as positive upward, we have the following relationships:

$$V_1 = V_1' \qquad \text{(conservation of flow)}$$

$$Q = \rho S_0 V_z = \rho S V_1' = \rho S_2 V_2 \qquad \text{(conservation of flow)}$$

$$p_2 = p_0 \qquad \text{(stream equilibrium at infinity downstream)} \tag{2-6}$$

$$p_0 + \tfrac{1}{2}\rho V_2^2 = p_1 + \tfrac{1}{2}\rho V_1^2 \qquad \text{(Bernoulli's Law)}$$

$$p_0 + \tfrac{1}{2}\rho V_2^2 = p_1' + \tfrac{1}{2}\rho V_1^2 \qquad \text{(Bernoulli's Law)}$$

On the other hand, $F_N = (p_1' - p_1)$, combined with the two latter equations, /26 gives

$$F_N = \tfrac{1}{2}\rho S \left(V_2^2 - V_2^2 \right) \tag{2-7}$$

In other respects F_N is calculated by the momentum theorem as in section 2.11.

$$F_N = Q \left(V_2 - V_2 \right) = \rho S V_1 \left(V_2 - V_2 \right) \tag{2-8}$$

On comparing (2-7) and (2-8) we obtain

$$2 V_1 \left(V_2 - V_2 \right) = V_2^2 - V_2^2$$

or

$$V_1 = \frac{V_2 + V_2}{2}$$

which demonstrates the general property pointed out in Section 2.11 for this particular case.

These relationships can be written:

$$F_N = 2\rho S \left| V_1 \right| \left(V_1 - V_2 \right) = 2\rho S \left| V_2 + V_i \right| V_i \tag{2-9}$$

$$P = F_N \cdot V_1 = F_N (V_z + V_i)$$

$$\frac{S_o}{S} = \frac{V_1}{V_z} = 1 + \frac{V_i}{V_z} \qquad (2\text{-}9)$$

$$\frac{S_2}{S} = \frac{V_1}{V_2} = \frac{1 + \frac{V_i}{V_z}}{1 + \frac{2V_i}{V_z}}$$

We shall study the cases of hovering, ascent and descent using these relationships.

2.1311. Hovering ($V_z = 0$) /27

Equations (2-9) are written:

$$F_N = 2\rho S V_{i_o}^2 \qquad \text{ou} \qquad \underline{V_{i_o} = \sqrt{\frac{F_N}{2\rho S}}}$$

$$P_{i_o} = F_N \cdot V_{i_o} = 2\rho S V_{i_o}^3 = \underline{F_N \sqrt{\frac{F_N}{2\rho S}}} \qquad (2\text{-}10)$$

$$\frac{S_o}{S} = \infty$$

$$\frac{S_2}{S} = \frac{1}{2}$$

The flow has the appearance shown in Fig. 2.9. The actual flow (Fig. 2.10) differs slightly from this due to air viscosity, which tends to homogenize the velocities, and air which has not traversed the rotor will be partially entrained. The velocities in the stream are reduced and its diameter increases. At infinity downstream the momentum, equal to the lift, is conserved; only the total energy of air has diminished, part having been dissipated by friction. This phenomenon is of little consequence for rotor performance. On the other hand, the remaining factors cause the power taken up by the rotor to exceed that of formula (2-10) due to losses from blade drag and "induced" losses which we shall examine in detail:

(1) The separation layer at the boundary of the stream is not infinitely thin, but has some thickness which reduces the "useful" surface of the rotor (Fig. 2.10); these are the losses at the blade tips and we shall subsequently specify their exact origin.

(2) The induced velocity is never uniform as has been assumed, and induced tangential components of the velocity exist as well. /28

- If the induced tangential velocities are ignored one feels intuitively — and it can easily be demonstrated — that uniform distribution of induced velocity requires less power for a given lift*. Any deviation from this optimum therefore entails an increase in induced power.

*For those readers not acquainted with the theorems of the calculus of variations, which shows this directly, it will be demonstrated by elementary reasoning. For an arbitrary distribution, the lift and power are written:

$$F_N = \int_S 2\rho \, d\sigma \, V_i^2$$

$$P = \int_S 2\rho \, d\sigma \, V_i^3$$

Let us assume that the optimum distribution of induced velocity has been found (giving minimum P for a given F_N). If we slightly change the induced velocities at two points A and B, preserving the lift F_N, we will have simultaneously

$$\Delta F_N = 0 \quad \text{(lift conserved)}$$

$$\Delta P = 0 \quad \text{(maximum power)}$$

or

$$d\sigma_A \, V_{i_A} \, \Delta V_{i_A} + d\sigma_B \, V_{i_B} \, \Delta V_{i_B} = 0$$

$$d\sigma_A \, V_{i_A}^2 \, \Delta V_{i_A} + d\sigma_B \, V_{i_B}^2 \, \Delta V_{i_B} = 0$$

These two equations require that $V_{i_A} = V_{i_B}$.

This reasoning can be applied to any point of the disc and we thus derive the condition V_i = const.

-As regards the tangential velocities, on examination of the air equilibrium in the stream at infintity downstream it is seen that these velocities bring about a pressure reduction that lowers the lift, the power consumed remaining the same.

The efficiency of a real rotor is to be characterized by comparing it with Froude's ideal rotor of the same diameter. /29

The induced factor (losses at the blade tips and non-uniformity of induced velocities) is:

$$\eta_i = \frac{P_{i_0}}{P'_{i_0}} \begin{matrix} \text{(theoretical induced power)} \\ \text{(actual induced power)} \end{matrix} = \frac{F_N}{P'_{i_0}} \sqrt{\frac{F_N}{2\rho S}} \qquad (2\text{-}11)$$

Likewise, if the total power P_T expended on the rotor is considered, the lift factor is introduced:

$$\eta_s = \frac{F_N}{P_T} \sqrt{\frac{F_N}{2\rho S}} \qquad (2\text{-}12)$$

η_i and η_s are obviously less than unity, and approach unity as the rotor is more "perfect". Practical orders of magnitude are $\eta_i = 0.8$ to 0.9 and $\eta_s = 0.6$ to 0.8.

2.1312. Vertical Climb ($V_z > 0$).

The flow is quite similar to that for hovering and has the appearance shown in Fig. 2.11.

It is convenient to write Eq. (2-9) in dimensionless form, taking as reference the theoretical velocity V_{i_0} induced in hovering with the same lift F_N:

$$V_{i_o} = \sqrt{\frac{F_N}{2\rho S}}$$

$$\left(\frac{V_Z}{V_{i_o}} + \frac{V_i}{V_{i_o}}\right)\frac{V_i}{V_{i_o}} = 1 \qquad (2\text{-}13)$$

$$P = F_N \cdot V_{i_o}\left(\frac{V_Z + V_i}{V_{i_o}}\right) = P_{i_o}\left(\frac{V_Z}{V_{i_o}} + \frac{V_i}{V_{i_o}}\right) = \frac{P_{i_o}}{V_i/V_{i_o}}$$

Knowing V_Z, V_i and P are easily found using the diagram of Plate II-1, which is a graphical representation of equation (2-13). /30

In practice V_i will be increased by a coefficient to account for the induced losses.

It is interesting to compute P for small values of V_Z ($\frac{V_Z}{V_{i_o}} < 0{,}25$, which covers most of the usual values). Since $\frac{V_Z}{V_{i_o}}$ is small, the second equation in (2-13) can be differentiated:

$$d\left(\frac{V_Z}{V_{i_o}}\right)\cdot\frac{V_i}{V_{i_o}} + d\left(\frac{V_i}{V_{i_o}}\right)\cdot\left(\frac{V_Z}{V_{i_o}} + \frac{2V_i}{V_{i_o}}\right) = 0$$

On setting $V_i/V_{i_o} = 1$, $V_Z/V_{i_o} = 0$, we find $V_i = V_{i_o} - V_Z/2$, and

$$P = P_{i_o} + \frac{F_N \cdot V_Z}{2} \qquad (2\text{-}14)$$

The power required for vertical ascent at velocity V_Z is equal to the power induced in hovering increased by one-half the power required to cause the weight sustained by the rotor to rise at velocity V_Z.

The principle of conservation of energy is of course not violated, since the decrease in work to overcome gravity is only apparent and stems from the saving realized in induced power due to the axial velocity V_Z.

On the other hand, for high values of V_Z/V_{i_o}, we find from eqs. (2-13):

$$P \simeq F_N \cdot V_Z$$

This is the classical equation for the screw propellor of unity efficiency (very small induced velocity).

2.1313. Vertical Descent $V_Z < 0$ /31

In these modes, V_Z and V_i are in opposition.

In rapid descent ($|V_Z| > 2V_i$) the flow has the appearance shown in Fig. 2.12. The following equations, analagous to formulas (2-13), are derived from eqs. (2-9):

$$\left(\frac{V_Z}{V_{i_o}} + \frac{V_i}{V_{i_o}}\right) \times \frac{V_i}{V_{i_o}} = -1$$

$$P = P_{i_o}\left(\frac{V_Z}{V_{i_o}} + \frac{V_i}{V_{i_o}}\right) = -\frac{P_{i_o}}{\frac{V_i}{V_{i_o}}} \qquad (2\text{-}15)$$

We note especially that P is negative and the air gives up power to the rotor: this is the "windmill-breaking" region.

A rotor operating in this way can be described by its efficiency — the ratio of the power received to the power theoretically available. We shall not dwell on this since this case is hardly ever used in gyro-aviation.

In descent at medium or slow speeds the limit for this flow is obtained for $|V_Z| = 2V_i$ would be that of Fig. 2.13(a), which is still a "windmill-breaking" mode $V_i < |V_Z| \leq 2V_i$. But owing to air viscosity, the blown-out stream is entrained in the direction of V_Z and the mode in fact established is characteristized by the appearance of vortex rings at the rotor level (Fig. 2.13(b)). This is the case pointed out earlier, when the air "does not follow the arrows" indicated for it by the theory. Equations (2-15) become inapplicable.

It is the same for the descent at very low speed mode ($|V_z| < V_i$) the helicopter ranges ($P > 0$). The theoretical flow should be that of Fig. 2.14(a), and this is in fact observed for three very low-speed descents, but after V_Z attains an appreciable value, the flow becomes that of Fig. 2.14(b), which is quite comparable with that of the preceeding case. Note that the vortex is more prominent and is located below the rotor. A physical explanation of the phenomenon is that the rotor, in descending, "swallows" its own slipstream, which explains the turbulent nature of the flow observed here. /32

From $V_Z = 0$ to $V_Z = -2V_i$ we are thus dealing with the same type of flow, characterized by the presence of vortex ring in the vicinity of the rotor. This operating mode is described as follows:

(1) The air has "detached" above the rotor, forming a wake.

(2) The phenomenon is not stationary: the vortex tied to the rotor periodically allows ring vortices to escape which are entrained in the wake.

The similarity of this process and that produced behind a poorly-streamlined body will be noted. In the case of interest to us, the lift, parallel to the velocity relative to the air, and in the same sense, is in fact a drag.

In general, however, the rotor cannot be compared to an inert body since, contrary to this, it exchanges energy with the air except in the special case when $P = 0$ (vertical autorotation) which we shall now examine.

Vertical autorotation represents the boundary between the helicopter ranges ($P > 0$, low speed of descent) and the windmill-braking ranges ($P < 0$, high speed of descent).

The theoretical flow is shown in Fig. 2.13(a). Figure 2.15(b), which refers to the actual flow, shows that the role of the rotor in this case is to impede the air flowing through it. It generates a slipstream above the disc that is quite similar to that of a circular plate of the same area perpendicular to the wind. Wind-tunnel studies confirm this similarity qualitatively and quantitatively. We shall return to it later in the general investigation of autorotation*.

*It is noted in passing that the "ideal air" of the theoreticians would be little appreciated by a pilot led to make an autorotation in it inasmuch as eq. (2.15) shows that the descent velocity would be infinite! ... This of course, is related to a particular form of d'Alembert's paradox, as shown in Fig. 2.15(a).

As we have seen, these vortex ring regimes are not explainable by Froude's theory, and the uniform induced velocity term no longer has the same meaning, even as an approximation. Neverthless one can introduce the concept of an effective induced velocity, defining it by the relationship /33

$$P = -\vec{F}_N \times (\vec{V}_z + \vec{V}_i)$$

By making use of experimental data (wind-tunnel and flight tests) it is also possible to determine V_i as a function of V_z* (see next section).

2.1314. Summary of Results for Vertical Flight

Plate II-2 is an arbitrary grouping of the sum total of the phenomena relating to vertical flight.

The induced and vertical velocities are shown as ratios with respect to V_{i_o}. The solid curve relates to experimental data.

For fast ascent and descent the curve approaches the theoretical curves of Froude (dotted). The differences in these regions correspond to the average corrections attributable to the induced losses.

Let us examine in greater detail that part of the curve corresponding to the vortex ring regime. We have given many experimental curves from various sources for this region; they show that a marked dispersion exists, as distinguished from Froude's flow regions. This is due to the fact that viscosity phenomena exert a major influence on the flow — the scale effect in particular will be important.

The shape of the curve merits some comment.

On the diagram the straight lines parallel to the diagonal of the second quadrant are the iso-power curves

---

*V_i can also be determined by equating the measured lift of the rotor and the lift calculated as a function of blade pitch, with the mode of operation and V_1 assumed to be unchanged (see the formula of Chapter 4). There is no reason that the two values of V_i thus found should coincide rigorously.

$$\frac{V_i}{V_{i_o}} + \frac{V_z}{V_{i_o}} = C^{te}$$

and the figurative point of "ideal" autorotation lies on the line

$$\frac{V_i}{V_{i_o}} + \frac{V_z}{V_{i_o}} = 0$$

Real cases of autorotation are actually cases of "windmill-breaking": a certain energy is taken up by the rotor to overcome the drag of the blades, friction in the transmission, to drive the accessories or the anti-torque, etc... Moreover, it is seen from the plate that the reduction is power in this operating mode has but little influence on the velocity of descent. /34

On the other hand, in the range of low velocity of descent $\left(\left|\frac{V_z}{V_{i_o}}\right| < 1.2\right)$ the tred of the curve is very nearly the same as that of the equal power curve: A very small change in power brings about large variations in speed of descent*.

This, coupled with the "choppy" nature of the ring vortex region below the rotor, is the cause of the control difficulties experienced by pilots who get into this flight mode.

In the language of the users, the vortex ring regime characterizes this difficult region with the exception of autorotation and its windmill-braking ranges, which do not show these properties.

The diagram of Plate II-2 takes into account in an overall manner the losses due to non-uniformity of the flow.

If a more precise estimate is desired, it may be obtained by applying the equations of Froude's theory to rings that are sufficiently close.

We shall see the application of this method in Chapter 4, in the treatment of performance calculation.

---

*Another way of interpreting this fact is to say that vertical damping is lacking in this case.

2.132. ELEMENTS OF ROTOR VORTEX THEORY— APPLICATIONS TO VERTICAL FLIGHT

In this section we shall investigate rotor operation from a fresh viewpoint — vortex theory.

The mathematical side of the problem has been somewhat sacrificed to a presentation that is as physical as possible. The few guidelines that will be given should not be taken as replacing specialized treatments; they should be looked on primarily as a means of making understandable how the rotor differs from the lifting disc we have considered thus far.

Moreover, this will be a preparation for the study of forward flight, for which the "vortex viewpoint" is least adapted.

2.1321. PRINCIPLES OF VORTEX THEORY /35

Vortex theory consists of calculating the velocities induced at each point of space by the vortices created by operation of the rotor. The attached vortices carried by the blades are distinguished from the free vortices, which escape and are carried along in the slipstream.

Fluid mechanics tells us that the velocities inside a fluid can be computed if the vortex intensities are known at each point of space. Each vortex element of length dl and intensity Γ will give, at a point M, an induced velocity

$$d\vec{V}_i = \frac{\Gamma \overrightarrow{d\ell} \wedge \overrightarrow{OM}}{4\pi |\overrightarrow{OM}|^3}$$ (see Fig. 2.16)

This formula is known to be the same within a constant factor as the Biot and Savart formula of electromagnetism. The following rule will be useful to those readers better aquainted with this subject: The induced velocity field created by a vortex system is identical to the electromagnetic field produced by currents of intensity $\frac{\Gamma}{4\pi}$ flowing in the vortex filaments.

In general the difficulties of vortex theory are twofold:

(1) It is often difficult to locate the free vortices in space.

(2) In any given case the calculations are extremely complicated and must be more or less grossely approximated to be handled satisfactorily.

To illustrate the method let us now apply it to vertical flight.

2.1322. APPLICATION TO THE ROTOR IN VERTICAL FLIGHT

We begin with the simple case of the blade in constant rotation. Consider Fig. 2.17, where we have assumed a single blade to facilitate comprehension. The blade represents a bearing segment characterized by uniform rotation Γ. /36
Free vortices of intensity Γ escape from its two extremities.

To the right of a blade, in the plane of the disc, the induced velocity due to attached vortices is zero (by reason of symmetry), and the same situation exists at infinity downstream. We shall thus study the induced velocities caused by free vortices only.

The vortex issuing from the root of the blade is disposed along the rotor axis. It creates on induced tangential velocity V_t in the plane of the disc and $2V_t$ inside the stream.

This induced tangential velocity does not exist in lifting disc theory; it is the new element introduced by the fact that the rotor is a rotating, lifting airfoil.

The value of V_t is obtained by writing that the circulation along a circle of radius r is equal to $\frac{\Gamma}{2}$:

$$V_t = \frac{\Gamma}{4\pi r} \qquad (2\text{-}16)$$

The vortex that escapes from the blade tip describes a helix.

The surface on which it coils up is evidently the surface separating the blown-out stream from the rest of the air. In vortex theory terms the surface of discontinuity in velocity is a vortex sheet.

The helix formed by the tip-vortex is similar to a solenoid: It creates an axial field which is precisely the induced velocity of the Froude theory. We shall assume that the turns of this solenoid are closely-spaced so that the usual formulas of electromagnetism are applicable. This hypothesis a large number of blades and a rapidly turning rotor (tip velocity much greater than axial velocity).

It is known that in this case the field inside the solenoid has the following characteristics:

- The field remote from the extremities is axial and uniform, and its intensity is given by the formula $H = 4\pi n i$ (n = numbers of turns per unit length, i = strength of current flowing through each turn).

- At the entrance the axial component of the field is uniform and equal to $2\pi n i$ one-half the previous value. /37

Thus we find the property that the velocity induced at infinity downstream is twice the velocity induced on traversing the disc.

The pitch of the helix formed by the tip-vortex must be known to calculate the magnitude of the induced velocity. We obtain this by describing the free vortex to be in equilibrium — that is, not subjected to force at any point. The force on one element of the vortex being of the form $\rho \vec{V}_A \vec{\Gamma} d\vec{\ell}$, we write that the tangent to the helix is parallel to the velocity relative to the air at every point. We will then have (Fig. 2.17):

$$\operatorname{tg} \phi = \frac{V_z + V_i}{\omega r - V_t} \quad (*)$$

where r is the radius (at infinity downstream) of the cylinder on which the solenoid is developed and the axial distance separating two turns is

$$\ell = 2\pi r \operatorname{tg} \phi = \frac{2\pi}{\omega} \times \frac{V_z + V_i}{1 - \frac{V_t}{\omega r}}$$

or

$$n = \frac{1}{\ell} = \frac{1}{2\pi r \operatorname{tg} \phi} = \frac{\omega}{2\pi} \times \frac{1 - \frac{V_t}{\omega r}}{V_z + V_i} \qquad (2\text{-}17)$$

*It is located in exes fixed with respect to the blades; the air is set into rotational motion - ω. The induced velocities to be considered are V_i and V_t, and not $2V_i$ and $2V_t$, since we are on the surface of discontinuity outside of which these induced velocities are zero.

The induced velocity V_i is given by

$$V_i = 2\pi \times \frac{\Gamma}{4\pi} \times \frac{\omega}{2\pi} \times \frac{\left(1 - \frac{V_t}{\omega r}\right)}{V_z + V_i}$$

or

$$V_i \left(V_z + V_i\right) = \Gamma \frac{\omega}{4\pi} \left(1 - \frac{V_t}{\omega r}\right) \qquad (2\text{-}18)$$

$V_t/\omega r$ is usually negligible with respect to unity and we can write /38

$$V_i \left(V_z + V_i\right) = \Gamma \frac{\omega}{4\pi} \qquad (2\text{-}18')$$

The Relationship between V_i and V_t: According to formula (2.17), V_i can be written

$$V_i = 2\pi \cdot \frac{\Gamma}{4\pi} \cdot \frac{1}{2\pi r \operatorname{tg} \phi} = \frac{\Gamma}{4\pi r \operatorname{tg} \phi}$$

and, considering (2.16), we have

$$V_t = V_i \operatorname{tg} \phi$$

whose interpretation is that the total induced velocity is perpendicular to the relative velocity of the air at each point, and especially to the right of the blade; this represents a generalization to the propellor of a property of the finite-span wing.

Calculation of Power and Lift: The lift of a blade element having a horizontal velocity wr - V_t is

$$dF_N = \rho \Gamma dr \left(\omega r - \frac{\Gamma}{4\pi r}\right)$$

and the total lift is

$$F_N = \rho \Gamma \int_0^R \left(\omega r - \frac{\Gamma}{4\pi r}\right) dr \qquad (2\text{-}19)$$

For the moment let us ignore the correction represented by insertion of the tangential velocity V_t. Eq. (2-19) becomes:

$$F_N = \rho \Gamma \int_0^R \omega r \, dr = \rho \Gamma \omega \frac{R^2}{2} \qquad (2\text{-}19')$$

On replacing Γ by its value taken from (2-18'), we find

$$F_N = 2\rho S V_i \left(V_z + V_i\right) \qquad (2\text{-}20)$$

Power: The axial velocity gives rise to a drag of form $\rho \Gamma dr \left(V_z + V_i\right)$, /39
and the power is given by

$$P = \int_0^R \rho \left(V_z + V_i\right) \Gamma \, dr \, \omega r \qquad (2\text{-}21)$$

$$P = \rho (V_z + V_i) \Gamma \omega \frac{R^2}{2} \qquad (2\text{-}22)$$

Taking (2-19') into account, we find

$$P = (V_z + V_i) F_N \qquad (2\text{-}23)$$

Equations (2-20) and (2-23) are identical to Eq. (2-9). We thus see the value of Froude's theory: It corresponds to the case of an ideal rotor with a large number of blades (solenoid with closely-spaced turns), for which the action of the induced tangential velocities is ignored. The circulation along the blades is constant.

The corresponding vortex picture would be a closely-shaped series of vortex rings shed by the edges of the rotor disc and distributed uniformly along the surfaces of discontinuity of the slipstream.

We shall now look into what corrections need be made to the theory to provide a more precise analysis of real rotors — the effect of the induced tangential velocity and the finite number of blades.

Effect of the Tangential Component of Induced Velocity.. In attempting to integrate Eq. (2-19):

$$F_N = \rho \int_0^R \Gamma \left(\omega r - \frac{\Gamma}{4\pi r} \right) dr$$

we see that negative lifts appear which tends to infinity at the root of the blade*. This suggests to us that the scheme $\Gamma = C^{te}$, with V_i uniform over the entire disc — which was the optimum was derived from the theory of the lifting disc — is not optimum when the fact that the rotor is a rotating-lifter is taken into account.

*These negative lifts are the translation into vortex language of the losses of lift we have mentioned in 2.1211 and which are due to the diminution of pressure in the slipstream as a consequence of the existence of tangential velocities.

We are therefore led to consider a distribution of circulation along the blade and to seek the law $\Gamma(\bar{r})$ that is optimum with respect to efficiency.

Figure 2.18 shows that the vortex at the root of the blade is replaced by a layer of vortex filaments, which are shed all along the length of the blade. Their intensity is $\frac{d\Gamma}{d\bar{r}}$ and they form helicoidal systems that induce, inside the cylinder they surround, velocities directed upward if $\frac{d\Gamma}{d\bar{r}}$ is positive. /40

The mathematical developments for computing the optimum distribution of induced velocities for hovering flight — the most important case practice — will be found in Appendix III-1. The results are plotted on Plate II-3.

It is noted, as might be expected, that correction with respect to the law of uniform velocities occurs principally toward the root of the blade, where the velocities are strongly reduced. The distribution approaches more closely the law V_i = Const. as the ratio V_i/U becomes smaller (i.e. low blade loading).

In practice the correction is only important in precisely that region where, due to the mode of construction of the rotor, it is impossible to obtain significant induced velocities ($\bar{r} \leq 0,2$). Therefore it should not be regretted that the induced velocities cannot be held constant up to the center of the rotor.

Even when the optimum distribution of induced velocities is obtained, it is clear that the operating power is necessarily greater than that indicated by the Froude theory. The optimum helix has an efficiency slightly lower than that of the optimum lifting disc; also one can say that it was not "cricket" to estimate the induced efficiency of a rotor using formula (2-11), since its rotating-lifter nature handicaps it with respect to the lifting disc.

To give a feeling for the orders of magnitude, Plate II-3 shows a diagram giving the maximum efficiency attainable by a rotor as a function of its "load" F_N. For practical values of F_N it is seen that the loss in efficiency is very small.

Losses at the Blade Tips. Until now we have assumed (explicitly or implicitly) the number of rotor blades to be infinite. The fact that real rotors have only a small number of blades entails modifying the theory, which now involves the blade tips.

It would be beyond the scope of this course to go into the details of this.

The corrections to be made to vortex theory are given in [6]; they entail a rapid reduction in lift at the blade tip. We shall content ourselves to show the physical reason for these losses. /41

As a consequence of the fact that the turns of the solenoid formed by the vortices at the blade tip are not joined, a vortex forms around them which reduces the useful cross-section of the stream (see Fig. 2.19).

One might say figuratively that the wall of the blown-out stream "skips" between the vortices. We again see the fact already mentioned that the useful cross-section of the stream is reduced, and therefore there is a loss of lift called the blade-tip loss (or tip-loss).

One should therefore expect the optimum induced velocity distribution at the blade tip to deviate from the law $V_i = \text{const.}$ (which, moreover, cannot be realized in practice).

In Chapter 4 we shall point out how to take these losses into account at each point of the blade (see 4.214). In practice they occur only over the last few percent of the rotor radius, and usually we are satisifed to introduce them by replacing the rotor radius R by an effective radius BR ($B < 1$). There are many formulas for B; the most practical one is that of Prandtl

$$B = 1 - \frac{1.386}{b} \frac{\lambda'}{\sqrt{1+\lambda'^2}}$$

where λ', (in-flow parameter) is equal to $(V_2 + V_i)/u$ and b is the number of blades.

In the case of hovering

$$\lambda' = \sqrt{\frac{F_N}{2\rho S u^2}}$$

On using the reduced lift coefficient

$$f_N = \frac{F_N}{\frac{\rho}{2} S u^2},$$

we obtain the approximate formula

$$B \simeq 1 - \frac{\sqrt{\frac{F_N}{2}}}{b} \qquad (2\text{-}24)$$

Remark. The analytic form of Prandtl's formula is intuitive: the reduction in radius is the larger the more widely spaced the tip-vortices are. There spacing ℓ, deduced from formula (2-17), is written /42

$$\frac{\ell}{R} = \frac{1}{b} \times 2\pi \frac{V_z + V_i}{\omega R} = 2\pi \frac{\lambda'}{b}$$

To recapitulate what vortex theory has taught us regarding the behavior of the rotor, we shall say that it shows that the maximum induced efficiency η_i it is possible to attain is slightly less than unity.

The optimum distribution of induced velocities is not strictly uniform; it calls for reducing these velocities at the root and tip of the blade.

A summary of the induced velocities for an actual rotor is shown on Plate II-4 as an example.

2.133. FORWARD FLIGHT

As we have indicated, this is the most difficult case to analyze, by reason of the complexity of the air flow.

2.1331. GENERAL CONSIDERATIONS

A preliminary comparison of the modes of operation of a propellor in vertical flight and the finite-span airfoil will help to understand better the role of the rotor. Let us consider Fig. 2.20.

Figure 2.20(a) corresponds to a rotor in vertical flight. The lift $\vec{F}_N$ is parallel to the velocity $\vec{V}_1$ and, as we have seen, this results in an increase in total pressure below the rotor. At infinity downstream this shows up as an

increase in velocity of the air which has traversed the rotor

$$|\vec{V}_2| > |\vec{V}_0|$$

We now consider the finite-span airfoil. As known, the formulas from Prandtl's theory allow us to write

$$\vec{F}_N = -2\rho S |\vec{V}_0| \vec{V}_i$$

where $\vec{F}_N$ is the lift of the airfoil, $\vec{V}_i$ is the induced velocity to the right of the airfoil $\vec{V}_0$ is the velocity at infinity upstream and S is the area of the circle having the airfoil span as its diameter. /43

In consideration of the fact that the induced velocity at infinity downstream is equal to $2\vec{V}_i$ in the slipstream, this formula is generally interpreted as expressing that the lift results from the downward deflection at velocity $2\vec{V}_i$ of a stream of air of cross-section S. Thus presented, this interpretation is a simple mnemonic device. We shall show that this formula is based on a physical reality. Consider Fig. 2.20(b).

The vortex system that is shed by the airfoil is not precisely parallel to $\vec{V}_0$. Its equilibrium requires that is be deflected downward at an angle ϵ (function of $\vec{V}_i$ and $\vec{V}_0$). The molecules of this layer are moved with velocity $\vec{V}_2'$. Study of the streamlines then leads to a separation of the air into two portions by a surface Σ enclosing the vortex layer.

The filaments of air (1) outline Σ; at infinity downstream their velocity is again $\vec{V}_0$. The filaments of air (2) are confined inside Σ and describe helices with axes parallel to $\vec{V}_2'$.

From this point of view, the lift is obtained by the deviation of the air contained in Σ (without variation in total pressure, since no energy is exchanged between the airfoil and the air). Calling S_Σ the right section of Σ, we have

$$-\vec{F}_N = \rho S_\Sigma |\vec{V}_0| (\vec{V}_2' - \vec{V}_0)$$

which, compared with the earlier formula, gives

$$2\rho S \left|\vec{V}_o\right| \cdot \left|\vec{V}_i\right| = \rho S_\Sigma \left|\vec{V}_o\right| \cdot \left|\vec{V}_o\right| \sin \varepsilon$$

Two Important Remarks: (1) An examination of Fig. 2.20(b) shows that the induced velocity $2V_i$ at the center of the vortex system is greater than the average velocity of deflection of the stream $V_o \sin \varepsilon$. The induced velocity increment serves to create air eddies to permit the existence of the stream Σ. The relationship $S_\Sigma \left|\vec{V}_o\right| \sin \varepsilon = 2 S V_i$ shows that the section S_Σ is greater than S. (2) Σ is not a surface of discontinuity of the flow; it separates molecules air that "take a short trip together" but whose destinations will be different at infinity downstream. /44

We can now better understand the mode of operation of the rotor in translatory motion (Fig. 2.20(c)).

The lift $\vec{F}_N$ can be decomposed into $\vec{F}_{N_1}$, perpendicular to $\vec{V}_1$ and $\vec{F}_{N_2}$ parallel to $\vec{V}_1$.

Qualitatively at least, one can then say that the rotor has two functions: to create $\vec{F}_{N_1}$ it acts as an airfoil and causes the deflection of a stream of air Σ; to create $\vec{F}_{N_2}$ it acts as a propellor operating axially and imposes a variation in total pressure on the air passing through it that is recovered as an increase in velocity at infinity downstream.

The air is thus separated into three regions: (1) the filaments of air of type (1) that enclose Σ and recover velocity $\vec{V}_o$ at infinity downstream. (2) the filaments of air of type $\vec{F}_{N_1}$ that are confined within Σ without having traversed the rotor. Their total pressure does not change and they contribute to the lift $\vec{F}_{N_1}$ by their average deflection. (3) Filaments of type (3) that traverse the rotor. These streams are deflected and undergo a change in a total pressure. Roughly speaking, they create $\vec{F}_{N_2}$ due to their change in total pressure and contribute to the setting-up of $\vec{F}_{N_1}$ by their deflection. The filaments (2) and (3) are tightly interlaced inside Σ.

Remarks: /45

The mode of operation of the rotor can be compared schematically to that of an airfoil equipped with propellors over its entire span.

Figure 2.20(c) shows the heterogeneity of the velocities in the slipstream: The assumption of uniform velocity $\vec{V}_2$ has only the sense of a mean value intended for performance calculations.

Moreover, in practice the air viscosity brings about a certain homogenization of the velocities in the slipstream.

One or other of the modes of operation of the rotor will predominate, depending on the direction of the velocity $\vec{V}_1$.

For example, on leaving hovering flight and introducing an increasing horizontal velocity, we will pass from the type of flow with a stream expelled vertically ("propellor" operation) to a type of flow having a deflected stream ("wing" operation) (see Fig. 2.21).

The range of velocities where change from one type to the other occurs is called the "transition zone". It is characterized by an unequal distribution of induced velocities over the disc and some flow turbulence which makes flight in this zone disagreeable — strong vibration, severe alternating stresses in the blades, etc...

This region is located near the value $V_x/V_{i_0} = 1.3$, being in practice between 30 and 70 km/hr depending on blade loading.

2.1332. QUANTITATIVE ANALYSIS

We have already stated that Froude's method cannot be used and that only vortex theory permits a satisfactory approach to the analysis problem.

These vortex theories are as yet quite crude and subject to uncertainty in detail. The difficulty is connected with determining the vortex systems and solving the equations giving the induced velocities.

The hypotheses usually made consists of assuming constant circulation along blades and encirclement of the oblique cylinder generated by the rotor disc moving in the direction $\vec{V}_1 = \vec{V}_o + \vec{V}_i$ by the free vortices.

A more accurate analysis leads to the introduction of a variable circulation with the azimuth such that uniform lift is maintained despite variations in velocity relative to the air. This introduces a lateral asymmetry into the distribution of induced velocities. /46

We shall not go into more detail here and refer the reader to specialized studies of the question (see particularly [4] and [5]). We shall merely point out the main properties of the rotor in forward flight.

Determination of Average Induced Velocity

Apart from the case analagous to vortex ring regions, we can use the relationship

$$\vec{F_N} = -2\rho S \left| \vec{V_0} + \vec{V_i} \right| \vec{V_i} \quad (*) \qquad (2\text{-}2')$$

In the general case there is no simple, rigorous proof of this formula. It is justified by the following considerations:

(1) It is the generalization of a formula applicable both to the finite-span wing and to the rotor in vertical flight. The considerations developed in the last section, according to which the rotor has a mixed propellor-wing operation, constitutes the kernel of the demonstration.

(2) Vortex theories give the same relationship (see formula (2-27) given below).

(3) It is confirmed with satisfactory accuracy by experiment — performance measures and slipstream deviation measurements in flight and in the wind-tunnel.

In the case of horizontal motion ($V_Z = 0$), V_i is conveniently obtained from the diagram of Plate II-5, which graphically portrays Eq. (2-2'), expressed here as

$$\left(\frac{F_N}{2\rho S}\right)^2 = V_i^2 \left(V_x^2 + V_i^2\right)$$

*We shall see that V_i is not uniform over the disc. The value calculated is an average value obtained at the center of the rotor.

or

$$\left(\frac{V_{i_o}}{V_i}\right)^2 = \left(\frac{V_x}{V_{i_o}}\right)^2 + \left(\frac{V_i}{V_{i_o}}\right)^2 \qquad (2\text{-}25)$$

In practice the velocity found is increased by a factor to account for the induced losses, as in vertical flight. Lacking information to the contrary, a coefficient of the same order of magnitude may be used. /47

In the most general case, Eq. (2-4) will be expressed by the relationship

$$\boxed{\left(\frac{V_{i_o}}{V_i}\right)^2 = \left(\frac{V_x}{V_{i_o}}\right)^2 + \left(\frac{V_z + V_i}{V_{i_o}}\right)^2} \qquad (2\text{-}26)$$

Note that if V_i/V_{i_0} is taken as a parameter the curves of V_x/V_{i_0} as a function of V_Z/V_{i_0} are circles centered on the $V_x = 0$ axis.

Such a representation is given by the diagram of Plate II-6; the graphs have been adjusted experimentally to take account of various factors that modify Eq. (2-26) in practice (in particular the vortex-ring zone).

The curves of equal-$(V_Z + V_i)/V_{i_0}$, which are the equi-powers referred to P_{i_0}, are also plotted on the diagram.

Remark:

In vertical flight in the vicinity of hovering, we have shown that it is possible to use an $\vec{F}_N$ with an apparent output greater than 1, since the additional power required to increase $\vec{F}_N$ to velocity V_Z is only $(F_N \times V_Z)/2$.

It is interesting to see what this is for horizontal flight: Starting from the operational case where the lift F_N is perpendicular to $V_o(V_Z = 0)$, what is the power increment to be furnished to insure the same lift with a given component V_Z? (in practice this corresponds to using the rotor to overcome parasitic drags or to ascedn obliquely).

It is easily seen from the diagram of Plate II-6 that for velocities used in practice the supplemental power to be supplied is slightly less than the work of propulsion done by the rotor. The rotor is a device having an apparent thrust output somewhat greater than unity (even if induced losses are included). An output will not be taken into account here as was done when the work of propulsion was accomplished by a propellor.

The Slipstream /48

Some idea of the actual flow configuration can be had by examining Figs. 2.22, 2.23, and 2.24. Figure 2.24, in particular, shows the arrangement of the tip-vortices as determined from wind-tunnel pictures made by Mr. Valensi at IMF, Marseille.

Note that the helices are distorted at slow velocities of advance. This phenomenon, caused by the non-uniformity of the velocities induced on the disc (which we shall discuss later) shows the uncertainty of the theoretical diagrams usually adopted.

Since the horizontal velocity is significant the slipstream becomes quite like that of a wing. The vortex layers are coiled around the two tip cells shed by the edges of the rotor disc*.

Distribution of Induced Velocities on the Disc

The induced velocities are not uniform over the disc; almost zero on the leading edge of the disc, they are of the order of twice the average value on the trailing edge, laterally they are decreased on the advancing side and strengthened on the retreating side (Fig. 2.25). In certain cases opposite induced velocities can even be observed on the forward edge of the disc and in the vicinity of the root of the retreating blade. These irregularities obviously stem from the bisymmetric structure of the vortex system in forward flight.

Some formulas and charts are available from which the velocities induced on the disc can be calculated.

The formulas worked out from calculations made by Mr. Meijer Drees [5] are given here:

*Excellant examples of these vortices can be seen by observing a helicopter engaged in crop treatment (dusting or spraying).

$$
\begin{aligned}
V_i &= V_{im} + V_{ic}\frac{r}{R}\cos\psi - V_{is}\frac{r}{R}\sin\psi \\
\frac{V_{im}}{V_{io}} &= \frac{1}{\left(1-\frac{3}{2}\mu^2\right)\sqrt{\left(\frac{V_x}{V_{io}}\right)^2+\left(\frac{V_z+V_{im}}{V_{io}}\right)^2}} \\
V_{ic} &= V_{im}\times\frac{4}{3}\times\frac{1-1{,}8\,\mu^2-\sin\alpha}{\cos\alpha} \\
V_{is} &= 2\mu V_{im} \\
\operatorname{tg}\alpha &= \frac{V_z+V_{im}}{V_x}
\end{aligned}
\qquad (2\text{-}27)
$$

A diagram from another source (Coleman) is given in Plate II-7; the portion of the induced velocity modulated in $\cos\psi$ (the most useful to know) can be ascertained quickly from this diagram. On Plates II-8 and II-9 are found as well the velocity distributions as calculated along the axes $\psi = 0$, $\psi = \frac{\pi}{2}$. /49

2.134. AUTOROTATION

Before beginning the quantitative study it is useful to understand the mechanism that allows the rotor to function in this mode.

We shall begin with vertical autorotation (Fig. 2.26a). It has already been explained (2.12) that if the airfoil drag is neglected the lift on a blade element is accompanied by a drag or a thrust component, depending on whether the air traverses the rotor from above the rotor downward or upward from below (see Fig. 2.6). The autorotation mode is established in such a way that the total torque on the blade is zero. Figure 2.26a shows that the center of the rotor operates in windmill-breaking and gives up the power received to the tip, which itself operates in the propellor mode. The air traverses the rotor to the center and is expelled by the outer part, which assures that the air sets the rotor disc into motion.

If the drag due to blade shape is considered, the air must furnish the power to overcome it; the air flow traversing the rotor will not be exactly zero but the

*This formula differs slightly from that of [5] where certain terms have been ignored in the calculation.

/Tr. Note: In-text collout for this footnote missing in original text./

flow pattern is not appreciably modified. Neverthless we note the existence of a flutter zone at the root of the blade, where the angle of attack on the airfoil is excessive.

In forward flight we again find the windmill-braking - and helicopter - zones (Fig. 2.26b).

Figure 2.7 shows that in this case the windmill-braking zone has moved from the side of the retreating blade.

IMPORTANT REMARKS

(1) Figure 2.26,a, illustrates why autorotation takes place at a pitch much lower than that for normal flight — since the velocities relative to the air are redirected upward, the trim of the airfoils must be reduced to maintain a suitable angle of attack.

(2) What has been said about the role of the central portion of the disc as the power source shows the importance of this portion of the rotor for autorotation.

Quantitative Study

The data on autorotation already appear on Plates II-2 and II-6. We shall take up the question again somewhat differently.

A rotor turning freely on its axis and adjusted to a given collective pitch will assume a precisely defined autorotation mode (rotational speed, drag and lift) under the effect of a relative air motion. It is therefore possible to plot the polar diagram by introducing the notions of C_x and C_z as for the wing; the reference surface is the surface S swept out by the disc. /50

The polar diagram will obviously depend on the given pitch angle and on the blade construction.

On Plate II-10 is shown (from Lapresse) a complete polar diagram of a model rotor compared with a diagram for a flat disc; they are seen to be quantitatively similar with the exception of an anomalous region for the disc.

We have also plotted as an example the theoretical polar diagram of the rotor as derived from Eq. (2-1), (2-2) and (2-3). As noted earlier, we again see that these equations give completely erroneous results except for low angles of attack of the disc. The effect of pitch is seen in Plate II-11, where actual values obtained

in the large wind-tunnel at Chalais-Meudon and in the Langley Field installation are also shown for portions of the polar diagrams of full-scale rotors. Theoretically, the greater the pitch the better the autorotation, but one must use low pitches in practice. For a given lift, the rotor regime degrades with increasing pitch and the angles of attack increase (see Fig. 2.26). It is mandatory to avoid reaching stalling angles of attack and to maintain an adequate rotor range (see Chapter 4).

2.14. THE GROUND EFFECT

Until now it has been implicitly assumed that the rotor was operating in open air, without nearby obstacles. For flight in the immediate vicinity of the ground this assumption is not valid. For example, in hovering flight the air can no longer flow axially below the rotor and it escapes radially along the ground (Fig. 2.27).

This interaction is in fact favorable in that it reduces the induced velocities and hence the power required to generate a given lift.

This phenomenon is complex quantitatively and depends on many parameters, such as rotor speed, Reynold's number, quality of the profiles used, nature of the ground*, etc. But the dominant factor is the ratio of height above ground to rotor diameter.

Plate II-12 shows a diagram giving the change in lift as a function of Z/2R at constant power.

Two important properties are retained in all usual cases: (1) the ground effect has essentially disappeared for $\frac{Z}{2R} > 1$, (2) the ground effect used, which corresponds to lifting the helicopter from 1 meter to 1.5 meters above the ground (Z/R = 0.35 - 0.40), is equivalent to a power requirement reduction varying from 5 - 20%, depending on the circumstances. /51

Effect of Forward Motion on the Ground Effect

It is clear that a horizontal component of wind will tend to eliminate the ground effect by "sweeping away" the air blown out by the rotor. Starting a forward motion in the ground effect will be equivalent at very low velocities to an increase in the power required as a function of the velocity, contrary to what happens outside the ground effect (see Fig. 2.28). A helicopter taking off

*For example, the ground effect is better above a cement surface than above a vegetation-covered terrain, which opposes the radial flow of air.

vertically in ghe ground effect and set into forward flight at constant power will have a tendency to "fall back".

2.15. MULTI-ROTORS

We have mentioned the perturbations created by the presence of obstacles in the vicinity of the rotor. Another case in which the rotor does not exactly obey the laws studied earlier is that of many rotors in proximity — coaxial configuration, tandem or side-by-side. The interactions in vertical flight, forward flight and autorotation are far from negligible, and they must be taken into account for correct performance calculations.

We shall merely give some general comments on this subject.

Coaxial Configuration (Fig. 2.29, a).

If the two rotors are far enough apart, their effectiveness in vertical flight is greater than that of single-rotor of the same diameter, due to the aspiration of air that occurs between the two rotors. For a given diameter this allows operating on a larger mass of air. Also, the induced tangential velocities are zero or weak.

Tandem Configuration (Fig. 2.29, b)

There is a slight improvement in efficiency for hovering flight in the ground effect. In forward flight, if the rear rotor is in the wash of the forward rotor, everything takes place aerodynamically as if it were operating in ascent (velocity relative to the air directed downward). The induced power consumed in forward flight will be larger than for a single-rotor of the same loading per square meter. This is one reason for usually trying to remove the rear rotor from the wash of the forward rotor by elevating it. /52

Side-By-Side Configuration (Fig. 2.29, c)

As with the tandem configuration, there is a slight improvement in efficiency for hovering flight in the ground effect.

In fast, level flight, the induced power required is less than for a single-rotor of the same loading per square meter.

This is due to the "span" effect of the configuration. To calculate the induced velocity, the rotor diameter is replaced by the separation L between the

outside edges of the two rotor discs:

$$F_N = 2\rho \frac{\pi L^2}{4} |\vec{V}_1| V_i \quad \text{instead of} \quad \frac{F_N}{2} = 2\rho \pi R^2 |\vec{V}_1| V_i \ .$$

To fix the orders of magnitude, Plate II-13 shows the results of comparative tests on models of various configurations.

2.16. THE DUCTED PROPELLOR

Certain machines related to the helicopter make use of ducted rotors (Fig. 1.26 and 2.30).

The aerodynamic interest of this device relates to the decrease in induced power needed to generate a given lift with a rotor of given diameter.

Figure 2.30 showed that the cross-section of the passage across the propellor is equal to the stream cross-section at infinity downstream, as a result of the suppression of constriction of the stream due to the convergent.

We thus have $S = S_2$ rather than $S = 2S_2$. Application of Froude's formulas then gives

$$P_{i_0} = \frac{1}{\sqrt{2}} \frac{F_N^{3/2}}{\sqrt{2\rho S}} \quad \text{instead of} \quad \frac{F_N^{3/2}}{\sqrt{2\rho S}}$$

for a free propellor, 30% of the induced power is saved.

One can proceed still further by using a convergent-divergent. Theoretically, a flow like that of Fig. 2.30,b, is in fact possible. The power to be supplied is written

$$P_{i_0} = \frac{F_N^{3/2}}{2\sqrt{\rho S_2}} = \frac{1}{\sqrt{2\frac{S_2}{S}}} \frac{F_N^{3/2}}{\sqrt{2\rho S}} \ ,$$

which is smaller the larger the ratio of S_2 to S_0.

The practical difficulty is in obtaining a divergent that will allow this type of flow to occur in a stable fashion. /53

Encouraging research from various sides is presently underway on this subject.

2.17. NON-STATIONARY AERODYNAMICS OF THE ROTOR

In studying certain problems involving the behavior of the rotor in different modes, the question comes up as to whether the response time of the aerodynamic flow should not be considered, as it is with the fixed wing.

The question comes up in two different contexts: (1) the working conditions of the blades, and (2) the induced flow.

With regard to the blades, we shall see in Chapter 3 that the angle of attack of the airfoil varies with azimuth in forward flight or during a manoeuver. Should the concepts of non-stationary aerodynamics enter into the calculation of the forces applied to the blades?

The numerical application of the usual two-dimensional formulas shows that if they are restricted to frequencies not exceeding the rotor regime the necessary corrections are small and can usually be neglected. This justifies the calculations of flapping to be made in Chapter 3, where the lift is assumed to be established on the airfoils without delay. The corrections are not negligible if higher frequencies are considered, such as higher-order flapping harmonics, blade stresses etc...

The second viewpoint relates to a large-scale phenomenon, the time of establishment of the induced flow. Its practical interest is in how the induced velocities to the right of the rotor evolve after a rapid change in operating mode, such as variation of cyclic pitch or collective pitch, or variation in trim. Since the behavior of the flow affects the lift of the blades, it is rather important from the standpoint of the flight properties of the machine — the rapidity and nature of the response to rapid actuation of the controls.

This subject is still little explored. However, the available experimental data do show that the time constants, which, moreover, are variable from one operating condition to another, are of the order of one second.

As an example, consult the NACA TN 3 044 study.

2.2. AERODYNAMICS OF THE ANTI-TORQUE ROTOR /54

The principles governing the aerodynamics of the anti-torque rotor are of course the same as those we have just studied. We have merely withheld it for separate discussion to call attention to the fact that it is subject to stringent operating conditions. In forward flight it is located so that it is supplied with air from the awhs of the main rotor. Moreover, during evolutions involving yawing

motion it is frequently located in vortexring regions. These two circumstances explain why the anti-torque rotor is at times the seat of severe vibration which can endanger the operation of its components.

In addition to torque balancing and yaw control, the anti-torque plays a less obvious but important role in contributing to the yaw stability of the fuselage by acting as a centerboard. It is easily seen on inspecting Fig. 2.31 that an anti-torque propellor acts as a vertical centerboard — i.e. by introducing aerodynamic restoring forces proportional to displacement and damping proportional to rate of displacement.

Cited here is a formula the reader will encounter among the methods pointed out in Chapter 4 and which gives the equivalent area S_e of a solid disc having the same efficiency as a centerboard as does the anti-torque rotor:

$$S_e = S \times \frac{1,32}{1+3,1 \dfrac{\mu}{\sigma \left(\dfrac{dC_z}{di}\right)_\infty \bar{G}_1}}$$

The notation is that of Appendix II.

This formula is useful when examining the yaw stability of an unpowered model in a wind-tunnel. The anti-torque is replaced by a solid disc of area S_e (it will be considered that the anti-torque is unaffected by the fuselag slip-stream). It will be noted that S_e decreases with $\mu = \frac{V}{u}$ and the stabilizing effect of the anti-torque rotor diminishes with flight speed.

2.3. AERODYNAMICS OF THE FUSELAGE /55

The reason for discussing this is that helicopter fuselages, for reasons of lightness and simplicity, still have shapes quite unlike good airplane fuselages. This is particularly marked for single-rotors with anti-torque propellors, where a long and relatively slender tail is joined to the rear of a compact ensemble consisting of the cabin and engine unit that is not usually streamlined.

Under these conditions it is not surprising that two disadvantages appear:

- the drag built up at the midship-frame is considerable, 3-4 times the figure for an airplane fuselage. To fix these notions more firmly in mind we note that the fuselage drag of a standard 2- or 3- place helicopter is about double that of the fuselage of a heavy, 4-motor transport...

- the existence of a sizeable slipstream behing the cabin complex makes the surfaces installed at the extremity of the tail to attain stability in forward flight of little use.

We have seen that fortunately the anti-torque rotor is often enough to insure yaw stability. In pitch, on the other hand, the positioning and dimensioning of stabilizers that are effective under all circumstances of flight poses difficult problems.

Improvement of the fuselage aerodymanics is important only if high crusing speeds are desired; reduction of drag-power and pitch stability are then indispensible conditions.

The methods used to reduce helicopter fuselage drag are the standard methods of continuous streamlining, elimination of undesirable protuberances, fairing or retracting the landing gear, etc.

Nevertheless, it should be taken into consideration that the fuselage works over an extended range of angles of attack. This creates a special problem in fixing the placement of the static and dynamic pressure sensors that feed the on-board instruments such as the altimeter and the anemometer...

Chapter 3

ROTOR MECHANICS

This chapter deals with the blade motion and the forces transmitted by the blades to the hub, which implies a "refined" aerodynamic study of the rotor, that is, a knowledge of the local working conditions of the blade sections. This section is therefore an extension of the system aerodynamics treated in the preceding chapter. /57

We know that the rotors of modern rotorcraft consist of blades mounted on a hub by means of multiple hinges (Fig. 3-1).

These hinges led the rotor very specific properties, which must be thoroughly understood. Unforunately, a detailed study takes on a rather complex mathematical form, making it somewhat forbidding and running the danger of clouding the important facts to be retained. Therefore these mathematical developments have been reduced to the minimum that is still consistent with rigorous presentation.

3.1. THE ORIGIN OF FLAPPING HINGES

Consider a rigid rotor (Fig. 3.2). In hovering flight, the distribution of lift-generated bending moments over the blade is of the type shown in the figure. The maximum moment is at the blade root and may be quite large. The situation deteriorates in forward motion: the diagrams in Fig. 3.3 do not require much comment. The advancing blade has a greater lift than the retreating blade because the relative air velocities are unequal. The result is a distribution of bending moments similar to the one shown in Fig. 3.3,b. The blade housing moments are not only high, but alternating, rising a difficult problem that of material strength. Besides, it is evident that a rolling moment is produced, increasing with speed, and this may make it difficult to balance the forces in forward flight.

Angular displacement of the rotor shaft (from stick action and manoeuvres) would have the same consequence (the gyroscopic effect).

Flapping Hinges

The above-mentioned problems were obviously of no great importance as long as helicopters were restricted to short hops above the ground, but when Juan de la Cierva developed his first autogyros, he was induced to take up the highly ingenious idea of Renard and Breguet to hinge the blades to a socket about an axis /58

perpendicular to the driving shaft; this is the flapping hinge (see Fig. 3.1). Thus the blade thrust moment is canceled. We now have, so to speak, a cable-rigged wing, the cables being the centrifugal force (Fig. 3.4, a), which restores the blade to the driving plane (the plane perpendicular to the rotor shaft).

In addition, there is no longer nay appreciable rolling moment in forward flight, since the only forces that can now be transmitted by the blades are the shear forces, which are essentially vertical (Fig. 3.4, c).

. The blades no longer rotate in a plane, rather they describe a very open cone (Fig. 3.4, b). In practice, the flapping axis is not always on the axis of rotation, but separated from it by a distance that is small as compared with the rotor radius.

. Feathering Hinges

In order to control the lift of the rotor, it must be possible to vary its pitch, as is done in a propellor. This is the reason for introducing a second hinge, the pitch change (feathering) hinge, which is parallel to the span of the blade (Fig. 3-1).

This degree of freedom makes it possible to control not only the lift be regulating the mean pitch, but also to control the plane of rotation of the blades by cyclic feathering of the form: $\theta = \theta_0 - \theta_1 \cos \omega t - \theta_2 \sin \omega t$ (see Section 3.212). The result is a blade flapping relation of the same form, causing the blade to describe a cone whose axis, called the no-flapping axis, no longer coincides with that of the hub. Since the resultant of the forces applied by the blades to the hub changes direction simultaneously with the rotor plane, it is evident that torques can be intorduced about the helicopter's center of gravity, that is, it can be piloted. The feathering axis passes near the aerodynamic center of the airfoils so as to get sensitive control forces (usually between 20 and 25% of the chord).

Lag Hinges

The essential reason why it is necessary to have lag hinges is that the slapping axes may generate a plane of blade rotation which differs from the plane perpendicular to the drive shaft.

Suppose that a rotor rotates with a coning angle of a_0 in a plane different from the driving plane. The diagram in Fig. 3.5 shows that the blade tips do not rotate uniformly in their plane. In equal periods, corresponding to 1/4 revolution of the rotor shaft, they describe arcs of 12, 23, 34, 41; the inequality of these

arcs is proportional to the magnitude of a_1 and a_0.* Thus forces of inertia are generated which cause bending forces in the plane of the blade. The moments /59
are eliminated by a procedure analogous to the one used in flapping; that is, by hinging the blade about a drag axis which is essentially parallel to the rotor axis (Fig. 3.1). The blade is brought back into line by centrifugal force, which requires tilting of the drag axis (Fig. 3.6). Unfortunately, the blades have a tendency to make poor use of the additional degree of freedom granted to them: their oscillations in the drag plane may result in unstable coupling with the elastic deformation modes of the airframe, particularly helicopter vibration on the ground, on its undercarriage. This is the origin of helicopter ground resonance, which will be studied later on (Section 6.2). Let us state immediately that to avoid this effect it is necessary to take various measures in the drag axis; e.g., damping by viscous or dry dampers; elastic restoration by springs or by "distributor cables".

Remarks

There are some designs in which the hinges are not located as indicated in Fig. 3.1. We will see a few examples in Chapter 9, entitled Technology. Note only that the hinged blade always has the same properties we have described; that is, flapping, cyclic and collective pitch control, and cancellation of the drag forces. We will also see that a return to the rigid rotor is taking shape for certain applications.

3.2. PROPERTIES OF AN ARTICULATED ROTOR

The study is presented progressively from the simple to the complex, beginning with elementary considerations, not always rigorous, and then proceeding gradually to a more exact study.

The general hypotheses to be made are as follows:

- The chord and thickness of the blade are negligible as compared with its span.

- The flapping angles are always small enough to permit application of the small-angle method.

*Another way of looking at the situation is to note that the tip of the blade is at a variable distance from the rotor shaft, which causes variations in tangential speed during rotation.

- The weight of the blade is negligible as compared with the aerodynamic and inertial moments.

- The blade is not deformable.

3.21. STUDY OF FLAPPING

3.211. The Rotor in Vacuum

This means that we will begin our study by ignoring aerodynamic forces. The motion of the blade about its flapping axis is expressed by the following relation, in axes fixed to the rotor (Fig. 3.7): /60

$$I_p \ddot{\beta} = \text{centrifugal force moment}$$

(pendulum equation: I_p blade inertia about its hinge).

For small angles let

$$I_p \ddot{\beta} = -\int_0^R dm\, \omega^2 r \times r\beta = -\omega^2 \beta \int_0^R dm\, r^2 = -I_p \omega^2 \beta$$

or

$$\boxed{I_p (\ddot{\beta} + \omega^2 \beta) = 0} \qquad (3\text{-}1)$$

This is a differential equation with general solution of the form

$$\beta = -a_1 \cos \omega t - b_1 \sin \omega t$$

or

$$\boxed{\beta = -a_1 \cos \psi - b_1 \sin \psi} \qquad (\psi = \omega t) \qquad (3\text{-}1)$$

It can be readily seen that this is the same as saying that the blade describes a fixed plane in space, determined by the flapping angles a_1 and b_1 (Fig. 3.8);* a_1 and b_1 are arbitrary and depend only on the initial conditions.

The characteristics flapping frequency is equal to the angular rotor speed.

Since the hinge cannot transmit flapping moments to the blade, angular motion of the rotor shaft will not result in any change in orientation of the rotor plane relative to the absolute axes.

Theorem. A hinged blade that is not subjected to aerodynamic forces describes a fixed plane, with respect to absolute axes, whose orientation depends only on the initial conditions.

Remarks.

1) This theorm makes the blade similar to a gyroscope; in fact, the physical phenomenon is the same. The preceding demonstration could be made by considering the kinetic moment of the blade as being invariant with respect to the center of the rotor.

2) Instead of using the driving plane as a plane of reference for the flapping, we take any plane of orientation. The equation of motion of the blade will still be of the form: $\beta = -a_1 \cos\psi - b_1 \sin\psi$. /61

3) Equation (3-1) is rigorous only if the flapping hinge lies in the axis of rotation; if not, we must write (Fig. 3-9).

$$I_p \ddot{\beta} = -\int_0^R dm\,\omega^2(r+a)\,r\beta = -I_p\omega^2\beta - \omega^2 a\cdot m_s\cdot\beta$$

where m_s is the static moment of the blade about the flapping axis.

Equation (3-1) must be replaced by the equation

$$I_p\left[\ddot{\beta} + \omega^2\left(1+\frac{a\cdot m_s}{I_p}\right)\beta\right] = 0 \qquad (3\text{-}1')$$

*Equation (3-2) can be interpreted as a linear relation between $r\beta$, $r\cos\psi$, and $r\sin\psi$ which are the coordinates in fixed axes of some point along the blade.

the rootes of which are of the form

$$\beta = -a_1 \cos \omega' t - b_1 \sin \omega' t \qquad \left(\omega' = \omega \sqrt{1 + \frac{a \cdot m_s}{I_p}}\right)$$

Now the blade no longer describes a fixed plane in space. An observer fixed to the absolute axes will see that the rotor plane rotates about the driving axis at the speed

$$-\omega \left(\sqrt{1 + \frac{a \cdot m_s}{I_p}} - 1\right)$$

It would also be seen that the angular motions of the rotor shaft are no longer without effect on the blade motion in absolute axes.

However, the quantity am_s/I_p is always sufficiently small in the usual designs for the rotor actually to have the properties ensuing from Eq. (3-1).

The rest of the study will be made under this hypothesis.

3.212. Simplified Study of the Effect of Aerodynamic Forces

If aerodynamic forces are taken into account, Eq. (3-1) becomes

$$I_p (\ddot{\beta} + \omega^2 \beta) = M \text{ (where } M \text{ is the aerodynamic force moment).} \qquad (3\text{-}3)$$

Let us consider a blade section obtained by truncating the blade in a plane perpendicular to its span (Fig. 3-10).

Rotor theory is developed under the assumption that the aerodynamic force exerted on the airfoil at this point stem uniquely from the relative velocity component $\vec{v}_r$ of the air in this plane. (The influence of the radial velocity component is neglected.)

Let us give a few definitions: /62

Pitch: the angle θ formed by the zero-lift chord of the airfoil with a reference plane (Fig. 3-10):

Angle of attack: angle formed by the zero-lift chord of the airfoild with $\vec{v}_r$.

According to Fig. 3-10 it is evident that in setting up the velocities we have

$$i = \theta - \frac{v_3 + r\dot{\beta}}{v_x}$$

or

$$\boxed{i = \theta - \frac{r\dot{\beta}}{v_x} - \frac{v_3}{v_x}} \qquad (3\text{-}4)$$

Remark

θ and β must obviously be referred to the same reference plane, which, however, may be arbitrary.

The value of i does not depend on the choice of this plane.

The lift of a surface element ds will be written as

$$dF_3 = \frac{1}{2}\rho\, ds\, v_r^2 \frac{dC_3}{di}\left(\theta - \frac{r\dot{\beta}}{v_x} - \frac{v_3}{v_x}\right)$$

and the moment with respect to the flapping axis is written

$$dM = \frac{1}{2}\rho\, ds\, r\, v_r^2 \frac{dC_3}{di}\left(\theta - \frac{r\dot{\beta}}{v_x} - \frac{v_3}{v_x}\right) \qquad (3\text{-}5)$$

Note that flapping is manifested by a damping moment on the blade (the term in $-\dot{\beta}$).

This very important property, which is similar to the "gyroscopic" properties of the blade, as mentioned in Section 3.211, will give us a clue to the entire behavior of the rotor.

In fact, by intergrating (3-5) and substituting it into the second term of formula (3-3) we can write

$$I_p \left(\ddot{\beta} + \omega^2 \beta \right) + \frac{K \dot{\beta}}{\omega} = M_0 \qquad (3\text{-}6)$$

where M_0 denotes the aerodynamic moment exerted on the wing if there is no flapping.

This equation shows that the wing, observed in a system of axes linked to the rotor, behaves like a second-order damped system with the angular rotor speed as the characteristic frequency.*

The solution to the equation without the second term is of the form

$$\beta = e^{-kt} (-a_1 \cos \omega' t - b_1 \sin \omega' t) \qquad (\omega' < \omega)$$

that is, damped sinusoidal motion.

From this we can deduce the following properties:

a) The case $M_0 = 0$ (hovering rotor, zero pitch).

In equilibrium, the plane of blade rotation is the plane perpendicular to the rotor shaft: if the direction of this shaft is altered, the rotor will follow through with a time constant determined by the factor k.

b) The case $M_0 = \text{const}$: $V_x = 0$, θ and v_z are constant in Eq. (3-5). (The case of vertical flight.)

*Here the characteristic frequency is defined as the frequency which makes the terms $\ddot{\beta}$ and β vanish in the first member of the equation.

We arrive at the same conclusions as before, except that in equilibrium β has a non-zero value: $\beta = a_0$ (coning angle): the blade describes a cone of revolution whose axis coincides with the rotor shaft.

c) The case where M_0 varies cyclicly during one revolution of the rotor.

As we have seen in Section 3.1, e.g., this is the case of the rotor in horizontal flight: the advancing blade has a greater lift tendency than the retreating blade, because of the relative speed difference v_x.

The blade reacts in the same way as any damped linear system excited at its characteristic frequency, that is, at the excitation frequency and with a phase lag of 90°.

From this we can derive some of the basic properties of the rotor:

1) In forward flight the blade will take the highest position one quarter of a revolution after maximum resultant horizontal speed had been reached, that is, it will be in the forward position.

Horizontal displacement speed makes the plane of equilibrium of an aritculated-blade rotor tilt backward (Fig. 3-11).*

Because of its importance, let us immediately note a property which will be demonstrated later on, namely, blade flapping takes place in such a way that the aerodynamic moments applied to the blade are constant during rotation. /64

This property is intuitive, provided we consider that when the blade rotates in its plane of equilibrium, no perturbing moment can appear.

2) Let us impose on the rotor an angular rotary speed $\vec{\Omega}$ (Fig. 3-12): the terms due to Coriolis forces $-2\,dm\,\vec{\Omega} \wedge \vec{V}$ relative must be added to the terms of Eq. (3-5). It can be seen in the figure that this shows up in the blade as periodic moments of frequency ω, the effect of which is to shift the rotor plane backward from the direction of motion.

3) Finally, cyclic variation of M can be used to control the rotor plane. Instead of uniform pitch, let us give the pitch a cyclic variation of the form $\theta_0 - \theta_1 \cos \omega t - \theta_2 \sin \omega t$. The result is to tilt the plane of the blades; the maximum blade flapping will take place one quarter of a revolution after the maximum pitch value has been passed.

*We will show later on the lateral tilt of lower amplitude is also produced, because of the coning angle.

Figure 3-13 shows a diagram of blade momement in the most general case.

3.213 THE ROTOR IN VERTICAL FLIGHT

3.2131. Solution of the Flapping Equation

The aerodynamic moment exerted on the blade can be obtained by integrating the moments of the elementary forces given by formula (3-5):

$$I_p\left(\ddot{\beta}+\omega^2\beta\right)=\int_0^R \frac{1}{2}\rho l\, dr\, \omega^2 r^3 \frac{dC_z}{di}\left(\theta_0-\theta_1\cos\omega t-\theta_2\sin\omega t-\frac{\dot{\beta}}{\omega}-\frac{v_i+V_z}{\omega r}\right) \tag{3-7}$$

where l, θ_0 and v_i are functions of r.

If the constant terms and the sine and cosine terms are cancelled, this equation will enable us to find the flapping of the blade:

$$\beta = a_0 - a_1\cos\omega t - b_1\sin\omega t$$

$$a_0 = \frac{1}{I_p}\int_0^R \frac{\rho}{2}\times\frac{dC_z}{di}\left(\theta_0-\frac{v_i+V_z}{\omega r}\right)r^3 l\, dr$$

$$\dot{\beta} = -\omega\left(\theta_1\cos\omega t+\theta_2\sin\omega t\right)$$

from which we get: $\beta = a_0+\theta_2\cos\omega t-\theta_1\sin\omega t$

Tilting of the rotor plane is of the same amplitude as that of the cyclic variation and is shifted relative to the latter by an angle of 90°. /65

Approximate value of a_0:

Assume that the blade is rectangular and that the angle-of-attack distribution

is constant. We have

$$a_0 = \frac{\rho}{2} \times \frac{dC_z}{di} \times i \times \ell \times \frac{R^4}{4}$$

The lift is given by

$$\frac{F_N}{b} = \int_0^R \frac{\rho}{2} \frac{dC_z}{di} i \omega^2 r^2 \ell \, dr = \frac{\rho}{2} \frac{dC_z}{di} \omega^2 i \ell \frac{R^3}{3}$$

from which we get

$$\boxed{a_0 = \frac{F_N}{b} \times \frac{0{,}75\ R}{I_p \omega^2}}$$

This formula, applied to modern blades, gives a sufficient approximation. It shows that the coning angle increases as the lift in the constant working state and as $1/\omega^2$ at constant lift.

It can also be easily seen that the coning angle increases with blade tapering (because $U = \omega R$ is limited for aerodynamic considerations).

Order of magnitude of the coning angle.

It is a few degrees, usually less than 8°.

3.2132. Rotor Response Time.

Equation (3-6) is written taking (3-7) into account:

$$I_p \ddot{\beta} + \omega^2 G_3 \frac{\dot{\beta}}{\omega} + I_p \omega^2 \beta = M_0$$

with

$$G_3 = \int_0^R \frac{\rho}{2} \frac{dC_z}{di} l r^3 dr$$

Thus blade motion is characterized by the time constant

$$\boxed{\tau_0 = \frac{2}{\frac{G_3}{I_p} \cdot \omega}} \qquad (3\text{-}8)$$

Sometimes the "Lock number" of the blade is used, defined by $\bar{\gamma} = \frac{8 G_3}{I_p}$ /66
then τ_0 is given by

$$\boxed{\tau_0 = \frac{16}{\omega \bar{\gamma}}} \qquad (3\text{-}8')$$

Evidently this time constant applies also to the way in which the plane of the blades returns to its equilibrium position. We will se in Chapter 5 how important this case is for problems of stability and piloting. The value of τ_0 is 0.05 seconds ("light" blades) to 0.2 second ("heavy"blades). Formula (3-8) shows that, all things being equal, τ_0 varies as I_p, $\frac{1}{\rho}$ and $1/\omega$: Altitude and reduction of the angular rotor speed increase τ_0. Likewise, τ_0 generally increases with tapering of the blades.

3.2133. Pitch-Flap Coupling

So far we have assumed that the control kinetics were such that the pitch was not altered by blade flapping. Actually, a link is sometimes introduced to reduce the pitch when the blade flaps:

$$\Delta\theta = -k \Delta\beta$$

Figure (3-14) shows one example of kinematic response to this condition: the device is sometimes called the k-link, after the coefficient $k = \tan \varphi$.

Let us examine its properties. In Eq. (3-7) the terms giving the angle of attack must be supplemented by a term in $-k\beta$:

$$I_p(\ddot{\beta} + \omega^2\beta) = \int_0^R \frac{\rho}{2} l\, dr\, \omega^2 r^3 \frac{dC_z}{di}$$

$$\left(\theta_0 - \theta_1 \cos \omega t - \theta_2 \sin \omega t - k\beta - \frac{\dot{\beta}}{\omega} - \frac{v_i + V_\beta}{\omega r}\right)$$

The term $\frac{\dot{\beta}}{\omega}$ is replaced by $\frac{\dot{\beta}}{\omega} + k\beta$. The response in β, taking the k-effect into account, is obtained by multiplying the response in β without k-effect by the symbolic operator $\frac{1}{1 + k\frac{\omega}{p}}$.

Therefore, for excitation of angular frequency ω (1st harmonic of the motion), the amplitude of the response is attentuated by a factor of $\frac{1}{\sqrt{1+k^2}} = \cos\varphi$ /67

and its phase lags by the angle $\varphi = \arctan k$. The response is no longer orthogonal to the excitation (because of the supplementary β term; the characteristic angular frequency of the blade in flapping is no longer equal to ω).

3.214. ROTOR IN FORWARD FLIGHT

3.2141. Solution of the Flapping Equation

Here we must confess that we have cheated a bit in the simplified study when we wrote the equation

$$I_p(\ddot{\beta} + \omega^2\beta) + K\frac{\dot{\beta}}{\omega} = M_0 \qquad (3\text{-}6)$$

In our reasoning it was assumed that K was a constant coefficient; this is not exactly true, however, because when the aerodynamic moments are completely integrated on the basis of Eq. (3-5) we find the relation:

$$I_p\left(\ddot{\beta}+\omega^2\beta\right)+\dot{\beta}\left(G_3\omega+V_x G_2\sin\omega t\right)+\beta\left[\left(V_x\omega G_2\cos\omega t\right)+\frac{V_x^2}{2}G_1\sin 2\omega t\right]$$

$$=\int_0^R\frac{\rho}{2}\rho_r\frac{dC_z}{di}\theta\left(\omega r+V_x\sin\omega t\right)^2 dr-\left(v_i+V_z\right)\left(\omega G_2+V_x G_1\sin\omega t\right) \qquad (3\text{-}9)$$

where G_1, G_2, G_3 are the characteristic blade constants defined in Appendix III.2.

Note that the coefficients of the terms β and $\dot{\beta}$ are not constant, but contain terms modulated in ω and 2ω. A rigorous quantitative calculation can therefore not be made on the basis of the preceding analysis.

In order to find the flapping, Eq. (3-9) is solved by trigonometric series, with β in the form

$$\beta = a_0 - a_1\cos\omega t - b_1\sin\omega t - a_2\cos 2\omega t - b_2\sin 2\omega t - \ldots\ldots$$

This expansion is introduced in Eq. (3-9) and the coefficients of the same trigonometric lines are set identical to zero.

Given in Appendix III.2 are formulas for the coefficients a_0, a_1, b_1 obtained by this method.

We will examine in particular those formulas in which the different terms have been grouped in such a way as to reveal the influence of the important factors, namely, lift, inflow, etc. /68

Note the following!

Coning Angle a_0. This term, by far the most important one, is identical with the expression given for the coning angle in Section 3.213.

Flapping a_1. Note that the tilt is essentially proportional to $\mu = \frac{V_x}{\omega R}$ for medium values of this coefficient ($\mu < 0.35$, which corresponds to all the practical cases).

Note also that at equal lift the magnitude of the flapping is proportional to the axial velocity component ($V_z + V_i$) of the wind: all things being equal, flapping will be stronger in helicopter flight than in autogyro flight.

Flapping b_1. The first term shows that the relative wind speed V_x will also cause lateral tilt, in addition to the backward tilt already mentioned. This is explained by the modulated axial velocity component produced by the coning (Fig. 3.15). This leads to variations in angle of attack, and therefore in lift, the result of which is to make the retreating blade rise. Since this effect is proportional to μ, the coning angle is much smaller than the tilt angle a_1.

Remarks.

1) The basic equation of flapping

$$I_p(\ddot{\beta} + \omega^2\beta) = M \qquad (3\text{-}3)$$

is written as

$$I_p a_0 \omega^2 = M$$

provided we do not go beyond first-order flapping terms ($\beta \approx a_0 - a_1 \cos \omega t - b_1 \sin \omega t$). This shows that the aerodynamic moment exerted on an articulated blade is constant during blade rotation.

If displacement of the aerodynamic thrust center along the blade is neglected, we can assume that the lift will remain essentially constant, which makes it possible to see that an articulated rotor can be considered similar to a lifting disk even in forward flight (uniformity distributed lift).

This property is true only insofar as the starting hypothesis is valid, that is, /69 that flapping harmonics of higher than first order can be neglected. This is true in practice in the case of flight at low and medium speeds. In high-speed flight ($\mu > 0,3$) second order harmonics can no longer be neglected and Eq. (3-3) becomes

$$I_p \omega^2 (a_0 + 3a_2 \cos 2\omega t + 3b_2 \sin 2\omega t) = M$$

by substituting flapping of the form $\beta = a_0 - a_1 \cos \omega t - b_1 \sin \omega t - a_2 \cos 2\omega t - b_1 \sin \omega t$. The moment is 2ω- modulated. Note that the moments are equal on two diametrically opposite blades.

2) We have not given the formulas for flapping with the k-link, because they beeome rather complex. A good approximation, however, may consist in doing what was done in vertical flight, that is, in multiplying the flapping amplitude by $\cos\varphi$ and phase-shifting by $-\varphi$. At low values of k this amounts to adding a term $-ka_1$ to the lateral tilt term b_1 of formula III-2-4. If k is suitably chosen, lateral tilt of the rotor due to forward flight can be eliminated. In this way we avoid increasing lateral stick displacement with speed, which can be troublesome. This is the principal reason for using the k-link.

The preceding formulas have been established under the assumption of uniform induced velocity, but this is only an approximation. We have seen in Chapter 2 that in reality the induced velocities in forward flight were of the approximate form

$$v_i = v_{i_m} + \frac{r}{R} V_{i_c} \cos\psi - \frac{r}{R} V_{i_s} \sin\psi$$

The term V_{i_c} is the most important, having the tendency to produce lateral tilt, which will be calculated as follows:

At a distance of r, the variation in angle of attack as a result of this term is of the form

$$\Delta i = \frac{1}{\omega r} \cdot \frac{r}{R} \cdot V_{i_c} \cdot \cos\psi = \frac{V_{ic}}{U} \cos\psi \quad , \quad \text{independent of r.}$$

Thus the effect is the same as that from cyclic variation of the form $-\theta_1 \cos\omega t$. In other words, the rotor will tilt laterally at an angle of V_{i_c}/U, the retreating blade being in the higher position.

This phenomenon can be seen quite well if we examine the lateral displacement curves of the control stick as a function of the speed of a helicopter. We note a bosse at low velocities (30 to 50 km/h) which decays as V_x increases (see formulas 2-27 or the diagram of plate II-7). /70

Shown in plate III-1 are experimental and calculated curves giving the variations of a_0, a_1, b_1 as a function of the forward flight speed. Therefore, we will be able to give due regard to the orders of magnitude and to the precision obtained by calculation.

3.215. REFERENCE PLANES

To conclude this study of flapping, let us present or recall below the definitions for the various planes of reference used.

Reference Plane. Any plane to which the flapping and pitch are referred. Some reference planes are particularly convenient to use.

Horizontal plane.

Driving plane, perpendicular to the rotor shaft. It has no privileged function from the point of view of flapping, but it is convenient as a reference plane fixed to the fuselage. Moreover, flapping should be referred to this plane in order to evaluate the mechanical wear of the pieces to which the blades are attached.

Tip-path plane, described by the blade tips.

Control plane. When the blades describe this plane their pitch, referred to this plane, is constant; therefore, it coincides with the tip-path plane in hovering or vertical flight.*

No-feathering plane. Plane with respect to which the blades have a constant pitch as they rotate. In vertical flight, this plane coincides with the control plane. In forward flight, it coincides only if there is no pitch-flap coupling.

The following table shows the forms taken by the pitch and flap, referred to these reference planes.

The diagrams in Fig. 3.16 show the relative locations of the reference planes in any flight mode. /71

3.216. THE ROTOR IN HIGH-SPEED FORWARD FLIGHT

Reverse flow circle. Figure 3.17 shows that in the retreating-blade position at a part of the blade close to the hub the flow reverses from the trailing to the leading edge. It can be easily seen that the area of the plane in which this phenomenon occurs is a circle of diameter μR, located as shown in Fig. 3.17. This reverse flow has been neglected in the preceding calculations; such an approximation is justified as long as the values of μ are small ($< 0,4$) since the aerodynamic forces on the corresponding part of the wing have no appreciable

*Although not absolutely necessary, the control kinematics are often designed in such a way that the control plane is parallel to that of the swash plate.

Reference Plane	Flap β	Pitch θ
Arbitrary plane	$\beta = a_0 - a_1 \cos\psi - b_1 \sin\psi$	Vertical flight $\theta = \theta_0 - b_1 \cos\psi + a_1 \sin\psi$
	$\beta = a_0 - a_1 \cos\psi - b_1 \sin\psi$	Forward flight $\theta = \theta_0 - \theta_1 \cos\psi - \theta_2 \sin\psi$
Tip-path plane	$\beta = a_0$ (coning)	Vertical flight $\theta = \theta_0$ Forward flight $\theta = \theta_0 - \theta_1 \cos\psi - \theta_2 \sin\psi$
Control plane	$\beta = a_0$	Vertical flight $\theta = \theta_0$
	$\beta = a_0 - a_1 \cos\psi - b_1 \sin\psi$	Forward flight $\theta = \theta_0 + k a_1 \cos\psi + k b_1 \sin\psi$
No-feathering plane	$\beta = a_0$ $\beta = a_0 - a_1 \cos\psi - b_1 \sin\psi$	Vertical flight $\theta = \theta_0$ Forward flight $\theta = \theta_0$

effect on the flapping. This is no longer true if μ reaches high values and the blade motion is perturbed.

Stalling. We will see in addition that this retreating blade courts disaster because outside this circle it may stall at large μ. In fact, it has been shown in 3.214 that if we do not go beyond first-order flapping terms, the equation /72

$$I_p (\ddot{\beta} + \omega^2 \beta) = M \qquad (3\text{-}3)$$

shows that the articulated rotor ensures that the aerodynamic moments acting on the blade during rotation are constant.

The consequence is that in the advancing blade region (Fig. 3.3,a) blade section subjected to high relative velocities operate at small angles of attack, but that in the retreating blade region blade sections subjected to low relative velocities operate at high angles of attack. Note that at a certain forward speed V_X, stalling angles will be reached by the retreating blade, causing increased drag, strong vibrations (higher-harmonic flapping) and even loss of control. Thus, we are confronted with a limit to the intrinsic speed of an articulated

rotor. Figure 3.18 shows one example of angle-of-attack distribution over the disk.

We will now make a quantitative analysis of the phenomenon. Let us find the angle of attack at the tip of the retreating blade. Taking the rotor plane as a reference, this angle is written

$$i = \theta_0 + \theta_2 - \frac{V_z + V_i}{\omega R - V_x} = \theta_{0,7} + \Delta\theta + \theta_2 - \frac{\lambda + \frac{V_i}{u}}{1-\mu}$$

$\theta_{0.7}$ and θ_2 are calculated on the basis of the equations given in Appendix III-2. $\theta_{0.7}$ can be derived from the lift equation III-2-1:

$$\theta_{0,7} \simeq \frac{1}{\bar{G}_2}\left[\frac{f_N}{\sigma \frac{dC_z}{di}} + \bar{G}_1\left(\lambda + \frac{V_i}{u}\right) - \left(\bar{L}_2 + \frac{\mu^2}{2}\bar{L}_0\right)\right]$$

θ_2 is obtained by writing $a_1 = 0$, the reference plane being the tip-path plane (Eq. 3-2-3):

$$\theta_2 = \mu\left[2\theta_{0,7}\frac{\bar{G}_2}{\bar{G}_3} - \frac{\bar{G}_1}{\bar{G}_3}\left(\lambda + \frac{V_i}{u}\right) + 2\frac{\bar{L}_2}{\bar{G}_3}\right]$$

If these values are substituted into the equation for the angle of attack, we get:

$$i = \underbrace{\frac{1}{\bar{G}_2} \times \frac{f_N}{\sigma \frac{dC_z}{di}}}_{①} + \underbrace{\mu \times \frac{2 f_N}{\bar{G}_3 \sigma \frac{dC_z}{di}}}_{②} + \underbrace{\left(\lambda + \frac{V_i}{u}\right)\left[\frac{\bar{G}_1}{\bar{G}_2}\left(\frac{1}{\bar{G}_2} + \frac{\mu}{\bar{G}_3}\right) - \frac{1}{1-\mu}\right]}_{④} + \underbrace{\left(\Delta\theta - \frac{\bar{L}_2}{\bar{G}_2}\right)}_{③} \quad (3\text{-}10)$$

For the usual blades, almost rectangular in form and linearly twisted, this

equation is written:

$$i = 3\frac{f_N}{\sigma \frac{dC_z}{di}} + \mu\, 8\frac{f_N}{\sigma \frac{dC_z}{di}} - 0{,}25\,\theta_v + \left(\lambda + \frac{V_i}{u}\right)\left[\frac{3}{2} + 2\mu - \frac{1}{1-\mu}\right] \quad (3\text{-}10')$$

Interpretation of the Various Terms:

① This is an expression which is essentially equal to mean blade angle of attack. Its magnitude is proportional to the lift.

② - This is the principal term expressing the increase in angle of attack of the retreating blade due to forward motion; it is proportional to μ and to the mean angle of attack.

③ Effect of twist. It is evident that positive twist (decreasing pitch from the root to the tip of the blade) is favorable, because it leads to reduced pitch at the blade tip for any given lift.

④ From Eq. (3-10') it can be seen that this term is always positive for the values of μ being considered. It expresses the effect of the inflow over the rotor.

Everything else being equal, the angle of attack at the tip of the retreating blade is greater if the rotor is working in the helicopter state than if it is operating in the gyrodyne or autogyro condition.

Figure 3.19 shows the origin of this effect: positive inflow is equivalent to negative twist, and is therefore not favorable from the standpoint of blade-tip angle of attack.

Conclusions

At given lift and operating conditions the angle of attack at the tip of the retreating blade increases with μ. All things being equal, the helicopter state is less favorable than the autogyro state. Positive blade twist is favorable.

If i is taken as the airfoil stall angle (12 to 16°), we can derive $\frac{f_N}{\sigma}$ from Eq. (3-10) and plot the values obtained as a function of μ for various values of

inflow and twist. Diagram III-2 gives such a representation for an untwisted rectangular blade. This diagram makes it possible to find the forward speed at which tip stalling of the retreating blade appears for any case of blade loading. /74

Remarks

1) The calculations we have made neglect flapping of order greater than 1. This is not exactly correct, because such flapping becomes appreciable at large μ and has an effect on the angle of attack.

2) We have seen that positive twist reduces the tip angle of attack of the retreating blade. But this procedure has a limited effectiveness because, as can be easily determined, it shifts the aerodynamic load inboard along the blade. When the twist exceeds the optimum value, the blade tip will operate at a low angle of attack, but stalling will occur within the disk.

3) The admissible speed limit of a rotor is not necessarily the one which triggers tip stalling of the retreating blade: flight can be maintained with partial stall along the disk. In practice, vibration and the danger of loss of control are the factors which determine the limiting speed.

It is not without interest to define the conditions in which a rotor will operate with an extended stall area on the retreating blade side. The aerodynamic moments acting on the blade are no longer constant during rotation because second-harmonic flapping appears. If higher-order flapping is disregarded, it has been shown in 3.2141 that the aerodynamic moments are equal for diametrally opposite blade positions. The result is that the rotor disk will exhibit two high-lift areas, one fore and one aft, and two lateral low-lift areas (since the angles of attack, and therefore the lift of the advancing blades, decrease in order to "compensate" for the stall area of the retreating blade).

Insofar as the flapping is concerned, the blade tip, because of the second harmonics, no longer describes a circle, but a curve comparable to the "brim of a Stetson hat." Note that second-order flapping is phase-shifted 180° with respect to the excitation: the high points of the blade trajectories correspond to low-lift regions (advancing and retreating blades).

Plate III-3 shows a diagram based on statistical data which will permit rapid determination of the order of magnitude of the limiting speed that is acceptable, from the stalling viewpoint, for conventional helicopters. Recent experience shows that a certain magrin should be taken with respect to velocities determined in this manner (C_z max = 0.9 instead of 1.2).

3.217. DYNAMIC BEHAVIOR OF THE ROTOR

So far we have constructed the formulas which give the equilibrium position of a rotor in the constant operating state. It remains to determine the variable case. This aspect is important for studies of the stability and piloting of a helicopter. It would go beyond the framework of this course to go into the computational details, and therefore, we will restrict ourselves to presenting the formulas relating to motion in hovering flight, which is the most useful case to analyze. /75

The formulas are given in the form of transfer functions; the input data consists of the control (deflection δ_p of the control plane)*, the helicopter trim (γ) and the speed of horizontal displacement $\mu = \frac{V_x}{\omega R}$. The output data are the the flapping angles a_1 and b_1, referred to a plane fixed in the absolute axes. (See the notation of Appendix III-4.)

$$\left\{\begin{aligned}
a_1 &= -\frac{G_3}{I_p} \times \frac{\left(2\frac{p}{\omega}+\frac{G_3}{I_p}\right)+k\left(\frac{p^2}{\omega^2}+\frac{G_3}{I_p}\frac{p}{\omega}+\frac{G_3}{I_p}k\right)}{\left(\frac{p^2}{\omega^2}+\frac{G_3}{I_p}\frac{p}{\omega}+\frac{G_3}{I_p}k\right)^2+\left(\frac{2p}{\omega}+\frac{G_3}{I_p}\right)^2}(\delta_p+\gamma)\\
b_1 &= -\frac{G_3}{I_p} \times \frac{\left(\frac{p^2}{\omega^2}+\frac{G_3}{I_p}\frac{p}{\omega}+\frac{G_3}{I_p}k\right)-k\left(2\frac{p}{\omega}+\frac{G_3}{I_p}\right)}{\left(\frac{p^2}{\omega^2}+\frac{G_3}{I_p}\frac{p}{\omega}+\frac{G_3}{I_p}k\right)^2+\left(\frac{2p}{\omega}+\frac{G_3}{I_p}\right)^2}(\delta_p+\gamma)\\
a_1 &= \frac{G_3}{I_p} \times \frac{\left(\frac{2p}{\omega}+\frac{G_3}{I_p}\right)+K\left(\frac{p^2}{\omega^2}+\frac{G_3}{I_p}\frac{p}{\omega}+\frac{G_3}{I_p}k\right)}{\left(\frac{p^2}{\omega^2}+\frac{G_3}{I_p}\frac{p}{\omega}+\frac{G_3}{I_p}k\right)^2+\left(\frac{2p}{\omega}+\frac{G_3}{I_p}\right)^2}A\mu.\mu\\
b_1 &= \frac{G_3}{I_p} \times \frac{\left(\frac{p^2}{\omega^2}+\frac{G_3}{I_p}\frac{p}{\omega}+\frac{G_3}{I_p}k\right)-K\left(\frac{2p}{\omega}+\frac{G_3}{I_p}\right)}{\left(\frac{p^2}{\omega^2}+\frac{G_3}{I_p}\frac{p}{\omega}+\frac{G_3}{I_p}k\right)^2+\left(\frac{2p}{\omega}+\frac{G_3}{I_p}\right)^2}A\mu.\mu
\end{aligned}\right.$$

*in depth.

$$\begin{cases} A\mu = \dfrac{\partial a_1}{\partial \mu} \\ K = \dfrac{\partial b_1 / \partial \mu}{\partial a_1 / \partial \mu} \quad \text{or} \quad \mu = 0 \end{cases}$$

Taken from the equations of Appendix III-2.

Remarks /76

1) The three inputs have a similar effect, namely, δ_p and γ are rigorous (the factor that counts is the absolute trim of the control plane: $\gamma + \delta_p$). In the case of μ, the functions differ slightly because k (pitch-flap coupling) has been replaced in the numerator by K. We have already mentioned that k is usually assigned a value which will permit the static displacement b_1 to be cancelled, and this is done by setting k = K. Under these conditions, the two groups of equations become similar.

2) These transfer functions are characterized by a velocity error:

$$\underline{\underline{\varepsilon_V = \frac{\frac{2I_p}{G_3} + k}{1 + k^2} \times \frac{\dot{\delta}_p + \dot{\gamma}}{\omega}}}$$

This is rearward rotor tilt in response to uniform rate of fuselage rotation, which has already been mentioned in 3.212.

3) For the majority of practical applications, in particular insofar as control and stability are concerned, the asympototic values of these functions are sufficient (frequency lower than 1 cycle). Assuming that $K \simeq k$, we get

$$a_1 = \frac{1}{1 + \frac{k + \tau_0 \omega}{1 + k^2} \times \frac{p}{\omega}} \left[-(\delta_p + \gamma) + A\mu \cdot \mu \right]$$

$$b_1 = \frac{1 - k\tau_0\omega}{1+k^2} \times \frac{p}{\omega}\left[-(\delta_p + \gamma) + A\mu\cdot\mu\right]$$

$$\left(\tau_0 = \frac{2}{\frac{G_3}{I_p}\omega}\right)$$

The preceding calculations assume that the inflow is uniform in azimuth. To be completely rigorous, it would be necessary to account for two phenomena: 1) the flow inertia induced at high frequencies, which modifies primarily the response in b_1; and 2) the asymmetry of the induced velocities, necessarily associated with the absolute movements of rotor trim, the "gyroscope" formed by these blades, for "precession," must be subjected to an aerodynamic force moment, and this is why the induced velocities in the azimuth direction are unequal, affecting response in a_1.

Sissingh has proposed a simple correction to account for this effect. It consists in replacing G_3 by a corrected value G_3^*, given by the relation: /77

$$\frac{G_3^*}{G_3} = 1 - \frac{\frac{dC_z}{di} B^3 \sigma}{4{,}2\sqrt{f_N}}$$

We see that τ_0 is modified in inverse proportion: $\frac{\tau_0^*}{\tau_0} = \frac{G_3}{G_3^*}$; this correction makes the rotor "sluggish."

Plate III-4 facilitates calculation of the correction; we see that it is far from being negligible.

3.22. STUDY OF LAG MOTION

By a calculation similar to the one made in 3.211, we obtain the equation for lag motion (see Fig. 3-6):

$$I_p\ddot{\delta} + C_\delta\dot{\delta} + \delta(\omega^2 . e . m_0 + K_\delta) = 0 \qquad (3\text{-}11)$$

where K_δ and C_δ characterize the dampers and spring restorers, mounted on the hinge, if necessary; m_o is the static moment of the blade about the lag axis; it is in practice equal to the corresponding value of the flapping axis. The angular velocity of the characteristic motion is written

$$\Omega_\delta = \omega \sqrt{\frac{e.m_\Delta}{I_p} + \frac{K_\delta}{\omega^2.I_p}}$$

In the case of a homogeneous blade, $\frac{m_\Delta}{I_p} = \frac{3}{2R}$. From this get, for $K_\delta = 0$,

$$\boxed{\Omega_\delta = \omega \sqrt{\frac{3}{2}\frac{e}{R}}}$$

In general, this equation will give a satisfactory approximation.

The natural frequency of a blade about its lag axis is always lower than the angular rotor speed (in practice, it is of the order of 1/4 or 1/3). This natural frequency is an important factor in analyzing ground resonance.

Calculation of Lag Angles /78

The constant lag δ_o due to aerodynamic drag is calculated without difficulty by Eq. (3-11), provided that the engine torque M_N/b is known.

$$\delta_o = \frac{M_N}{b\,(\omega^2 e.m_\Delta + K_\delta)}$$

Drag Flapping

We have seen in (3-1) that lag hinges permit blade motion induced by vertical flapping. In what follows we will provide means for calculating this motion. Figure 3-20 shows the forces to which the blade is subjected.

1) With blade flapping, the rotating axes of the rotor shaft are subjected to horizontal Coriolis forces of the form $d\vec{F}_c = -2\,dm\,\vec{\omega} \wedge \vec{r\dot{\beta}}$. They yield a moment about the lag axis:

$$r\,dF_c = r \times 2\,dm\,(\omega\beta \times r\dot{\beta})$$

In other words, by integrating we have the moment $M_{F_c} = 2\,dm\,r^2\omega\beta\dot{\beta}$ or $M_{F_c} = 2I_p\,\omega\beta\dot{\beta}$.

2) The aerodynamic lifting forces which induced blade flapping are perpendicular to the tip-path plane, and therefore the moment due to these forces has an axial drag component equal to $-M \sin \varepsilon$ (ε is the angle between the no-flapping and lag axes). M is given by the flapping equation:

$$I_p\left(\ddot{\beta} + \omega^2\beta\right) = M\cos\varepsilon \simeq M$$

and ε by the relation

$$\varepsilon \simeq \frac{\dot{\beta}R}{\omega R} = \frac{\dot{\beta}}{\omega}$$

from which we get the moment $-I_p\frac{\dot{\beta}}{\omega}\left(\ddot{\beta} + \omega^2\beta\right)$ on the lag axis.

If these moments are substituted into Eq. (3-11) we get

$$I_p\ddot{\delta} + C_\delta\dot{\delta} + \delta\left(\omega^2 e.m_\delta + K_\delta\right) = 2I_p\omega\beta\dot{\beta} - I_p\frac{\dot{\beta}}{\omega}\left(\ddot{\beta} + \omega^2\beta\right)$$

Assuming that β is of the form $\beta = a_o - a_1\cos\omega t$ /79

$$\beta\dot{\beta} = \omega a_o a_1 \sin\omega t - \frac{a_1^2\omega}{2}\sin 2\omega t$$

$$\ddot{\beta} + \omega^2\beta = \omega^2 a_o$$

Neglecting the effect of damping C_δ, and substituting these values into the above equation we find that

$$\delta = -\frac{a_0 a_1 \sin \omega t}{1-\left(\frac{\Omega}{\omega}\right)^2} + \frac{a_1^2 \sin 2\omega t}{4\left[1-\left(\frac{\Omega}{2\omega}\right)^2\right]}$$

Remember that the flapping amplitude, which is of the order of $a_0 a_1$ and a_1^2, is of the second order with respect to the vertical flapping and is therefore always very low (it is hardly more than 1° in practice).

Remarks

1) The reader will be able to verify that the above expression for drag flapping shows the blade motion to be essentially uniform in its plane.

2) In high-speed flight, the aerodynamic drag forces are modulated (dissymetry between the advancing and retreating blades), resulting in additional drag flapping, which can be easily calculated.

3.3. THE FORCES TRANSMITTED BY THE ROTOR

We know how to calculate the blade motion; it remains only to derive the constant and alternating forces that this motion transmits to the parts to which they are connected, namely, the hub and the controls. It is essential to know these forces in order to study a number of important problems. These are 1) the forces transmitted to the hub: the constant forces, which must be known in order to study flight characteristics (balance of forces), and the alternating forces, stemming from vibrations transmitted to the airframe, and 2) the forces /80
transmitted to the controls: the constant forces, which govern the forces in the controls, and eventually their stability, and the alternating forces, stemming from control vibrations.

3.31. FORCES TRANSMITTED TO THE HUB

3.311. CONSTANT FORCES

Obviously the elementary forces (aerodynamic and mass) produced at each point on the blade can be integrated, yielding the mean value of the forces exerted

on the hub by the set of blades. Complete calculations show that they can be obtained by the following rules (Fig. 3-21):

1) Lift $\vec{F}_N$ perpendicular to the tip-patch plane. This is the lift applied to the center of the hub when the flapping hinges are located directly on the rotor axis, but it is lacking if the hinges are offset. It then passes through a point situated above the rotor, called the thrust center F.

2) Drag T_X in the tip-path plane, parallel to V_X.

3) A component T_Y orthogonal to the velocity, also in the tip-path plane. This force is quite small and can generally be neglected.

An expression for T_X will given in Chapter 4.

At the present we will restrict ourselves to proving the existence of the rotor thrust center.

Suppose we have a four-bladed rotor whose plane of blade rotation forms an angle of a_1 with the drive shaft. We have seen that if we consider only first-order flapping, the blades have uniform motion about the no-flapping axis. The forces transmitted to the hinges consist of the aerodynamic lift and the resultant of the centrifugal force. The aerodynamic lift varies little in intensity (especially in the force and the positions in forward flight when the distribution of aerodynamic forces is equal). Therefore the aerodynamic lift will not introduce asymmetric forces which could produce a moment.

What remains is the centrifugal force, which is perpendicular to the no-flapping axis and has the intensity $\int_0^R \omega^2 dm\, r = \omega^2 m_\Delta$. It produces a moment of $M = -2a_1 \times a \times \omega^2 m_\Delta$ (Fig. 3.22).

The lift $\vec{F}_N$ perpendicular to the disk and the moment M can be replaced by a single force passing through a point F, located in the rotor axis above the hub at a distance of $h_f = \frac{2a\omega^2 m_\Delta}{F_N}$. This is the rotor thrust center. /81

For an arbitrary number of blades, it can be easily seen that we would have

$$h_f = \frac{b}{2} \frac{a \cdot \omega^2 \cdot m_\Delta}{F_N}$$

An expression is often given for h_f as a function of the coning angle. For a homogeneous blade we have

$$\begin{cases} m_\delta = m \frac{R}{2} \\ I_p = m \frac{R^2}{3} \end{cases}$$

and

$$a_o \simeq \frac{F_N}{b} \times \frac{R}{I_p \omega^2} \times \frac{3}{4} .$$

If these values are substituted into the above equation we get

$$\boxed{h_f \simeq \frac{1}{2} \frac{a}{a_o}}$$

3.312. PERIODIC FORCES

There would be no sense in making a quantitative study of these forces, because the results depend essentially on the aerodynamic and dynamic properties of the blades. We propose only to show how the numerous periodic aerodynamic forces and masses produced on the blades are transmitted to the machine.

3.3121. General Properties

The forces transmitted by one blade to its bearings vary periodically with the frequency of rotor rotation. Therefore, their components in rotation axes tied to the rotor can be written using a Fourier expansion as

$$F = F_o + F_1 \cos(\omega t + \varphi_1) + F_2 \cos(2\omega t + \varphi_2) + \dots + F_n \cos(n\omega t + \varphi_n) + \dots$$

In order to study the vibrations transmitted to the airframe, we must refer to fixed axes. We distinguish between the case of vertical forces (or, more exactly, those parallel to the rotor axis), which are transmitted without change, and that of horizontal forces (or, more exactly, those in a plane perpendicular to the rotor axis). Their components along the fixed axes become /82

$$\begin{cases} f_0 \cos \omega t + f_1 \cos(\omega t + \varphi_1) \cos \omega t + \dots + f_n \cos(n\omega t + \varphi_n) \cos \omega t + \dots \\ f_0 \sin \omega t + f_1 \cos(\omega t + \varphi_1) \sin \omega t + \dots + f_n \cos(n\omega t + \varphi_n) \sin \omega t + \dots \end{cases}$$

which can be written

$$\begin{cases} f_0 \cos \omega t + \frac{f_1}{2}\left[\cos \varphi_1 + \cos(2\omega t + \varphi_1)\right] + \dots + \frac{f_n}{2}\left\{\cos\left[(n-1)\omega t + \varphi_n\right] + \cos\left[(n+1)\omega t + \varphi_n\right]\right\} \\ f_0 \sin \omega t + \frac{f_1}{2}\left[-\sin \varphi_1 + \sin(2\omega t + \varphi_1)\right] + \dots + \frac{f_n}{2}\left\{-\sin\left[(n-1)\omega t + \varphi_n\right] + \sin\left[(n+1)\omega t + \varphi_n\right]\right\} \end{cases}$$

When fixed axes are used, each frequency n is divided into two new frequencies, n + 1 and n-1. The effect is analogous to that of two vanes, one rotating at a speed of $(n + 1)\omega$, the other at $-(n - 1)\omega$. What has been just said shows that all the forces transmitted by one blade to the fuselage are of the form:

$$F_0 + F_1 \cos(\omega t + \varphi_1) + F_2 \cos(2\omega t + \varphi_2) + \dots + F_n \cos(n\omega t + \varphi_n) + \dots$$

What is of interest to us from the viewpoint of vibrations transmitted to the fuselag are the forces resulting from the action of a set of b blades.

The alternating forces are summed by the formula

$$\sum_{p=1}^{p=b} F_n \cos\left(n\omega t + \varphi_n + \frac{2\pi}{b} np\right)$$

According to a well-known theorem of trigonometry, these sums are zero except when n is a multiple of b:* /83

> Theorem: a perfectly balanced rotor transmits only alternating forces of a frequency which is a multiple of the angular rotor speed times the number of blades.

Examples:

A two-blade rotor will transmit forces of frequency 2, 4, 6, etc.

A three-blade rotor will transmit those of frequency 3, 6, 9.

3.3122. Principal Sources of Alternating Forces

Vertical Forces. They are modulated primarily by the aerodynamic dissymetry produced by horizontal velocity. However, because of the tendency of the flapping hinge to equalize these forces, they remain very small except at high velocities, when flutter and flapping of frequency 2 become important.

Forces in the plane of the disk. Those which are by far the most important are the forces stemming from variations in blade drag. These are induced drag variation at low velocities (transition zone) due to unequal distribution of induced velocities over the disk. Figure 3.23 shows how these forces appear; they

---

*This theorem can be easily demonstrated by considering that the expression

$$\sum_{p=1}^{p=b} F_n \cos\left(n\omega t + \varphi_n + \frac{2\pi}{b} np\right)$$

represents the projection of a closed polygon contour onto an axis.

result primarily in lateral vibration of fundamental frequency 2. Variations in profile drag at high speeds (dissymmetry between the advancing and retreating blades). They produce longitudinal and lateral vibrations of fundamental frequency 2, and may be as high, in order of magnitude, as several percent of the lift.

The following table recapitulates the principal alternating forces produced by the blades and the way in which they are transmitted to the airframe. /84

Important Remarks /85

1) From the viewpoint of vibrations, note how important it is to increase the number of blades. This is one of the reasons why high-speed helicopters have rotors of four or even more blades. The two-bladed rotor is very unfavorable because its hub receives forces modulated at a frequency of 2 from cyclic variations in drag at a frequency of 1. These are by far the most "mischievous." This is why it is absolutely necessary for a two-bladed rotor to be flexibly mounted in order to attanuate the transmission of these vibrations to the fuselage.

2) The study which has just been made assumes that the rotor is perfect (identical blades). Unfortunately, perfection is not of this world (particularly insofar as rotorcraft are concerned!) and there may exist small mass and aerodynamic differences between the blades. Therefore, vibrations of any frequency may be generated, especially of frequency 1 and 2. A rotor vibrating at a frequency which is not an integral multiple of its number of blades is faulty, that is, the mass balance is poor or the aerodynamic properties of the blades are unequal. The latter case of faulty functioning is rather frequent in service, especially when the blades are made of wood.

3.32. FORCES TRANSMITTED TO THE CONTROLS

3.321. CALCULATION OF THE MOMENTS ABOUT THE FEATHERING AXIS OF A BLADE

These moments can be obtained by adding the moments due to aerodynamic forces and the forces of inertia. The latter are calculated by applying the kinetic moment theory to the feathering axis. In order not to encumber the text, the complete calculation is presented in Appendix III-3.

We will limit ourselves to presenting a physical interpretation of the equation we obtained.

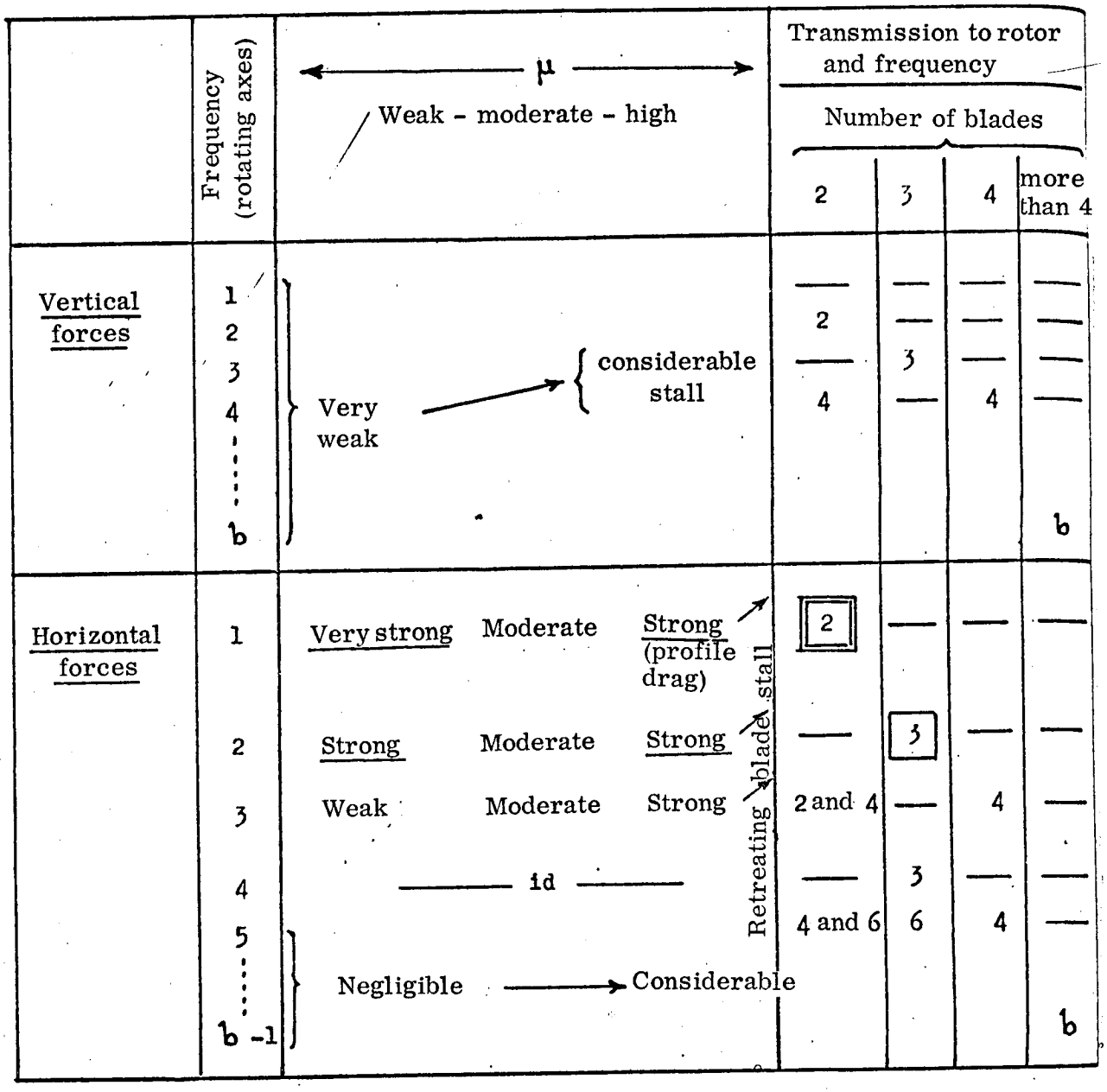
Frequency (rotating axes)
μ
Weak - moderate - high
Transmission to rotor and frequency
Number of blades
2
3
4
more than 4
Vertical forces
1
2
3
4
b
Very weak
considerable stall
Horizontal forces
1
Very strong
Moderate
Strong (profile drag)
2
Strong
Moderate
Strong
3
Weak
Moderate
Strong
4
id
5
b -1
Negligible
Considerable
Retreating blade stall
2 and 4
4 and 6
6

In the case of a freely articulated blade the moment applied to the controls is written as

$$M_\theta = -\left\{ A\left(\ddot{\theta} + \omega^2\theta\right) + \left(A + B - C\right)\omega^2\left(\frac{\dot{\beta}}{\omega} - \theta\right) + F\left(\omega^2\beta + \ddot{\beta}\right)\right\} \qquad (3\text{-}12)$$

$\longleftarrow$ forces of inertia $\longrightarrow$

$$+ F_A y_A + C M_o$$

aerodynamic forces

$A = \Sigma m\left(y^2 + z^2\right)$, the moment of inertia of the blade about its feathering axis will be denoted by i_θ .

$B = \Sigma m\left(z^2 + x^2\right) = I_p$

$C = \Sigma m\left(x^2 + y^2\right)$

$F = \Sigma m x y$ (the coefficients $D = \Sigma m y z$, $E = \Sigma m z x$ are assumed to be zero). /86

CM_o aerodynamic moment due to the profile drag (Cm_o)

F_A aerodynamic force exerted on the blade

Y_A coordinate of the point where the force F_A is applied.

The term $\left(A + B - C\right)\omega^2\left(\frac{\dot{\beta}}{\omega} - \theta\right)$:

The vertical flight the alternating part of this term is zero because $\frac{\dot{\beta}}{\omega} - \theta$ is constant (basic law of flapping). In addition, $A + B - C = 2\Sigma m z^2$ is very small as compared with the other terms and can therefore be neglected (which is equivalent to assuming that the blade is infinitely thin).

The term $F\left(\omega^2\beta + \ddot{\beta}\right) = \Sigma m x y\left(\omega^2\beta + \ddot{\beta}\right)$.

This is the moment resulting from the fact that the blade is no longer articulated about a principal axis of inertia. More simply, it is the sum of the moments due to centrifugal force and flapping acceleration $m\left(\omega^2\beta + \beta\right)x$ applied at a distance of y from the axis.

This term can be written

$$\left(\omega^2\beta + \ddot{\beta}\right) m_\delta \times y_G \text{ with } y_G = \frac{F}{m_s}$$

It should be noted that a relation exists between the resultant of the forces of inertia $\left(\omega^2\beta + \ddot{\beta}\right) m_\delta$ and that of the aerodynamic forces F_A, that is, the fundamental vertical flapping relation

$$I_p\left(\omega^2\beta + \ddot{\beta}\right) = M$$

which can be written

$$\left(\omega^2\beta + \ddot{\beta}\right) m_\delta r_G = F_A r_A$$

$r_G = x_G = \frac{I_p}{m_\delta}$ coordinate of the point where the resultant of the forces of inertia is applied.

$r_A = x_A = \frac{M}{F_A}$ coordinate of the point where the resultant of the aerodynamic forces is applied.

The coordinate point $y_G r_G$, the point where the resultant of the forces of inertia are applied, is the elastic center of the blade corresponding to the flapping axis. /87

The coordinate point $y_A r_A$, the point where the resultant of the aerodynamic forces is applied, will be called the aerodynamic center, by way of generalizing the fact that at every blade section the elementary lift is applied to the aerodynamic center of the airfoil.

Under these conditions the equation is written

$$M_\theta = -i_\theta\left(\ddot{\theta} + \omega^2\theta\right) + F_A\left(y_A - y_G\frac{r_A}{r_G}\right) + C_{M_0} \qquad (3\text{-}13)$$

Interpretation

The forces of inertia are given only by the term $-i_\theta(\ddot{\theta}+\omega^2\theta)$, which shows that the natural frequency of the blade about its cyclic pitch axis is equal to the angular velocity of the rotor.

Therefore the forces of inertia stemming from cyclic pitch control at a frequency of one will be zero.

This term can be reduced to the constant term $-i_\theta \omega^2 \theta_0$, which is a restoring force produced by the forces of inertia (the blade has a tendency to return to the "flat" position).

The terms due to aerodynamic forces yield moments which are modulated in forward flight; C_{M_0}, F_A, y_A and r_A vary slightly with azimuth.

These moments are disturbing because the forces and vibrations are transmitted to the controls, and therefore efforts are made to reduce them to a minimum. This is why it is attampted to get blades with airfoils of low c_{m_0}. In addition the blade is designed in such a way as to make the expression $y_A - y_G r_A/r_G$ as low as possible, or, preferably, to cancel y_A and y_G. It is easy to see that this results in practice to coincidence of the pitch-change axis, the center-of-gravity line of the sections and the aerodynamic-center line of the airfoils.

Remarks

1) There are some blades which are attached in such a way that a pitch restoring moment is created. It is sufficient to account for this fact by introducing this supplementary term in the equation.

2) In some cases we cannot avoid modifying the M_θ forces by mounting suitable counterweights on the blades. Their effect can be estimated from the resultant change in the parameters A, B, C, D, and F in the equation given in Appendix III-3. /88

3.322. TRANSMISSION OF FORCES TO THE FLIGHT CONTROLS

The forces from b blades are transmitted to the cylic and collective pitch controls by the same rules studied in Section 3.312 relative to vibrations transmitted to the fuselage. They have been summarized in the following table.

	Frequency (rotating axes)	Transmission to the controls and frequency			
		Number of blades			
		2	3	4	more than 4
Forces in the collective pitch control	1	—	—	—	—
	2	2	—	—	—
	3	—	3	—	—
	4	4	—	4	—
	⋮				
Forces in the cyclic pitch control	1	Constant force + 2	Constant force	Constant force	Constant force
	2	—	3	—	—
	3	2 and 4	—	4	—
	4	—	3	—	—
	5	4 and 6	6	4	—
	⋮				

Chapter 4

PERFORMANCE

4.1. GENERAL

Every calculation of performance consists in comparing the available power with the power required for a given flight situation. /89

The different methods are charactized by the way in which the required power is calculated. In the case of a helicopter, these methods are numerous. They can be classified in two main families.

1) Those which are carried out be intergrating the elementary effects exerted at every point of the blade. Their precision is often very rough because of the approximations to be made in order to avoid intricate calculations. Therefore they are rarely used, except in the study of vertical flight.

2) Those which decompose the required power into a certain number of terms computed separately. These are the methods that are called "balance of power" methods. The elementary terms are obtained by formulas or graphs, more or less complex, depending on the degree of precision desired. Even in their simplest forms these methods yield satisfactory results in the hands of experienced analysts.

This chapter is not intended to provide the reader with a detailed presentation of the calculation procedures used by special research bureaus. It is intended rather to point out the properties which are peculiar to the helicopter from a performance standpoint. This is why we will use primarily the balance of power method, in its simplest form, while at the same time providing the means for proceeding to more precise calculations.

4.11. POWER BALANCE

In the general case the power balance is written

$$P_N = P_{\text{total required}} = P_i + P_p + P_f + P_a,$$

where $P_i = GXV_i$ is the induced power required for lift, P_p is the power expended as a result of blade drag, P_f is the power expended to overcome fuselag drag, and $P_a = GXV_a$ is the power required to bring the machine to a speed of V_a (negative if the machine is descending).

P_N will be comparable to the available rotor power, P_D, and should be less or equal to it.

4.12. DETERMINATION OF THE POWER AVAILABLE IN THE ROTOR OR ROTORS

Case of Mechanically-Driven Machines

Under given atmospheric conditions (altitude and temperature) and a given engine and rotor speed of rotation, we know the maximum power P_M that the engine can develop (reciprocal or turbine engine). This power is transmitted to the rotor only with certain losses; the losses depend on the type of machine. Two characteristic balances are given below by way of example.

Single rotor with anti-torque propellor. Reciprocating engine.

Losses:
- Engine cooling (fan) = 4 to 6%
- Anti-torque rotor drive = 7 to 9%
- Transmissions losses = 2 to 3%
- Total = $\simeq$ 15%

Available rotor power: $P_D \simeq 0.85\ P_M$

Single rotor with anti-torque propellor. Turbine engine.

Losses:
- Anti-torque rotor drive = 7 to 9%
- Transmission losses = 4 to 5%
- Total $\simeq$ 12%

Available rotor power: $P_D \simeq 0.88\ P_M$

Case of Jet-Propelled Machines. /91

It is expedient to know the net thrust available at the blade tip as a function of the atmospheric and rotor conditions. These characteristics, which vary considerably from one system to the other, are the subject of a more detailed study in Chapter 8.

4.13. LEVEL FLIGHT

If we plot P_i, P_p, P_f as a function of V_x, we get curves of the form shown in plate IV-9 (helicopter A).

If these three powers are summed, we obtain the total power curve. The dashed curve shows the power required with ground effect accounted for. This curve is being mentioned at the beginning of this chapter in order to emphasize the important fact that it has a distinct minimum which, in modern designs, represents 60 to 70% of the power required for landing out of ground effect; this minimum becomes effective in the range of 70-100 km/h.

The result is that from hovering onward the power required decreases with level-flight speed.

4.14. THE THREE CEILINGS OF A HELICOPTER

For a given weight the helicopter will be characterized by three ceilings (see Fig. 4.1):

1) The vertical-flight ceiling out of ground effect (flight at point A);

2) The vertical-flight ceiling in ground effect (flight at point B);

3) The forward-flight ceiling (flight at minimum power: point C).

In fact, the last ceiling, which requires infinite time to be reached, is replaced by the service ceiling (altitude at which the optimum rate of climb is 0.50 m/sec).

These ceilings are classified in increasing altitude; the power required is in decreasing order. For a reciprocating-engine helicopter without a compressor (the case which is still prevalent), we will see that the ceiling levels are approximately.

z_0: vertical-flight ceiling out of ground effect;

$z_0 + 1,200$ m: vertical-flight ceiling in ground effect;

$z_0 + 3,500$ m; service ceiling.

4.2. VERTICAL FLIGHT PERFORMANCE /92

4.21. HOVERING PERFORMANCE OUT OF GROUND EFFECT.

We have seen in 2.1311 that the power required for hovering was of the form

$$P_N = \frac{P_{i\,theor.}}{\eta_s} = \frac{1}{\eta_s} \times F_N \sqrt{\frac{F_N}{2\rho S}}$$

In this equation F_N represents the "apparent" weight of the helicopter, that is, its real weight G, to which is added the drag on the fuselage caused by rotor downwash. In general, the drag correction is small and can be neglected in the first approximation. However, in the case of heavily loaded rotors and a heavy fuselage, it may make an appreciable contribution to the total value of the real weight (up to 10%).

The correction may even be greater in the case of a compound or convertiplane because of the vertical drag of the auxiliary wing.

Before presenting the various methods which will enable more or less precise calculation of P_N, let us first introduce the concept of "rotor polar".

We define the dimensionless coefficients f_N, m_N by the relations

$$\begin{cases} F_N = \frac{\rho}{2} S u^2 f_N \\ P_N = \frac{\rho}{2} S u^3 m_N \quad (\text{ou : } M_N = \frac{\rho}{2} S u^2 R m_N) \end{cases} \tag{4.1}$$

For a given rotor, each value of the collective pitch corresponds to a pair of values f_N, m_N. When the collective pitch changes, the coordinate point f_N, m_N describes a curve called the rotor polar (Fig. 4.2). A numerical example is given in Plate IV.1.

Remarks.

1) The reference pitch that is usually used is that of a blade section at a distance of r = 0.7R from the center; note the symbol $\theta_{0.7}$

2) It can be easily seen that $\eta_s = \frac{f_N^{3/2}}{2 m_N}$. /93

3) During hovering in the ground effect the power required to lift a given weight is reduced, and therefore the preceding polar is no longer valid. It is expedient to use a new polar that is characteristic of the new operating state.

4.211. APPROXIMATE CALCULATION

We can write $P_N = P_i + P_p$.

Calculation of P_i.

This calculation consists in adding the induced losses to the theoretical induced power. As we have seen in Chapter 2, these losses stem from blade tip losses and losses from nonuniform induced velocities.

Blade Tip Losses

These losses are accounted for in an overall manner by calculating the lift with BR replacing R, where B is equal to $1 - \frac{\sqrt{f_N/2}}{b}$ (see 2.1322). In practice B lies between 0.95 and 1. For an approximate calculation the value 0.97 is often used.

Losses for Nonuniform Induced Velocities

In the absence of any information on the distribution of the induced velocities of the rotor being studied the distribution can be assumed to be linear: $v_i = V_i\, r/R$ is always close to reality (see Plate II-4) and unfavorable. Under these conditions, if the lift and induced power are calculated by Eq. (2.10), as applied to annular rings:

$$F_N = \int_0^R 2\rho \cdot 2\pi r\, dr\, V_i^2 \frac{r^2}{R^2} = \rho S V_i^2$$

$$P_i = \int_0^R 2\rho \cdot 2\pi r\, dr\, V_i^3 \frac{r^3}{R^3} = \frac{4}{5}\rho S V_i^3$$

Taking the blade tip losses into account we get (replacing S by B^2S): /94

$$\begin{cases} F_N = \rho S V_i^2 B^2 \\ P_i = \frac{4}{5} \rho S V_i^3 B^2 , \end{cases}$$

and applying Eq. (2.11):

$$\eta_i = \frac{P_{i\,\text{theoretical}}}{P_{i\,\text{real}}} = \frac{F_N^{3/2}}{P_i \sqrt{2\rho S}} = \frac{(\rho S B^2 V_i^2)^{3/2}}{\frac{4}{5} \rho S B^2 V_i^3 \sqrt{2\rho S}}$$

that is,

$$\eta_i = \frac{B}{1,13}$$

and therefore

$$\boxed{P_i = \frac{1,13}{B} \frac{F_N^{3/2}}{\sqrt{2\rho S}}} \qquad (4.2)$$

If instead of a linear induced velocity distribution we assume a parabolic one of the form $v_i = V_i(2\bar{r} - \bar{r}^2)$, even though we are being somewhat optimistic this time, we get a coefficient $\eta_i = B/1.06$. Real rotors lie between these two limiting cases. Taking into account the nominal values for B, the additive power factor $1/\eta_i$ will vary between 1.10 and 1.20.

Calculation of P_p

This factor can be obtained by the following approximate calculation. A mean C_z is determined by the formula

$$F_N = b \int_0^{BR} \frac{\rho}{2} \omega^2 r^2 \ell_{0,7} C_{z_m} \, dr$$

where the blade section chord is assumed to be constant, equal to its value at 0.7R. We obtain /95

$$C_{zm} = 3\frac{F_N}{b\frac{\rho}{2}\omega^2 R^3 \ell_{0,7} B^3} = \frac{3F_N}{\frac{\rho}{2} S\sigma u^2 B^3} = \frac{3f_N}{\sigma B^3} \qquad (4.3)$$

The coefficient $\sigma = \frac{b\ell_{0,7}}{\pi R}$ is called the rotor "solidity". It represents the ratio of the "effective" blade area to the rotor disk area.

The C_{xp} (in infinite aspect ratio) corresponding to the mean C_z and to the Reynolds number is determined as 0.7R (0.7 u·$\ell_{0.7}$/ v)*.

We then have

$$P_p = \omega \int_0^R \frac{\rho}{2} \omega^2 r^3 \ell_{0,7} C_{xp}\, dr \quad **$$

that is

$$P_p = \frac{\rho}{8} C_{xp} S\sigma u^3 \qquad (4.4)$$

*It would be appropriate to increase the experimentally deduced C_{xp} (on models) by a coefficient accounting for the lace of perfection in constructing airfoils and for possible deformation. This is especially true of wood or fabric-covered blades. The factor accounting for this increase may be of the order of 1.1 to 1.7, depending on the case.

**In the case of drag it is expedient to integrate up to R and not up to BR, because the blade tips drag is they do not lift.

The total power is

$$P_N = P_i + P_p = \frac{1,13}{B} \frac{F_N^{3/2}}{\sqrt{2\rho S}} + \frac{\rho}{8} C_{xp} S \sigma u^3$$

Remark.

The integrations carried out above have been simplified by assuming that certain variables were constant, equal to their value at 0.7 R . (ℓ, C_z, C_{xp}). This deserves a few comments:

This type of mathematical reasoning is justified by the well-known formula of analysis /96

$$\int_a^b f(x)\, g(x)\, dx = f(c) \int_a^b g(x)\, dx \qquad (a < c < b)$$

II

The difficulty lies in determining C, the value of which depends on the analytical value of f(x) and g(x). In the case at hand, therefore, we should expect, if we are to be completely rigorous, that the reference blade span will depend on each specific rotor configuration and on the problem being treated (i.e., calculation of lift, induced torque, frictional couple). This implies that depending on the author and the problem to be solved we will find reference blade spans that differ somewhat (0.7, 0.75, 0.8).* The resulting deviations are in practice small for calculations of peformance and can be neglected without degrading the accuracy of the formulas. For this reason all the formulas given in this course use the single reference point 0.7R, so as to simply representation.

---

*By way of example let us calculate the exact reference blade span x for the lift calculation. The formula to be used is

$$F_N = \int_0^R \frac{\rho}{2} \omega^2 r^2 (\ell C_z)_r \, dr$$

Assume that the variation of ℓC_z as a function of r is small enough to be expressed in the useful parts of the blade by a linear relation of the form

Note: Footnote continued on following page.

4.212. SIMPLIFIED EQUATIONS FOR THE ROTOR POLAR

Returning to Eqs. (4.2), (4.3), (4.4), we can express f_N and m_N by the relations

$$\begin{cases} f_N = \dfrac{\sigma B^3}{3} C_{3m} \\ m_N = \dfrac{1}{\eta_i} \dfrac{\sigma^{3/2} B^{9/2} C_{3m}^{3/2}}{6\sqrt{3}} + \dfrac{C_{xp}}{4} \sigma \end{cases} \tag{4.5}$$

Approximate Relation Between the Lift and the Rotor Pitch /97

We can write

$$C_{3m} = \frac{dC_3}{di}\left(\theta_{0,7} - \frac{V_{i\,0,7}}{0,7\,u}\right)$$

where $v_{i_{0.7}}$ is given by the relation

$$V_{i\,0.7} = \frac{1}{B}\sqrt{\frac{F_N}{\rho S}} \times 0.7$$

$$(\ell C_3)_r = (\ell C_3)_x \left[1 + \alpha(r - x)\right]$$

We get

$$F_N = \int_0^R \frac{\rho}{2} \omega^2 r^2 (\ell C_3)_x \, dr + \int_0^R \alpha (\ell C_3)_x \frac{\rho}{2} \omega^2 (r - x) r^2 dr.$$

The desired condition is that the second integral be zero:

$$\frac{R^4}{4} - x\frac{R^3}{3} = 0 \quad \text{from which} \quad \underline{x = 0,75\ R}$$

Note: Footnote continued from page 98.

assuming that the induced velocity is lineary distributed (see 4.211). From this we get

$$f_N = \frac{\sigma B^3}{3} \frac{dC_z}{di} \left(\theta_{0,7} - \frac{1}{B} \sqrt{\frac{F_N}{\rho S}} \times \frac{1}{u} \right)$$

Taking the relation

$$\frac{F_N}{\frac{\rho}{2} S u^2} = f_N ,$$

into account, we get

$$f_N = \frac{\sigma B^3}{3} \frac{dC_z}{di} \left(\theta_{0,7} - \frac{1}{B} \sqrt{\frac{f_N}{2}} \right)$$

which permits calculation of $\theta_{0.7}$ if f_N is known and vice versa.

4.213. PRECISE CALCULATION

In what follows we present the method of elementary rings, which is an example of a calculation which takes exact account of the aerodynamic effects at every point of the blade. The presentation we have adopted is due to Chief Engineer Garry.

In order to avoid eventual repetitions we will first give the equations in the general case of vertical climb.

Consider an elementary ring of radius r and thickness dr. The principle of the method consists in assuming that the elementary lift and power relative to the ring can be determined regardless of what happens anywhere else on the blade. Figure 4.3 gives a diagram of the distribution of velocities and forces over a blade element.

Since ϕ is always small in the case of a rotor (contrary to the case of a tractor propellor), the following approximations will be made.

The tangential induced velocity (equal to $V_i \tan \phi$; see 2.1322) will be neglected:

$$\left| \begin{array}{l} \phi = \operatorname{arc\,tg} \dfrac{V_1}{\omega r} \simeq \dfrac{V_1}{\omega r} \\ dF_N \simeq \dfrac{\rho}{2} d\sigma\, \omega^2 r^2 C_z \\ dF_T \simeq \dfrac{\rho}{2} d\sigma\, \omega^2 r^2 (C_z \phi + C_{x_p}) \end{array} \right.$$

The lift is written in two ways.

1) Profile lift:

$$dF_N = \frac{\rho}{2} b l\, dr.\omega^2 r^2 C_z = \frac{\rho}{2} \pi R^2 \omega^2 R^2 \frac{bl}{\pi R} \left(\frac{r}{R}\right)^2 \left(\frac{dC_z}{di}\right)_\infty (\theta - \phi) \times \frac{dr}{R}$$

or, setting $\frac{l}{R} = \bar{l}$, $\frac{r}{R} = \bar{r}$.

$$dF_N = \frac{\rho}{2} \sigma u^2 \pi \bar{r}^2 \frac{b\bar{l}}{\pi} \left(\frac{dC_z}{di}\right)_\infty \bar{r}^2 (\phi - \theta)\, dr$$

2) Momentum theorem (see Eqs. (2.9)):

$$dF_N = 2\rho . 2\pi r\, dr (V_1 - V_2) V_1 = \frac{\rho}{2} S u^2 8 \bar{r}^3 \phi \left(\phi - \frac{V_2}{u\bar{r}}\right) dr$$

By comparing the two expressions we get the equation

$$\phi \left(\phi - \frac{V_2}{u\bar{r}}\right) = \frac{b\bar{l}}{8\pi \bar{r}} \left(\frac{dC_z}{di}\right)_\infty (\theta - \phi) \qquad (4.6)$$

which permits calculation of ϕ at any point of the blade.

Then, by integration, we can calculate F_N and P_N:

$$F_N = \frac{\rho}{2} S u^2 f_N \quad \text{with} \quad f_N = \int_0^B \frac{b\bar{\ell}}{\pi} \left(\frac{dC_z}{di}\right)_\infty \bar{r}^2 (\theta - \phi)\, d\bar{r}$$

(Integration is carried out only up to the radius BR in order to account for blade tip losses); /99

$$P_N = \int_0^R \frac{\rho}{2} b\ell\, dr . \omega^2 r^2 . \omega r (C_z \phi + C_{xp})$$

or

$$P_N = \frac{\rho}{2} S u^3 m_N \quad \text{avec} \quad m_N = \int_0^1 \frac{b\bar{\ell}}{\pi} (C_z \phi + C_{xp}) \bar{r}^3 d\bar{r} \qquad (4.8)$$

where C_{xp} is the drag coeffieicnt of an airfoil of infinite aspect ratio at local conditions of angle of attack, Reynolds number (in a nonturbulent atmosphere) and of compressibility; C_z is considered to be zero for $\bar{r} > B$.

The graphs in Plate IV-2, which are due to Aeronautical Engr. Linot, make it possible to solve Eq. (4.6) and to obtain values of V_i and C_z at every point of the blade.

Remark. Examination of Eq. (4.8) shows that the expression for power contains two terms, one in $C_z \phi$, which is the induced power P_i, and one in C_{x_p}, which is the profile power. The first is independent of , the second dependent on the Reynolds number.

It is because of this term that deviations have been noted between the value of m_N in models and in full-scale machines.

Case of Hovering Flight.

Setting $V_Z = 0$, Eq. (4.6) becomes

$$\boxed{\phi^2 = \frac{b\bar{\ell}}{8\pi\bar{r}}\left(\frac{dC_3}{di}\right)_\infty (\theta-\phi)} \qquad (4.9)$$

which can be solved accurately by means of a graph constructed by Mr. Normand and given in Plate IV-3.

According to (4.7) we have /100

$$f_N = \int_0^B \frac{b\bar{\ell}}{\pi}\left(\frac{dC_3}{di}\right)_\infty \bar{r}^2 (\theta-\phi)\, d\bar{r}$$

or, taking (4.9) into account,

$$\boxed{f_N = \frac{F_N}{\frac{\rho}{2} S u^2} = \int_0^B 8\phi^2\bar{r}^3 d\bar{r} = \int_0^B 2\phi^2 d(\bar{r}^4)} \qquad (4.10)$$

The same is true for the calculation of m_N:

The induced power is

$$m_{N_i} = \int_0^B b\frac{\bar{\ell}}{\pi} C_3\, \phi\, \bar{r}^3 d\bar{r} = \int_0^B 8\phi^2\bar{r}.\phi.\bar{r}^3 d\bar{r} = \int_0^B \frac{8}{5}\phi^3 d(\bar{r}^5)$$

Since the angle of attack at every point of the blade $i = \theta-\phi$ is known, the corresponding profile drag factor is deduced from it and the profile power is

$$m_{N_p} = \int_0^1 \frac{b\bar{\ell}}{\pi} C_{xp}\, \bar{r}^3 d\bar{r} = \int_0^1 \frac{b\bar{\ell}}{5\pi\bar{r}}\, C_{xp}\, d(\bar{r}^5)$$

and therefore

$$m_N = \frac{M_N}{\frac{\rho}{2} S u^3} = \int_0^B \frac{8}{5} \phi^3 d(\bar{r}^5) + \int_0^1 \frac{b\bar{\ell}}{5\pi\bar{r}} C_{xp}\, d(\bar{r}^5) \qquad (4.11)$$

Integration of Eqs. (4.10) and (4.11) is greatly facilitated by using the diagrams of Plates IV-3 and IV-4, where the abscissas are proportional to $\bar{r}^4$ and $\bar{r}^5$, respectively. Then the operation reduces to simple measurement of plane surfaces.

Remarks

1) Examination of the diagrams in Plates IV-4 and IV-5 reveals the importance from the performance standpoint of sections some distance from the center of the rotor and, in contrast, the lack of importance of sections located within the first quarter of the radius. The consequence of this fact is that it is hardly worthwhile to give close attention to this region of the blade insofar as aerodynamics is concerned. This is why, for structural and weight economy reasons, the blades are often not streamlined in this region, without essentially affecting the performance.

2) The proportion between induced and profile power is of the order of 3 to 1 in present-day designs. /101

4.214. REFINEMENTS TO THE PRECEDING METHOD

Tip Losses.

The calculation of the preceding section has accounted, in an overall fashion for blade tip losses by limiting the lift to a radius of BR. Given the importance of the blade tip from the performance standpoint, it may be useful to make a more precise analysis. To do so, it is necessary to rely on the rotor vortex theory. Lock and Yeatman [6] give tables for a coefficient K as a function of the number of blades, of the relative radius $\bar{r}$ and of the local angle ϕ. This coefficient serves to correct Eq. (4.6), which becomes

$$K\phi\left(\phi - \frac{V_z}{u\bar{r}}\right) = \frac{b\bar{\ell}}{8\pi\bar{r}} \left(\frac{dC_z}{di}\right)_\infty (\theta - \phi) \qquad (4.6')$$

Plate IV-6, after Payne, presents the useful values of K in graphic form. Since K is a function of ϕ, we proceed by the method of successive approximations. In practice the correction is not appreciable except beyond 0.7R.

Remarks.

1) As can be seen from Eq. (4.6'), the introduction of the factor $K (< 1)$ increases the induced velocities toward the tip of the blade. Contrary to what is expected at first glance, this does not enhance the lift of the rotor, but reduces it. As we have seen in 2.1322, an increase in induced velocity corresponds to a vortex (or "spilling") effect, which reappears at infinity downstream in the form of momentum. The reduction in lift is evident if we consider that the local C_z is proportional to

$$\theta - \phi = \theta - \frac{V_i}{\omega r}$$

2) The "scholarly" aspect of these corrections for tip losses ought not lead to deception: they correspond to only a rather crude solution of a complicated mathematical problem, and agreement with experiment is far from being perfect. This is why many analysts restrict themselves to the preceding overall corrections.

Influence of Tangential Induced Velocities

We know that the approximation in which these velocities were neglected is not valid near the root of the blade. In particular, if we wish to assess the behavior of the airfoils in this region precisely, it will be expedient to introduce the appropriate corrections. /102

Given below are the formulas relating to hovering flight. In this case, the relations between ϕ, V_i and V_t are as follows (see 2.1322):

$$V_t = V_i \operatorname{tg} \phi$$

$$\operatorname{tg} \phi = \frac{V_i}{\omega r - V_i \operatorname{tg} \phi} \text{ which is written } V_i = \omega r \sin \phi \cos \phi$$

Equation (4.9), which relates θ and ϕ, must be replaced by

$$\sin^2\phi = \frac{b\bar{\rho}}{8\pi\bar{r}}\left(\frac{dC_z}{di}\right)_\infty(\theta-\phi) \qquad (4.9')$$

This equation differs from (4.9) only in that $\sin^2\phi$ is substituted for ϕ^2. The deviation is appreciable only if the angles ϕ are large.

4.215. THE OPTIMUM ROTOR IN HOVERING FLIGHT

In this section we propose to find the answer to the question which is asked when any helicopter is designed, namely, "what is the optimum rotor?" Such a question is meaningful only if it is translated into precise a mathematical form.

In the present case, the problem is to determine the rotor characteristics (operating state and geometry) which will permit a given lift to be obtained with minimum power (the case of a mechanically driven machine) or minimum thrust at the blade tip (case of a jet machine).

Stated in this general form, the problem is unsolvable, as we will show further on. Given any rotor, it is always possible to find an infinite number of rotors which will yield the same lift at a lower power (or blade tip thrust).

On the other hand, if certain supplementary conditions are imposed (rotor diameter, tip speed, etc.) we will see that there are optimum values for the parameters, and these are to be defined.

We will now study this question in detail, because of the particular interest it presents for helicopter engineering and because of the numerous false ideas prevalent in the literature in this regard.

The study will be divided into two parts, one dealing with mechanically driven rotors, the other with jet-driven rotors. We will indeed see that the conclusions reached are different in the two cases.

1) Case of the Mechanically Driven Rotor

In this case the desired result is to obtain a given lift F_N with a minimum of power P_N.

Let us introduce the formulas of Section 4.211:

$$\begin{cases} F_N = \dfrac{\rho}{6} S \sigma u^2 C_{xm} \\ P_N = \dfrac{1}{\eta_i} \dfrac{F_N^{3/2}}{\sqrt{2\rho S}} + \dfrac{\rho}{8} C_{xp} S \sigma u^3 \end{cases} \quad (4.12)$$

*

These equations involve four structural parameters; namely, S, the rotor disk area; σ, the rotor solidity; i, the working angle of attack of the blades (which fixes the values of C_{xp} and C_{z_m}); and u, the tip speed.

- If F_N is given, these four parameters, related by the first Eq. (4.12), are not independent, and the relation between F_N and P_N can be written several ways, depending on which three independent variables are chosen:

$$\begin{cases} P_N = \dfrac{1}{\eta_i} \dfrac{F_N^{3/2}}{\sqrt{2\rho S}} + \dfrac{3}{4} \dfrac{C_{xp}}{C_{xm}} F_N u & \text{(S, i, u are the independent variables)} \\ P_N = \dfrac{1}{\eta_i} \dfrac{F_N^{3/2}}{\sqrt{2\rho S}} + 3\sqrt{\dfrac{3}{4}} \times \dfrac{C_{xp}}{C_{xm}^{3/2}} \times \dfrac{1}{\sqrt{\sigma}} \dfrac{F_N^{3/2}}{\sqrt{2\rho S}} & \text{(S, i, } \sigma \text{ are the independent variables)} \end{cases} \quad (4.13)$$

Using the notation

$$V_{i_o} = \sqrt{\frac{F_N}{2\rho S}}$$

the formulas can be written

/104

$$\frac{P_N}{\dfrac{F_N^{3/2}}{\sqrt{2\rho S}}} = \frac{1}{\eta_s} = \frac{1}{\eta_i} + \frac{3}{4} \frac{C_{xp}}{C_{xm}} \cdot \frac{u}{V_{i_o}} = \frac{1}{\eta_i} + 3\sqrt{\frac{3}{4}} \frac{C_{xp}}{C_{xm}^{3/2}} \cdot \frac{1}{\sqrt{\sigma}} \quad \text{power equation} \quad (4.14)$$

*We have taken B = 1 to simplify the written expressions.

$$\frac{F_N}{2\rho S u^2} = \left(\frac{V_{i_0}}{u}\right)^2 = \frac{\sigma \cdot C_{z_m}}{12} \quad \text{— lift equation} \tag{4.15}$$

These formulas show that the actual power is obtained by multiplying the minimum theoretical power $P_{i_0} = \frac{F_N^{3/2}}{\sqrt{2\rho S}}$ by the factor $\frac{1}{\eta_s}$, which does not depend on S, provided we take the independent variables to be i and σ, or i and $\left(\frac{u}{V_{i_0}}\right)$.

The result is that, all things being equal, the required power will be as low as the disk loading; from the theoretical standpoint the optimum rotor radius is infinite.

From the practical standpoint, this conclusion is obviously absurd, because the weight of the rotor itself also tends to infinity!

This reminds us that power economy is not an end in itself, but a means of obtaining an optimally "efficient" machine.

Therefore power economy should be strived for only if it does not otherwise result in excessive disadvantages which would run counter to the desired goal. The choice of disk loading should not, therefore, stem from aerodynamic considerations alone. As a matter of fact, this choice follows primarily from structural considerations, which we will point out in Chapter 10.

In what follows, therefore, we will assume that the disk loading is given as F_N/S.

We still have to try to minimize $\frac{1}{\eta_s}$. This problem in turn reduces to two problems, the reduction of induced losses and of drag losses.

Minimum Drag Losses

Equations (4.14) and (4.15) show that here too there is no optimum from the theoretical viewpoint: Whatever the working angle of attack of the blades, the profile losses can be made as small as desired; it is enough to assign (u/V_{i_0}) a sufficiently low value and, correlatively, a sufficiently large value to σ.

From the point of view in which we now find ourselves, however, there is no optimum blade angle of attack, contrary to what is often said. On the other hand,

if one of the structural parameters σ or u is imposed, there is an optimum a angle of attack. If the tip velocity u is specified, the angle of attack minimizes C_{x_p}/C_{z_m} (maximum aerodynamic efficiency). This case is equivalent to seeking the optimum blade chord when the transmission of power (and therefore u) is defined.

If the solidity σ is specified, the angle of attack minimizes $\frac{C_{xp}}{C_{zm}^{3/2}}$ ("climb" angle of attack). This case is equivalent to seeking optimum speed of rotation for a geometrically defined rotor; in other words, it corresponds to the point of maximum lift efficiency on the rotor polar.

The graph in Plate IV-7-1, which illustrates Eq. (4.14) in a particular case, will help us to better understand this problem. Plate IV-8-1 gives a different representation for another family of rotors.

In practice, the reduction of drag losses is limited by structural weight considerations. In fact, we have seen that such reduction implies low tip speeds, associated with rather high values of rotor solidity, two characteristics which cost weight: an increase in solidity, and therefore of blade area, increases the weight of the rotor, while a reduction in tip speed increases the driving torque to be transmitted to the rotor, which increases the weight of the transmission system.*

This demonstrates why, although there may not be an "optimum blade angle of attack", it is still of interest to utilize high angles of attack, because for a given value of profile loss, high angles of attack permit us to use the solidity and tip speed values which will be most favorable from a structural standpoint (see Plate IV-7-1). The exact choice of the angel of attack depends on the particular case. Most often we will use a C_{z_m} as high as possible, compatible with a certain number of conditions. These conditions are: 1) to permit the application of a loading factor which will be sufficient for maneuverability (of the order of 2); 2) to avoid excessive angles of attack when the rotor is overloaded and at high altitudes; 3) to pervent tip speeds for resulting in detrimental compressibility effects; and 4) to avoid retreating-blade stall in high-speed flight (see Section 4.32).

Minimum Induced Losses

Since the preceding consideration have permitted specification of the rotor diameter, solidity and working state, the determination of minimum induced

*In the case of an anti-torque rotor configuration, it is also necessary to take into account the increased thrust that this component must provide when the tip speed is reduced.

losses will make it possible to choose the blade "plan form" and the rules governing profile pitch setting. The problem is to get as close as possible to the optimum distribution of induced velocities studied in Chapter 2. Let us recall that except near the blade root and tip this optimum distribution corresponds in practice to the law

$$V_i(\bar{r}) = cte$$

Equation (4.9) permits us to find the relations between the chord, the angle of attack and the induced velocity, which can be written

$$b\bar{l}C_z = 8\pi \frac{V_i^2}{u^2\bar{r}} \quad *$$

If the law V_i = const is imposed, the product $\bar{l}C_z$ will vary as 1/r. It goes without saying that it is desirable that C_z be essentially constant and equal to the chosen C_{z_m}. In these conditions the blade chord should vary as 1/r, and the blade pitch setting θ will vary as

$$\theta = i_m + \frac{V_i}{u\bar{r}}$$

The blade chord and pitch setting must decrease from the root to the tip of the blade. In reality, in the immediate vicinity of the blade root the optimum induced velocity tends to zero and the same is true of the blade chord.

The blades most frequently used in practice have a trapezoidal or even a rectangular shape and the twist is linear. /107

A trapezoidal blade is defined by its taper:

$$t = 1 - \frac{l_1}{l_0}$$

where l_1 is the chord for $\bar{r} = 1$ and l_0 is the chord for $\bar{r} = 0$. Plate IV-9 gives a few typical examples of distributions of induced velocity and of C_z as a function

*This formula must be corrected by the factor K, as in 4.214, if we wish to account for blade tip losses.

of the blade shape. In Plate II-4 can also be seen an example of the distribution of induced velocities over an actual rotor.

2) Case of a Jet-Driven Rotor

Suppose the drive system is characterized by a total blade tip thrust T, independent of u. This is a condition which, except in the case of rockets, has not been rigorously realized by machines actually in use.

The problem we have set ourselves is to obtain the maximum value of the ratio F_N/T, called the aerodynamic efficiency of the rotor.

Taking the relation $P_N = T \cdot u$ into account, Eq. (4.13) can be written as

$$\begin{cases} \dfrac{T}{F_N} = \dfrac{1}{\eta_i} \dfrac{V_{i_0}}{u} + \dfrac{3}{4} \dfrac{C_{xp}}{C_{z_m}} & \text{(S, i, u are the independent variables)} \\ \dfrac{T}{F_N} = \dfrac{1}{\eta_i} \sqrt{\dfrac{\sigma C_{z_m}}{12}} + \dfrac{3}{4} \dfrac{C_{xp}}{C_{z_m}} & \text{(S, i, } \sigma \text{ are the independent variables)} \end{cases} \tag{4.13'}$$

$$\left(\frac{V_{i_0}}{u}\right)^2 = \frac{\sigma C_{z_m}}{12} \tag{4.15}$$

These formulas are illustrated for particular cases in the diagrams of Plate IV-7-2 and IV-8-2. The following remarks can be made.

1) The area S occurs only as the ratio V_{i_0}/u: for a given value of this parameter, the aerodynamic efficiency of the rotor is not affected by the disk loading. The reason why this is true is that the increase is induced power as a result of reducing the area S is compensated by an equivalent increase in driving power, because $u(V_{i_0}/u = \text{const})$ is increased. Driven to the extreme, this result would /108 lead to a rotor of zero area, which is too good to be true.

We have just seen that such a reduction is accompanied by an increase in tip speed, which is limited in practice for two reasons: 1) because it is necessary to keep below the critical Mach number of the blade, and 2) because the majority of jet propulsion systems of rotors (except for ramjets and rockets) exhibit a reduction in thrust with tip speed. Since u is limited by these considerations, it is

of interest to reduce the induced drag, which is proportional to V_{i_o}/u, to decrease V_{i_o}, and therefore, in the end run, to use low disk loading. At the same time, the solidity σ will also have to be reduced (Eq. 4.15).

Let us also note that in the case of a jet rotor, structural considerations are not of great importance, because the weight of the rotor increases slowly with diameter (the solidity must decrease), and because no driving torque need be transmitted and compensated for.

2) This time, insofar as profile losses are concerned, there exists an optimum angle of attack, namely, the one which will yield maximum aerodynamic efficiency. Contrary to what happens with a mechanically driven rotor, the profile drag cannot drop below a minimum.

- It is evident that it is necessary to dimension a jet rotor in a manner different from a mechanically driven rotor. That is, solidity must be low and the tip speed as high as possible, in conformity with the restrictions already mentioned, which is exactly the opposite of what is expected for a mechanically driven rotor. On the other hand, an increase in rotor area always has a favorable effect.

The methods which will permit minimization of the induced losses are the same as those presented in the case of a mechanically driven rotor; that is, the optimum distribution of induced velocities is determined.

4.22. GROUND EFFECT. TAKEOFF LIMIT

We have seen in Chapter 2 how these factors come into play. The diagram in Plate II-12 permits us to estimate the increase in lift at a given power caused by the presence of the ground.

Let us remember that the enhancement of lift is in practice from 10 to 15%. /109
At a given weight, the reduction in required power due to the ground effect is of the same order of magnitude.

Take-Off Limit

The ground effect is of interest in that it permits the helicopter to take off without taxiing (or sliding) with a load greater than would be possible without the ground effect. In this case the take-off procedure is as follows: the machine hovers near the ground and then accelerates horizontally until climbing speed is reached. We can even go farther than this and imagine vertical take-off at a

weight greater than would be possible with flight in the ground effect. To do so it will be necessary to use the kinetic energy of the rotor for take-off and to put the machine in forward flight at a speed in which flight is possible in the stabilized operating state: this is the "jump take-off" method which is done by driving the rotor at high rpm at a low pitch before taking off.

A helicopter driven mechanically by a reciprocating engine (or by a fixed-turbine engine) is capable of only low increments in rpm and this maneuver is somewhat acrobatic: the limiting take-off weight will be the same as in flight in the ground effect (skids about 1.5 m from the ground).

On the other hand, jet or turbine helicopters are capable of large increments in rpm. In the most favorable cases (high-inertia rotors) the take-off limit can be extended to the altitude of the forward-flight ceiling (flight at minimum power).

4.23. VERTICAL CLIMB

Obviously the complete calculation can be made by means of Eqs. (4.6), (4.7) and (4.8) of Section 4.213; in practice, however, the following approximate calculation will be sufficient for low climbing speeds, since such performance is not of great importance.

Equation (4.7) can be written

$$P_N = \frac{\rho}{2} S u^3 \int_0^1 \frac{b\bar{l}}{\pi} \left(C_z \times \frac{V_i + V_a}{u\bar{r}} + C_{xp} \right) \bar{r}^3 \, d\bar{r}$$

We have seen in Section 2.1312 that V_i decreases by $-V_a/2$ when the rotor rises /assuming that the local lift remains constant (C_z const) and that V_a is small as compared with V_{i_o} $\left(\frac{V_a}{V_{i_o}} < 0.5\right)$]. Taking this relation into account, the power is written /110

$$P_N = \frac{\rho}{2} S u^3 \int_0^1 \frac{b\bar{l}}{\pi} C_{xp} \bar{r}^3 \, d\bar{r} + \frac{\rho}{2} S u^2 \int_0^1 \frac{b\bar{l}}{\pi} C_z V_{i_o} \cdot \bar{r}^2 \, d\bar{r}$$
$$+ \frac{V_a}{2} \times \frac{\rho}{2} S u^2 \int_0^1 \frac{b\bar{l}}{\pi} C_z \bar{r}^2 d\bar{r}.$$

Since the C_{xp} have the same value as in hovering (the same C_z), the first two terms represent the power required in hovering; the third is equal to $\frac{V_a}{2} F_N \simeq \frac{V_a}{2} G$ (stable climb), from which we get the relation

$$P_N(V_a) - P_N(V_a = 0) \simeq \frac{V_a}{2} \times G \qquad (4.16)$$

This relation generalizes the property stated in 2.1312 for a perfect rotor to the case of a real rotor; V_a is essentially double the value that would be calculated if the power increment were written as being devoted to accelerate a weight of G to a velocity of V_a.

Example. In the case of Plate IV-10, the vertical-climb velocity for a weight of 950 kg is

$$V_a = 2 \times \frac{164 - 145}{950} \times 75 = 3 \text{ m/s} .$$

For climbing velocities that a relatively large as compared with V_{i_o}, this calculation is optimistic. A more exact calculation will be obtained by successive approximation, calculating the induced velocity for a series of V_a-values (we will make use, e.g., of Plate II-1).

4.3. LEVEL FLIGHT

4.31. CALCULATION OF THE REQUIRED POWER

In level forward flight the balance-of-power equation is written

$$P_N = P_i + P_p + P_f$$

where P_i is the induced power, equal to $F_N \times V_i$ (see Chapter 2) and P_p is the power absorbed by blade drag. The latter consists of two terms, as will be shown. The first term comes from the drag torque M_{N_p} exerted on the rotor. The power to be furnished is ωM_{N_p}. The second term comes from a drag term $\vec{T}_x$ in the

/111

rotor plane. Its value is $\vec{V}_x \vec{T}_x$; that is, in practice it is $V_x \times T_x$.* The quantity P_f is the fuselage drag power, which is equal to $T_f V_x$ (T_f is the drag of the fuselage)*.

Calculation of the Various Terms

1) $T_f = \frac{1}{2} \rho \Sigma C_{xf} V_\infty^2$, where Σ is the mid-action of the fuselage and C_{xf} is the fuselage drap coefficient. It is advisable to increase the C_{xf}, as measured on unpowered models, by a rotor/fuselage interaction factor of the order of 1.2 and not to forget the pylon drag (including the non-streamlined parts of the rotor), which is often considerable.

2) Calculation of T_x

This factor ensues from integration of the drag forces over the blade in the velocity direction. We have

/112

$$T_x = \int_0^{2\pi} \frac{\sin\psi \, d\psi}{2\pi} \int_0^R b \frac{\rho}{2} (\omega r + V_x \sin\psi)^2 C_{xp} \rho \, dr$$

$$= \frac{1}{4} \rho C_{xp} S \sigma U^2 \mu.$$

As before, C_{xp} is deduced from the C_{zm} of the rotor $\left(\frac{3 f_N}{B^3 \sigma}\right)$**.

---

*The mechanism by which the drag terms T_x and T_f require power to be expended on the rotor is easy to understand: to compensate for these terms it is necessary to tilt the rotor forward (a propelling component; see Fig. 4.4). This makes the rotor work with a relative axial wind component V_z which, as we have seen in Chapter 2, results in an expenditure of power $F_N V_z$.

**In reality, a more exact C_{zm} is obtained by integrating the lift as a function of the azimuth and radius and by assuming that C_z varies sinusoidally, so that the aerodynamic moment on the blade is independent of the azimuth (fundamental law of flapping). The reader can verify that we than find $C_{zm} = \frac{3 f_N}{\sigma B^3 \left(1 + \frac{\mu^2}{18}\right)}$ (and not $\frac{3 f_N}{\sigma B^3 \left(1 + \frac{3}{2}\mu^2\right)}$, as many authors suggest).

Remarks

1) This calculation does not account for the drag exerted by the radial air components on the blades. To take this into account, the preceding drag is usually multiplied by a corrective factor. Let

$$T_x = 1{,}825 \times \frac{1}{4} \rho C_{xp} S \sigma u^2 \mu.$$

2) Reverse-Flow Drag

The preceding calculation is incorrect insofar as the reverse-flow circle is concerned. Not only does the drag change direction, but the reverse-flow effect of the trailing edge results in much higher C_{xp}. Therefore it is expedient to make a correction when this area exerts a noticeable effect ($\mu > 0{,}3$).

If we take $C_{xp} = 0.07$ and integrate for a rectangular blade, we find

$$\Delta T_x \text{ reverse-flow circle} = \rho \times \frac{11}{64} \left(0{,}07 + C_{xp}\right) S \sigma \mu^3 u^2;$$

in other words, we have approximately $\Delta T_x = \frac{\rho}{64} S \sigma u^2 \mu^3$.

3) Calculation of M_{Np} /113

This factor is determined in hovering by intergating the drag torques:

$$M_{Np} = \int_0^{2\pi} \frac{d\psi}{2\pi} \int_0^R \frac{\rho}{2} C_{xp} b l_{0,7} \, dr \, (\omega r + V_x \sin\psi)^2 r$$

$$= \frac{\rho}{8} S \sigma u^2 R C_{xp} (1 + \mu^2)$$

Remark

It would also be appropriate to make a correction in order to take the reverse-flow circle into account, but it is neglected because it is so small, is favorable, and is of the order of magnitude of the errors introduced by the calculation that has already been made.

4) Calculation of $P_i = F_N \times V_i$

V_i is calculated by the methods indicated in Chapter 2. For example, the diagrams in Plates II-5 or II-6 could be used.

Although a generally sufficient approximation is obtained by neglecting the effect of the axial component V_z, a more precise calculation can be made by taking this component into account, as given by the relation

$$V_z = V_x \alpha \quad \text{with} \quad \alpha = \frac{T_x + T_f}{F_N}$$

(see Fig. 4.4); balance of longitudinal forces. At high forward speed the asymptotic formula

$$V_i = \frac{F_N}{2 \rho S V_x}$$

will be sufficient. As for hovering flight, V_i must be increased by an induced loss factor (which can be taken equal to the factor used for hovering flight).

The total power is written by adding the terms which have just been calculated:

$$P_N = F_N V_i + \frac{\rho}{8} S \sigma u^3 C_{x_p} (1 + \mu^2) + V_x \left(\frac{\rho}{2} \Sigma C_{x_f} V_x^2 + 1{,}825 \frac{\rho}{4} S \sigma u^2 C_{x_p} \mu + \frac{\rho}{64} S \sigma u^2 \mu^3 \right)$$

which can also be written /114

$$\boxed{P_N = F_N V_i + \frac{\rho}{8} S \sigma u^3 C_{x_p} (1 + 4{,}65 \mu^2) + \frac{\rho}{64} S \sigma u^3 \mu^4 + \frac{\rho}{2} \Sigma C_{x_f} V_x^3} \qquad (4.17)$$

In order to illustrate this formula, a breakdown of the balance of power as a function of the velocity is given for an actual case in Plate IV-10. This diagram

permits us to determine various flight cases, for instance, minimum-power flight (point C), flight at maximum speed (point D), and flight at maximum range.

In the case of a drive system where the fuel consumed is proportional to the power developed (which is essentially the case for piston engines), the operating point is point E, which corresponds to a maximum speed/power ratio.

In fact, the desired goal is to obtain a maximum ratio of distance covered to fuel consumed; that is, to obtain a maximum ratio of speed/fuel consumed per hour, equal to speed/power times the specific fuel consumption, by dividing the two parts of the ratio by the time. If the specific fuel consumption is assumed to be constant, the condition to be met is simply the one given above. On the other hand, in the case of turbines, the specific consumption increases with power. It can be easily seen that this results in greater speed for maximum range than is consistent with the point E. All things being equal, the optimum cruising speed of a turbine helicopter is higher than that of a piston engine. In practice, the best cruising speed of such a helicopter is the maximum velocity that is consistent with the endurance of the engine, the flight stability, and the aerodynamic stall of the rotor.

4.32. THE OPTIMUM ROTOR IN FORWARD FLIGHT

Adaptation of a rotor to cruising flight conditions is determined by criteria which differ considerably from those adopted for hovering. On the one hand, the induced power represents a small fraction of the power balance, and therefore the disk loading per m^2 is only of secondary importance. In addition, insofar as /115
blade drag losses are concerned, the rules which allow the influence of the principal parameters (tip speed, mean C_z and solidity) to be estimated are the same as those for vertical flight (see Eq. 4.17). On the other hand, there is one condition to be met which may lead to a departure from the optimum with respect to performance. This is the necessity of avoiding retreating-blade stall. We have seen in 3.216 that this requires the use of C_{zm}- values lower than a limiting value, as a function of the flight mode being considered. Therefore, rotor adaptation must represent a compromise between the desire for maximum hovering efficiency (which governs the take-off weight), for good performance in cruising flight (speed and fuel expenditure per km) and correct aerodynamic functioning of the rotor.

For example, in the case of a mechanically driven rotor, the ideal would be to have a variable-speed rotor with a "slow" speed in hovering (maximum take-off weight) and a "high" speed in cruising flight (to avoid rotor stall).

This condition can be easily realized if the engine is a free-turbine engine (see Chapter 8); on the other hand, it is incompatible with the operating conditions of a piston engine or of a fixed-turbine engine, which furnishes maximum power

(used for take-off) at maximum speed. In this case, the mean blade operating angle of attack and the tip speed must be determined by allowing simultaneously for operation in hovering and in cruising flight.

4.33. METHODS FOR DETAILED ANALYSIS OF FORWARD-FLIGHT PERFORMANCE

There exist numerous methods which permit account to be taken of the various factors involved in forward-flight performance, namely, blade plan form, twist, induced velocity distribution, etc., in greater detail than in the above method. It would go beyond the scope of this course to outline them all, and therefore we refer the reader to the specialized papers: /1/, method of calculation by Tables, /7 and 8/, use of charts, and /9/, calculation by a high-speed computer.

It should be noted, however, that the additional precision obtained by these methods is often deceptive, in that some of the basic data are not well founded (C_{xp}, local induced velocities, etc.). /116

4.4.. OPTIMUM CLIMBING CONDITIONS

Here we propose to determine the conditions which will allow maximum rate of climb. This factor can obviously be found from level flight at the speed of minimum power.

Let V_m and P_m be the relative velocity and power in this flight mode. Assuming that the helicopter rises at a speed along path of V_m and that the maximum power available on the rotor shaft is P_D, we have

$$P_D = P_m + V_a \times F_N, \text{ which permits us to find } V_a.$$

Example. In the case of Plate IV-10:

$$V_a = \frac{(164 - 91) \times 75}{950} = 5{,}75 \text{ m/sec.}$$

Remark. This reasoning does not allow for the fact that an increase in the axial component of ascent (at constant total velocity) results in a loss of induced velocity (an effect which was already noted in the case of vertical climb). We can see in Plate II-6, however, that in the region being considered (V_x/V_{i_o} = 2 to 3), this effect is much weaker and can be ignored in all normal cases. We obtain a

somewhat pessimistic calculation compensating for the small increment in fuselage drag due to the less favorable angle of attack as compared with level flight (see Fig. 4.5).

In this regard, note how such behavior is different from that of an aircraft, whose trim is governed by its flight path, whereas in our case the trim of the machine remains constant with respect to the absolute axes at any speed along path. (Compare the balance of forces in Figs. 4.4 and 4.5). From this fact we can deduce the following rule, which is valid for paths not too close to the vertical.

At any given speed along path, the absolute trim of the fuselage and rotor are, in the first approximation, independent of the slope of the flight path, and consequently of the power.

This rule is no longer exact if the control surfaces of the helicopter are large. /117

4.5. INFLUENCE OF VARIOUS FACTORS ON PERFORMANCE

4.51. VARIATION IN REQUIRED POWER AS A FUNCTION OF THE TOTAL WEIGHT, THE ALTITUDE AND THE TEMPERATURE

Weight. For a given flight situation the required power obviously increases with the total weight.

In hovering, the law of variation depends on the point of matching along the rotor polar, $f_N m_N$ (see Fig. 4.2). In most cases, however, matching occurs near the point of maximum aerodynamic efficiency (f_N/m_N maximum). The formulas

$$\begin{cases} F_N = \frac{\rho}{2} S u^2 f_N \\ P_N = \frac{\rho}{2} S u^3 m_N = F_N . u . \frac{m_N}{f_N} \end{cases}$$

show (at constant speed u) that in this case the power increases in proportion to the total weight.

Thus, the influence of weight is less important than one might be tempted to believe when referring to the formula $P_{i_o} = \frac{F_N^{3/2}}{\sqrt{2\rho S}}$, which indicates that an increase in lift increase the efficiency η_s, the maximum being reached at maximum $\frac{F_N^{1/2}}{m_N}$. It is when operating at this point that the power varies as the 3/2 power of the weight, which may occur with heavy overloading or at high altitudes.

In forward flight, the weight effect is less important; it is exerted primarily on the induced power, which decreases with speed. The power is unaffected in practice by the total weight, in particular at high speeds. See the diagram in Plate IV-9, which gives the power required for two different weights.

Altitude and Temperature come into play in that they cause a variation in specific air mass. /118

Variations in ρ With Altitude and Temperature

In the lower layers of the atmosphere, ρ decreases by 10% per 1,000 m. A 10° -increase in temperature over the standard represents a variation in specific mass of 3.5%. From this circumstance we get the following rule: from the viewpoint of power required, a 10° -increase in temperature is equivalent to a 300-m increase in altitude.

Influence of Air Density on Performance

Suppose we have a situation characterized by a given weight, velocities u and V, and specific mass ρ_o.

If the specific mass is replaced by ρ_1 we obtain the same reduced operating parameters by multiplying u and V by $\sqrt{\frac{\rho_o}{\rho_1}}$; the lift, proportional to ρu^2 is preserved, while the power, proportional to ρu^3, is multiplied by $\sqrt{\frac{\rho_o}{\rho_1}}$.

On the basis of the preceding considerations, we can thus conclude that the power required by a helicopter increases by 5% per 1,000 m.

In reality, this calculation is often psssimistic, because it is assumed that the tip speed increases with altitude, which is difficult with rotors driven mechanically by an engine in which the operating mode has only a very narrow range. Therefore, in order to get acceptable performance at various altitudes, rotor have

been adapted on the ground to rather low lift-drag ratios, C_{zm}. At high altitudes, the lift-drag ratio, and consequently the rotor efficiency, increase under constant flight conditions. Thus the required power does not increase as much as indicated by the preceding calculation.

For example, for vertical-flight performance this power is often practically independent of the specific mass of the air (and therefore of the altitude and temperature).

This is due to the above-mentioned adaptation of rotors near the maximum f_N/m_N of the polar. The previously given formula

$$P_N = F_N \cdot u \frac{m_N}{f_N}$$

shows that ρ plays no part.* /119

Let us remember that in all cases the variation in required power as a function of altitude and temperature is small as compared with variations in available power.

4.52. VARIATIONS IN AVAILABLE POWER

In order to assess variations in performance, it is obviously necessary to know the variations in available power as a function of the altitude and temperature. This depends on each particular case. We will mention the most important cases.

Piston Engines (without compressors). Here the influence of altitude shows up as a 10% change in power available per 1,000 m altitude, while the temperature causes a 0.2% change per degree.

For Turbines (or, in the first approximation, thermal propulsion by a gas turbine), the characteristics vary from one type of machine to the other, since the limits depend on the maximum temperature permissible in the chamber and on the turbine (denoted by T_3). Assuming that the operating mode of the machines is

*In this case mutual compensation between the variation in induced power, which increases as ρ decreases, and the variation in drag power, which itself decreases, is evident.

constant, the following orders of magnitude can be given: altitude, 5.5 to 8.5% per 1,000 m; temperature, 0.75 to 1% per degree.

Note that the turbine is superior to the piston engine insofar as the altitude effect is concerned, whereas the opposite is true with respect to temperature.

It should be noted, however, that the power limitation of the turbine, given by T_3, is not an absolute limitation as in the case of a fully admitted piston engine. In some cases, e.g. for operation at high altitudes or in a warm atmosphere (cases which are exceptional in the life of an engine), T_3 can be exceeded without danger. Fall-off in power as a function of temperature and altitude will then be lower than indicated above.

4.53 Given below is a table which recapitulates the effects on performance of the factors which have just been studied and their order of magnitude. Obviously, the given figures should be taken as being only indicative and should not replace a precise study of performance in each particular case. /120

4.6. AUTOROTATION /121

The quality of autorotation governs the safety of the helicopter in case of engine failure. Landing in such a situation comprises two phases: 1) stabilized descent, and 2) near the ground, flare-out and flattening make it possible to touch down at low vertical and horizontal speeds.

In the first phase it is expedient to try for moderate vertical descent speeds and low-slope flight paths (permitting access to the desired landing site). This problem is exactly like gliding with an airplane, and it is sufficient to replace the wing polar by the rotor autorotation polar (see Plates II-10 and II-11).

An approximate calculation method consists in writing the power balance as in the case of climb: $V_d \times G$ = the power required in level flight at the same speed along path.

In particular, the minimum speed of descent corresponds to the velocity at minimum power in level flight:

$$V_{d\ mini} = \frac{P_m}{F_N\ (= Mg)}$$

As for climb, this procedure is not completely correct, because the variation in induced velocity as a result of descent is neglected (see Plate II-6). Thus we obtain slightly optimistic results.

		Piston engine	Turbine or thermal propulsion by turbine fluid generator
Variation in powers available as a function of	Altitude	-10% per 1,000 m	-5.5 to 8.5% per 1,000 m
	Temperature	-0.2% per °C above the normal temperature	0.75% per °C
Variation in required power for a given flight condition as a function of	Total weight	Essentially proportional to the total weight for hovering Very slight influence of high velocity	
	Altitude and temperature	Vary but slightly	
Approximate spread of the ceilings*	Hovering out of ground effect	Z_o	Z_c
	Hovering in ground effect	Z_o + 1200 m	Z_o + 1800 m
	Ceiling in forward flight	Z_o + 3500 m	Z_o + 5000 m

*No allowance has been made for compressibility and retreating-blade stall phenomena, which, if they occur, may seriously alter this arrangement.

Example: in the case of Plate IV-10:

$$V_d = \frac{91 \times 75}{950} = -7,2 \text{ m/s}$$

An experimental autorotation polar can be found in Plate IV-11 for the same machine. Let us remember the following points: 1) the minimum speed of descent is approximately one-half the vertical speed of descent, and 2) the minimum path slope is 20°, that is, a maximum negotiable horizontal distance that is 2.7 times the altitude; in practice, when there is little wind, this slope increases appreciably (30 to 45°); then the maximum negotiable horizontal distance is greater than the altitude above the ground by a factor of 1 to 2. /122

Remarks:

1) As in the case of an airplane, if all things are equal, the speed of descent varies proportionally to $\sqrt{\frac{G}{S}}$.

2) We have already mentioned that the rotor pitch must be low to permit autorotation under favorable conditions, the pitch angle having an appreciable influence on the descent conditions (see Plate II-11). An increase in pitch reduces the speed of descent as well as the rotor operating state. In practice, the acceptable pitch will be the one that will give the rotor a working state that is at least equal to the normal working state so that the pilot will have sufficient kinetic energy available when he reaches the second stage, that is, touch-down proper. The factor which characterizes the quality of the machine in the latter phase is the ratio of kinetic rotor energy available to kinetic descent energy of the machine:

$$\frac{I_p (\omega^2 - \omega_{mini}^2)}{M V_d^2}$$

This explains why even helicopters with a heavy load per m^2 can have sufficient autorotation qualities, although "they descend rapidly".

4.7. NUMERICAL DATA

Several times during the course of this chapter we have been induced to emphasize that the dimensioning of rotors results in numerous compromises; these are, on the one hand, between the various performance factors, and on the other, insofar as questions of weight, structure, bulk, production facility etc. are concerned. Therefore, it seems useful to us to terminate this chapter by showing the results we finally end up with in practice.

4.71. CHOICE OF BLADE PROFILES

The main qualities expected of the blade profiles are low C_{xp}/C_z at the operating angles of attack, high stalling angle of attack, critical Mach number sufficiently high, and low or zero C_{m_o} and stable aerodynamic center (stresses in the controls, blade flutter). /123

Remarks

1) These qualities are required at rotor Reynolds numbers which are much lower than those used for airplanes, that is, 2 to 5 x 10^6.

2) Blade rotation is without doubt the reason for the varying behavior of blade sections in a rotor and in two dimensions. In particular, stalling is influenced by the fact that the blades operate in the unsteady state and at oblique incidence over a certain portion of the disk. These problems are poorly understood, and therefore it is expedient to be prudent when applying the results of wind-tunnel tests.

The profiles usually employed are the symmetrical NACA profiles of the 230 family. Plate IV-2 gives some data on the profile characteristics of interest. Laminar profiles of series 66 are sometimes used.

NACA has also studied special laminar profiles for helicopters; these have low C_{xp} at high angles of attack (series H).

However, laminar profiles are difficult to use because they have a tendency to become nonlaminar on slight pretexts, which abound in the case of a rotor; among these are roughness and defects in fabrication, deformation during operation operation, erosion, etc. (in this regard see Plate IV-13). Moreover, except for series-H profiles, the C_{xp} of laminar profiles increases rapidly even at a relatively low angle of attack, so that they are not always attractive from the performance point of view (above all in high-speed flight). However, some of these profiles are used on occasion because of their high stall angle of attack.

The usual relative thicknesses vary between 9 and 18%.

4.72. ORDER OF MAGNITUDE OF THE PRINCIPAL STRUCTURAL AND OPERATIONAL PARAMETERS OF THE ROTOR

Rotor Disk Loading

According to the case, this parameter varies from 8 to 48 kg/m^2, but the majority of rotors are loaded between 10 and 20 kg/m^2. The present tendency is

to use heavy loading (see the graphs in Appendix I). The induced velocity over the rotor, which is a function of the disk loading, varies between 5 and 13 m/sec (6 to 10 m/sec in the majority of cases).

The Number of Blades is 2 to 6.

The plan-form of the blades is rectangular or trapizoidal. In the latter case the taper ($t = 1 - \frac{l_1}{l_0}$) is usually of the order of 0.3 to 0.4.

Twist. The trim of the blade sections decreases linearly from the root to the tip, usually between 5 an 12° (between the sections $\bar{r} = 0$ and $\bar{r} = 1$).

The solidity ($\sigma = \frac{b l_{0,7}}{\pi R}$) is from 3 to 10%.

The collective pitch ($\theta_{0,7}$) is from 6 to 12° in power-on flight and 0 to 3° in autorotation.

The tip speed (u) is between 130 and 220 m/sec. The present tendency is to use the highest values.

The meaning operating C_z of the profiles is from 0.4 to 0.6.

The coefficients f_N, m_N are (under nominal operating conditions) 50 to 150 x 10^{-4} and 3 to 12 x 10^{-4}, respectively.

The aerodynamic efficiency of the rotor (f_N/m_N) is from 12 to 15.

The lift efficiency in vertical flight (η_s) is 0.6 to 0.7.

The advanced ratio ($\mu = \frac{V}{u}$) used in cruising flight is 0.25 to 0.35.

Finally, Appendix I (Section 3) contains a table which, by way of example, gives the characteristics of three rotors having different configurations: mechanical drive by reciprocating engine, by turbine and by jet drive.

Chapter 5

STABILITY AND FLIGHT PROPERTIES

This chapter makes no claim to be a complete treatment of the flight properties of the helicopter, a subject in itself deserving of an entire course. We intend simply to bring out certain special characteristics of the helicopter from this point of view. /125

Hovering will be given special emphasis; forward flight, maneuverability and safety properties are then discussed more summarily.

5.1. HOVERING FLIGHT

5.11. QUALITATIVE STUDY

As pointed out in Chapter 2, the instability of the helicopter in hovering flight is one of the special piloting difficulties of this type of machine.

An over-simplified argument that considers the helicopter to be suspended from its rotor like a light fixture from the ceiling would seem to bear out the stability of the machine with locked-stick. But this is not at all the case, since the suspension point is not fixed in space and the rotor (and hence the resultant $\vec{F}_N$) follows the angular motion of the fuselage. Calculation (corroborated, unforunately, by experience) shows that under these conditions a helicopter without special stabilizing devices has two characteristic motions:

(1). A strongly-damped, short-period (some seconds) oscillation in trim.

(2) A coupled motion in trim and horizontal displacement, resembling a rocking motion around a point located far above the machine (see Fig. 5-1). This motion is always unstable; its period varies from 9 to 20 seconds, depending on the machine. The doubling time of the oscillations is of the order of 1/2 - 2 periods.

It has been noted that the instability is less severe with high-inertia rotors (long response time, see Chapter 3). The gyroscopic effect of the rotor then becomes noticeable and it tends to maintain its plane fixed in space irrespective of fuselage motion. The comparison with a light fixture suspended from the ceiling becomes more appropriate and its approaches (without attaining) a stable pendulum motion (see Fig. 5-2). This effect would be more pronounced still if the control plane were to be maneuvered as as always to remain horizontal. Some designers have thought to obtain this effect by the use of auxiliary rotors with response times much greater than can be given the main rotor. By a /126

suitable combination of components, positive stability can even be attained. These are the inertial stabilizers, of which there are two characteristic forms:

(1) Hiller Rotormatic (Fig. 5-4)

The figure shows that the pilot controls the auxiliary rotor, whose movement in turn cyclically controls the pitch of the main blades. The control plane of the main rotor is precisely the plane of rotation of the vanes. Since the auxiliary rotor has a long time constant, it will remain essentially fixed in space, as will the main rotor whose trim it controls.

(2) The Bell Stabilizer Bar (Fig. 5-5)

It is seen that here the control plane of the main rotor is determined by the addition of the motion of the swash-plate and that of the gyroscopic bar. The stabilizing effect with locked-stick is comparable to that of the previous example. (The damping device mounted on the bar serves as the "erector"; in the stabilized position the plane of rotation of the bar is perpendicular to the rotor shaft.)

Unfortunately the locked-stick stability cannot be the sole criterion of the quality of flight at a fixed setting; objections are all too easy to make.

— It is claimed by some that the stability makes the machine awkward to control and that it would be better to have a machine that was unstable but easily controlled.

— Others say that if the stability criterion is applied to walking or to riding a bicycle it is found that these operations are more difficult than piloting any helicopter - which is not true (or at least so say the pilots...).

On reflection it appeared that these difficulties stem from the fact that the behavior of the helicopter is studied without considering its close associate — the pilot. This is why some years ago in France a new investigative technique was devised which attempts to define what might be called the "pilotability" if the word were not so unpalatable. The general problem can be stated as follows: /127
To investigate the dynamic properties permitting optimum control of a helicopter by a human operator.

In what follows we shall study the properties of a helicopter in hovering flight from the two viewpoints of inherent stability with locked-stick and inherent "pilotability".

5.12. CHARACTERISTIC MOTION OF A HELICOPTER IN HOVERING FLIGHT

As in all analagous situations, this is studied by the method of small displacements around the equilibrium position. The system possesses six degrees of freedom (linear and angular displacements referred to the three axes), but the complete calculation shows that the following simplifications can be made without changing the results significantly:

— The vertical displacement is negligible.

— Roll and pitch motions are not coupled.

The analysis then reduces to investigating the displacement of the fuselage in two degrees of freedom – horizontal displacement of the center of gravity and angular motion.

In order to set up the equation we must know the forces exerted by the rotor*, which may be best understood by inspecting Fig. 5-3.

The reactions of a fixed-blade rotor to linear and angular displacements of the fuselage are shown schematically in Fig. 5-3,a. We have seen in Chapter 4 that a relative component of air motion in the rotor plane creates a drag T_x opposed to the motion and proportional to the velocity. Figure 5-3,a, shows that this gives rise to (weak) damping in each degree of freedom, and also to a coupling effect (generally called "cross-derivatives" in stability theory).

Let us now consider the hinged-blade rotor (Fig. 5-3,b). The effect of motion of the rotor plane must be added to that of the drag T_x. We have seen in Chapter 3 that a hinged-blade rotor tilts backward from the motion under the effect of forward flight or angular rotation. Figure 5-3,b, shows that this phenomenon strongly enhances the damping and the coupling.

Setting Up the Equation of Motion

/128

This is done in symbolic form in Appendix III.4.

The characteristic equation is obtained by substituting r for the symbolic operator p in the first member of Eq. II-4.5 and equating the expression obtained

*The aerodynamic forces on the fuselage arising from movements of the machine are negligible since they are proportional to the square of the velocities, which averages out to zero.

to zero. From this we find

$$z^4 \frac{\tau_0}{\lambda_c^2} + z^3 \left[\frac{1}{\lambda_c^2} + \tau_0 \frac{T\mu}{F_N} \left(\frac{\lambda_q}{\lambda_c^2} + \frac{\rho_h}{\omega R} \right) \right] + z^2 \left[\tau_0 + \left(A\mu + \frac{T\mu}{F_N} \right) \left(\frac{\lambda_q}{\lambda_c^2} + \frac{\rho_h}{\omega R} \right) \right]$$

$$+ z \lambda_g \frac{T\mu}{F_N} \tau_0 + \lambda_g \left(A\mu + \frac{T\mu}{F_N} \right) = 0 \qquad (5.1)$$

(See the symbol definitions in Appendix II. 4).

The equation is a quartic and its solution brings out the two characteristic motions pointed out in 5.11:

— A rapidly damped oscillation

— A diverging oscillation of long period.

Simplified Analysis of the Stability of the Characteristic Motions

If the coefficients of Eq. 5-1 are assigned numerical values it is seen that the equation can be replaced by a cubic equation for the long-period characteristic motion:

$$z^3 + z^2 \tau_0 \lambda_c^2 + z \tau_0 \lambda_c^2 \lambda_g \frac{T\mu}{F_N} + \lambda_g \lambda_c^2 \left(A\mu + \frac{T\mu}{F_N} \right) = 0 \qquad (5\text{-}2)$$

of the form

$$z^3 + A z^2 + B z + C = 0$$

Such an equation is known to have stable roots if the following conditions (Routh conditions) are met:

$$A > 0 \quad , \quad B > 0, \quad C > 0 \quad , \quad AB - C > 0$$

In our case the first three conditions are met but the fourth is not

$$\lambda_g \lambda_c^2 \left[\frac{T\mu}{F_N} \left(\tau_o^2 \lambda_c^2 - 1 \right) - A\mu \right] > 0$$

As a matter of fact, with nominal values of τ_o and λ_c the first term in the paranthesis is negative (and, in any case, its absolute value is clearly less than that of $A\mu$). /129

This condition brings out the factors that influence stability:

— The term $A\mu$, which represents the rotor tilt under the effect of the horizontal displacement velocity, is the prime cause of the instability.

— Large blade inertia (τ_o large) and low fuselage inertia (λ_g^2 large), on the other hand, decreases the instability. Theoretically, stability can even be attained by assigning appropriate values to these parameters (values, however, not attainable in practice except by the artifice of auxiliary rotors, discussed in 5.11).

Remarks:

(1). In stability studies a system having static and dynamic stability is often discussed. It is useful to dwell a bit on the meaning of these terms.

Dynamic stability means that all characteristic motions are stable - that is, all roots of the characteristic equation have negative real parts. Let alone or subjected to transient perturbations the system will tend not to be dislodged from its equilibrium position. In the last analysis this is what counts from a practical viewpoint.

The concept of static stability is more subtle. For a system with a single degree of freedom there is no ambiguity: The condition of static stability is one of the two conditions to be met in order that the equation

$$z^2 + Az + B = 0$$

will have stable roots: $B > 0$.

As easily seen, the name "static stability" stems from the fact that this condition is equivalent to the existence in the system of a restoring force proportional to displacement.

The definition is less clear for a system having many degrees of freedom. The condition that the constant term in the characteristic equation be positive /130
is still one of the necessary conditions for dynamic stability*, but this condition is not equivalent, as before, to the existence of restoring forces proportional to displacements in the various degrees of freedom. This explains why the term "static stability" is used in two different senses.

1st Definition: The constant term in the characteristic equation is positive. This definition is the only one having a precise mathematical meaning from the standpoint of stability. For this reason it is tending to come into general use.

2nd Definition: The existence of restoring forces proportional to displacements in one or more degrees of freedom (static stability of trim, for example).

In all rigor, dynamic stability thus defined yields information only as to the sign of the "force derivatives" which appear in the characteristic equation, and does not permit drawing firm conclusions regarding the dynamic stability**. One can say only that dynamic stability will be favored by the existence of a positive static stability in each degree of freedom.

To conform to established usage and by reason of the simplification of language it allows we shall henceforth always use the second definition.

(2) As we have seen, the term causing the instability is the quantity $\lambda_g \lambda_c^2 A\mu$, which is proportional to $(h + h_f) A\mu$. This term corresponds to a "cross-derivative" which seems a priori to have been "tailor-made" by bringing about a bucking motion of the fuselage and consequently the appearance of a decceleration term under the effect of the horizontal displacement velocity (see Figs. 5-1 and 5-3). Calculation shows that this is not so and that it is in reality a destabilization effect.

(3) Motional inertia can be attained for $\lambda_c^2 = 0$, that is $h + h_f = 0$ (the thrust center of the rotor coincides with the center of gravity of the machine). Apart

---

*The Routh conditions.

**Note especially that these pseudo-conditions of static stability depend on the (arbitrary) choice of independent variables describing the motion of the system.

from the technical difficulties it implies, this arrangement has the disadvantage of making it impossible to control the machine by cyclic control of the rotor. However, it has been used in certain machines of special design (flying platforms, for example). What has been said above satisfactorily explains, contrary to what "intuition" may indicate, that placement of the rotor below the machine is not necessarily catastrophic from the stability viewpoint.

5.13. PRACTICAL CRITERIA OF THE QUALITY OF HOVERING FLIGHT /131

As we suggested at the beginning of this study, the stability proper of a helicopter is not the most important quality of consider. What should be sought for is to characterize its controllability - ease of stabilization of the one hand, and handling (or the way the machine responds to piloting commands) on the other. This pilotage capacity is estimated using criteria of empirical origin. We shall cite the "handling criterion" used in France by the CEV.

The response in trim of a helicopter to an echelon stick movement has the appearance shown in Fig. 5-6. The angular velocity passes through a maximum 1 - 2 seconds after application of force to the stick.

Experience leads to requiring - at least for light- and medium- helicopters - that this maximum angular velocity be 8 - 10° per second for a stick movement of 10% of its total travel.

Below 6° the machine is too "soft" (handling inadequate).

Above 12° it is too "touchy" (stabilization difficult).

Moreover, the "coupling" of the motions must not be excessive (by coupling is meant the motion induced on one axis by a control displacement along another axis - see, as an example, Fig. 5-6). A coupling of 30% for angular velocities appears to be a maximum that should not be exceeded.

5.14. STUDY OF LIGHT QUALITY BY HARMONIC ANALYSIS

Criteria similar to that expressed in the last section are at bottom simply the conditions imposed on the helicopter dynamics so that it will be easily controllable by the pilot. It is therefore normal to hope to come to a deeper understanding of the subject by using the method of harmonics, which permits extracting all desired information regarding the dynamics of any mechanical system.

We have set down the main results obtained using this method in an AGARD report, to which we refer for detailed study (Study Report CEV No. 197/E).

PRECEDING PAGE BLANK NOT FILMED.

Examination of These Curves Elicits the Following Remarks:

(1) The prominent maximum of the amplitudes corresponds to the characteristic unstable period whose properties can be determined from the diagram by the classical methods of harmonic analysis.

(2) In the range of periods from 1 - 5 seconds, which, as we shall see later is the useful range to be considered for piloting, the curve of $\bar{A}_\gamma$ follows the curve labeled V, the response of the helicopter with very much simplified dynamics - a flywheel articulated at the center of gravity G and subject to the action of an inertia-free rotor (lift applied without delay and perpendicularly to the control plane (Fig. 5.7)). At these frequencies the helicopter thus behaves, to a first approximation, like a flywheel whose acceleration is commanded by the pilot (however, there are important differences as regards the phases). /133

(3) Comparison of Plates V.3.1 and V.3.2 brings out a well-known property of helicopters. Rapid stick movements result principally in changes in trim without marked horizontal displacement. On the other hand, slow movements give rise to horizontal displacements with slight variations in trim.

Let us now examine Plate V-4, which points up the two decisive factors in the dynamic behavior of the helicopter - the time constant of the rotor and the inertia of the fuselage.

Plate V-4.1 shows the response in trim of a machine not differing essentially from helicopter B except for a much greater rotor time constant (0.15 second instead of 0.05 second). This is the jet-helicopter S 0 1 120, whose blades are weighted at their tips by the jet-nozzles. For purpose of comparison, the curve for helicopter B has been dotted in on the diagram. The difference is seen to be considerable. The characteristic period is much increased, 15 seconds rather than 9, the amplitudes are much lower in the pilotage frequency band and the phase is clearly increased.

The roll and pitch responses for the same machine (S 0 1 120) are compared in Pelate V-4.2. The dynamics are not different except for the disparity in fuselag inertias around the two axes (about 1 to 2.5). The characteristic period of motion is seen to be little affected. A more accurate comparison shows that the pitch instability is greater.

Before concluding this section we call attention to the simplified Eq. III.4.7 of Appendix III.4,

$$\gamma\left(\frac{p^2}{\lambda_c^2}+\frac{\tau_0 p}{1+\tau_0 p}\right)=\frac{\delta_p}{1+\tau_0 p}$$

which shows that in the pilotage frequency range, only τ_0 and λ_c^2 $\left[= \frac{G(h+h_F)}{I}\right]$ enter.

The properties just pointed out regarding the role of τ_0 and I are again found on using the graph of Plate V-2. /134

We shall reiterate once again the essential point that even a slight modification of the time constant of the rotor has important consequences for the response curve (particularly in roll).

5.142. TRANSFER FUNCTION OF THE PILOT

It would take too long here to dwell on the considerations that lead to a choice of this transfer function. We shall merely state that it complies with the following considerations:

(1) Simple in analytical form.

(2) The numerical values introduced into it are based on physiological experiments made in analogue control studies.

(3) It does not purport to represent the exact behavior of the pilot, but does serve for intercomparison of machines from the viewpoint of ease of piloting.

We have assumed a tangible response to the angular deviation observed, described by a delay time τ_r, a time constant τ_{op} and a gain R_p (see Fig. 5-8). We have taken $\tau_r = 0.3$ second, $\tau_{op} = 0.1$ second and R_p to be the gain between the control plane and the stick (the pilot gain itself is equal to unity).

This function is written symbolically as

$$\frac{\delta_p}{\tau_r - \tau} = R_p F_p = \frac{R_p e^{-\tau_r p}}{1 + \tau_{op} p}$$

5.143. THE BEHAVIOR OF THE HELICOPTER-PILOT SYSTEM

This is studied as a closed-loop system. The most familiar method is to pilot the Nyquist curve in the complex plane, replacing R_p, F_p and F_γ by pure imaginary values of p.

The plot of this curve for helicopter B has the appearance shown in Plate V-5.1. The portion of interest from the viewpoint of stability is seen to be the region in the vicinity of the point -1, that is, the range of periods from 1 - 5 seconds. The inverse criterion indicates that the system is unstable (the point -1 remains to the right when the curve is traversed in the sense of increasing frequency). /135

Plate V-5.2, the analagous curve for an airplane, given as a comparison, brings out the causes of the piloting difficulty of the helicopter. Sizeable variations in gain and phase (delays) can be tolerated by the airplane without compromising stability*. The helicopter, on the other hand, is critical in this respect.

We shall now look into what must be done to obtain satisfactory control. In applying the considerations developed in the last section, two approaches are apparent: (1) reduce the gain, and (2) advance the phase.

Each of these methods breaks down into two categories, depending on whether it is a question of pilot response or machine response.

We shall examine the possibilities of using these two methods in turn, first as applied to the pilot (drive) and then to the machine (improvement in flight properties).

Pilot Training

(1) Gain Reduction

Piloting must be accomplished with small movements. The mistake of over-reacting made by beginning pilots is well known - this is called "overcontrol" in the Anglo-Saxon literature, and was the cause of many helicopter crashes during the "Heroic Age" of the helicopter.

A method of piloting based solely on gain reduction would present a grave disadvantage; by compelling very slight hand movements it would prejudice the precision of piloting. It should therefore by combined with the next method.

(2) Phase Advance

/136

A first approach is to reduce the sources of delay τ_r and τ_{op} to the minimum.

*Although in the example selected the airplane by itself is also unstable (spin instability).

This approach is quickly limited by the properties of the human machine. It is possible to impose constants somewhat lower than those taken as a basis, but the attention demanded, and the resulting fatigue, are substantially increased.

One solution remain - to train the pilot. Despite what it may seem, this is not a platitude, since we shall show that the methods of control taught to student-polots have as their object the inculcation of a type of response characterized by a marked advance in phase.

It is in fact easy to observe that the reaction of a pilot to a control stimulus is of the "counter-movement" type (Fig. 5.9).

A response of this type corresponds to a transfer function of the form

$$K \times \frac{1 + a\tau_1 p}{1 + \tau_1 p + 1 p^2}$$

with $a \gg 1$.

It is now easy to see that this function yields a phase advance.

Another way of stating this is to say that the pilot reacts not only to γ, but also to its serivatives, $\dot{\gamma}$ and $\ddot{\gamma}$, in particular. This is shown by converting the above function into an expansion in p:

$$\gamma (K_0 + K_1 p + K_2 p^2 + \ldots)$$

And this leads to a new physical interpretation. The expression $K_0 \gamma(t) + K_1 \dot{\gamma}(t) + K_2 \ddot{\gamma}(t)$ can be considered to be the Taylor series representation of $\gamma(t)$ at time $t + \Delta t$. Thus the various delays introduced into the response are compensated by an advance that is obtained by predicting what the error would be at time $t + \Delta t$.

Improvement of the Helicopter

(1) Gain Reduction

One can conceive of modifying the kinematics linking the swash-plate and

stick so as to improve stick action. This method is actually used and can bring about some improvement, but it is soon limited by the requirement for maintaining adequate maneuverability under all flight circumstances (minimum cyclic variation to be established for total stick travel). /137

Thereis one other way to realize the same effect - to arrange for a gain reduction of F_γ in the useful range. One method that is effective is to increase the response time of the rotor, for example by increasing the blade weight. Comparison of the properties of the "classical" helicopter B and the SO 1 120 clearly shows this effect.

We have already pointed out the much lower gain of the SO 1 120 in the high frequency range attributable to the masses at the blade tips (see Plate V-4). The resulting improvement from the viewpoint of piloting is brought out by comparing Plates V-5.1 and V-5.3, which show the critical curves in roll for helicopter B and the SO 1 120, respectively.

The gain on the real axis is seen to be a factor of three smaller for the SO 1 120, which makes the system stable. We infer from this that the SO 1 120 is easier to pilot than a "classical" helicopter, which is borne out by experience.

It will be noted that the gain reduction is accompanied by a perceptible phase advance, which is also favorable.

(2) Phase Advance

We have just seen that this effect can be used by increasing the response time of the rotor. Another way is to use stabilizers.

Compare the two critical curves of Plate V-6; the curves refer to the same machine (C), without stabilizer (Plate V-6.1) and with a gyroscopic stabilizer (Plate V-6.2). We see that the presence of the stabilizer shows up as some reduction in gain, but primarily as a strong phase advance in the pilotage frequency range. Without going into the details of the methematical analysis, this is convincingly demonstrated by the fact that the gyroscopic stabilizer, by at first opposing the motion commanded by the stick, produces a cyclic control of counter-motion similar to that shown in Fig. 5-9.

As seen, the method of analysis used here leads to evaluating stabilizer systems by new criteria. We are no longer primarily interested in the locked-stick stability of the machine but in the degree to which the device is a phase advancer in the pilotage frequency band. This explains the disappointing results sometimes obtained with stabilizers that are otherwise effective - although matched to the helicopter characteristics they were not adapted to those of the pilot.

The study we have just made was intended primarily to bring out the various phenomēna that enter into piloting a helicopter. /138

We shall conclude this section with some thoughts on the practical application of the method of harmonics.

The critical curves we have established are, in the final analysis, merely a convenient way to bring out the portion of the helicopter transfer function important to pilotage. From this point of view the arbitrary nature of the transfer function of the pilot is no longer objectionable. In particular, the fact that the critical curve has an unstable configuration should not force the conclusion that it is impossible to pilot the machine. The human pilot will simply have to show himself to be more versatile than his mathematical caricature; examination of the critical curve gives an appreciation of this degree of skill and, therefore, the piloting difficulty in comparison with machines taken as reference*. One can hope that when more significant practical experience is acquired it will be possible to define precisely the conditions to be met by the critical curve in order for a helicopter to be satisfactory.

5.2. FORWARD FLIGHT

The behavior of the helicopter is forward flight approaches that of the airplane - but a medicore airplane.

Yaw and roll stability are assured on "normal" machines. On the other hand, the pitch instability characteristic of hovering flight disappears or diminishes above some flight speed, to reappear and grow larger at high spees.

At druising speeds one seeks to obtain, if not a positive stability, an instability that is at least easily controllable. A typical example of the characteristic motion is shown in Fig. 5-10. The motion is similar to the longitudinal hunting of an airplane.

What has just been said explains why prolonged piloting of an helicopter is tiring and why the practice of blind flying is tricky.

5.21. STUDY OF STABILITY IN FORWARD FLIGHT

Theoretical analysis of the behavior of the helicopter in forward flight is

*Note that case of pilotage depends on factors that do not appear in the critical curve, such as the visibility afforded the pilot, force required on the controls, etc... It is advisable to consider these factors when comparing two machines.

difficult by reason of the poorly-known factors that enter, such as aerodynamic effects on the fuselage, the interaction of the rotor slipstream and the control surfaces and the coupling between all motions. We shall limit ourselves here to giving a qualitative analysis.

Yaw Stability

Yaw stability is generally good for helicopters equipped with an anti-torque propellor (see 2.2). The stabilizing action of this device is sometimes supplemented with that of a fin. The other configurations are less favorable and they must be provided with rather extensive systems of control surfaces. We shall come back later to this question of control surfaces and the special case of the double-rotor in tendem.

Pitch Stability

We shall first examine the forces applied to the fuselage by the rotor a consequence of perturbations to flight equilibrium such as changes in horizontal or vertical velocity or variations in trim.

In this connection we shall speak of "static stability (or instability)" with respect to the various degrees of freedom, keeping in mind as was stressed in 5.12 that this does not have a precise meaning in terms of the motional stability of the ensemble. One can only say that static instability in the direction of a degree of freedom is a factor unfavorable to the stability of the characteristic motion.

(1) The Helicopter Possesses Static Stability in Level Flight

Let us imagine a random increase in flight speed V. The rotor will tilt backward in proportion to the velocity differential, and this will introduce a drag component that tends to slow the machine (see Fig. 5-11, a).

(2) The Helicopter Possesses Static Stability in Vertical Flight

Suppose the helicopter takes an an upware velocity V_z; the angle of attack of the blades is decreased and, consequently, so in the lift. A vertical force proportional to V_z and directed downward appears to counteract the motion (see Fig. 5-11, b).

(3) A helicopter without a system of control surfaces is statically unstable in trim.

Suppose the rotor tilts. The axial flow across the rotor decreases which, with constant pitch, increases the lift and accentuates the flapping a_1 (see the flapping equations in Appendix III.2). These two factors create a destabilization moment around the center of gravity (see Fig. 5-11, c).

Note that a rotor mounted on a fixed support is stable in trim, contrary to what is sometimes stated. It is the ensemble of rotor and fuselage that is not stable. This phenomenon is comparable to the unstable behavior of an airplane that is aerodynamically centered too for to the rear. Just as in this case, it can be remedied by a horizontal control surface to produce the stabilizing static restoring forces and damping (see (Fig. 5-12). /140

In fact, this is essentially what must be done to improve the behavior of a helicopter at cruising speed (in yaw and pitch).

However, the difficulties often encountered in obtaining satisfactory results (fuselage slipstream, interaction of the main rotor) have been pointed out in Chapter 2.

On examination of Fig. 5-12 we also note that while the static stability effect of a system of control surfaces is proportional to L, its damping effect is proportional to L^2 (L is the distance of the surface from the center of gravity). This is why short-tailed machines should have substantial horizontal and vertical surfaces (see the examples of Figs. 1-17 and 1-21).

The Special Case of Double-Rotors in Tandem.

This type of helicopter poses delicate problems with regard to its forward flight properties. Two unfavorable factors enter:

(1) Interaction of the forward- and rear- rotors, which increases the pitch instability. The effect is reduced by elevating the rear rotor.

(2) The shape of the fuselage is like the hull of a dirigible, which is known to be unstable in a wind since the center of thrust of the aerodynamic forces is located in front of its aft extremity (see Course in Aerodynamics).

To insure satisfactory stability in yaw and pitch it will therefore be necessary to equip this type helicopter with rather extensive control surfaces.

Remarks:

(1) The rotor design affects the forward flight stability. Favorable (or unfavorable) effects can be obtained with special kinematic configurations of the rotor attachment, such as the non-flutter coupling (k-link, see Section 3.2133) or the pitch-coning coupling, which modifies the "force derivatives" of the rotor.

(2) Apart from flight speed, two other factors have considerable effect on the longitudinal stability: the altitude (unfavorable effect) and the slope of the flight path (instability generally stronger in ascent than during descent at the same speed).

(3) The stability may be further impaired by carrying large bodies or external loads on the fuselage such as litters, packing creates, floats... (not to mention appurtenances arranged for by the owner such as advertising placards, booms, etc.). In some cases* the flight properties can become dangerous and require a reduction in flight speed. /141

5.22. PRACTICAL CRITERIA FOR THE QUALITY OF FORWARD FLIGHT

To be judged acceptable a helicopter must meet a certain number of criteria at normal operational speeds. We shall dite the main ones of these.

(1) In case of dynamic instability, the period and the time for reducing the amplitudes by a factor of two must be long enough to permit easy correction (minimum of the order of 10 seconds). Figure 5-10 shows an example of a ma chine judged to be satisfactory.

(2) The slope of the stick-displacement curve as a function of velocity must be positive for reasons of piloting ease, but its sign is not necessarily linked to the positive- or negative- nature of the static stability as it is with the airplane**. Moreover, this condition is difficult to meet over the entire speed range. Control surfaces are important here.

(3) Tests made in the U.S.A. have shown that ease of handling in pitch is associated with the shape of the curve representing the development of the normal

---

*However in other cases the stability is clearly improved, to the consternation of the "experts".

**Yet one can show that this is true for certain configurations - the "classical" single-rotor, for example.

acceleration following a deep-stick movement. The machine is deemed acceptable if, for echelon stick movement of about 10% of the total stick travel, the curve becomes concave after less than 2 seconds (see Fig. 5-13).

5.3. MANEUVERABILITY

This quality describes the ease and safety with which the evolutions for which the craft was designed can be made. We shall cite the main characteristics of the many that are jointly considered in defining this complicated concept: the concept of "handling" which we have already examined and shall not go over again, and the maximum load factor attainable by the machine.

This depends in part on the design conditions of the machine, but also on the /142
difference between the maximum C_z of the blade sections and their normal operating C_z. A load factor of 2 is usually considered to cover most practical requirements. We note in this regard that helicopters take on high accelerations with difficulty, by reason of the "transparency" of the rotor, and that the factor 2 is obtained only by "searching for it", by a joint maneuver of collective pitch and blade chord.

Action of the Controls

With respect to their limit-stops and over the entire useable range, the controls shouls have a position that permits adequate maneuvering margin (generally fixed at about 10% of the total flapping).

Cyclic Pitch Control: Its flapping leads to defining the acceptable margins of trim compensation (longitudinally and laterally). As an indication, the total cyclic amplitude variation for a single-rotor is of the order of 15-20° longitudinally and 8-10° laterally.

Collective Pitch Control. Its action should be such that the low limit-stop permits a satisfactorily stabilized autorotation and the high limit-stop allows adequate damping of touchdown impact during an unpowered landing. Example: low pitch, 3°; high pitch, 18°.

Yaw Control: Hovering flight is the most critical condition with respect to yaw control. Stabilization of the machine in all headings with a wind of minimum intensity (30 km/hr, for example) is usually required.

Forces in the Controls

The reactions in the control will obviously have an effect on the ease of piloting. We have seen the origin of these forces in Chapter 3 (Section 3.32).

These forces must be easily overcome by the pilot in every case. For flights of long duration, in addition, the reactions of the cyclic- and collective-pitch controls are required to be zero (or at least very small). This stipulation leads to the use of various devices that will be discussed in Chapter 9. We mention here that in cargo helicopters the forces transmitted to the controls can become excessive and require the installation of servo-control. /143

5.4. IMPROVEMENT OF FLIGHT CHARACTERISTICS BY AUXILIARY ARRANGEMENTS

Many arrangements have been tried or proposed to facilitate the pilot's taks, and certain of these are already in general use.

— Inertial stabilizers, of which two examples were given at the beginning of this chapter.

— Automatic Pilots, which are installed on machines intended for flights of long duration, blind flying or missions requiring precise stabilization.

— Servo-Dampers. Similar arrangements installed on the controls of certain high-speed aircraft have been tested with success. Their function in acting in parallel with the pilot is to confer artificially to the machine a good stability on its three axes.

5.5. SAFETY LIMITS

The mode of use of a helicopter should be fixed to avoid the appearance of circumstances that comprise safety. We shall pass over the limitations set by structural considerations to bring out those related to the flight behavior of the machine.

5.51. MAXIMUM SPEED

The maximum authorized speed is fixed with regard to dangerous phenomena that may be produced if it is exceeded: excessive instability, especially longitudinal, and retreating blade stall, causing vibrations, stresses in the control and possible loss of control.

5.52. VORTEX RINGS

We saw in Chapter 2 that during descent at low vertical and horizontal speeds the rotor has a particular mode of operation called "vortex-ring regime". This regime is characterized by the impossibility of obtaining a stabilized rate of descent and a partial loss of cyclic control. Moreover, the pilot may have difficulty in arresting the descent rapidly despite a major application of power ("power-settling"). One pulls out of this by increasing the speed along path.

5.53. THE "DEAD MAN'S ZONE" /144

This macabre term denotes the limited zone in an altitude-speed diagram where operation is not recommended under pain - in case of engine failure - of arriving at the ground with a very high touchdown velocity. This diagram has the shape shown in Fig. 5-14.

In the case of helicopters having a large reserve a kinetic energy in the rotor (or several rotors) this zone may be very much reduced or even disappear*.

*The Djinn helicopter is an example of this.

Chapter 6

SOME "PITFALLS" OF THE HELICOPTER /145

Some special problems of helicopters are grouped together for study under this heading. We have culled out those problems that are met with most frequently or whose nature is such as to influence the machine design.

6.1. VIBRATIONS

It was shown in Chapter 3 that the rotor gives rise to a host of alternating, low-frequency forces that are transmitted to the fuselage and controls. This made veritable "Black Marias" of the earliest helicopters. The situation has improved somewhat since then, but the problem of vibration remains an important one for the helicopter, as testified to by the plethora of pilot's cant on this subject. (Unfortunately, propriety prevents us from citing the most picturesque examples ...)

In what follows we shall study only the vibrations attributable to the rotor and pass over those of more conventional origin (engine and transmission).

In the final analysis the vibration level at some point of the helicopter depends basically on three categories of phenomena, which we shall take up in order:

(1) The intensity of the alternating forces appearing on the rotor.

(2) The transmission of exciting forces to the fuselage or to certain components: This is the suspension problem.

(3) Possible amplification of vibrations by structural resonances.

6.11. THE ROTOR AS A SOURCE OF ALTERNATING FORCES

The first and obvious thing to do is to eliminate or attenuate possible vibrations at the source. In Chapter 3 (Section 3.312) we have seen the mechanism by which alternating excitations are created on the rotor and controls. Let us recall the important facts: /146

(1) The intensity of the alternating forces applied to the rotor obviously depends on the flight mode. It is particularly high for high speeds and in the transition zone. We add that the level of air turbulence also has a marked effect.

(2) A well-balanced rotor transmits only vibrations whose frequency is a multiple of the number of blades. If vibrations of different frequency appear it is because the blades are not identical. In practice this is always to some extent the case and the consequences for vibration level can be substantial. Therefore we cannot insist too strongly on the importance of attaining - and maintaining in service - an identity of blades* as perfect as possible with respect to aerodynamics and masses. In Chapter 9 we shall see what means are adopted to accomplish this.

6.12. SUSPENSIONS

With the superficial vibrations eleminated, the vibrations inherent in the operation of the rotor remain to the dealt with. An attempt can be made to filter them by appropriate elastic arrangements:

— Damping at the fuselage level (for comfort and protection of the airframe) by elastic suspension of the rotor.

— Damping at the level of sensitive components (radio, on-board instruments and expecially the instrument -flight panel) by elastic suspension of these units.

The efficiency in these two cases is defined by the transmission coefficient:

— In the first case, the ratio of the amplitude of the forces transmitted to the fuselage to the amplitude of the forces applied to the rotor.

— The ratio of the amplitudes of the displacements or accelerations of the suspended unit of the amplitudes of the fuselage displacements or accelerations at the point in question.

If the mass of the suspended items (rotor, accessories) can be considered to be small compared to the mass of the fuselage, the transmission curves as a function of frequency are as shown in Plate VI-1 (second-order system described by a mass m, a spring of stiffness K and a linear damper with coefficient C). Examination of these curves is very instractive:

(1) In order that the remedy not be worse than the disease, the natural frequency of the suspension should be somewhat lower than the lowest of the frequencies to be filtered: $\Omega_n < 0,7\,\Omega$. Otherwise the suspension will amplify /147

*The identity must of course also obtain for the components attached to the blades: drag dampers, distributor cables, etc.

rather than damp the vibrations (resonance phenomenon). If this condition cannot be met the best results are obtained with a rigid mounting ($\Omega_n \gg \Omega$).

(2) The presence of dampers on the suspension is deterimental (unless the suspension is poorly adapted, in which case they prevent it from being catastrophic).

These considerations point up the special difficulty in designing suspensions for the helicopter: The vibrations to be filtered are low-frequency (4 - 15 cycles) and, as we have just seen, to be effective the suspension should have a characteristic frequency that is lower still. One is thus led to use very weak suspensions which are subject to large motional amplitudes, which entails serious mechanical difficulties, especially for the rotor suspension.

In addition, as we shall see in the next section, softening the rotor suspension goes contrary to the elimination of the ground resonance regime outside its effective zone. This is why it is usually preferred to abandon the weak suspension and to mount rotors of more than two blades with lag hinges very rigidly onto the fuselage.

For the double-blades the situation is something else. First, we have seen in Chapter 3 that they transmit much more severe vibration than do other rotors (frequencies producing the drag variations in the ratio of 2 to 1). It is absolutely necessary to filter these (horizontal) vibrations. Second, the double-blades are not usually provided with lag axes (see-saw mounted on the universal, see Chapter 9) so that instability on the ground is of no concern. Therefore the double-blades are commonly equipped with a flexible suspension to filter the frequency 2.

This axiom of gyro-aviation (which one must know how to interpret) stems from these considerations:

— Weak suspension for rigid rotor (in drag).

— Rigid suspension for flexible rotor (in drag).

The position adopted is usually the same regarding the suspension of sensitive units: Rigid mounting unless absolutely necessary. Instrument pannels in particular are usually mounted rigidly. A mounting weak enough to filter the high-frequency vibrations (engine and transmission) and rigid enough not to amplify the low-frequency vibrations (rotor) is used in certain cases.

Remark:

The blades themselves are a dynamic system capable of transmitting -

attenuated or amplified - the alternating force inputs they receive from the air. They can be considered simply in analogy with the classical example of the pendulum subjected to a shock. The shock is transmitted to the axis with a greater or less intensity according to the location of its point of application with respect to the center of percussion of the system (if the forces are applied at this point they are entirely filtered out). /148

A blade subject to periodic vertical and horizontal forces is comparable to this - although the mathematical theory is quite complicated*. We shall present only the main features that significantly affect the force levels transmitted to the hub: Natural frequency of lag, distribution of masses over the span, characteristic deformation modes (vertically and in torsion).

6.13. PENDULUM DAMPERS

To suppress or attenuate vibrations in the controls, pendulum dampers consisting of a spring-mass system (Fig. 6.1a) are sometimes used. In view of the incorrect explanations of the operation of this system extant, although the theory is classical, it may be appropriate to dwell briefly on this.

Let us set up the equations in the most simple form (Fig. 6.1,b).

Suppose a mass M to be subjected to an alternating force

$$F = F_0 \cos \Omega t$$

It is proposed to eliminate the resulting vibrations byinserting a mass-spring system coupled to M, as shown in the figure. (For the intended application, M represents the equivalent mass of the control gear and the mass-spring system is the pendulum damper.)

The equations of motion are written as

$$\begin{cases} M X'' - K x = F_0 \cos \Omega t \\ m (X'' + x'') + K x = 0 \end{cases}$$

*Deformation of the blade in vertical flexure and in torsion must especially be taken into account; they can influence the vibration level by a resonance effect.

We now seek the amplitudes of the forced vibration of the mass M subjected to the force F. On solving these two equations in the standard way we have

$$X'' = \frac{F_0 \cos \Omega t}{M + \dfrac{K}{\dfrac{K}{m} - \Omega^2}}$$

The attenuation A provided by the pendulum damper is obtained by forming the ratio of the acceleration amplitude of M to that existing without the pendulum damper: /149

$$\frac{F_0 \cos \Omega t}{M} ,$$

from which

$$A = \frac{1}{1 + \dfrac{\dfrac{K}{M}}{\dfrac{K}{m} - \Omega^2}}$$

The vibrations will be completely eliminated at frequency $\Omega = \sqrt{\frac{K}{m}}$, that is, when the exciting frequency is equal to the natural frequency of the pendulum damper with M held fixed.

The mechanism is as follows: The pendulum damper oscillates at its frequency with an amplitude and phase such that the forces transmitted to the mass M by the spring exactly balance the forces F at each instant.

Note that it is not properly speaking a question of resonance:

(1) The amplitudes do not tend to infinity in the absence of damping, but become stable at a well-defined level, (2) The resonance occurs at the characteristic frequency of the system, which is not $\sqrt{\frac{K}{m}}$ but $\sqrt{\frac{K}{m}\left(1 + \frac{m}{M}\right)}$; it is at this frequency that the elongations would become infinite.

The diagram of Plate VI-2 shows the variation of A as a function of the frequency Ω for several valuesof the ratio m/M.

We note here the optimum operating point ($A = 0$, $\Omega = \sqrt{\frac{K}{m}}$) and the resonance point where A tends to infinity.

Note the important point that the "tuning" to be effected to obtain a satisfactory result becomes "sharper" the smaller the ratio m/M.

6.14. · STRUCTURAL RESONANCES /150

With vibration being attenuated as much as possible, it is further necessary to prevent airframe resonances with the exciting frequencies. This problem can severe, particularly for tandems or single-rotors, with an anti-torque propellor, where the tail carries at its extremity relatively large masses that have natural frequencies of the same order of magnitude as the harmonics of the rational mode of the rotor. The attempt is made to attain an optimum intercalation and resonance spectra by systematic tests of the fuselage vibrations. Plate VI-3 shows a significant example of this overlapping.

6.15. SUMMARY

A good modern helicopter has an acceptable vibration level in cruising flight. (We cite a mean order of magnitude of 0.2g). Nonetheless vibrations are important at low speeds (transition zone: 30-50 km/hr) and at high speeds (large aerodynamic asymmetries, significant flapping, stalling, compressibility effects, etc...)

All else being equal, the situation is improved as the number of blades is increased and with the precision of construction and adjustment of the blades.

On the other hand, poorly-considered design characteristics such as badly-matched suspensions, blade or structural resonances, can be injurious.

In conclusion, we emphasize a practical aspect of vibrations: Their level can be quite different from machine to machine end, for the same machine, from one day (or hour) to then ext.

This is easily explained on the basis of various factors that crop up in practice, such as air turbulence, minor disorders, blade deformations condensation of water in the blades, etc ...

6.2. GROUND RESONANCE

On the ground with rotor turning the helicopter is somewhat like the albatross of whom the poet said "His giant's wings prevent him from walking". To speak more precisely he is subject to the phenomenon of dynamic instability known as "ground resonance". This name derives from the fact that the instability generally appears when the rotor is set into operation on the ground, or after landing, and disappears as soon as the machine takes off.

What, exactly, is this? We shall first give the testimony of eye-witnesses:

"A Western Rodos" .... writes one experimenter still under the stress of emotion. Another, less terse, gives us a basic idea of the nature of the phenomnon:

"A helicopter with vertical and horizontal flapping hinges is taken to the test /151
field for the first time. The individual check-out tests have all been completed satisfactorily and the completely assembled machine is to be turned over for the first time. The frequency of the machine resting on its wheels has been measured for roll and pitch, with the rotor replaced by a single section of metal of the same total weight placed at the center of the rotor head; 100 cycles/min in pitch and 125 cycles/min in roll are established. We therefore expect two critical rotor frequencies, 100 r.p.m. and 125 r.p.m. The rotor is started, and in the vicinity of 90 r.p.m. strong oscillations of the machine in roll are observed; at about 115 r.p.m. strong oscillations again occur, this time in pitch. Thus far nothing unexpected has happened except that the resonance speeds are smaller than anticipated. The rotor speed is further increased and toward 140 r.p.m. new oscillations appear, this time so violent that, if maintained, the machine capsizes".

This phenomenon remained a mystery for a long time. La Cierva, who encountered it with autogiros, suggested that it could by eliminated by mounting sufficiently powerful dampers on the landing gear and bladelag hinges. The first correct explanation of the phenomenon was published by Coleman in 1943 and since then the analytical investigation has been pushed far toward revealing the role of the many factors that enter*. But now it is time for some mechanics.

6.21. QUALITATIVE ANALYSIS

We shall begin with the simple case of a helicopter having a fixed-blade rotor. The rotor head can be displaced horizontally by elastic deformations of

*Mssrs. Gilly and Normand particularly have made at SNCASE a very complete study, from which we have borrowed liberally for the mathematical portions of this account.

the airframe (particularly vibrations of the machine on its landing gear). The behavior of the system is similar to that of a flywheel mounted on a flexible shaft (Fig. 6.2).

The theory given in textbooks on mechanics leads to the following conclusions:

Let ω_c be the angular frequency of the characteristic oscillation of the flywheel (taken to be stopped, which corresponds to oscillation of the helicopter on its landing gear). Suppose that the flywheel shows an imbalance described by the offset ε of its center of gravity.

The rotational mode is ω. If $\omega < \omega_c$, the flywheel turns as shown in Fig. 6.2,a. The configuration is stable.

If $\omega = \omega_c$ there is instability: In this region the vibrations tend to infinity (resonance) in the absence of damping. /152

ω_c is called the critical velocity of the system.

For $\omega > \omega_c$ a new position of stable equilibrium is established, as shown in the diagram of Fig. 6.2,b.

For $\omega = \infty$, $x = \varepsilon$, the flywheel turns around G.

In the case of a helicopter with a rigid rotor there will thus be as many critical regions as there are natural frequencies of oscillation of the rotor head (usually the two fundamentals in roll and pitch). In the neighborhood of these regions the vibrations caused by rotor imbalance will be considerably amplified.

A rotor with hinged blades is much more complicated, since the lag motions of the blades permits a variable displacement of the center of gravity of the moving masses, as shown in Fig. 6.3. This has two consequences:

(1) The critical regions are modified and no longer exactly coincide with the natural frequencies of oscillation of the fixed blade. (See the description of this phenomenon at the beginning of the section.)

(2) A new effect appears: In certain ranges (usually near the critical regions) divergent oscillations are produced, even without any initial imbalance.

This is a matter of an unstable coupling between the oscillations of the rotor head and the blade lag oscillations. Stated differently, a "negative damping" exists comparable to the "negative resistance" of unstably-coupled radio circuits.

The energy required to produce this effect is obviously supplied by the engine that drives the rotor.

The term "ground resonance" thus includes two distinct effects for a hinged-blade rotor:

(1) Resonance properly so-called, which occurs with rigid rotors as well.

(2) Instability on the ground.

Before setting about the mathematical analysis let us bring out qualitatively the important facts. The instability shows up at rotational speeds where the characteristic blade lag frequency (observed in the fixed axes) is close to one of the natural frequencies of the rotor head. /153

The methods available to eliminate it from the operating ranges are the following:

(1) Shift the location of the unstable zones by modifying the natural frequencies of the rotor head and blades. This can be done by experimenting with the stiffness of the landing gear and the mode of attachment of the blades to the hub, by selecting an appropriate value of drag-hinge offset, with auxiliary devices such as "distributor cables", elastic inter-blade ties, and the like.

(2) A damping great enough to overcome the effect of the negative damping created by the unstable coupling. To be effective the damping must act simultaneously on the motions of rotor head and blades.

This accounts for the arrangements one is led to use in practice. On helicopters equipped with a wheeled landing-gear, which strongly damps the fuselage motion, it is above all necessary to mount dampers on the blades. On the other hand, on helicopters with lag-hinged blades equipped with a skid landing-gear the fuselage motion may perhaps be checked with suitable dampers (An example is the SE 3130, Figs. I.22 and IX.16).

Some Important Remarks:

(1) Given the essential roles of the damping and the vibrational frequencies of the machine, the appearance of ground resonance will in practice depend on many factors, such as tire inflation, damper adjustment, load conditions and ground consistency, the nature of the terrain, etc... Actually, it can be stated without risk of contradiction that it is possible to find a configuration for all present hinged-blade helicopters where resonance appears to some degree. What is finally important, and not always easy to obtain, is that no objectionable or dangerous effects occur in normal operating conditions.

(2) As with any unstable process, ground resonance shows up more strongly as the force inputs capable of exciting it grow larger. The inputs stem from poor rotor balance, wind, rough handling of the controls, hard landings, etc... We note particularly the effect of solid friction on the landing-gear and blades. Below a certain threshold the machine is "frozen", but above this threshold instability sets in and builds up as the damping effect of solid friction diminished with the amplitude of motion.

These considerations may explain why certain "off-beat" machines are viewed by pilots as having a rather disconcerting and capricious behavior from the standpoint of instability on the ground. /154

(3) We have stated that the resonance disappears as soon as the machine loses contact with the ground. If it is possible, then, take-off is the most effective way to escape from a difficult situation.

6.22. MATHEMATICAL STUDY

The characteristics of the two dynamic motions are shown in Fig. 6.3.
Elastic Displacement of the Rotor Head: The motion is defined along the two axes OX and OY (pitch and roll) by its angular frequency Ω and the associated equivalent mass M (from the relationship $M = \frac{K}{\Omega^2}$, where K is the elastic restoring coefficient of the rotor head.

	Pitch	Roll
Displacement	x	y
Natural Angular Frequency	Ω_x	Ω_y
Associated mass	M_x	M_y

Blade Motions: We assume a three-blade rotor. The blade nomenclature is as follows:

Lag angles of the three blades: δ_1, δ_2, δ_3.

Mass of blade: m

Static moment of blade around lag axis: m_s

Moment of inertia of blade around lag axis; I_p

Distance between lag hinge and rotor axis: e

Coefficient of elasticity of blade: K_δ.

These parameters are not all independent and setting them into equations shows that they may be replaced by the following:

$$\begin{cases} \Omega_x \\ \Omega_y \\ \bar{e} = e\,\dfrac{m_\delta}{I_p} & \text{(value approaches } 3e/2R \text{ for a homogeneous blade.} \\ \bar{m}_x = \dfrac{3\,m_\delta^2}{M_x\,I_p} & \text{(value approaches } 9m/4M_x \text{ for a homogeneous blade.} \\ \bar{m}_y = \dfrac{3\,m_\delta^2}{M_y\,I_p} & \text{(value approaches } 9m/4M_y \text{ for a homogeneous blade.} \\ \Omega_{\delta_0} = \sqrt{\dfrac{K_\delta}{I_p}} & \text{(natural angular frequency of flapping of blade lag for } \omega = 0. \end{cases}$$

6.221. EQUATIONS OF MOTION

The equation is set up (we shall leave this operation to the reader) by calculating the total potential and total kinetic energy and applying Lagrange's equations to each degree of freedom x , y , δ_1 , δ_2 , δ_3 . A system of differential equations is thus obtained whose solution yields the characteristics of the system. This calculation shows that δ_1 , δ_2 and δ_3 can be replaced by two degrees of freedom, X_G' and Y_G', the coordinates of the center of gravity of the blade ensemble in the fixed axes tied to the rotor head (Fig. 6.3).

Using the following reduced coordinates

$$\begin{cases} \bar{x} = x \cdot \dfrac{m_\delta}{I_p} & u = 6\,x_G' \cdot \dfrac{m}{m_\delta} \\ \bar{y} = y \cdot \dfrac{m_\delta}{I_p} & v = 6\,y_G' \cdot \dfrac{m}{m_\delta} \end{cases}$$

the equations of motion are written as:

$$\begin{cases} \ddot{\bar{x}} + \Omega_x^2 \bar{x} + \frac{m_x}{2} \ddot{u} = 0 \\ \ddot{\bar{y}} + \Omega_y^2 \bar{y} + \frac{m_y}{2} \ddot{v} = 0 \\ \ddot{u} + 2\omega \dot{v} - \left[\omega^2 - (\Omega_{\delta_0}^2 + \bar{e}\omega^2)\right] u + \ddot{\bar{x}} = 0 \\ \ddot{v} - 2\omega \dot{u} - \left[\omega^2 - (\Omega_{\delta_0}^2 + \bar{e}\omega^2)\right] v + \ddot{\bar{y}} = 0 \end{cases}$$

In seeking roots of the system of the form

$$\bar{x} = \bar{x}_0 e^{i\Omega t} \quad , \quad u = u_0 e^{i\Omega t} \quad , \quad \ldots \text{ etc } \ldots ,$$

we must solve the equation

$$\left\{(\Omega^2 - \Omega_x^2)\left[\Omega^2 + \omega^2 - (\Omega_{\delta_0}^2 + \bar{e}\omega^2)\right] - \frac{\bar{m}_x}{2}\Omega^4\right\} \times \left\{(\Omega^2 - \Omega_y^2)\left[\Omega^2 + \omega^2 - (\Omega_{\delta_0}^2 + \bar{e}\omega^2)\right] - \frac{\bar{m}_y}{2}\Omega^4\right\} = 4\omega^2\Omega^2(\Omega^2 - \Omega_x^2)(\Omega^2 - \Omega_y^2) \tag{6-1}$$

Remarks:

(1) It can be shown that these equations are also valid for rotors with more than three blades.

(2) On the other hand they are not the same for a double-blade (rotor not isotropic). We shall pass over this case since double-rotors do not usually have lag axes and therefore ground resonances are not a problem.

To study the stability of the roots of Eq. (6-1) we plot the curves of Ω as a function of ω, as shown in Plate VI-4. The values of ω for which all roots in Ω are imaginary corresponds to instability.

6.222. INTERPRETATION OF THE DIAGRAMS

/157

In case $m_x = m_y = 0$ (mass of blades negligible with respect to the mass of the fuselage), Eq. (6-1) reduces to a set of equations

$$\begin{cases} \Omega^2 - \Omega_x^2 = 0 \\ \Omega^2 - \Omega_y^2 = 0 \\ \Omega^2 \pm 2\omega\Omega + \omega^2 - (\Omega_{\delta_0}^2 + \bar{e}\,\omega^2) = 0 \end{cases} \tag{6-2}$$

corresponding to uncoupled fuselage- and blade- oscillations.

The point is obvious for the first two equations. For the last equation we can write

$$|\Omega \pm \omega| = \Omega_\delta \quad , \text{ in setting } \Omega_\delta = \sqrt{\Omega_{\delta_0}^2 + \bar{e}\,\omega^2} \ .$$

Ω_δ is the natural lag frequency of the blade in axes tied to the rotor as calculated in 3.22.

$\Omega = |\Omega_\delta \pm \omega|$ gives the characteristic frequencies of blade lag as seen in the fixed axes (separation into two frequencies by a process similar to that pointed out in 3.3121).

If $\Omega_{\delta_0} = 0$ (elastic restoration not present in blades) the describing curves are the straight lines given by equations

$$\Omega = \omega(1 \pm \sqrt{\bar{e}}) \ .$$

If $\Omega_{\delta_0} \neq 0$, the curves are hyperbolas with these straight lines as asymptotes.

The lines or curves representing Eq. (6-2) have been plotted (dashed) in the diagrams of Plate VI-4. Obviously there is no instability in this case.

Case $\bar{m}_x \neq 0$, $m_y \neq 0$. : Since $\bar{m}_x$ and $\bar{m}_y$ are always comparatively weak, the curves of Ω as a function of ω lie very close around the curves and lines of the preceding case. Two special cases are plotted on the diagram of Plate VI-4.1:

(1) $\bar{m}_x$, $\bar{m}_y$ very small (dotted) yields, by way of example, two small zones of instability. /158

(2) Usual values of $\bar{m}_x$ and $\bar{m}_y$ (solid lines) yield a single, very large zone of instability.

On inspecting the diagram one can state intuitively the following results, which are confirmed by an exact calculation with Eq. (6-1): The mid-point of the zone (or zones) of instability is:

Two zones: $\omega_1 \simeq \frac{\Omega_x}{1-\sqrt{\bar{e}}}$ (intersection of the lines $\Omega = \Omega_x$, $\Omega = \Omega_y$, with the line $\Omega = \omega(1-\sqrt{\bar{e}})$.

$\omega_2 \simeq \frac{\Omega_y}{1-\sqrt{\bar{e}}}$

Single zone: $\omega = \frac{1}{2} \cdot \frac{\Omega_x + \Omega_y}{1-\sqrt{\bar{e}}}$

These formulas are valid only if Ω_{δ_0} is small (less than Ω_x and Ω_y), which is always the case the hinged blades. If Ω_{δ_0} is large, comparison of the diagrams VI-4.1 and VI-4.2 shows that the instability has been shifted toward higher frequencies (blades mounted inflexibly in lag).

Conclusion: The instability appears at higher frequencies as Ω_x, Ω_y, $\bar{e}$, and Ω_{δ_0} becomes larger. It disappears for $\bar{e} \gg 1$. The size of the band (or bands) of instability grows as $\bar{m}_x$ and $\bar{m}_y$ becomes larger (since the unstable coupling is made by the mass of the blades).

6.223. EFFECT OF DAMPING

The action of dampers on the blades of fuselage has not been considered in the formulas. We cannot treat friction effects in detail, but shall simply give the formula with which the damping required to eliminate an unstable zone lacking

in friction can be computed. Since the damping is given in the form of a force $-C_x\dot{x}$, $-C_y\dot{y}$ on the rotor head and as a moment $-C_\delta\dot{\delta}$ on the blades, we must have

$$C_x C_\delta > \frac{b}{4} m_\beta^2 \frac{\Omega_0^3(1-\bar{e})}{\Omega_0 \bar{e}+\sqrt{\Omega_0^2 \bar{e} + \Omega_{\delta_0}^2(1-\bar{e})}}$$

in case of two distinct zones of instability, and /159

$$\frac{C_x C_y}{C_x+C_y} C_\delta > \frac{b}{4} m_\beta^2 \frac{\Omega_0^3(1-\bar{e})}{\Omega_0^2 \bar{e}+\sqrt{\Omega_0^2 \bar{e} + \Omega_{\delta_0}^2(1-\bar{e})}}$$

for a single zone $\left(\Omega_0 = \frac{\Omega_x + \Omega_y}{2}\right)$.

These formulas are not valid except when C_x, C_y and C_δ are not too large and Ω_x not too different from Ω_y, which is also the situation in practice. The important thing to remember - as pointed out earlier in 6.21 - is that these conditions require dampers both on the landing gear and on the blades.

6.224. DISTRIBUTOR CABLES

The principle is simple: Cables equipped with inertia weights that tie the blades one to the other according to the scheme of Fig. 6.4. If the angles between the three blades become unequal it is clear from the figure that the changes in direction of the cable sections produce moments to restore the blades to the 120° position (moreover, the cables limit the angles possible between two blades).

This arrangement, then, has an effect of the same nature as the offset $\bar{e}$ of the blade lag hinges. In effect, the calculation shows that if the mass of the inertial weights is small compared with the masses of the blades, and if the cables have little slack ($\gamma \ll 1$, see Fig. 6.4), the effect is to augment $\bar{e}$ by the quantity

$$\Delta\bar{e} = \frac{9}{16}\frac{M r_T^2}{I_p}\frac{1}{y^3}$$

where M is the mass of each inertial weight, r_T the distance between cable attachments and rotor axis and y is as defined in Fig. 6.4.

. We saw in Section 3.22 that in practice $\bar{e}$ is always small compared to unity, when it should be at least equal to one to suppress the instability on the ground without dampers. The distributor cables provide a convenient means of accomplishing this, or at least of shifting the zone of instability away from the operating range.

6.225. RESONANCE PROPER

/16

Using these equations let us examine the possibility of resonance in the usual sense. We recall that this is a question (as in the case of the rigid rotor presented in 6.21) of establishing the critical regions where any unbalanced residual can induce significant vibration of the machine by resonance effects.

It is clear that these regions are reached when the excitations due to imbalance coincide with one of the natural frequencies of the overall fuselage-rotor system.

In the diagrams of Plate VI-4 the critical frequencies lie at the intersection of the line $\Omega = \omega$ with the curves of Ω as a function of ω. We find two resonances for the case $\Omega_{\delta_0} = 0$ and three for $\Omega_{\delta_0} \neq 0$.

The complete calculation shows that actually only one region (marked R on the diagrams) is truly dangerous, since the amplification in the other regions is feeble (these resonances disappear completely for $\Omega_x = \Omega_y$, $\bar{m}_x = \bar{m}_y =$ isopropic support). Here there is a danger region, usually lower than the operating speeds, in which one must not linger.

The amplitude of the resonance is clearly attenuated by the dampers on the landing gear, but is not affected by the dampers on the blades, since the alternating lag motions are zero are resonances as is easily seen from the equations.

6.23. CONCLUDING REMARKS

(1) The analysis we have made shows that "ground" resonance can indeed theoretically be produced in "flight"; it is only necessary that the airframe support

elastic deformations at the required frequencies. This has actually been observed, but it is much rarer than at the ground.

(2) Instability can appear with rotors without lag hinges if the blades are flexible enough in their plane to resemble hinged blades with elastic restoration.

(3) The real situation is often more complicated than the calculations which have been made. Each mode of deformation can be superposed on the fundamental modes Ω_x and Ω_y to complicate the phenomenon. Moreover, as was pointed out in the last section, so may factors enter into the values of the characteristics Ω_x, Ω_y, M_x, M_y, C_x, C_y,... that it would not be surprising to find that the machine did not conform rigorously to the calculation. The important thing is to understand what is happening and to know what to do.

6.3. ROTOR INSTABILITY /161

In this category can be placed a number of effects originating with pitch instability and vertical flapping of the blades. The result is more or less violent vibration and control instability:

— instability of the cyclic pitch control, which jitters in turning on its bearings.

— instability of the collective pitch control, which passes abruptly from high to low pitch.

Such effects, which according to their intensity made the machine disagreeable or even dangerous, should obviously be eliminated. We shall not study the causes of instability that occur most frequently.

6.31. POOR CHORDWISE CENTERING OF THE BLADES

If the blades are made so that the center of gravity of the blade section is somewhat behind the aerodynamic thrust center instability becomes a problem.

The expression for the moment exerted by the blade around its feathering axis was given in Section 3.321. Retaining only the important terms, it is written

$$M_\theta = -i_\theta(\ddot{\theta} + \omega^2\theta) + F_A\left(y_A - y_G\frac{z_A}{z_G}\right) + CM_0 \qquad (3\text{-}13)$$

where i_θ is the moment of inertia of the blade around its feathering axis, F_A is the lift of the blade, y_A and r_A are the coordinates of the aerodynamic center of the blade, y_G and r_G the coordinates of the elastic center of the blade and CM_o the moment due to the Cm_o of the blade section.

We shall find the static stability of the blade around its feathering axis; this depends on the sign of $\frac{dM_\theta}{d\theta}$. We have /162

$$\frac{dM_\theta}{d\theta} = -i_\theta \omega^2 + \frac{dF_A}{d\theta}\left(y_A - y_G \frac{r_A}{r_G}\right) \qquad (6\text{-}3)$$

$\frac{dF_A}{d\theta}$ is obviously positive (the lift increases with pitch). The blade will therefore be statically unstable if $y_A - y_G \frac{r_A}{r_G}$ is positive and sufficiently large - i.e. if the blade is centered too far to the rear.

Let us look into what happens on a helicopter whose blades possess this static instability. We assume the controls to be reversible and in neutral. It is clear that the collective pitch control is unstable. Left to itself it will tend to take on high pitch or low at the slightest provocation.

As for the cyclic control, Fig. 6.5 shows what takes place. The swash-plate is in unstable equilibrium, displaced from its original position. It is subject via the blades to forces df_1, df_2 and df_3, which cause it to hit its limit-stop as shown in the figure. The plate, thus tilted, turns with the rotor, inducing a circular motion on the cyclic control stick in the same sense and at the rotor rate.

We have shown in 3.321 that the troublesome forces on the blade can be completely eliminated in all flight modes if the pitch variation axis, the line of the thrust centers and the line of the centers of gravity coincide. This is represented by the conditions $y_G = 0$, $y_A = 0$, which eliminates the unstable term in Eq. (6-3).

Nevertheless, for technical reasons it is often difficult to realize this condition, so it may be necessary to guard against the tendencies to instability that sometimes turn up by using the appropriate devices - frictional dampers, anti-backlash, sero controls.

Remark:

Examination of the above equations leads to understanding a fact that is at

first glance confusing - the tendency toward instability at high pitches can exist even in stabilized flight when the collective pitch lever has a tendency to drop (and a forteriori if it is in equilibrium).

Bad chordwise centering of the blades can also, as with airplane wings, give rise to flutter effects. We note, moreover, that the static pitch instability studied earlier is in short merely a special case of divergent flutter.

With blades of standard construction, if the precautions of aerodynamic centering given above are taken, flutter is normally not a problem. /163

6.32. WEAVING

This is a malady characteristic of double-blade rotors mounted on the universal (Fig. 6.6). In this mounting the combination of hub and blades makes up a rigid Vee articulated at 0. Such a rotor can exhibit an instability called "weaving" in the Anglo-Saxon literature*.

The aficionados of rational mechanics will recognize this as the classical problem of the stability of rotation of a tip around a mean principle axis of inertia. The diagram of Fig. 6.6 shows that due to the coning and displacement of the universal joint (which essentially coincides with the center of gravity of the aggregate) the following relationships exist between the principal moments of inertia:

$$I_x < I_z < I_y .$$

We know that rotation around 0_z is unstable under these conditions.

For a helicopter rotor it is necessary to consider aerodynamic forces and forces stemming from the cyclic control (elastic restoration on the warp axis).

The equation of the problem is developed in Appendix III. 5, from which we abstract the critical stability criterion:

*The name stems from the appearance of the effect. Since the plane of rotation of the blades is unstable their tip paths will cross over each other like the threads of a fabric.

$$(I_z - I_x)\left(I_z - I_y + \frac{K_\theta}{\omega^2} - \frac{M y_A}{\omega^2}\right) > 0$$

where K_θ is the coefficient of elastic restoration on the warp axis, M is the aerodynamic constant, y_A the distance of the aerodynamic thrust center of the blade from the warp axis. Disregarding elastic restoring- and aerodynamic - forces, the stability criterion

$$(I_z - I_x)(I_z - I_y) > 0$$

shows clearly the instability of the rotation if 0_z is the mean axis of inertia.

If the general case $I_z - I_x$ is always positive and the stability condition is written

$$\omega^2 (I_z - I_y) + K_\theta - M y_A > 0 .$$

This suggests what should be done to remedy weaving (Fig. 6.7). /164

(a) Frictional dampers or, better, anti-blacklash on the cyclic control (factor K_θ).

(b) Addition of masses on arms that are fixed rigidly to the hub, perpendicular to the plane of the Vee formed by the blades. This makes $I_z - I_y$ positive.

(c) Offsetting the blades behind the warp axis (y_A negative).

As an example we note that all these means are used simultaneously on the Bell 47, which in its early days was subject to weaving (the function of the inverse counterweights is taken over by the stabilizer bars, see (Fig. 5.5).

Remark: Weaving can of course be produced in the same way with a hub double-blade of the Djinn type (Fig. 9.6) where the universal is replaced by a spherical bearing. This explains the purpose of the transverse counterweights (Fig. 1.21) mounted on the hub.

Chapter 7

STRENGTH OF MATERIALS /165

The special nature of the problems of strength of materials peculiar to the helicopter is the considerable role of fatigue. Moreover, since the forces applied to the rotor are essentially periodic, the many critical components are ranked according to their endurance under alternating stress. Thorough ground tests on complete or partial assemblies are necessary to insure their service integrity.

We are thus led to classify the various components of hovercraft into categories in terms of their operating conditions:

Predominantly static forces: Fuselage, landing gear, engine mounting, hub, etc...

Predominantly alternating forces: Blades, controls, transmission, etc.

7.1. STATIC FORCES

The design conditions of the fuselage do not differ materially from those of an airplane. Two load conditions are the determining factors:

(1) Pull-out

We have seen in Chapter 5 (Section 5.3) that a load factor of 2 essentially covers the present requirements. On the other hand the rotor is usually "saturated" at factors between 2 and 3* and it is much more "transparent" to gusts then is a fixed wing. Unintentional load factors considerably above 2 are therefore not a matter for concern.

This is why most regulations require that safe load factors be calculated between 2 and 2.5 (4 to 5 to breakdown). Negative pull-out at safe load factors between 0.33 and 0.66 are likewise provided for.

(2) Landing /166

The calculations for wheeled landing-gear are similar to the methods used with aircraft. Different special cases must be considered, such as the normal landing, tail down (autorotation), and the skid landing. The touchdown velocities

*Saturation is reached when the blade profiles work at their maximum angle of attack (stall).

specified vary, depending on the expected use. As an example we cite the normal conditions from the American regulations (C.A.R. Parts 6 and 7):

Drop Height: 0.33 meters, or a touchdown velocity of 2.55 meters per second. During the take-up of the landing gear the rotor is assumed to lighten the hovercraft by one-half its weight.

The above method does not apply directly to the skid landing-gear mounted on elastic cross-bars without dampers, such as are frequently used on light helicopters. It is usually permissible to calculate such a landing-gear on the basis of absorption of the energy resulting from a given touchdown velocity by plastic deformation. The American regulations just quoted require the same drop height as for the wheeled landing-gear.

7.2. ALTERNATING FORCES

In this section we shall give first consideration to the main rotor blade, the vital component whose operating conditions are themost difficult to foresee and to measure.

7.21. BLADE

The critical forces for this component are three in number: traction (due to centrifugal force), a continuous force, permanent vertical flexure, and alternating vertical flexure due to variations in the distribution of lift during rotation.

Drag and torsonal forces, just as the shear forces, are most often small and are only of secondary importance for blade endurance.

7.211. CALCULATION OF BLADE FORCES

The stresses attributable to centrifugal force present no difficulty. On the other hand, the calculation of vertical flexure is quite intricate and the results are rather unreliable.

We shall restrict our consideration to outlining the principle of most of the methods in use: /167

(1) Determination of the natural vertical deformation modes of the blade in rotation (see Fig. 7.1 for the natural deformations and frequencies).

(2) - Calculation of the aerodynamic force distribution as a function of radius and azimuth for each flight mode. The blade is assumed to be rigid and its flapping is calculated using formulas similar to those given in Chapter 3.

(3) Calculation of the forced deformation due to aerodynamic forces using an expansion in terms of the natural modes of deformation (orthogonal functions). The deformation corresponding to each mode is itself obtained by a Fourier expansion of the form

$$M = M_0 + M_1 \cos(\omega t + \varphi_1) + \dots + M_n \cos(n\omega t + \varphi_n) + \dots$$

This permits a qualitative understanding of the blade operating conditions.

A permanent deformation stemming from the terms in M_0 is added to the deformation modulated in ω, 2ω, ... $n\omega$. The magnitude of the deformation for a given harmonic is a function of two factors: (1) the intensity of the corresponding excitation, which varies considerably with flight mode but decreases with the order of the harmonic, and (2) the dynamic amplification produced when the exciting frequency approaches the natural modes of the blade (resonance).

Remark:

The level of the alternating flexural stresses is influenced by the chordwise centering of the blade.

If the blade has a torsonal flexibility that is large enough and if the line of the centers of gravity of the blade sections is located behind the line of the aerodynamic centers, the lift forces induce "diverging" moments that increase the angle of attack of the blade profiles and therefore increases the aerodynamic lift. Finally, the alternating stresses are increased. Conversely, a forward centering of the blades has a favorable effect on the level of the alternating stresses.

The reasons these computational procedures cannot yield satisfactory numerical results are:

— Knowledge of the local aerodynamic forces is not precise enough (particularly with regard to the damping they cause in each of the natural modes).

— The critical flight cases are least amenable to calculation: flight in the transition zone (30 - 50 km/hr), maneuvering, pull-out landing, etc. /168

— Although the natural modes of the blades can be calculated accurately enough as regards deformation and frequencies, their structural damping (which is important when operating close to a resonance) is difficult to evaluate.

These considerations suffice to show that at the investigative level the working conditions of the blade are not known beyond a rather doubtful precision. It is therefore mandatory from the standpoint of safety to make up for the inadequacies of calculation by flight tests.

7.212. FLIGHT MEASUREMENTS

The now standard technique of strain-gages is used. The major difficulty is that the measurements must be made on moving parts and therefore electrical pick-ups must be used that are good enough not to perturb the measurements.

In France, the method of mounting the entire measuring package (including the recorder) on the hub has also been used with success.

7.213. STUDY OF FLEXURAL FORCES IN A BLADE

Let us examine the results recorded using these methods.

Plate VII-1 shows example of the distribution of forces on a blade for the various flight modes. Plate VII-2 shows, for the same blade, the development of the maximum alternating stress as a function of speed.

Finally, Plate VII-3 shows the resonance diagram, again for the same blade, giving the natural frequencies (calculated) and the excitation frequencies. An example of the harmonic analysis of the recorded alternating forces is also shown.

We note the following facts, which are valid for all standard blades: In a general way the forces in helicopter flight and in autorotation are very different.

Average Moments:

In helicopter flight the blade is flexed upward with a maximum moment of about 0.20R. In autogiro flight the blade exhibits a double curvature - concave upward near the hub, concave downward at the tip.

The explanation for these features can be found in Fig. 7.3.

For the ideal case of a blade with a uniform distribution of mass and constant induced velocity*, the equilibrium of the forces of lift and centrifugal restoring force is made as shown in the diagram of Fig. 7.3,a. The force components normal to the blade are balanced at each point and the blade exhibits no permanent deformations. /169

As we know, the induced velocity is actually not uniformly distributed and the lift is concentrated at the outer portion of the blades. Figure 7.3,b, illustrates the force balancing under these conditions. The blade is curved upward, which explains the deformation noted for helicopter flight in Plate VII-1.

We shall now look at the case of a blade that is mass-loaded at its tip - large counterweight, ram-jet, pulse-jet, etc. The normal component of centrifugal force is larger than the lift at the blade tip and the tip is deflected downward (Fig. 7.3,c).

Finally, Fig. 7.3,d, shows what takes place in autorotation. We know that in this case the lifts are displaced toward the inner part of the blade, which exhibits a double curvature similar to that of Plate VII-1.

Alternating Moments: In the helicopter mode, very low-speed flight in the transition zone (30 km/hr) is quite severe (see Plate VII-1 and Plate VII-2). This stems from the strong inequality in distribution of the induced velocities characteristic of the transition zone.

In practice this says that no matter how little wind there is, hovering (or stationary on the ground) can generate significant fatigue in the blades, contrary to what might be thought a priori.

Alternating forces again become important at elevated speeds, where there is great dissymmetry between the working conditions of the advancing and retreating blades.

Harmonic Contributions to the Alternating Stresses (Plate VII-3):

---

*For an elementary annulus of radius r, the lift is given by the relationship

$$dF_N = 2\rho V_i V_1 2\pi r\, dr,$$

which, taking V_i to be constant, is of the form $dF_N/dr = kr$.

The spectrum of the excitation always contains many harmonics. Their proportions can vary considerably from one type of flight to another, but in a general way the 1st, 2nd and 3rd harmonics, always present, are by far the most important. As pointed out in 7.211, some one harmonic, even of higher order, can become important if it resonates with a natural frequency of the blade (see the 9th harmonic in the example of Plate VII-3).

This makes clear the importance of the rigidity characteristics and mass of the blade from the viewpoint of alternating forces. For example, in the case shown in Plate VII-3, making the blade rigid would be deleterious since this would risk locating the resonance point of the 1st mode/3ω inside the operational range. /170

We note in this regard that calculations of the natural frequency of the blades as a function of rotor speed can be made with good enough accuracy to avoid at this stage the study of dangerous resonances.

7.214. DETERMINATION OF BLADE LIFETIME

The process is as follows: (1) Survey the forces applied to the blade in service, (2) determine in the laboratory the fatigue behavior of the blade, and (3) calculate a safe lifetime from these data.

7.2141. BLADE FORCE STATISTICS FOR THE VARIOUS FLIGHT MODES

When surveying the alternating forces in all operational cases (stabilized flights and maneuvers) one can, by taking into account the relative duration of flight in each case, separate the forces into several groups, graded according to increasing stress. Since the permanent stresses are little variable and less critical, the alternating stresses are used in the classification. In practice three groupings are enough; an example is shown in the Table.

7.2142. FATIGUE TESTS

Elements having the structural characteristics of the critical areas of the blade and about two meters long are usually used. The three categories or critical forces are applied to them - tension, constant and alternating flexure, and the test is continued to breakdown.

The difficulty with this type of test is to avoid stress concentrations due to application of the loads or to the fastenings.

/171

Flight mode	Examples (the most important are underlined)	Percentage of total flight time	Maximum alternating force for each category (exemplary) in mapz* in the stee
(A) Continuously controlled flight	Level flight at cruising and maximum speeds, climb, descent with and without engines, etc.	90 %	6
(B) Quasi-continuous evolutions and maneuvers	Over-velocitie, pull-out, lateral and rearward flight, level flight at low speeds, etc.	9 %	8
(C) Short-duration or exceptional maneuvers	Sudden stick movements, approach to quick-stop landing,** etc.	1 %	10

The fatigue test-bench used for testing blades in France by STAe is shown on Fig. 7-2. A is a horizontal frame of great iregidity, about 9 meters long, B is a fixed hinge of the element under test E, C is a second hinge of the element under test, displaced vertically by a crank-tie-rod system D with adjustable speed and cam (700 to 2500 rev/min). F are steel cables placing the element E in tension by means of an air-jack I centrifugal force). H is a controllable pressure chamber permanent deflection). This chamber is sometimes difficult to use and could probably be replaced by shocks applied at appropriate points of the blade.

/172

*) The corresponding response time, which is variable, depending on the type, is of the order of a few seconds.

A cam rotation somewhat lower than the natural frequency of the element is used. The element is set into "spindle-like" motion under the effect of the inertial forces. The maximum flexure is produced toward the middle of the element, in a region that is not perturbed by the attachments.

By proper regulation of the rotation and cam the desired alternating stresses can be generated.

The fatigue diagram of the blade can be charted by running tests on many elements with a series of loads. Enough tests should be run to permit a sufficiently accurate determination of the dispersion.

7.2143. CALCULATION OF BLADE LIFETIME

The principle is simple. The useful lifetime with negligible probability of breakage is calculated by the appropriate statistical methods from the laboratory test results and the stress levels taken in flight.

Some useful developments in methodology are found in Appendix III.6. We shall here merely emphasize by a numerical example a difficulty in principle common to all problems of determining a safe lifetime for a critical component working under fatigue conditions.

Suppose there are 100 three-blade helicopters in service and it is desired that the probability of a single breakage in the aggregate of these machines be very low, say 1/1000. We must therefore establish the blade lifetime so that the probability of fracture in service is less than 1/ 1000 x 3 x 100) or 1/300,000.

At this level of probability an experimental knowledge of the dispersion curve assumes that at least 300,000 tests have been made, which is clearly out of the question in practice. Perhaps 30 test results are available under the best of circumstances.

The experimental data must therefore be extrapolated rather far by using empirical or theoretical rules that are often of dubious validity.

However these considerations should not deter the reader from boarding a helicopter. The very uncertainity of the methods used is conducive to great prudence in establishing a compromise between safety and economics.

Blade ruptures in flight are in fact rare and are usually isolated instances. /173

*Tr. note: mega-pieze 1 pz = 10^2 bar).

**Quick-stop obtained bya joint maneuver of cyclic- and collective-pitch.

7.22. OTHER VITAL COMPONENTS WORKING UNDER FATIGUE CONDITIONS

We shall mention only the most important of these.

7.221. FLIGHT CONTROLS

These components also elude calculation. Designed on the basis of rigidity considerations, they are always very much overdesigned with respect to the calculated forces. However, accidents, often with tragic consequences, have resulted from their failure in flight due to forces much higher than were calculated, local vibration, abnormal forces caused by seizing of ball-out-socket linkages, etc.

For this reason they are handled in the same way as the blades; the real forces are determined in flight and fatigue tests are made in the laboratory.

7.222. TRANSMISSION

We shall pass over the methods of calculation that present no special features with regard to engine design.

Endurance is usually established by a ground test. A machine including all the major components (transmissions, rotors, flight controls) is given operational tests following a procedure adopted from engine proof-testing (150 hr at the various speed ranges). These tests attempt to reproduce control forces in the blades similar to those encountered in flight.

In addition, certain critical parts - the rotor shaft, for example - are subjected to special static and dynamic tests.

7.223. COMPONENTS SUBJECT TO WEAR

Certain components can deteriorate so as to be unacceptable in service without presenting a risk of failure from fatigue. Hinges and blade attachments are examples of this; they usually require rollers or bearings that are subjected to large forces (the centrifugal force varies from 5 tons for small machines to several tens of tons for medium or heavy machines). In the case of rollers, which do not rotate but execute small oscillations around some average position, these forces are very harmful and the impression marks on the ways (Brinelling) are a cause of roughness and vibration in the controls. It is well to check the behavior of these parts in the laboratory as well.

Chapter 8

ROTOR DRIVE ASSEMBLIES /175

In the course of this chapter we intend to examine in greater detail the advantages and disadvantages of the various rotor drive mechanisms mentioned in Chapter 1. We will restrict ourselves to systems that have actually been employed or tested. The guideline for this study will be the deadweight-fuel consumption balance, which governs the economic aspects. Compared with this factor, all other considerations are relatively secondary. In this regard, a preliminary remark is appropriate: the helicopter is a machine whose missions are usually of short duration, i.e., from one-half to two hours, and therefore no fundamental importance will be attached to an increase in specific fuel consumption if it results in an appreciable reduction in deadweight. This is why helicopters have seen the light of day; this is why piston engines have given way to turbine engines* and why in choosing the latter we can accept an engine with a high specific fuel consumption as long as it is simple and light.

We will begin by examining the relative merits of jet and mechanical drive systems, and then we will study the various engines that can be used for mechanical drive.**

8.1. JET AND MECHANICAL DRIVE

Generally speaking, the advantages of jets for propulsion are as follows. They are light and simple to construct, because they have no transmission, clutch, free wheel, or anti-torque rotor, and are therefore cheaper to buy and maintain. They have better flight qualities and greater range of application. The advantages accruing to variable rotor speed over a broad range have been studied in Chapter 4 and 5. Let us recall them briefly. The variable speed /176

*The term turbine engine designates any power generator that uses turbines for the internal drive system. Depending on the way in which the useful power is furnished, we distinguish between a turbojet (thrust), a turboprop (mechanical power), and a high-pressure turbine (hot compressed gas). To simplify the language, we will sometimes use the term turbine in this course, since, although incorrect, it has been hallowed by usage.

**For a more detailed study of the characteristics and technical aspects of various types of engines, the reader is referred to the specialized courses of E.N.S.A.

can be regulated for optimum rotor operating conditions as a function of the weight, altitude and flight velocity. In particular, we have seen that it was of interest in high-speed cruising flight to use angluar rotor speeds higher than those used in hovering (to avoid retreating-blade stall). In addition, overload take-off by the "jump take-off" method is easy. Finally, the safety is greater because there is a reserve of kinetic energy which is available for use by the rotor; in other words, the "deadman's zone" is reduced or eliminated.

On the debit side of jet drive we find that the fuel consumption is very high, and therefore the endurance is limited. In addition, the noise level is often excessive. Helicopters in which combustion takes place at the blade tips have some very delicate regulation and control problems.

Given below is a classified list of the various jet-propulsion systems that may be considered (they are classified in decreasing order of fuel consumption; see Fig. 8-1):

a) Balde-tip Generators: rockets, ramjets, pulsejets, and turbojets. Only the ramjets and pulsejets come in question since the rocket (solid or liquid) has been set aside for highly specific applications, because of its low endurance, while the turbojet is destined for the giant helicopters of the future (provided the mechanical problems of blade-tip mounting are solved).

b) Mixed System. An air generator located in the fuselage forces air through hollow blades at the tips of which combustion chambers are mounted. The air generator consists of a specially adapted turbine with a high-pressure cycle (the air compression ratio is from 2.5 to 4).

c) Fuselage Generator Systems. These are comparable to the preceding, but do not have blade-tip combustion. We distinguish between high-pressure cycles in which pure air is compressed at a ratio of 2.5 to 4, and low-pressure cycles, in which hot gas issues from a specially adapted reactor at compression ratios of 1.4 to 1.8. Insofar as this system is concerned, the reactors can be mechanically driven by piston or turbine engines.

There is no better way of judging the respective merits of each type than by examining the comparative table given below, where the figures represent mean values, corresponding to the present status of airframe and engine engineering. /177

Comments Regarding the Table

1) Note the frequently enormous handicap of all jet systems from the fuel consumption point of view: the best still consumes three times as much as a piston engine and twice as much as a turbine engine.

2) Comparison of the empty weight of types ④, ⑤ and ⑥ may surprise the reader who has been indoctrinated with the idea that jets are synonymous with lightness, but these figures are not arbitrary - they have been computed on the basis of real data. The explanation can be readily found; namely, a mechanical reduction gear does not weigh as much as a turbine, in fact, its weight is of the same order of magnitude. If it is done away with, it must be compensated by mounting engines approximately twice as powerful because of the poor transmission efficiency. On the other hand, elimination of the anti-torque rotor makes it necessary to incorporate a yaw-control device, which makes the rotor (hub and blades) heavier.

It should be emphasized, however, that the figures given for types ③, ④ and ⑤ correspond to the use of turbine generators. The use of reciprocating - engine generators leads to prohibitive deadweight.

The possibilities for employing the various types of helicopters are illustrated in the payload-endurance diagram of Plate VIII-1, which was set up on the basis of the same data used in the table just described.

Compare also the deadweight estimates of the three CDE machines given in Appendix I, from which it can be concluded that jet helicopters are reserved for the execution of short-duration missions, which puts a considerable restraint on their flexibility. Therefore, such machines do not seem to be destined to come into general use.

In Chapter 10 we will point out the reasons which nevertheless militate in favor of jet helicopters in certain cases.

Before leaving this subject, we have given in Plate VIII-2 some indications of the efficiency of various jet-propulsion systems as a function of the tip speed of the rotor. These data make it possible to make a better choice of the optimum /179 operating state in each case.

The decrease in thrust with tip speed u of systems of type ③, ④ and ⑤ merits some explanation. The "net" thrust is the difference between the "gross" thrust developed by the nozzle and the "drag resulting from setting the fluid in motion" (to bring the fluid to the velocity u it is necessary to expend energy). The fluid drag obviously increases with u and cannot be totally recovered in the form of an increase in gross thrust.

Types of drive system	Empty (1) weight (% of total weight)	Fuel consumption (g per hp/hr on the rotor shaft	Transmission efficiency	Noise	Remarks	Examples of machines using this system
① Ramjets	35/40	3,000 to 4,000	↗ (2)	Noisy	Poor autorotation qualities very high kinetic rotor energy	Hiller Hornet
② Pulsejets	35/40	2,000 to (6) 3,000	↗	Very violent and distressing (5)	Poor autorotation qualities very high kinetic rotor energy	American Helicopter xA 5, xH26
③ High-pressure air generator with combustion at the blade tips	50/55	1,300 to 1,500	(2) ≃ 100%	Violent and distressing	Good autorotation considerable kinetic rotor energy "normal rotor	50 1120 ariel Fariey Rotodyne Fariey ultra-light
④ High-pressure air generator without blade-tip combustish	50/60	1,200 to 1,500	(2) 40 to 30%	Turbine noise can be sound-proofed	Simple fabrication large-diameter rotor	50 1221 Djinn
⑤ Low-pressure gas generator	60/65	750 to (4) 1,000	60 to (4) 45%	Turbine noise can be sound-proofed	Complex generator and hub "thick blades" (for gas transport)	Girania LP 10 Dorand DH 011
⑥ Mechanical drive by turbine engine	50/55	500 to (3)(4) 350	95% (3)(4)	Turbine noise can be sound-proofed	Less complex than ⑦	SE 3130 alouette Bell H 40 Kaman K 600 Westland Wessex etc.

Mechanical drive by reciprocating engine ⑦	60/70	(3)(4) 250 to 280	(3)(4) 93%	Engine noise can be sound-proofed	Mechanically complex	The majority of machines in current service

(1) With the same equipment, the total weight corresponds to vertical flights out of ground effect at om (standard atm)

(2) Ratio of the available rotor power to the mechanical power extractable from the exhaust of the fuselage-mounted engine.

(3) With due regard to the losses involved in running the fan.

(4) In a single-rotor machine, account must also be taken of the power expanded on the anti-torque rotor (about 8%).

(5) The americans have named one of their pulsejet helicopter(American Helicopter xA 5) "top sergeant" because of the waving noise it makes.

(6) Their figures are valid for "tangential" pulsejet lower fuel consumption can be obtained, theoretically, by using "radical" pulsejets.

8.2. ENGINES FOR MECHANICALLY-DRIVEN HELICOPTERS

8.21. PISTON OR TURBINE ENGINES

The case is decided in advance in favor of the turbine engine. It is enough to look at the preceding table and Plate VIII-1 to see why the turbine engine is presently in such great favor. Let us examine its records in greater detail.

a) Much lower specific weight: 0.30 to 0.15 kg/hp for turbine engines at the present state of the art as compared with 0.9 to 0.4 kg/hp for piston engines.

b) Simple engine installation: less space is required, the fan is eliminated, the oil circuit is simplified, etc.

c) Less distrubing vibration.

d) No cyclic irregularity in the drive torque a and therefore better response of the transmission system.

e) Better high-altitude performance (see 4.52).

f) Elimination of engine warm-up makes it possible to start the engine instantaneously.

g) Simplification of pilot handling since the angular speed of the rotor does not have to be closely miontored by the pilot (see 8.221).

h) Increased safety. There are much fewer causes of failure and, most important, they are usually not sudden, and consequently the necessary safety precautions can be taken in time.

On the other hand, the turbine engine is not so favorable in hot weather, and long-duration missions are unfavorable because of its relatively high fuel consumption. Finally, the endurance of these engines is generally lower than that /180
of a good piston engine (it is true that even such an engine is rare in a helicopter, where the working conditions are so severe: fluctuating cooling, prolonged operation at high power, frequent bursts of speed, etc.).

It should be noted, however, that the power per mass, the fuel consumption* and the endurance of turbine engines will not fail to improve long after piston engine technology has reached its peak.

8.22. FIXED-TURBINE OR FREE-TURBINE ENGINES

Let us recall the definition of these two types of engines (see Fig. 8-2). In the former, the turbine engine forms a single spool: power is transmitted directly by means of a reduction gear and is furnished at a rate that can vary only within a very narrow range. In the latter, the energy is supplied by a turbine which is separate from the rotor proper, called a working or free wheel. The power is furnished with high efficiency over a very broad operating range.

There is a lively discussion between the proponents of the two different systems, exhibiting different operational characteristics, which we propose to examine.

8.221. CONTROL AND REGULATION

This is the main subject of controversy, and we will begin by putting the skids to a tenacious legend to the effect that the torque characteristics of a fixed turbine engine make it improper for use in a helicopter. For those who have not

*Some turbine drive systems already have specific fuel consumption rates which are comparable to those of piston engines.

been cured of this prejudice by the highly satisfactory results obtained with this type of engine, let us analyze the problem in some detail.

8.2211. CONTROL AND REGULATION OF A FIXED-TURBINE ENGINE

Plate VIII-3 gives diagrams for the drive and opposing torques as a function of the rotor speed in the case of a fixed-turbine engine. The opposing torque of the rotor (at constant pitch) as a function of the angular speed in parabolic*. The system is stable in motion only if the drive torque increases less with speed than the opposing torque.

It can be clearly seen that the problem of stability is meaningless unless the mode of turbine regulation is defined (and a mode always exists in the broadest sense, namely, that the control parameter is held constant). /181

We studied three typical cases: 1) constant fuel supply (the simplest control mode); 2) constant speed (speed governor); and 3) T_3 constant (this is essentially the case of thermal regulation).

Referring to the four characteristic points of Plate VIII-3 we see that operational stability exists for the three types of regulation at B_1, B_2 and A_2. But thermal regulation is unstable at A_1, while the other two types of regulation are stable. This is the same as saying that a satisfactory regulation system can be found in all cases.

In general, constant-velocity regulation is adopted; it is particularly attractive because automatic control of the angular speed can be assured. Gas control is then eliminated, and the pilot needs only to actuate the collective pitch level to obtain more or less lift at will; the governor takes care of everything else. Let us also mention that the power response of the engine is almost instantaneous.

Remarks

1) Stabilization of the rotor speed at a precise value is of particular importance with this type of turbine engine, which, as has already been said, must operate

*This is not rigorously true if the machine is on the ground. In flight this amounts to neglecting the influence of vertical motion of the machine, an approximation which has been verified by the complete calculation.

within a narrow range. The maximum mode is specified by the mechanical handling conditions of the rotary system. The minimum mode is specified at high power in order to avoid hot starts and compressor surge.

2) This method of control requires perfect functioning of the governor because deviations or fluctuations in rpm may have serious effects on the engine, the transmission or the rotor.

8.2222. Control and Regulation of a Free-Turbine Engine

Plate VIII-4, which gives the drive and opposing torques for such an engine along the easiest method of control to be used, shows that the operational stability is excellent.

If it is desired to maintain constant rotor speed, as in the preceding case, /182
we would have to solve a delicate regulation problem stemming from the response inertia of the generator assmebly (which works at a variable speed)*. But this result is of little practical interest because we will show that with such turbine engines it is not necessary to hold the rotor speed within the narrow limits of a helicopter with piston engines (or with a fixed-turbine engine).

As a matter of fact, while a piston engine has good operating characteristics only at very specific rpm, which cannot be greatly exceeded, at high power such as engine is not capable of ensuring helicopter lift if the rpm is allowed to drop too low. Diagram VIII-5 gives the variation of opposing torque with rpm at constant lift in an actual case of rotor adjustment. The curves for drive torque at full throttle are also given in the case of piston and free-turbine engines.

Case of a Piston Engine

Supposing that the pilot has allowed the operating rpm to drop below n_{min}; it can be seen that it will become impossible to maintain the lift. The angular rotor speed decreases and the helicopter descends: this is "overcoupling", which may cause involuntary touch-down when evolutions are carried out near the ground with a heavy load. This is why pilots are always tempted to turn at

---

The corresponding response time, which is variable, depending on the type, is of the order of a few seconds.

over-velocity, a maneuver which is deleterious to the life-expectancy of the engine*.

Case of the Free-Turbine Engine.

It is evident that the danger of overcoupling is less acute. In addition, it is no problem for the engine to bring the rotor to overvelocity in difficult situations.

Conclusion

Piloting is simplified not only because the rotor speed is maintained automatically constant, but also because the consequences of any possible change in rpm are less embarrassing. On the other hand, experience shows that the power response time in this type of engine is no problem for piloting.

8.222. INSTALLATION /183

As one of the assets of the free-turbine engine note that it does not require a clutch between the turbine and rotor, a component which is relatively heavy and always sensitive.

It is true that in some cases (single-engine machines) it is also possible to eliminate the clutch by using a fixed-turbine engine, proviced a sufficiently powerful starter is installed (starter and battery).

In contrast, one fault of the fixed-turbine engine is that it is bulkier (especially in regard to length) and that the exhaust often follows a more "torturous" path. In some makes the fact that the drive coupling is to the rear of the turbine may also complicate installation.

Remark

In both cases a free wheel must be introduced in the transmission to permit autorotation in the event of engine failure, since the unloaded turbine requires prohibitive power.

---

*A procedure used by pilots to recover rotor rpm in the case of overcoupling is pumping, that is, rapid alternating displacement of the collective pitch and low-amplitude lever. The Americans call this "milking the cow", which is of limited effectiveness when the helicopter is a "calf".

8.223. PERFORMANCE AND SAFETY

With regard to these two factors, the free-turbine engine, which permits considerable variations in rotor speed, may lay claim to the same advantages as the jet engine, which have been mentioned at the beginning of Section 8.1.

8.224. CASE OF MULTIPLE ENGINES

Free-turbine engines are ideally suited for multiple mounting since they require neither clutches or any particular regulation. Appreciable changes in the load of various engines can be tolerated without any inconvenience.

8.225. RECAPITULATION /184

The following table redapitulates the pros and cons of each type.

After having "counted the points" we are tempted to declare a "tie". This is why both engines are being used at the present time and why we can expect excellent (and deficient) machines using these two types.

In spite of everything that has been said, two tendencies can be detected: development of low- or medium-weight helicopters with one or two engines, the fixed-turbine engine being of great interest, since it is light, simple to install, and has an automatic speed governor; the other tendency is to build heavy, multi-engine helicopters.

The free-turbine engine seems to be the better solution, since it is easy to install and control and has better performance, especially when overloaded.

	Fixed-turbine engine	Free-turbine engine
Weight	very light	heavier*
Installation	not bulky	Does not require a clutch
Protection and regulation	Risk of overheating and surging if operated too close to maximum power.	No risk of overheating or surging.

Handling ease	Automatic governing of rotor speed (elimination of throttle). Instantaneous power response.	Rotor speed can vary without disadvantage. Relatively slow power response.
Performance	Better residual thrust recovery (direct exhaust.)	Permits adjustment of rotor speed to each flight situation. Easy overload take-off.
Multi-engine installation		Easier

*The difference tends to disappear with high-power high-gain turbines.

Chapter 9

TECHNOLOGY

/187

The title of this chapter may lead to some confusion. Actually, it is devoted to an examination of how the different components of rotorcraft are constructed, but it will not deal with the technological details. An attempt will be made in particular to present the lines of reasoning which guide designers toward this or that solution.

9.1. AIRFRAME

There is nothing particularly remarkable about airframe design procedures, except that the goal pursued is not always for perfect aerodynamic properties, as can be readily noticed with regard to some of the machines reproduced in the figures. An arrangement in which the principal components are exposed to the atmosphere is often adopted for light helicopters because it lends itself to lightness and ease of maintanance. The frame is made either of soldered steel tubing, closed or not closed, or with a hull of light alloys.

The landing gears deserve particular mention. Up to the present time they have been rigid (simple and light), but this is no reason why retractable landing gears may not become widespread for high-speed rotorcraft, in fact, some current prototypes are equipped with them. The landing-gear configurations are widely varied (Fig. 9-1).

Wheeled, Tricycle or Quadricycle Landing Gears. Here one or several wheels are free to swivel so as to facilitate ground handling, but it is preferable to be able to lock them in operation. Besides, it is better to have locking brakes, especially for touch-down on sloping terrain. As in airplanes, differential brakes are often provided to facilitate taxiing. In single-rotor helicopters equipped with tricycle landing gears, in which one wheel is forward, a tail skid protects the anti-torque rotor, at least in principle, in case of excessively rough landings.

The skid landing gear is much favored for light machines of up to 500 kg total weight since it is simple, light and highly regarded by pilots. It carries small auxiliary wheels (retractable) for ease in ground handling.

To be mentioned also are the special-purpose landing gears such as floats and skis.

9.2. ROTOR HUBS /188

9.21. MAIN ROTOR HUBS

Conventional Hub. We will not dwell long on the design of this hub because it has been the subject of study for quite some time. Each blade is connected to the hub by a three-fold hinge. The structural principle is given in Fig. 9-2. Two typical production models are shown in Fig. 9-3:

a) Blade attached to the hub by means of a strap;

b) Blade attached to the hub by means of a cross-pin Cardan joint whose two axes permit flapping and lag. This type of hub is the one most frequently used at the present time.

See-saw Rotor. This is a configuration used especially for two-bladed rotors. The principle is as follows. Restricting ourselves to first-order flapping, it can be seen that when one of the blades rises, the other descends by an equal amount but phase-shifted by 180°. For the time being let us ignore coning and lagging. Then the blade can be considered as being mounted rigidly on the same centerpiece, which is hinged to the rotor shaft for vertical flapping. Thus we have spared one hinge. In order to guard against the constant flectural forces stemming from lift, the blades are designed in such a way as to give the blades a suitable calculated coning angle. Moreover, this is the solution used with flexible blades whose vertical bending also attenuates the bearing thrust forces. Note that such a rotor can be further simplified by applying the same reasoning to the cyclic control; that is, when the pitch of one blade increases, that of the other decreases by an equal amount. Therefore it will be possible to obtain cyclic control by tilting the assembly of hub and two blades about an axis parallel to the span of the blades, the warp axis. In other words, it will be possible to obtain vertical flapping and feathering by means of a single universal joint (see Fig. 9-4).

Does such a hub require lag axes? Let us assume that the blades are mounted for lag. In stabilized hovering flight the control plane and the tip-path plane coincide, and the blade-hub assembly describes uniform rotational motion about the no-flapping axis. In such a case lag hinges are useless.

On the other hand, in forward flight or when changing course, the tip-path /189
plane and the control plane no longer coincide, and the blades because of coning, no longer describe uniform rotational motion (see Section 3.1). This results in alternating forces being applied to the hub, blades and controls. To eliminate these forces lag hinges are necessary, in theory. In practice, however, they can be avoided by mounting the universal joint about the hub, essentially on a

level with the center of gravity of the rotary system (see Fig. 9-4). It can be easily seen that the alternating forces of inertia are considerably reduced by this expedient, which achieves the equivalent of a rotor with zero coning angle.

In contrast, it is not possible to eliminate individual pitch hinges, because it is necessary to be able to change the collective pitch, by which a special arrangement equalizes the pitch of the two blades relative to the hub.

An example of a see-saw rotor is given in Fig. 9-4,b.

The advantages of such rotors are reduced hub weight because the design is compact and the centrifugal forces on the flapping and feathering hinges are eliminated, and the hinges may therefore be much lighter. Lag hinges and their dampers may also be done away with.

The disadvantages are that residual alternating forces remain in the controls and there is a risk of weaving (see Section 6.32). This is why hubs often require irreversible controls or servo-controls. The latter is true of the Hiller Rotormatic, Fig. 5-4, where the rotor paddles constitute veritable servo-controls.

In addition, the blades must be flexible in vertical bending; if they are not, they must be hinged individually for flapping and the system loses its simplicity.

Floating Hub. This is a hub mounted in such a way that it can rotate in the blade plane, thus eliminating the necessity for lag axes. The result is achieved by attaching the hub to the rotor shaft with a universal joint (Fig. 9-5). This solution, although interesting from a vibration standpoint, is not often used in mechanical systems because of its relative complexity. However, it is just the thing for jet helicopters, where it is sufficient, e.g., to mount the hub on a spherical bearing (see the example in Fig. 9-6).

Rigid Rotor. We have seen in Chapter 3 that the purpose of blade flapping hinges is to reduce to a considerable extent the fatigue forces at the blade socket. Advances in technology allow the consideration of higher working levels. In fact, some designers are presently attempting to develop rigid rotors for light helicopters. In reality, the problem involved here is rather semi-rigid rotors, since the flexibility of the mounting method appreciably attenuates the /190
bearing thrust forces.

Of primary importance is the substantial technological simplification achieved by eliminating the flapping and lag axes. Other advantages are the elimination of ground resonance problems and the gyroscopic stability conferred on the helicopter by the rotor.

On the other hand, such a design leads necessarily to an appreciable increase in the rotor weight. This is the price paid for simplification, and precautions must be taken to prevent the introduction of excessive control moments on the rotor, especially when the machine is on the ground.

9.22. ANTI-TORQUE ROTOR HUBS

These hubs are comparable to those of the main rotor, i.e., conventional, see-saw, and floating, but they do not have lag hinges, for reasons of simplicity (because of the small rotor diameter, the alternating lag forces applied from the blades are much less critical).

9.3. BLADE ATTACHMENT

The conventional solution is to provide the feathering hinge with ball or roller thrust bearings to take up the centrifugal force. We have already mentioned the poor working condition of these bearings, since the powerful forces and the small clearance result in scoring of the ball races and in stiffening the controls. We have the resort to over-size extra-quality bearings, and consequently they are expensive, heavy and bulky.

For these reasons some designers bypass such bearings by taking up the centrifugal force with torsion bar concentric to the spindle or with leaf springs. See, for example, the hubs shown in Fig. 9-7 (torsion bar), 9-3, a, and 9-6 (spring attachment). In the case of Fig. 9-6 the leaf springs also allow vertical flapping. Attempts have also been made to use cables, but it is almost impossible to keep them from gradually stretching during service, despite precautions.

9.4. HUB ACCESSORIES

Drag Dampers

Drag dampers are of two main types: friction (see Figs. 9-3 and 9-7) or viscous (see Fig. 9-3,b). The former are simpler and lighter, but of mediocre efficiency and reliability, and therefore hydraulic dampers are usually preferred. The latter are double-action and have valves which limit the forces applied to the blade. Most frequently they have an oil reserve for automatic compensation of leakage.

Despite their basic simplicity, such cables, which are designed to counteract ground resonance (see Section 6.2), must be made with precision. They are difficult to attach to the blades, because perturbing forces are transmitted to the cyclic pitch stick. For one example see Fig. 9-3,a. This type of equipment is tending to disappear in modern rotors.

An analogous function is sometimes fulfilled by elastic inter-blade ties (see the example in Fig. 9-7).

9.5. BLADES

If we recall the numerous sections, namely, performance, vibration level, forces in the controls, and safety, in which the blades played an essential part, it will not appear exaggerated to say that the first condition to be fulfilled in making good helicopters is to make good blades. This is why designers devote, or should devote, so much care to their manufacture.

9.51. GENERAL DESIGN PRINCIPLES

Because of their conditions of operation and use, the blades must be designed with a view toward respecting a certain number of general rules, the main ones of which are outlined in what follows.

Strength. The blade is a vital component operating under alternating forces. Therefore, manufacturing procedures which may be injurious from a fatigue point of view are prohibited; pitting, stress concentration, and contact erosion must be meticulously avoided. This explains why almost nobody assembles blades with rivets or bolts and why cementing is becoming more and more popular (wood-to-metal and metal-to-metal).

A particularly sensitive region of the blade is the region of strap attachment. The assembly method must be carefully studied with a view toward maximum possible distribution of forces; the links are bevelled, the bolt holes are precisely drilled, plastic films are placed between the metal surfaces which are susceptible to contact erosion, etc.

We have seen in Chapter 7 that alternating and constant flectural forces are high at 20% of the radius. In case the blade is anchored in this region (this is the case, e.g., of the hub shown in Fig. 9-3,a), extra precautions must be taken.

Precision

Blade fabrication is a high-precision task insofar as mass and geometry are concerned. The tolerances imposed are comparable to those in practice for propellors. Precision is necessary for two reasons: 1) the airfoils must have good aerodynamic qualities, i.e., low C_{xp} and sufficiently high $C_{z\ max}$; and 2) the blades must be as identical as possible. In fact, we have shown that blade identity has a considerable influence on the vibration level of the helicopter (see Section 6.1). /192

In Section 9.52 we will return to the principal characteristics to be respected in this regard.

Chordwise Centering and Placement of the Feathering Axis

It was demonstrated in Section 6.31 that to avoid disturbing or dangerous effects on the blades and controls, it is necessary to align the feathering axis, the aerodynamic and elastic centers and the center of gravity of the blade elements, insofar as this is possible.

This means in practice that the chordwise center of mass of the blade element is located at the 20/25% chord point. For this reason, the way in which a rotor blade is produced must be very different from that of a propellor; the structure is composite, the forward portion being heavy, the rear portion as light as possible.

Thus, J. Shapiro [1] illustrates the structural repercussions of this centering requirement. A hollow blade with an envelope of uniform thickness is centered at the 48% chord point, and a solid blade at 41%. A blade having a tubular steel spar and an aluminum covering of uniform thickness is centered at about 32%. Based on this configuration, any forward displacement of 1% from the centering point (by weights placed at the leading edge) results in a 10% increase in weight. When the blade is centered at 22%, its weight doubles.

Characteristics Associated with Use

The blade must suitable resist humidity and erosion. The leading edge of the outboard part of the blade must be protected against erosion from rain or dust. For this reason it often has a sheath made of stainless steel. Finally, in service the blades must not be subjected to excessive deformation, or they must at least have the necessary control devices to compensate for such deformation. When rotors consist of more than two blades, the latter are usually fixed to the hub in such a way that they can be folded back, thus saving on parking space.

9.52. BLADE CONTROL AND ADJUSTMENT

The principal structural parameters which characterize the "identity" of blades and which consequently must be precisely respected are as follows.

Mass Characteristics

The essential characteristics are the spanwise static moment (with respect to the center of the hub) which governs the static balance of the rotor, and the spanwise, and above all the chordwise placement of the elastic flapping center, /193
which govern the forces in the controls and their stability.

The secondary characteristics are the weight, the chordwise static moment, and the moment of vertical flapping inertia.

Aerodynamic Characteristics

Care must be taken with respect to the airfoils (thickness and curvature) and with respect to the blade setting as a function of the span (twist).

The precision required is such that, despite the care taken in fabrication, it cannot be obtained except by special adjusting expedients. For the mass balance these expedients are small counterweights, usually placed at the tip of the blade, the size and chordwise emplacement of which are varied. For aerodynamic adjustment tabs are used or else the trailing edge is reshaped. In addition, the setting of each blade can be adjusted with respect to the hub (usually by adjusting the length of the pitch control arms).

The current tendency is for final control and adjustment of the blades on a rotating test bench equipped with a hub similar to the one of the helicopter. The moments about the feathering axis are measured at different rpm and angles of attack and are then compared with reference values.

In service the adjustment of the blades is checked by "tracking". The machine is fastened to the ground, in a calm wind, the blades are rotated at different collective pitch values, and it is observed whether all the blades describe the same plane. This is done either by sight or by the "flag" method, whereby the blade tips are coated with paint or chalk of different colors and, while rotating, are made to brush a piece of fabric stretched over a frame. This makes it possible to determine the discrepancies existing between blades and to make the appropriate corrections.

Improved instruments that permit observation of blade motion in flight are beginning to be used.

The ideal from the maintenance point of view would be to have individually interchangeable blades. This is still an exceptionable event, and almost all blades presently in service must be balanced for mismatch.

9.53. STUDY OF VARIOUS TYPES OF BLADES

The first blades made for helicopters were of the mixed wood-metal type with a tubular spar and ribs covered with plywood and fabric (Fig. 9-9, a). This construction is light and easily adaptable to any laws governing plan form, thickness and twist.

But such blades have many disadvantages, and therefore they have now been abandoned. Among these disadvantages are high manufacturing cost, mediocre airfoil precision and poor surface appearance (their "ribs" can always be seen) and, above all, deformation during service.

Figures 9-9 B and C, show two types of wooden blades, one solid and one hollow. (The metal strip seen in Fig. 9-9 B, does not contribute to the strength, but serves to ensure correct chordwise centering.) These blades, despite the use of select impregnated wood, exhibit to some degree the disadvantages mentioned above. This is why the majority of constructors have now turned to metallic construction, several types of which we will describe. /194

Figure 9-9, D and E, show two aluminum alloy blades with forward parts consisting of a cast spar and an aft part of alloyed honeycomb spar units.

In the type shown in Fig. 9-9, E, the units are thermocemented to the spar. In the type shown in Fig. 9-9, D, however, which corresponds to a blade for a jet helicopter, the Djinn, the compressed-air temperature would impair the strength of the cement, and therefore the trailing edge is attached to the spar by piano-wire stringing. Note also the conical shape of the airfoil at the blade socket, which was formed by forging.

Figure 9-9, F, shows one type of design with a solid spar and all-round covering.

Figure 9-9, G, shows a metal blade with a forward part consisting of a steel spar, which is more favorable from the fatigue standpoint than duraluminum.

New techniques are continually cropping up. Some manufacturers are making steel blades in which some components are put together by arc brazing.

Others are trying to use fiberglass/resin complexes, either for the trailing edges or for the entire blade.

To conclude this rapid study, let us note that the present tendency is to develop cylindrical designs, of constant thickness and chord, to facilitate fabrication, since the slight losses in induced efficiency are largely compensated by the gain in drag due to precision in shape and surface smoothness. Twisting is generally useful and does not present any appreciable difficulties.

9.54. ANTI-TORQUE ROTOR BLADES

The engineering problems connected with anti-torque rotor blades are comparable to those of the main blades. There are, however, a few deviations from the general principles outlined in 9.51, especially in regard to light helicopters. In particular, it is not always certain that the chord point will be centered in line with the aerodynamic and elastic centers. This lack of strict adherence to the rules is justified (sometimes) because the anti-torque rotor is thin, the blade bending is less pronounced, and cyclic control is absent.

9.6. FLIGHT CONTROLS /195

We will treat only cyclic and collective pitch control of the blades. Depending on the case, such controls are handled by two types of arrangements which are identical in principle, but differ in technological aspects.

The swashplate and the spider are shown, respectively, in the diagrams of Figs. 9-10, a and 9-11. The collective pitch is varied by raising or lowering these and the cyclic pitch by varying the orientation.

Design examples for the swashplate can be found in Fig. 9-10,b, and for the spider in Figs. 9-6 and 9-7. These components are connected to the flight controls by appropriate kinematic combinations, depending on the type of helicopter. We have already seen in Chapter 1 how the cyclic and collective pitch stick functions in a single-rotor machine (see Section 1.316). Figure 9-12 gives the control principle for a tandem two-rotor machine.

In all cases we have no choice but to introduce auxiliary assemblies designed to obtain suitable force conditions in the control systems so as to avoid any possible instability and to attenuate vibration. Among these assemblies are friction governors, which can often be adjusted in flight, viscous dampers, pendulum dampers (see Section 6.13), irreversible systems, and force-compensation systems (springs, bungees, or even pneumatic jacks in turbine helicopters). In most cases they can be adjusted in flight. In machines of a certain

gross weight the preceding arrangements are completely or partially eliminated by the use of irreversible servo-controls.

9.7. TRANSMISSION /196

Reduction Gears. Since the rotors have angular speeds of 400 to 150 rpm, while the engine or turbine outputs have speeds of 2,000 to 6,000 rpm, the reduction ratios are usually between 10 and 20. In other words, several reduction stages are required, but the number of stages hardly ever exceeds four. Most often epicyclic gears with one or stages are used. This is the most compact and the lightest solution, an example of which is shown in Fig. 9-8. An example of a different type of reduction gear is shown in Fig. 9-7.

Clutches. The clutches are by preference of the centrifugal type, a system which is more gradual at a rate which is not left to the whim (sometimes disastrous) of the operator. The operation may be either dry (as in an automobile) or wet (oil). The response to rotational speed is controlled in most cases by means of governor weights which react to the centrifugal force; and example is shown in Fig. 9-13. Note also the original design of a mercury clutch given in Fig. 9-14.

Free Wheels. Except for rare cases, free wheels make use of the load-equalizing principle. Figure 9-15 shows an example of one type.

Jet Helicopters. Insofar as jet-driven rotors with fuselage generators are concerned, the essential power transmission component is the hub arrangement for transmitting the fluid. A typical example is the arrangement used in the Djinn, which is shown in Fig. 9-6.

9.8. OPERATIONAL EQUIPMENT

We must still describe some of the equipment which enables the helicopter to carry out the various tasks of which it is capable.

Winch. This item of equipment enables a helicopter hovering above a site where it cannot land to hoist men or material on board. The nominal characteristics of a winch are as follows: 1) cable about 30 m long; 2) hoisting rate of 0.5 to 1 m/sec; and 3) capacity of 100 to 300 kg, depending on the model. /197

The conventional arrangement consists in a hydraulic engine drive. In the case of helicopters with turbine engines, a light and neat solution consists in using a compressed-air engine supplied by tapping the turbine. A shearing

device makes it possible to cut the cable in case of danger, e.g., if the cable gets hung up on an obstacle, if the load balance becomes uncontrollable, etc.

Sling. This component makes it possible to carry bulky loads attached under the fuselage. The load can be dropped in two ways, either manually by the pilot, or automatically by releasing the sling when the load reaches the ground.

Medical Evacuation Equipment. In helicopters of sufficient total weight, the way in which the fuselage is outfitted for such a task is similar to that of an aircraft. For light helicopters, however, where the cabin is not spacious enough to accomodate stretchers, pods fixed to the side of the fuselage fulfill the same purpose.

Rotor Brake. The purpose of the rotor brake is to bring the blades to a quick stop and to keep them immobile while stopped. This accessory is especially important when there is a high wind, primarily for loaded helicopters. For an example see Fig. 9-7.

Blade De-icers. This place of equipment is on the agenda, but has not yet become a mass-produced item with Western manufacturers. Some Russian helicopters, however, have been equipped with a liquid de-icing system. One example is given in Fig. 9-18.

9.9. INTEGRATED DESIGN /198

Perspective drawings illustrating a few typical designs can be seen in Figs. 9-16, 9-17, 9-18 and 9-19.

Chapter 10

SYNTHESIS

/199

This chapter, the last of the course to be devoted to the unadultered helicopter, calls upon the body of knowledge acquired up to this point to intercompare the various helicopter designs, to "take a fix" on present techniques and to look briefly at the new trends.

10.1. THE VARIOUS TYPES OF HELICOPTERS

In what follows we shall review the inherent advantages and disadvantages of the various designs already discussed briefly in Chapter 1.

10.11. MECHANICAL HELICOPTERS

These are the most widely used by far because of the flexibility in use made possible by their moderate fuel consumption.

Single-Rotor With Anti-Torque Propellor

This is the most prevalent model, particularly among the light- and medium-machines (although very large machines of this type do exist). Its simplicity and light construction are the major reasons for its success. We note also that it can quite easily be given acceptable flight qualities. Some criticisms of this helicopter are:

(1) Loading Conditions: Since the center of gravity must remain near the rotor axis, some loading precautions must be taken, such a load distribution or compensation by suitable counterweights. (On light machines this if often accomplished by providing several battery locations,)

(2) The shape of the ensemble is generally not good aerodynamically (long tail), which gives it mediocre aerodynamic efficiency in forward flight.

(3) Finally, and most important, "in cauda venenum", as the Ancients would certainly have said had they known such a device. The tail rotor is indeed the source of a number of aggravations in use. It is dangerous to personnel moving about the machine, there is danger of its striking the ground or obstacles during operations in difficult terrain, and the adverse conditions under which it operates (high vibration level) makes it quite difficult to realize good mechanical integrity.

Meshed, Side-By-Side:

This design is quite like the single-rotor just discussed, but we note in its favor that it has to anti-torque, that the fuselage design is cleaner and that it possesses very good handling properties (low inertia in pitch) and better aerodynamic efficiency in level flight.

On the other hand it is obviously somewhat more complex mechanically, and it is rather tricky to give it good on-course stability due to its short tail (see 5.21). Finally, yaw control on this type machine is essentially established by differential variation of the engine torques applied to the two rotors. This mode of control is characterized by a sluggishness of response that can be inconvenient in autorotation at low speed.

This design, little seen today, could perhaps come back into favor.

Side-By-Side, Not Meshed.

This design differs from the meshed design in being less compact from the structural and mechanical viewpoint, and therefore heavier. Theoretically, this configuration is the best from the standpoint of "induced aerodynamic efficiency" in level flight (see (3.15). However, the gain in performance resulting from this is in practice partially or totally compensated by the drag of the arms exhibit interference phenomena near the ground that can create problems as regard flight properties.

Helicopters of this type are not presently in service.

Coaxial:

This design can be given a fuselage of good aerodynamic efficiency and excellent rotor efficiency in hovering (see 3.15), but it has many defects, among them its heavy, complicate and bulky mechanisms (transmissions and controls).

Moreover, it has a special fault of aerodynamic origin, of which we shall give some details: We saw in Chapter 3 (3.2141) that a hinged-rotor tilts to one side at low forward speeds because the retreating blade rises due to the inequality in the distribution of induced velocities. In the coaxial design, with rotors revolving in opposite directions, this results in a drawing together of the two rotor discs at low velocities, with danger of the blades striking each other. To avoid this the rotors must be spaced far enough apart and this makes a veritable "giraffe" of the machine. The weight estimate and aerodynamic efficiency in forward flight make this appear far from profitable. In addition, as with the

meshed side-by-side and for the same reason, control in yaw is sluggish in autorotation at low speed. /201

This design appears to have been abandoned today other than for special applications.

Double-Rotor in Tandem:

This design has some important advantages; it has a roomy fuselage and is very tolerant with regard to aerodynamic centering. It is in truth a "flying bus", which can be a valuable property for many applications. For a given gross weight its rotors and reduction gears can be somewhat smaller than those of the single-rotor design, and this is appreciable for large machines. For example, the tendem Bristol 173 results from mounting two engine-transmission rotor units identical to those of the Briston single-rotor 171 at the two ends of the fuselage. Finally, its streamlined shape makes the airframe suitable for high speeds.

Unfortunately, there are some clouds in this picture. The design is rather complicated due to the dispersal of the mechanical units (synchronizing transmissions for the two rotors, unification of controls, etc...).

Its structure and mass distribution are favorable to the appearance of variable zones of vibration or ground resonance.

Good flight properties are difficult to obtain in forward flight due to rotor interaction, high inertia, yaw instability of the fuselage, etc...

The weight of this helicopter design compared to that of the single-rotor is a debatable matter. It is generally admitted that the single-rotor is less heavy for small loads and, on the other hand, that beyond 5-7 tons of total weight the tandem presents a slight advantage. The mere fact that the question remains open proves that the weight differences are not decisive in choosing between the two.

To sum up, this design is preferred for large loads, where it can give excellent results, but it is not within anyone's reach.

Helicopter With More than Two Main Rotors:

These designs seem to have been completely abandoned because of their enormous complexity. As the most recent example we can mention the Air-Horse

prototype with three identical rotors, which was designed in England by the La Cierva Company but whose development has not been pursued.

10.11. JET HELICOPTERS

It was pointed out in Chapter 8 that jet helicopters are by nature short-endurance machines that cannot compete with the mechanical helicopter in all its uses.

The rocket, ram- and pulse-jet-machines are set apart for very special applications such as sport or one-man helicopters. /202

The machines with combustion at the blade tips, although there is some interest in them from the standpoint of payload transported over short distances, are much handicapped by their noise, which practically inderdicts their entry into inhabited areas.

The disign most likely to take its place alongside the mechanical helicopter is the blade-tip pod-jet without post-combustion. If this concept is economical and simple to build, and convenient and robust in use, it could be a valuable runabout or air-jeep for certain tasks. Another interesting application of the jet is in the construction of very large tonnage cranes, where the mechanical solution is difficult and in any case very expensive.

10.2. CHOICE OF STRUCTURAL CHARACTERISTICS OF THE ROTOR

Certain of these characteristics, such as solidity, nature of the blade profiles, twist, plan form of the blades and to a lesser degree tip speed, are essentially set by performance considerations (see Chapter 4). On the other hand, two parameters having considerable influence on the design of the helicopter must be fixed by compromise between the conflicting demands. These are the rotor diameter (or the disc loading) and the number of blades.

10.21. CHOICE OF ROTOR DISC LOADING

The objective of every designer is to create a physical implement that is as "profitable" as possible. Of course this "profitability" cannot be rigorously described by some absolute number; it depends strictly on the conditions of use. However, one factor that is always critical in this respect is the "structural efficiency", defined as the ratio of the payload to the empty weight (it expresses, more or less, the way the material making up the helicopter is utilized). Hence

it is always desirable to obtain a high value of this ratio (or the ratio of payload to total weight, which varies in the same sense).

It is easy to see for a given state of airframe and engine engineering that the choice of the diameter of the rotor (or torors) will have a considerable effect on the weight specification, as Plate X-1 illustrates quantitatively. In practice, of course, many other parameters enter (the load, for example) so that such a graph should be considered to be a simplified demonstration.

Expressed in percent of total weight it includes: /203

— The weight of the airframe and equipment, essentially independent of G/S, the rotor disc loading.

— The weight of the transmission plus tail rotor (if it exists), also almost independent of G/S, which might seem surprising since the power to transmitted to the rotor varies as $\sqrt{\frac{G}{S}}$. The explanation of this paradox is that at constant tip speed (fixed by aerodynamic considerations) the engine torque to be transmitted to the rotors is constant. The factor determining the transmission weight, then, is the torque.

— The rotor weight, which decreases with S, as is quite understandable.

— The weight of the engine and its appurtenances, which varies as $\sqrt{\frac{G}{S}}$. Different curves of engine weight have been plotted: piston engines (1.2-0.7 kg/hp: present turbines (0.4 - 0.2 kg/hp; "future" turbines between 0.2 and 0.1 kg/hp. The last value is quite futuristic and should be considered to be a limit that will not be attained in the near future.

The sum of all these partial weights represents the empty weight of the helicopter. The payload if the difference between 100 and the empty weight.

It is seen that for a given engine the payload passes through a maximum at a larger value of G/S the smaller the specific weight of the engine. For piston engines this maximum occurs between 7 and 20 kg/m^2 and for "future" turbines between 40 and 100 kg/m^2.

As pointed out at the beginning of this section, a rotor disc loading near that corresponding to maximum payload is desired. However we note that the curves are quite flat, so that some latitude is available to cover the special needs of each program.

A more compact machine is obtained by adopting a disc loading higher than the optimum, and it is less clumsy and faster in cruising flight (as we shall show in Section 10.31).

On the other hand, if a disc loading less than the optimum is chosen, the fuel consumption in slow flight is reduced (low induced power). /204

All things being equal, the autorotation properties improve with a smaller disc loading.

The statistical diagrams given in Appendix I show the values adopted in practice. A steady trend with time is noted toward higher values of rotor disc loading and, correlatively, the power specified. In view of the earlier considerations, this is explained by the progress made in engine technology (increase in power/weight ratio).

10.22. CHOICE OF NUMBER OF BLADES

The number of rotor blades is relatively unimportant from the standpoint of performance (what counts here is the solidity, or, stated differently, the total blade surface). The choice is made taking the following factors into account.

Arguments in Favor of a Large Number of Blades:

— The rotor efficiency is somewhat improved (see 2.1322).

— The vibrational forces transmitted to the airframe and controls are reduced (see 3.312); this is of special interest for fast helicopters (see 10.3).

— Better production facilities for the large machines.

Arguments in Favor of a Small Number of Blades:

— Lower rotor weight.

— Easier to fold up on the ground.

Most present rotors are three-bladed. Light helicopters are often two-bladed for reasons of the simple and light construction using the "SEE-SAW" hub (see 9.21) which, moreover, suppresses the annoyance of ground resonance and reduces the space occupied on the ground without removing the blades.

Medium- and heavy- helicopters usually have 4-, 5-, or 6- blade rotors and the present tendency is to increase the number of blades.

10.3. ADAPTATION OF THE HELICOPTER TO RAPID FLIGHT

/205

Fast flight with a helicopter brings with it problems of two sorts:

(1) Available Power: The mediocre aerodynamic efficiency of the helicopter causes the power required for flight to increase rapidly with speed. Apart from all other factors, the cruising speed is thus limited by the maximum long-term power that can be furnished by the engine.

(2) The aerodynamic and mechanical behavior of the rotor operating with a high parameter of advance:

— Retreating blade tip-stall (see 3.216).

— Compressibility at the blade tips, which shows up not only at the tip of the advancing blade, but also in the area of the retreating blade where the critical Mach number is lower due to the high angles of attack.

— Blade flapping, which becomes severe and rich in higher harmonics at high values of μ.

The aggregate of these phenomena adds up to an increase in power required, to a higher level of vibration and finally to control difficulties.

We shall now examine what can be done to reconcile best these various limitations.

10.31. IMPROVEMENT OF THE POWER RATIO

The solution for this is evident - reduce the power needed and increase the power available.

The fuselage drag consumes most power in cruising flight. The poor aerodynamic design of the standard fuselage has already been mentioned in Chapter 2; a theoretical investigation of fuselage shapes is needed. Parasitic drags must be reduced as much as possible. It is especially profitable to make use of a faired- or retractible- landing-gear.

As for increasing the power, its only drawback is to tax the weight estimate. In the last section we saw that the use of engines of low specific weight theoretically leads to an increase in rotor disc loading and therefore to an increase in the power requirement.

We shall show that this leads to a power ratio favorable to the attainment of high cruising speeds. /206

As a matter of fact we see from Plate X-2 (contrary to the situation in hovering flight) that the power required for cruising flight depends only slightly on the rotor disc loading since the induced power here is relatively low. The diagrams show the net gain in cruising speed resulting from the increase in G/S. The gain is even more marked if turbo-engines are used since they can be used at higher cruising powers than can piston engines. (In the example selected we have taken 90% of the maximum power for the turbo-engine against 80% for the piston engine.) The diagrams shown also the benefits to be expected from improving the aerodynamic efficiency of the fuselage when high flight speeds are reached.

10.32. ADAPTATION OF ROTORS TO HIGH SPEEDS

Essentially this the problem of avoiding the troublesome retreating blade stalls. In Chapter 3 (3.216) we saw that retreating blade stall appeared at a critical value of the parameter of advance $\mu = \frac{V}{u}$ as a function of the mean C_Z of the blades (porportional to $\frac{f_N}{\sigma}$).

The relationship $\frac{f_N}{\sigma} = \frac{2F_N}{\rho S \sigma u^2}$ indicates the direction to go to obtain a critical speed V as high as possible for a given lift:

(1) Increase u: This is an efficient method. $\frac{f_N}{\sigma}$ decreases, and for a given velocity V the value of μ is reduced. Unfortunately the increase in u is limited by the need to avoid too-pronounced compressibility effects.

(2) Increase $S\sigma$: This means to increase the blade area, either by increasing the solidity or the diameter.

These two solutions have the drawback of requiring power, since the drag power of the blades rises as the mean operating angle of attack of the blade profile decreases.

This says that to attain high speeds without stalling it is necessary to make sacrifices in the aerodynamic efficiency of the rotor in forward flight and

accept a loss of efficiency in hovering in case the rotor speed cannot vary over wide limits (operation at values of $\frac{f_N}{\sigma}$ much lower than optimum).

In conclusion we recall some steps to be taken to improve the behavior of the rotor with respect to stalling: /207

— large blade twist

— use of blade sections with very high maximum C_z

— operation with a small axial flow $V_z + V_i$. Since this axial flow is a function of the propulsion component required of the engine, the reduction of fuselage drag is here also a favorable element.

— use of rotors having a large number of blades (since the limitation to speed caused by retreating blade stall can generally be traced to the appearance of a prohibitive level of vibration.

In summary, the efficient way to increase the cruising speed of helicopters is to combine aerodynamic refinement of the fuselage with a power installation that is adequate to permit adaptation of the rotor to the expected flight conditions. We shall quote some figures to fix these ideas: The present speed record is 350 km/hr (Sud-Aviation SA 3210) and the cruising speeds of service helicopters is between 100 and 250 km/hr.

10.4. DISADVANTAGES OF THE MODERN HELICOPTER

It is only necessary to re-read the earlier chapters and the beginning of this one to come up with an impressive list of grievances. If we pass over its appearance, which is not usually particularly aesthetic, the grievances can be grouped under four major headings:

(1) The helicopter is a complicated and delicate machine, with the attendant consequences. Its first cost and upkeep are high, and to maintain it in service requires an extensive organization and highly-qualified personnel.

(2) Its performance with regard to load carried, service ceiling and speed is inadequate for certain applications.

(3) From the piloting standpoint these machines require special training and are fatigueing because of the unremitting attention they demand and the mediocre comfort due to vibration. Instrument flying at present cannot be done in an up-to-date way. These disadvantages evidently run counter to an intensive use of personnel and material.

(4) Its safety with a single engine is only moderate. This is especially disturbing to civil operations subject to the constraints of routes and clearances not always easy to find in inhabited areas.

10.5. MAIN MODERN TRENDS IN HELICOPTER DESIGN /208

For the designers this is obviously a question of eliminating the defective points brought up by the users (and which have been summarized in the last section) and to develop models that have better economic factors and performance.

10.51. USE OF TURBO-MACHINES

This is the most significant technical improvement since it alone permits improving the helicopter in almost every point where it is critical. The many advantages this machine offers in theory have been studied in detail in Chapter 8 (see 8.21). The advantages are so positive that at present hardly any piston-engine helicopters are under development.

Let us emphasize once again the profound conceptual modifications to the helicopter brought about by the adoption of the turbo-engine: High power, high rotor disc loading, high tip velocities (simplification of transmission and adaptation to rapid flight).

10.52. SIMPLIFICATION AND RUGGEDNESS

In this area we are in good shape, since designers are now at the stage of knowing how to make mechanical components that will stand up under the demanding performance required by the helicopter.

Although at present the major units have overhaul times of the order of 200-600 hours and must often be replaced before this, one can hope to obtain machines capable of going 1000 hours without overhaul in the near future. At least this is what is now being written into many specifications, and the result seems more creditable if it is considered that it corresponds to something like 50,000 kilometers between overhaul for an automobile. The automobile reached this point only recently, although its working rate is much lower.

10.53. INCREASING THE CRUISING SPEED

The methods that can be used to increase cruising speed - increased power and proper streamlining of the airframe - were discussed in Section 10.32. We

have also seen that in theory the use of turbines leads quite naturally to relatively fast machines.

This explains why helicopters now under development generally have cruising speeds in the range of 200 - 300 km/hr.

However, it is appropriate to stress that the inherent limiting factors of standard hinged rotors apparently will not permit attaining speeds of more than 300 km/hr without heavily penalizing its other properties. This is why research is underway to apply "revolutionary" methods and to develop new types of rotorcraft that are better adapted than the helicopter to rapid flight. These new rotorcraft will be discussed briefly in the next chapter. Let us sketch the revolutionary approaches that are capable of improving the pure helicopter. These methods aim at raising the critical stall value $\left(3\frac{f_N}{\sigma}\right)$. with respect to the mean angle of attack of the rotor blades. /209

Blowing of the profiles (at the leading or trailing edge).

This blowing, by increasing (perhaps substantially) the maximum C_z of the blade profiles, inhibits the appearance of detachments.

The method is particularly well adapted to blades driven by thermo-propulsion with low pressure gas. The fluid is available, and using it for not only does not take power, but economizes on it (improvement in aerodynamic efficiency of the blade profiles by the "ejector effect"). Its application to mechanically-driven rotors is also under study.

In the same category, tests of blade profile hyper-lift by suction have also been made, but apparently this is less promising.

Multi-Cyclic Pilotage

The basic idea here is to introduce cyclic pitch control of the blades at the rate 2ω so as to reduce the lift of the blades in the advancing and retreating positions and to increase it in the fore and aft sectors (see Fig. 10.1). The rotor is thus compelled to lift in regions where the aerodynamic dissymmetry is small and is relieved of this task in the difficult regions. To obtain a positive result by this procedure may seem to contradict the demonstration of Chapter 3, where it was shown that to a first approximation the torques, and therefore essentially the blade lifts, are constant during rotation with a rotor having flapping hinges. But it is not at all contradictory. The demonstration was based on the fundamental relationship

$$I_p\left(\ddot{\beta} + \omega^2\beta\right) = M_{aérodyn.}$$

The first term of this expression is constant only if β flaps at the frequency ω (the natural frequency of flapping at moderate speeds of advance and with "monocyclic" control). But if flapping at a rate of 2ω is induced by a cyclic pitch control, the first term is modulated at this frequency; this is also true for the lift and angle of attack, which may thus be reduced at the desired locations. It is possible to go further and seek a law of multi-cycle variation in 2ω, 3ω, etc... that is optimum from the standpoint of flutter and aerodynamic efficiency. /210 However it may be asked whether such a procedure could really succed: The wing-tip stalls are annoying primarily because of the vibrations they excite, and could not the creation of flapping at 2 and 3 to be remedy worse than the disease from this point of view? Any calculation of the matter is deceptive and only experience will permit making a judgement. Moreover, apart from the mechanical complexity, which does not seem excessive, there is still another objection to be made. Although the forces of monocyclic pitch variation are small because the natural motion of the blade has a frequency very close to the rotor rotation, these forces become large when pitch variations are made at higher frequencies. This introduces large forces into the control elements.

Use of Vertical Flapping Hinges With Large Offsets.

The effect of such an arrangement is to make the natural angular frequency of flapping of the blade somewhat higher than ω. The law of constancy of torque during rotation is no longer valid and the blade behaves with respect to the periodic inputs in ω as if it were semi-rigid. It is easily seen that this results in a decrease in the angles of attack in the region of the retreating blade.

The disadvantage of this solution is that it becomes heavy from the structural viewpoint (hub) and has some vibration problems.

We point out that the "revolutionary" methods we have just examined are as yet merely in the study and preliminary trial stage.

The Derschmidt Rotor

Suppose that the blade were to be subjected to large-amplitude flapping around its lag hinge such that its angular velocity slows down in the advancing position and increases in the retreating position. The modulation in relative airspeed due to the forward motion can thus be compensated, which equalizes the angles of attack over the rotor disc. For a normally mounted blade, such as arrangement is out of the question due to the enormous forces that must be applied at the blade socket to obtain the desired motion. This difficulty can be avoided by an artifice that consists of making the natural frequency of the

blade in lag equal to the rotor rotation. The control forces under these conditions can be very small. This is obtained by a large offset of the lag axis, of the order of 40% of the radius. This is the principle of the Derschmidt patent that allows its author to claim the possibility of speeds in the range of 400 - 500 km/hr.

The device itself is in the research stage and should very soon be undergoing flight test on an experimental machine (Belkow Company) in Germany.

10.54. IMPROVEMENT OF FLIGHT PROPERTIES AND APPLICATION POSSIBILITIES

/211

A substantial effort along several lines is underway, including studies of stabilizers and automatic pilots, development of navigation methods adapted to the helicopter and equipment for all-weather flying (blind-flying gear, rotor deicers, etc.).

10.55. EXTENSION OF THE GROSS WEIGHT RANGE

Let us refer back to Fig. 1.30 and inspect the categories that go beyond those already in service.

The medium- and heavy- transports are already represented by operational machines that are even beginning to be delivered in quantity, such as the SIKORSKY S 56 and the Soviet helicopter of comparable weight, the YAK 24. The machines in this category are multi-engined.

Over and beyond these machines are the crane helicopters designed to manipulate very heavy loads.

At the other end of the scale is the appearance of the one-man helicopter.

The development of these two latter types faces several difficulties. Specifications and crane helicopter projects are being established, mainly in the United States. Hook loads of 10, 20 and even 50 tons are freely mentioned. The extrapolation of present engineering techniques meets with great difficulties, both technical and financial. As already mentioned, this is why the use of jet propulsion can be of interest.

Despite what it may seem the one-man helicopter also poses a large-size problem. The difficulty is not to construct and to make fly such a machine. Many prototypes, conceived in various designs, have flown successfully, but none has met all of the conditions set by the users, as follows: (1) It should be

very inexpensive, (2) easy to fly and maintain, (3) safe, (4) not clumsy and easy to handle on the ground and (5) be, in fact, a helicopter.

The reader is by now aware that the fifth condition seems incompatible with the first four. /212

This is of course why the one-man helicopter cannot be a scaled-down standard helicopter, but rather must be a specially-designed machine.

The "flying platforms", some prototypes of which are flying in the United States, represent an attempt in this direction. Furthermore they are only in the prototype development stage and some serious problems remain to be solved.

10.56: CIVIL TRANSPORT MACHINES

For some time designers of heavy helicopters have sought to meet the special requirements of civil transport. Although very divergent opinions still exist on this subject, some general conditions to be met can be distinguished:

(1) First, they must be large enough to be economically profitable. The 25- to 40- place types would seem to meet immediate needs.

(2) They should be sufficiently fast and capable of IFR flight for scheduled operations. There is general agreement that the speed should be between 200 and 300 km/hr.

(3) They should be multi-engined in the interest of safety. The trimotor configuration seems to be the best compromise between complexity and safety.

Chapter 11

NEW TYPES OF ROTORCRAFT COMPETITORS OF THE HELICOPTER

/213

Earlier chapters have dealt almost exclusively with the helicopter, the only rotorcraft in general use at present. If only to justify the title of this course, we should still examine, however briefly, the other members of the family - the compounds and convertiplanes.

It also seems an opportune time to round off the course with some basic considerations concerning the comparative evaluation of the helicopter and the new forms of short- or vertical-takeoff- aircraft.

11.1. NEW TYPES OF ROTORCRAFT

As we have seen in Chapter 10, the attempt to obtain high cruising speeds with the helicopter proper runs headlong into a number of technical difficulties. For this reason some designers have investigated or developed special rotorcraft that are better adapted to rapid flight.

11.11. THE COMPOUNDS

Let us return to the problem of increasing the critical stall value μ on the retreating blade by lowering the $\frac{f_N}{\sigma}$ ratio of the rotor. This can be done by reducing the lift required from the rotor in forward flight, with the remaining weight of the craft being borne by an auxiliary wing. There are different types of compounds depending on the mode of operation of the rotor.

(1) Helicopter-Airplane Compound: The rotor is relieved of some part of the weight but continues to provide the propulsion. Its forward tilt must be rather large to compensate for the reduction in lift. We have seen that this is unfavorable with respect to stalling, which results in losing part of the improvement realized. In addition, it can lead to excessive flapping amplitudes. For this reason this first and rather simple design cannot improve on the performance of the pure helicopter to any important degree (it is generally accepted that mounting an auxiliary wing on a helicopter brings about a gain of some tens of kilometers per hour).

(2) Gyrodyne-Airplane Compound: This is the same design as (1) with the addition of an auxiliary propellor charged with furnishing all or part of the propulsion. The disadvantages pointed out earlier no longer exist. /214

(3) Autogiro-Airplane Compound: This compound has the same components as the gyrodyne-airplane; however, the rotor is not powered in cruising flight but turns in autorotation. The lift of the wing is of the order of 50-75% of the total weight. Of the three configurations described, this one permits the highest speeds.

Apart from their inherent capacity for speed, we might ask if the aerodynamic efficiency of these designs is superior to that of a helicopter designed to fly at the same speed and, if the answer is in the affirmative, if one is better than the others.

The question is not clearly resolved. Calculations and wind-tunnel tests show that the overall differences are small. It appears that the gyrodyne is somewhat superior to the helicopter and autogiro. The presence of the auxiliary wing does little to improve the aerodynamic efficiency unless the rotor is almost completely load-free, a condition difficult to realize.

Many prototypes of autogiro compound have been built. We list the following:

SO 1310 Farfadet (France) (Fig. 1.25) - Experimental machine, first flight in 1953.

McDonnell (U.S.A.) - Experimental. Reached 320 km/hr in tests.

Fairey Rotodyne (England) - Heavy civil transport, 40 passengers. First flight at end of 1957.

Kamov Vintokryl (U.S.S.R) - Transport for 80-100 passengers. First appeared in public in 1961. Has held the speed record for convertiplanes over 15-25 km at 356.3 km/hr since then.

The major handicap of the compound is that common to all hybrid-machines - complexity and considerable dead weight (never on paper, but always on the scales). This explains why in most of the prototypes the rotor is jet-powered in takeoff* and placed in autorotation when cruising. The weight of the rotor propulsion system is thus reduced without the problem of the high fuel consumption characteristic of jet drive, since the jets are not in use except for short periods.

*The "Doblhoff cycle", named for the engineer who first used it - blade tip jets fed with compressed air from a fuselage generator.

11.12. THE CONVERTIPLANES

The definition of these machines was given in Chapter 1. Their interest lies in the elimination of the rotor as such in cruising configuration. At the same time the disadvantages resulting from the poor behavior of the rotor at high speeds and its poor aerodynamic efficiency are avoided. The convertiplane is the fastest rotorcraft. Let us recall some proposed designs:

(1) After takeoff as a helicopter the rotors are tilted by 90° to serve as propellors. /215

(2) A double-blade rotor stopped parallel with, or perpendicular to, the fuselage in cruising flight; in the latter case the lenticular-profile blades serve as a wing.

(3) Rotor stopped in flight and retracted into the fuselage.

(4) The entire machine is tilted by 90° in cruising flight. The vertical-takeoff airplanes so much discussed recently are seen to be a limiting case.

Designs involving rotor tilt present a problem during the transition phase, when the rotors tend to generate severe vibration (oblique attack). As for those requiring stopping and starting the rotor in flight, it is not necessary to stress the delicacy of this maneuver.

The complexity and dead weight of these machines is of still mote concern that it is with the compounds. It serves no purpose to go fast if nothing can be carried.

We shall not pursue this further, since the several prototypes constructed (in the U.S.A.) are in the preliminary test stage.

11.13. CONCLUSIONS

In most of its applications the helicopter does not appear to be threatened by the new types of rotorcraft just mentioned. First, they need not often fly particularly fast and, second, it is possible to make improvements, notably by using engines of high power-to-weight ratio. Nevertheless, for certain special applications, such as scheduled transport over medium and long distances, the compound could be an interesting development.

11.2. RIVALS OF THE HELICOPTER

In view of the proliferation of new vertical-takeoff (VTO) and short-takeoff- and landing- (STOL) designs and the advantages they present (at least on paper, the question might be asked whether the helicopter and the autogiro are not sooner or later fated to disappear. This might be demoralizing to the reader who is obliged to "sweat out" this course, and the following considerations are intended to reassure him....

First of all, we recall that the helicopter at present does many tasks for which it is not particularly suited. This is the case, for example, for transport between confined or undeveloped areas. Short-takeoff airplanes, once perfected, could do equally well and would probably be more economical (for example, hyper-lift airplanes or those with a wing in the propellor wash, of the Breguet 940 type). On the other hand, the STOL cannot be used when it is a question of well-controlled vertical flight or landing and takeoff without roll, which is often the case when it is necessary to sit down on a mountain peak, on a field encumbered with obstacles or even on a hillside.

Here the helicopter has no rival other than the various designs permitting vertical flight, and we shall see why the helicopter retains its interest.

11.21. COMPARATIVE STUDY OF PERFORMANCE IN VERTICAL FLIGHT

Until we have found means to defy gravity (which will not be tomorrow despite the pronouncements of certain "experts") everything heavier than air will have to use the same physical process for its lift in vertical flight as does the helicopter - the downward acceleration of a stream of air of finite cross-section.

The various designs are classified according to the loading per square meter of the supporting stream:

Helicopters: 15-20 kg/m^2.

VTO with or without ducted propellors: 100-800 kg/m^2.

VTO with jets: 5000 - 8000 kg/m^2*.

*Taking the mid-frame section of the jet engine as reference.

An idea of the power to be provided in each case can be derived from the /217
formula $P = F_N \sqrt{\frac{F_N}{2\rho S}}$, which gives the minimum induced power required to sustain a given weight. It varies as $\sqrt{\frac{F_N}{S}}$. On setting the power required by a helicopter loaded to 25 kg/m^2 equal to unity we obtain 2 - 6 for the VTO with propellor, and 14 - 18 for the VTO with jets.

These figures explain the characteristics of the different machines from the standpoint of structural weight and fuel consumption.

Design Weight. The engine weight increases considerably with loading per square meter, but two important factors must be considered:

(1) As we have seen, in choosing the optimum loading of the rotor disc of a helicopter, the penalties of engine weight are partially compensated by the decrease in weight of the other components of the lifting system - the rotors and transmissions. This is especially noticeable for the VTO with jets, where transmission and rotors are totally lacking.

(2) With jets the energy transformation is made using a cycle more favorable for obtaining a high power-to-weight ratio (particularly the elimination of all internal reduction in the engine).

In practice one can already conceive to VTO jets (or double flow) having a ratio of empty weight to total weight comparable to that of the helicopter (0.5 - 0.6).

In the present state of the art it is difficult with turbo-machines to obtain a result comparable to the VTO with propellors (present order of magnitude of the ratio of empty weight to total weight of 75%).

Fuel Consumption:

In practice the fuel consumptions are essentially in the ratio of the minimum induced powers* (although the cycles are not always comparable).

This leads to the following conclusions as to performances: /218

*For example: 0.06 kg/hr per kg of total weight lifted by the comparison helicopter and 1 kg/hr per kg of weight lifted by the jet VTO.

(1) If it is a question only of vertical landing and takeoff, the reaction jet VTO's are presently comparable to the helicopter from the standpoint of payload*. The propellor VTO's with heavily loaded propellors are of no great interest with the present state of the art. They will not take over in the future unless a considerable weight reduction is realized in engines, transmission and propellors.

(2) If it is necessary to make a hovering flight or a slow flight somewhat longer than usual, the helicopter is substantially better due to its lower fuel consumption. The probability that this difference in fuel consumption can be materially decreased in the future is rather low.

11.22. OTHER COMPARATIVE FACTORS

But it is necessary to consider factors other than performance in missions that have hitherto been reserved for the helicopter.

Efficiency and Precision of Control

Although the helicopter is now satisfactory in this respect, the question remains to be resolved for the other types of VTO's, and no doubt there are still some problems. However, it seems likely that these will be overcome rather quickly. There is in principle no obstacle to making jet or propellor VTO's as easily controllable, if not more so, than standard helicopters. (If necessary with the assistance of the "little black boxes"). **

Downwash of the Lifting Stream

The downwash of a helicopter rotor operating near the ground still presents difficulties, especially by raising clouds of dust objectionable to the crew and ground personnel (not to mention its effect on the hats of the male onlookers and the skirts of the females ...).

---

*The heaviness of the VTO resulting from its adaptation for rapid flight, such as wind, control surfaces, etc... are not taken into account. Such a VTO would be comparable to the compounds or convertiplanes.

**A picturesque term by which automatic stabilizer devices are described in the Angle-Saxon literature.

The jets of the VTO's, whose energy is much more concentrated, will be still more objectionable and could even be dangerous to personnel and material on the ground.

Safety

This is perhaps the trump card of the helicopter, which has a permanently deployed parachute above it - the rotor - which can always be set into autorotation in case of engine failure or loss of power. This is possible, but very tricky, even with heavily loaded rotors.

With VTO's the only safety measure is the installation of a large number of lifters and automatic control arrangements. /219

11.23. CONCLUSIONS

The helicopter can do but one job, namely, vertical and slow flight, but it does this one job very well.

Its area of application will be reduced inasmuch as it will probably be supplanted in its "marginal" uses by other, better adapted, machines, such as the STOL for medium-speed transport and the VTO when high cruising speed coupled with vertical takeoff is required. On the other hand, in its own sphere the helicopter will be with us yet for a long time without serious rival and its applications will certainly expand considerably.

APPENDIX I

/A.1

NUMERICAL DATA

I-1 CHARACTERISTICS OF THE WORLD'S PRINCIPAL HELICOPTERS

Configuration

- M: Single-rotor
- BC: Coaxial double-rotor
- BE: Meshed double-rotor
- BT: Tandem double-rotor

Mode of Rotor Drive

- MP: Mechanical drive, piston engines
- MT: Turbo-engine drive
- RF: Direct rocket drive
- RP: Direct pulse-jet drive
- RS: Direct ram-jet drive
- RTA: Direct drive by compressed air jet without blade-tip combustion
- RTC: Direct drive by compressed air jet with blade-tip combustion

State

- P: Prototype
- PS: Pre-production
- S: In production

Note: The weight and performance numbers are given as examples. Their correctness varies with the source of the data. A question mark is affixed to individual items that are most uncertain. The empty weights relate to various stages of equipment. The performance figures in principle relate to the total standard weight.

PRINCIPAL LIGHT HELICOPTERS OF THE WORLD
(Total weight less than 2500 kg)

Designation	KH-15	Hoppi-Copter C-1	Kolibrie H-3	Airborne platform 1031-A	Héli-Vector DH 4
Builder	KELLET	CAPITAL	N H I	HILLER	DELACKNER
Country	U.S.A.	U.S.A.	HOLLANDE	U.S.A.	U.S.A.
Configuration	M	M	M	BC faired	B.C.
Number of blades per rotor	2	2	2	2	2
Diameter of rotors (meters)	5.5	5.49	10,06	1,50 (fairing 1.80)	4.60
Type of drive	R F	R P	RS	M P	M P
Number of engines	2	2	2	2	1
Type of engines	XLR-32		NHI-TJS	H-59	MK 56 Mercury
Builder	Réaction Motors	NRL	NHI	Nelson	Kickhaefer
Maximum thrust (csn)	2 x 7.25	2 x 10.4			
Maximum power (h.p.)	—		2 x 55	2 x 42	44
Empty weight (kg)	106	59	200	100 (?)	80
Total standard weight (kg)	290	204	600	210	220
Total overloaded weight (kg)			700	-	-
Maximum speed (km/hr)	97	144		25	110
Crusing speed (km/hr)		96	85/100		
Ceiling outside ground effect (meters)					1500
Ceiling in ground effect (meters)		3050			
Service ceiling (meters)					
Fuel consumption, crusing (kg/hr)	450	40	300		13
Normal tank capacity (liters)	2 x 50	60.5	350		16
Range (km) with normal tank capacity	26	140	80		100
Number of places	1	1	1	1	1
State at end of 1963	P	P	P S	P	P

PRINCIPAL LIGHT HELICOPTERS OF THE WORLD

(Total weight less than 2500 kg)

Skeeter MKG	Hornet HJ-1 H.32-H OEI	Ultra-light	Djinn SO.1221	47.G1	UH 12B H 23B	47.J
SAUNDERS-ROE	HILLER	FAIREY	SUD-AVIATION	BELL	HILLER	BELL
G.B.	U.S.A.	G.B.	FRANCE	U.S.A.	U.S.A.	U.S.A.
M	M	M	M	M	M	M
3	2	2	2	2	2	2
9.76	7	8,53	11	10,70	10.67	11.30
MP	RS	RTC	RTA	MP	MP	MP
1	2	1	1	1	1	1
Gipsy-Major 201	8RJ-2B	Palouste	Palouste	GV-4-200	GV-4-200	VO-435
de Havilland	Hiller	Turbomeca Blackburn	Turbomeca	Franklin	Franklin	Lycoming
–	2x18	–	2x18,5	–	–	–
200	97	260	260 (92 on the rotor)	200	200	240
738	246	430	376	651	788	730
980	490	–	760	1067	1135	1086
1000	–	860	800	1140	–	1270
170	130	160	130	150	135	170
135	110	130	105	128	114	150
335	–	–	–	–	–	
1250	–	3067	600	1700		3600
3930	2100	6000	2000	3720	3505	5000
30	380	164	100	44	39	47
105	196,5	275	250	172	106	134
350	55	185	210	360	220	310
2	2	2	2	3	3	4
S	P	P	S	S	S	S

PRINCIPAL LIGHT HELICOPTERS OF THE WORLD
(Total weight less than 2500 kg)

K.600 HOK-1 H-43	171-4	Alouette II SE-3130	Alouette III SE-3160	Wasp	Rotorcycle GCA-59	269 A
KAMAN	BRISTOL	SUD-AVIATION	SUD-AVIATION	WESTLAND	GYRODYNE	HUGUES
U.S.A.	G.B.	FRANCE	FRANCE	G.B.	U.S.A	U.S.A
B.E.	M	M	M	M	B.C.	M
2	3	3	3	4	2	3
14.30	14.80	10.20	11	9.85	6.10	7.62
MP	MP	MT	MT	MT	MP	MP
1	1	1	1	1	1	1
R-1340-48	Leonides Mk 73	Artouste IIB	Artouste IIIB	Nimbus MK103	YO-95-6	O-360-C2E
Pratt et Whitney	Alvis	Turboméca	Turboméca	Bristol-Siddeley	Porsche	Lycoming
-	-	-	-	-	-	-
600	520	400	550	720	72	180
1835	1850	830	1125	1535	250	413
2631	2450	1500	2100	2404	377	704
3084	-	1600	-	2495	411	-
176	204	185	210	195	125	138
120/160	146	170	190	178	96	135
	1220	1400	500	2073	1555	1220
3660		2200	2000	3048	2225	1920
5500	4725	4000	4000	3810	3780	3355
	72	155	180	225	32	
378	300	575	550	709	38	94.5
	480	550	550	487	88	
4/5	5	5	7	5	1	2
S	S	S	S	S	P	S

Designation	HUP-2 H-25-A Army-Mule	S-55 H-19-A HRS-1	Mi-4 Hound
Builder	Vertol	Sikorsky	M. L. MIL
Country	U.S.A.	U.S.A.	U.R.S.S.
Configuration	B.T.	M	M
Number of blades per rotor	3	3	4
Diameter of rotors (meters)	10.67	16.15	21
Type of drive	MP	MP	MP
Number of engines	1	1	1
Type of engines	R.975.46	R-1340	Ash-82 V
Builder	Continental	Pratt et Whitney	
Maximum thrust (csn)*	-	-	-
Maximum power (h.p.)	550	500	1700
Empty weight (kg)	1782	2300	4450
Total standard weight (kg)	2608	3263	6800
Total overloaded weight (kg)	2767	3583	7200
Maximum speed (km/hr)	180	187	210
Cruising speed (km/hr)	130	150	160
Ceiling outside ground effect (meters)		1585	
Ceiling in ground effect (meters)		2620	
Service ceiling (meters)	3050	3660	4880
Fuel consumption, cruising (kg/hr)		109	
Normal tank capacity (liters)		700	
Range (km) with normal tank capacity	630	650	400
Number of places	6	10	16
State at end of 1963	S	S	S

*Translator's note: csn = 100 sthène; 1 sthène = 103 Newtons

192 Belvedere	S-58 H-34 HSS-1	H-21 Work-Horse	S-56 H-37 HR 2S-1	Yak-24 Horse	Rotodyne
Westland	Sikorsky	Vertol	Sikorsky	Yakovlev	Westland
G.B.	U.S.A.	U.S.A.	U.S.A.	U.R.S.S.	G.B.
B.T. 4 14.91 MT	M 4 17.07 MP	B.T. 3 13.42 MP	M 5 21.95 MP	B.T. 4 24 MP	Combiné 4 27.4 RTC
2 Gazelle NGA-2 Napier - 2 x 1650	1 R. 1820-84 Wright - 1525	1 R. 1820-103 Wright - 1425	2 R. 2800 Pratt et Whitney - 2 x 2100	2 Ash-82 V 2 x 1700	2 ELAND N. EL. 3 Napier - 2 x 3000
5234 8620 9072	3600 5400 6000	4100 6000 6800	9448 14000	12000 16000	10000 15000 17700 (with Eland 7)
220 185	210 150/170	209 140/160	209 185	175 155	 260
1830 3050	1500 2260 3660	1670 2400 3000	335 2650	 5500	
   695	205 970 560	230 1135 525	 233	 200	 3410 740
20	12/15	22	25/40	40	40
S	S	S	S	S	P

Mi-6	UH-2A Seasprite	107 II1	T14 Chinook	S 61 L
M. L. MIL	Kaman	Vertol	Vertol	Sikorsky
U.R.S.S.	U.S.A.	U.S.A.	U.S.A.	U.S.A.
M 5 35 MT	M 4 13.41 MT	B.T. 3 15.24 MT	B.T. 3 17.98 MT	M 5 18.9 MT
2 TB-2BM Soloviev 2 x 4635	1 T58 GE 8 General Electric 1250	2 T 58 GE 8 General Electric 2 x 1250	2 YT 55 L 5 Lycoming 2 x 2200	2 T 58 GE 8 General Electric 2 x 1250
18600 32200 39000	2390 3445 4953	4355 8370 8618	14970	4933 8483 8620
300 270	261 236	250 240	282 240	240 219
	3415 4420 6735	1980 2375 4175		1700 2040 3970
500	1045 980	480 1040 420	2385	480 1550 470
70/80	14	28	35	27
S (?)	S	S	S	S

64 Skycrane	SA 3210 Super Frelon	HU 1 B Iroquois
Sikorsky	Sud Aviation	Bell
U.S.A.	France	U.S.A.
M 6 21.95 MT	M 6 18.9 MT	M 2 13.4 MT
2 JFTD 12 A-1 Pratt et Whitney 2 x 4050	3 Turmo III C 3 Turboméca 3 x 1500	1 T 53 L 9 Lycoming 1100
7820 17240	6350 11000 12000	2042 2994 3856
269 177	280 250	203 222
1435 2950 3200	3700 3300 4800	3810
1565 3332 307	750 3560 850	 625 418
5	33	10
PS	PS	S

EVOLUTION OF POWER

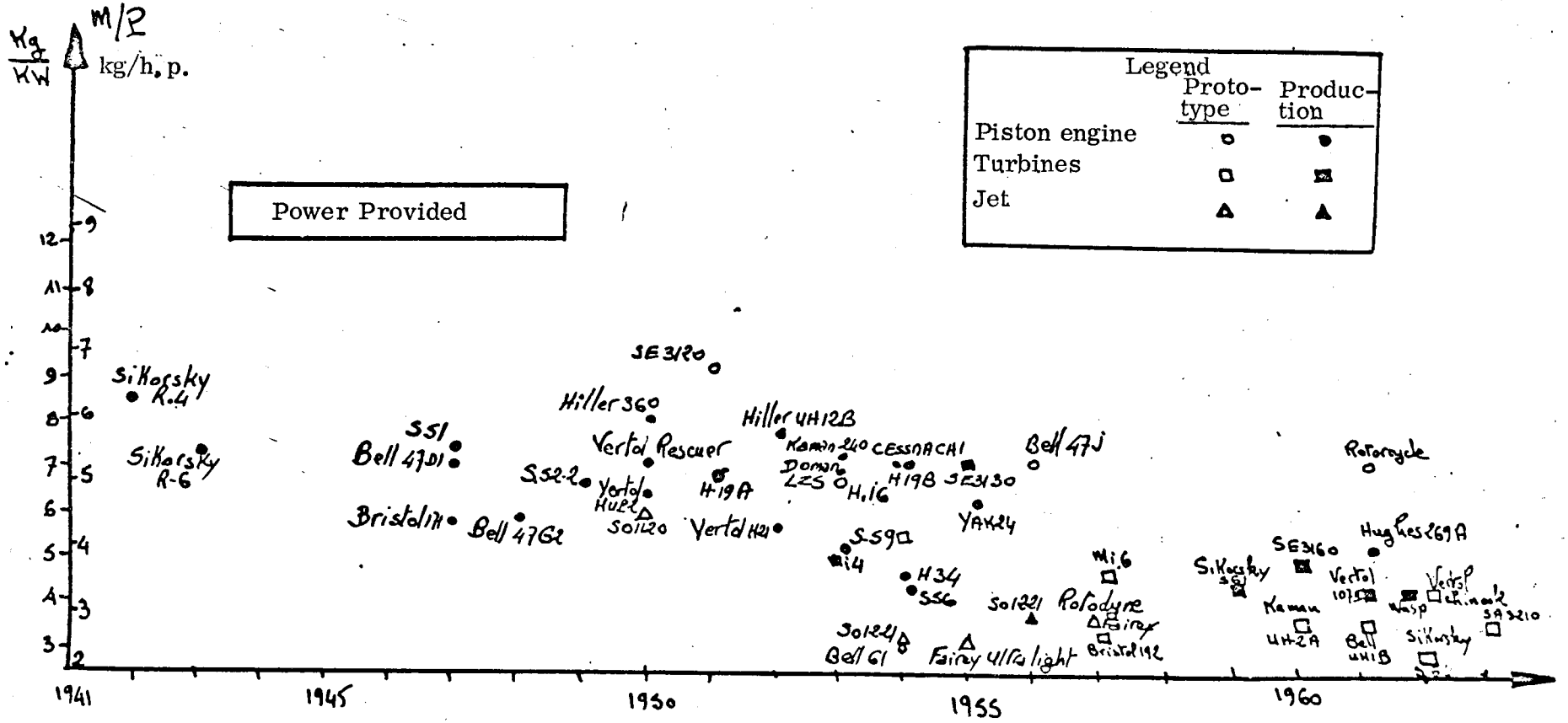

EVOLUTION OF ROTOR SURFACES

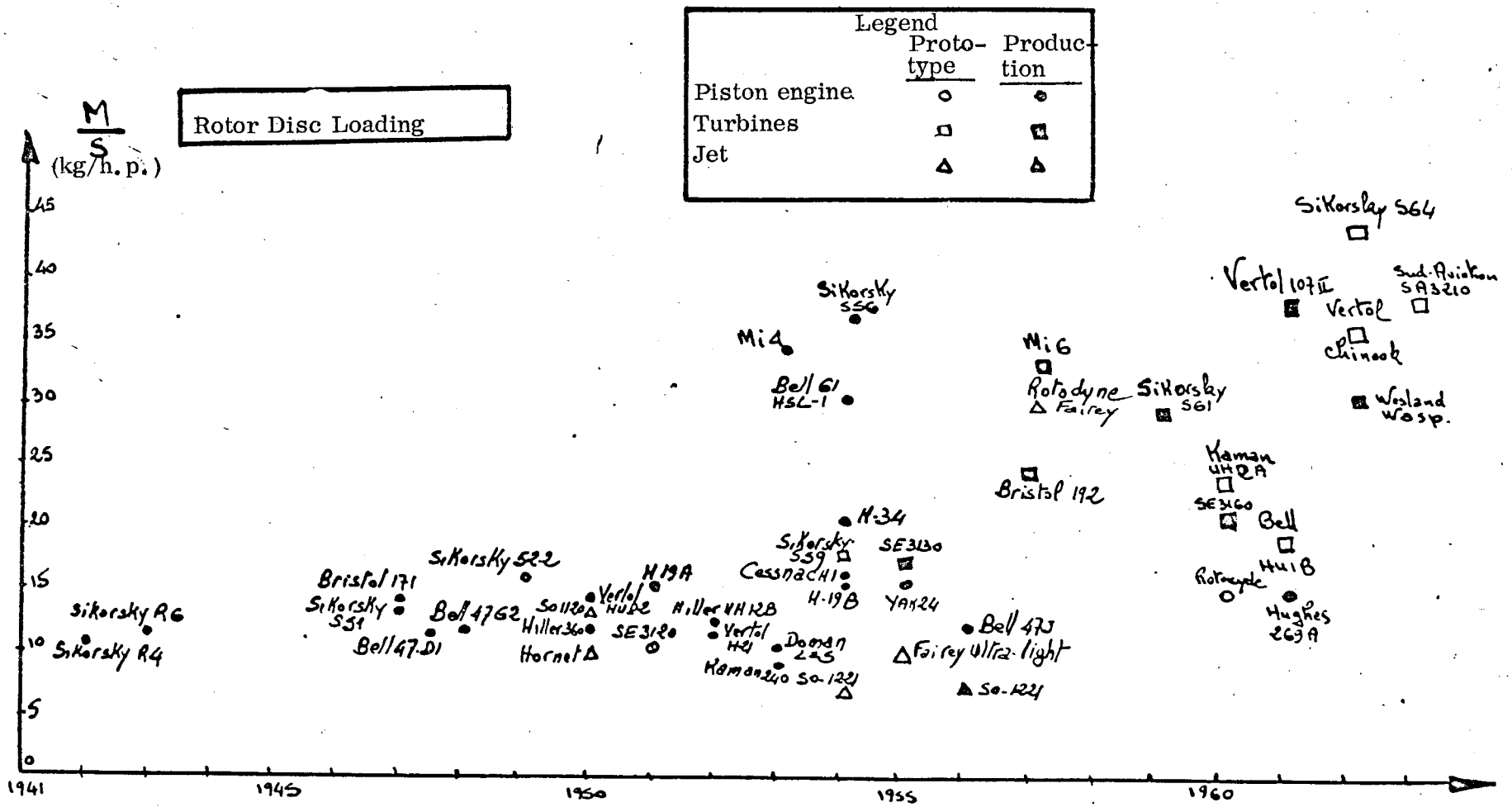

I-2 Evolution of the Major International Records for Helicopters

a- Altitude and Speed

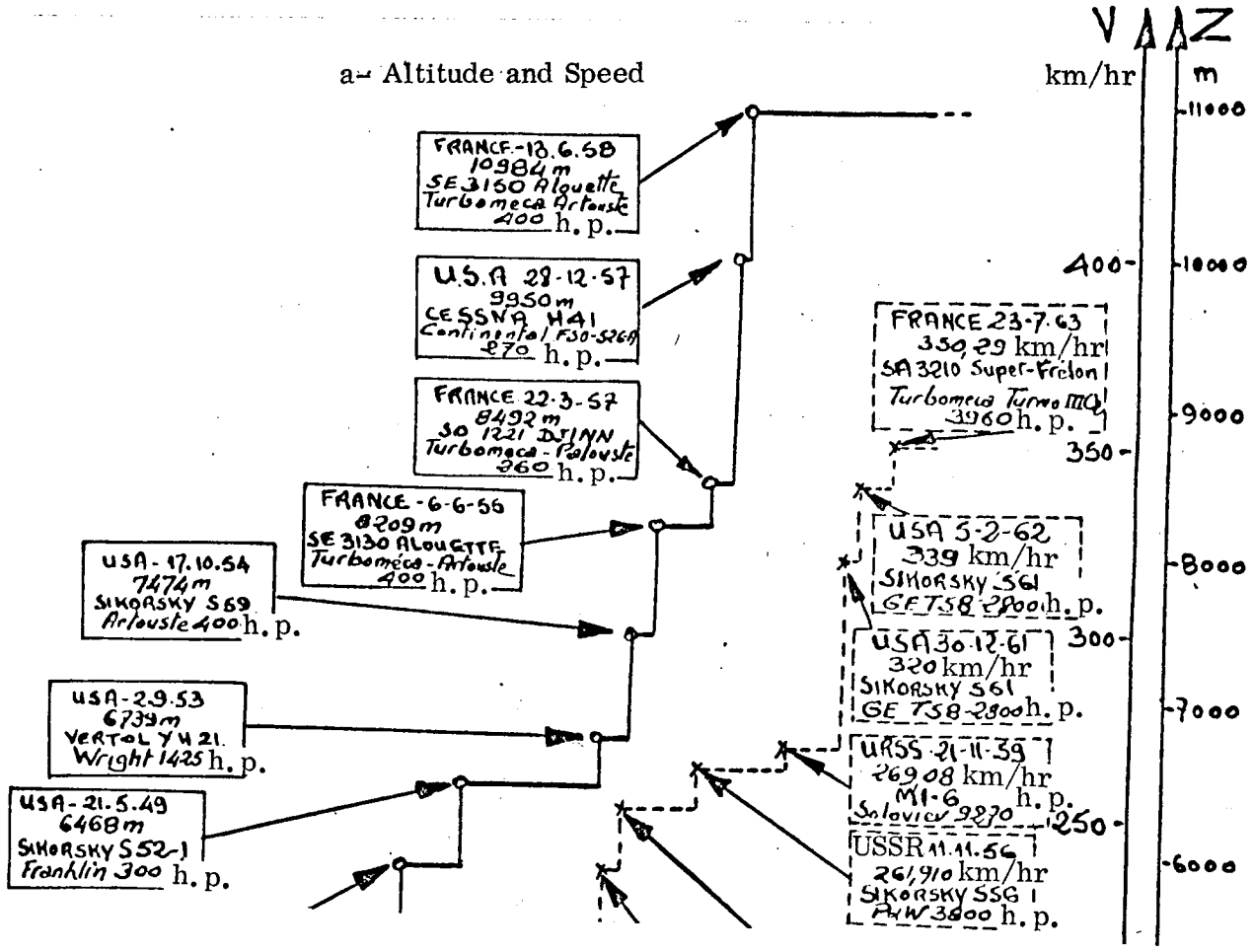

I-2 Evolution of the Major International Records for Helicopters

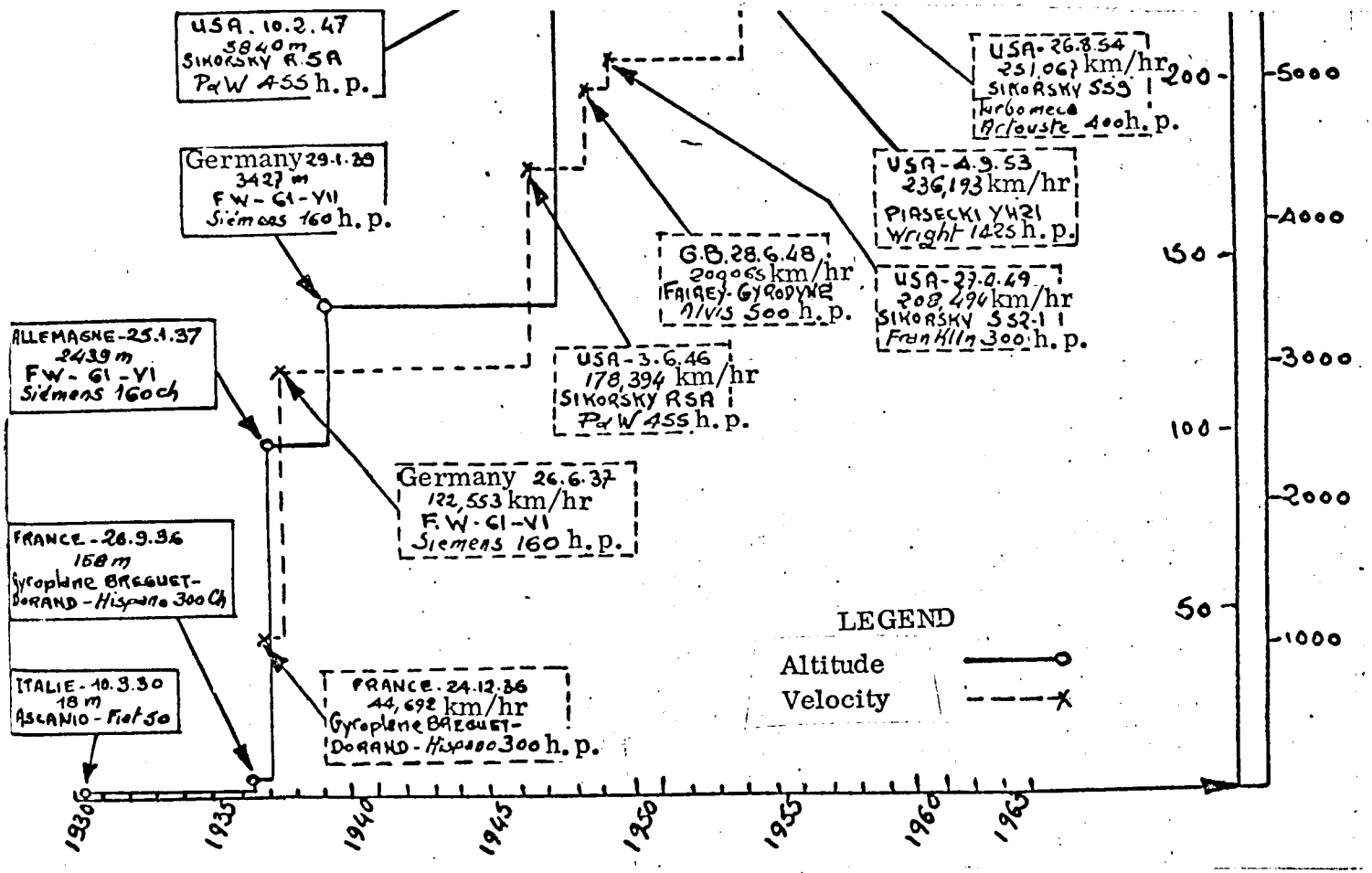

b- Ranges

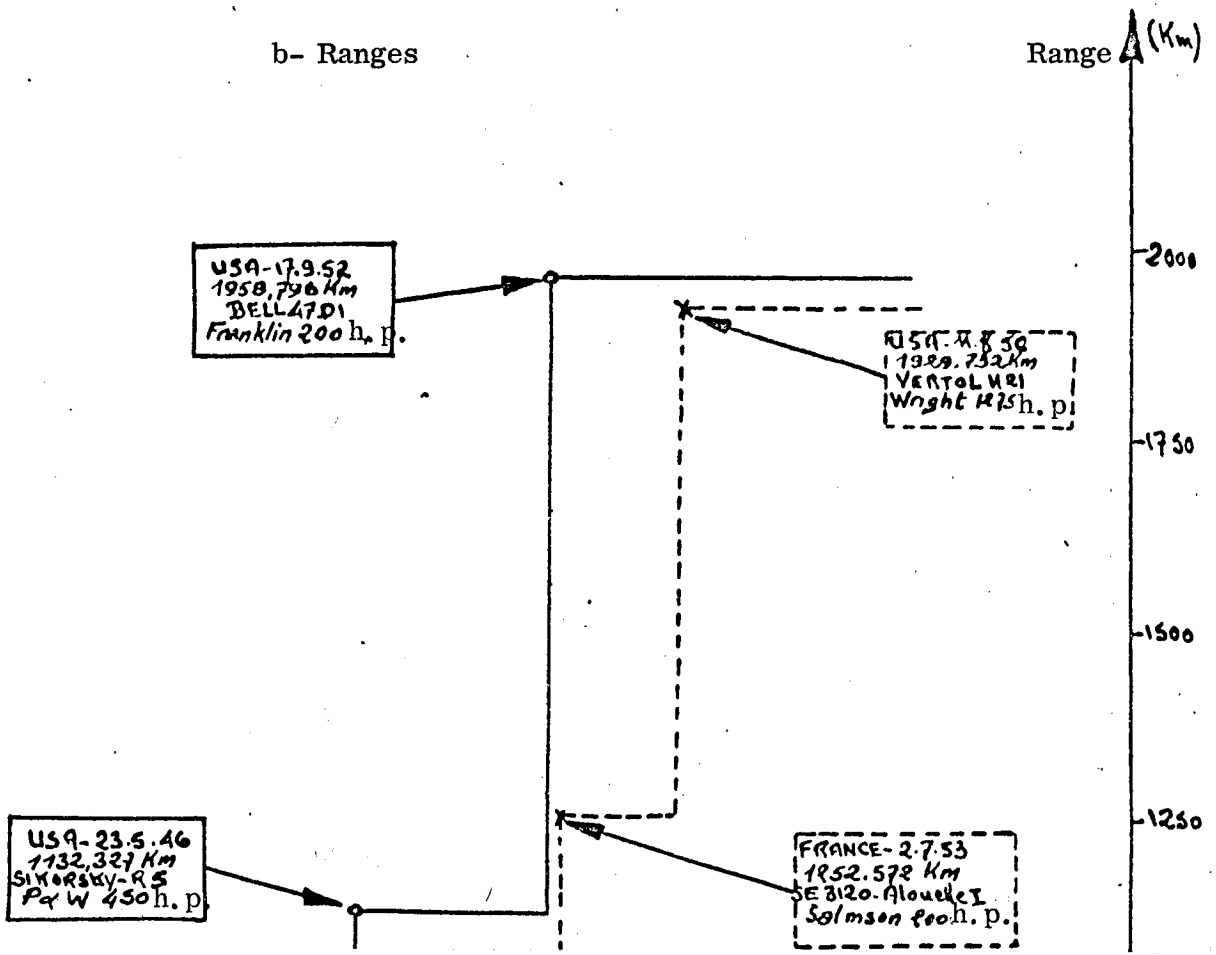
Range (Km)
2000
1750
1500
1250
USA-17.9.52
1958,796 Km
BELL 47 D1
Franklin 200 h.p.
USA-23.5.46
1732,327 Km
SIKORSKY-R5
P&W 450 h.p.
USA-?.?.50
1929,732 Km
VERTOL H21
Wright R75 h.p.
FRANCE-2.7.53
1952,572 Km
SE 3120-Alouette I
Salmson 200 h.p.

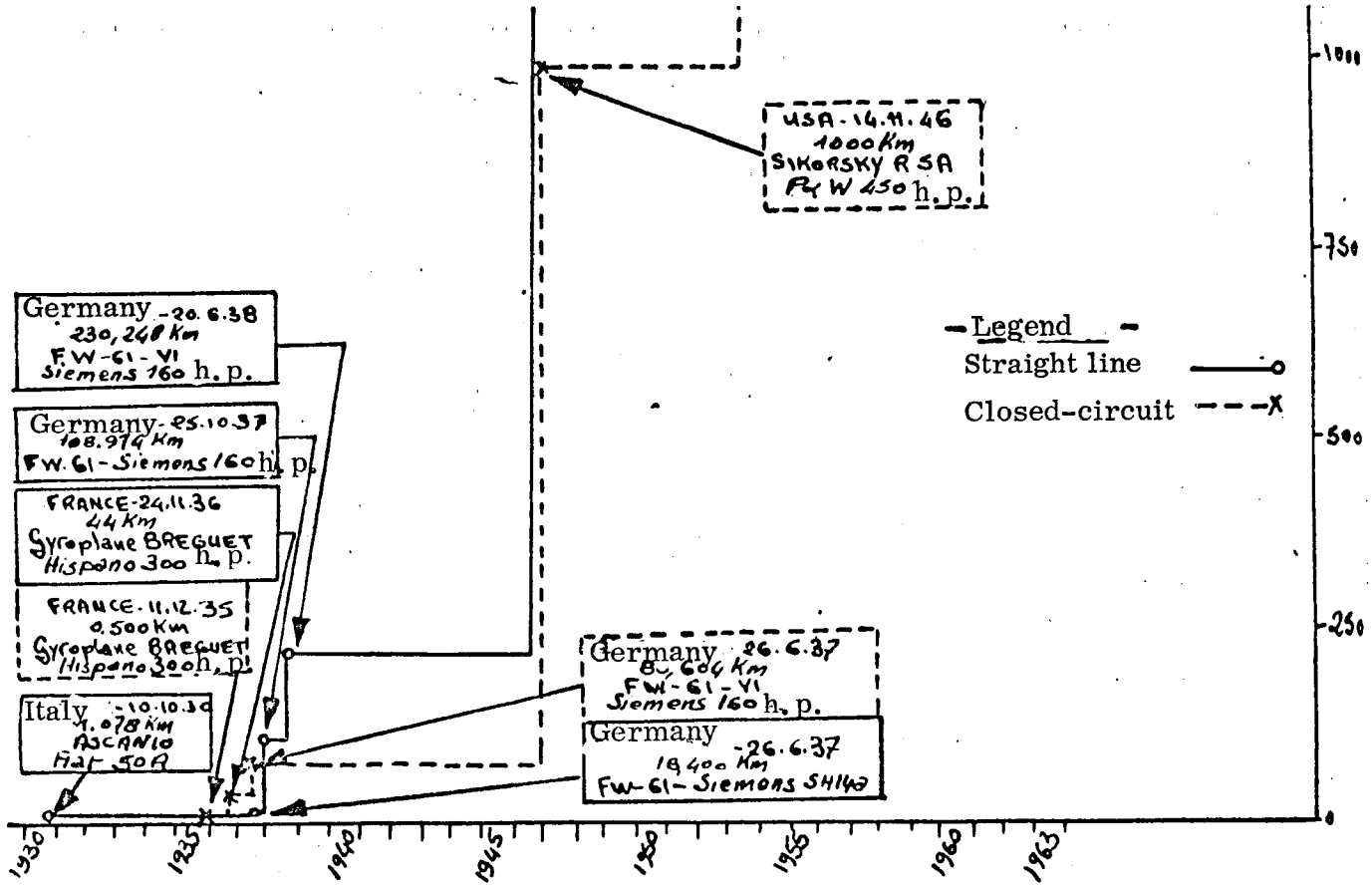
USA - 14.11.46
1000 Km
SIKORSKY R SA
P&W 450 h.p.
Germany - 20.6.38
230, 248 Km
FW-61-VI
Siemens 160 h.p.
Germany - 25.10.37
108.974 Km
FW. 61 - Siemens 160 h.p.
FRANCE - 24.11.36
44 Km
Gyroplane BREGUET
Hispano 300 h.p.
FRANCE - 11.12.35
0.500 Km
Gyroplane BREGUET
Hispano 300 h.p.
Italy - 10.10.34
1.078 Km
ASCANIO
Fiat 50 A
Germany - 26.6.37
8.604 Km
FW-61-VI
Siemens 160 h.p.
Germany - 26.6.37
19.400 Km
FW-61 - Siemens SH14a
Legend
Straight line
Closed-circuit
1000
750
500
250
0
1930
1935
1940
1945
1950
1955
1960
1963

I-3 AERODYNAMIC CHARACTERISTICS OF ROTORS

Type of helicopter	Single-rotor with piston-engine - three-place (C)	Single-rotor with fixed-wheel turbine - five-place (D)	Single-rotor jet (ejection of compressed air at blade tip) - two-place (E)
Mass M (kg)	1150	1500	690
Diameter of rotor D (m)	11.60	10.20	11
Disc loading $10^3 \frac{M}{S}$ (kg/m^2)	10.8	18.5	7.26
Tip velocity u (m/sec)	138	186	185
Number of blades b	3	3	2
Blade shape (plan)	trapezoidal $l_{0.7} = 0.336$ m	rectangular $l = 0.265$ m	rectangular $l = 0.235$ m
Thickness relative to profile	16 %	12 %	18 %
Blade twist (degrees)	-8	-8	-4.5
Solidity $\sigma = \frac{b l_{0.7}}{\pi R}$	0.055	0.0496	0.027
$f_N \left(\frac{f_N}{\sigma}\right)$ (%)	0.0094 (0.17)	0.00975 (0.196)	0.0035 (0.13)

I-3 AERODYNAMIC CHARACTERISTICS OF ROTORS

m_N (%) (m_N induced, in %)	0.000735 (71)	0.000750 (73)	0.00019 (54)
$\eta_s = \frac{f_N^{3/2}}{2 m_N}$ (%)	0.62	0.645	0.53
Aerodynamic efficiency f_n/m_n*	12.8	13	18
Maximum power (or thrust) avialable on the rotor* (h.p.)	166	290	thrust 37 csn* power 92 h.p.
Ceiling in vertical flight without ground effect (m)	300	1400	0
Ceiling in vertical flight with ground effect (m)	1500	2200	2000
Service ceiling (m)	2400	4100	3100
Flight speed at minimum power* (km/hr)	60	90	65
Maximum speed of climb (m/sec)	3.80	4.5	3.7

*At the vertical ceiling altitude outside of ground effect.

I-4 HELICOPTER WEIGHT ESTIMATES

1) Effect of Type of Propulsion

Type (7) (See Chapter VIII) (C) Single-rotor with piston engine drive, 3-place

Type (6) (See Chapter VIII) (D) Single-rotor with turbine drive, 5-place

Type (4) (See Chapter VIII) (E) Jet single-rotor (ejection of compressed air at blade tips), 2-place.

	(C) Mass		(D) Mass		(E) Masse	
	kg	% M_T (*)	kg	% M_T (*)	kg	% M_T (*)
Blades	91	17.9	85	5	71,5	10,3
Hub	46.5	4	98	5.8	29,5	4,3
Airframe	206	18	261	15.5	100	14,5
Flight controls	41	3,5	40	2.4	19	2,8
Propulsion system	223.5	19.4	158	9.4	103,5	15
Transmissions	75	6.5	120	7.2	2,5	0,4
Fixed equipment (without radio)	50	4.3	85	5	36	5,2
Empty weight	733	63.6	847	50.3	362	52,5
Payload	417	36.4	833	49.7	328	47,5
Total weight*	1 150	100	1 680	100	690	100

*M_T: Total mass corresponding to vertical flight outside the ground effect at 0 meters, standard atmosphere.

2) Comparison of the single-rotor and the double-rotor in tandem for high gross weights (D'apres R. Hafner - Journal of the helicopter association of Great - Britian. vol 8 no. 4 April 1955).

	(F) Single-rotor Mass		(G) Double-rotor tandem Mass	
	kg	% M_T (*)	kg	% M_T (*)
Forward or main rotor — blades	670	7.45	236	2.62
Forward or main rotor — hub	410	4.55	204	2.26
Rear rotor or anti-torque rotor — blades	23	0.25	236	2.62
Rear rotor or anti-torque rotor — hub	23	0.25	204	2.26
Total, rotors	1 126	12.50	880	9.76
Fuselage	1 520	16.90	1 420	15.80
Flight controls	154	1.70	120	1.33
Transmissions**	700	7.80	680	7.56
Total	3 500	38.90	3 100	34.45

*M_r: total mass: 9,000 kg.

**The power provided is assumed to be the same for the two machines.

APPENDIX II

PRINCIPAL NOTATION

Reference axes

O_{xyz} is any arbitrary reference trihedron. If it serves as a reference system for the relative airspeeds with respect to the rotor, oz is directed upward; of, O_z contain the relative airspeed.

OXYZ is a particular reference trihedron used in the rotor theory. OZ is perpendicular to the rotor disk and is directed upward. OX, OZ contain the relative airspreed with respect to the rotor. OX is directed in the sense of velocity. ψ is the azimuth of a blade.

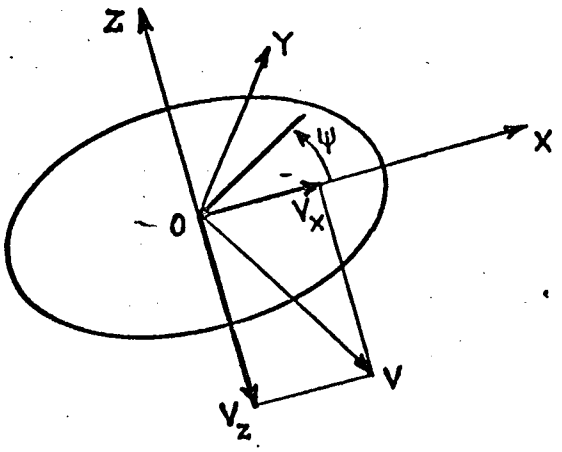

Velocities

ω = rotor angular velocity w.f. = ωt)

u = blade tip velocity ($u = \omega R$)

V(or V_o) = airspeed at infinity upstream, with respect to the rotor

V_1 = airspeed at the center of the rotor.

V_2 = airspeed at infinity downstream of an airstream passing through the center of the rotor

V_x, $-V_z$, V_x, $-V_z$ = airspeed components along the reference axes.

Reduced Values of the Velocities:

$\Lambda = \frac{V}{u}$

$\mu = \frac{V_x}{u}$ tip-speed ratio (advancing)

$\lambda = \frac{V_z}{u}$ inflow ratio

$\lambda' = \frac{V_z + V_i}{u}$ total inflow ratio

α = angle of attack of V_o (or V_1) with respect to a reference plane (usually the tip - path plane OXY): tg $\alpha = V_z/V_x$ (or $V_z + V_i/V_x$)

Induced Velocities: /A.14

v_i = induced velocity at a point

v_{i_o} = theoretical induced velocity in hovering: $v_{i_o} = \sqrt{\frac{F_N}{2\rho S}}$

$$v_i = v_{im} + \frac{r}{R} v_{ic} \cos\psi + \frac{r}{R} v_{is} \sin\psi$$

series expansion of the induced velocity in the plane of the disk as a function of r and ψ.

BLADE CHARACTERISTICS

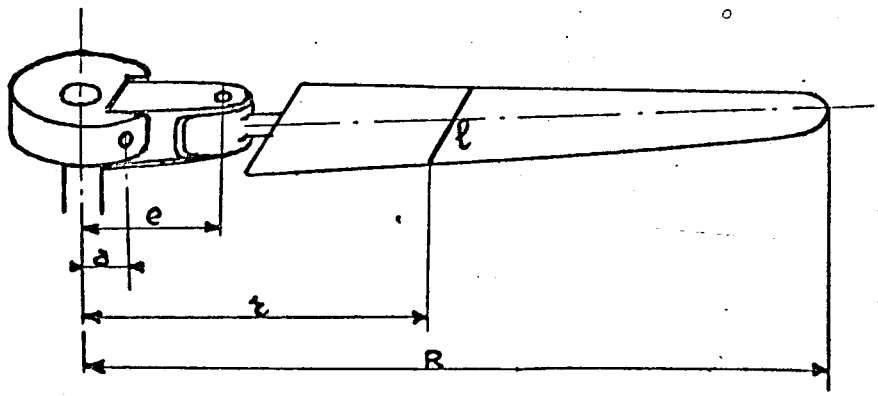

R = rotor blade radius /A.15

r = distance from blade element to rotor axis

$\bar{r} = r/R$: ratio of blade-element radius to rotor-blade radius

$S = \pi R^2$: rotor disk area

ℓ = blade section chord

$\ell_{0.7}$ = blade section chord at 0.7R

$t = 1 - \frac{\ell_1}{\ell_0}$ = blade taper ratio (ℓ_1 chord at the blade tip, ℓ_0, chord at the root).

b = number of blades

$\sigma = \frac{b c_{0.7}}{\pi R}$ rotor solidity. This is the ratio of the blade area to the rotor disk area if the blades are rectangular. In all other cases it is the ratio of the "effective" blade area to that of the disk

a = distance from flapping hinge to axis of rotation (hinge off-set)

e = distance from drag hinge to axis of rotation (off-set)

$G_0, G_1, G_2 \ldots \bar{G}_0, \bar{G}_1 \ldots$ blade plan form parameters. See Appendix III-2

θ = blade-section pitch angle (referred to an arbitrary plane)

$\theta_{0.7}$ = blade-section pitch angle at 0.7R

$\theta = \theta_0 - \theta_1 \cos \omega t - \theta_2 \sin \omega t - \theta_3 \cos 2\omega t - \theta_4 \sin 2\omega t \ldots$ series expansion of the cyclic pitch change

θ_V = twist angle, difference in pitch between the tip and root of the blade (positive if the pitch decrease from the root to the tip)

$L_0, L_1, L_2 \ldots \bar{L}_0, \bar{L}_1,$ blade twist parameter. See Appendix III-2.

m = blade mass

m_S = static moment of the blade with respect to lag (or flapping) hinges

I_p = moment of inertia of blade with respect to the lag (or flapping) hinges /A. 16

γ_L = lock number of the blade. See Appendix III-2

Blade Motion:

β = blade flapping angle with respect to a reference plane

$\beta = a_0 - a_1 \cos \omega t - b_1 \sin \omega t - a_2 \cos 2\omega t - b_2 \sin 2\omega t - \ldots$

Fourier series expansion of β

a_0 = rotor coning angle

$k = -\frac{\Delta\theta}{\Delta\beta}$: pitch-flap coupling (k-linkage).

$\varphi = \text{arc tg } k$

δ = blade drag angle.

$\delta = \delta_0 - \delta_1 \cos \omega t - \delta_2 \sin \omega t - \ldots\ldots$

Fourier series expansion of δ .

δ_0 = mean blade drag angle

Forces - Torques - Powers:

$$\left\{ \begin{array}{l} F_x, F_y, F_z \\ F_X = T_X \\ F_Y = T_Y \\ F_Z = F_N \end{array} \right\}$$

(Constant components of the force transmitted by the rotor to the hub along the reference axes)

h = height of the rotor above the center of gravity

h_f = height of the rotor thrust center above the rotor $\left(\simeq \frac{1}{2}\frac{a}{a_o}\right)$

M = mass of the helicopter

G = M_g = gross weight of helicopter

M_N = rotor-shaft torque

T = blade tip thrust (jet drive)

P = rotor-shaft power

P_D = power available on the rotor shaft

P_N = power required on the rotor shaft

P_i = induced power

P_p = blade profile power

P_f = drag of the fuselage

Σ = mid-section of the fuselage

Y_A, r_A = coordinates of the "aerodynamic center" of the blade (see the definition in Section 3.321).

Reduced Coefficients:

$f_N = \frac{F_N}{\frac{\rho}{2} S u^2}$; coefficient of the thrust ratio

$m_N = \frac{P_N}{\frac{\rho}{2} S u^3} = \frac{M_N}{\frac{\rho}{2} S u^2 R}$; coefficient of the torque ratio

$\eta_i = \frac{f_N^{3/2}}{2 m_N}$; lift efficiency of the rotor

$f = f_N/m_N$: aerodynamic efficiency of the rotor

M_{Ni}, m_{Ni}, η_i : induced torques and efficiency

B = blade tip-loss factor

M_{Np}, m_{Np} = blade profile-drag torques

$C_{zm} = C_z$ mean operating profile drag factor (in vertical flight $C_{zm} \simeq \frac{3 f_N}{\sigma B^3}$)

$C_{xp} = C_x$ mean blade drag factor

C_{xf} = fuselage drag

APPENDIX III

MATHEMATICAL DEVELOPMENTS

Appendix III-1

/A.21

DETERMINATION OF THE OPTIMUM INDUCED-VELOCITY DISTRIBUTION IN HOVERING

The problem of defining the optimum rotor in hovering with due regard to the induced tangential velocities is complex and cannot be rigorously solved by elementary methods. Given below as an example of mathematical examination are the elements necessary for setting up the equations without going into the details of the mathematical solution.

The rotor lift and power are obtained by the same formulas as those used in Section 2.1322:

$$F_N = \rho \int_0^R \Gamma (\omega r - V_t)\, dr \qquad \text{(III.1.1)}$$

$$P = \rho \int_0^R \omega r\, \Gamma V_i \qquad \text{(III.1.2)}$$

where V_t is calculated as in the mentioned section. The circulation along a circle of radius r is written as being equal to the half-sum of the vortex circulation across the circle:

$$2\pi r V_t = \frac{1}{2} \int_0^r \frac{d\Gamma}{dr}\, dr \qquad \text{(III.1.3)}$$

$$V_t = \frac{\Gamma}{4\pi r}$$

In view of these conditions III.1.1 is written

$$F_N = \rho \int_0^R \Gamma \omega r \left(1 - \frac{\Gamma}{4\pi\omega r^2}\right) dr \qquad \text{(III. 1. 1')}$$

V_i is difficult to calculate because the induced velocity at some point is the sum of all the elementary induced velocities produced by the free vortex filaments, $d\Gamma$, spilling off the blade (see Fig. 2-18). Here is one way of calculating it.

In the following figure consider the flow between the sections r and r + dr. /A.22
As in the case of the lifting disk it is permissiable to assume that

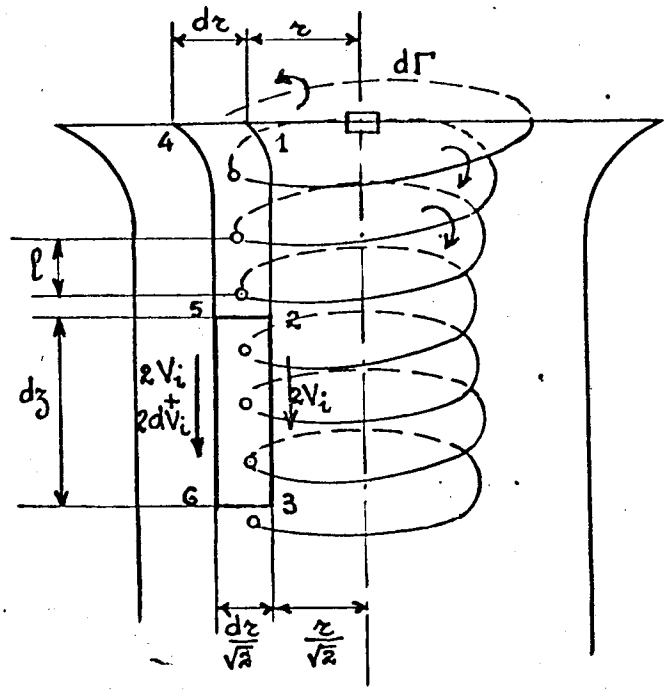

the induced velocities at infinity upstream are double those to the right of the rotor. The result is that the stream contracts in such a way that the sections at infintiy downstream are reduced by one-half (conservation of mass flow). The flow meridians are represented schematically by the Curves 1, 2, 3, and 4, 5, 6. These meridians contain the traces of the vortex $d\Gamma$ arranged so that they form a solenoid of pitch ℓ.

The circulation along the contours 2, 3, 6, 5 is written as being equal to the intensity of the vortices traversing its surface:

$$-dz\, 2V_i + dz\,(2V_i + 2dV_i) = \frac{dz}{\ell} d\Gamma,$$

that is,

$$2\,dV_i = \frac{d\Gamma}{\ell}$$

ℓ is calculated as in 2.1322

$$\ell = 2\pi \frac{r}{\sqrt{2}} \frac{2V_i}{\left(\omega \frac{r}{\sqrt{2}} - \frac{\Gamma}{2\pi \frac{r}{\sqrt{2}}}\right)} = \frac{4\pi}{\omega} \frac{V_i}{\left(1 - \frac{\Gamma}{\pi \omega r^2}\right)},$$

from which we get

/A.23

$$2V_i\, dV_i = dV_i^2 = \frac{\omega}{4\pi} d\Gamma \left(1 - \frac{\Gamma}{\pi \omega r^2}\right). \qquad \text{(III.1.4)}$$

Integration yields

$$V_{i(r)}^2 = \frac{\omega}{4\pi} \left[\Gamma_{(r)} - \int_0^r \frac{\Gamma_{(\alpha)}\, \Gamma'_{(\alpha)}\, d\alpha}{\pi \omega \alpha^2}\right] + C$$

or, if we integrate by parts,

$$V_i^2 = \frac{\omega}{4\pi} \left[\left(\Gamma - \frac{\Gamma^2}{2\pi \omega r^2}\right) - \int_0^r \frac{\Gamma^2(\alpha)}{\pi \omega \alpha^3}\, d\alpha\right] + C.$$

At the boundary of the stream (r = R) the induces velocity is produced by the solenoid of intensity $\Gamma(R)$ springing from the blade tip, and we have

$$V_i(R) = \frac{\omega}{4\pi} \Gamma \left(1 - \frac{\Gamma}{2\pi \omega R^2}\right),$$

which determines the integration constant C. Then $V_i(r)$ is given by

$$V_i^2(r) = \frac{\omega}{4\pi}\left[\Gamma(r)\left(1-\frac{\Gamma(r)}{2\pi\omega r^2}\right)+\int_r^R \frac{\Gamma^2(\alpha)}{\pi\omega\alpha^3}\,d\alpha\right]. \qquad \text{(III. 1. 5)}$$

By setting

$$\int_r^R \frac{\Gamma^2(\alpha)\,d\alpha}{4\pi^2\alpha^3} = -y(r),$$

we can express $\Gamma(r)$ and $V_i(r)$ as functions of y(r):

$$\Gamma(r) = 2\pi\sqrt{r^3 y'(r)}$$

$$V_i = \left[\frac{\omega}{2}\left(\sqrt{y' r^3} - r y'\right) - y\right]^{1/2}.$$

Substituting these values into Eqs. (III. 1. 1') and (III. 1. 2), we can express P and F_N by means of the unknown function y(r) and of its derivative y'(r). We have arrived at a classical problem of the calculus of variations: find the function y(r) such that the integral /A. 24

$$\int_0^R F(y y' r)\,dr \text{ is minimum,}$$

the integral $\int_0^R G(y, y', r)\,dr$ having an imposed value.

We know that the desired function y(r) obeys the differential equation

$$\frac{\partial F}{\partial y} - \frac{d}{dr}\left(\frac{\partial F}{\partial y'}\right) = K\left[\frac{\partial G}{\partial y} - \frac{d}{dr}\left(\frac{\partial G}{\partial y'}\right)\right],$$

where K is a constant depending on the value imposed on the second integral. The calculation will not be given in greater detail because it is very complex and of little practical interest.

Plate (III-3a) presents a typical example of induced velocity distribution.

Note. Some authors simplify the solution by neglecting the effect of the induced tangential velocities in the equation giving V_i as a function of Γ. Eq. (III.1.4) then becomes

$$dV_i^2 = \frac{\omega}{4\pi} d\Gamma \qquad \text{(III.1.4')}$$

from which we get

$$\underline{V_i^2 = \frac{\omega}{4\pi} \Gamma} .$$

If the value of Γ thus obtained as a function of V_i is substituted into (III.1.1) and (III.1.2) and the variational equation is written, the reader will be able to verify that the solution is

$$\frac{V_i}{u} = \frac{\bar{r}}{u} \left(-3K\bar{r} + \sqrt{32 + 9K^2\bar{r}^2} \right),$$

which allows us to get an idea of the form of the exact solution, but which leads to highly erroneous results in the region near the root of the blade.

APPENDIX III-2

SOLUTION OF THE FLAPPING EQUATION

Lift III-2.1

$$F_N = \frac{\rho}{2} S \sigma U^2 \frac{dC_z}{di} \left[\theta_{0,7}\left(\bar{G}_2 + \frac{\mu^2}{2}\bar{G}_0\right) - \bar{G}_1\left(\lambda + \frac{V_i}{U} + \theta_2 \mu\right) + \left(\bar{L}_2 + \frac{\mu^2}{2}\bar{L}_0\right)\right]$$

Approximate value for a rectangular blade :

$$F_N = \frac{\rho}{2} S \sigma U^2 \frac{dC_z}{di} \left[\frac{\theta_{0,7}}{3}\left(1 + \frac{3}{2}\mu^2\right) - \frac{1}{2}\left(\lambda + \frac{V_i}{U} + \theta_2 \mu\right)\right].$$

Coning angle II-2.2

$$a_0 = \underbrace{\frac{\rho}{2} U^2 \frac{S\sigma}{b} \frac{R}{I_p \omega^2} \frac{dC_z}{di}}_{(\gamma_L)} \left[\theta_{0,7}\left(\bar{G}_3 + \bar{G}_1 \frac{\mu^2}{2}\right) - \left(\lambda + \frac{V_i}{U} + \theta_2 \mu\right)\bar{G}_2 + \left(\bar{L}_3 + \bar{L}_1 \frac{\mu^2}{2}\right)\right]$$

$$a_0 = \frac{1 + \frac{\bar{G}_1}{\bar{G}_3}\frac{\mu^2}{2}}{1 + \frac{\bar{G}_0}{\bar{G}_2}\frac{\mu^2}{2}} \times \frac{\bar{G}_3}{\bar{G}_2} \left\{ \frac{F_N}{b} \frac{R}{I_p \omega^2} + \gamma_L \left[\left(\lambda + \frac{V_i}{U} + \theta_2 \mu\right)\left(\bar{G}_1 - \frac{\bar{G}_2 \cdot \bar{G}_3}{\bar{G}_3} \times \frac{1 + \frac{\bar{G}_0}{\bar{G}_2}\frac{\mu^2}{2}}{1 + \frac{\bar{G}_1}{\bar{G}_3}\frac{\mu^2}{2}}\right) + \left(\bar{L}_3 + \bar{L}_1 \frac{\mu^2}{2}\right) \right.\right.$$

$$\left.\left. \frac{\bar{G}_2}{\bar{G}_3} \times \frac{1 + \frac{\bar{G}_0}{\bar{G}_2}\frac{\mu^2}{2}}{1 + \frac{\bar{G}_1}{\bar{G}_3}\frac{\mu^2}{2}} - \left(\bar{L}_2 + \frac{\mu^2}{2}\bar{L}_0\right) \right] \right\}$$

Approximate value: $a_0 = \frac{\bar{G}_3}{\bar{G}_2} \frac{F_N}{b} \frac{R}{I_p \omega^2} \simeq \frac{3}{4} \cdot \frac{F_N}{b} \cdot \frac{R}{I_p \omega^2}$

APPENDIX III-2

SOLUTION OF THE FLAPPING EQUATION

Longitudinal tilt III-2.3

$$a_1 = \frac{\mu}{1 - \frac{\mu^2}{4}\frac{\bar{G}_1}{\bar{G}_3}} \left[2\,\theta_{0.7}\,\frac{\bar{G}_2}{\bar{G}_3} - \frac{\bar{G}_1}{\bar{G}_3}\cdot\left(\lambda + \frac{V_i}{u} + \theta_2\mu\right) + 2\,\frac{\bar{L}_2}{\bar{G}_3} \right] - \theta_2$$

$$a_1 = \frac{\mu}{\left(1 + \frac{\mu^2}{2}\frac{\bar{G}_0}{\bar{G}_2}\right)\left(1 - \frac{\mu^2}{4}\frac{\bar{G}_1}{\bar{G}_3}\right)} \left[\frac{2\,\frac{F_N}{b}\,R}{G_3\,\omega^2} + \left(\lambda + \frac{V_i}{u} + \theta_2\mu\right)\frac{\bar{G}_1}{\bar{G}_3}\left(1 - \frac{\mu^2}{2}\cdot\frac{\bar{G}_0}{\bar{G}_3}\right) + \mu^2\,\frac{\left(\bar{L}_2 \times \frac{\bar{G}_0}{\bar{G}_2} - \bar{L}_0\right)}{\bar{G}_3} \right] - \theta_2$$

Influence of lift | ← Influence of axial inflow → | Influence of twist (always negligible) | Influence of piloting

Approximate value : $a_1 + \theta_2 = 2\mu\left[\frac{F_N R}{b G_3 \omega^2} + \left(\lambda + \frac{V_i}{u} + \theta_2\mu\right)\right] \simeq 2\mu\left[\frac{4 f_N}{\sigma \frac{dC_z}{di}} + \lambda + \frac{V_i}{u} + \theta_2\mu\right]$

$= 2\mu\left[\frac{3}{4} i_m + \left(\lambda + \frac{V_i}{u} + \theta_2\mu\right)\right]$

Lateral tilt III-2.4

$$b_1 = \underbrace{\frac{\bar{G}_2}{\bar{G}_3}\,\frac{a_0}{1 + \frac{\mu^2}{4}\frac{\bar{G}_1}{\bar{G}_3}}\,\mu}_{\text{Influence of coning}} + \underbrace{\theta_1}_{\text{Influence of piloting}}$$

Approximate value : $b_1 = \frac{4}{3}\,\frac{a_0\,\mu}{1 + \frac{\mu^2}{2}} + \theta_1$

DEFINITIONS

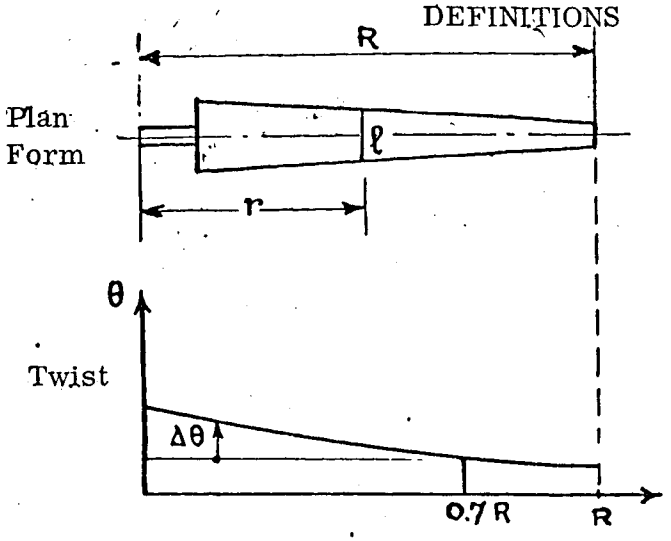

$$S = \pi R^2$$

$$\sigma = \frac{b\,\ell_{0,7}\,R}{\pi R^2}$$

$$f_N = \frac{F_N}{\frac{\rho}{2} S U^2}$$

$$C_{3m} = \frac{3 F_N}{\sigma} \quad ; \quad i_m = \frac{C_{3m}}{\frac{dC_3}{di}}$$

$$\gamma_L = \frac{\frac{\rho}{2}\frac{dC_3}{di} R^4 \ell_{0.7}}{I_p}$$

Form Parameters

Approximate values rectangular blade

$$G_0 = \int_0^{BR} \frac{\rho}{2}\frac{dC_3}{di}\,\ell\,dr \qquad \bar{G}_0 = \frac{G_0}{\frac{\rho}{2}\frac{dC_3}{di}\,\ell_{0.7}\,R} \qquad (1)$$

$$G_1 = \int_0^{BR} \frac{\rho}{2}\frac{dC_3}{di}\,\ell r\,dr \qquad \bar{G}_1 = \frac{G_1}{\frac{\rho}{2}\frac{dC_3}{di}\,\ell_{0.7}\,R^2} \qquad (\tfrac{1}{2})$$

$$G_2 = \int_0^{BR} \frac{\rho}{2}\frac{dC_3}{di}\,\ell r^2 dr \qquad \bar{G}_2 = \frac{G_2}{\frac{\rho}{2}\frac{dC_3}{di}\,\ell_{0.7}\,R^3} \qquad (\tfrac{1}{3})$$

$$G_3 = \int_0^{BR} \frac{\rho}{2}\frac{dC_3}{di}\,\ell r^3 dr \qquad \bar{G}_3 = \frac{G_3}{\frac{\rho}{2}\frac{dC_3}{di}\,\ell_{0.7}\,R^4} \qquad (\tfrac{1}{4})$$

Twist parameters

Linear twist $\Delta\theta = \theta_v\left(0.7 - \frac{r}{R}\right)$

$$L_0 = \int_0^{BR} \frac{\rho}{2}\frac{dC_3}{di}\,\ell\,\Delta\theta\,dr \qquad \bar{L}_0 = \frac{L_0}{\frac{\rho}{2}\frac{dC_3}{di}\,\ell_{0.7}\,R} \qquad (0.2\,\theta_v)$$

$$L_1 = \int_0^{BR} \frac{\rho}{2}\frac{dC_3}{di}\,\ell r\,\Delta\theta\,dr \qquad \bar{L}_1 = \frac{L_1}{\frac{\rho}{2}\frac{dC_3}{di}\,\ell_{0.7}\,R^2} \qquad (0.017\,\theta_v)$$

$$L_2 = \int_0^{BR} \frac{\rho}{2}\frac{dC_3}{di}\,\ell r^2\,\Delta\theta\,dr \qquad \bar{L}_2 = \frac{L_2}{\frac{\rho}{2}\frac{dC_3}{di}\,\ell_{0.7}\,R^3} \qquad (-0.017\,\theta_v)$$

$$L_3 = \int_0^{BR} \frac{\rho}{2}\frac{dC_3}{di}\,\ell r^3\,\Delta\theta\,dr \qquad \bar{L}_3 = \frac{L_3}{\frac{\rho}{2}\frac{dC_3}{di}\,\ell_{0.7}\,R^4} \qquad (-0.025\,\theta_v)$$

Note: B is the coefficient of blade tip losses.

APPENDIX III-3

CALCULATION OF THE MOMENTS ABOUT THE FEATHERING AXIS OF A BLADE

/A.27

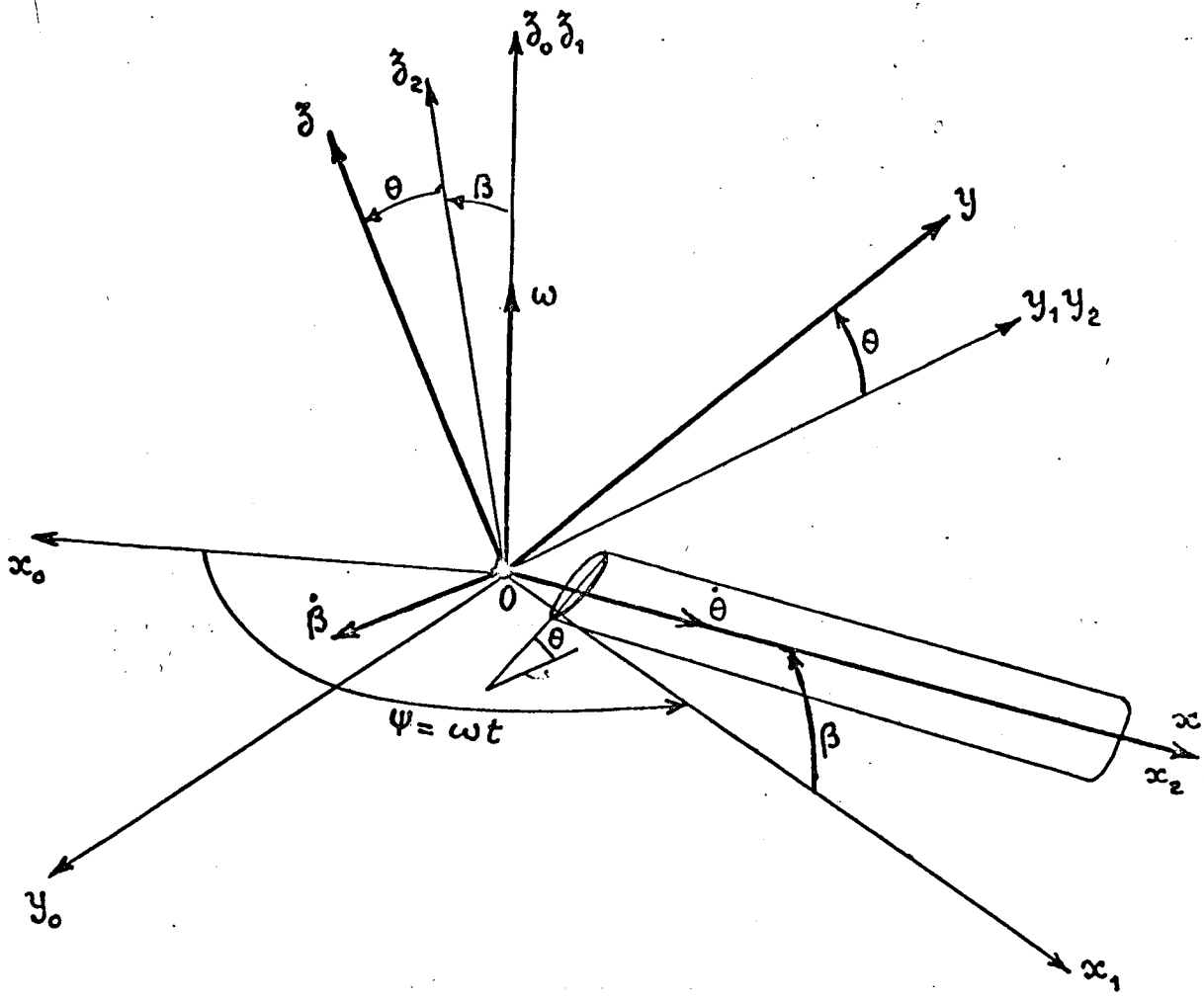

In the figure given above the blade motion is defined by the angles $\psi = \omega t$, β, and θ, which determine the position of the trihedron Oxyz fixed to the blade; Ox is the feathering axis of the blade.

Forces of Inertia

The moment on Ox due to the forces of inertia, which we will denote by M_I, is calculated by writing the equation for the kinetic moment on this axis.

The mass characteristics of the blade are given by the coefficients /A.28

$$\left|\begin{array}{l} A = \Sigma m (y^2 + z^2) \\ B = \Sigma m (z^2 + x^2) \\ C = \Sigma m (x^2 + y^2) \end{array}\right| \qquad \left|\begin{array}{l} D = \Sigma m\, yz \\ E = \Sigma m\, zx \\ F = \Sigma m\, xy \end{array}\right| .$$

The components of the instantaneous rotational velocity along the axes Oxyz are written with the small-angle approximation as

$$\left|\begin{array}{ll} \text{along } Ox: & p = \omega\beta + \dot{\theta} \\ \text{" } Oy: & q = -\dot{\beta} + \omega\theta \\ \text{" } Oz: & r = \omega \end{array}\right| .$$

The derivatives of p, q, r are written with the same approximation as

$$\left|\begin{array}{ll} \text{along } Ox: & \dfrac{dp}{dt} = \omega\dot{\beta} + \ddot{\theta} \\ \text{" } Oy: & \dfrac{dq}{dt} = -\ddot{\beta} + \omega\dot{\theta} \\ \text{" } Oz: & \dfrac{dr}{dt} = 0 \end{array}\right| .$$

The equation for the kinetic moment on the Ox-axis (the Euler equation) is written as

$$-M_I = A\frac{dp}{dt} - F\frac{dq}{dt} - E\frac{dr}{dt} + qr(C-B) - pqE + rpF + D(r^2 - q^2) .$$

That is, if p, q, r, dp/dt, etc. are replaced by their values and if we restrict

ourselves to first-order terms, we have

$$-M_I = A\left(\ddot{\theta} + \omega\dot{\beta}\right) - F\left(\omega\dot{\theta} - \ddot{\beta}\right) + (C-B)\left(\omega^2\theta - \omega\dot{\beta}\right) + F\left(\omega^2\beta + \omega\dot{\theta}\right) + D\omega^2,$$

which can be written /A.29

$$\underline{-M_I = A\left(\ddot{\theta} + \omega^2\theta\right) + (C-B-A)\omega^2\left(\theta - \frac{\dot{\beta}}{\omega}\right) + F\left(\ddot{\beta} + \omega^2\beta\right) + D\omega^2},$$

an equation which gives the moment M_I in the general case of a blade considered as a body of arbitrary shape.

This equation can be simplified by taking into account the particular geometrical shape of the blade and the location of the Ox-axis.

If the xyz-axes are chosen in such a way that xy is close to the "plane of the blade", then

$$C - B - A = -2\Sigma m z^2 \text{ is negligible,}$$

which is also true for $D = \Sigma m y z$ (rigorously zero if xy is the plane of symmetry).

The equation then reduces to

$$\underline{-M_I = A\left(\ddot{\theta} + \omega^2\theta\right) + F\left(\ddot{\beta} + \omega^2\beta\right)}.$$

If, in addition, the feathering axis Ox is the principal axis of inertia, $F = \Sigma m x y = 0$,

$$\underline{-M_I = A\left(\ddot{\theta} + \omega^2\theta\right)}.$$

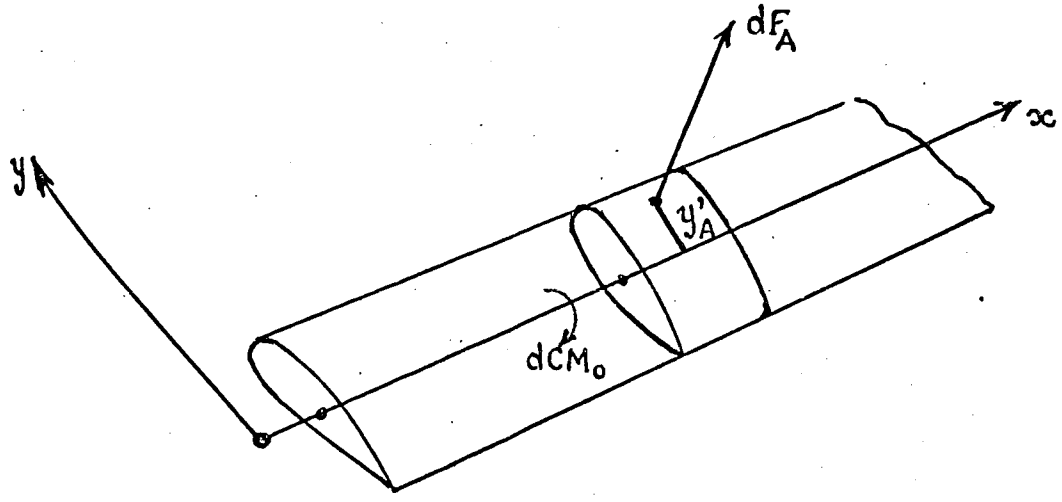

Every blade section is subjected to a moment about the Ox-axis of the form /A.30

$$dM_A = dCM_o + dF_A\, y'_A ,$$

where dCM_o is the aerodynamic moment due to the Cm_o of the blade section, dF_A is the lift of a blade element, and y_A is the coordinate of the aerodynamic center of the blade. For the entire blade assembly, the aerodynamic moment is of the form

$$\underline{M_A = CM_o + F_A y_A} ,$$

with

$$y_A = \frac{\int dF_A\, y'_A}{F_A} .$$

APPENDIX III-4

EQUATIONS OF THE HELICOPTER DYNAMICS IN HOVERING /A.31

The given formulas are simplifications which in general yield a good approximation. They concern the case of a helicopter without a stabilizer and with rigid rotor suspension. The thrust center f is assumed to be near the hub (h_f/h is small).

The equations are set up on the basis of the data given in the following diagram and are given in symbolic form.

Note. The angular displacements indicated in the figure correspond to positive values of the parameters. In particular, the motion of the rotor disk is referred to the angle a_1, which is considered to be positive when it is tilted forward, contrary to the convention adopted in the rest of the course.

Rotor Flapping (with respect to the absolute axes): /A.32

$$a_1 = \frac{1}{1+\tau_0 p}\left[\delta_p + \gamma - A\mu\left(\mu + \frac{h}{R\omega} p\gamma\right)\right]. \qquad \text{(III.4.1)}$$

Horizontal Force Applied to the Hub:

$$F_h = + F_N a_1 - T_x = F_N a_1 - T\mu\left(\mu + \frac{h}{R\omega} p\gamma\right). \qquad \text{(III.4.2)}$$

Helicopter Motion about the Center of Gravity:

$$(p^2 + \lambda_c^2)\gamma = \lambda_c^2 \frac{F_h}{F_N}. \qquad \text{(III.4.3)}$$

Displacement of the Center of Gravity:

$$p\mu = \lambda_g \frac{F_h}{F_N}.$$

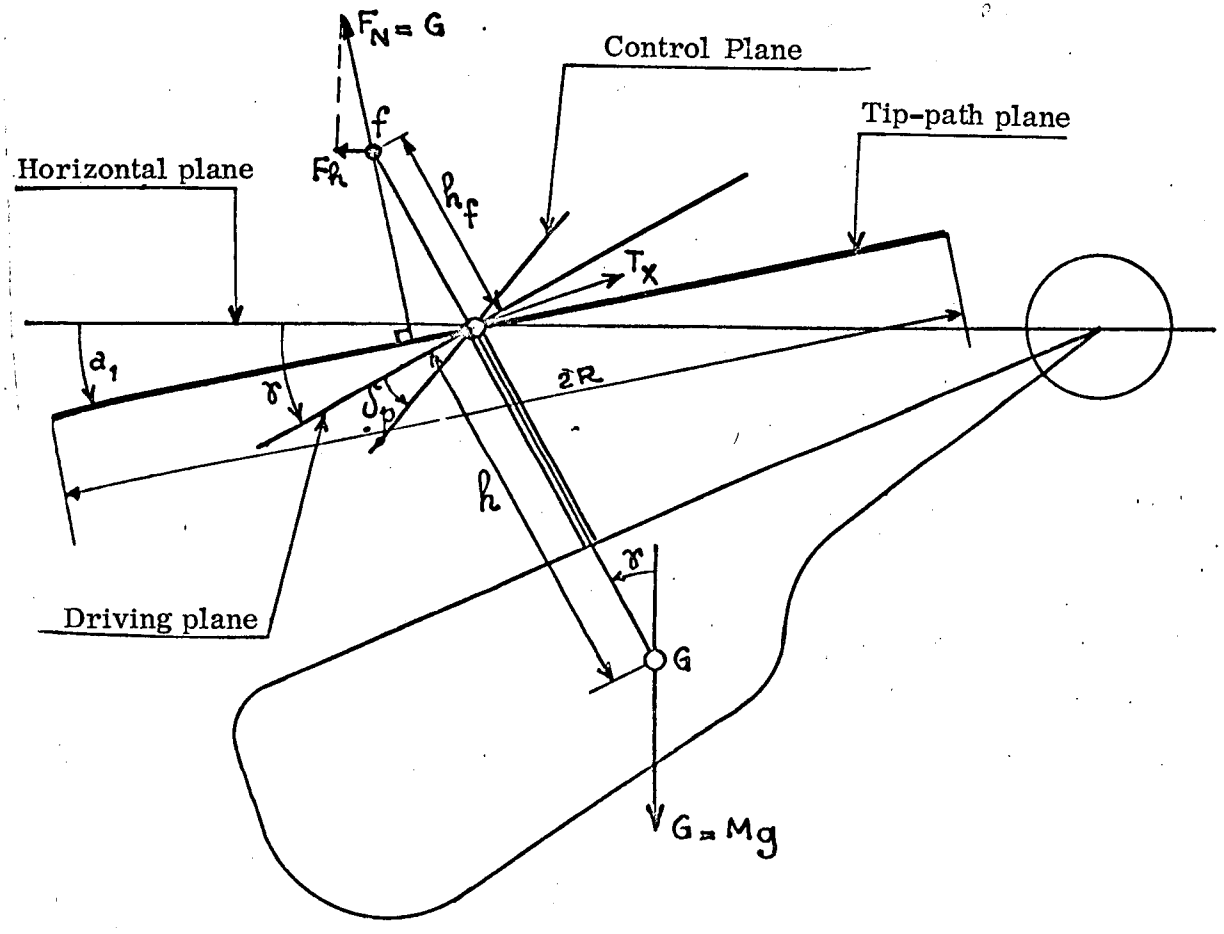
$F_N = G$
Control Plane
Tip-path plane
Horizontal plane
f
F_h
h_f
T_x
a_1
γ
δ_p
2R
h
γ
Driving plane
G
$G = Mg$

Transfer Function in γ

From the preceding equations we deduce the transfer function linking γ to δ_p by eliminating a_1, F_h, and μ:

$$\boxed{\gamma\left\{\frac{p^2}{\lambda_c^2}+\frac{\tau_0 p}{1+\tau_0 p}+\left[\frac{\lambda_q}{p}\left(\frac{p^2}{\lambda_c^2}+1\right)+\frac{hp}{R\omega}\right]\left(\frac{A_\mu}{1+\tau_0 p}+\frac{T_\mu}{F_N}\right)\right\}=\frac{\delta_p}{1+\tau_0 p}} \quad \text{(III.4.5)},$$

which can be written

$$\gamma\left[\frac{p^2}{\lambda_c^2}+\frac{\tau_0 p}{1+\tau_0 p}+F_\mu\left(\frac{A_\mu}{1+\tau_0 p}+T_\mu\right)\right]=\frac{\delta_p}{1+\tau_0 p} \quad \text{(III.4.5')}$$

by setting

$$F_\mu=\frac{\lambda_q}{p}\left(\frac{p^2}{\lambda_c^2}+1\right)+\frac{hp}{R\omega}. \quad \text{(III.4.6)}$$

F_μ is the transfer function linking μ_{rotor} to γ.

Meaning of the Symbols.

τ_0 = rotor response time

$$=\frac{1}{\omega}\times\frac{\left(2\frac{I_p}{G_3}+k\right)}{1+k^2}$$

$$G_3=\int_0^R \frac{\rho}{2}\frac{dC_z}{di}\,l\,r^3\,dr$$

I_p = inertia of the blade about its flapping axis.

ω = rotor speed in rad/sec

k = pitch-flap coupling: $k = -\frac{\Delta\theta}{\Delta\beta}$

A_μ = tilting of the rotor due to the relative airspeed

$$A_\mu = \frac{\partial a_1}{\partial \mu_{rotor}}$$

δ_p = position of the control plane (equilibrium position of the rotor at a stable speed and without relative airspeed)

τ_μ = rotor drag due to relative airspeed: $\tau_\mu = \frac{\partial T_x}{\partial \mu_{rotor}}$; $\left(\frac{\tau_\mu}{F_N} \simeq \frac{3}{4}\frac{C_{xp}}{C_{zm}}\right)$

$\lambda_g = \frac{g}{\omega R}$

$\lambda_c^2 = \frac{F_N(h+h_f)}{I}$ (negative if the thrust center is above the center of gravity of the helicopter)

I = inertia of the machine about the center of gravity

h = distance between the hub and the center of gravity

h_f = distance between the thrust center and the hub: 1/2 a/a_0 (a = off-set of the flapping hinges; a_0 = rotor coning angle)

Approximation Within the Range of Piloting Frequencies /A.34

Within the range of periods of 1 to 5 sec (angular velocities between 6 and 1.25 rad/sec), formula (4.5') can be simplified with good approximation by neglecting the terms in F_μ:

$$\gamma\left(\frac{p^2}{\lambda_c^2} + \frac{\tau_0 p}{1+\tau_0 p}\right) = \frac{\delta_p}{1+\tau_0 p}$$

The graph in Plate V-2 permits direct determination of the value of the transfer function for an angular velocity of 2 rad/sec (period = 3.14 sec).

APPENDIX III-5

MATHEMATICAL STUDY OF WEAVING

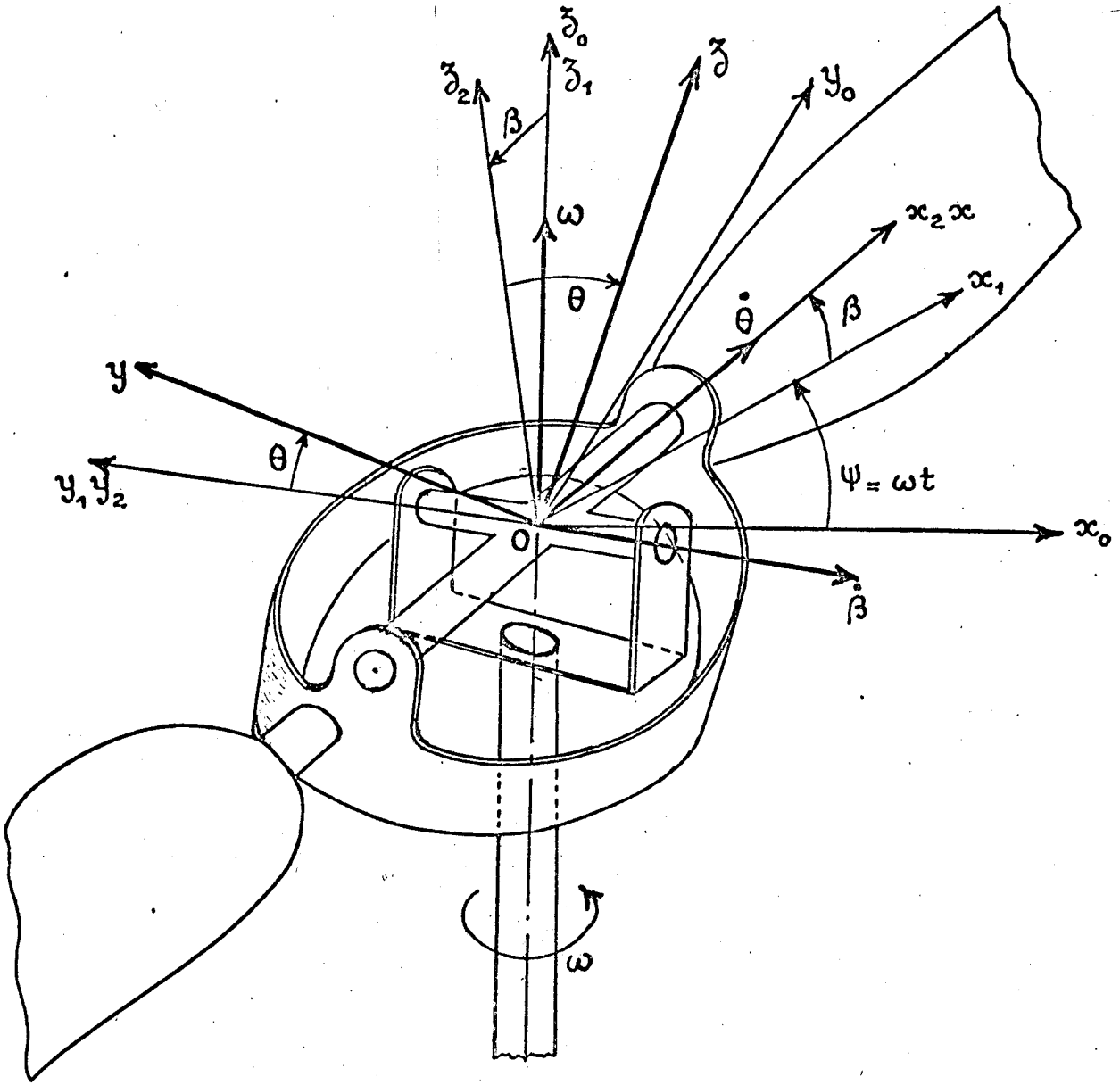

$0x_0y_0z_0$ = fixed reference trihedron. O_{z_0} is parallel to the rotor axis.

Oxyz = reference trihedron linked to the hub-blade assembly considered as a a solid body.

$Ox_1y_1z_1$, $Ox_2y_2z_2$ = intermediate reference trihedra.

The motion of the solid body made up of the hub and blades is defined by the angles $\Psi = \omega t$, β and θ, as shown in the preceding figure. /A.36

The trihedron Oxyz linked to the rotor is, by reason of symmetry, the principal trihedron of inertia.

The motion is studied by writing the equation for the kinetic moment on the two axes of the universal, Ox and Oy_1:

The instantaneous rotational velocity components are

$$\left|\begin{array}{ll} \text{on } Ox: & p = \dot{\theta} + \omega\beta \\ \text{" } Oy: & q = -\dot{\beta} + \omega\theta \\ \text{" } Oz: & r = \omega . \end{array}\right.$$

The components of the kinetic moment are

$$\left|\begin{array}{ll} \text{on } Ox: & I_x(\dot{\theta} + \omega\beta) \\ \text{" } Oy: & I_y(\omega\theta - \dot{\beta}) \\ \text{" } Oz: & I_z\omega , \end{array}\right.$$

where I_x, I_y, and I_z are the moments of inertia about the three axes Oxyz. The equation for the kinetic moment on Ox is

$$I_x(\ddot{\theta}+\omega\dot{\beta})+(I_z-I_y)\omega(\omega\theta-\dot{\beta})=M_{Ox}$$

where M_{Ox} denotes the moment of the applied external forces.

The Equation For the Kinetic Moment on Oy_1.

This can be obtained by projecting the velocities of the kinetic moment calculated on the principal axes Oy and Oz onto the axis Oy_1. It is easy to see that the equation for the kinetic moment on Oy is obtained to within the first order as

$$\cos\theta\left[I_y\frac{dq}{dt}+(I_x-I_z)rp\right]-\sin\theta\left[I_z\frac{dr}{dt}+(I_y-I_x)pq\right]=M_{Oy_1}.$$

If we restrict ourselves to first-order terms, the equation is written as /A.37

$$I_y(-\ddot{\beta}+\omega\dot{\theta})+(I_x-I_z)\omega(\dot{\theta}+\omega\beta)=M_{Oy_1}.$$

Before studying the stability of the system let us define M_{Ox} and M_{Oy1}. The forces that may appear are the differential aerodynamic forces stemming from blade flapping and from variations in blade angle of attack. A variation of pitch θ results in the appearance of a force dF_A applied to the "center of one blade and of a force $-dF_A$ applied to the same point on the other blade.

On Ox, therefore, we get a moment of the form

$$M\theta y_A,$$

where M is the aerodynamic constant characteristic of the rotor and is always positive,

and on Oy_1 we get a moment of the form

$$-M\theta z_A.$$

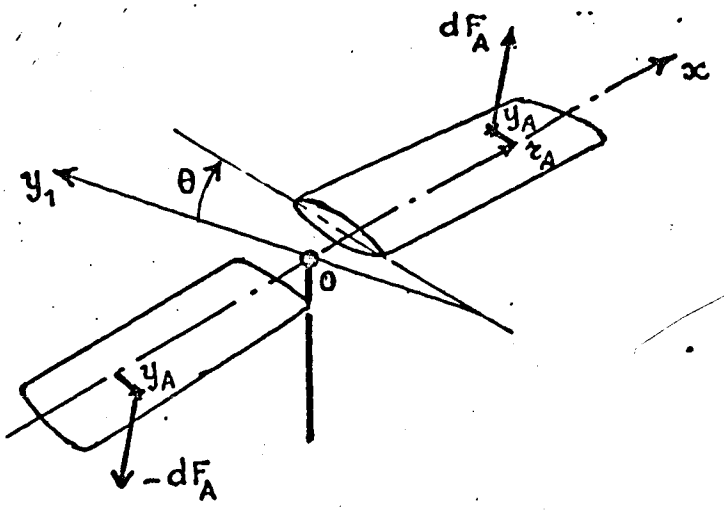

Insofar as the flapping β is concerned, we know that it is equivalent to a change in pitch of $-\beta/\omega$, and that it will therefore induce moments of the form

$$-M\frac{\dot{\beta}}{\omega}y_A \text{ on Ox and } -M\frac{\dot{\beta}}{\omega}z_A \text{ on } Oy_1.$$

Since the pitch motion θ is controlled by the cyclic control system, it will be assumed in addition that there will be elastic restoration of the form $-K_\theta\theta$ with respect to the degree of freedom. /A.38

Then the motion is characteristized by the system of two equations given below:*

$$I_x\left(\ddot{\theta}+\omega\dot{\beta}\right)+\left(I_z-I_y\right)\omega\left(\omega\theta-\dot{\beta}\right)=-K_\theta\theta+My_A\left(\theta-\frac{\dot{\beta}}{\omega}\right)$$
$$I_y\left(-\ddot{\beta}+\omega\dot{\theta}\right)+\left(I_x-I_z\right)\omega\left(\dot{\theta}+\omega\beta\right)=-Mz_A\left(\theta-\frac{\dot{\beta}}{\omega}\right)$$

The characteristic equation is obtained by the usual method as

*In case the aerodynamic force center is not located on the Ox-axis, it is expedient to account for the differential drag forces which produce a moment about Ox which is similar in form to that produced by differential lift. This effect has been neglected because in practice the center is very close to Ox.

The characteristic equation is obtained by the usual method as

$$\tau^4 I_x I_y + \tau^3 I_x \frac{M r_A}{\omega} + \tau^2 \omega^2 \left[I_z^2 + 2 I_x I_y - I_y I_z - I_x I_z + \frac{I_y K_\theta}{\omega^2} + \left(I_x - I_z\right) \frac{M y_A}{\omega^2} \right]$$

$$+ \tau . \frac{M r_A}{\omega} \left(K_\theta + I_x \omega^2\right) + \omega^4 \left(I_z - I_x\right)\left(I_z - I_y + K_\theta - M y_A\right) = 0$$

The stability can be studied by the Routh criteria. In practice the critical condition is the static stability:

$$\omega^4 \left(I_z - I_x\right)\left(I_z - I_y + \frac{K_\theta}{\omega^2} - \frac{M y_A}{\omega^2}\right) > 0.$$

Appendix III-6

METHOD OF CALCULATING THE LIFE-TIME OF HELOCOPTER BLADES

/A. 39

This method is especially suited for determining the lift-time of helicopter blades*, but it is obvious that it can be applied without modification to any problem of this nature; that is, the determination of the life-time of a vital component working under fatigue conditions which, if it fractured while in service, would result in a disaster.

The presentation is rather concise and assumes that the reader has considerable knowledge of the calculus of probabilities.

*The method was developed at S. T. Ae. by Mr. Soulez-Lariviere, Aeronautical Engr.

1. Introduction

Suppose that we know on the one hand the forces exerted on the blade during service and on the other hand the fatigue Curve S-N of the blade (the forces are the number of cycles leading to rupture). The life-time is calculated by means of the hypothesis of cumulative damage, viz., the damage caused by n_0 cycles at a stress of S_0 is defined by the ratio n_0/N_0, where N_0 denotes the number of cycles leading to rupture. If in addition the blade is subjected to n_1 cycles at a stress of S_1, n_2 cycles at a stress of S_2, etc., rupture will occur when the damage $n_0/N_0 + n_1/N_1$, $n_2/N_2 + \ldots = 1$. Thus we can evaluate the damage represented by one hour of flight and deduce the life-time from it.

Knowledge of the forces applied in service does not present any basic difficulty; it is sufficient to take a suitable margin to account for the dispersion inherent during operation. In contrast, determination of the Curve S-N to be used poses a problem of the calculus of probabilities.

Since fatigue is a phenomenon affected by dispersion, it is necessary to plot a "reliable" S-N Curve on the basis of test results and with the aid of appropriate statistical methods. By a reliable curve is meant a curve which reflects the risk of rupture occurring before the life-time limit it defines as being less than some value judged to be acceptable.

A particular difficulty derives from the fact that the tolerated risk is extremely low and that the corresponding law of probability is not accessible to experiment (as demonstrated in 7.2143). Therefore we must rely on a priori laws, which are in part arbitrary. /A.40

2. Determination of a Reliable S-N Curve

The experimental data represent a certain number n of rupture tests carried out with blade elements subjected to different loads levels*. These data are applied under the following assumptions:

1) The curves of equal probability are mutually affine along the S-axis, the mean curve being best fitted to the spread of points obtained with a certain number of form parameters. In general a linear law in 1/N and S is chosen (Fig. 1).

*A rupture test yields much more statistical information than a test without rupture; therefore it will be of interest to carry out the majority of tests at load levels slightly higher than those observed in flight.

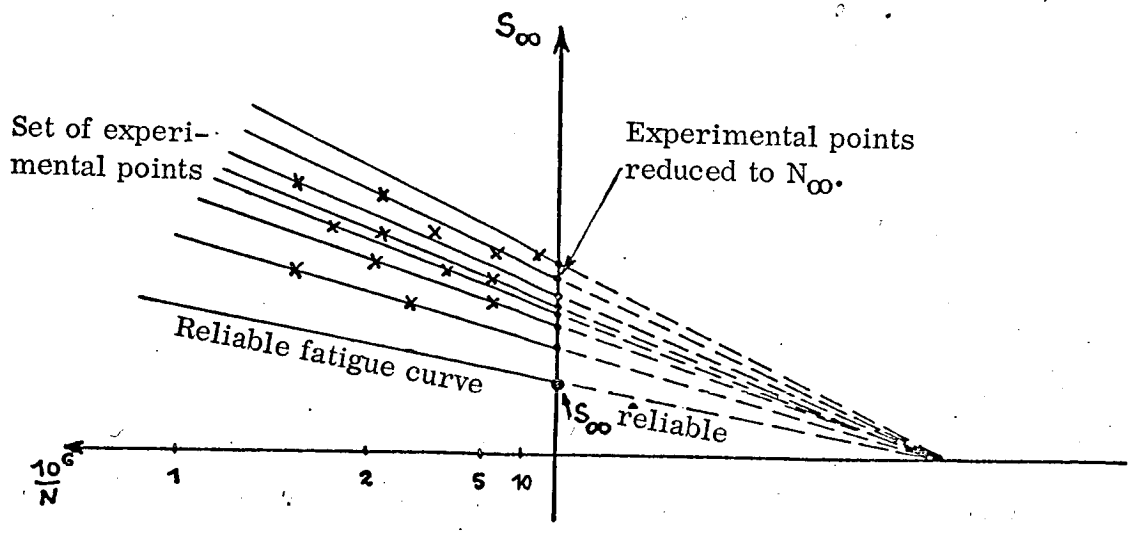

Figure 1.

2) The affinity parameter (the fatigue limit S_∞, for example) is considered as the only random variable subject to dispersion.

3) The first step to be taken is to arbitrarily extrapolate the probability law for S_∞ toward very small probabilities or, what is the same, to choose the function $x(S_\infty)$, which is assumed to obey the normal law. This will make it possible to reduce the problem to a rather well founded statistical domain (that of the Gaussian law). /A.41

The law $x(S_\infty)$ adopted in what follows is defined as in Fig. 2.

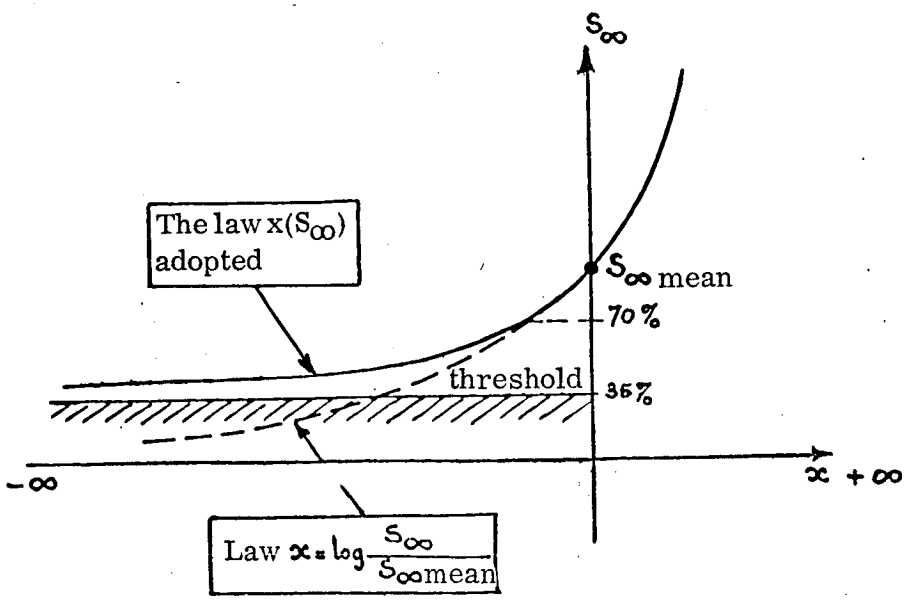

Figure 2.

a) Above 70% of S_∞ mean it is assumes that $x = \log S_\infty / S_\infty$ mean, which is normal. This results in quasi-equivalence between Δx and ΔS_∞ in the neighborhood of S_∞ mean (tangent at 45°) and is justified by the fact that the dispersion of log S_∞ is almost normal in this region of mean probability ($0.1 < p < 0.99$), which can be assessed experimentally.

b) It is presumed that there is a threshold at 35% of S_∞ mean. This threshold is necessary if we do not wish to be forced to accept the enormous and very probably excessive margins that would ensue from application of the normal law to S_∞ in this region. Moreover, this threshold is somewhat justified by the sum total of fatigue experience in all domains (billions of cases ?): "fatigue rupture has never been observed in parts that work at a very low stress level". It is also justified by the fact that a natural defect that would produce a decrease in strength of this order would never have passed undetected through thorough industrial quality control.

c) Between 70 and 35% we apply a linear reduction of the margin to be taken as a result of the effect of the normal law on log S_∞.

4) Thus we know n values of the normal random variable x, and it is enough /A.42
to find the value of X_0 which has little risk (r) of being exceeded and also to compute the risk of being deceived in stating that $Pr\{x < X_0\} \leqslant r$.

This is a problem of estimating parameters, and the results depend on the point of view taken. In what follows we use the method of the 90% confidence factor: the value of X_0 is taken to be equal to $m - k\ell\sqrt{\frac{n}{n-1}}$ (where m is the mean and 1 the typical deviation of the determined values of x_i) and k is given as a function of the risk r and of the number of tests n, both from Table (1).

Note that for $n = \infty$, the values of k are those of the normal law. In fact, in this case the parameters μ and λ (real mean and real typical deviation) are exactly known, equaling the experimental m and 1. If n is finite, μ and λ are found to be "near" the experimental values and, to account for this uncertainty, we have to choose a higher margin k so as to lend a certain "confidence" (here 90%) to the statement $Pr\{x < X_0\} \leqslant r$

From the table and the empirical law defined in 3) we deduced graph (2), which gives the reliable strength percentage directly as a function of the tolerated risk, the observed dispersion, and the number of tests performed. Note in particular how the number of available tests affect the margins to be taken and, in contrast, the relatively small influence of the number of blades to be checked.

Table of the Margins k to be Taken, Calculated as the Probable Runs Deviations as a Function of the Tolerated Risk r and of the Number n of Tests Performed (1)

90% confidence

n \ r	10^{-2}	10^{-3}	10^{-4}	10^{-5}	10^{-6}	10^{-7}
3	6.660	8.75	10.53	12.03	13.39	14.63
4	5.04	6.61	7.95	9.09	10.10	11.05
5	4.40	5.76	6.93	7.92	8.81	9.64
6	4.05	5.30	6.38	7.30	8.11	8.85
8	3.71	4.84	5.83	6.68	7.41	8.10
10	3.44	4.51	5.43	6.20	6.90	7.54
20	3.05	3.99	4.80	5.50	6.10	6.67
50	2.73	3.59	4.34	4.86	5.52	6.04
∞	2.33	3.09	3.74	4.29	4.78	5.23

$$k = \frac{k_r + k_q \sqrt{\frac{1}{n}\left(1 - \frac{k_q^2}{2(n-1)}\right) + \frac{k_r^2}{2(n-1)}}}{1 - \frac{k_q^2}{2(n-1)}}$$

k_r = margin corresponding to the risk n in the simple normal law

k_q = margin corresponding to the risk q in the simple normal law

q = confidence factor

Here q = 90% k_q = 1.28

Total Risk of Rupture Versus the Total Number of Blades in Service r-1/1000

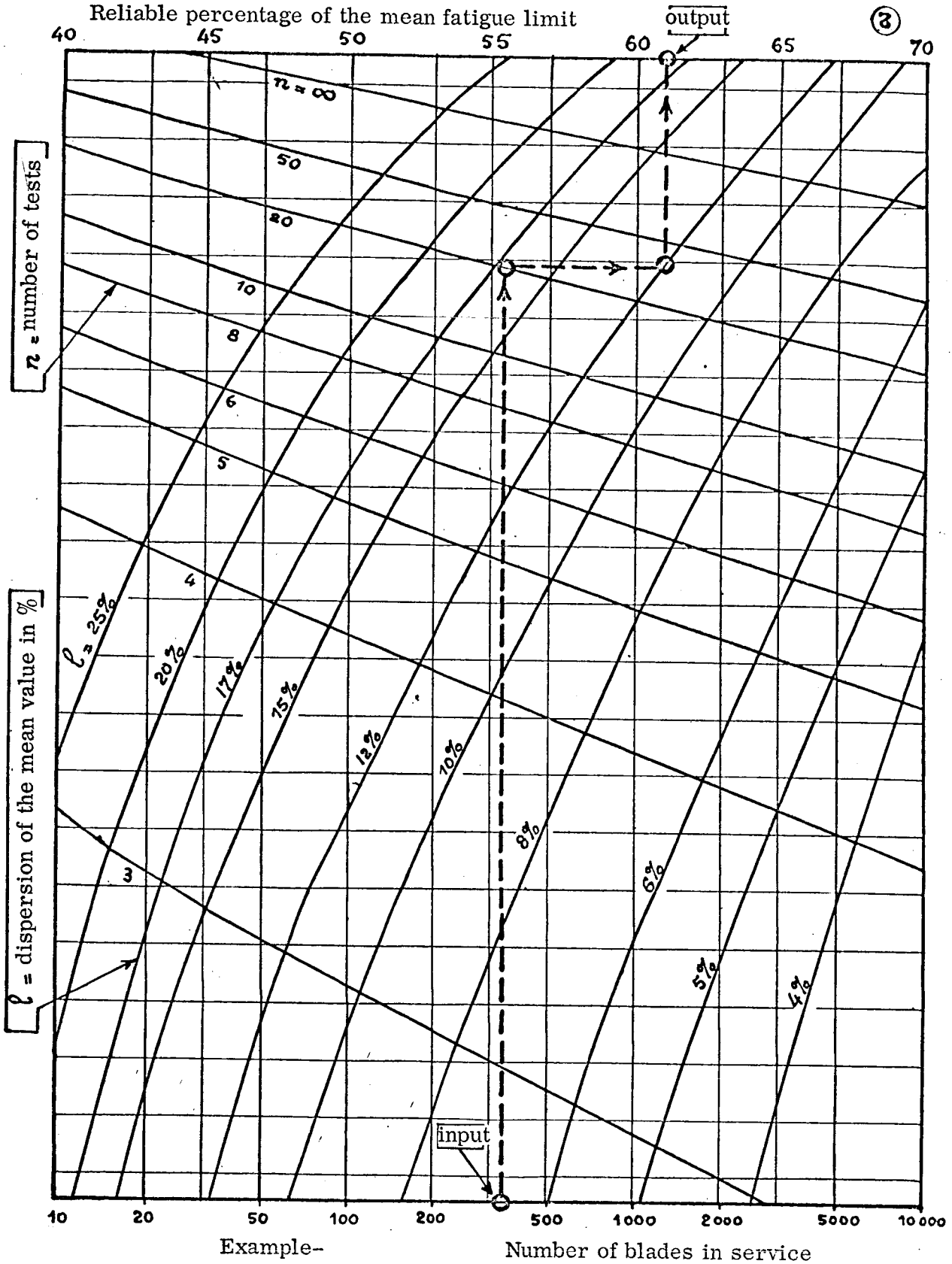

Example-

350 blades - 20 tests - dispersion: 12%

Reliable percentage of the mean fatigue limit: 61

APPENDIX IV

BRIEF ENGLISH-FRENCH GLOSSARY

Note: This glossary makes no claim to completeness; it is restricted to technical terms of specific application of the helicopter that are encountered most frequently. It should be noted that certain of these terms are used in different senses by different authors (in particular, some differences exist between English and American usages). The glossary proper is supplemented by a table showing the correspondence between the Anglo-Saxon notation and that used in this course.

AIRFOIL SECTION: Profile (blade)

AUTOGYRO: Autogire

AUXILIARY ROTOR (Trail Rotor, Angi-torque Rotor): rotor auxiliare (rotor de queue, rotor anti-couple)

BLADE: pale

BLADE PITCH (Blade angle, Blade feathering): pas de la pale (θ)

BRAKE: frein

CLUTCH: embrayage

COLLECTIVE PITCH (common pitch, meanpitch): pas collectif, pas général (θ_o)

CONING ANGLE: angle de conicité (a_o)

COOLING: refroidissement

CYCLIC FLAPPING ANGLE: angle de battement cyclique

CYCLIC PITCH: pas cyclique

DAMPER: amortisseur

DISC AREA: surface du disque (rotor)

DISC LOADING: charge du disque (rotor)

DRAG: traînée

DRAG HINGE: (vertical hinge, lagging hinge): articulation de traînée

ENDURANCE: autonomie

FAN: ventilateur

FEATHERING: variation de pas (of a blade)

FEATHERING HINGE (Torsion hinge): axe de variation de pas

NO FEATHERING AXIS (virtual axis): axe perpendiculaire an plan de base (voir ci-après)

NO FEATHERING PLANE: plan de base (Reference plane with respect to which the blades have constant pitch during rotation.

FIGURE OF MERIT: rapport de al sustentation créée par un rotor à celle créée par un rotor parfait de meme diamètre pour la même puissance (η_s 2/3). (There seems to be some confusion on this subject and certain authors use the term "Figure of Merit" to denote lifting efficiency).

FLAPPING: battement vertical, levée d'une pale (β)

FLAPPING HINGE (Horizontal hinge): articulation de battement vertical

FREE-WHEEL: roue libre

GEAR: engrenage

LANDING GEAR: atterrisseur

GYROPLANE: autogire (In France the term "gyroplane" has sometimes been used to denote special helicopters)

HOIST: treuil

HOVERING: vol stationnaire

HOVERING in ground effect: vol stationnaire dans l'effet de sol

HOVERING out of ground effect: vol stationnaire hors effet de sol

HUB: moyeu

LAGGING (drag motion, in-plane motion, hunting, swinging, sweeping): mouvement de traînée (of a blade)

LAGGING ANGLE: angle of de trainee (δ)

LIFTING EFFICIENCY: efficacité sustentatrice (η_s)

PITCH: pas (of the blades) /A.47

RANGE: distance franchissable

SERVICE CEILING: plafond pratique

SKIDS: patine

SOLIDITY: solidité, plénitude ($\sigma = \frac{b\ell_{0.7}}{\pi R}$)

SPIDER: araignée

STICK: manche (cyclic pitch)

SWASH-PLATE: plateau cyclique

TAIL BOOM: cône de queue

TIP SPEED: vitesse périphérique (rotor)

TWIST: vrillage

CORRESPONDENCE OF ANGLO-SAXON NOTATION WITH THE NOTATION USED IN THE COURSE /A.48

English	French	Notes
A	S	
A_0, A_1	θ_0, θ_1	
a	dC_z/di	
a_0	a_0	
a_1, a_2	a_1, a_2	

CORRESPONDENCE OF ANGLO-SAXON NOTATION WITH THE NOTATION USED IN THE COURSE

English	French	Notes
B	B	
B_1	θ_2	
b	b	
b_1, b_2	b_1, b_2	
C_D, C_L	C_x, C_z	$\frac{\text{Drag (or lift)}}{\frac{1}{2}\rho S V^2}$
C_d	C_{xp}	
C	ℓ	
C_ℓ	C_γ	
C_P, C_Q	m_N	Important: The Americans often use a different definition: $C_T = \frac{F_N}{\rho S u^2} = \frac{1}{2} f_N$; $C_P = \frac{P}{\rho S u^3} = \frac{1}{2} m_N$
C_T, C_H	f_N	
D		Rotor component parallel to the velocity (F_X in some cases)
d	e	
e	a	
H	$\simeq T_X$	Component of the rotor force in the plane of the disc
i	α	
L		Rotor component perpendicular to the velocity (F_Z in certain cases).
P	P	
P_t	P_d	
Q	M_N	
R	R	

CORRESPONDENCE OF ANGLO-SAXON NOTATION WITH THE NOTATION USED IN THE COURSE

English	French	Notes
t	t	
T	F_N	
U	V_1	
U_o	V_{i_o}	
U_1	V_2	
V	V (ou V_o)	
V_h	V_x	
V_v	V_3	
v	v_i	
W	G	
$x = \frac{z}{R}$	$\bar{z}$	
α	i	
β	β	
γ	γ_L	
$\delta_0, \delta_1, \delta_2$		Coefficients of the expansion of C_X as a function of the angle of attack $C_x = \delta_o + \delta_1 i + \delta_2 i^2$.
ζ	δ	
η_e	η_s	
θ	θ	
λ	λ'	
μ	μ	

CORRESPONDENCE OF ANGLO-SAXON NOTATION WITH THE NOTATION USED IN THE COURSE

English	French	Notes
μ_1	Λ	
Ω	ω	
χ		Inclination of flight path to horizon
ψ	Ψ	Angular velocity of induced flow, ω_o on traversing the rotor disc, ω_1 at infinity downstream.
$\omega, \omega_o, \omega_1$		

REFERENCES

The works cited were chosen from those easy to obtain or to consult in France. (Most of them will be found in the S.D.I.T. Library).

However, we have included some documents that are difficult of access because of their special interest.

Ref. No.

HISTORY

—VERTICAL FLIGHT - Lt-Colonel LAME - Paris-Blondel La Rougery -1934) (Many historical references in Parts 1 and 3).

PILOTAGE

—THE HELICOPTER - THEORY - PILOTAGE AND APPLICATION, J. Moine, (Edited by the Fenwick Society, Paris, 1953)

GENERAL THEORY

— Helicopter Analysis - A.A. Nikolsky (New-York, John Wiley and Sons, Inc.).

(1) —Principles of Helicopter Engineering - J. Shapiro, (London, Temple Press, 1955).

— Aerodynamics of the helicopter - Gessow A. and Myers G.G. (New-York, Mac Millian Co., 1953).

–Rotocraft, I.C. Garry (ENSA Course, 1953).
–Theory of single-rotor helicopters - J.J. Ginoux, (Brussels, Office of Publicity).
–Elements of Aerodynamics for Helicopter Pilots - Owen G. Niehaus and Richard Balchelder (Co. Translation C.E.V. No. 302). (Elementary work, but clear and quite complete). /A.52
–Helicopter Engineering - R.A. Young (New York, The Ronald Press Co., 1949).
–Introduction to Helicopter Aerodynamics - W.Z. Stepniewski, (Rotorcraft Publishing Committee, Morton Pa., (1956). (Theory and performance calculations simply presented for use by design bureaus).

FLIGHTS TESTS

–Helicopters - C.E.V. Report No. 194/E, E.P.N. Course, G. Petit. (For use by flight test personnel, general theory, flight test manual). A.G.A.R.D. Flight Test Manual (Translation SDIT, Paris, 1958).

AERODYNAMICS

–Review of Information on Induced Flow of a Lifting Rotor - Alfred Gessow, (NACA Technical Note 3238, 1954).
(3) –Induced Aerodynamics of Helicopters - P.R. Payne (Aircraft Engineering, February, March, April, May 1956).
–An Investigation in Flight of the Induced Velocity Distribution Under a Helicopter When Hovering - P. Brotherhood, (British ARC, R and M No. 2531).
–Flow through a helicopter rotor in vertical descent- P. Brotherhood (British ARC - R. and M. No. 2735 - 1952).
–Static Thrust Measurements of the Aerodynamic Loading on a Helicopter Rotor Blade - John P. Rabbot, Jr. (NACA T. N. 3688, 1956).
–An experimental investigation of the flow through a helicopter rotor in forward flight, P. Brotherhood (British ARC - R. and M. No. 2734, 1952).
–Empirical Relation Between Induced Velocity Thrust, and Rate of Descent of a Helicopter Rotor as Determined by Wind-Tunnel Tests on Four Model Rotors - Walter Gastles Jr. and Robin B. Gray (NACA T. N. 2474, 1951).
–Analysis and Comparison With Theory of Flow-Field Measurements Near a Lifting Rotor in the Langley Full Scale Tunnel - Harry H. Mayson (NACA T. N. 3691, 1956). /A.53
(4) –Evaluation of the Induced Velocity Field of an Idealized Helicopter Rotor- Robert P. Coleman, Arnold M. Feingold, Carl W. Stemphin, (NACA W.R.L. 126, 1945).

(5) –A Theory of Airflow Through Rotors and its Application to Some Helicopter Problems - Meijer Drees J. (Journal of the Helicopter Association of Great Britain, Vol. 3, No. 2, July, August, Sept. 1949).
–The Normal Component of the Induced Velocity in the Vicinity of a Lifting Rotor and Some Examples of its Application - Walter Castles Jr. and Jacob Henri de Leeww (NACA, Rep. 1184, 1954).
–Distribution of Normal Component of Induced Velocity in Lateral Plane of a Lifting Rotor - Walter Castles Jr. and Howard L. Durham Jr. (NACA T.N. 3841, 1956).

(6) –Tables for Use in an Improved Method of Airscrew Strip Theory Calculation- C.N.H. Lock and D. Yeatman (Aeronautical Research Committee, Reports and Memoranda, No. 1674, London, October 1934).
–Charts for Estimating Tail-Rotor Contribution to Helicopter Directional Stability and Control in Low-Speed Flight - Kennet B. Amer, Alfred Gessow (NACA, Technical Note 3156, 1954).
–Reduction of Helicopter Parasit Drag - Robert D. Harrington (NACA, T.N. 3234, 1954).
–A Balsa-Dust Technique for Air-Flow Visualization and its Application to Flow through Model Helicopter Rotors in Static Thrust - Marion K. Taylor (NACA, Technical Note, 2220, 1950).
–Full Scale Wind-Tunnel Tests of a P.C.A. 2 Autogiro Rotor - John B. Wheatley, Manely J. Hood (NACA, Report 515, 1935).
–Determination of Inflow Distributions from Experimental Aerodynamic Loading and Blade - Motion Data on a Model Helicopter Rotor in Hovering and Forward Flight - Gaetano Falabella Jr. and John R. Meyer Jr. (NACA, Technical Note 3492, 1955).
–The Low Speed Performance of a Helicopter - A.L. Oliver (Ministry of Supply, Report No. A.A.E.E/Res/264, 1952).
–Preliminary Results from Flow-Field Measurements Around Single and Tandem Rotors in the Langley Full Scale Tunnel - Harry H. Heysons, (NACA, Technical Note 3242, 1954). /A.54
–Wind-Tunnel Studies of the Performance of Multirotor Configurations - Richard C. Dingeldein (NACA, Technical Note 3236, 1954).
–Ground Effect on the Lifting Rotor - J. Zbrozek (R.A.E. Technical Note Aero 1903).
–Effect of a Rapid Blade-Pitch Increase on the Thrust and Induced Velocity Response of a Full-Scale Helicopter Rotor - Paul J. Carpenter and Bernard Fridovich (NACA, Technical Note 3044, 1953) (Study of the transient characteristics of a rotor in stationary hovering).
–Investigation of Vertical Drag and Periodic Airloads Acting on Flat Panels in a Rotor Slipstream - Robert A. Makofski and George F. Mankick (NACA, Technical Note 3900, 1956).
–Helicopter Dynamics and Aerodynamics - P.R. Payne (Pitman and Sons, London 1959).

ROTOR MECHANICS

–A Method for Studying the Transient Blade-Flapping Behaviour of Lifting Rotors at Extreme Operating Conditions - Alfred Gessow and Almer D. Crim (NACA, Technical Note 3366, 1955).

–Charts for Estimating Rotor Blade-Flapping Motion of High-Performance Helicopters - Robert J. Rapscott and Alfred Gessow (NACA, Technical Note 3616, 1956).

PERFORMANCE

–Full Scale Investigation of the Aerodynamic Characteristics of a Typical Single-Rotor Helicopter in Forward Flight - Richard C. Dingeldein and Raymond F. Scheafer (NACA, Report No. 905, 1948).

–A Method for rapid estimation of Helicopter performance - Q. Wald (Journal of the Aeronautical Sciences, April 1951).

–A direct Method of estimating the performance of a Helicopter in powered flight - W. Castles Jr. (Journal of the Aeronautical Sciences, October 1945).

–Charts for Estimation of the Characteristics of Helicopter Rotor in Forward Flight - F. J. Bailey Jr. and F.B. Gustafson (NACA, W.R.L. 110, 1944).

(8) –Charts for Estimating Performance of High-Performance Helicopters - Alfred Gessow and Robert J. Tapscott (NACA, Rep. 1266 - 1956). /A.55

(9) –Equations and Procedures for Numerically Calculating the Aerodynamic Characteristics of Lifting Rotors - Alfred Gessow (NACA, Technical Note 3747, 1956). (Method of calculating performance by integration of the local aerodynamic effects using a high-speed compter).

–Jet propulsion of the rotor blades of helicopters. A. Stepan (Translation SDIT M.R. 474, 1949).

–A Theorical Estimate of the Effects of Compressibility on the Performance of a Helicopter Rotor in Various Flight Conditions - Alfred Gessow and Almer D. Crim (NACA, Technical Note 3798, 1956).

–Hovering Performance of a Helicopter Rotor Using NACA 8-H-12 Airfoil Sections - Robert D. Powell, Jr. (NACA, Technical Note 3237, 1954). (Tests of a laminar-profile blade).

–Experimental Investigation on the Langley Helicopter Test Tower of Compressibility Effects on a Rotor Having NACA 63_2-015 Airfoil Sections - James P. Shivers and Paul J. Carpenter (NACA, Technical Note 3850, 1956).

–Research and Design Progress Towards High Performance Rotary Wing Aircraft - P.L. Michel (IAS Paper No. 60-27, 25.1.60).

PROPULSION SYSTEMS

–Comparison of helicopter rotor propulsion systems - Stuart J. III (American Helicopter Society, 8th Annual Forum, 1952).

–Investigation of the Propulsive Characteristics of a Helicopter-Type Pulse-Jet Engine over a Range of Mach Numbers and Angle of Yaw - Paul J. Carpenter, James P. Shivers and Edwin E. Lee, Jr. (NACA, Technical Note 3625, 1956).

–The Effect of Forward-Flight Speed on the Propulsive Characteristics of a Pulse-Jet Engine Mounted on a Helicopter Rotor - Robert D. Powell Jr. (NACA, Technical Note 3855, 1957).

–Some applications of gas turbine to helicopter propulsion - John Brown (Journal of the Helicopter Association of Great Britain, Vol. 8, No. 3, January 1955).

STABILITY AND FLIGHT PROPERITIES /A.56

– An Explanation of Some Important Stability Parameters That Influence Helicopter Flying Qualities - A. Gessow and K. B. Amer (New York Institute of Aeronautical Science).

–An Introduction to the Physical Aspects of Helicopter Stability - A. Gessow and K. B. Amer - (NACA, TR-993, 1950).

–Longitudinal Stability and Control of the Single-Rotor Helicopter, A.R.S. Bramwell (R.A.E. Report Naval 1: January 1957, Ministry of Supply, London, W.C. 2).

–Directional Stability Characteristic of Two Types of Tandem Helicopter Fuselage Models - James L. Williams (NACA, Technical Note 3201, 1954).

–Studies of the Lateral-Directional Flying Qualities of a Tandem Helicopter in Forward Flight - Kenneth B. Amer and Robert J. Tapscott (NACA, Technical Note 2984, 1953). (Special study of a tandem configuration, definition of the general criters of flight quality, comparison between theory and tests).

–Methods for Obtaining Desired Helicopter Stability Characteristics and Procedures for Stability Predictions - F.B. Gustafson and Robert J. Tapscott (NACA, Technical Note 3945, 1957).

–Application of harmonic methods in the analysis of the flight properties of helicopters. Principal Engineer LEGRAND (C.E.V. Study Report No. 197/E).

–Automatic piloting of helicopters - R. Larrieu (DOCAERO, January 1961).

GROUND RESONANCE

–Theory of Self-Excited Mechanical Oscillations of Helicopter Rotors with Hinged Rotor Blades - R.P. Coleman and Arnold M. Feingold (NACA, Technical Note 3844, 1957). (NACA, Report 1351, 1958).

–Ground stability of three-blade helicopters - J. Gilly and Y. Normand (Technique and Science Aeronautique, No. 6, 1952).

–Investigation of Ground Resonance in Helicopters With an Analog Computer - H. Fuchs (Journal of the Helicopter Association of Great Britain, Vol. 2, No. 5, October 1957).

STRENGTH OF MATERIALS /A.57

–In-flight measurements of the stresses in helicopter blades - G. Petit (C.E.V. Study Report No. 196/E).

–Flight Measurements and Analysis of Helicopter Normal Load Factors in Manoeuvers - F.B. Gustafson and A.D. Grim (NACA, Technical Note 2990, 1953).

–Normal Accelerations and Operating Conditions Encountered by a Helicopter in Air Mail Operations (NACA, Technical Note 2714, 1953).

–A Study of Normal Accelerations and Operating Conditions Experienced by Helicopters in Commerical and Military Operations - Marlin E. Hazen (NACA, Technical Note 3434, 1955).

–A Dynamic- Model Study of the Effect of Added Weights on Other Structural Variations on the Blade Bending Strains of an Experimental Two-Blade Jet Driven Helicopter in Hovering and Forward Flight - John Locke McCarty and George W. Broocks (NACA, Technical Note 3367, 1955).

–Gust-Tunnel Investigation of the Effect of a Sharp-Edge Gust on the Flap-Wise Blade Bending Moments of a Model Helicopter Rotor - Domenic J. Maglieri and Thomas D. Reisert (NACA, Technical Note 3470, 1955).

–Determination of the Structural Damping Coefficients of Six Full-Scale Helicopter Rotor Blades of Different Materials and Methods of Construction - Frederick W. Gibson (NACA, Technical Note 3862, 1956).

–Calculation of the Useful Lifetime of Helicopter Blades - J. Soulaz (Larivière Technical Note 165/STA/VT, August 1956).

MISCELLANEOUS

–Rotor heads for rotorcraft - E. Leygue and P. Lefort (S.D.I.T. Docaéro, No. 11).

–Design, Development, Production and Servicing of Rotor Blades - R. Allen Price and Frank L. Stulen (Journal of the Helicopter Association of Great Britain, Vol. 9, No. 2, October 1955).

–Two Bladed Rotor - A. M. Young (Bell Aircraft corporation Report 1945).
–French technology and the evolution of the helicopter - I. C. Legrand (Technique and Science Aeronautics, T. 2, 1957).

PUBLICATIONS AND PERIODICALS DEVOTED TO THE HELICOPTER

–American Helicopter, (U. S. A. monthly).
–Forums de l'American Helicopter Society (yearly).
–The Journal of the Helicopter Association of Great Britain (G. B., quarterly).

Translated for the National Aeronautics and Space Administration by Scripta Technica, Inc., NASw-1694.

HIGHER NATIONAL SCHOOL OF AERONAUTICS

ROTORCRAFT

by

F. Legrand
Chief Air Engineer
Director of Helicopter Studies at "Sud-Aviation"

Figures

1964

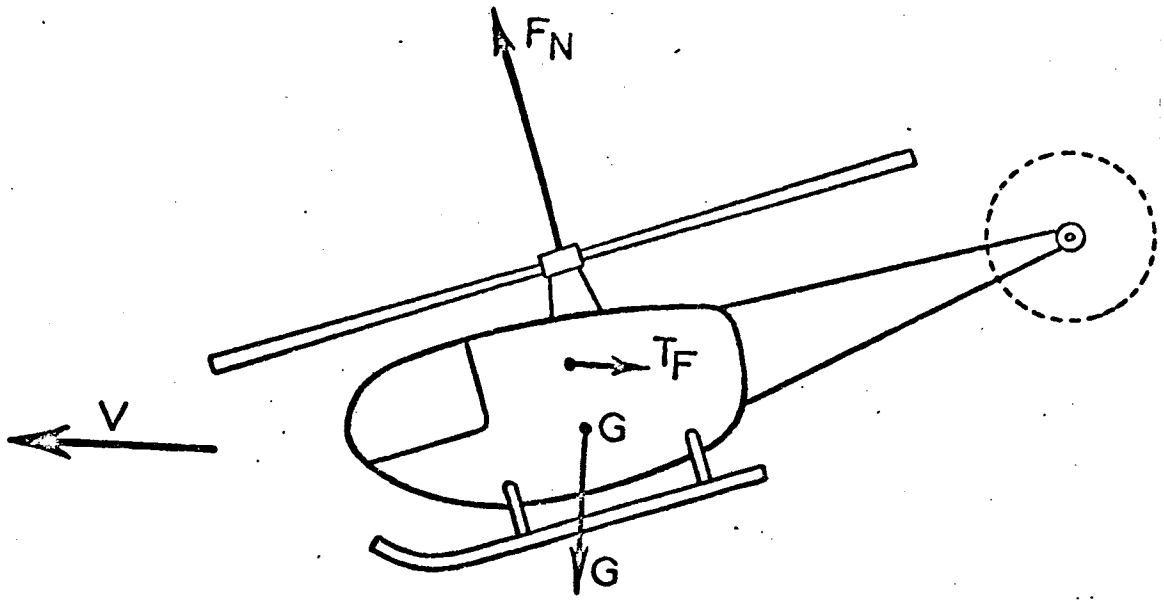

Figure 1-1. Helicopter.

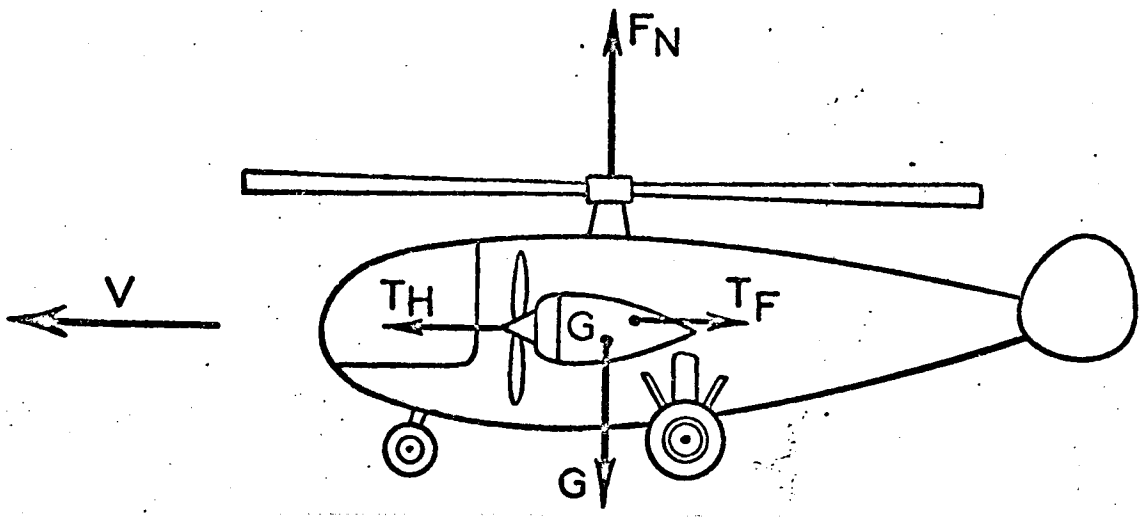

Figure 1-2. Gyrodyne.

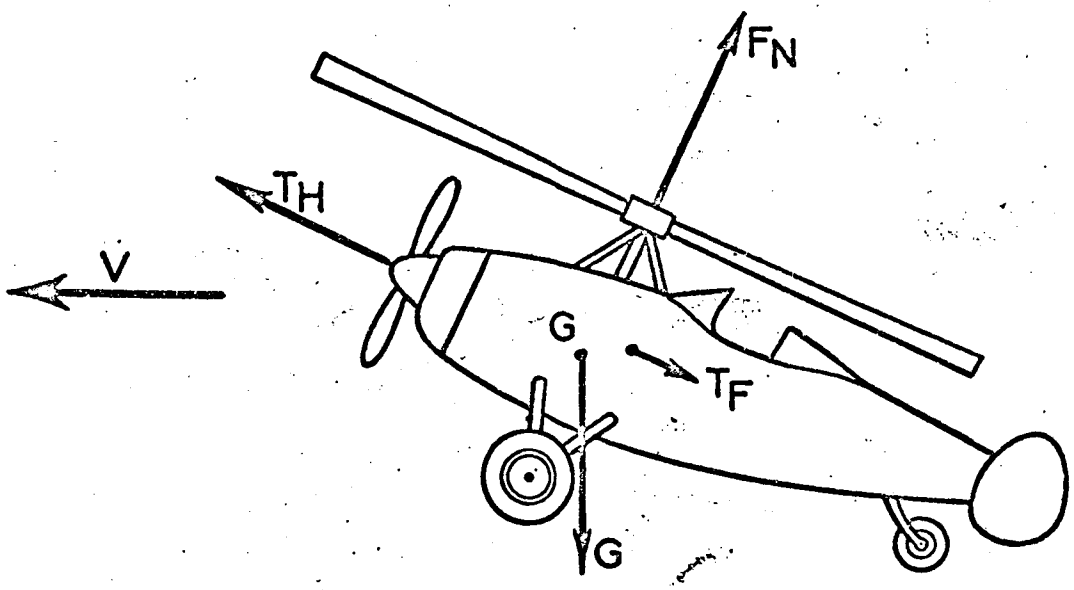

Figure 1-3. Autogyro.

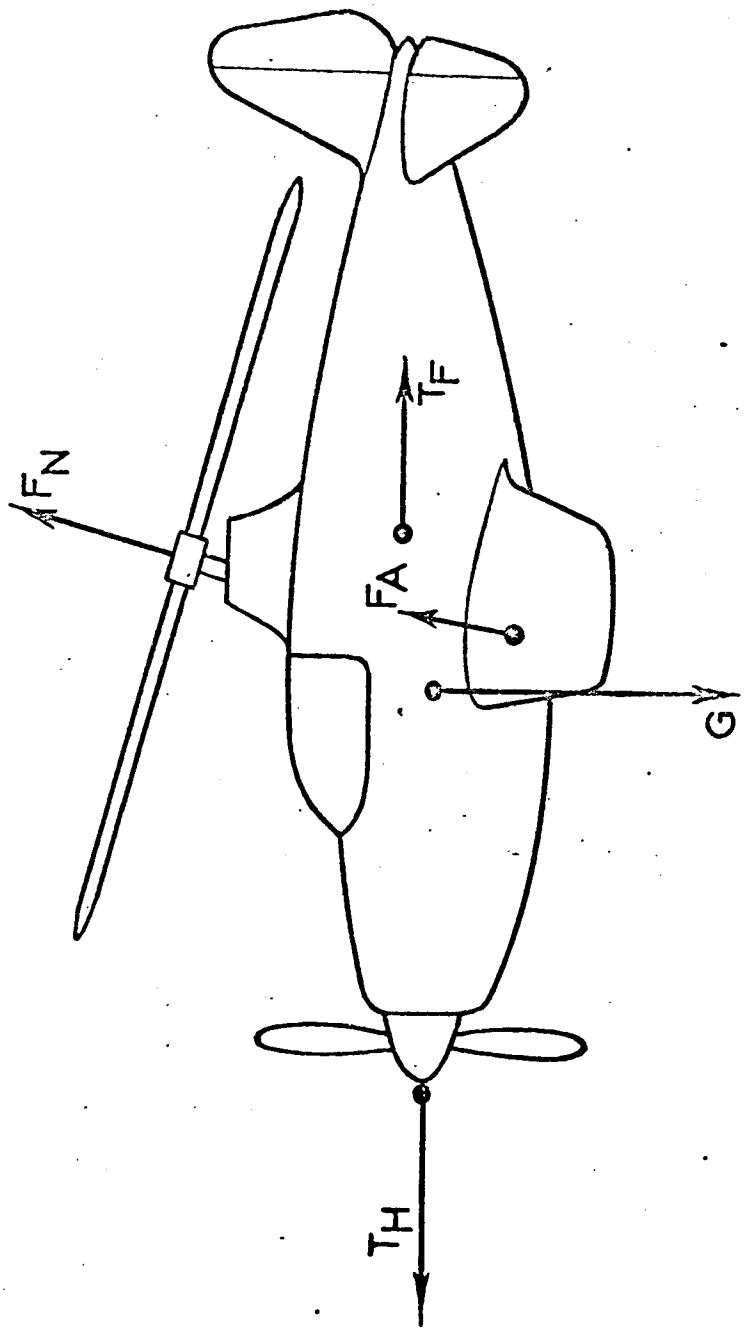

Figure 1-4. Compound.

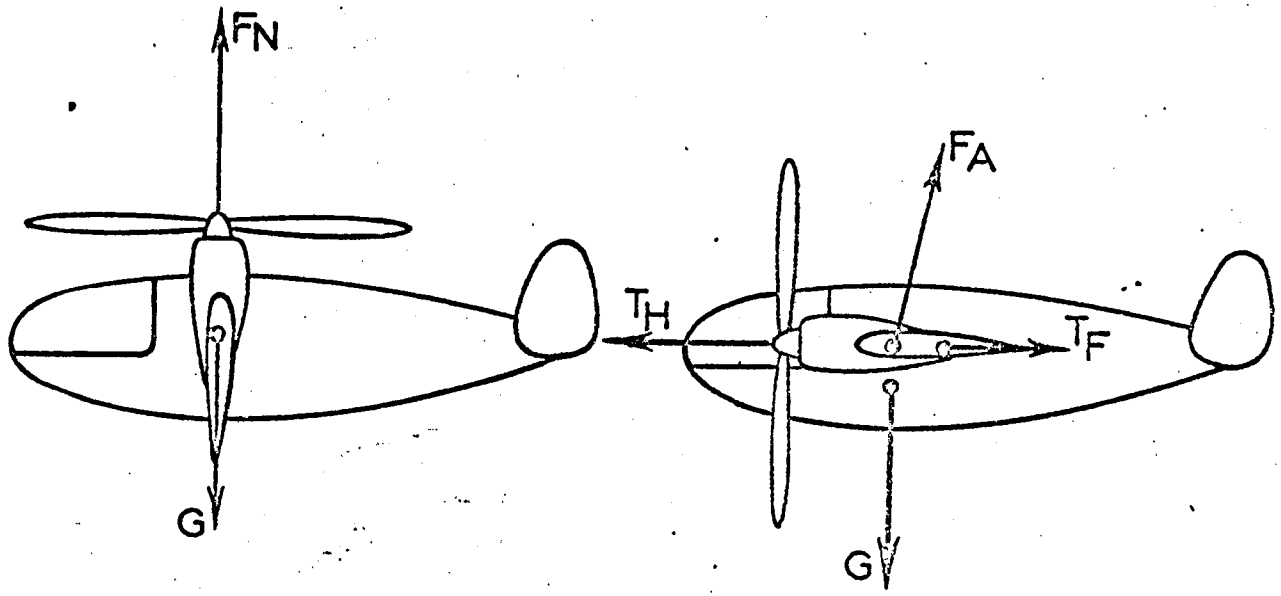

Vertical flight.

Cruising flight.

Figure 1-5. Convertiplane.

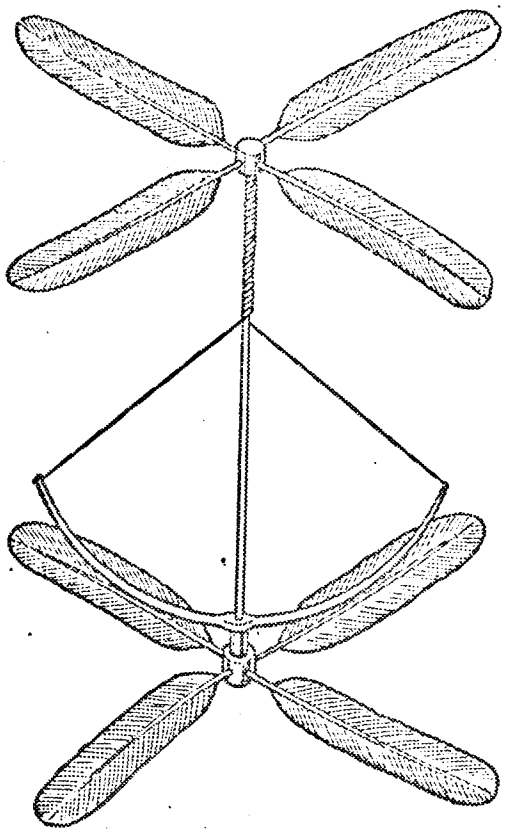

Figure 1-6. The Helicopter of Launoy and Bienvenu.

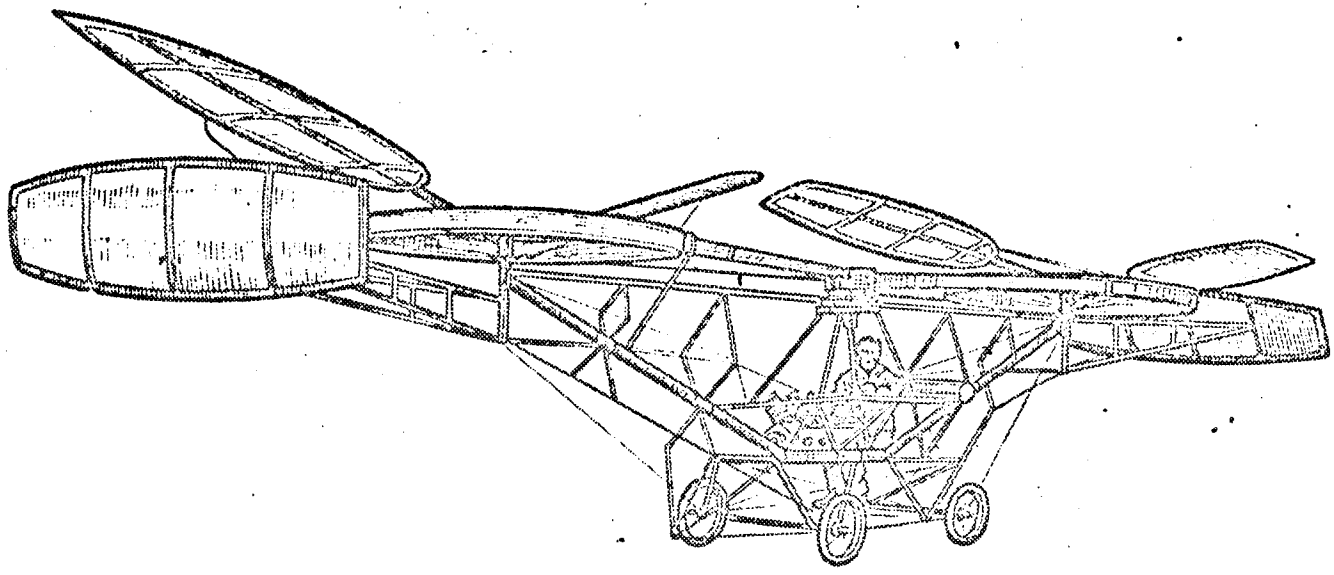

Figure 1-7. The Helicopter of Paul Cornu.

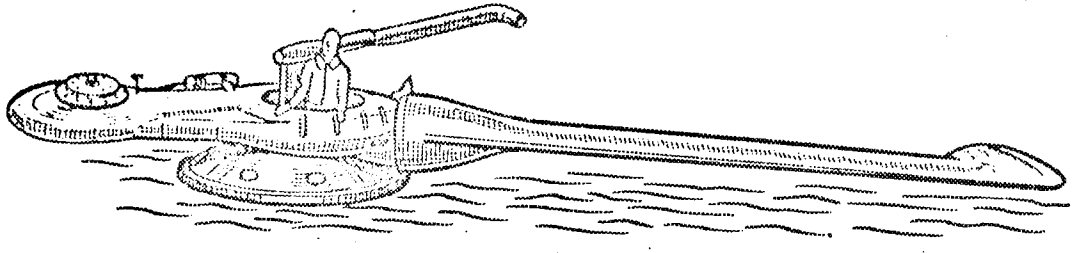

Figure 1-8. The First Jet-Powered Helicopter (Papin and Rouilly).

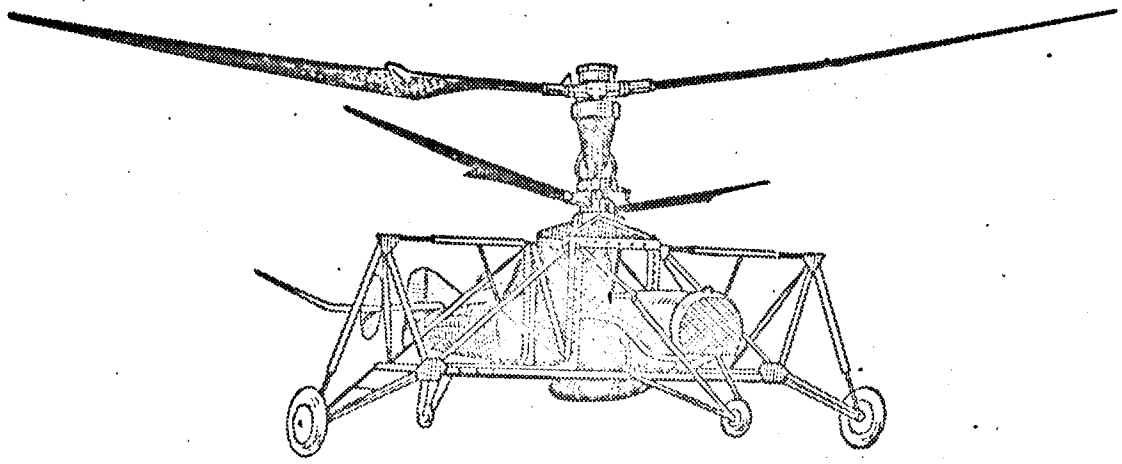

Figure 1-9. The Berguet-Dorand Gyroplane.

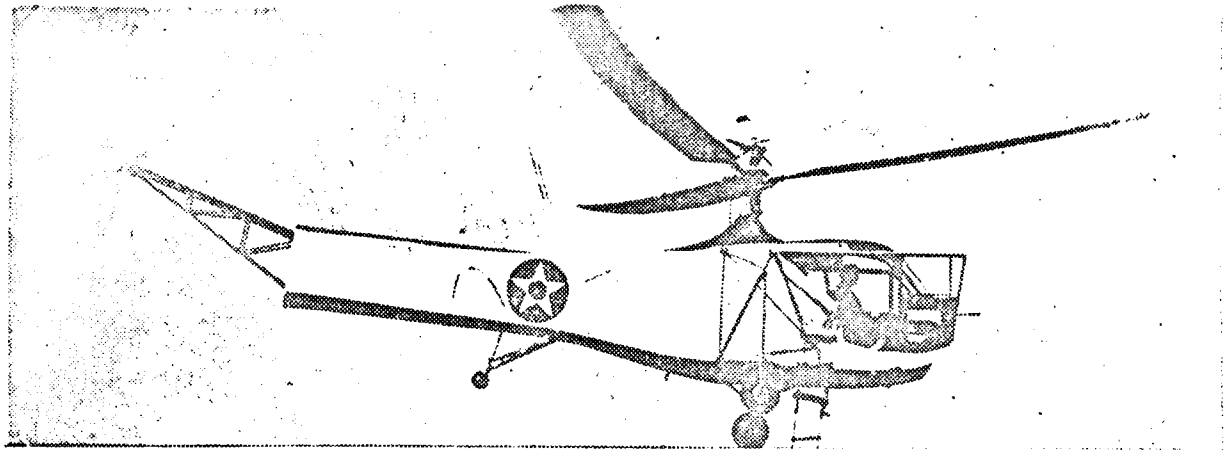

Figure 1-10. Sikorsky R-4.

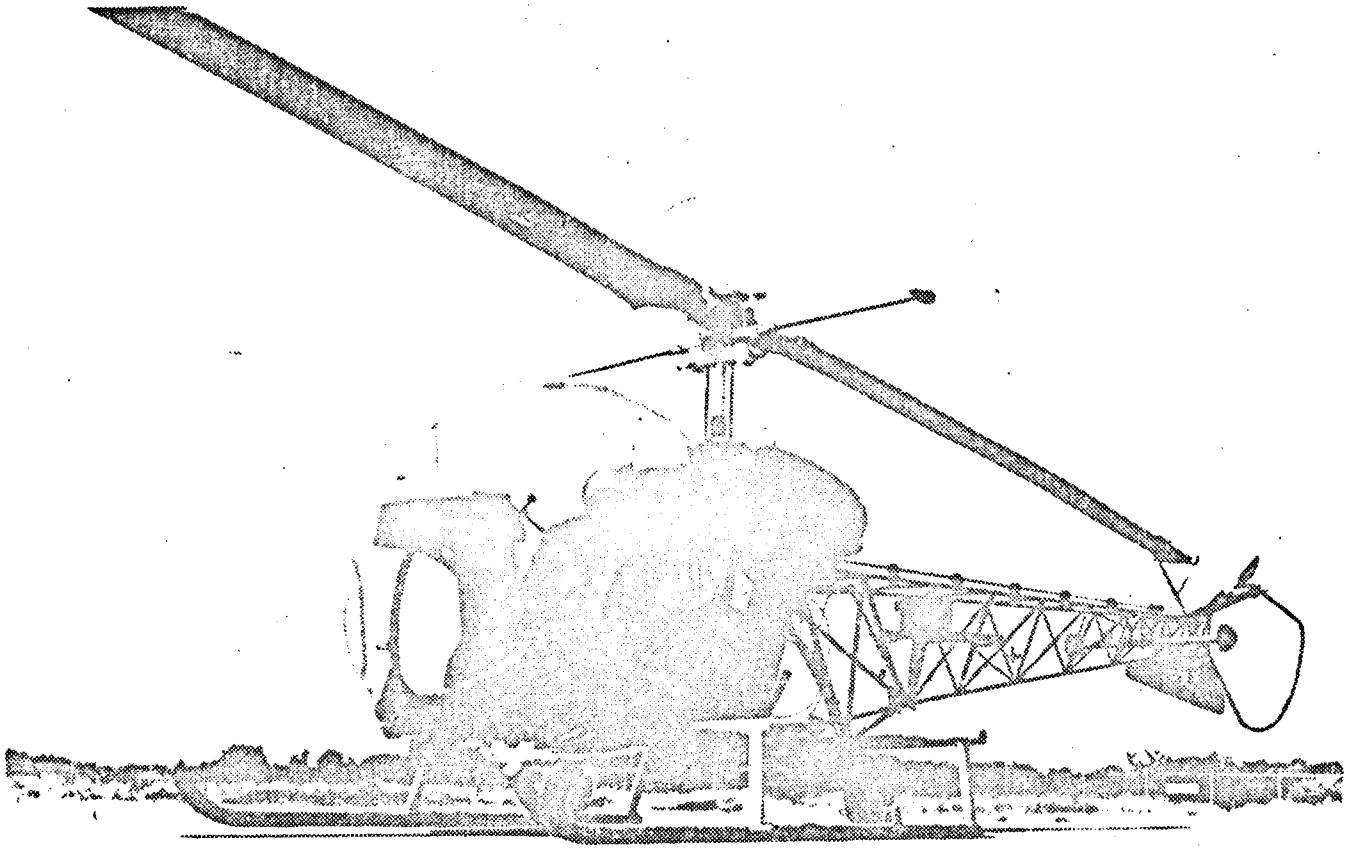

Figure 1-11. Bell 47-G Single Rotor.

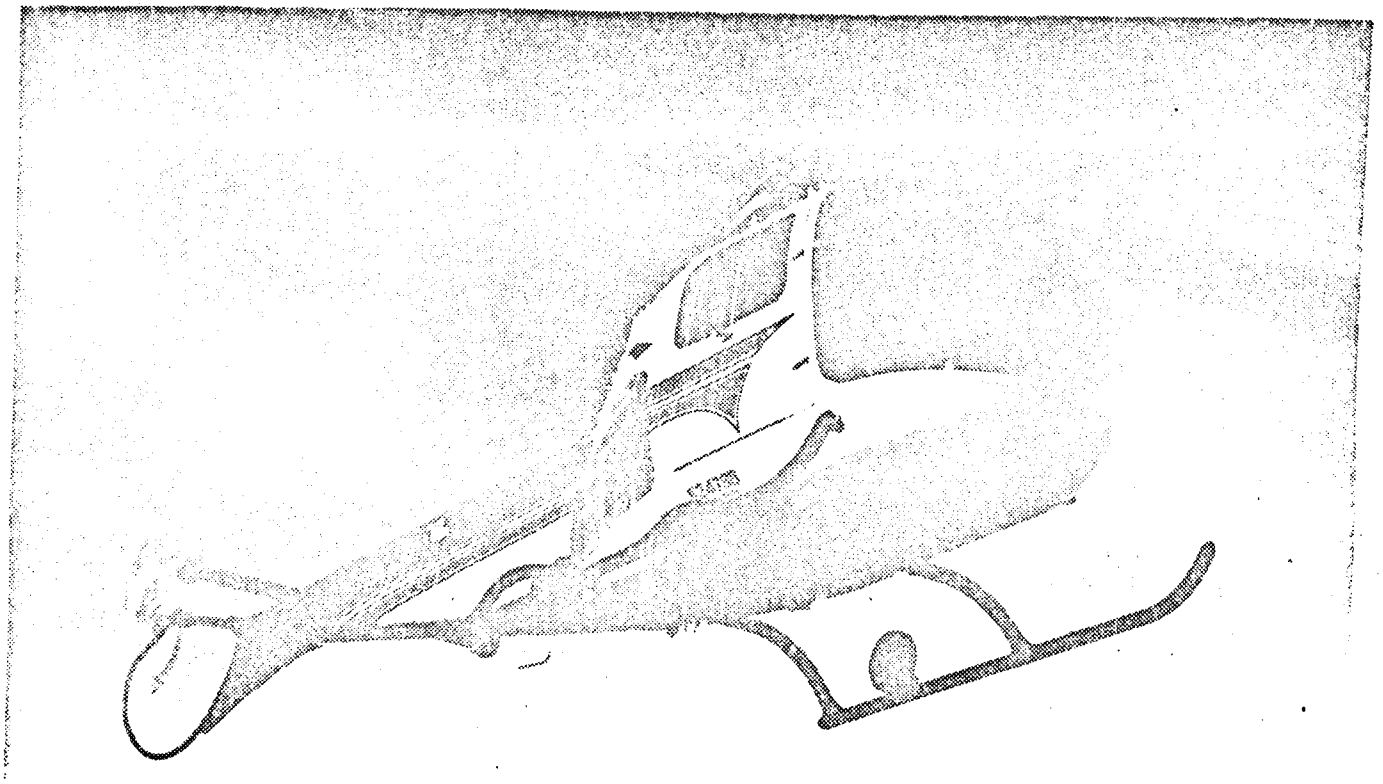

Figure 1-12. Bell 47-J Single Rotor.

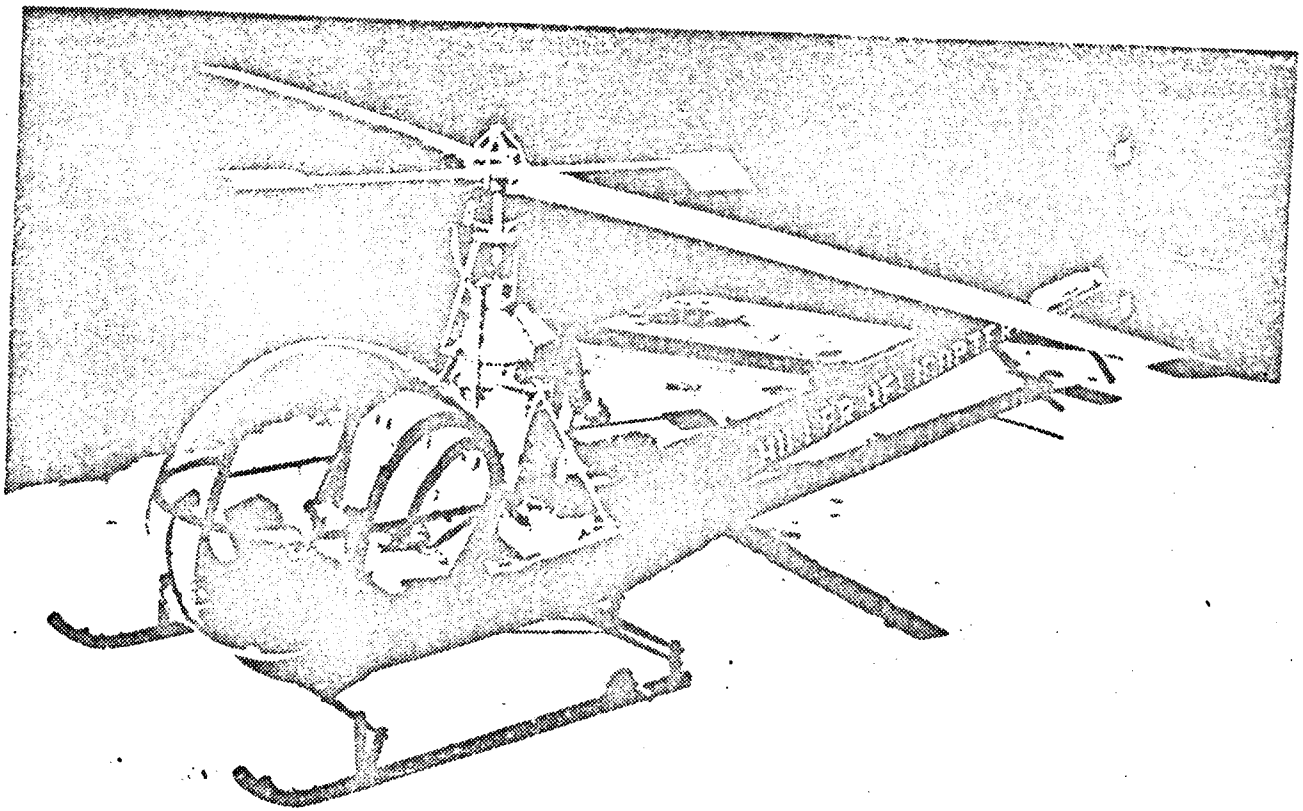

Figure 1-13. Hiller 12-C Single Rotor.

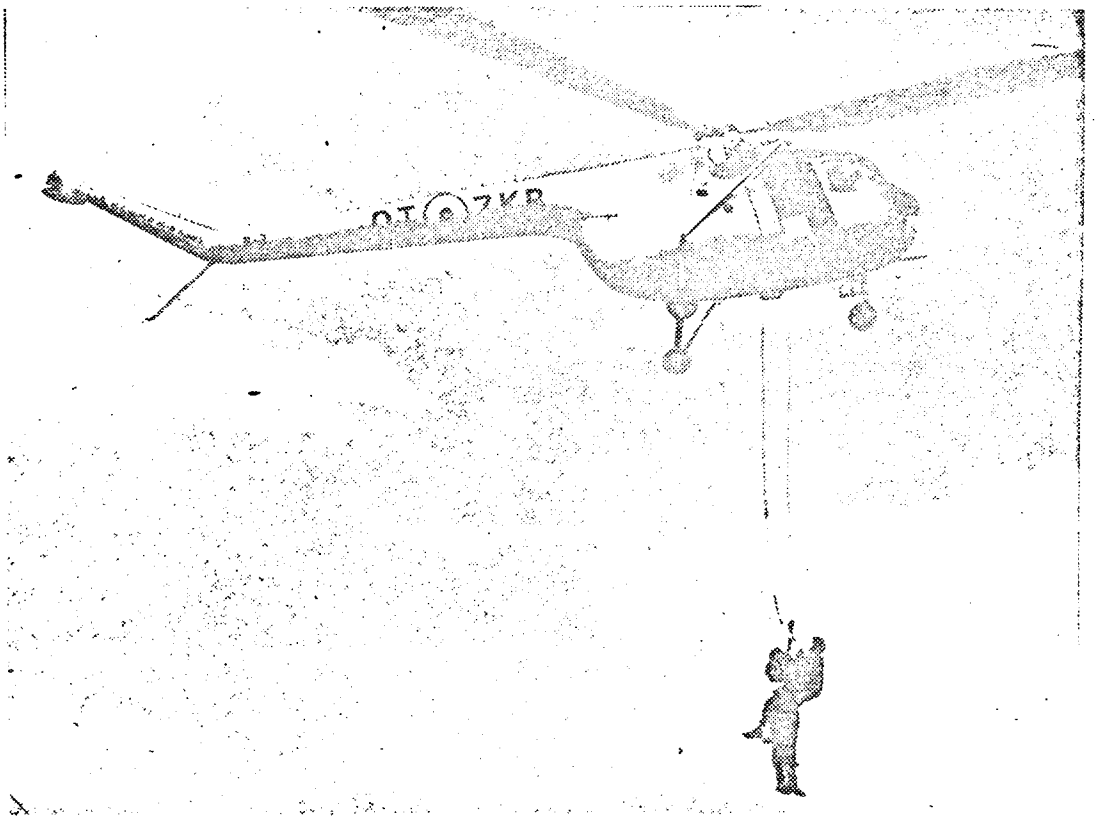

Figure 1-14. Bristol 171 Single Rotor.

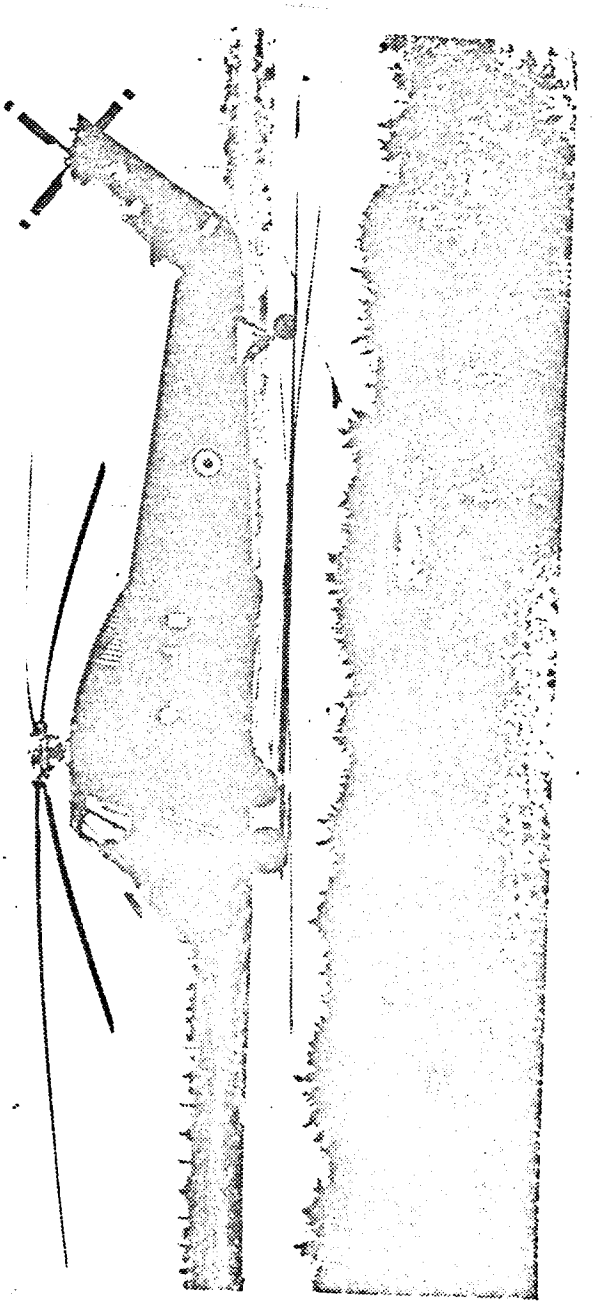

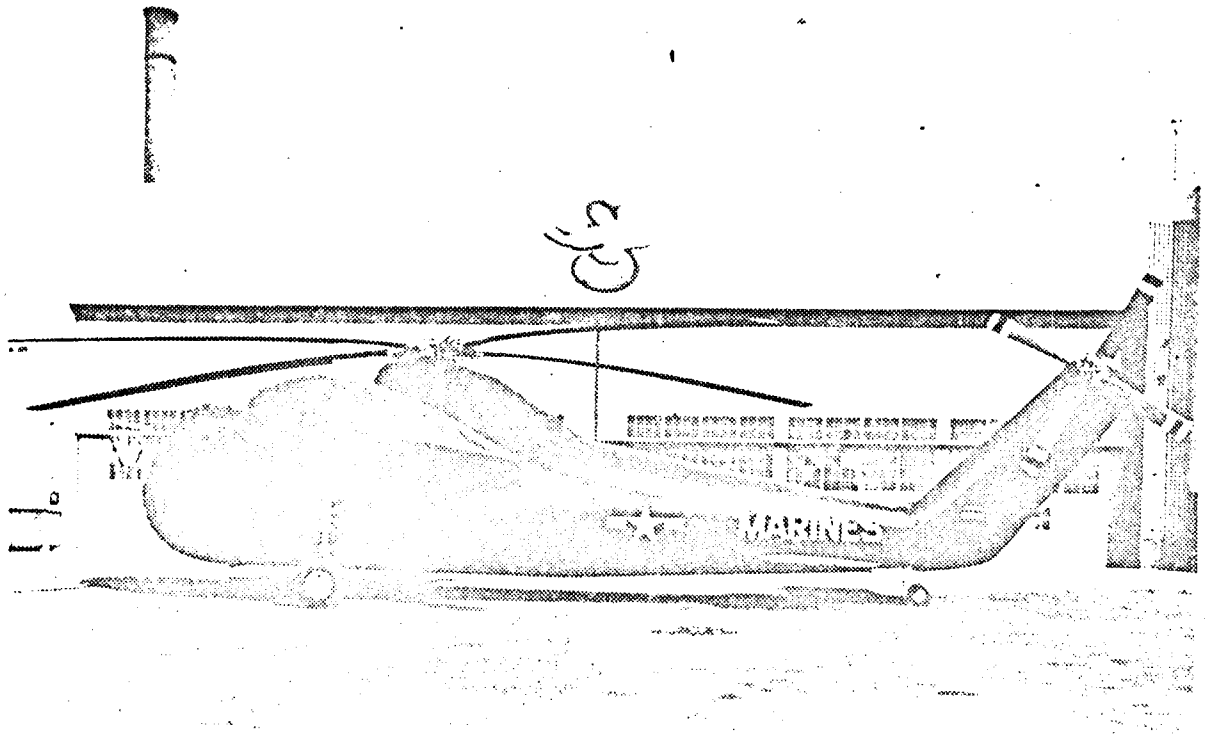

Figure 1-15. Sikorsky.
Single Rotors With Anti-Torque Rotor.

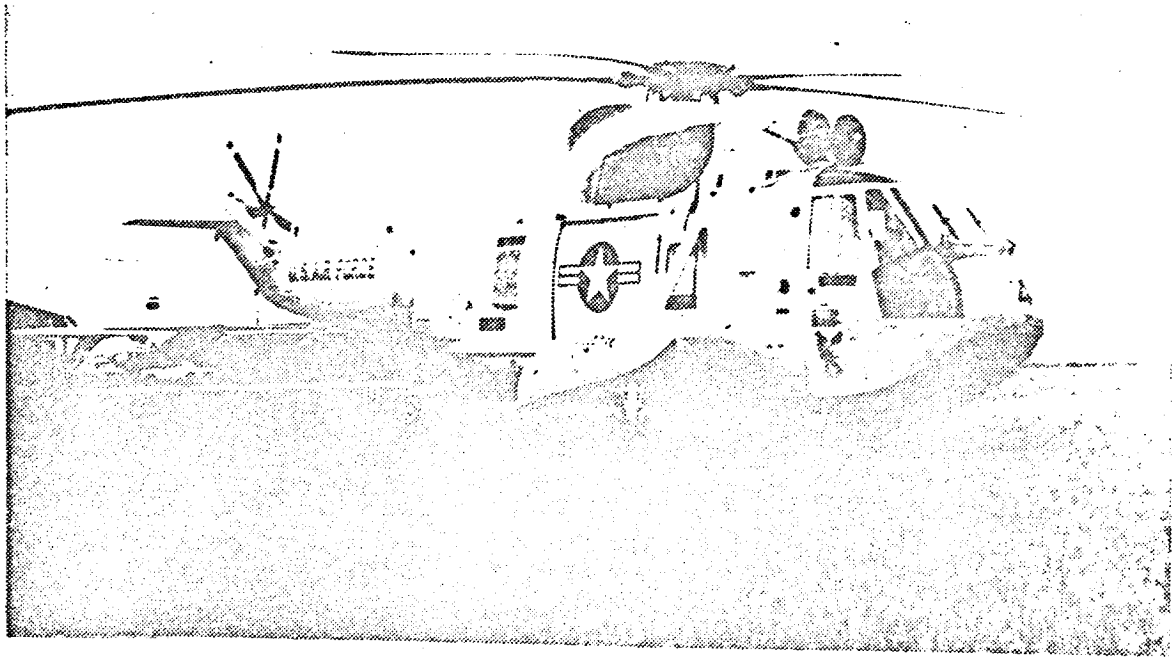

S-61-A

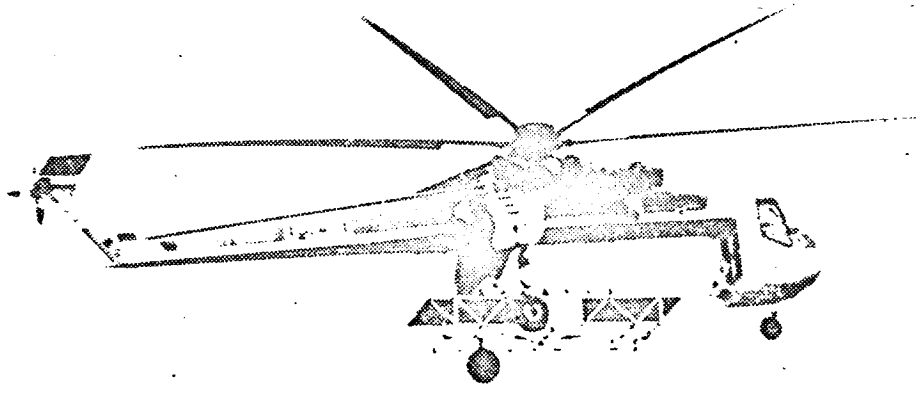

Figure 1-15. (Cont'd) - Sikorsky.
Single Rotors With Anti-Torque Rotor.

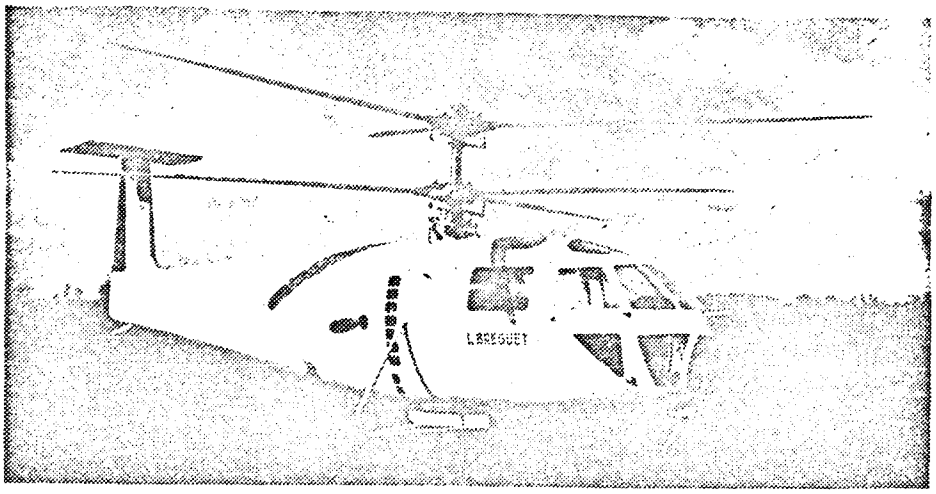

Figure 1-16. Breguet 11 E Coaxial.

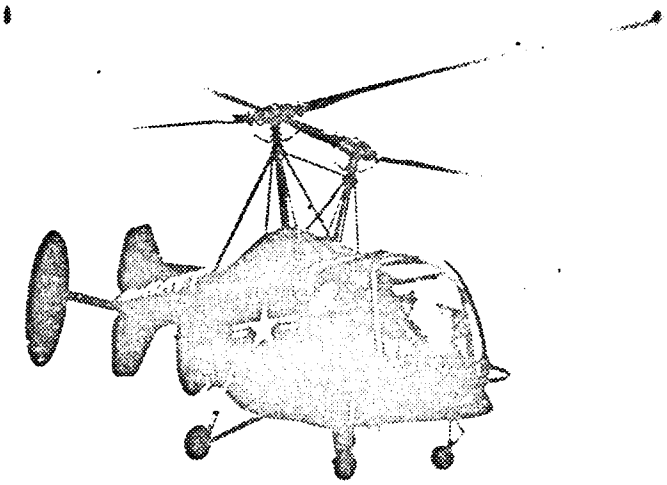

Figure 1-17. Kaman HTK-1.
Side-By-Side Intermeshing.

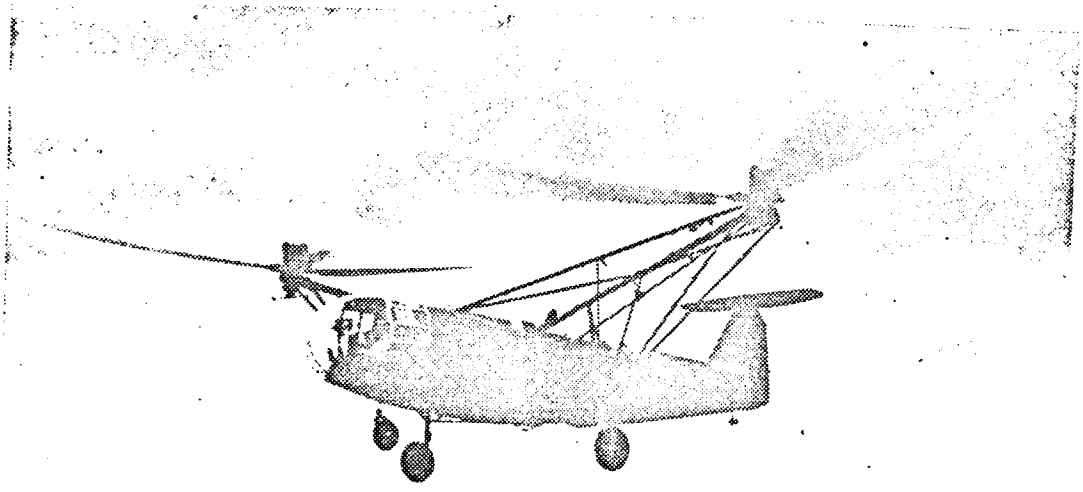

Figure 1-18. SE 3000.
Side-By-Side, Non-intermeshing.

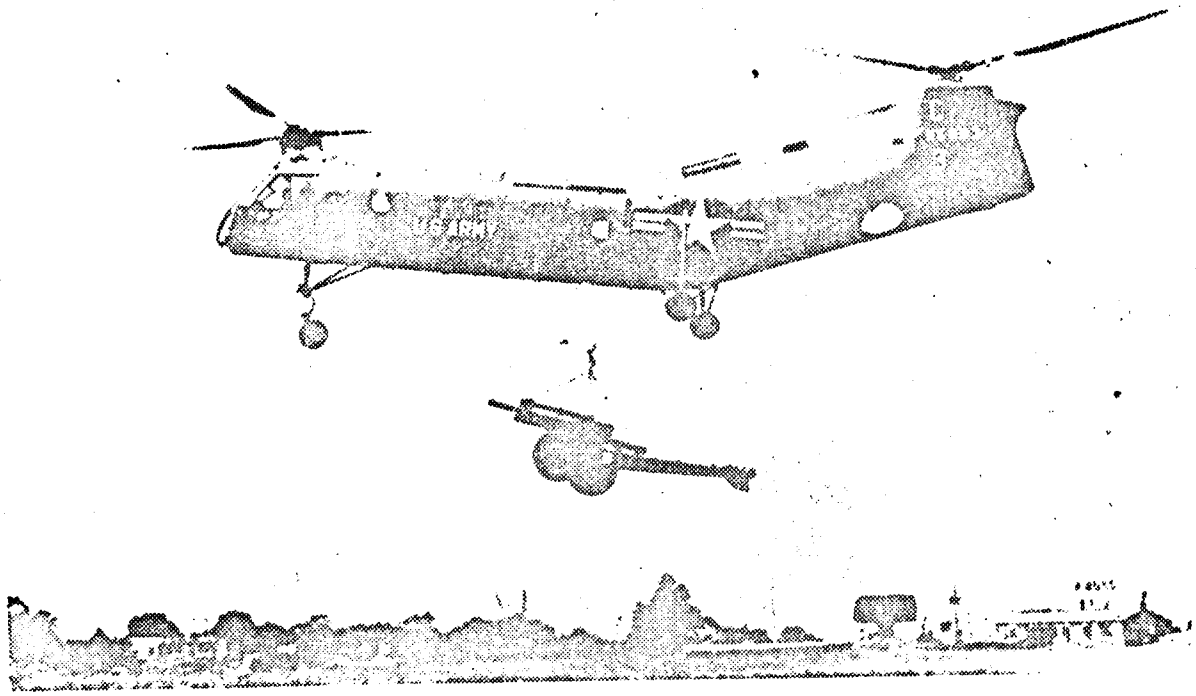

H-21

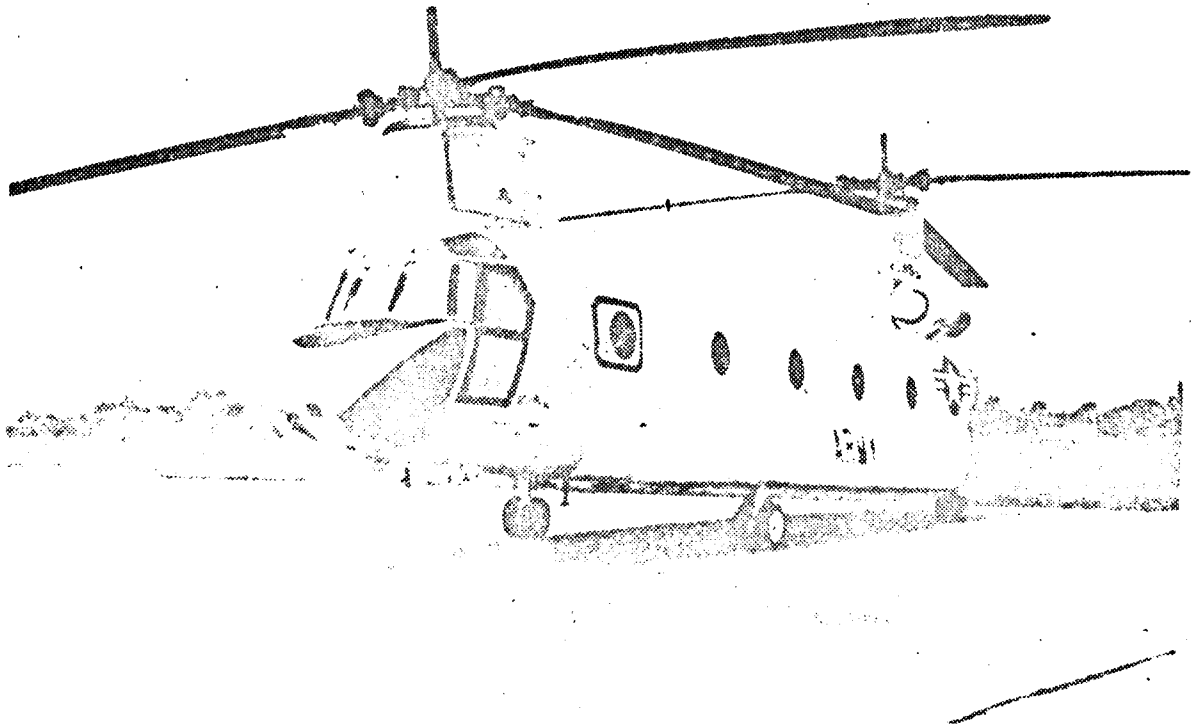

HC-1B-Chinook

Figure 1-19. Vertol (formerly Piasecki).
Two Rotors in Tandem.

Figure 1-20. SO 1120 Ariel.

Experimental Jet Helicopter Compressed Air is Ducted to the Blade Tip and Burned. Yaw is Controlled By the Turbine Exhaust at the Tail.

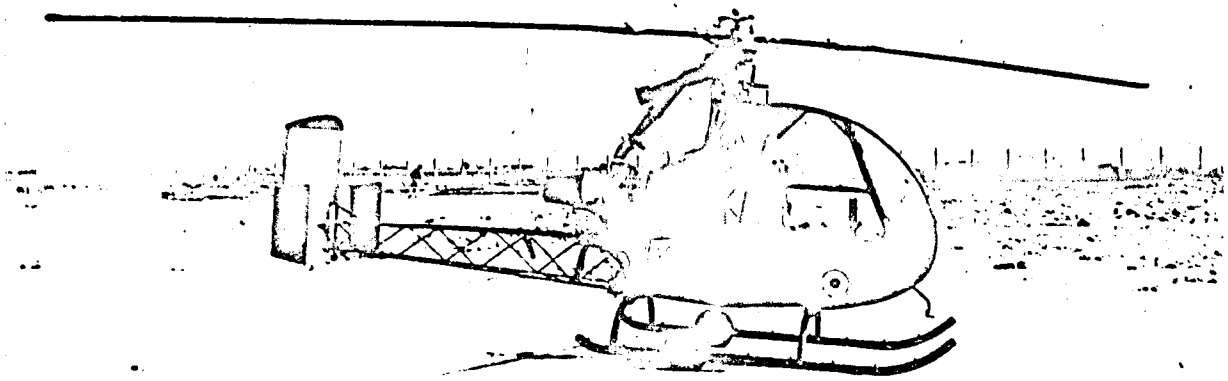

Figure 1-21. SO 1221-Djinn.

Jet-Driven Helicopter. Compressed Air is Ejected at the Blade Tip Without Combustion. Yaw is Controlled By the Turbine Exhaust Acting on the Rudder.

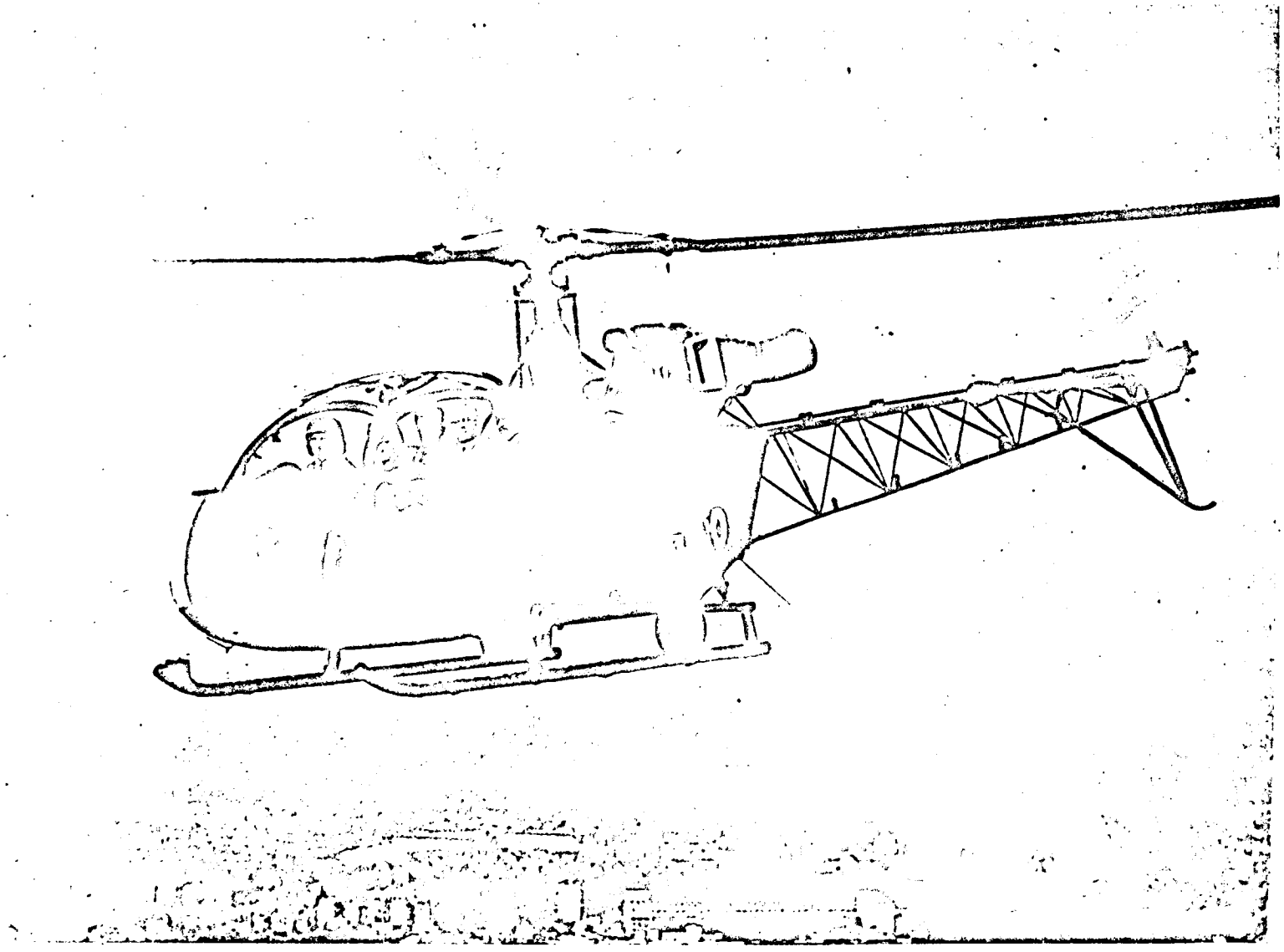

Figure 1-22. SE 3130 Alouette II.
Mechanical Turbine-Powered Single Rotor.

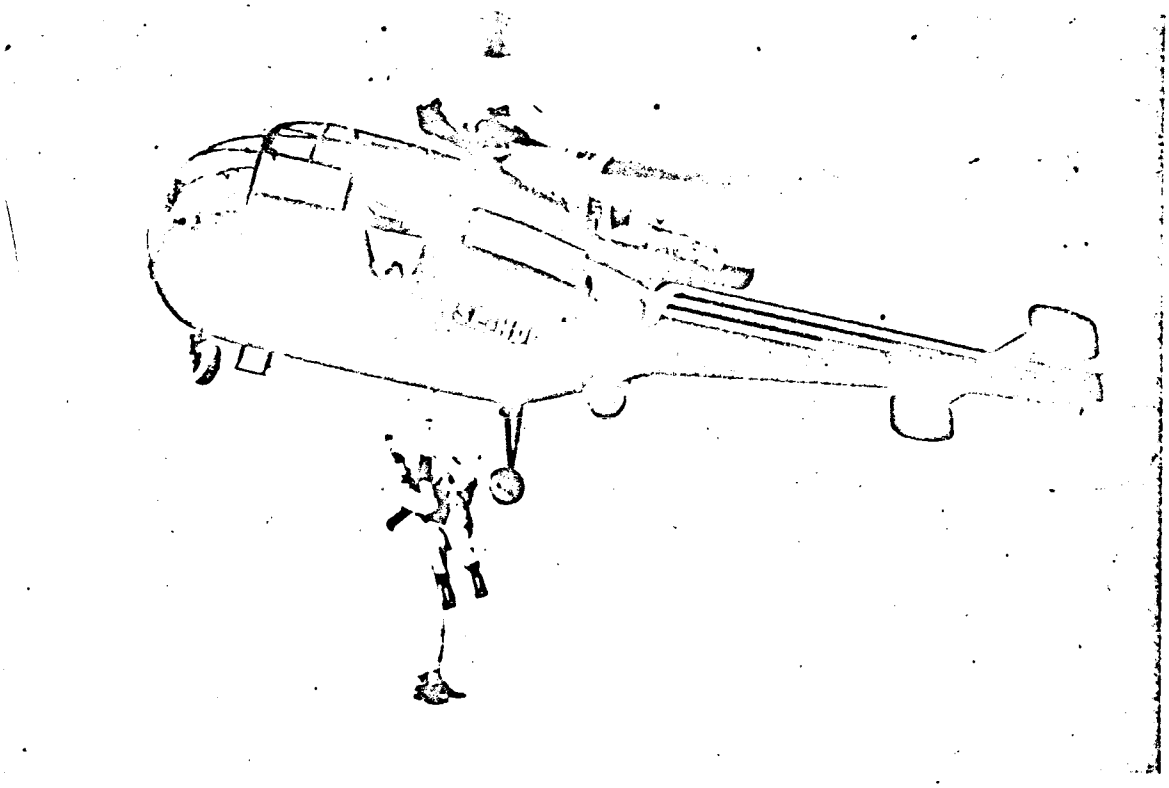

Figure 1-23. SA 3160-Alouette III-(Sud-Aviation).
Mechanical Turbine Power.

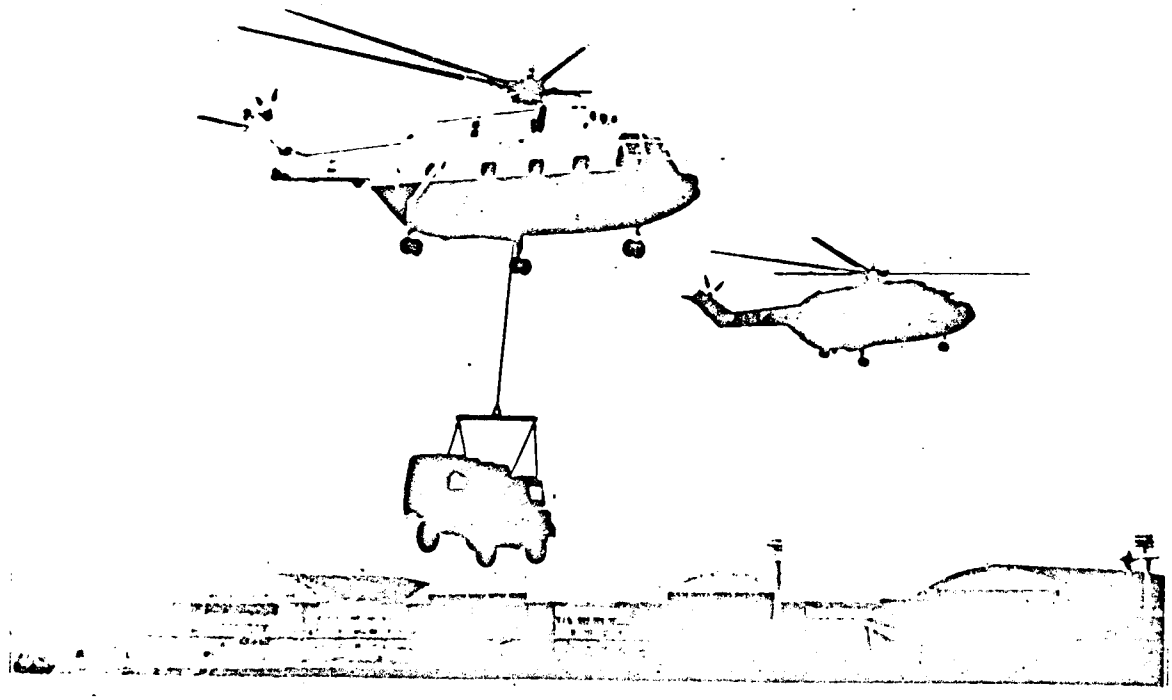

Figure 1-24. SA 3210 Super Frelon (Sud-Aviation).
Mechanical Powered By 3 Turbines. In the Foreground the Air-Ground Version, in the Background the Naval Version.

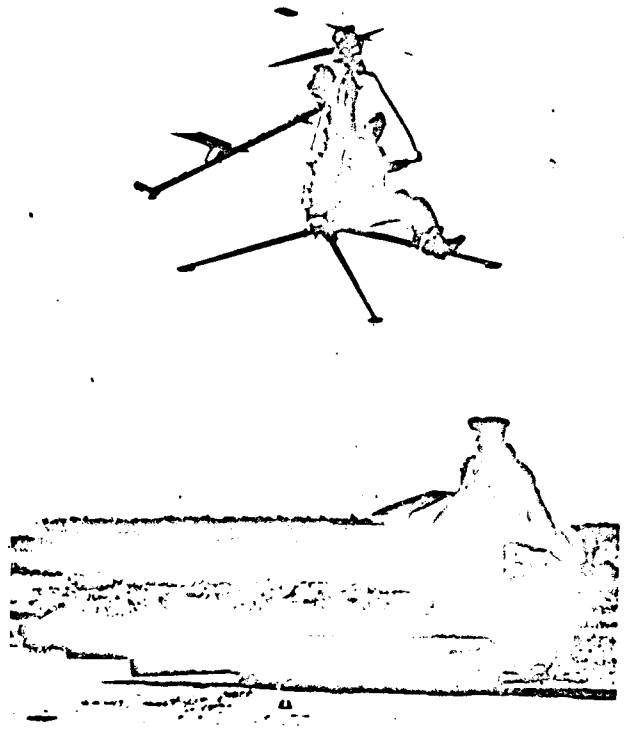

Figure 1-25. Hiller XROE-1 Rotorcycle.
One-Man Helicopter.

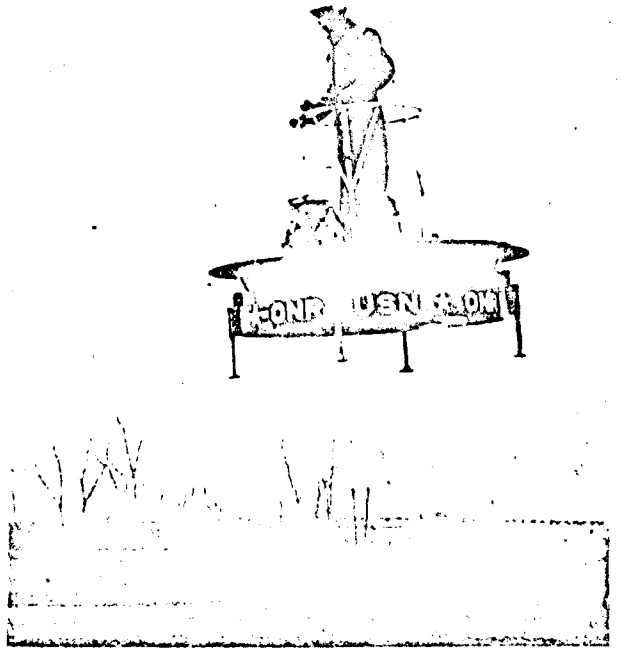

Figure 1-26. Hiller.
Flying Platform Ducted Rotor.

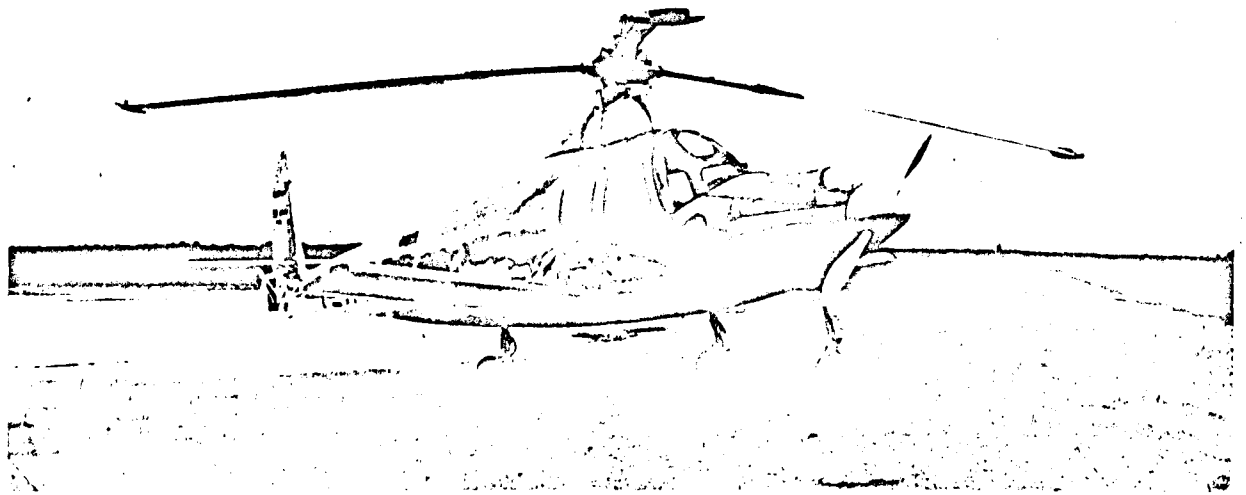

Figure 1-27. SO 1310 Farfadet.
Experimental Compound.

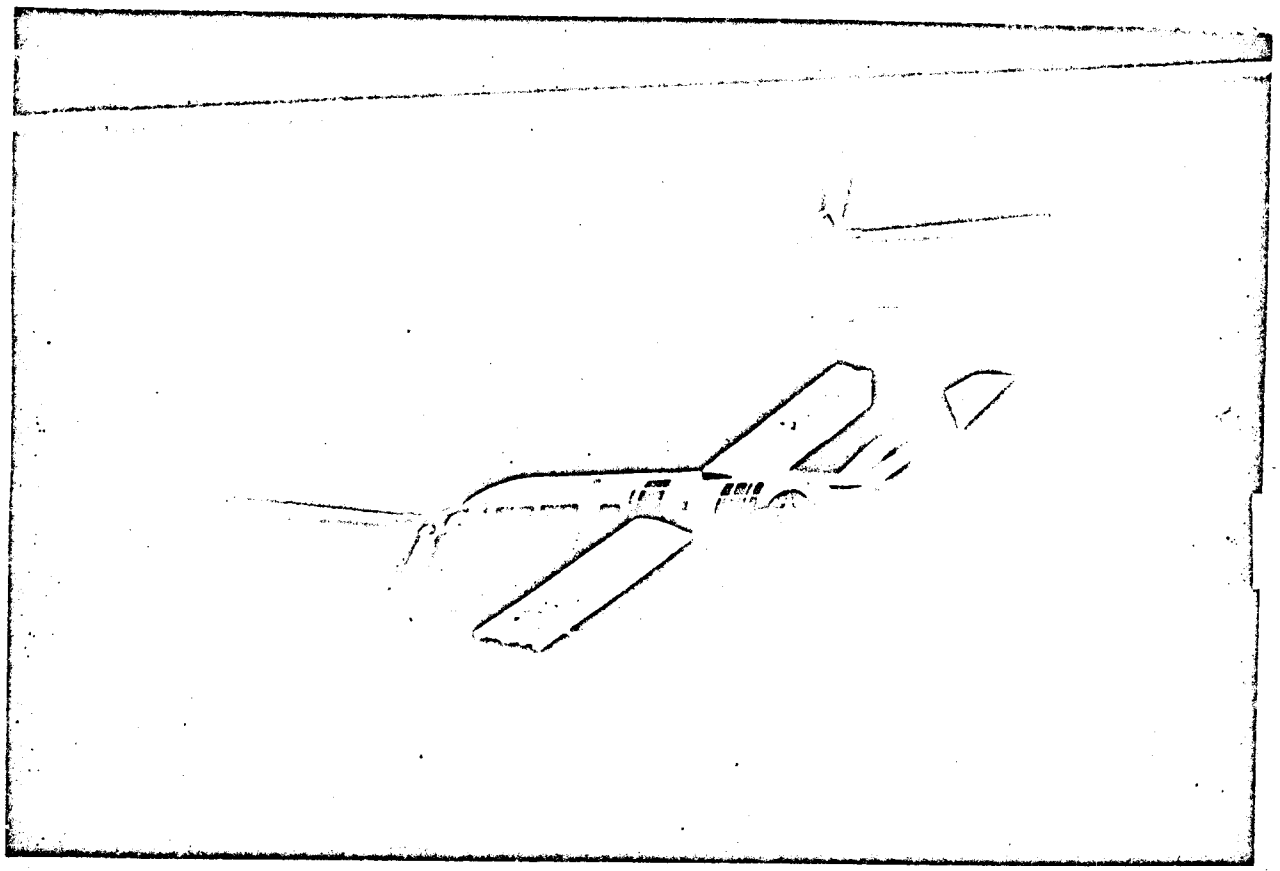

Figure 1-28. Bell XV-3.
Convertiplane.

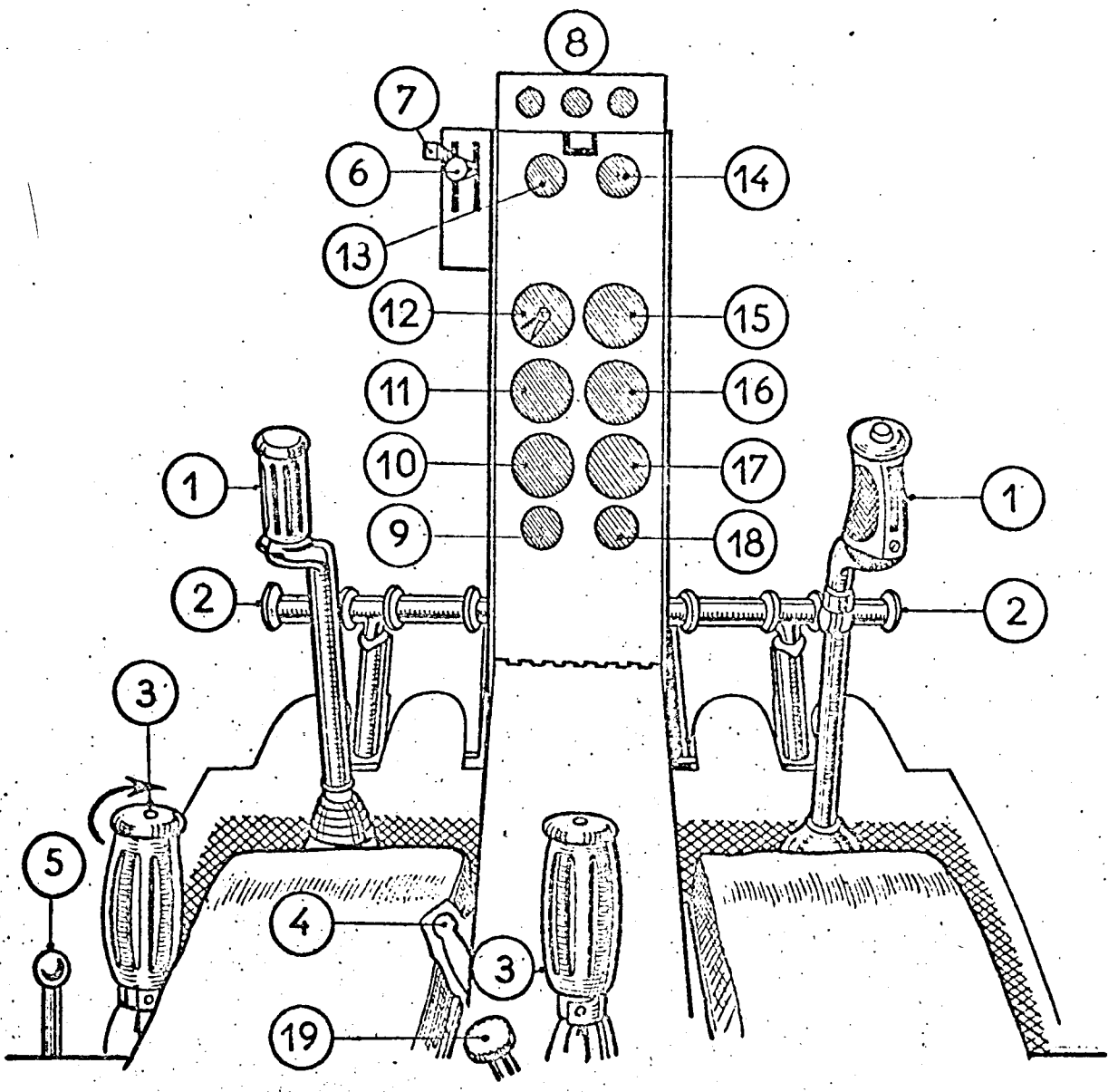

11. Manifold pressure
10. oil temperature and pressure
9. fuel gauge
8. radio panel
7. carburator heat
6. mixture control
5. fuel valve
4. starter
3. collective pitch control and throttle
2. rudder pedal
1. control stick

19. Collective friction control
18. ammeter
17. cylinder head temperature
16. altimeter
15. anemometer
14. ignition switch
13. carburator air temperature
12. rotor and engine tachometers

Figure 1-29. Cockpit of a Helicopter.

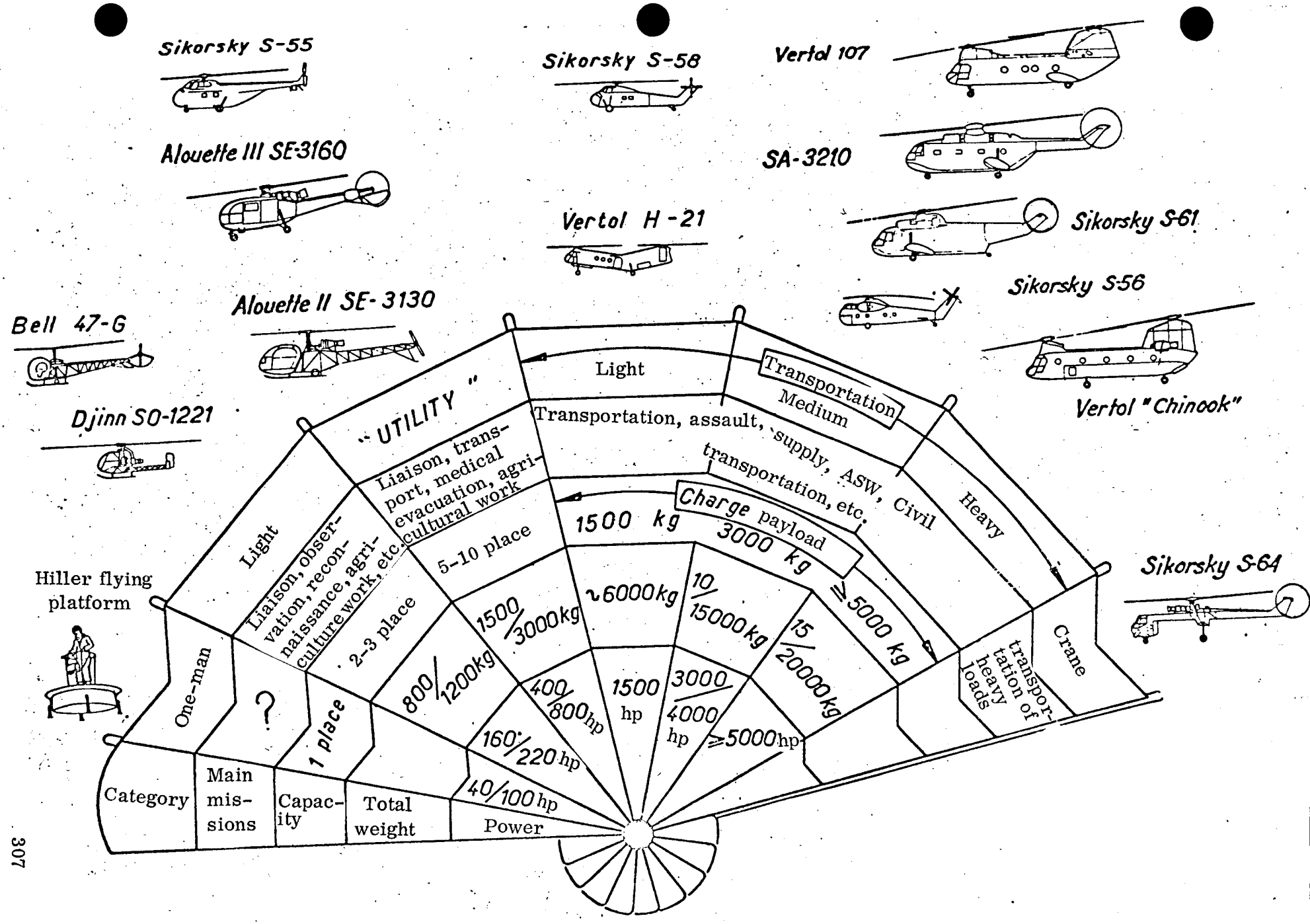

Figure 1-30. Range of Helicopter Types.

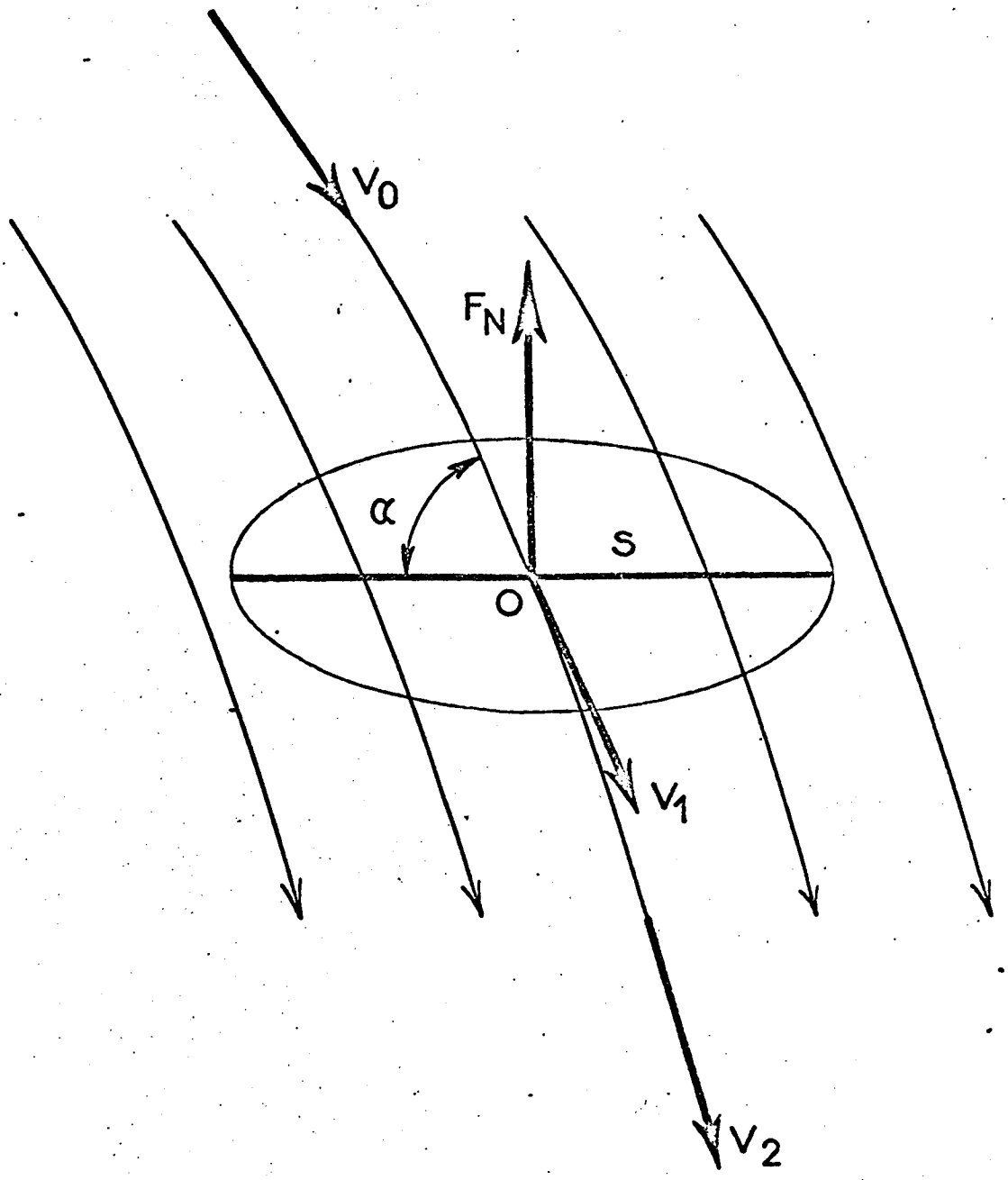

Figure 2-1.

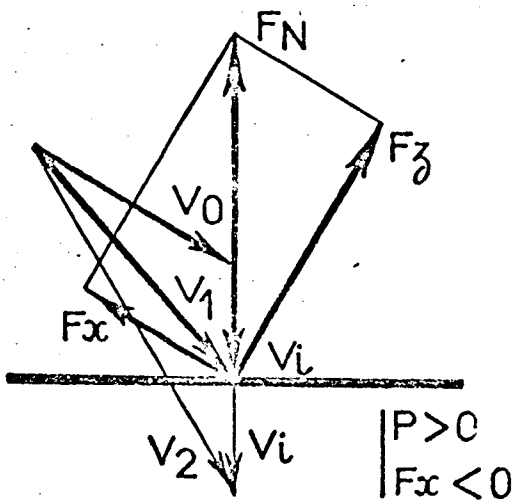

Figure 2-2. Helicopter Mode.

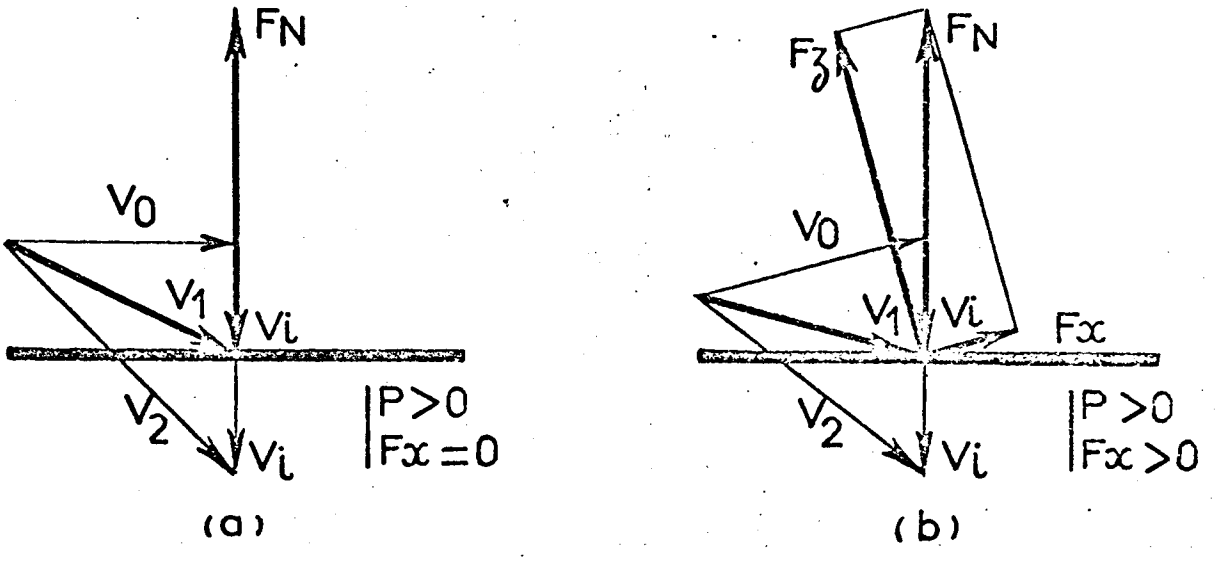

Figure 2-3. Gyrodyne Mode.

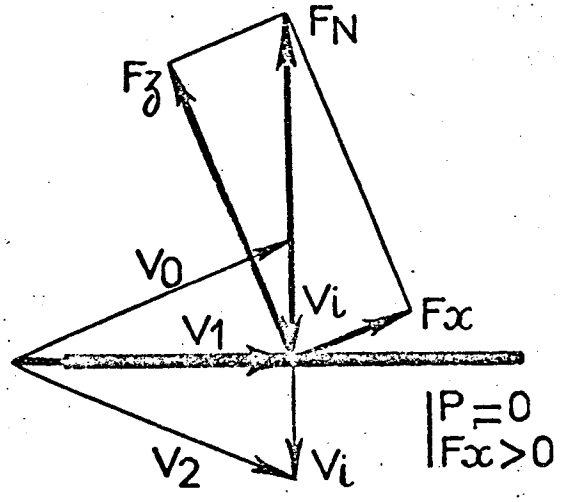

Figure 2-4. Autogiro Mode.

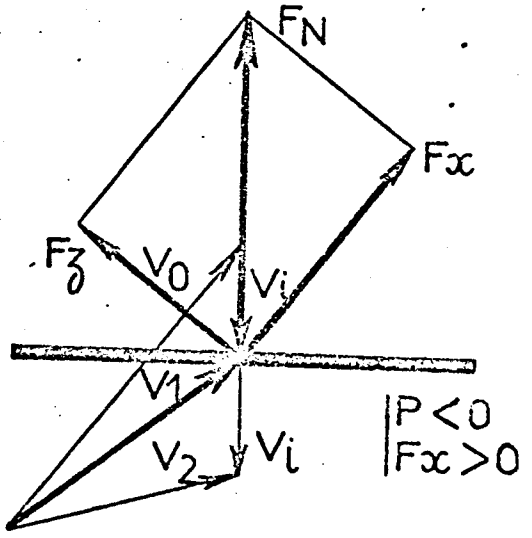

Figure 2-5. Windmill-Braking Mode.

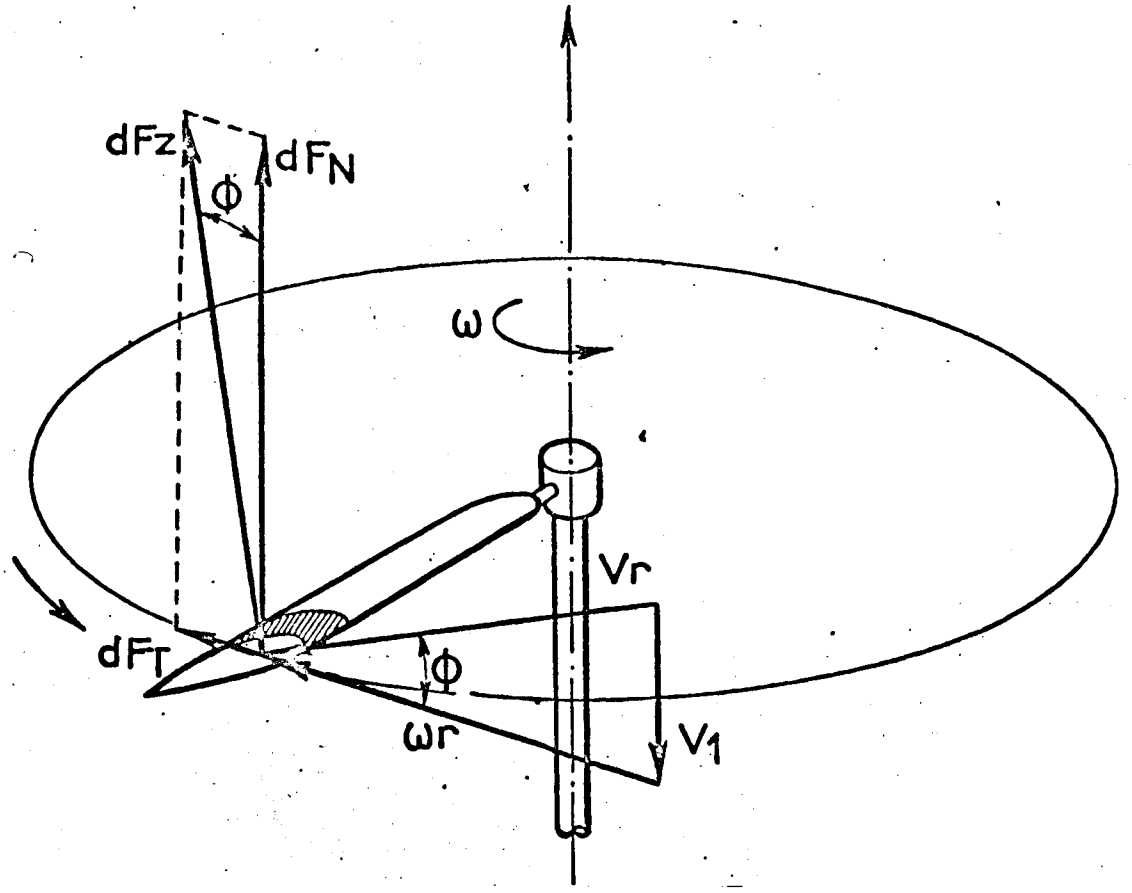

Figure 2-6.

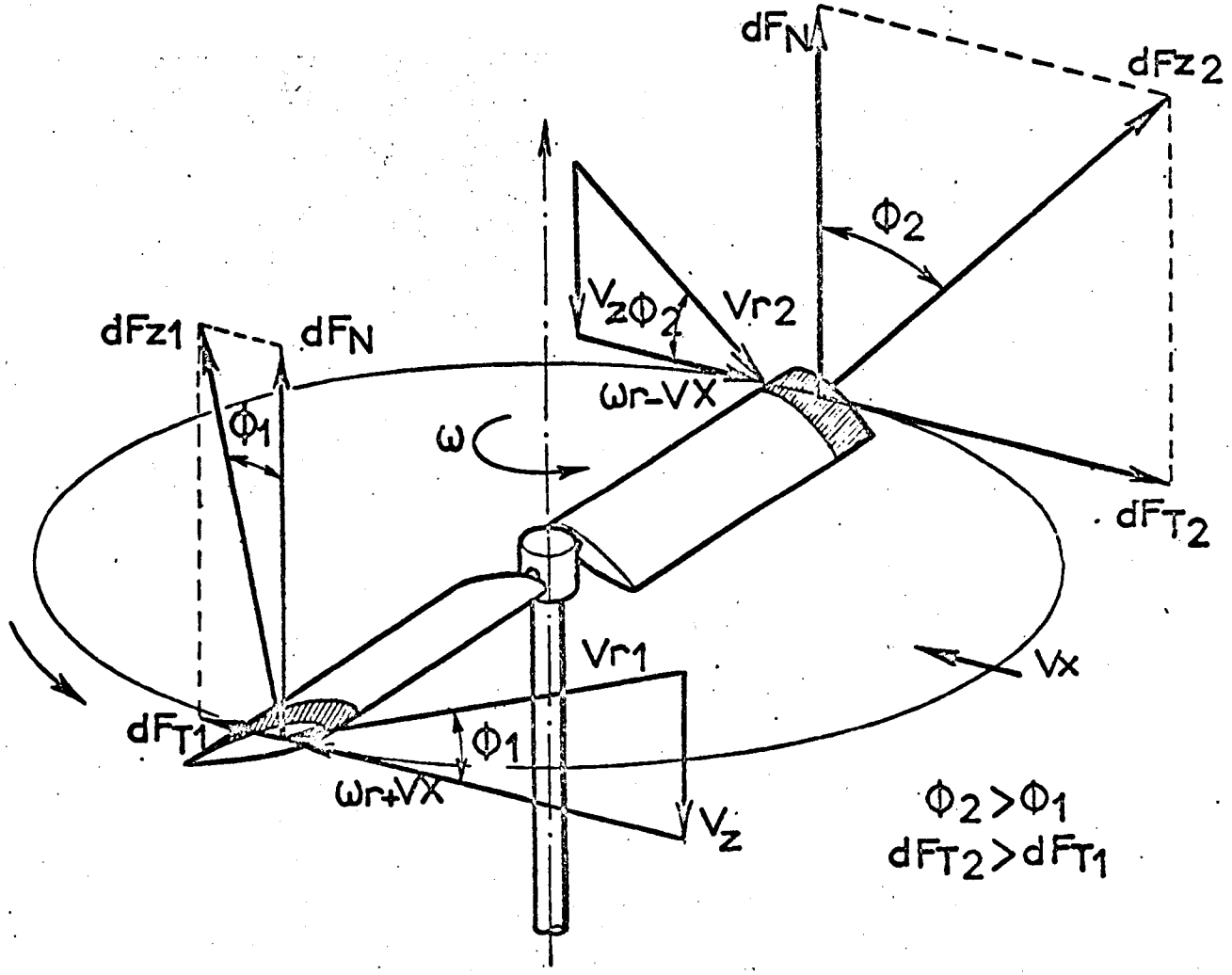
dFN
dFz2
Φ2
Vz Φ2
Vr2
dFz1
dFN
ωr-VX
Φ1
ω
dFT2
Vr1
Vx
dFT1
Φ1
ωr+VX
Vz
Φ2>Φ1
dFT2>dFT1

Figure 2-7.

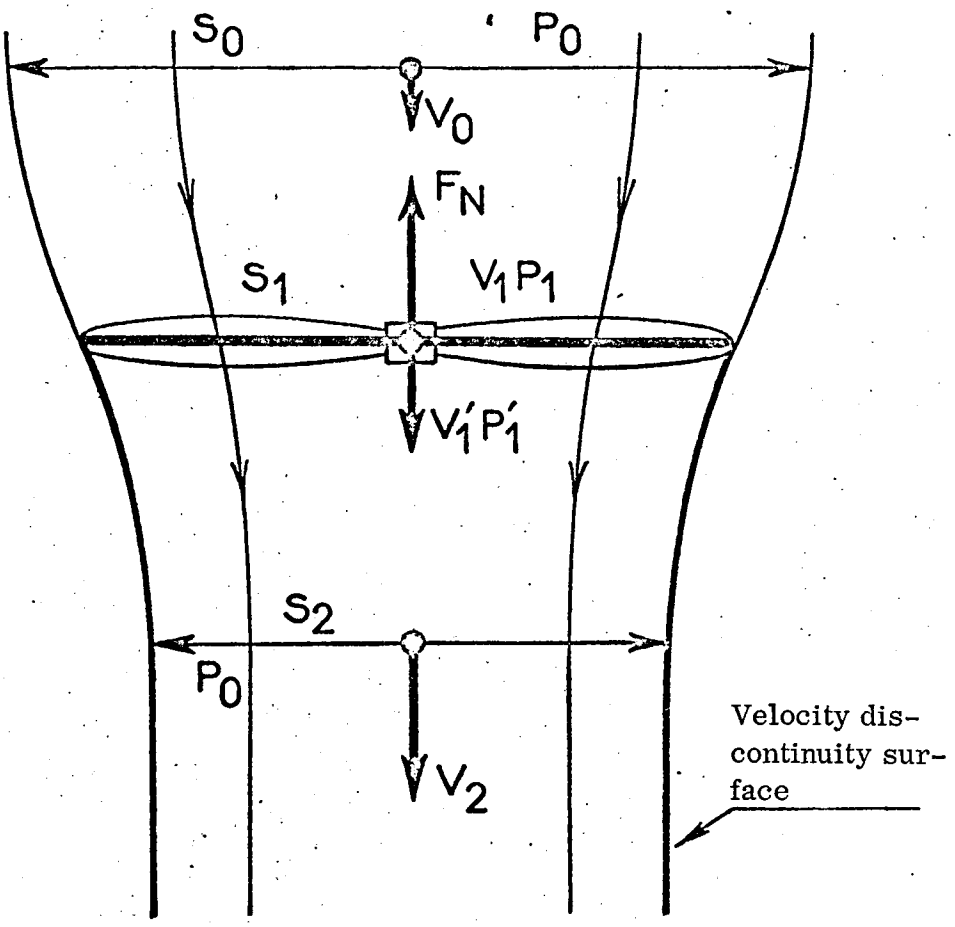

Figure 2-8.

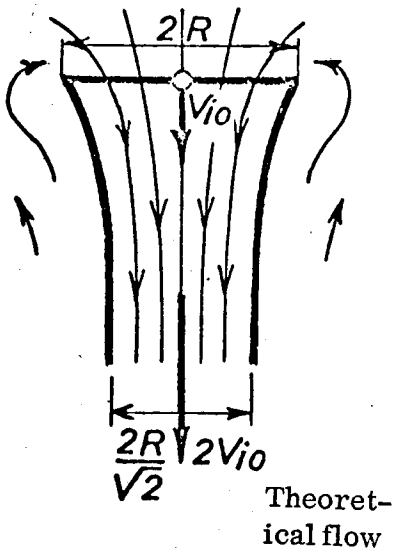

Figure 2-9. Hovering Flight

$V_z=0$

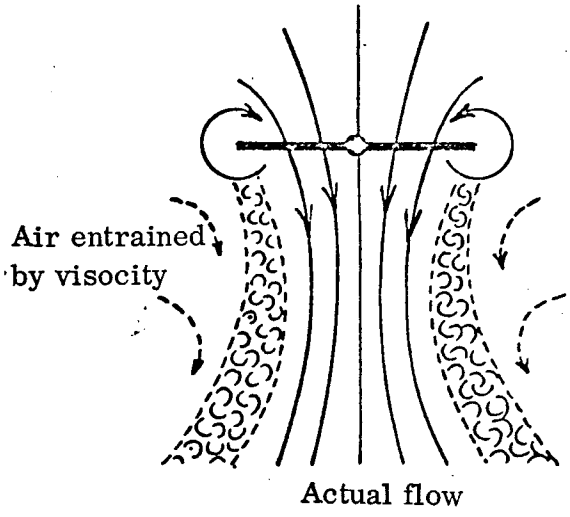

Figure 2-10. Hovering Flight.

$V_z=0$

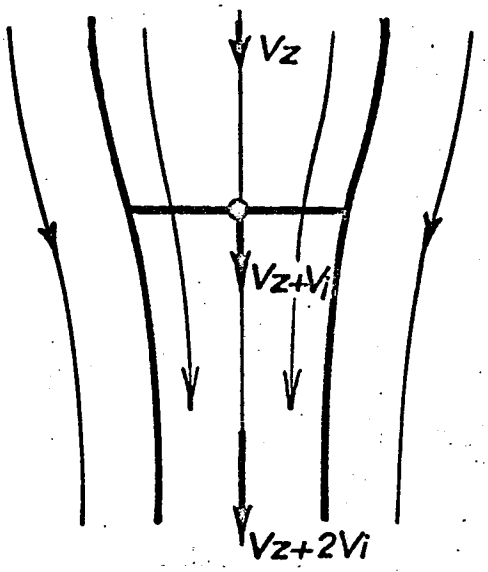

Figure 2-11. Ascent.

$V_z > 0$

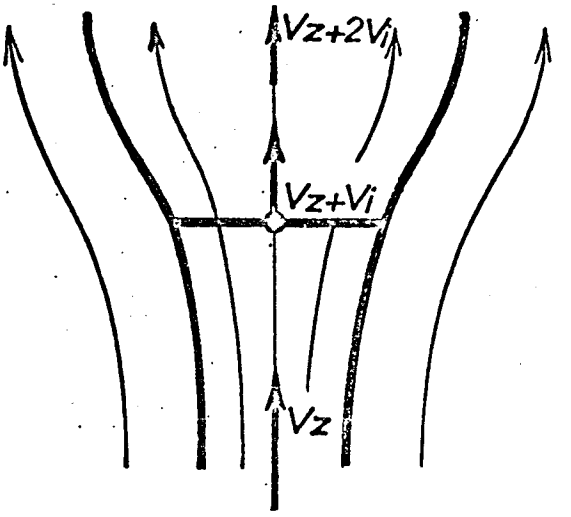

Figure 2-12. Rapid Let-Down in Windmill Braking.

$|V_z| > 2V_i$

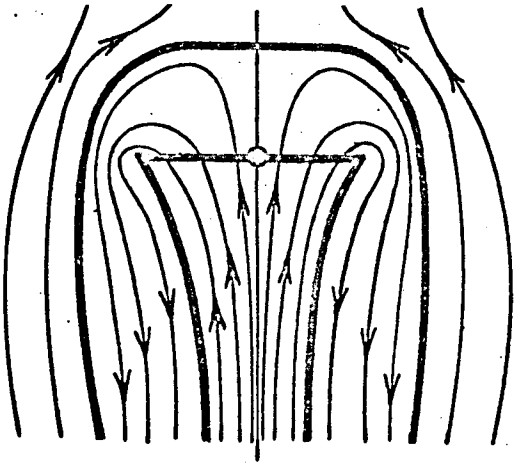

a) Theoretical flow

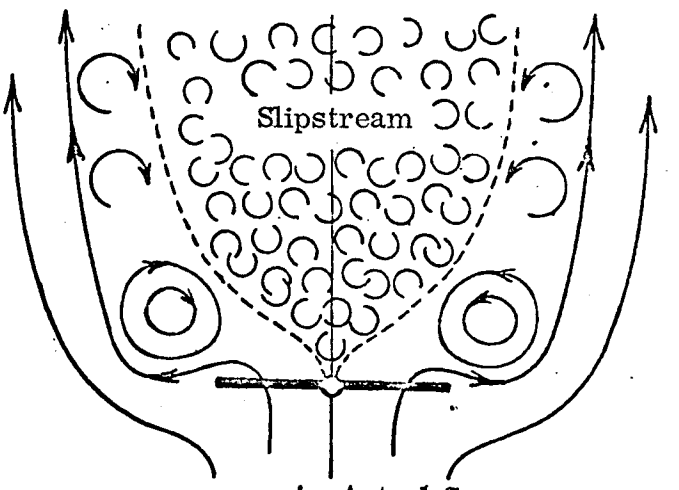

b) Actual flow vortex rings

Figure 2-13. Low-Speed Letdown in Windmill-Braking Mode.

$V_i < |V_z| < 2V_i$

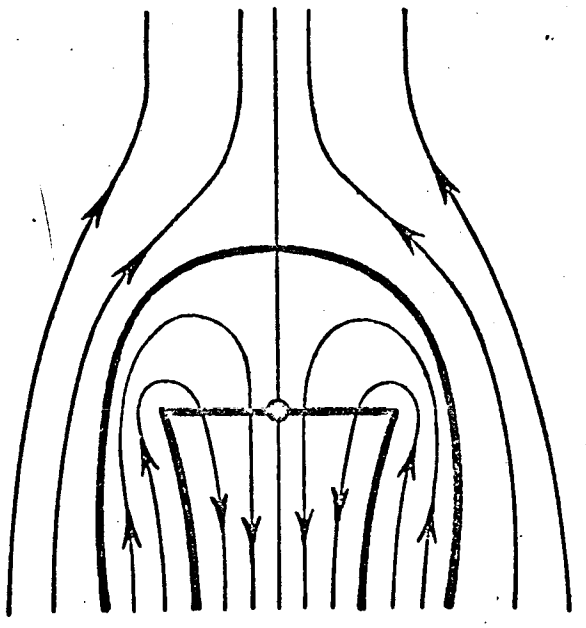

a) Theoretical flow

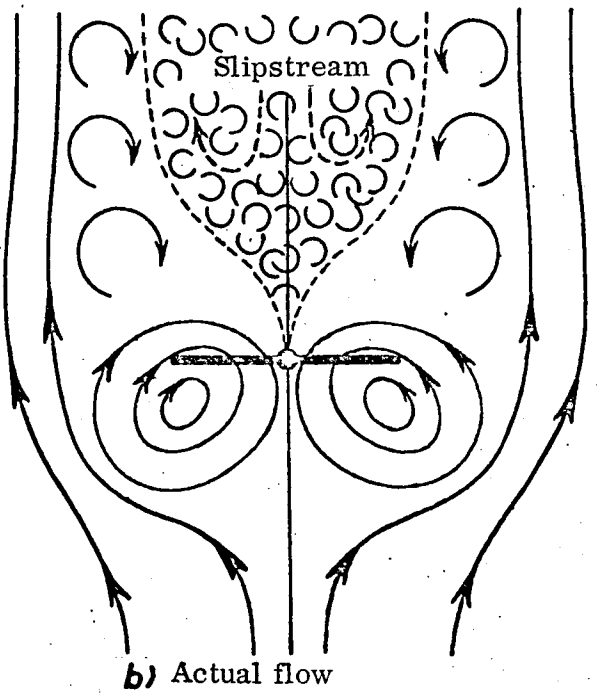

b) Actual flow
(vortex rings)

Figure 2-14. Low-Speed Letdown in the Helicopter Mode.

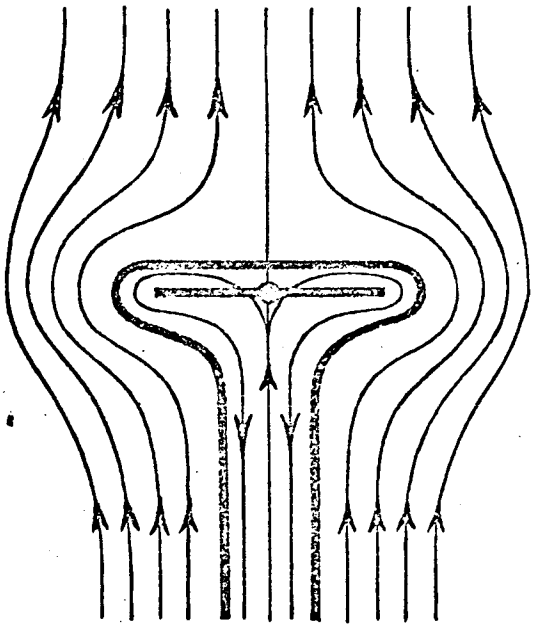

a) Theoretical flow

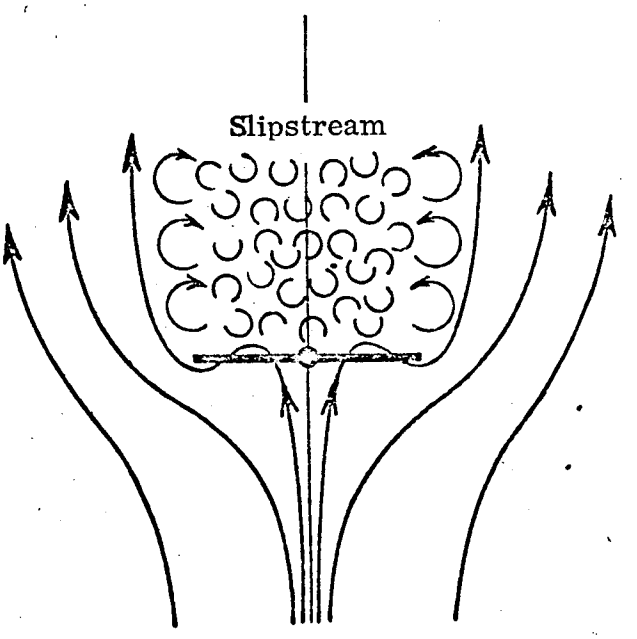

b) Actual flow

Figure 2-15. Autorotation.

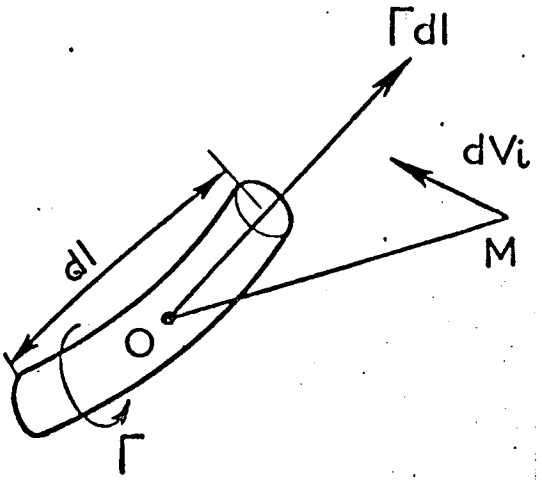

Figure 2-16. Velocity Induced By a Vortex Element.

$$d\vec{V}_i = \frac{\vec{\Gamma} d\vec{l} \wedge \vec{OM}}{4\pi OM^3}$$

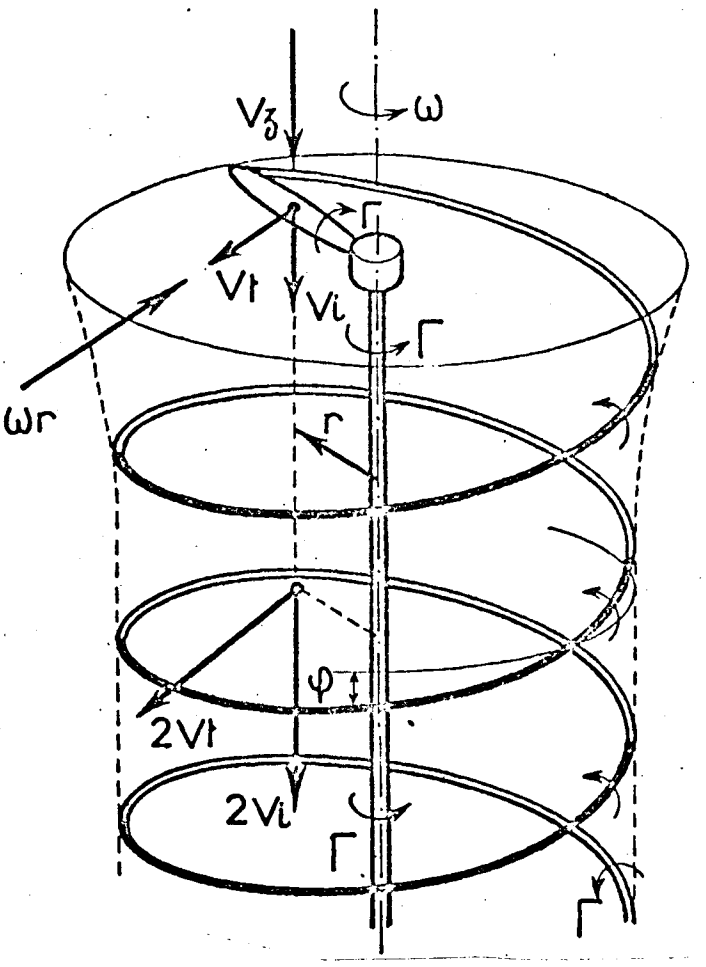

Figure 2-17.

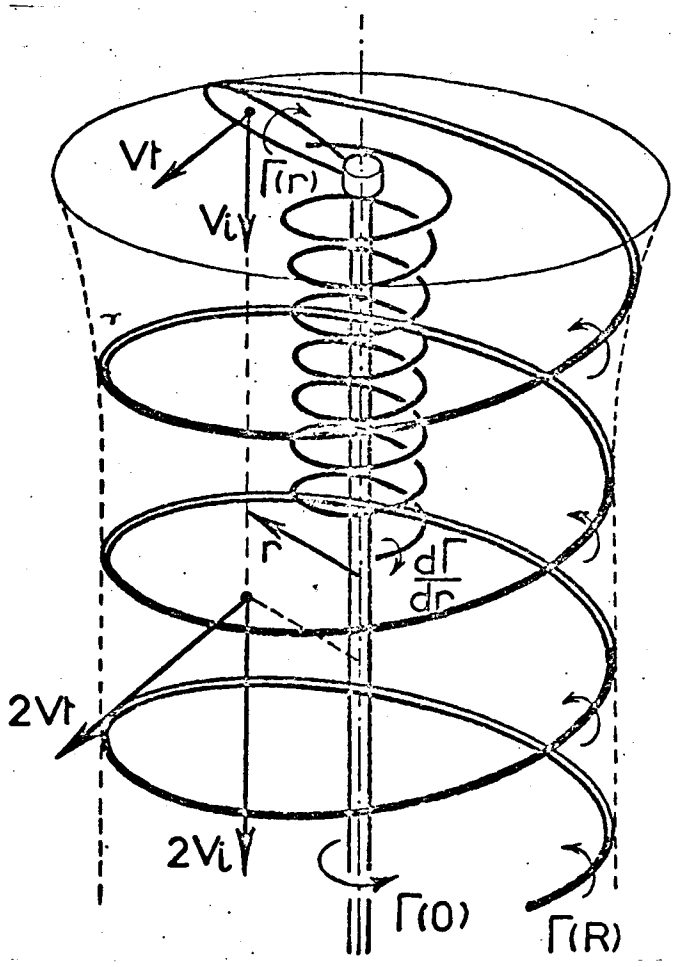

Figure 2-18

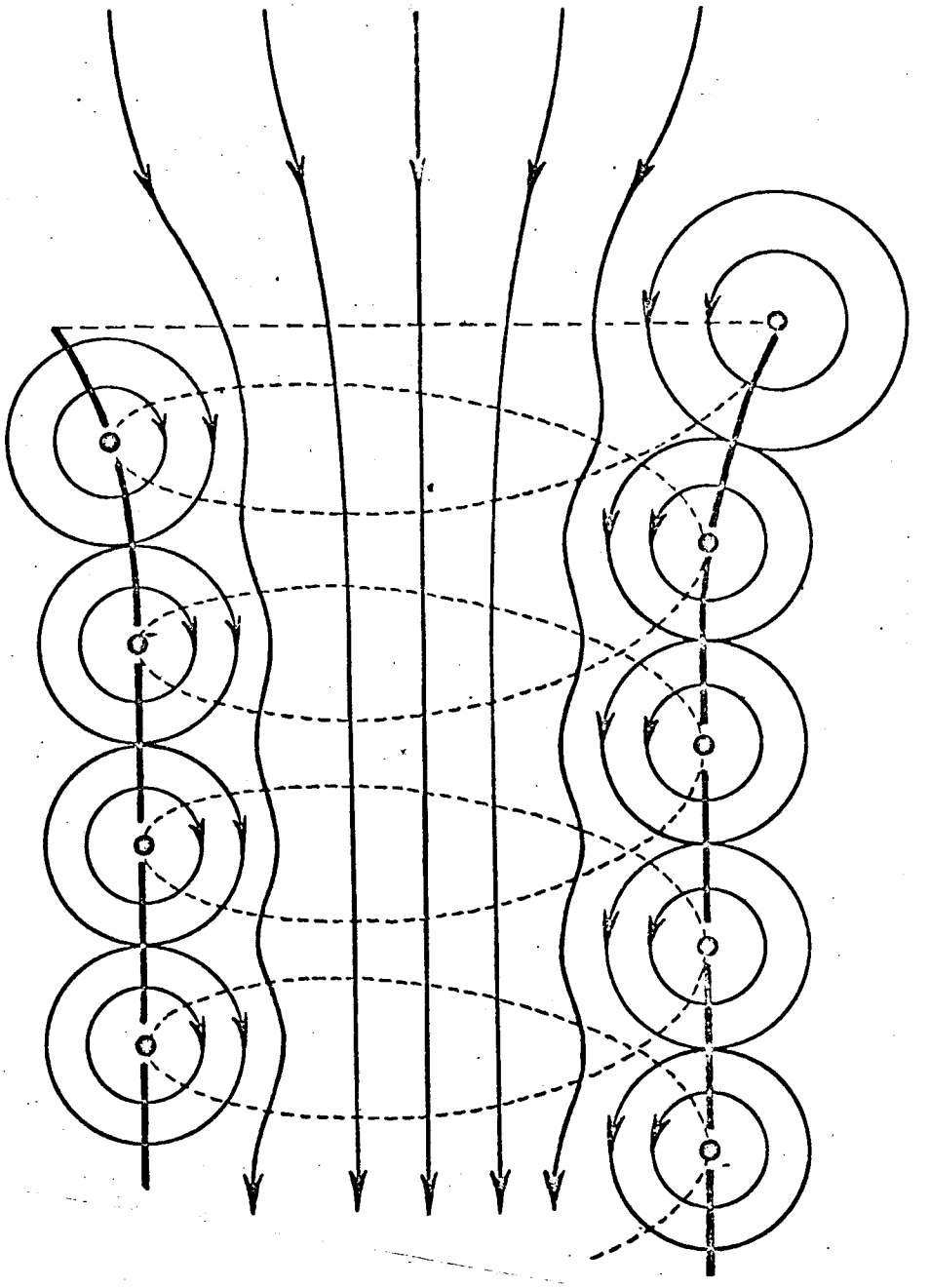

Figure 2-19. Tip Losses.

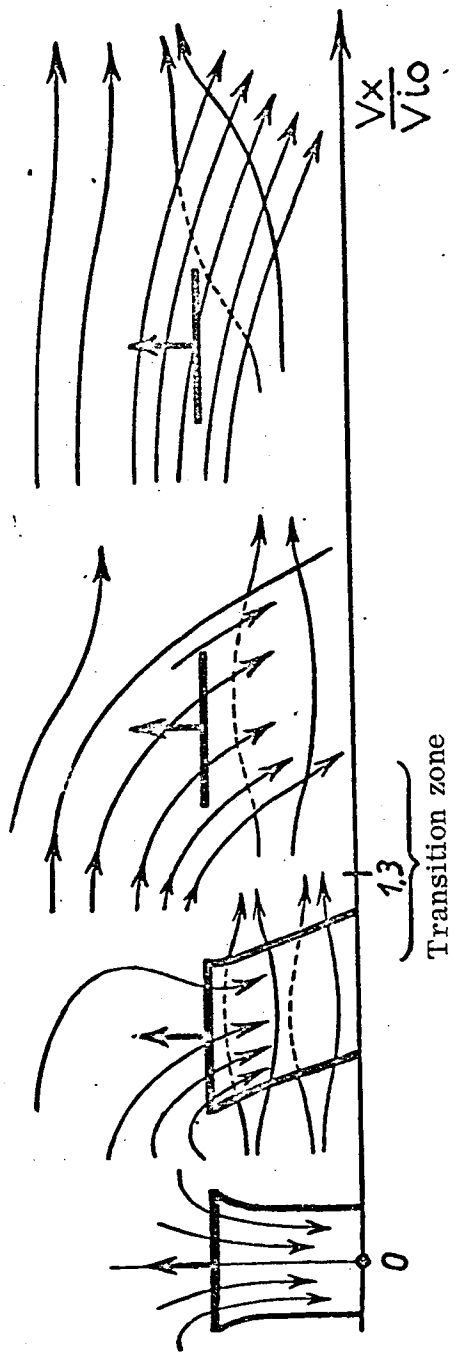

Figure 2-21. Different Types of Flow Across a Rotor in Forward Flight.

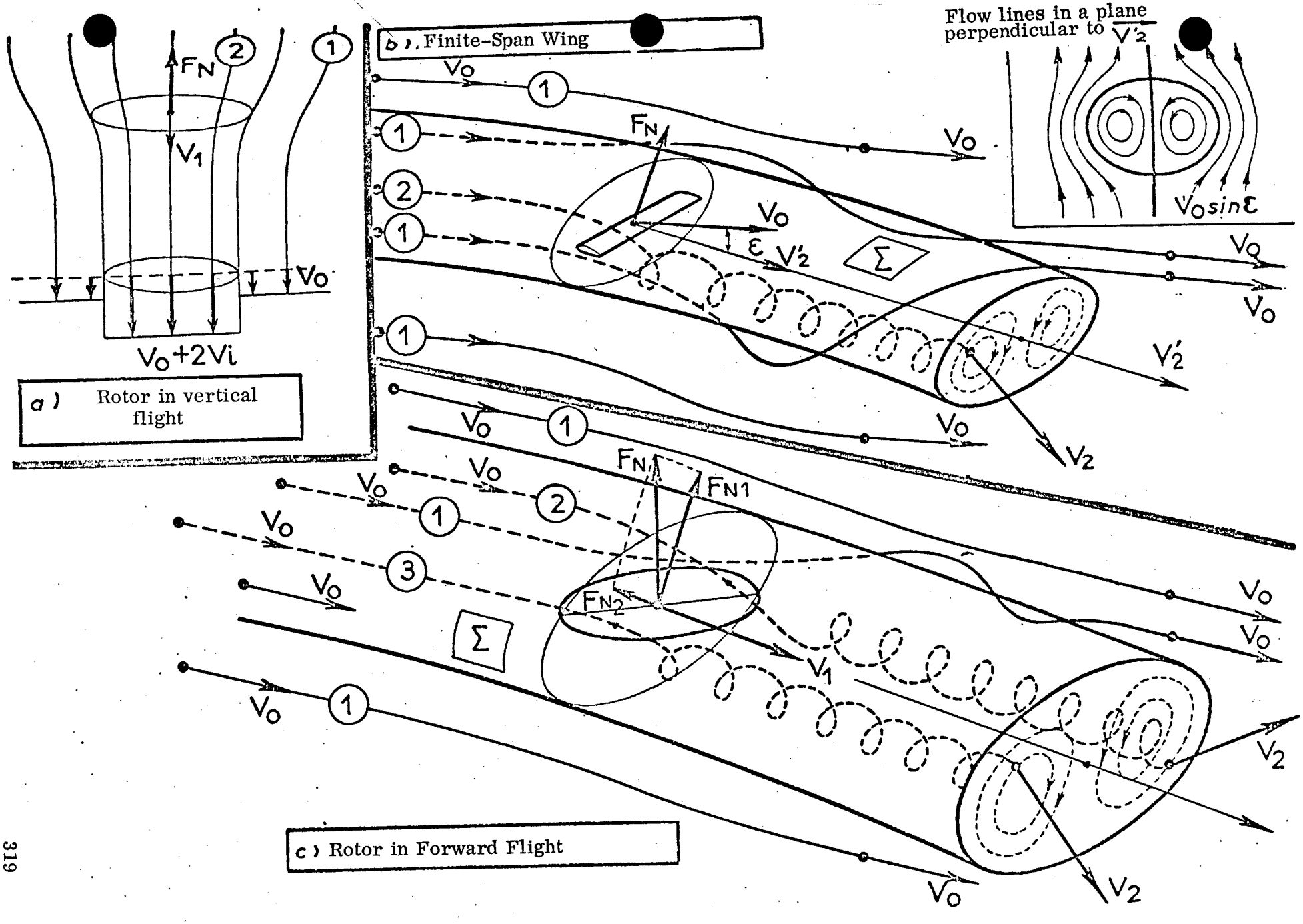
a) Rotor in vertical flight
F_N
V_1
V_o
V_o+2V_i
b) Finite-Span Wing
Flow lines in a plane perpendicular to V'_2
$V_o \sin\varepsilon$
ε
V'_2
Σ
V_2
F_{N1}
F_{N2}
c) Rotor in Forward Flight

Figure 2-20.

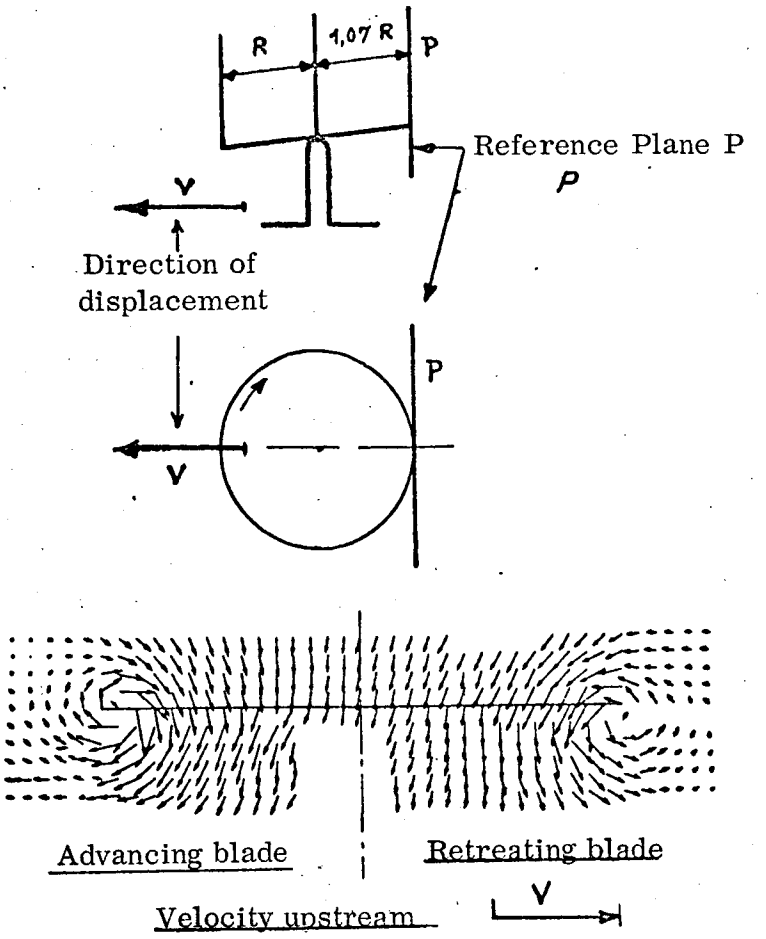

a) Induced velocities in plane P

Remarks (1). The discontinuity in horixontal velocities below the disc characteristic of the passage of a vortex sheet.

(2). The asymmetry between advancing and retreating blades.

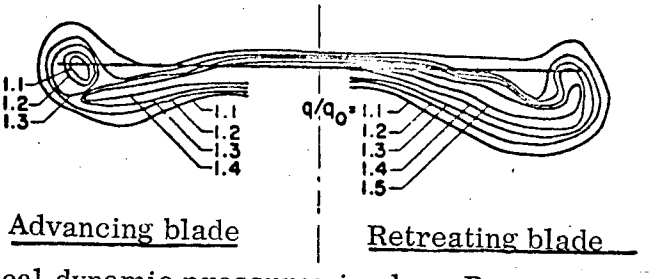

b) Local dynamic pressures in plane P

q: local dynamic pressure

q_0: dynamic pressure at infinity

Figure 2-22. Flow Behind a Rotor in Horizontal Flight.

$$\mu = 0{,}15 \frac{F_N}{\frac{1}{2}\rho S V^2} = 0{,}321$$

(From NACA TN 3242)

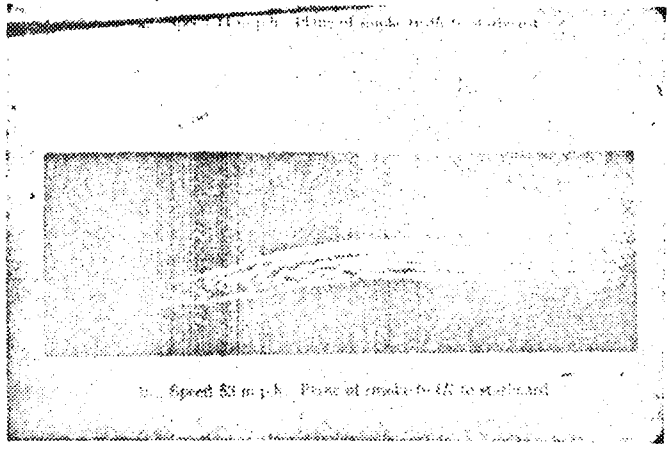

IN-FLIGHT FLOW VISUALIZATION (BROTHERHOOD)

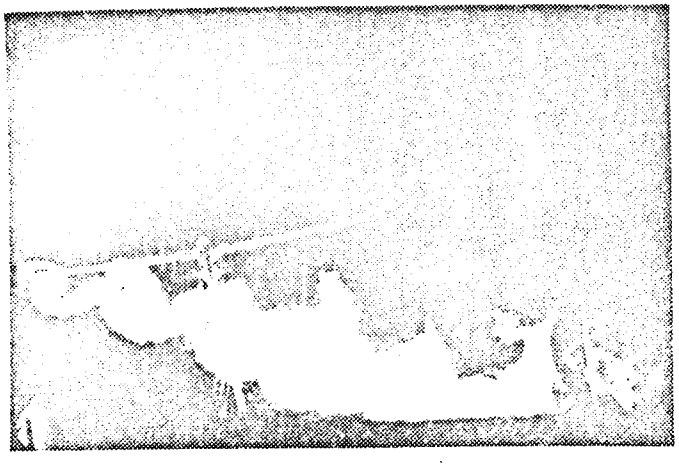

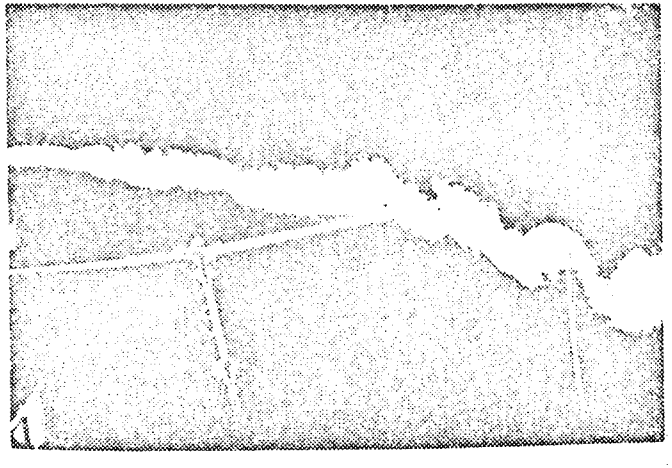

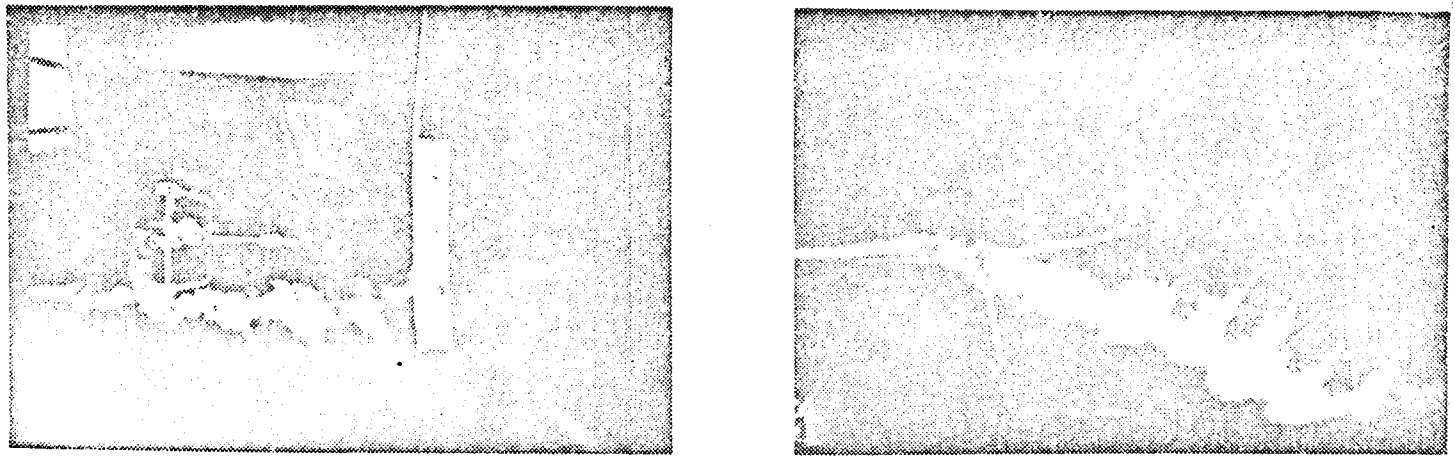

WIND-TUNNEL FLOW VISUALIZATIONS (I. M. F., MARSEILLE)

Figure 2-23. Visualizations of Flow Across a Rotor in Forward Flight.

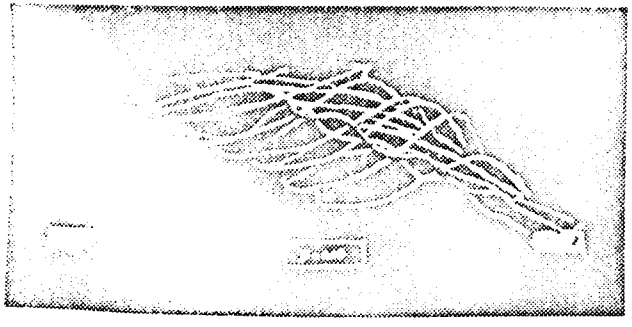

Side View

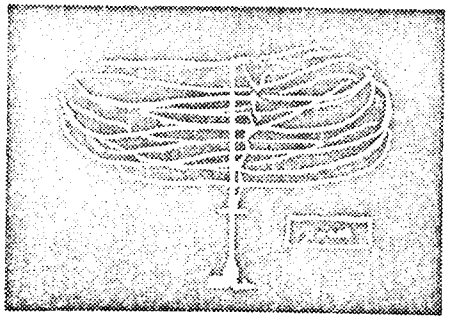

Front View

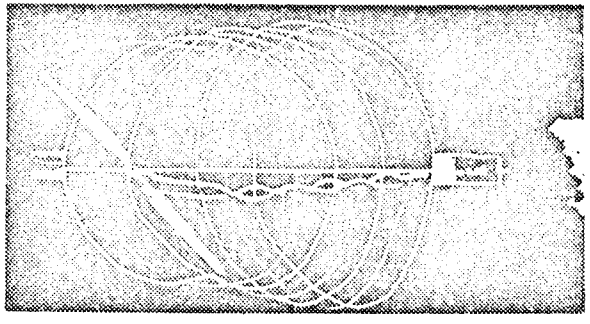

Plan View

$$\mu = 0{,}05 \; \frac{V_{i_0}}{V_\infty} \simeq 1$$

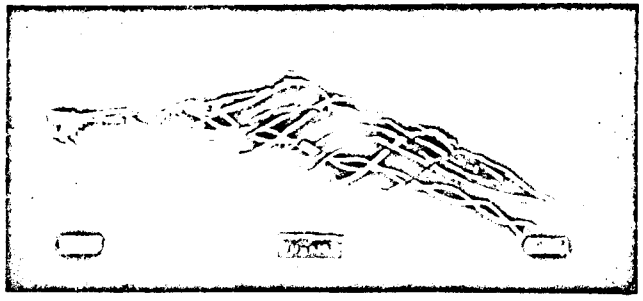

Side View

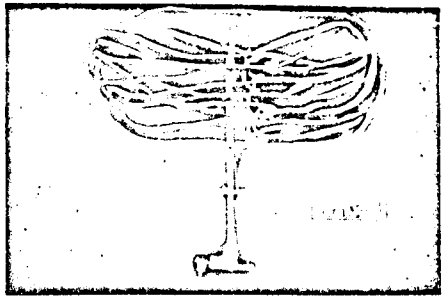

Front View

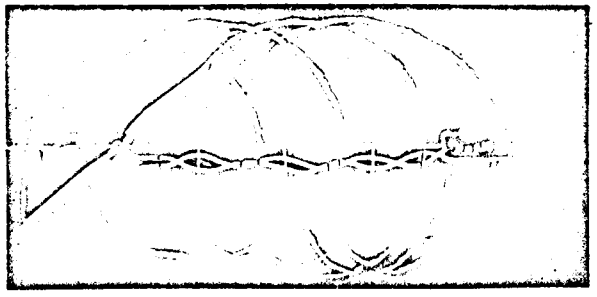

Plan View

$$\mu = 0{,}10 \ \frac{V_{i_o}}{V_x} \simeq 0{,}5$$

Figure 2-24. Reconstruction of Vortex Systems (I.M.F. Marseille).

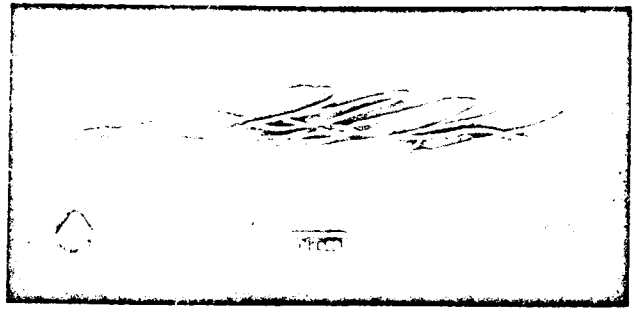

Side View

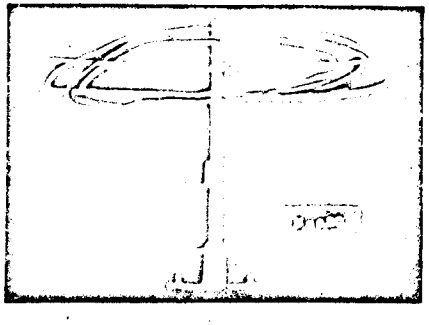

Front View

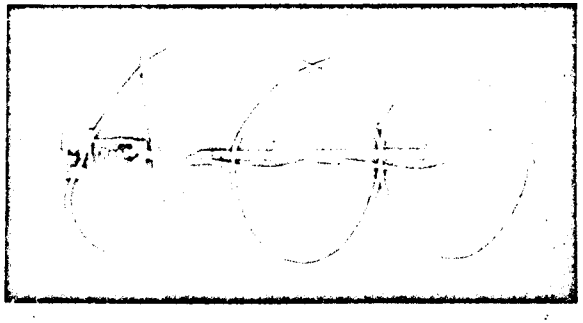

Plan View

$$\mu = 0{,}2 \ \frac{V_{i_o}}{V_x} \simeq 0{,}25$$

Figure 2-24. (Cont'd and Conclusion).
Reconstruction of Vortex Systems.

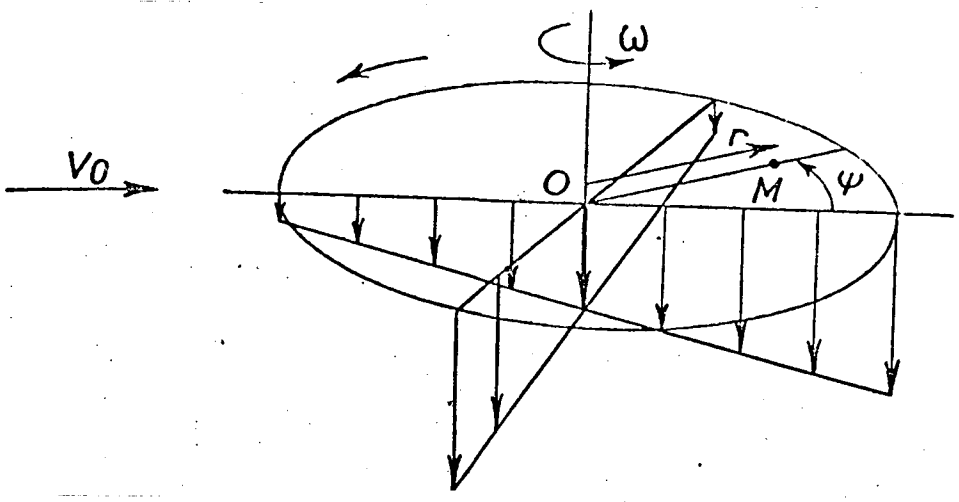

Figure 2-25. Distribution of Induced Velocities in Forward Flight.

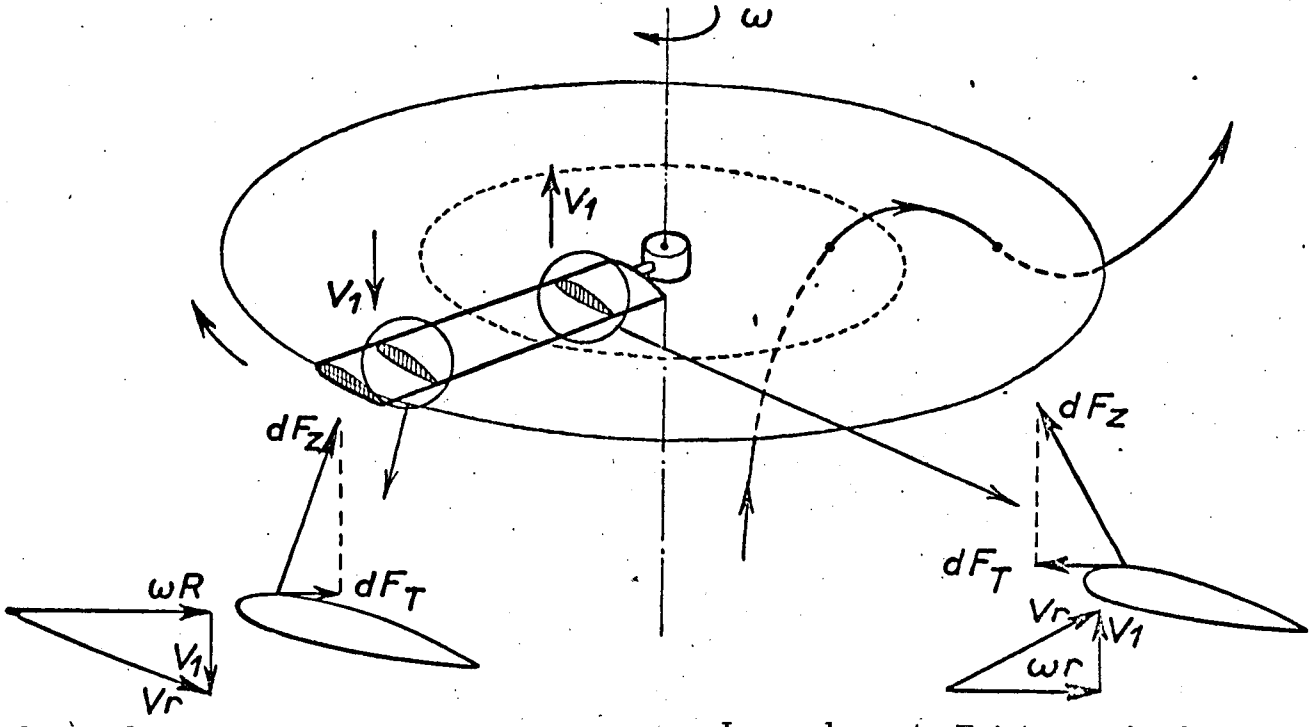

Outer Element: Existance of a drag; helicopter regime.

Inner element: Existence of a thrust component; windmill-braking regime.

b) Autoration in forward flight

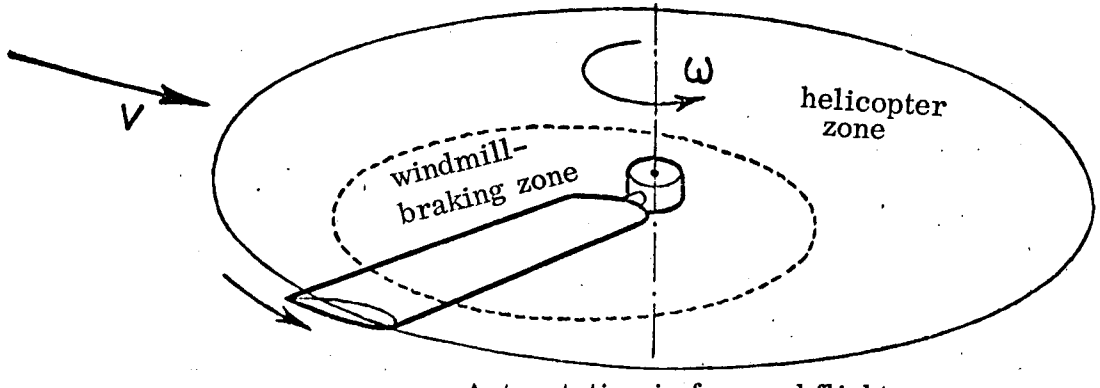

Autorotation in forward flight.

Figure 2-26. Mechanism of Autorotation.

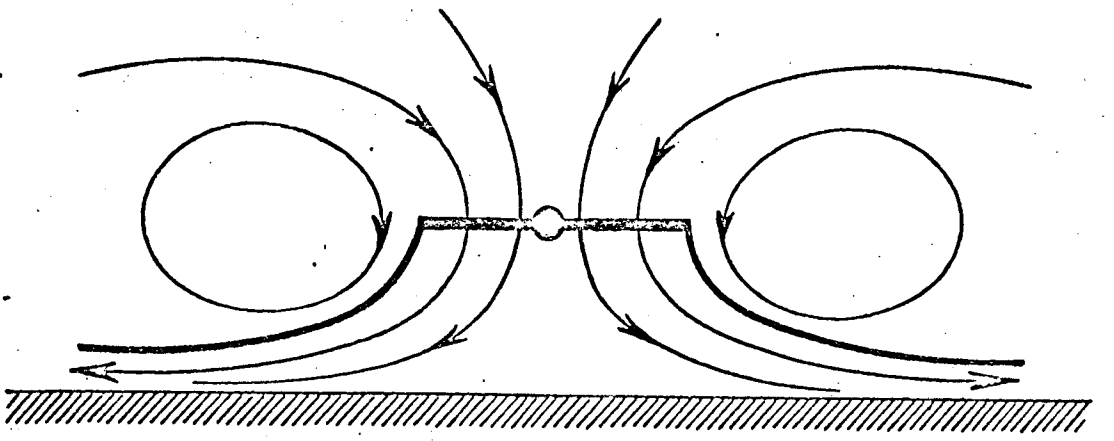

Figure 2-27. Ground Effect.

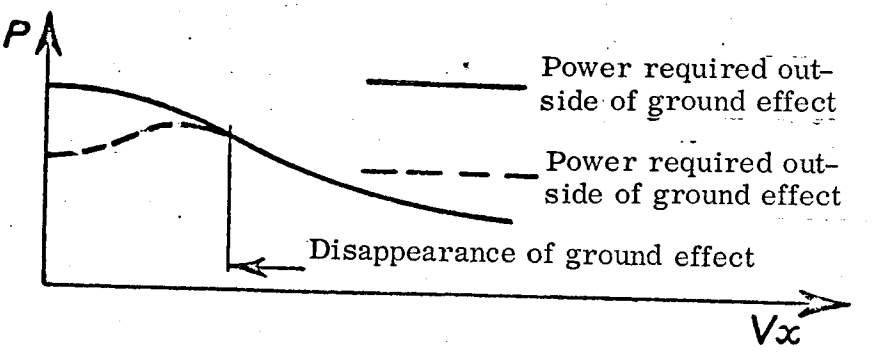

Figure 2-28. Influence of Horizontal Velocity on the Ground Effect.

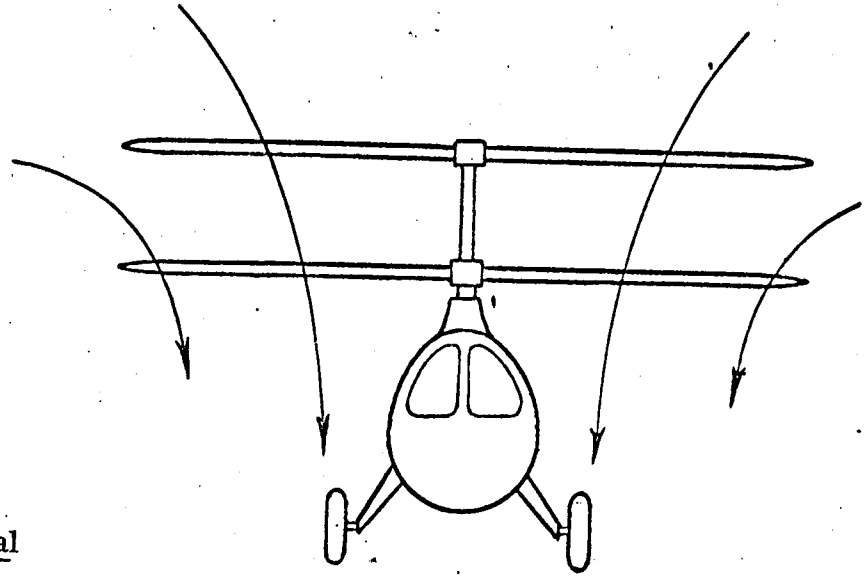

a) Coaxial

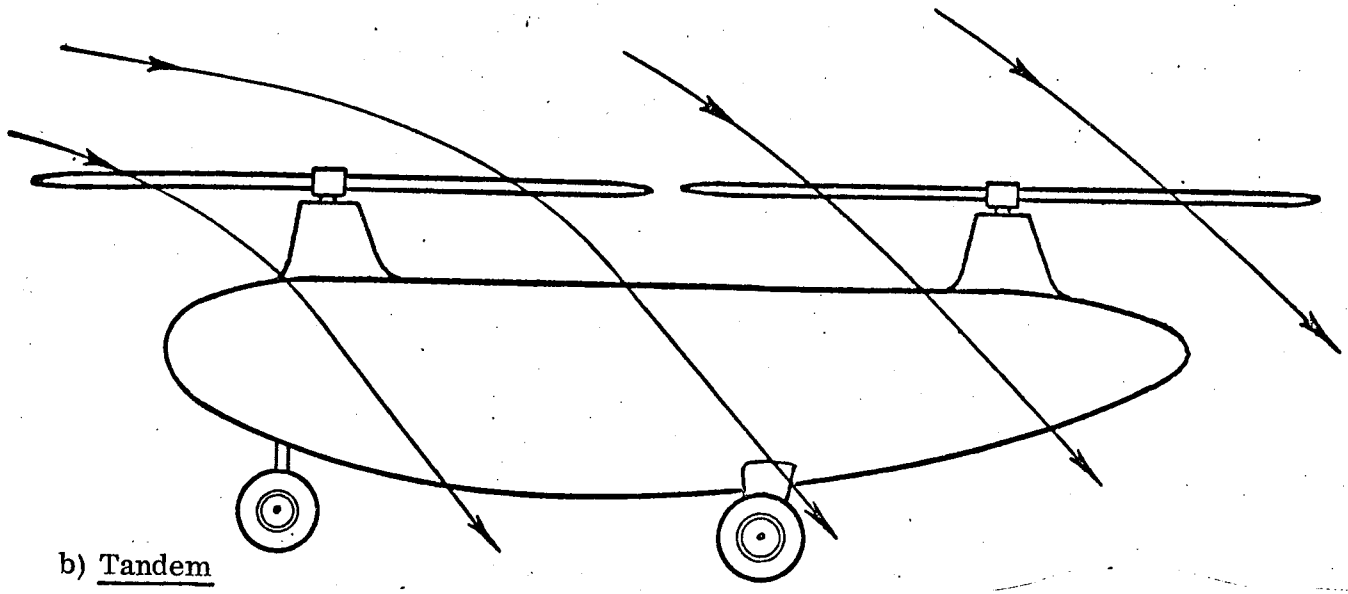

b) Tandem

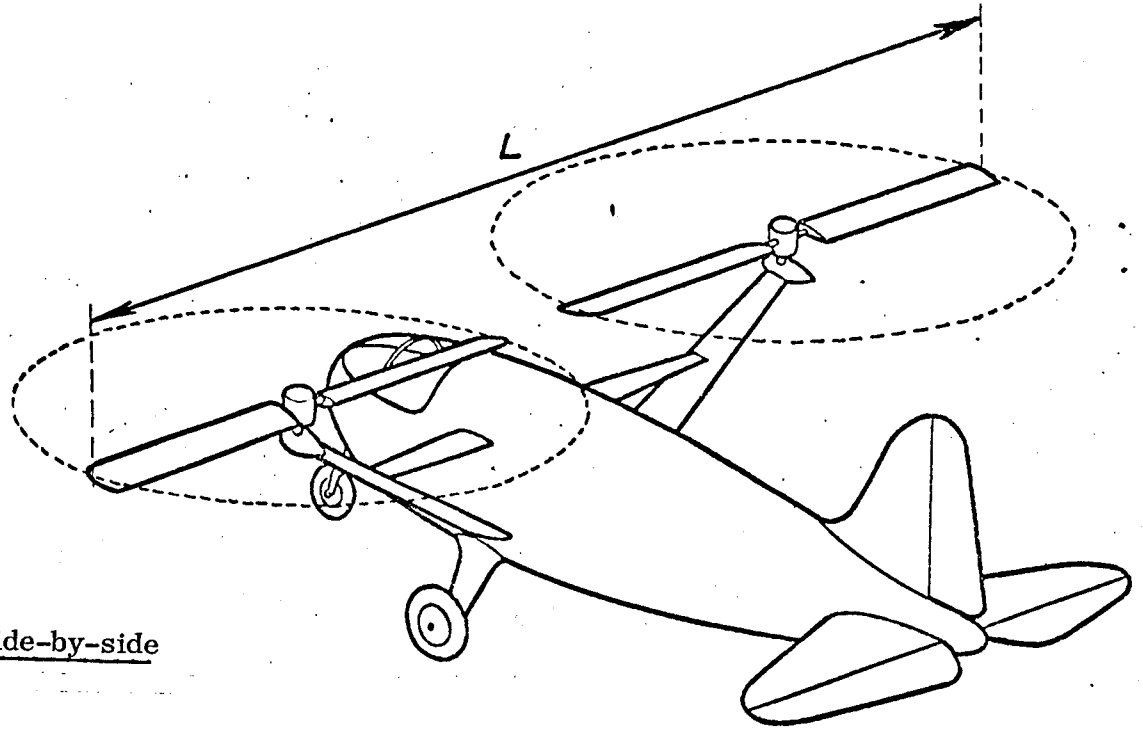

c) Side-by-side

Figure 2-29. Multirotors.

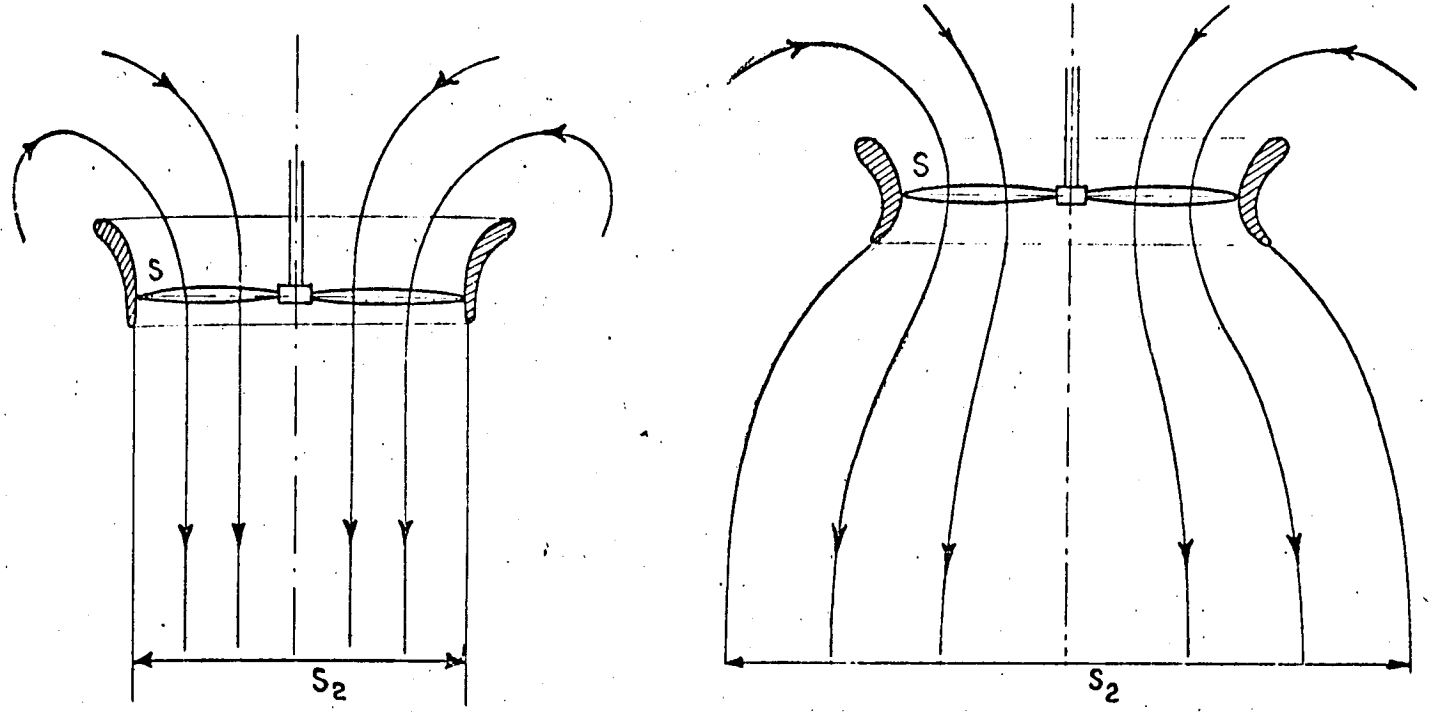

2.30-a-Convergent

2.30-b-Convergent-divergent

Figure 2-30. Ducted Propellor.

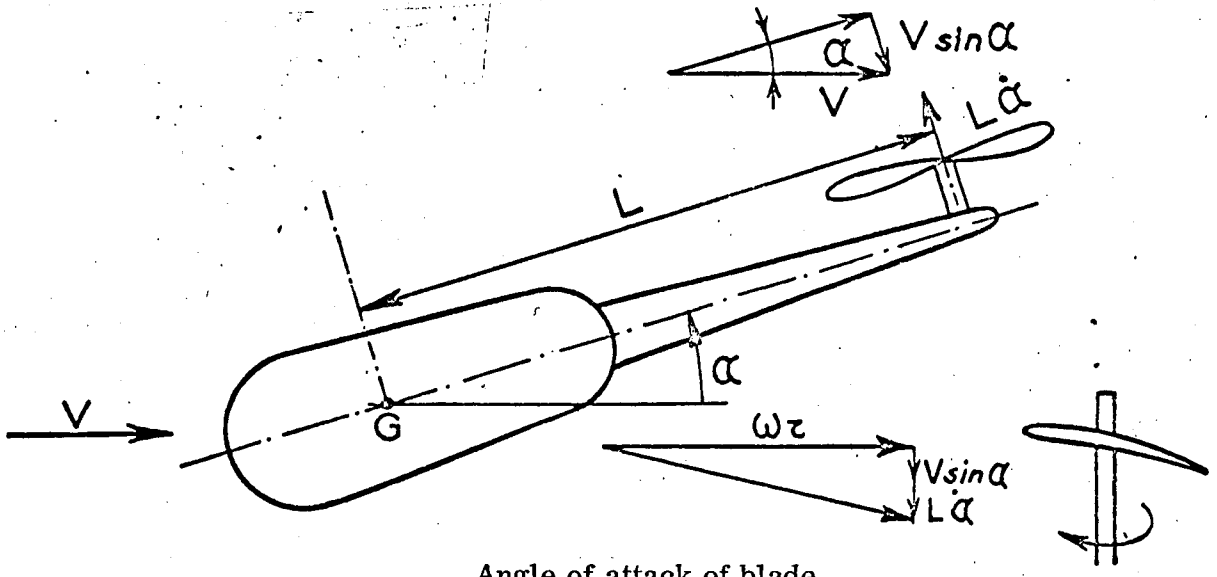

Angle of attack of blade is reduced: rotor traction diminishes

Figure 2-31. Stabilizing Function of the Anti-Torque Rotor.

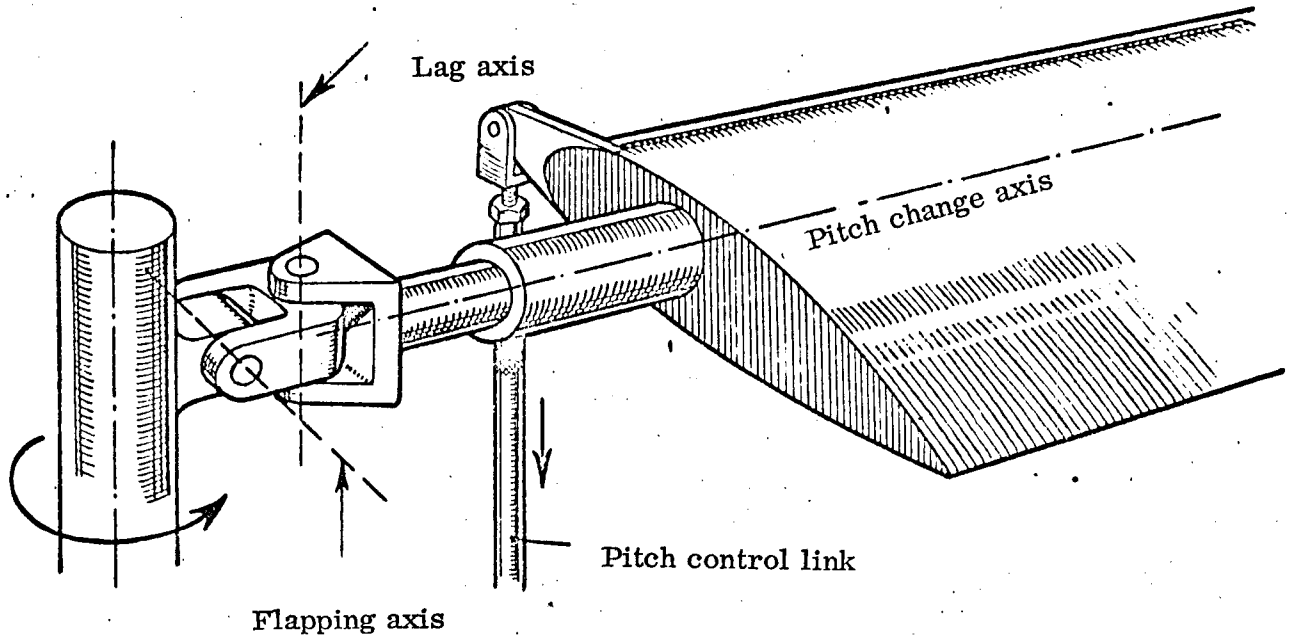

Figure 3-1. The Three Blade Articulations.

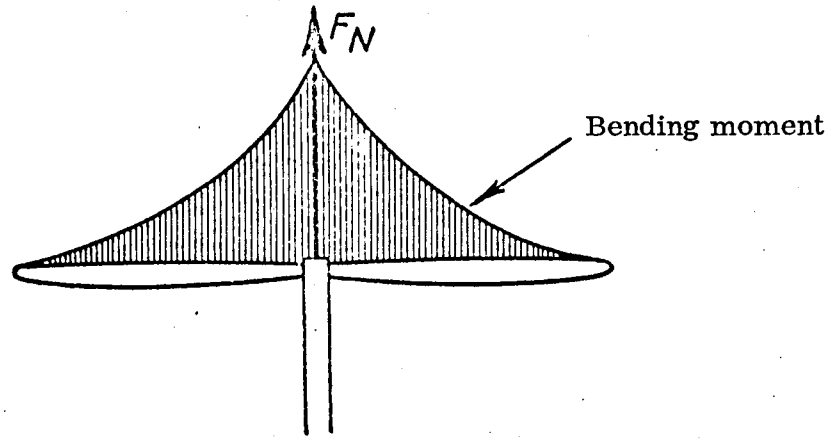

Figure 3-2. Rigid Rotor in Vertical Flight.

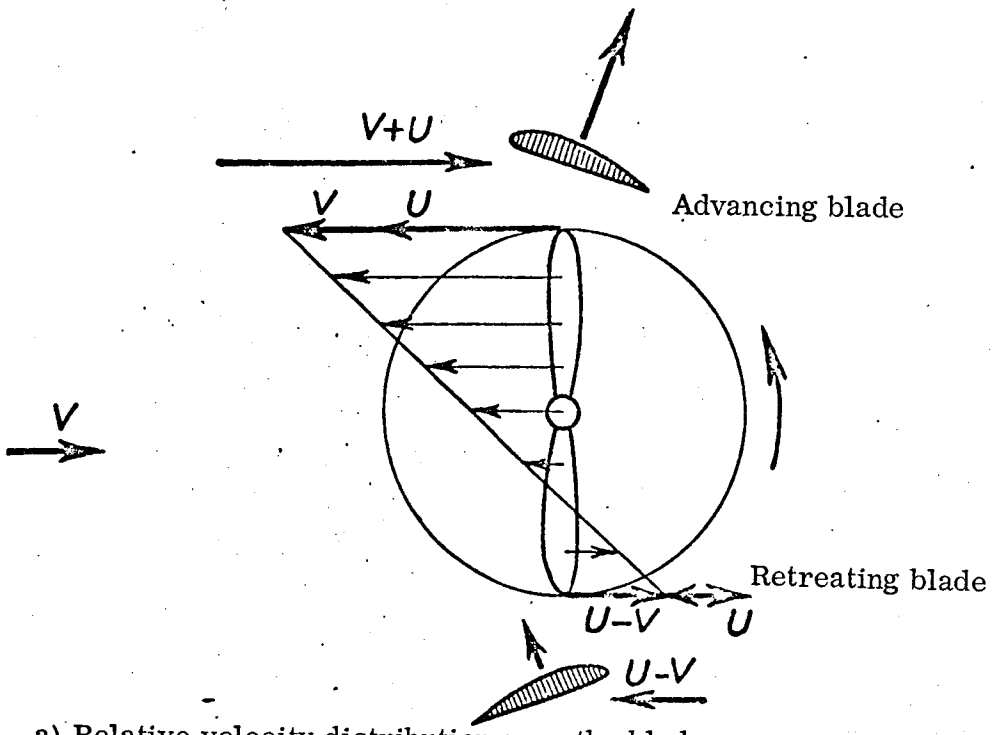

a) Relative velocity distribution over the blades.

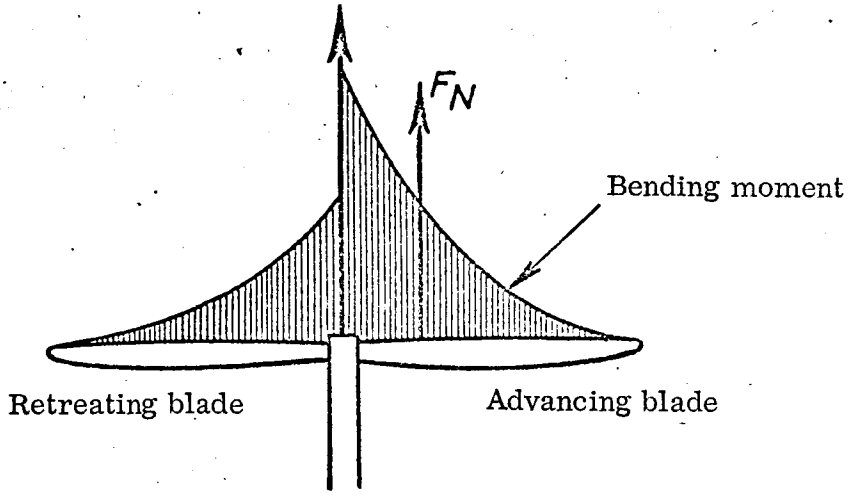

b) Distribution of bending moments over the blades

Figure 3-3. Rigid Rotor in Forward Motion.

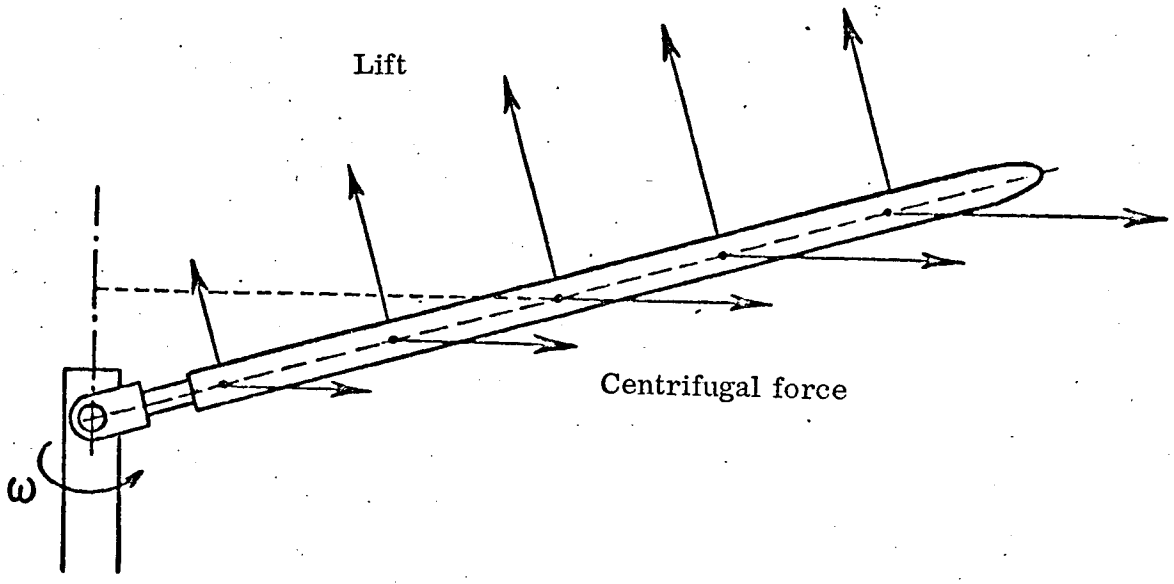

Figure 3-4, a. Balance of Forces over the Blade.

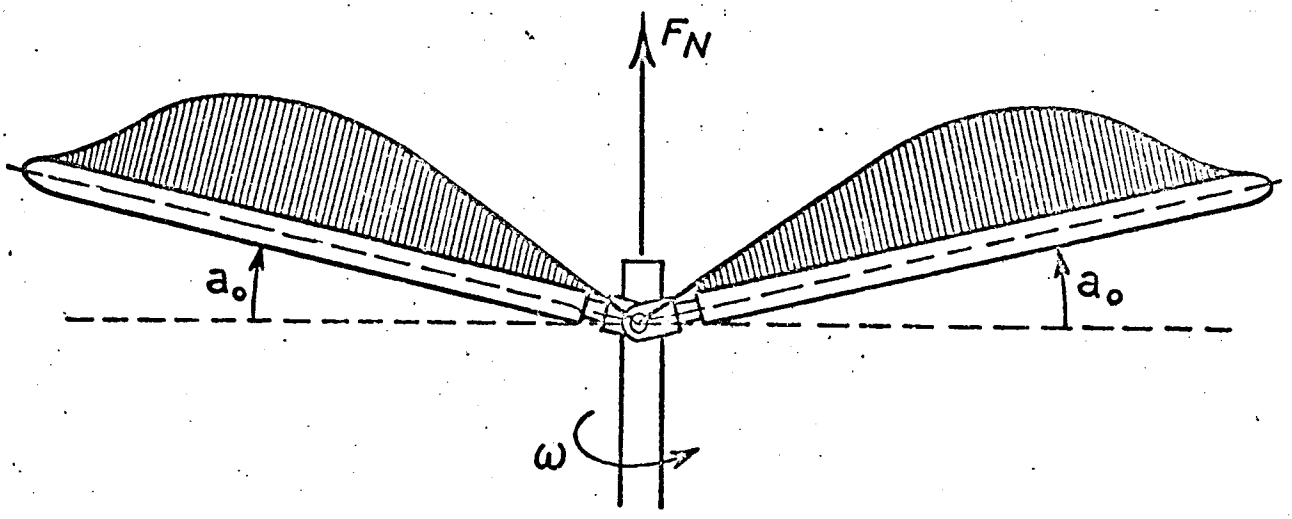

Figure 3.4, b. Distribution of Bending Moments in Vertical Flight.

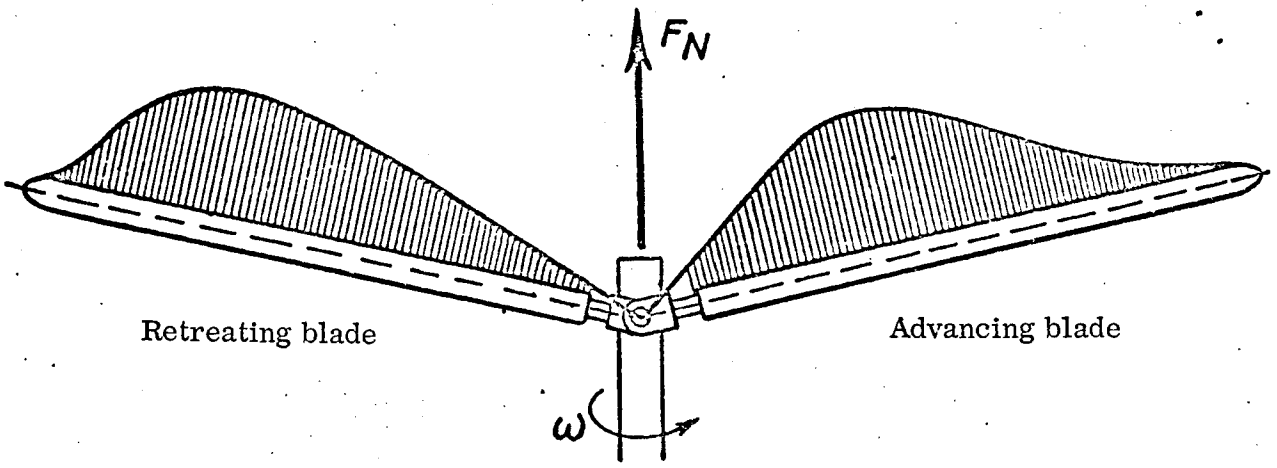

Figure 3-4, c. Distribution of Bending Moments in Forward Flight.

Figure 3-4. Rotor With Articulated Blades.

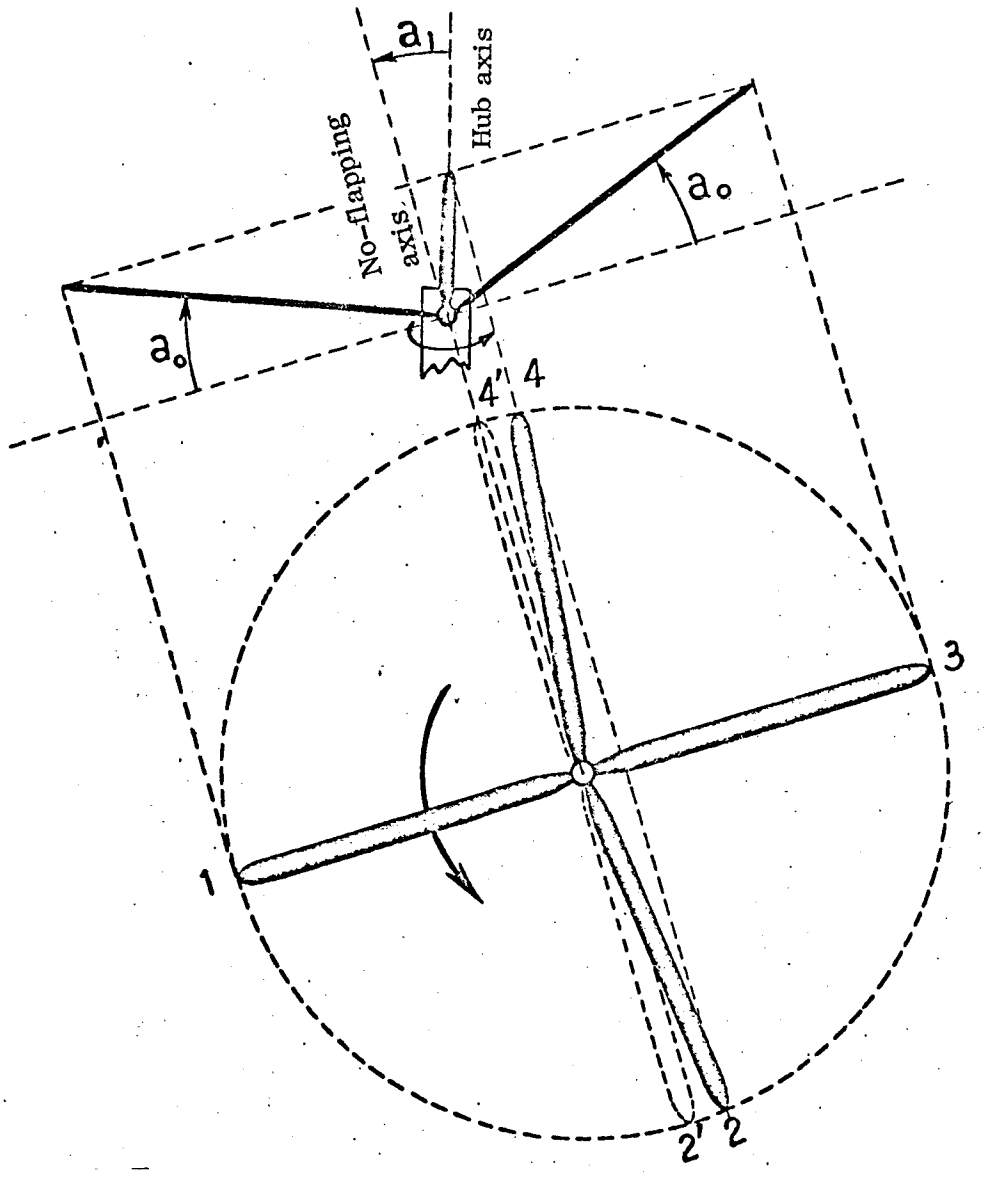

Figure 3-5.

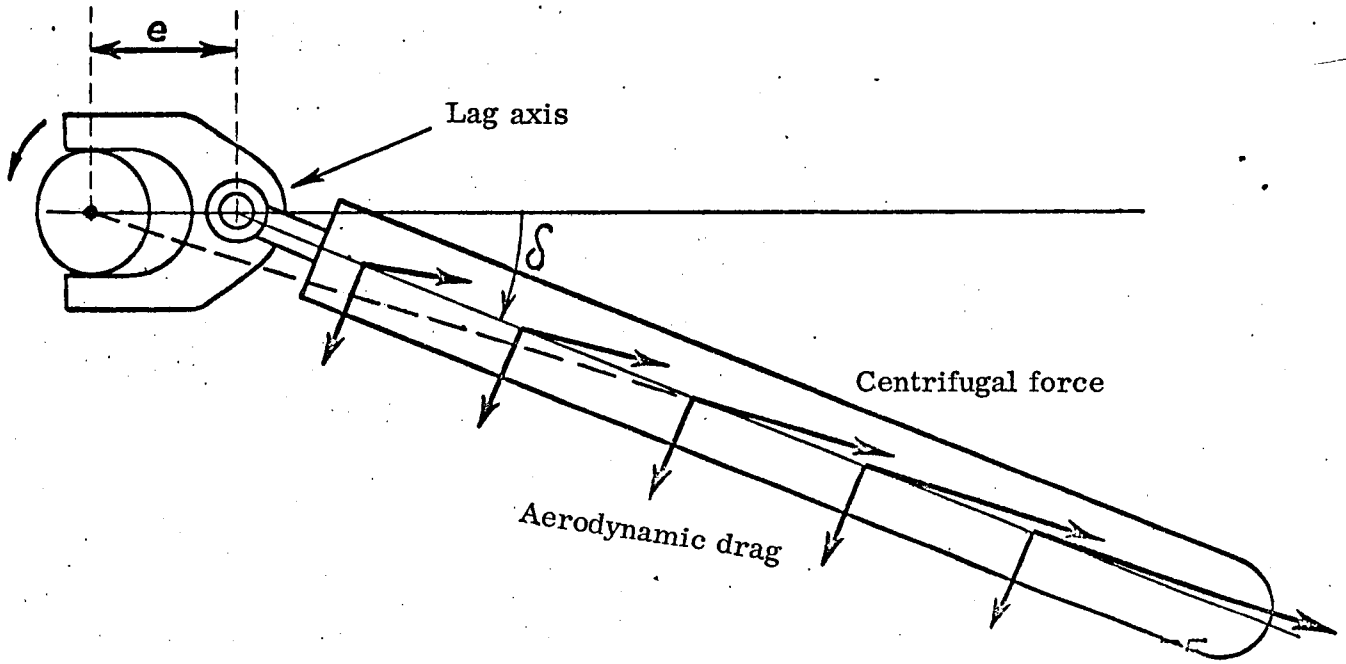

Figure 3-6. Balance of Forces About the Lag Axis.

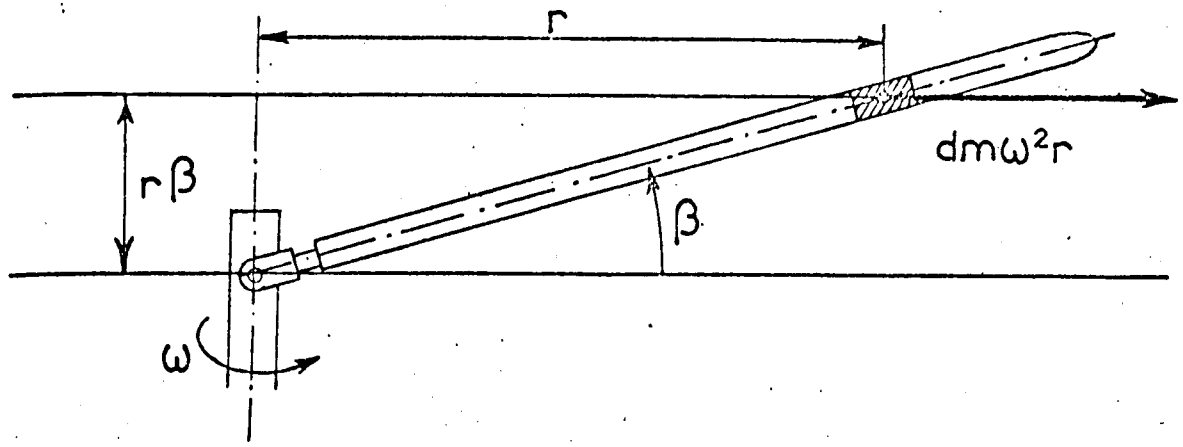

Figure 3-7.

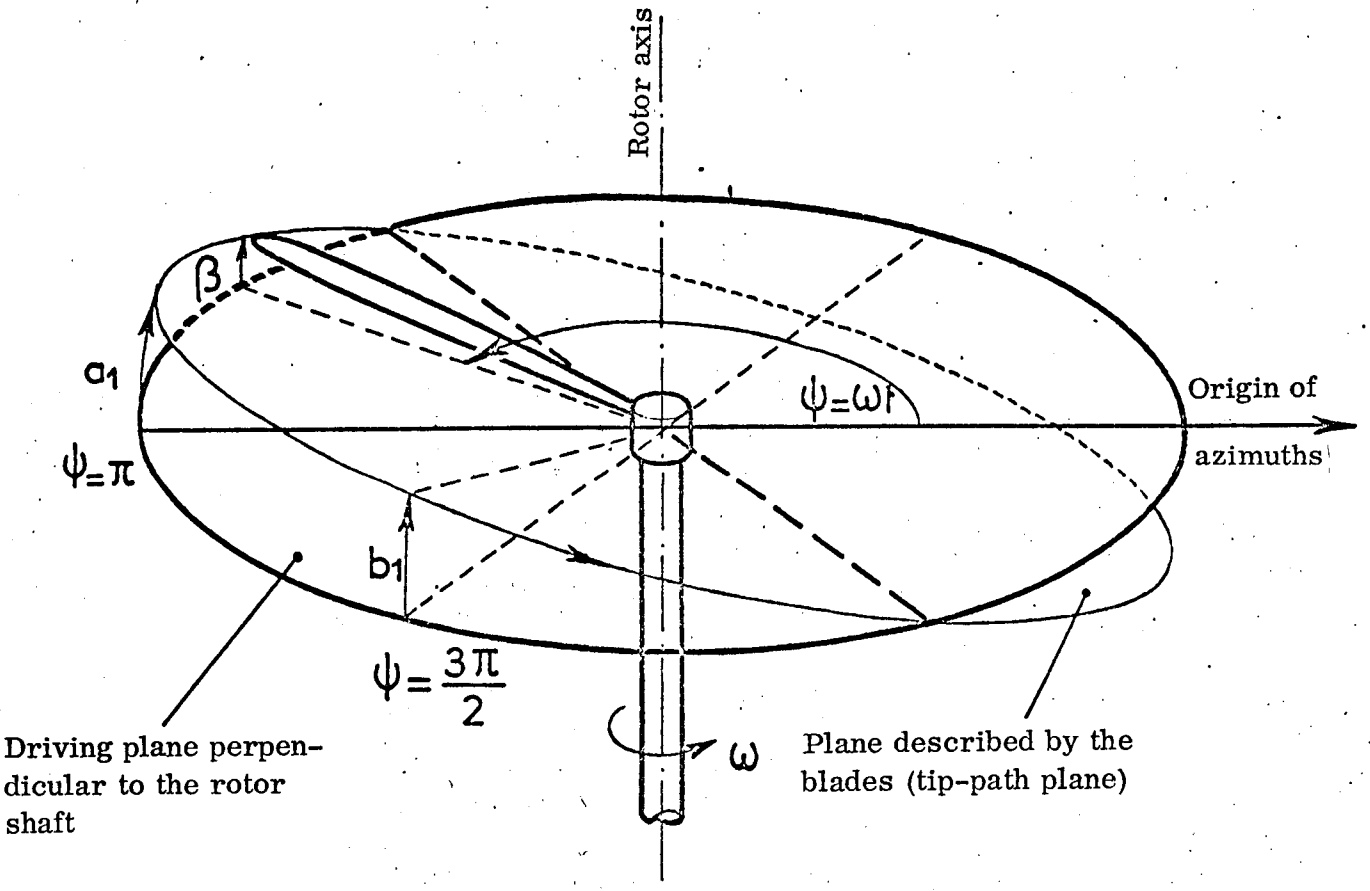
Rotor axis
β
a1
ψ=π
ψ=ωt
Origin of
azimuths
b1
ψ=3π/2
ω
Driving plane perpendicular to the rotor shaft
Plane described by the blades (tip-path plane)

Figure 3-8.

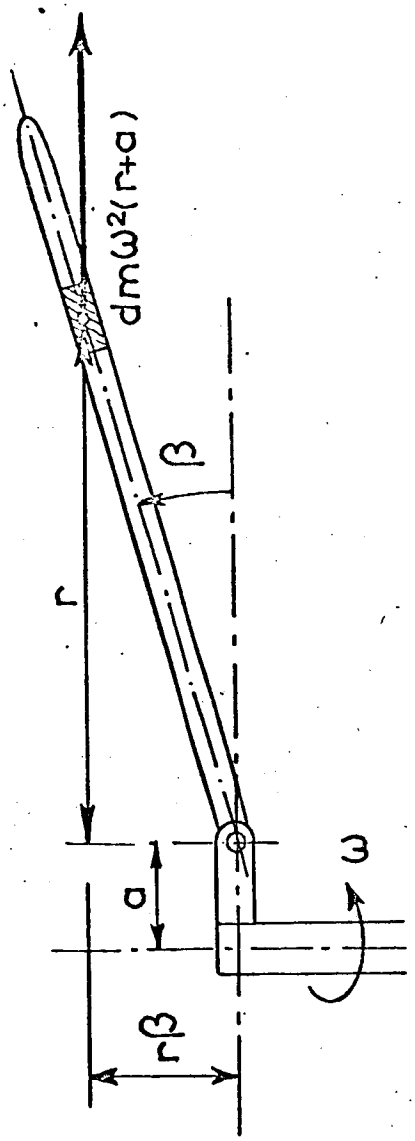

Figure 3-9. Offset Flapping Hinge.

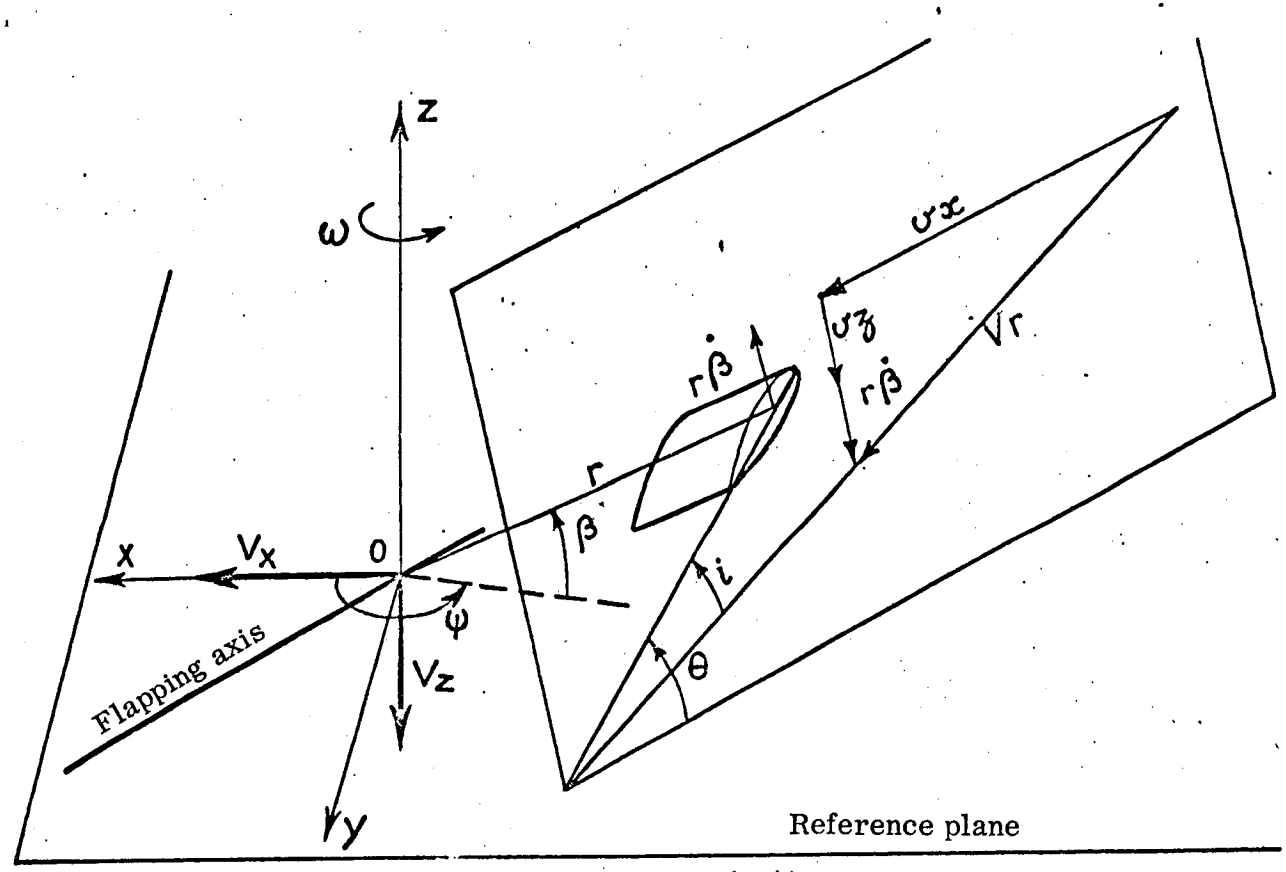

$$\upsilon_x \simeq \omega r + V_x \sin\psi$$

$$\upsilon_z \simeq V_z + v_i - V_x \cos\psi\,\beta \text{ (positive downward)}$$

Figure 3-10. Breakdown of the Resultant Velocities Over a Blade Section.

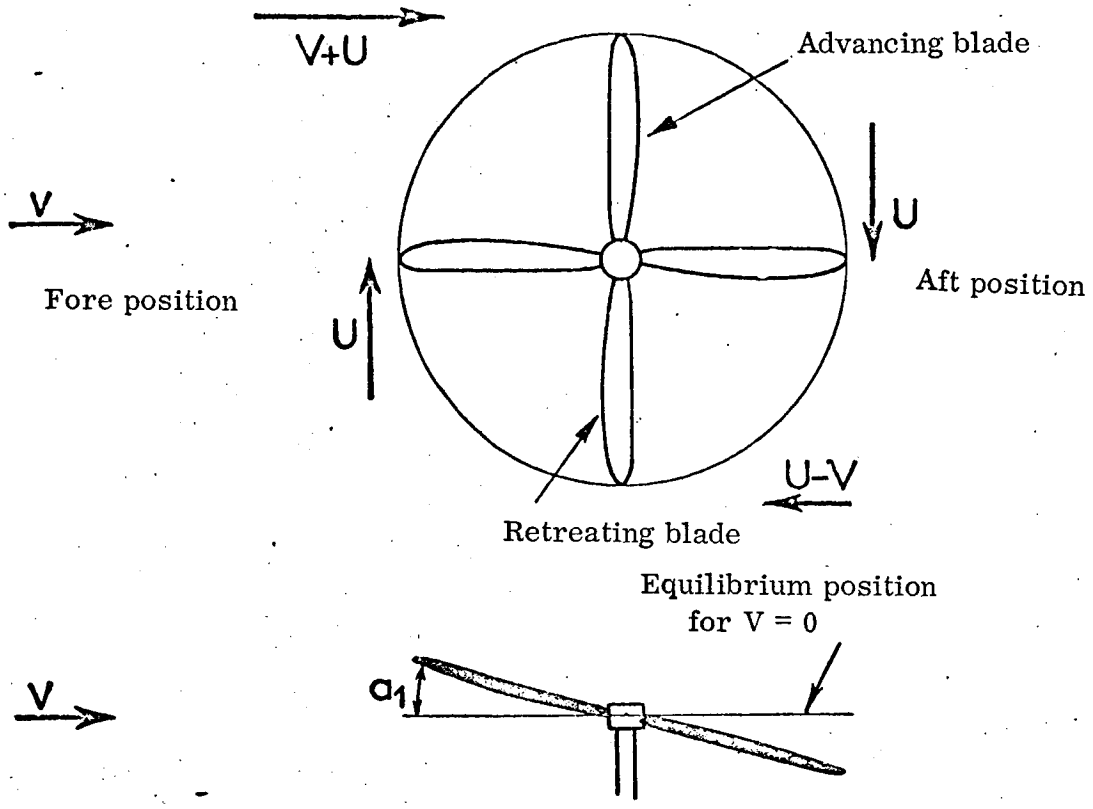

Figure 3-11. Effect of Horizontal Motion on a Articulated Rotor.

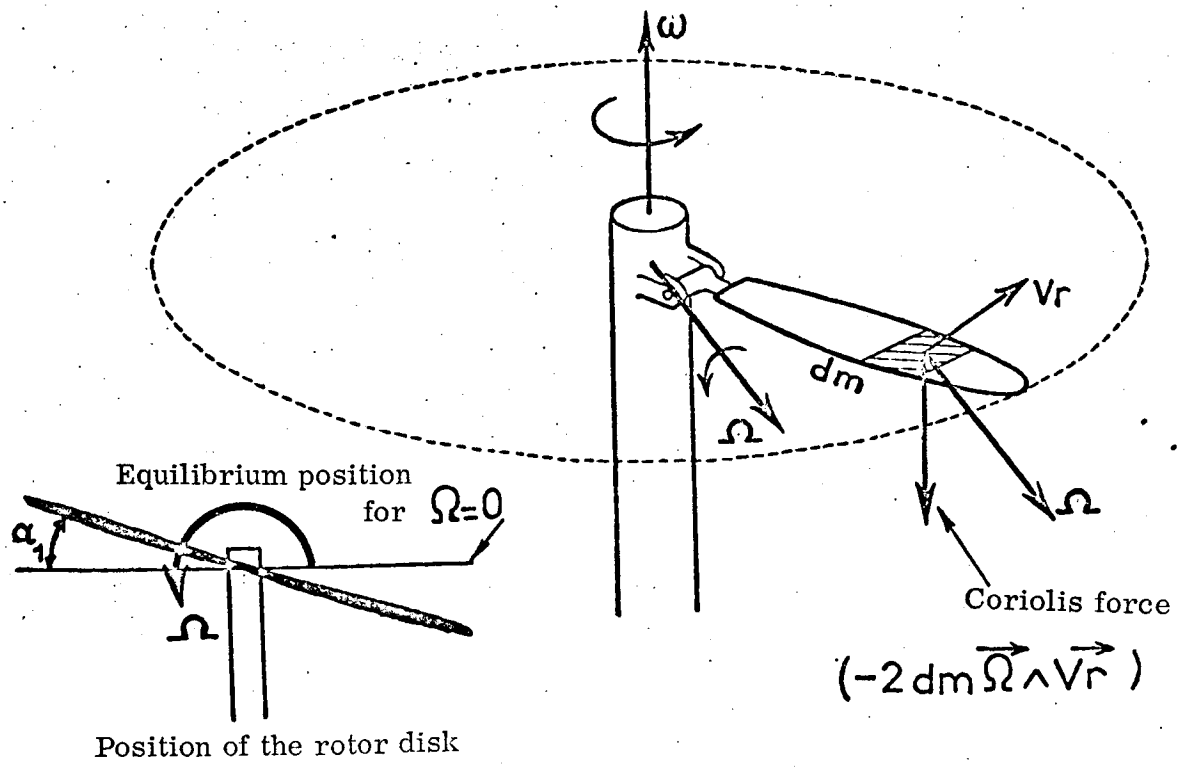

Figure 3-12. Effect of Uniform Rotor Speed on an Articulated Rotor.

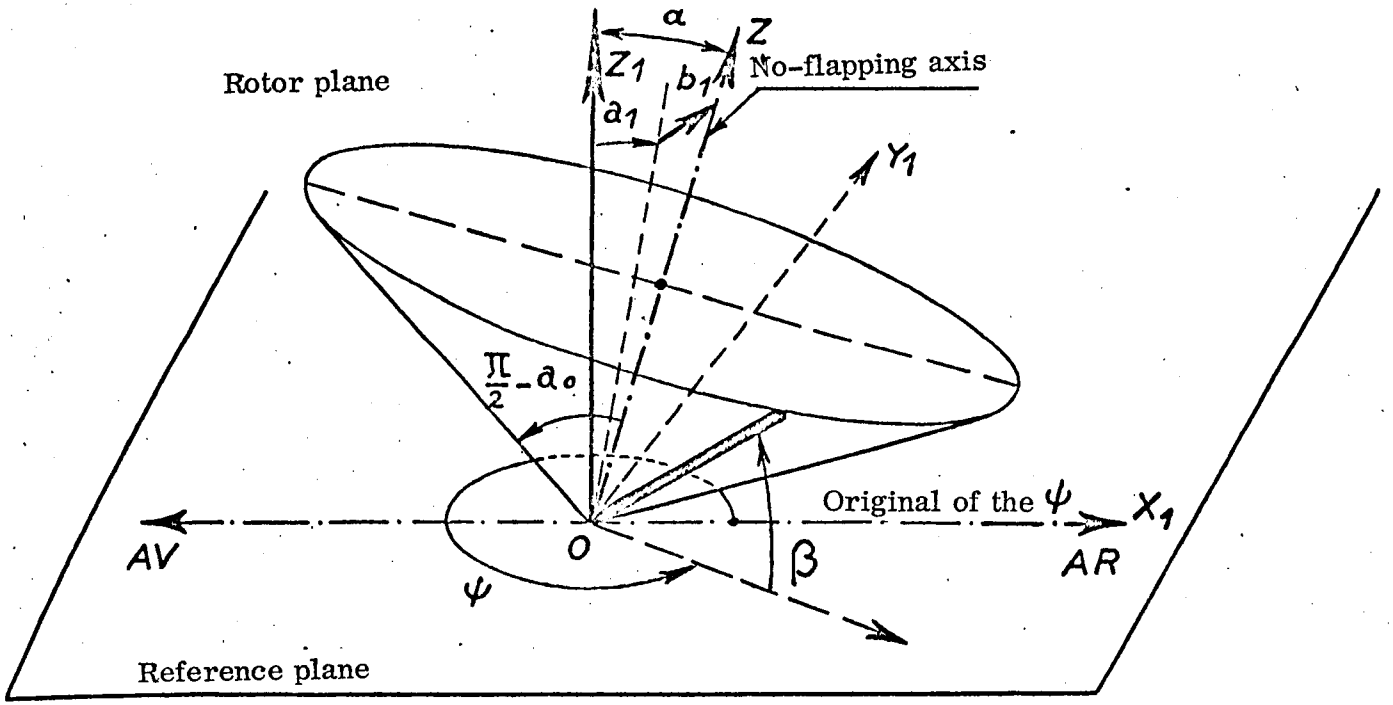
a
Z
Z1
b1
No-flapping axis
Rotor plane
a1
Y1
π/2 - a0
Original of the ψ
X1
AV
O
β
AR
ψ
Reference plane

Figure 3-13.

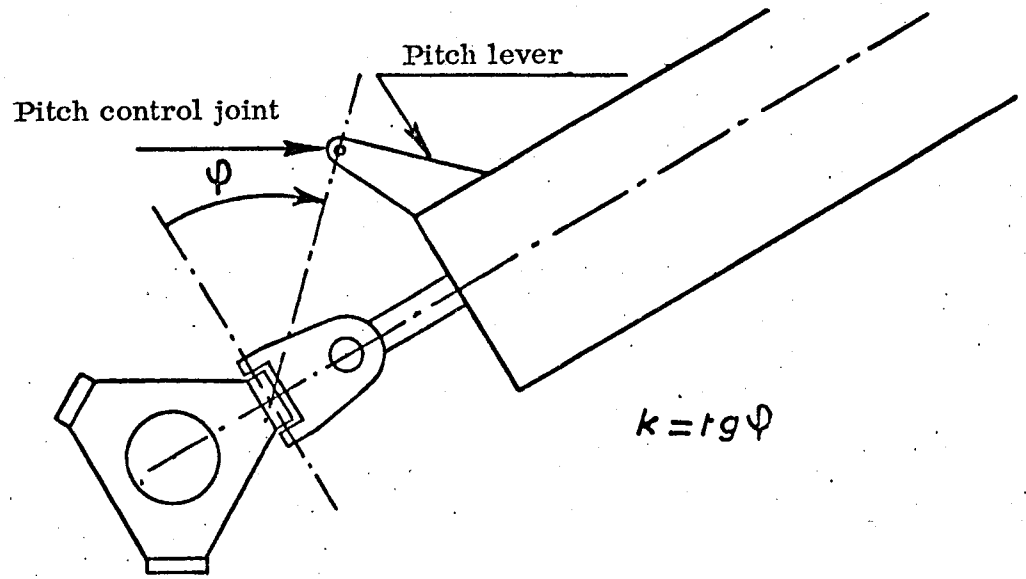

Figure 3-14. Pitch-Flap Coupling

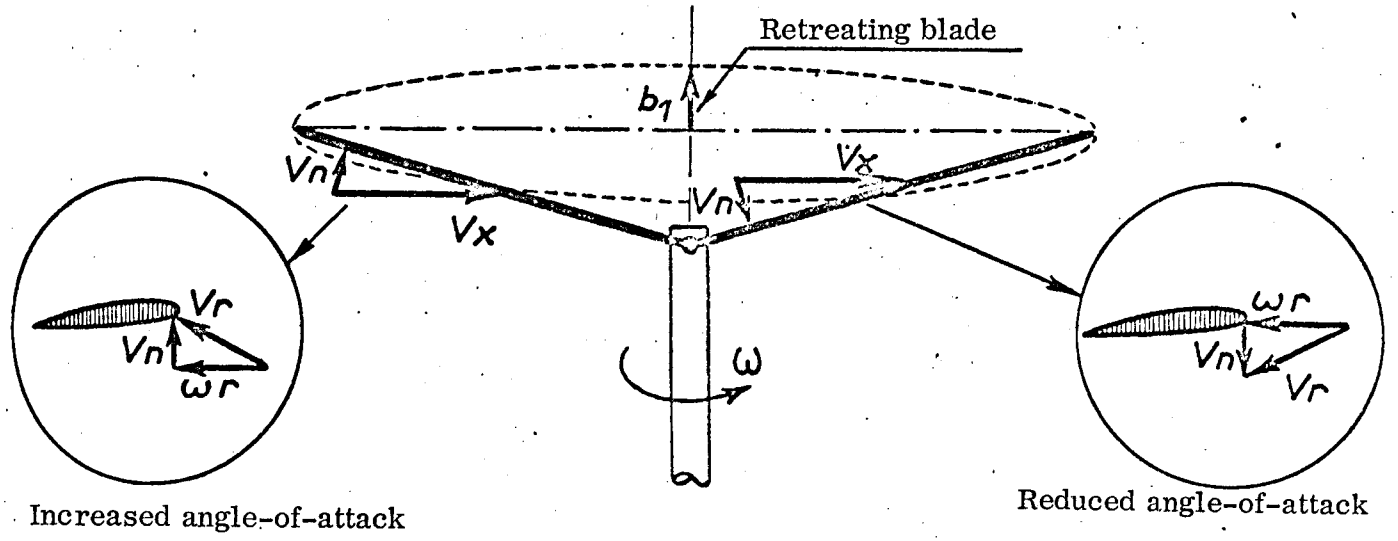

Figure 3-15. Coning Causes Lateral Rotor Tilt in Response to the Effect of Forward Speed.

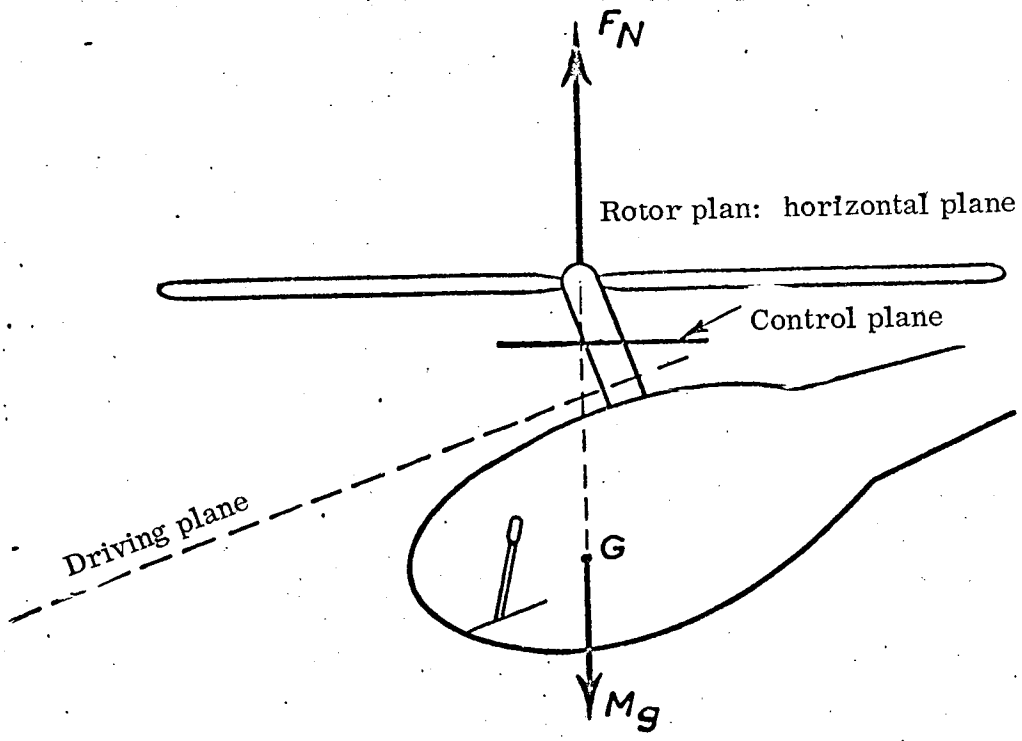

Figure 3-16, a. Vertical Flight (forward trim compensation).

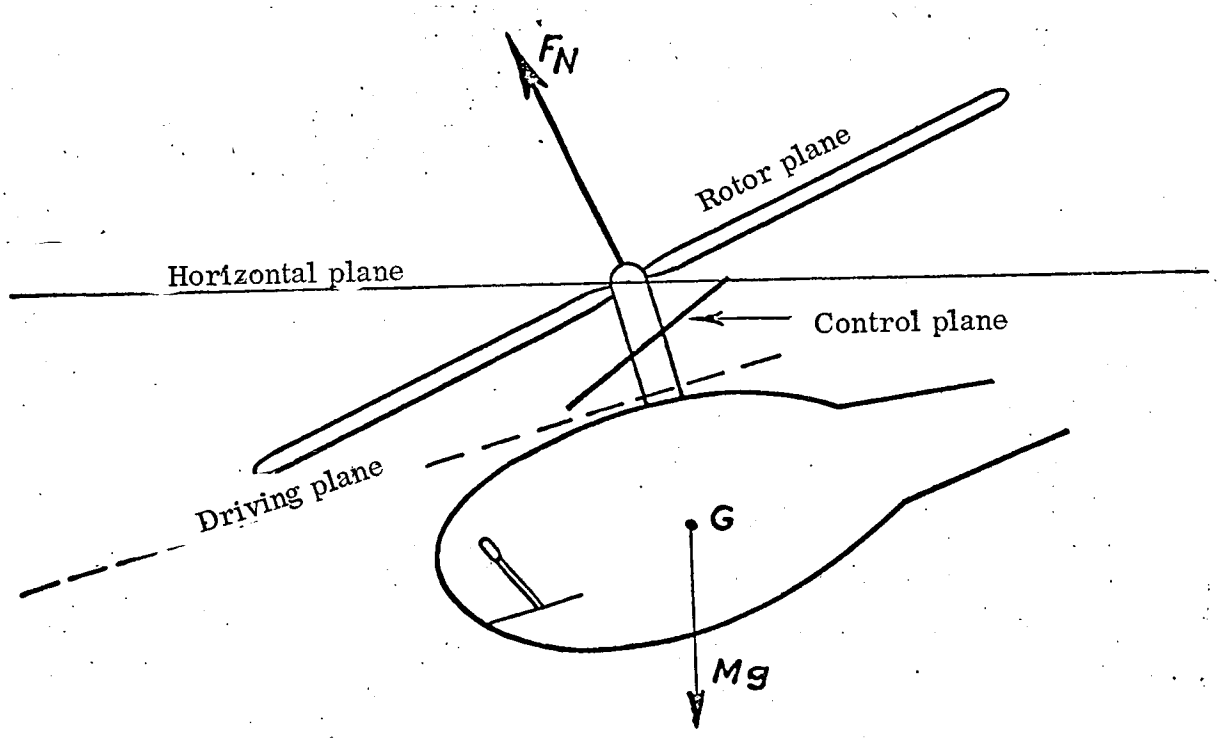

Figure 3-16, b. Translational Flight (helicopter state).

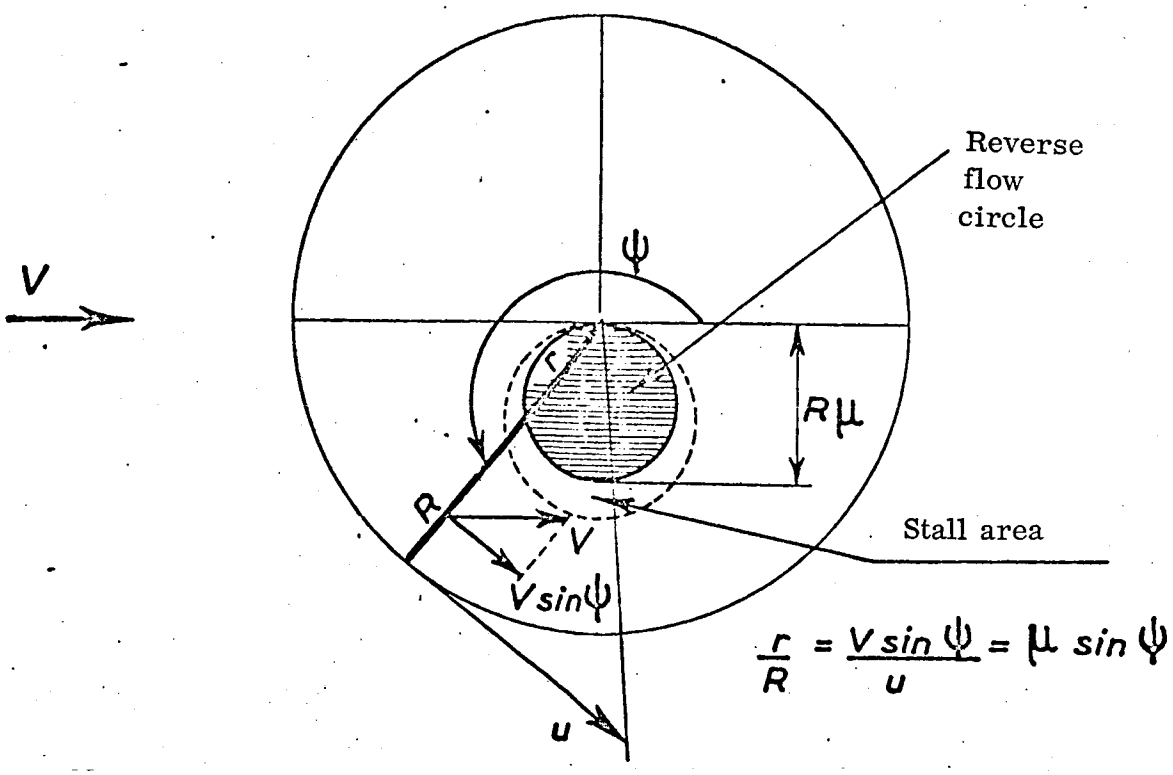

Figure 3-17. Reverse Flow Circle.

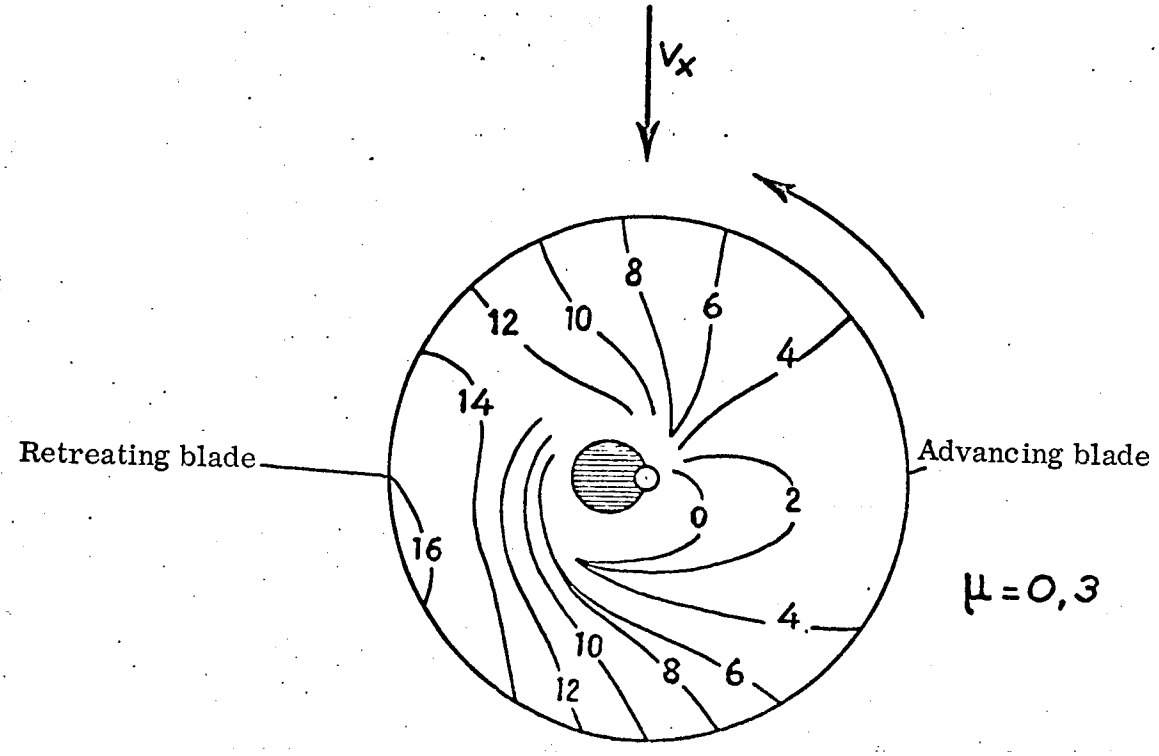

Figure 3-18. Angle-of-Attack-Contour Plot (in degrees) Over a Rotor in Horizontal Forward Flight.

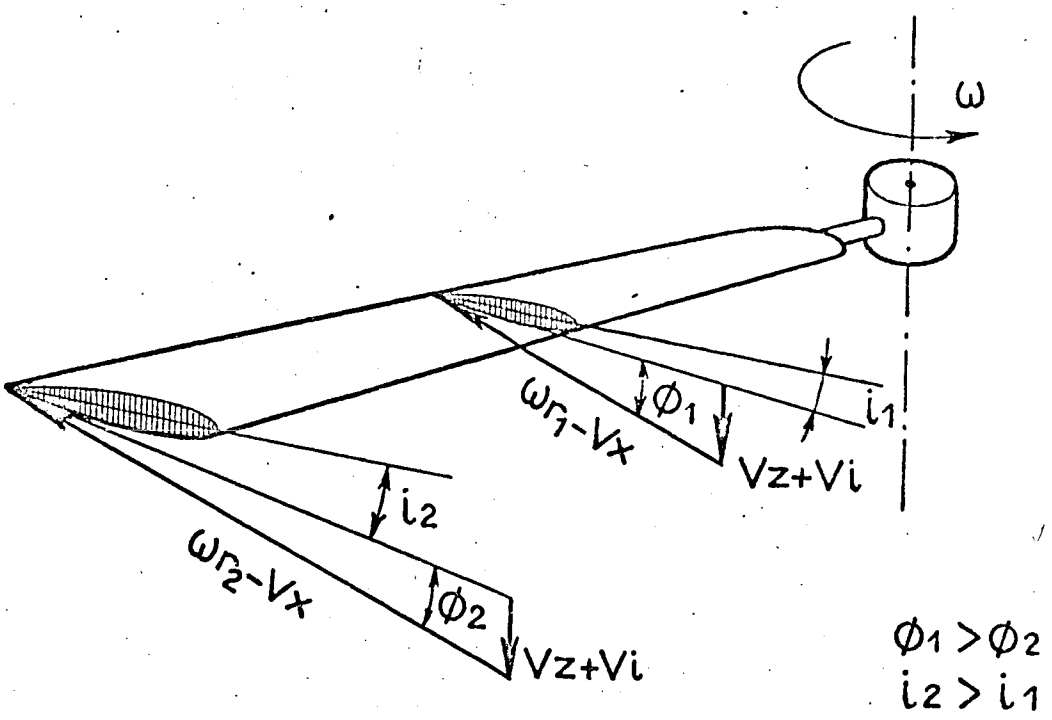

Figure 3-19. Influence of Rotor Inflow on the Angle of Attack at the Tip of a Retreating blade.

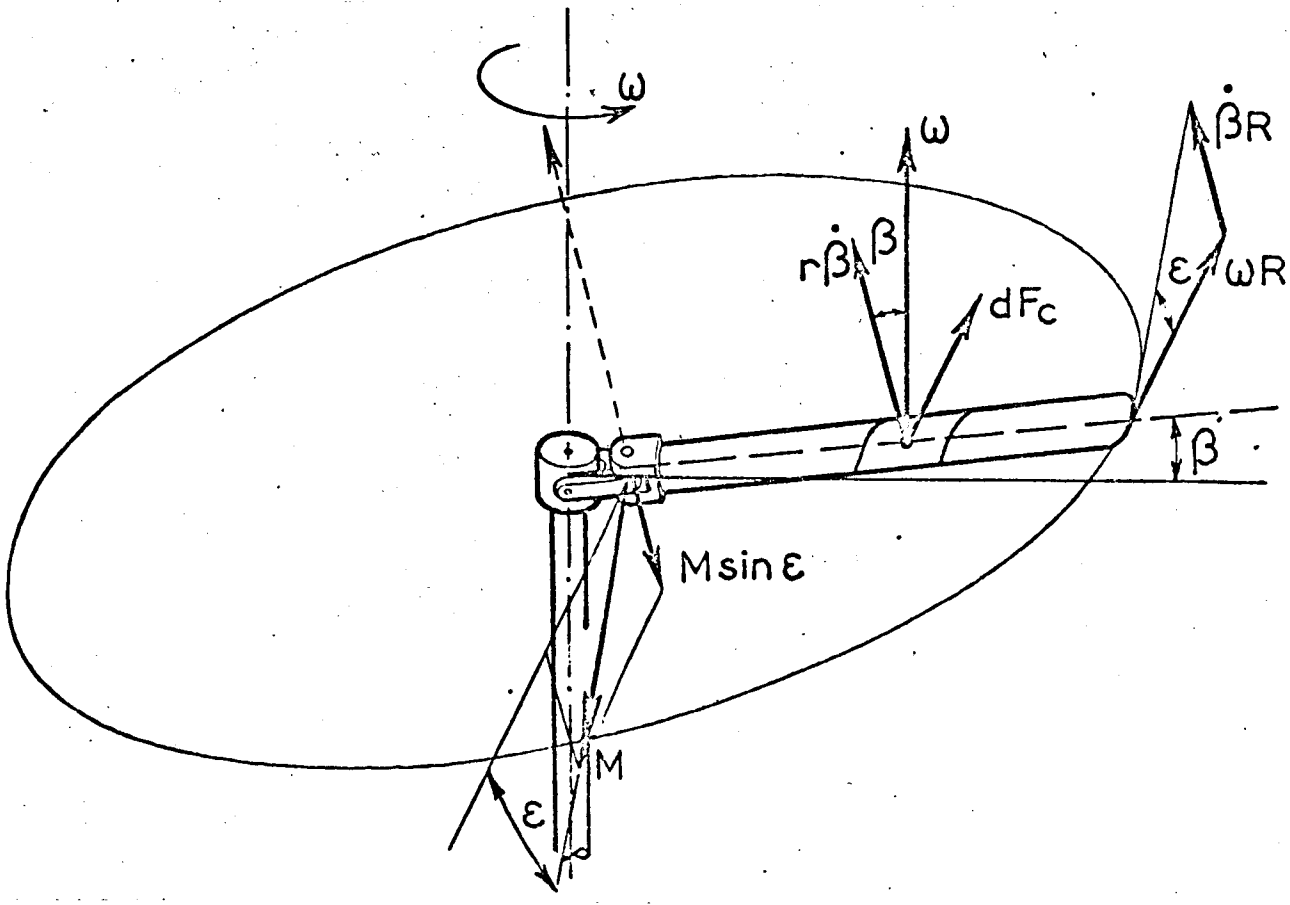

Figure 3-20. Formulation of the Equation for Lag Motion.

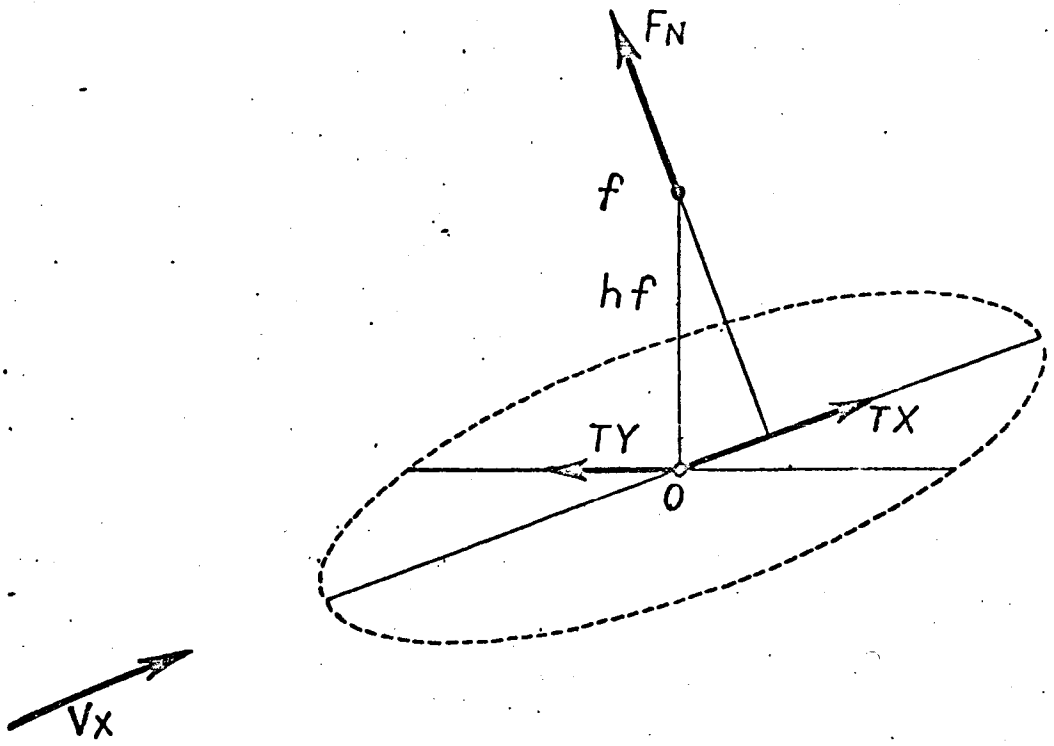

Figure 3-21. The Forces Applied to the Hub by the Blades.

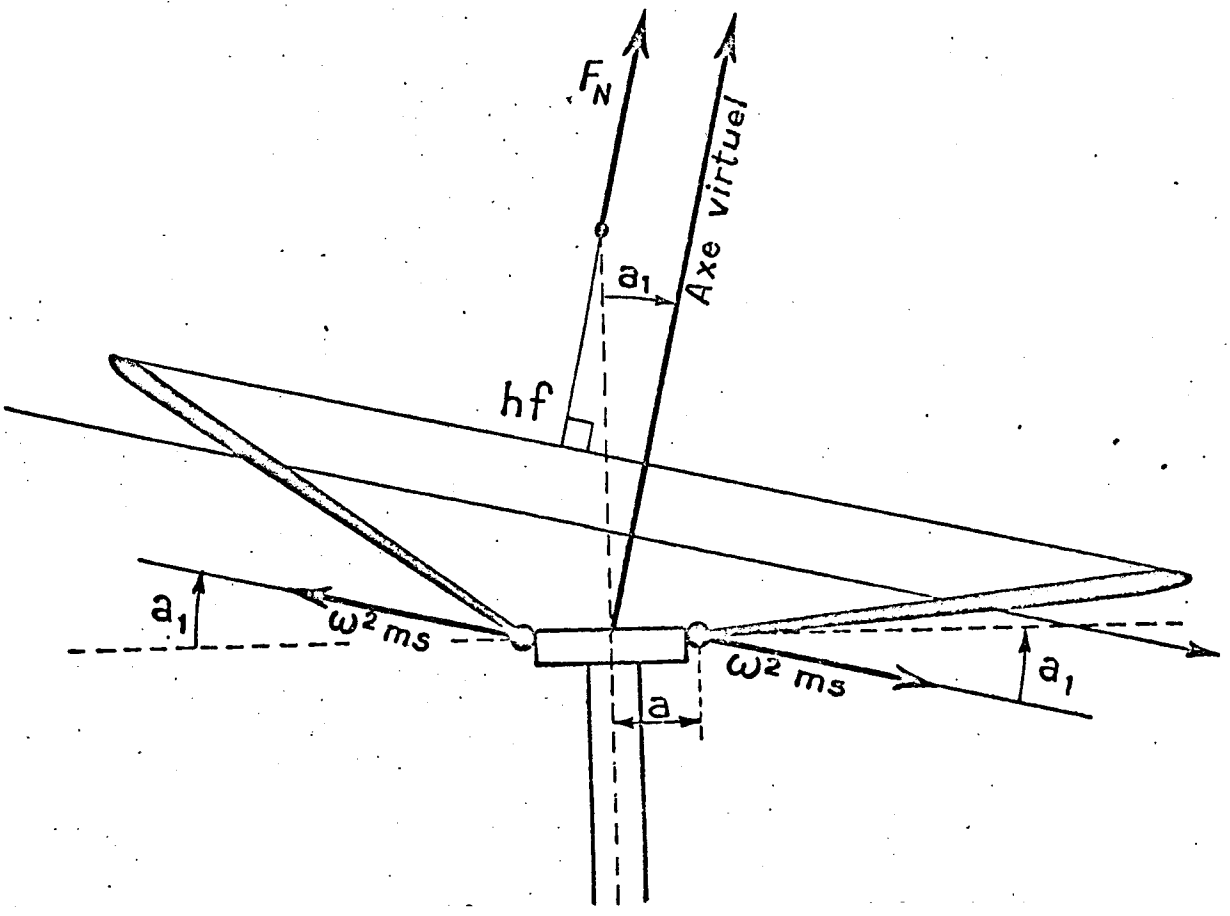

Figure 3-22. Rotor Thrust Center.

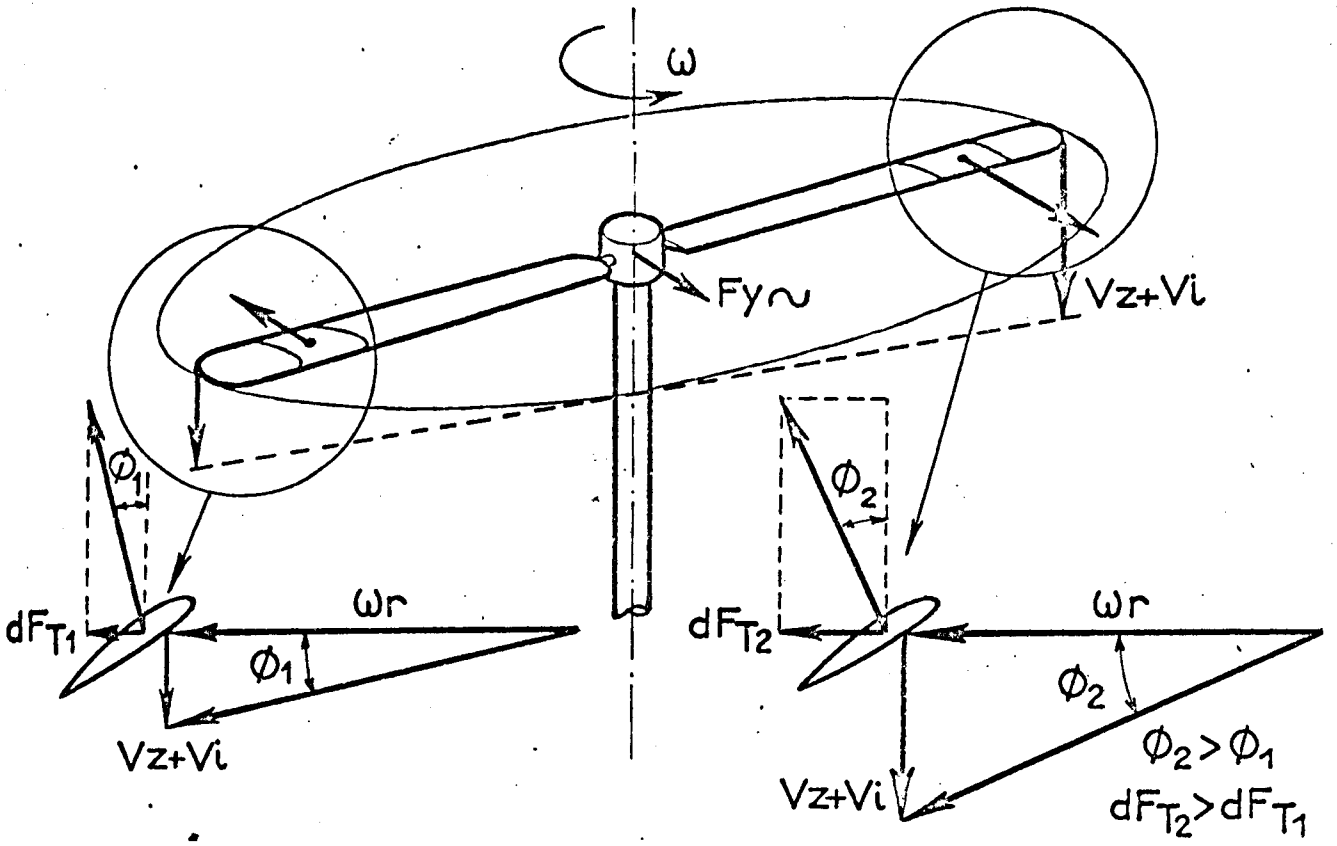

Figure 3-23. Alternating Forces Due to Unequal Distribution of Induced Velocities Over the disk.

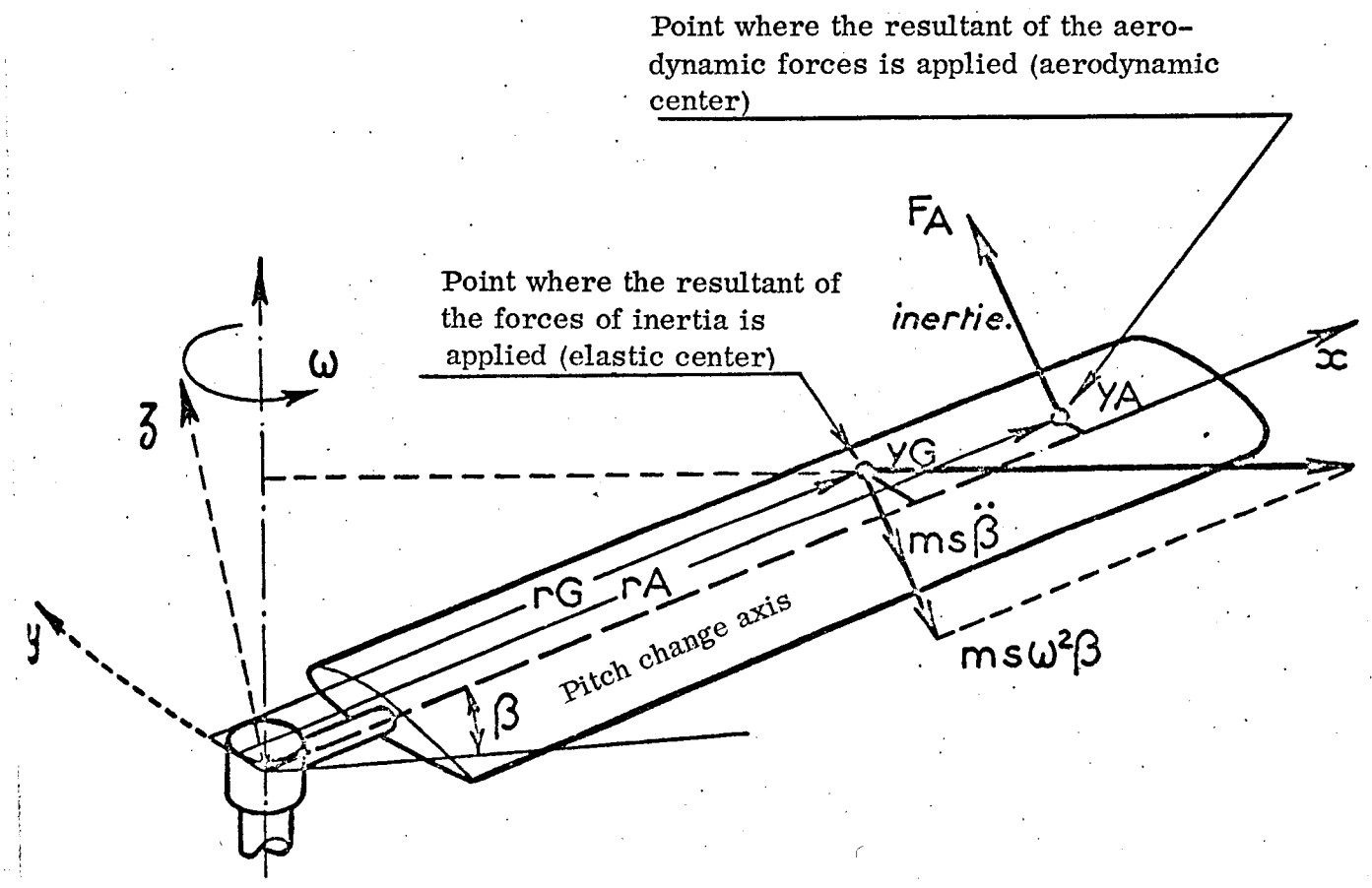

Figure 3-24. Moments About the Feathering Axis.

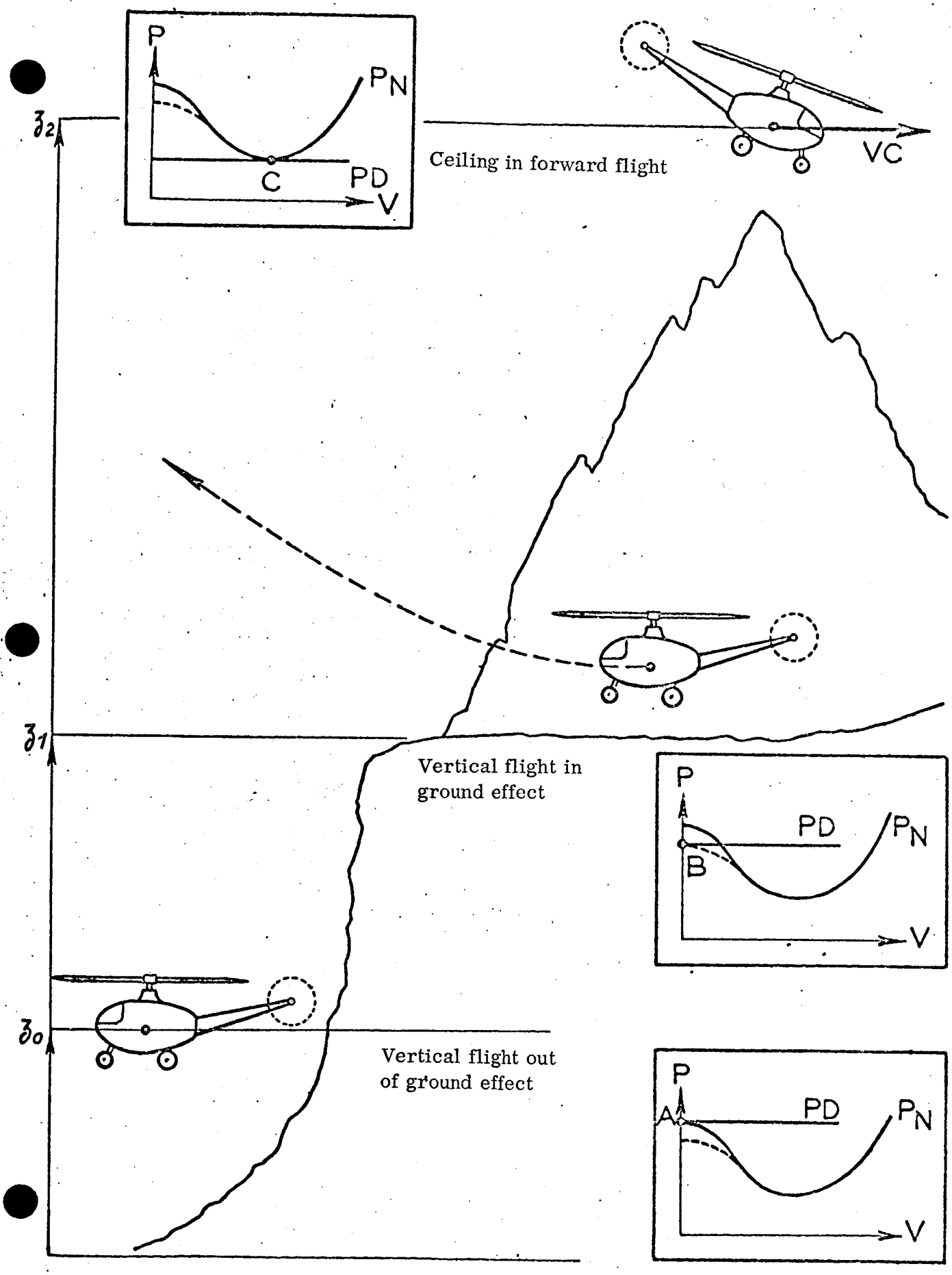

Figure 4-1. The Three Flight Ceilings of a Helicopter.

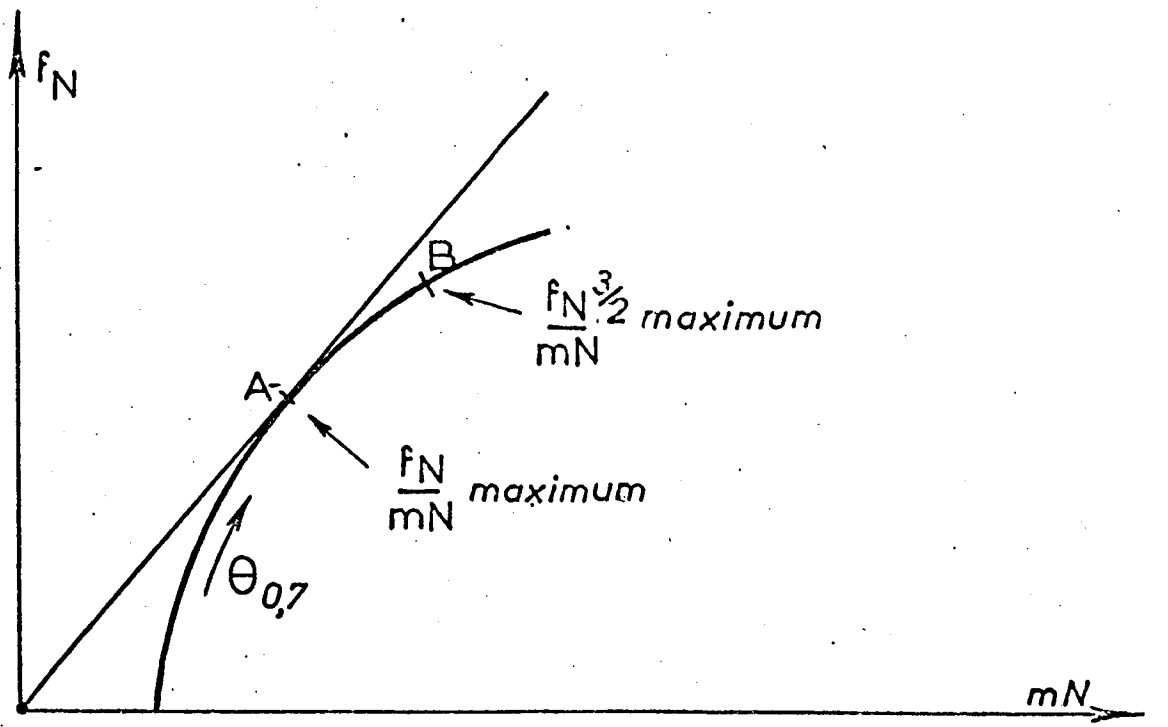

Figure 4-2.

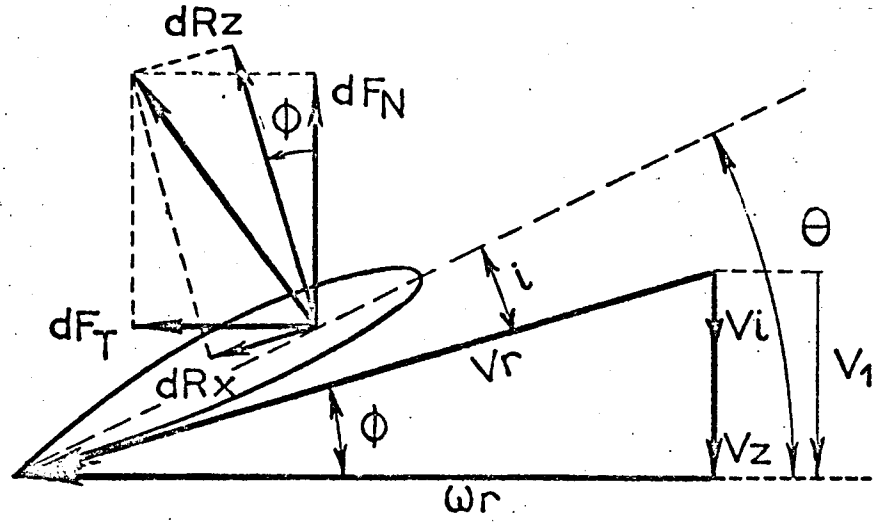

$$\phi = Arc\,tg\frac{V_1}{\omega r}$$

$$Vr = \frac{\omega r}{\cos\phi}$$

$$dRz = \frac{\rho}{2} ds \frac{\omega^2 r^2}{\cos^2\phi} Cz$$

$$dRx = \frac{\rho}{2} ds \frac{\omega^2 r^2}{\cos^2\phi} Cxp$$

$$dF_N = dRz\ \cos\phi - dRx\ \sin\phi$$

$$dF_T = dRz\ \sin\phi + dRx\ \cos\phi$$

Figure 4-3.

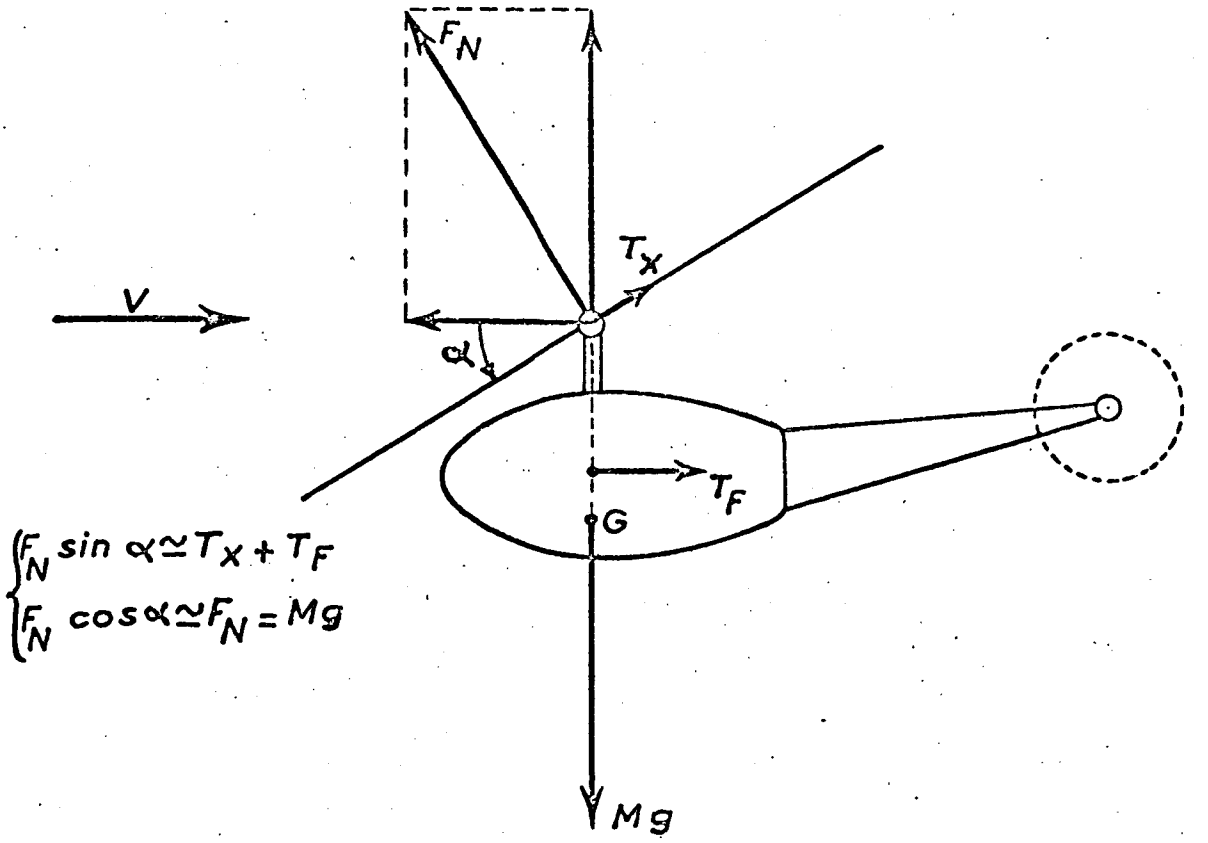

Figure 4-4. Balance of Longitudinal Forces in Level Flight.

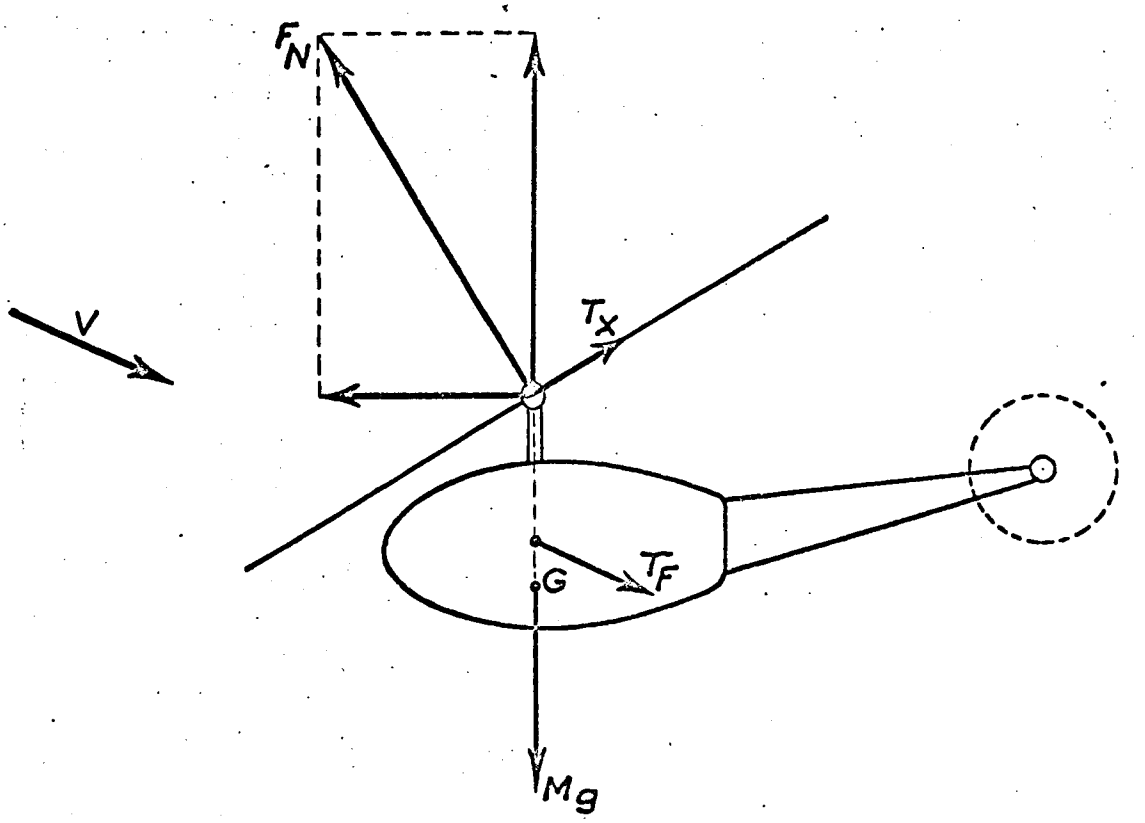

Figure 4-5. Balance of Longitudinal Forces During Climb at an Oblique.

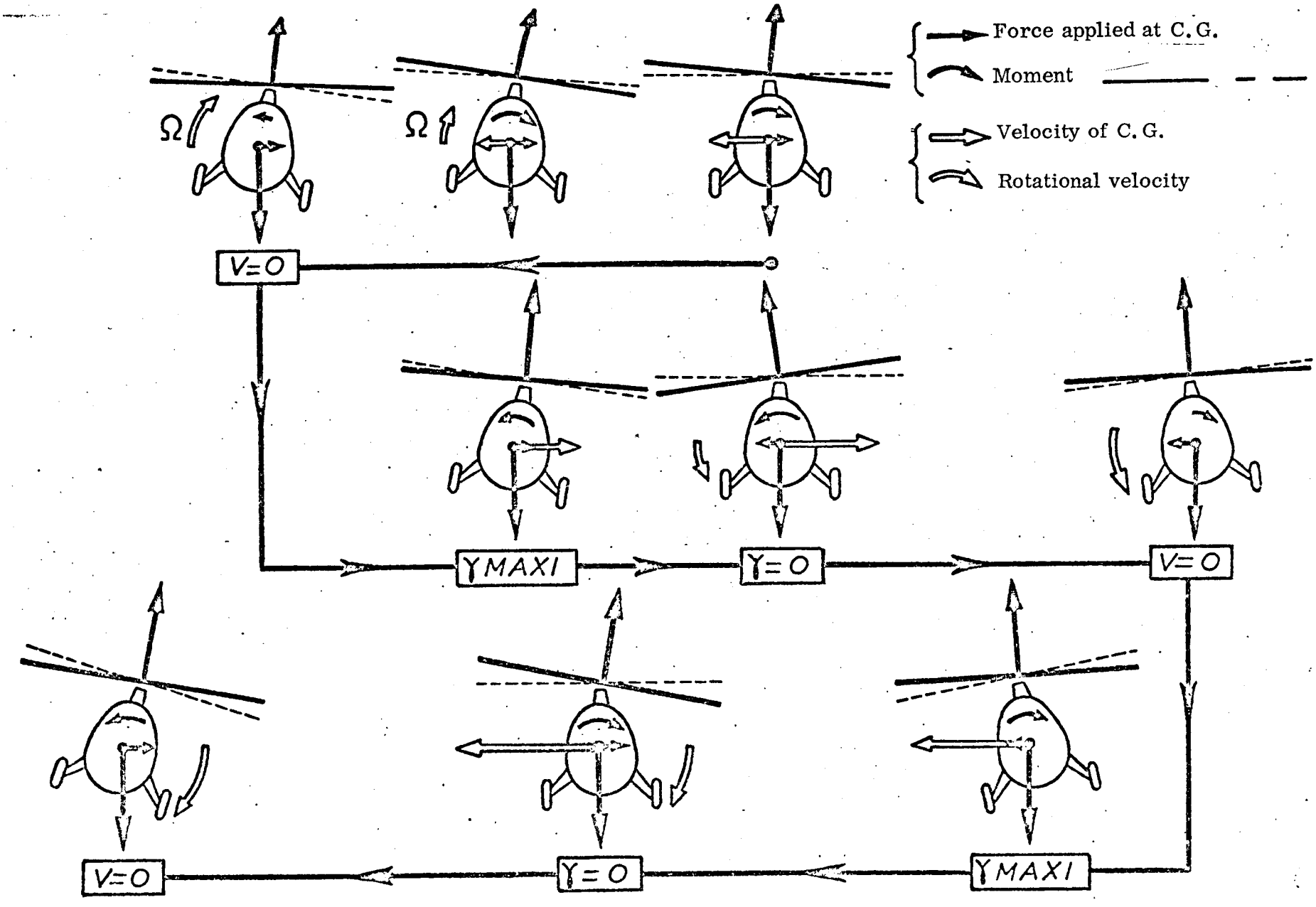

Figure 5-1. Characteristic Unstable Motion of the Helicopter in Hovering Flight.

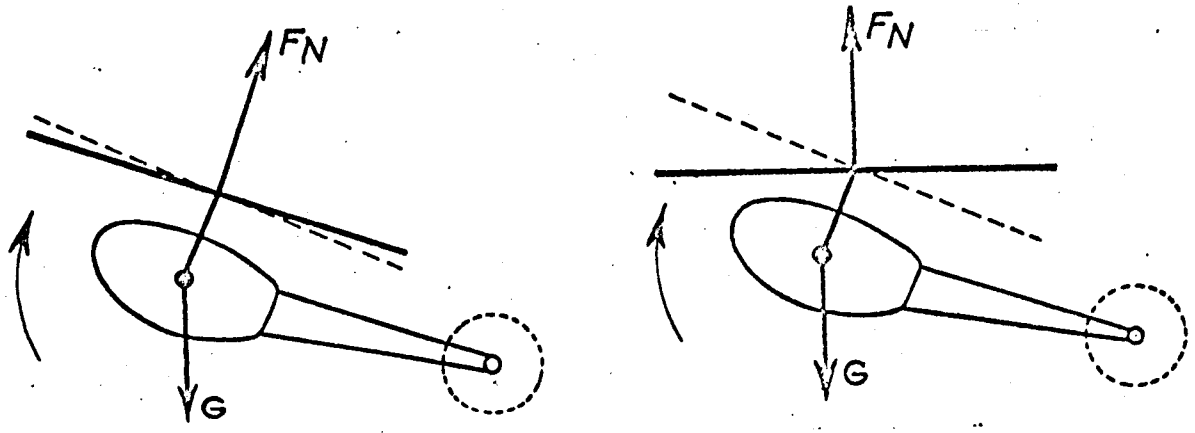

A - Blades "light" (Jo small) the rotor follows the fuselag

B - Blades "heavy" (Jo large). The rotor tends to remain fixed in space

Figure 5-2. Role of Rotor Response Time.

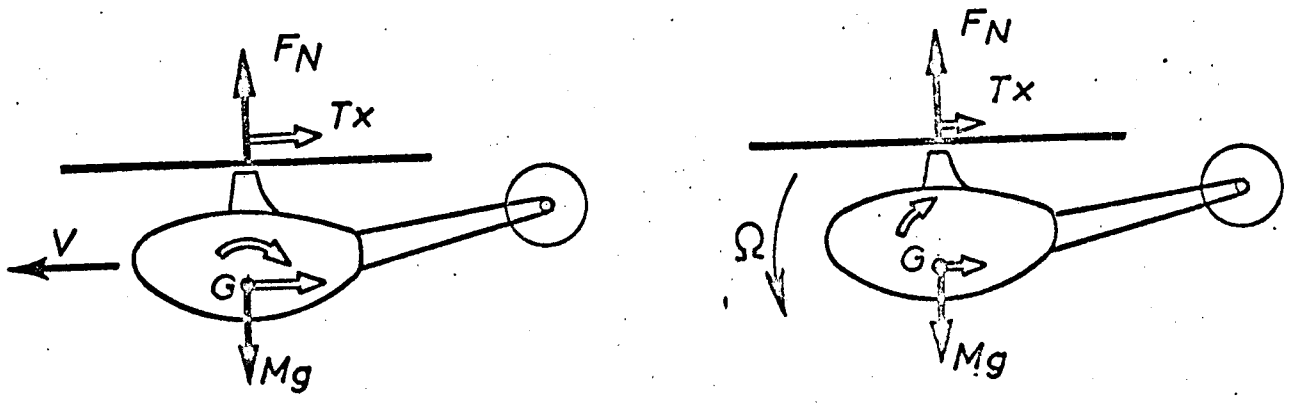

Horizontal displacement

Angular displacement

a) Fixed-blade rotor

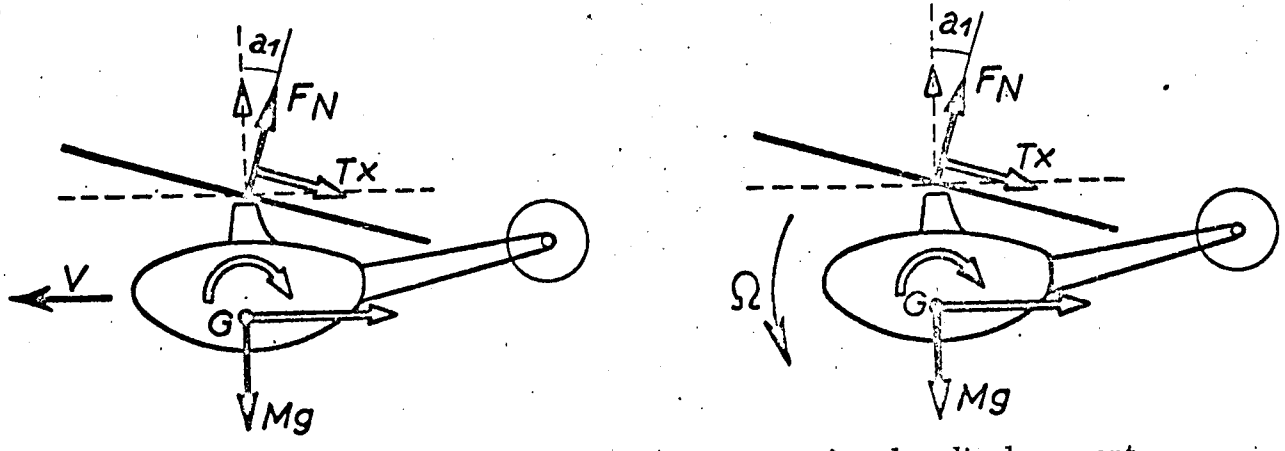

Horizontal displacement

Angular displacement

b) Hinged-blade rotor

Figure 5-3. Rotor Reactions to Fuselage Motions.

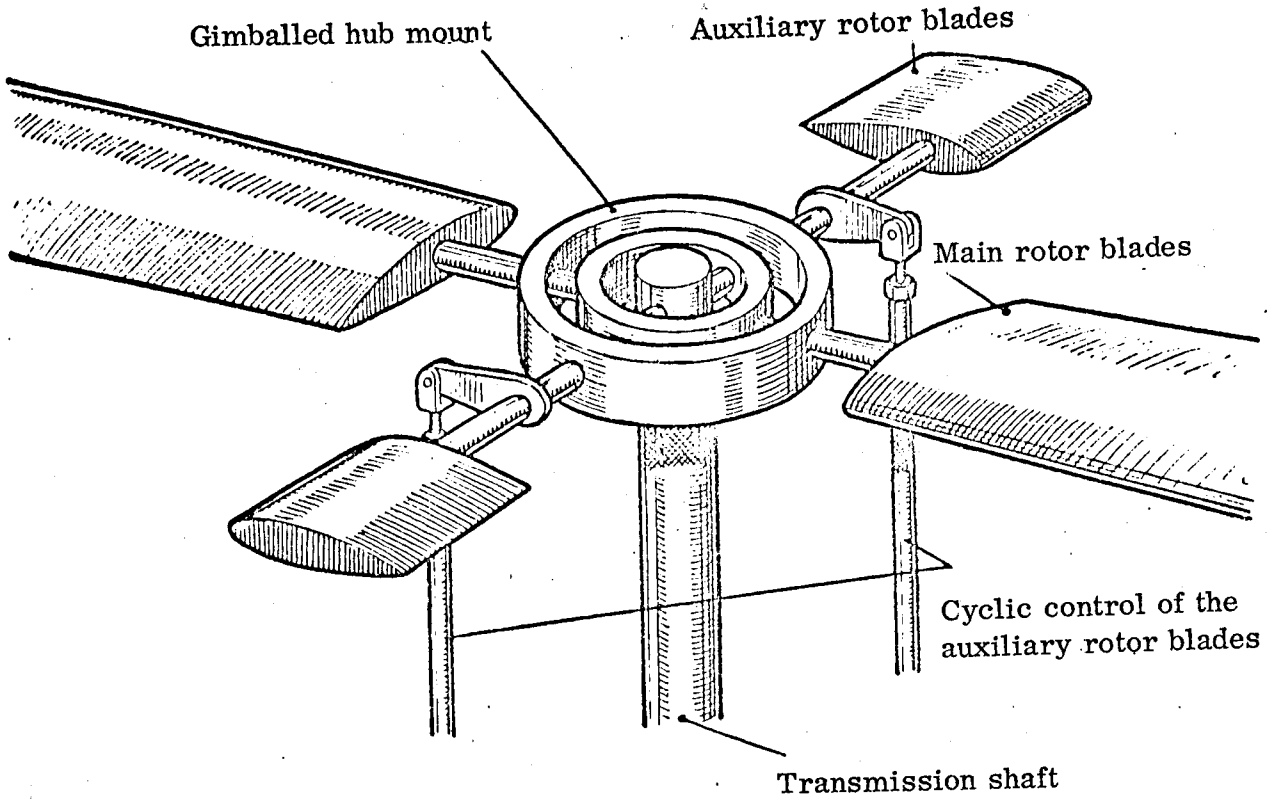

Figure 5-4. Hiller Rotor Matic (simplified diagram).

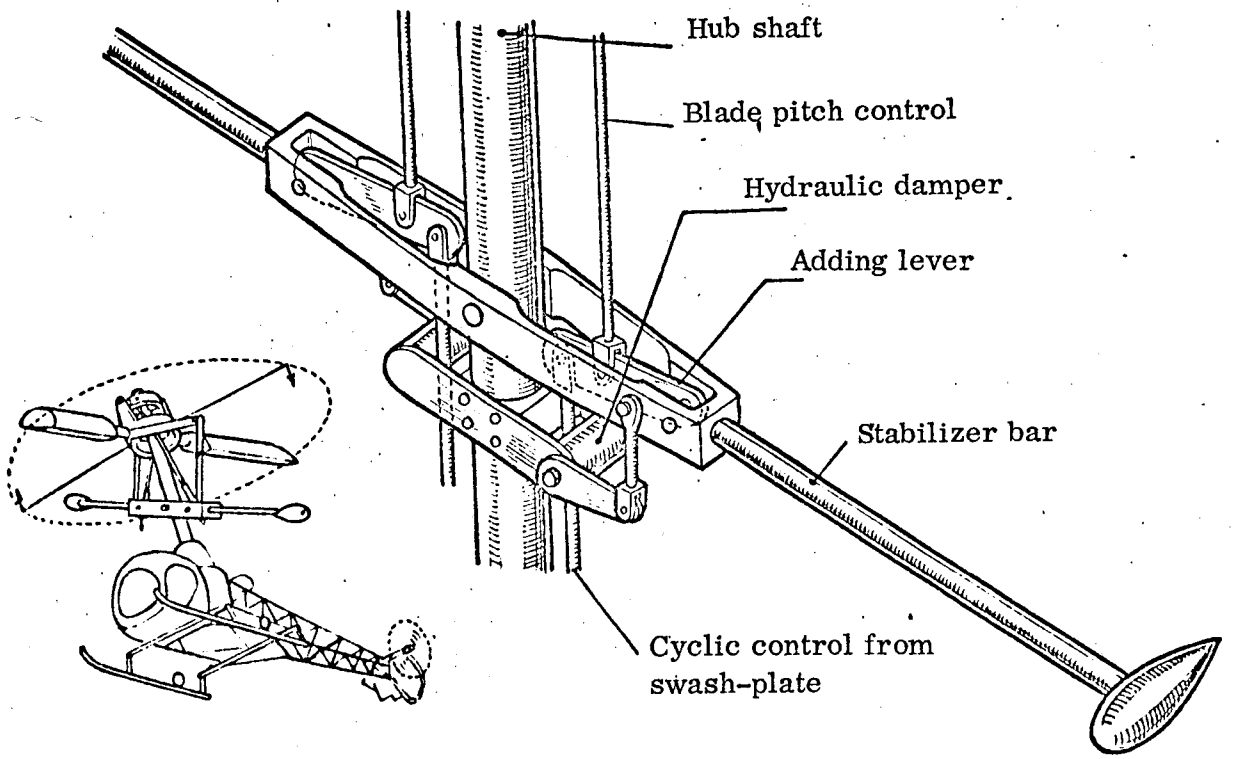

Figure 5-5. Bell Stabilizer Bar.

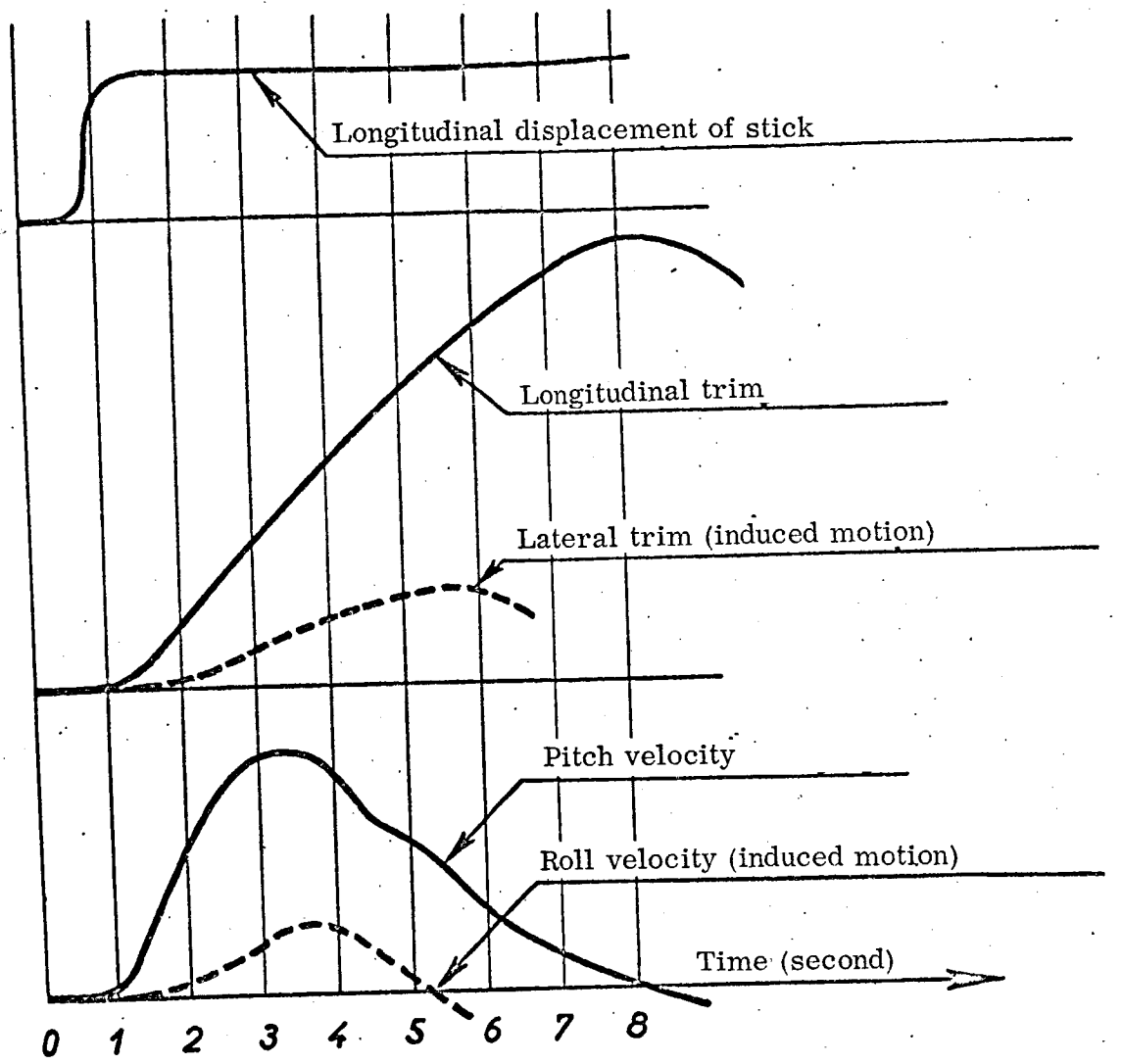

Figure 5-6. Typical Response of a Hovering Helicopter to a Echelon Stick Movement.

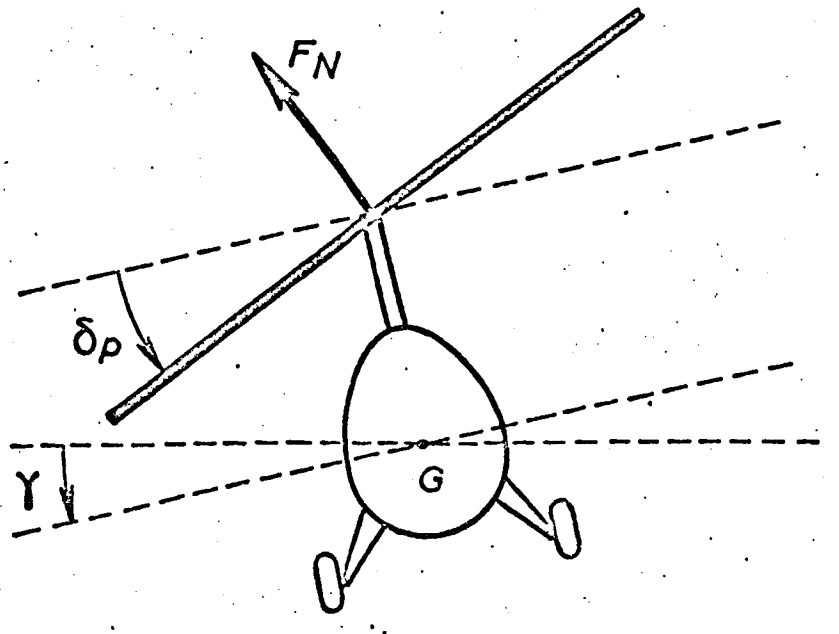

Figure 5-7.

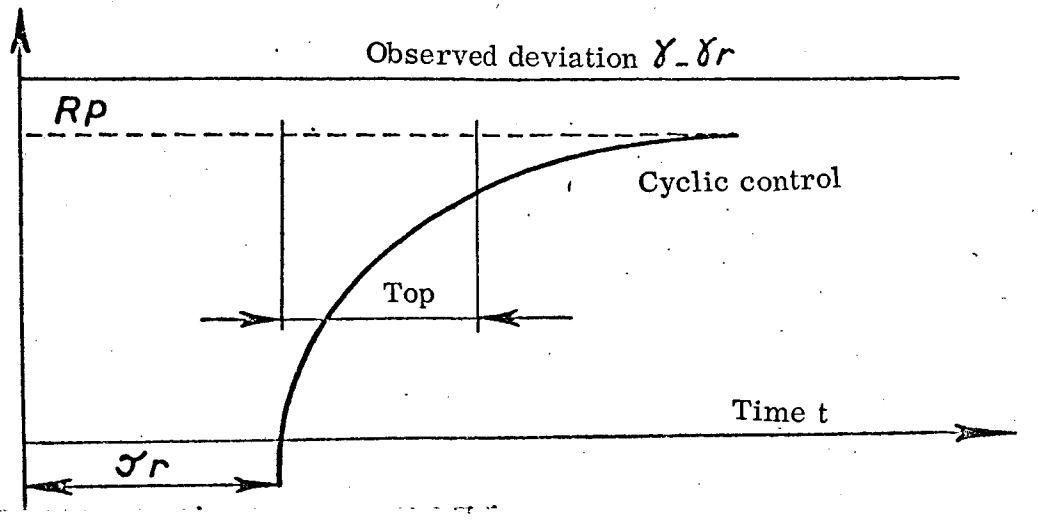

Figure 5-8. Pilot's Response.

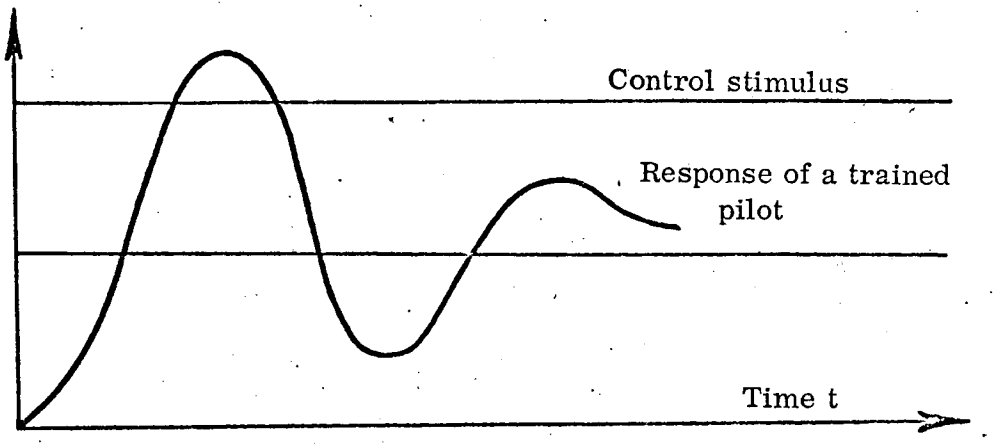

Figure 5-9.

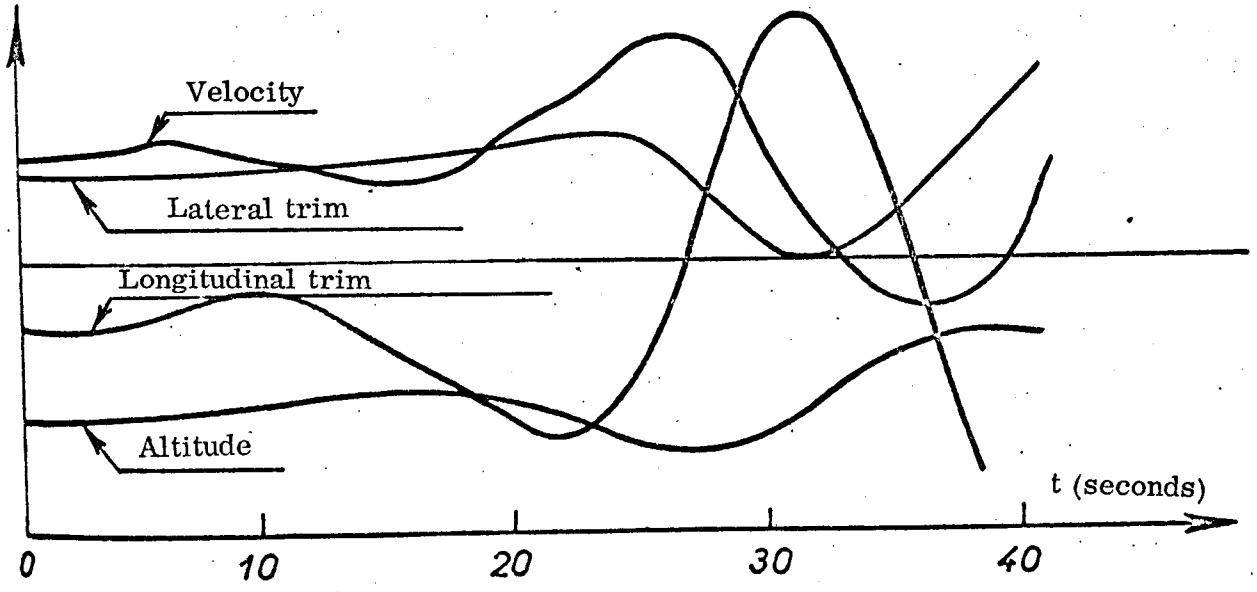

Figure 5-10. Characteristic Motion in Level Flight (V = 100 km/hr).

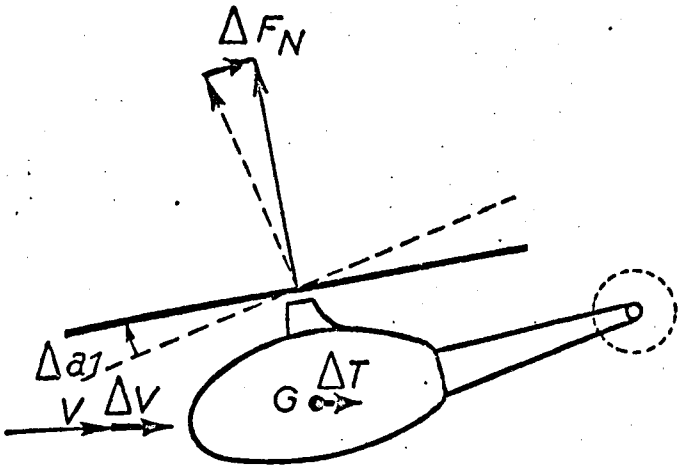

5-11, a. Velocity Stability

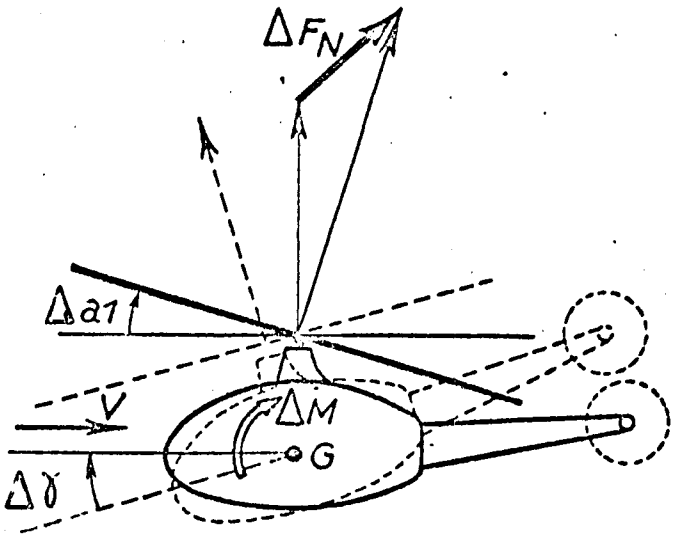

5-11, b. Trim Stability.

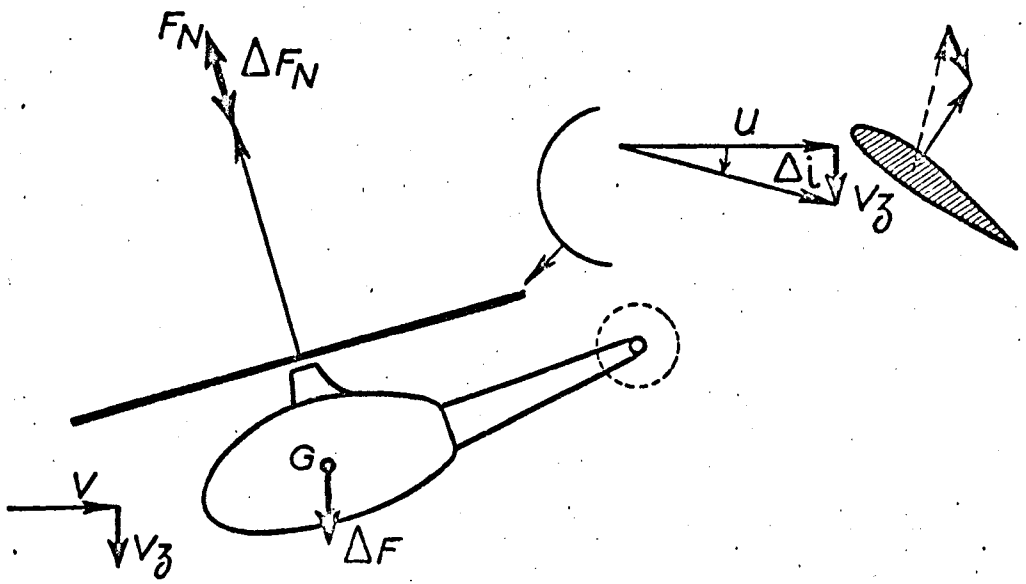

5-11, b. Altitude Stability.

Figure 5-11. Stability in Forward Flight.

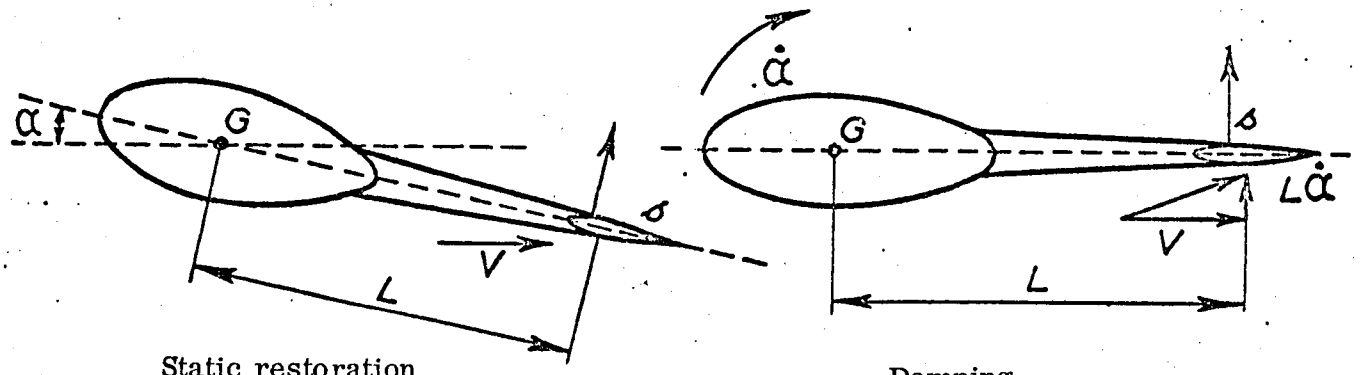

Figure 5-12. Stabilizing Effect of Control Surfaces.

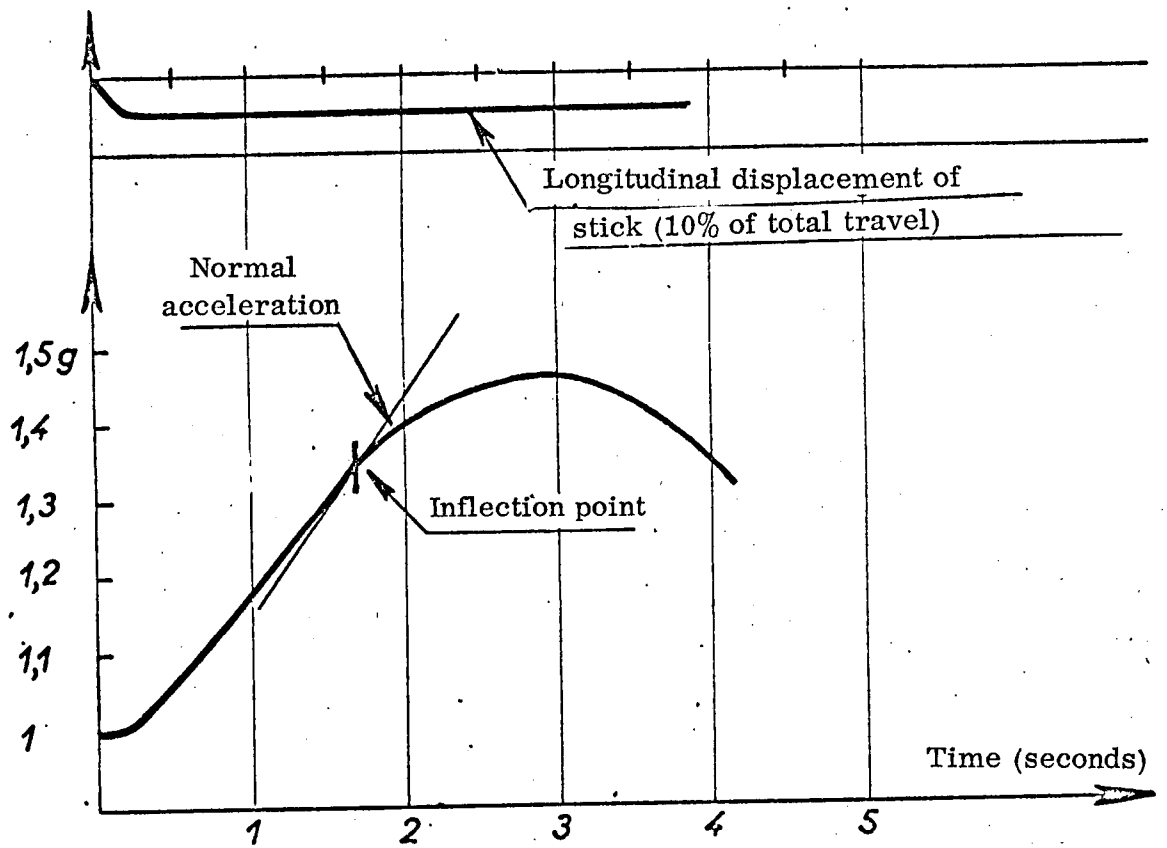

Figure 5-13. Response of a Helicopter in Cruising Flight to an Echelon Stick Movement.

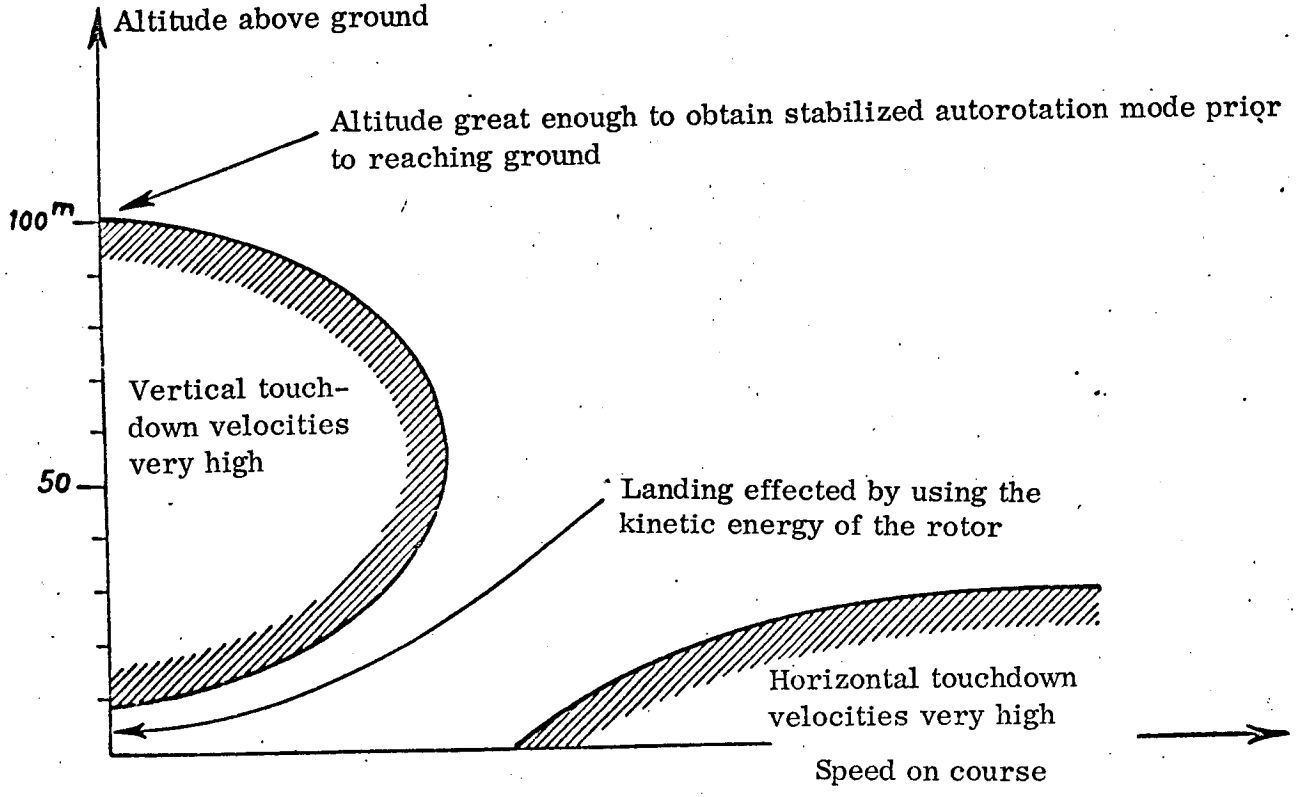

Crosshatched areas are forbidden zones

Figure 5-14. "Dead-Man's Zone".

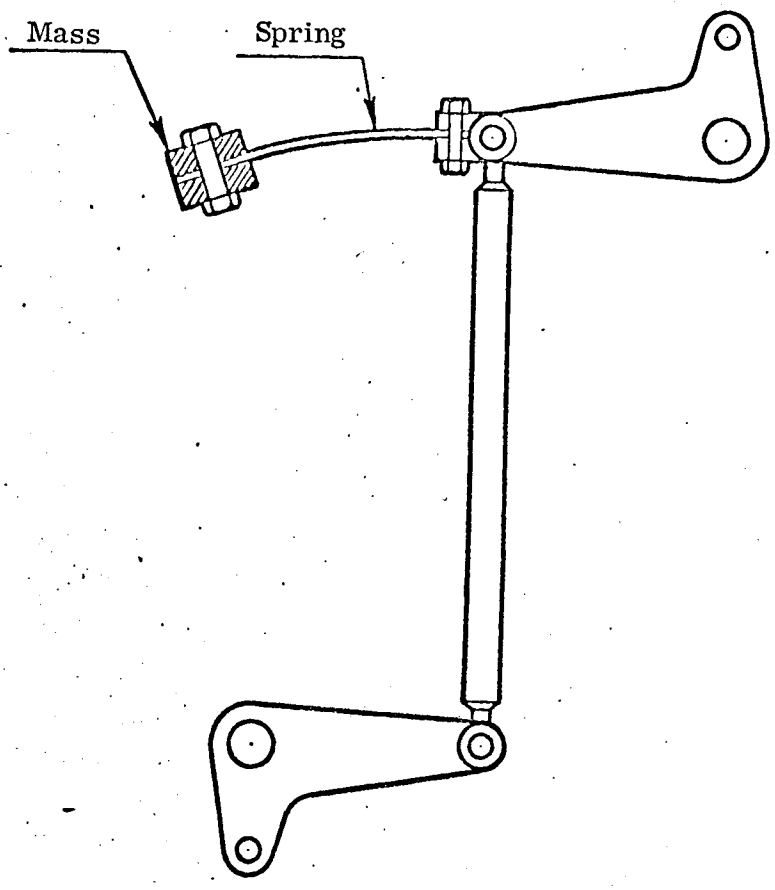

a) Example of mounting

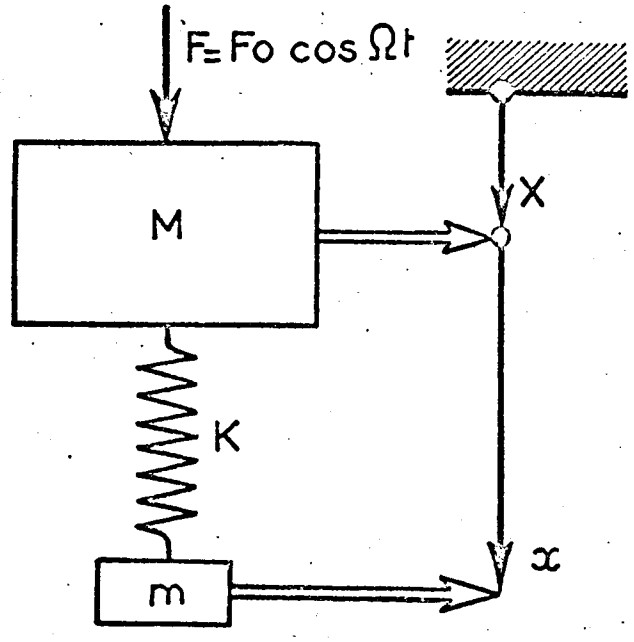

b) Simplified diagram

Figure 6-1. Pendulum Damper.

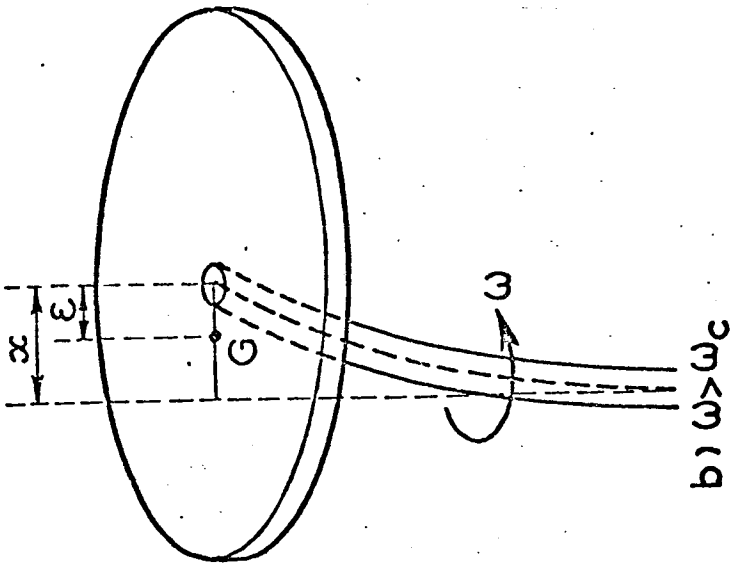

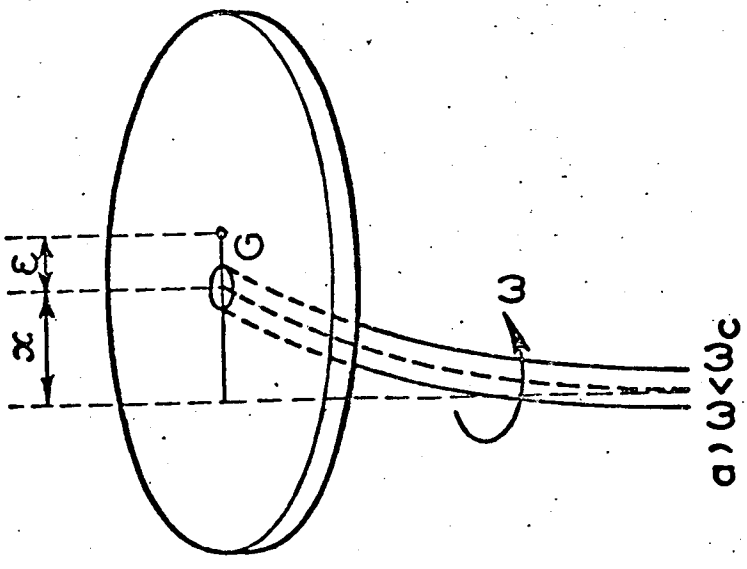

Figure 6-2.

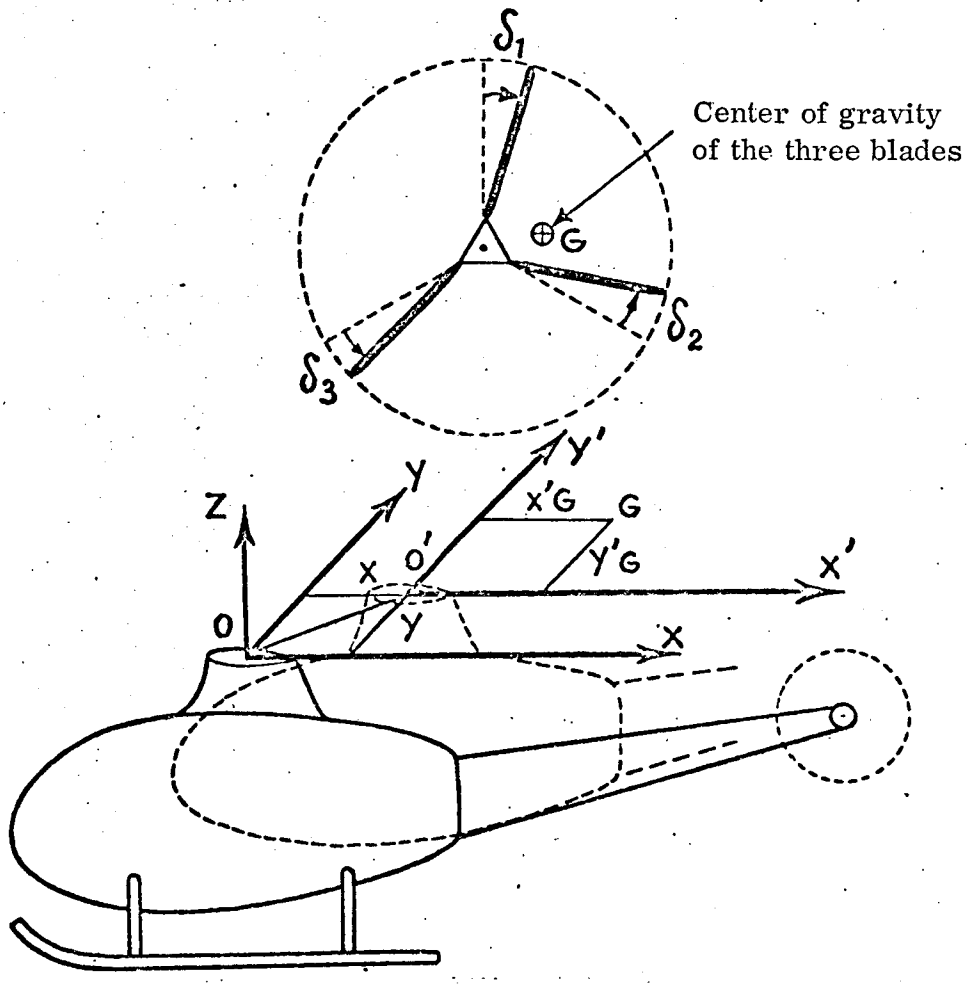
δ_1
Center of gravity
of the three blades
G
δ_2
δ_3
Y'
Y
Z
X'G
G
Y'G
X
O'
X'
O
Y
X

Figure 6-3.

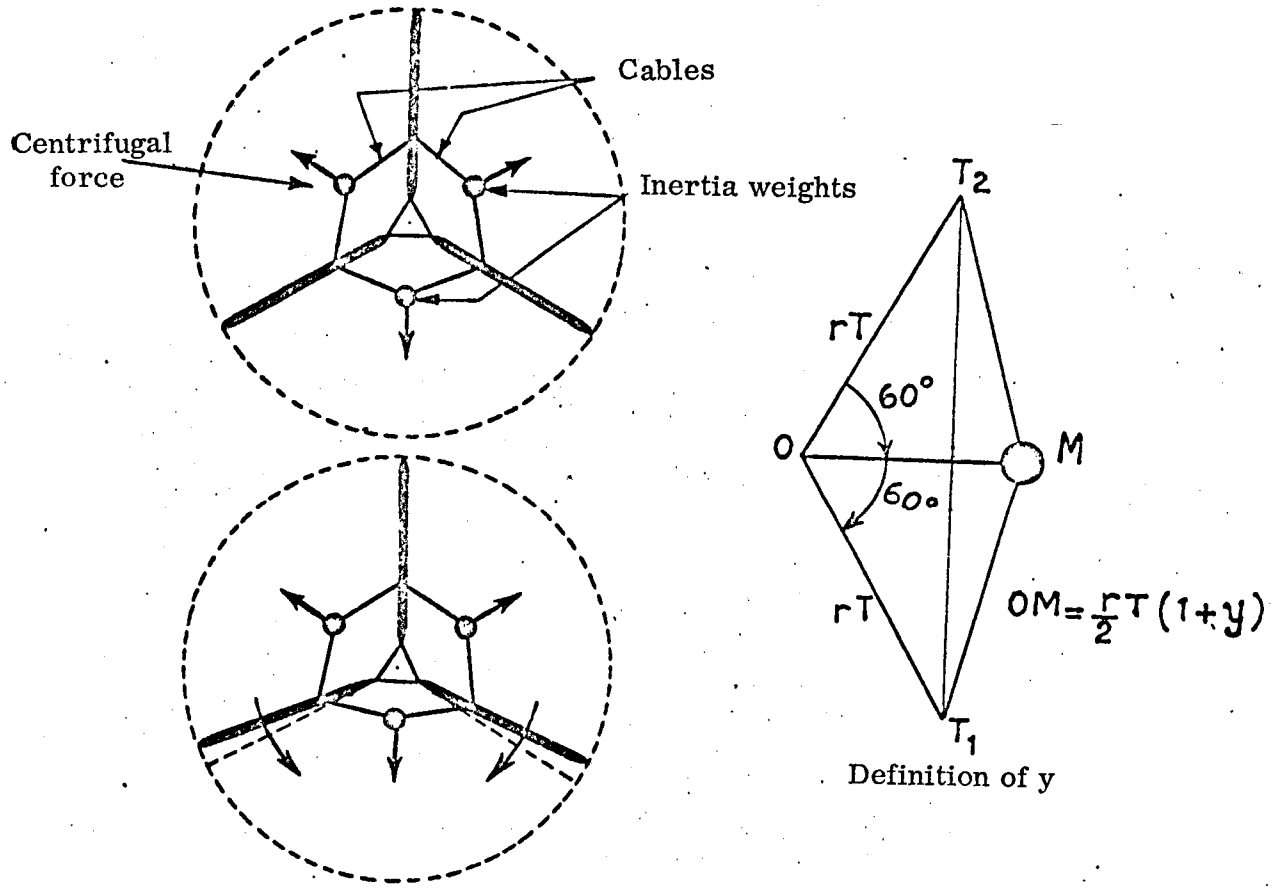

Figure 6-4. Distributor Cables.

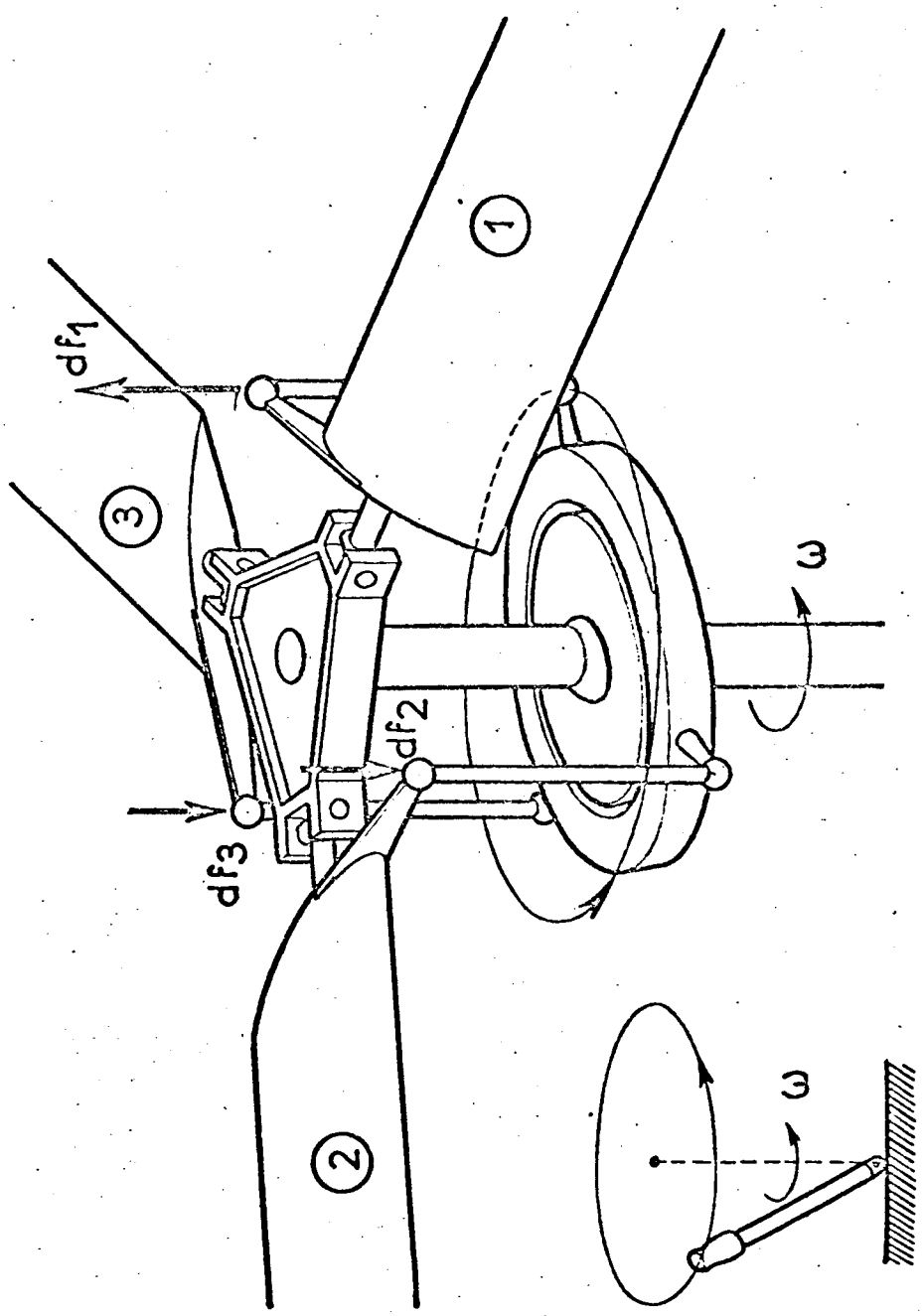

Figure 6-5. Cyclic-Control Instability.

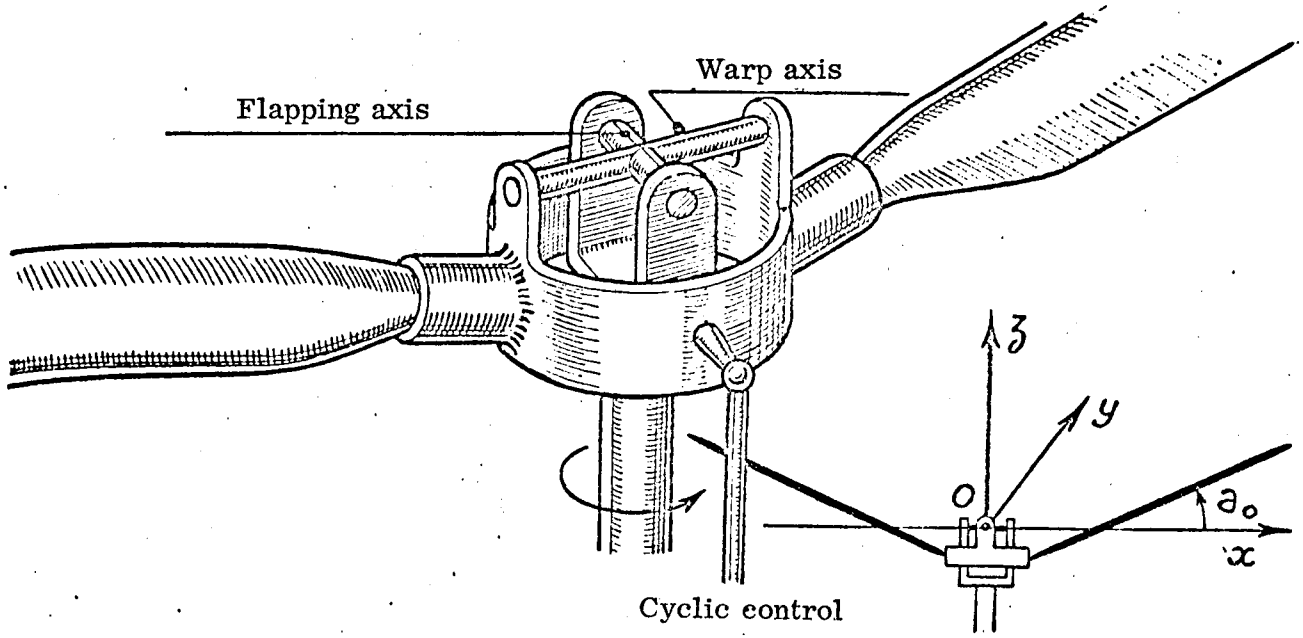

Figure 6-6. Weaving.

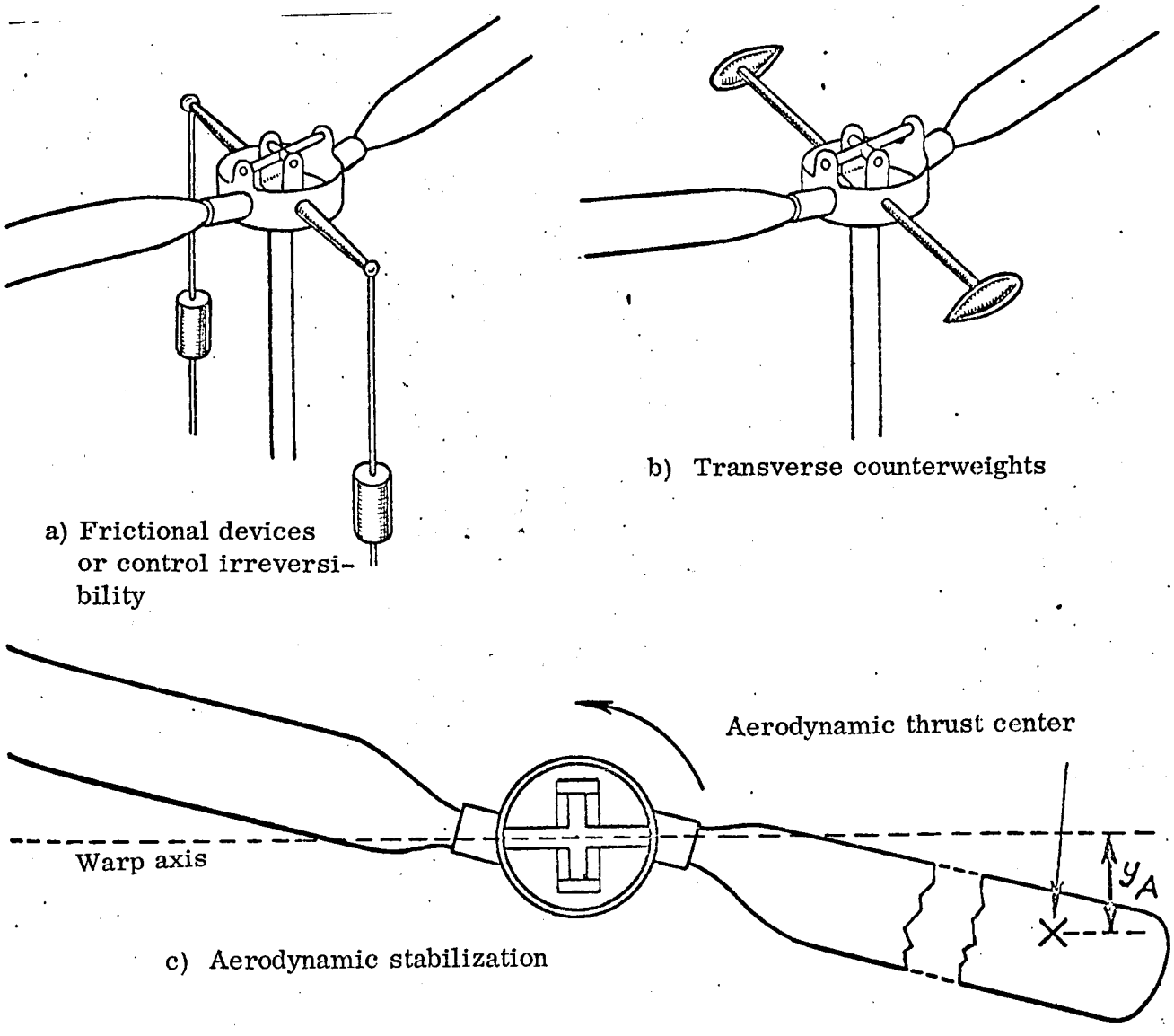

Figure 6-7. Methods for Suppressing Weaving.

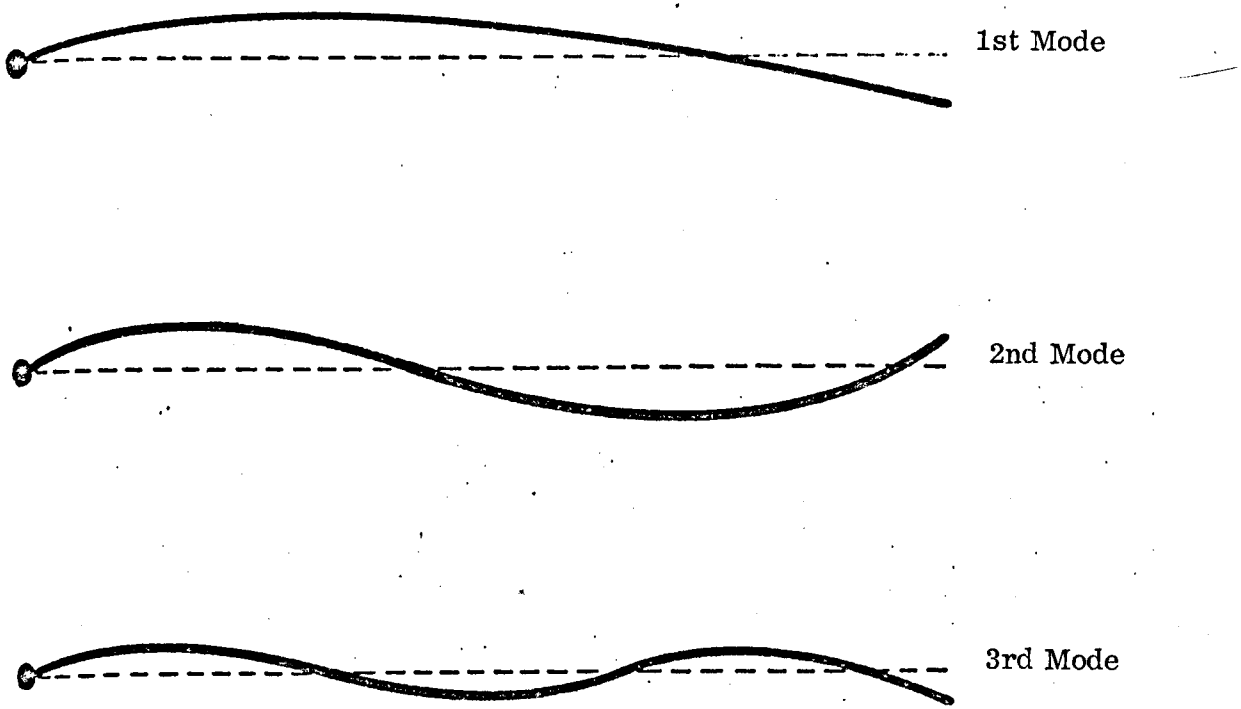

Figure 7-1. Natural Deformations of the Blade in Vertical Flexure.

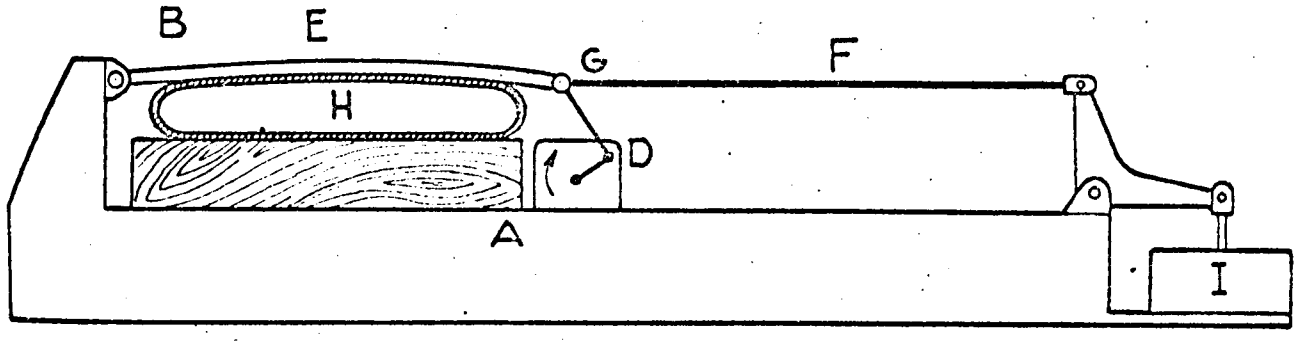

Figure 7-2. Blade Test Bench.

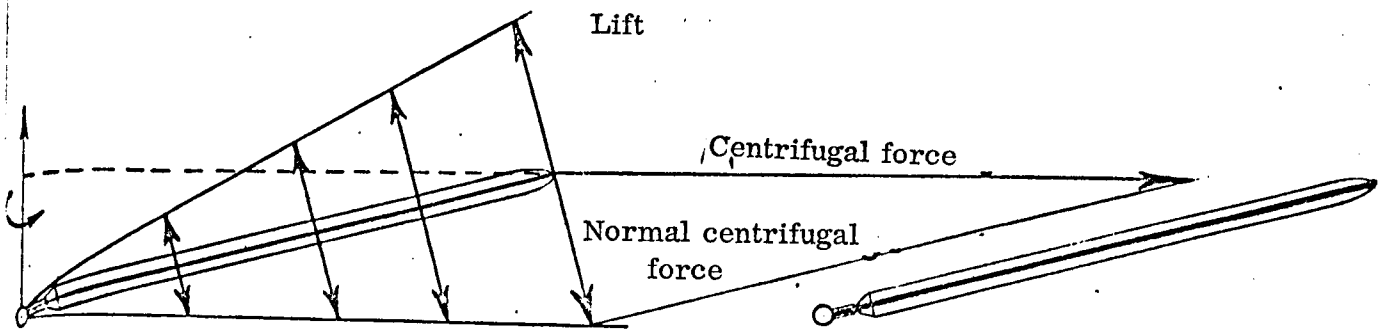

a) Homogeneous blade - Induced velocities uniform

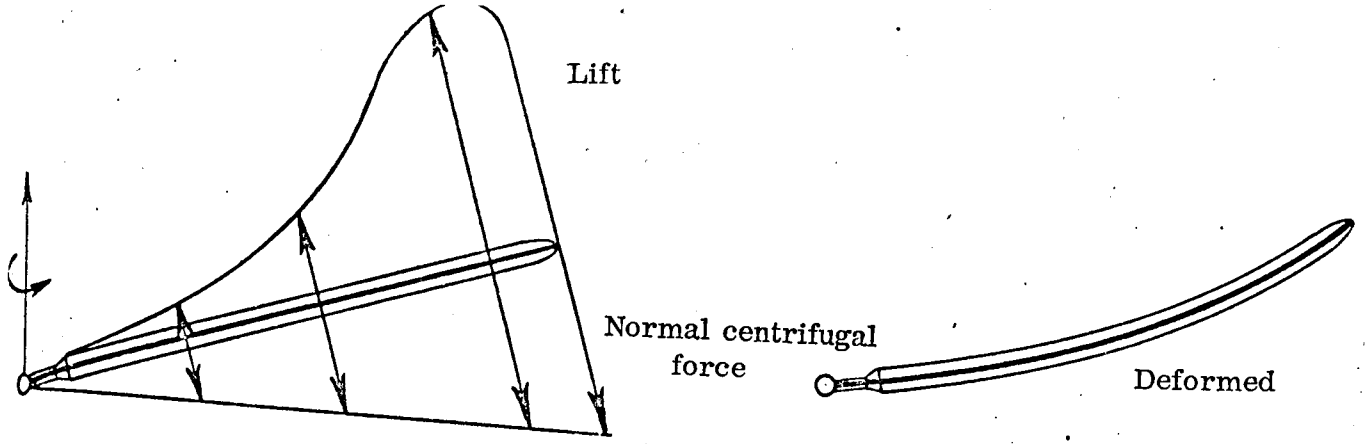

b) Homogeneous blade - Usual distribution of induced velocity

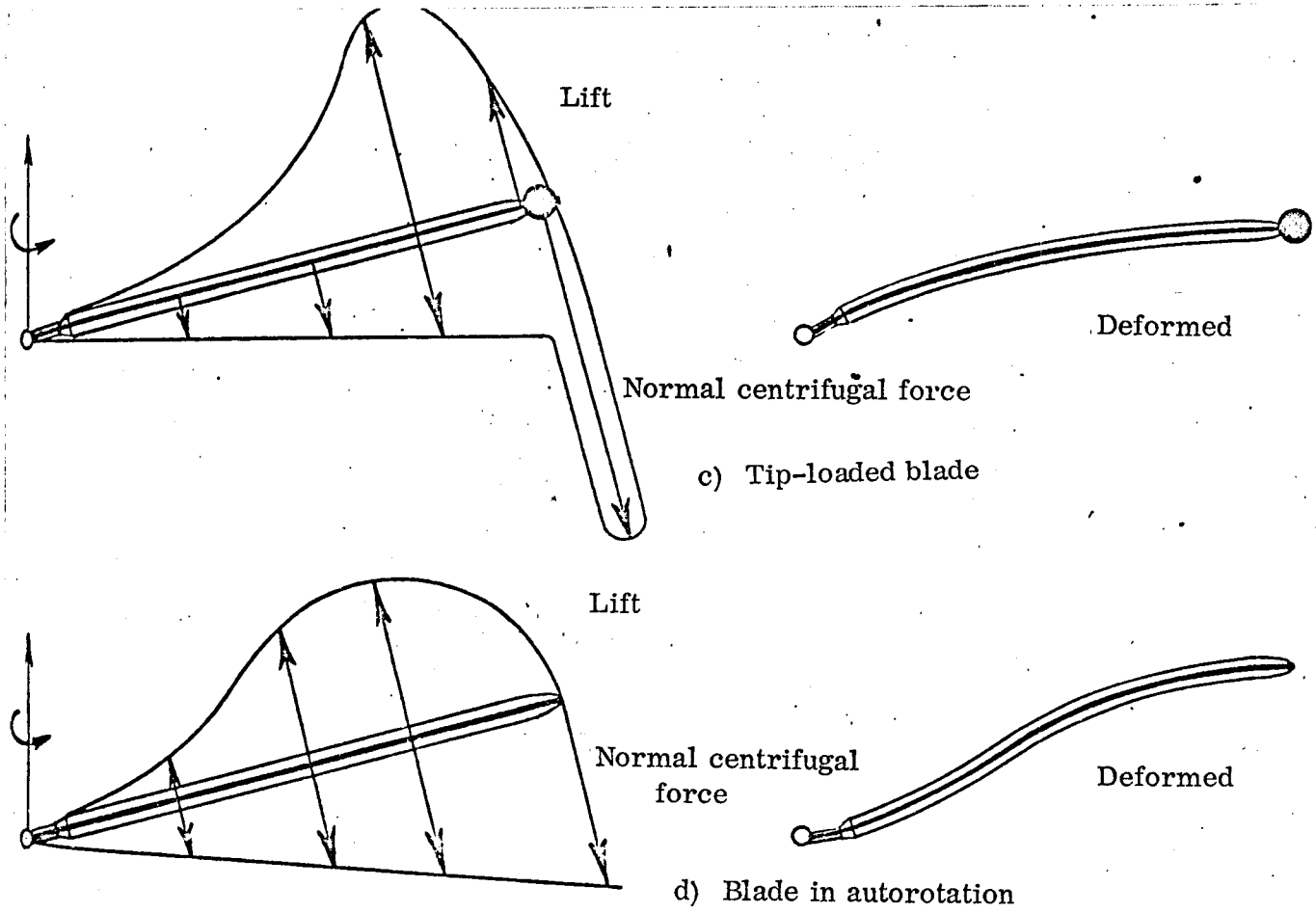

Figure 7-3. Permanent Vertical Flexure of a Blade.

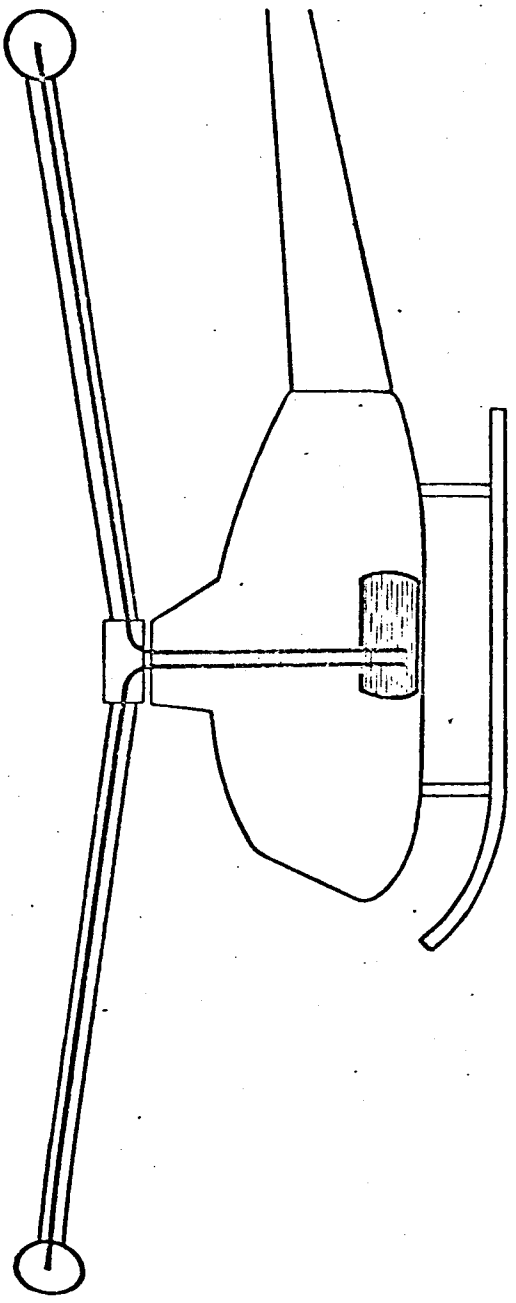

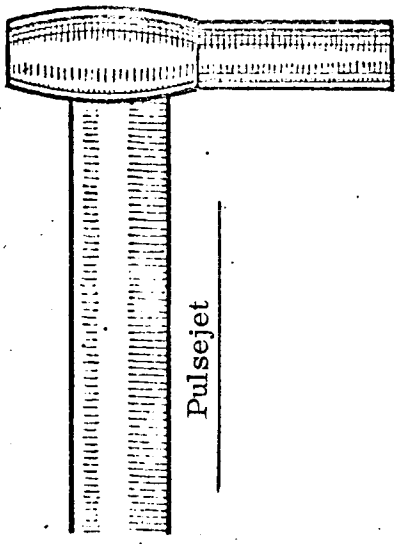

Pulsejet

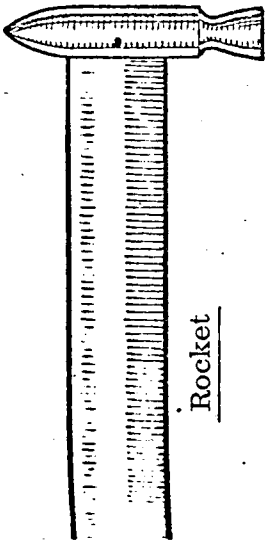

Rocket

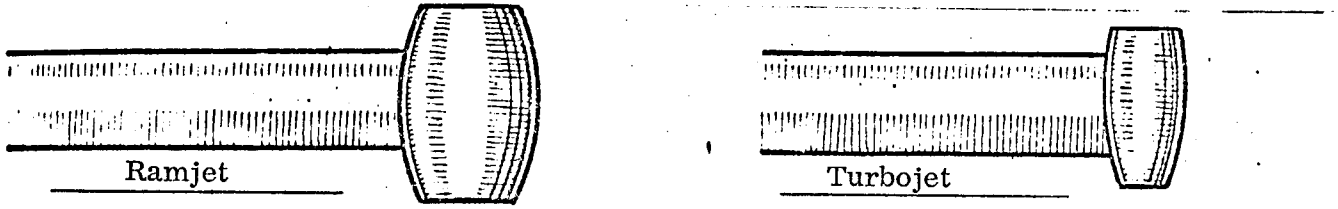

A – systems with blade-tip power generators

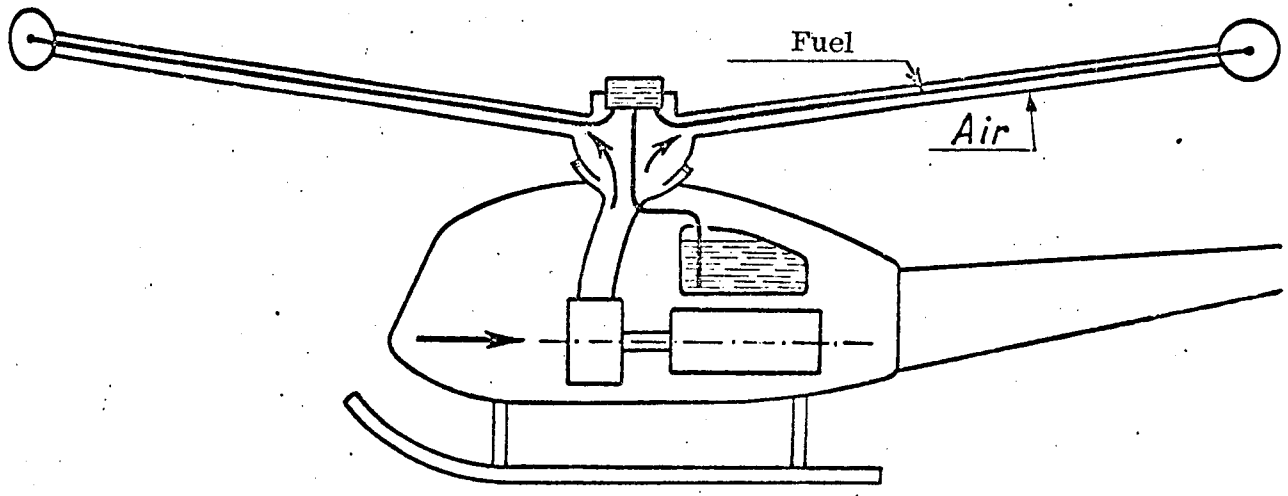

B – mixed system (high pressure)

Figure 8-1. Different Jet Propulsion Systems.

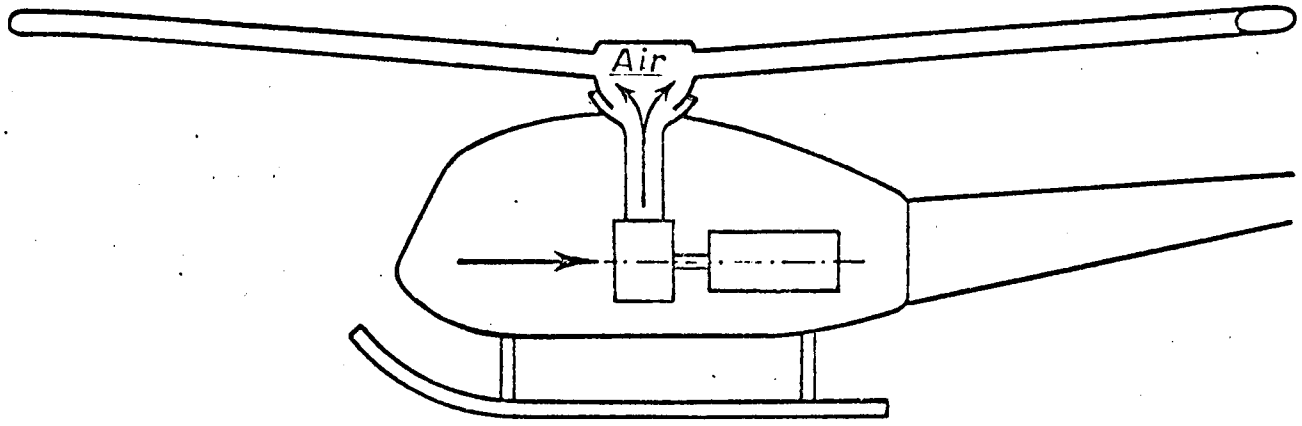

Pure air (high pressure)

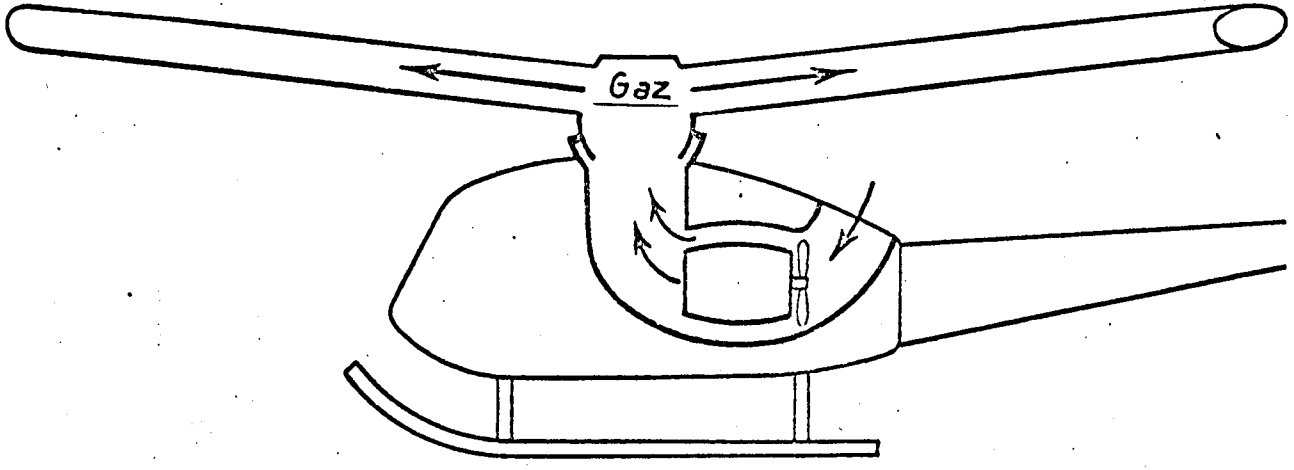

Hot gas (low pressure)

C - Generating systems unstalled in the fuselage

Figure 8-1. (Cont'd). Different Systems of Jet Propulsion.

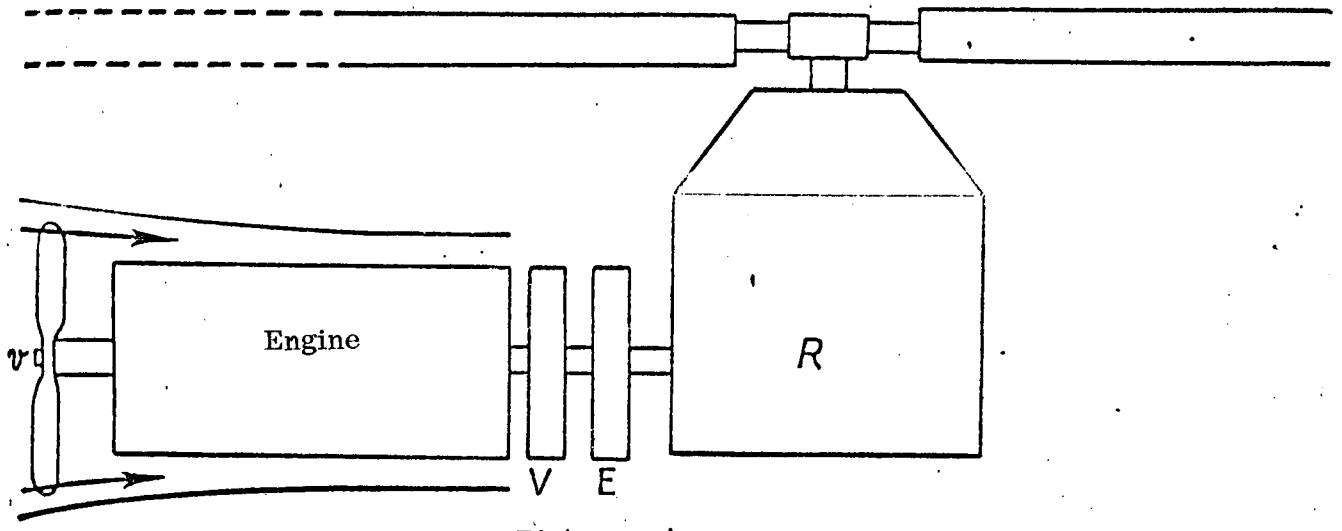

a) Piston engine

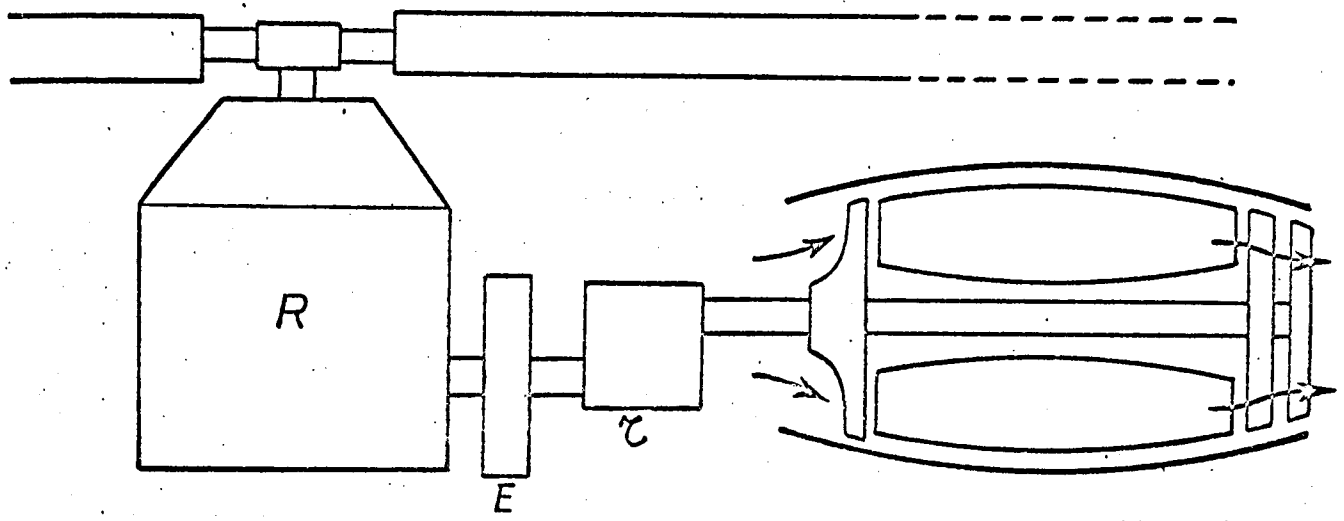

b) Fixed-turbine engine

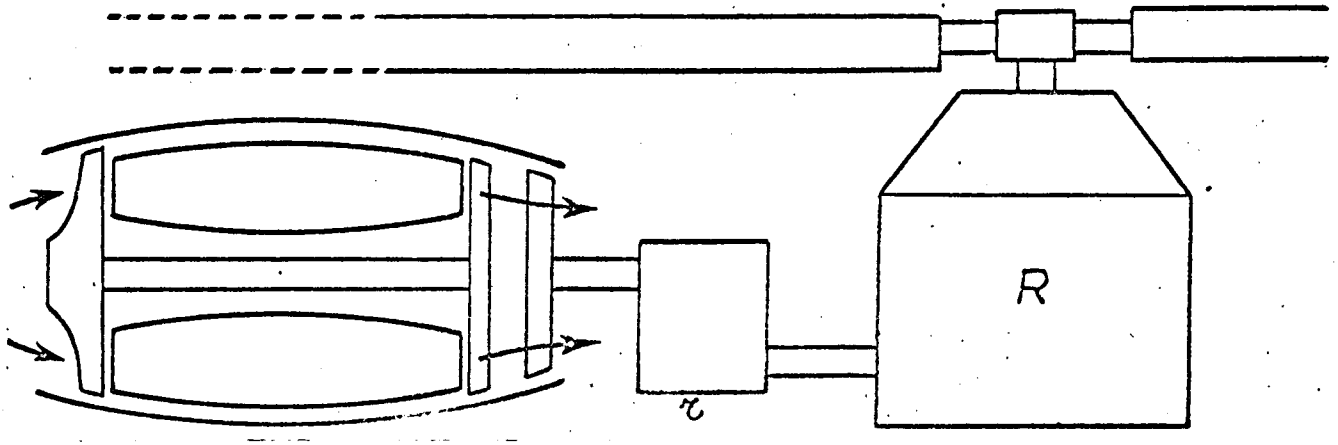

c) Free-turbine engine

E: Clutch V: Flywheel $\mathcal{V}$: Fan R: Main reduction gear
r: Turbine reduction gear.
Note: In all cases there is a free wheel between the engine and the rotor (variably emplaced).

Figure 8-2. Mechanical Rotor Drive.

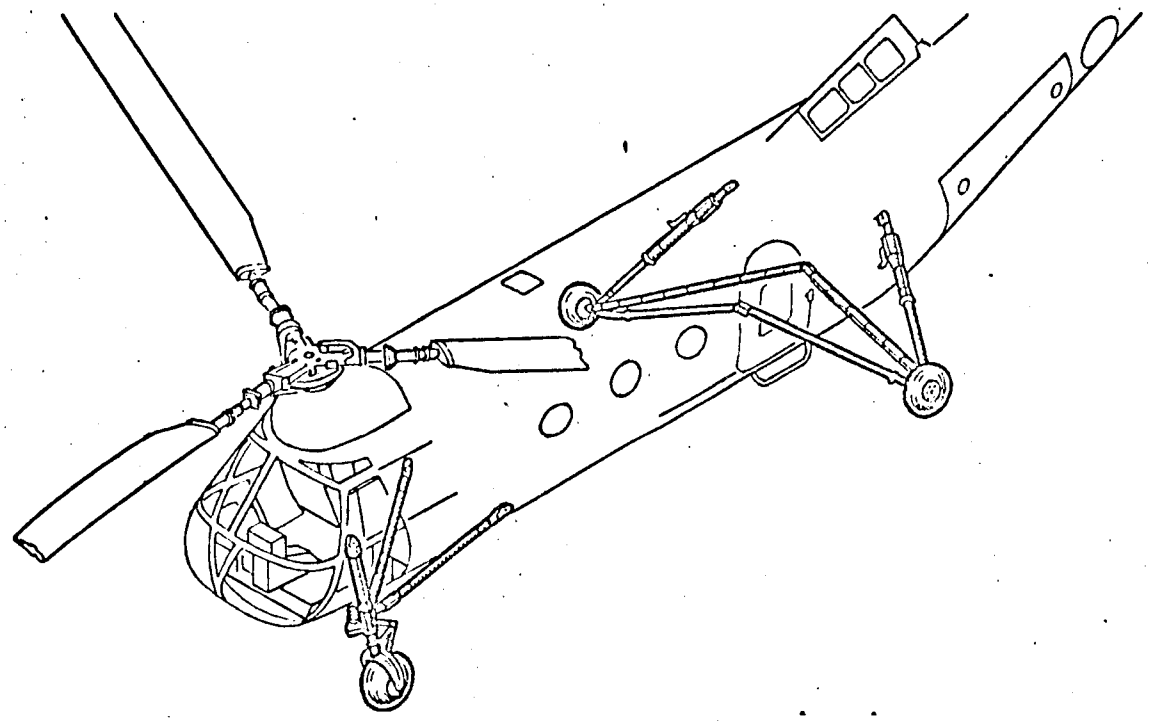

a) Tricycle landing gear

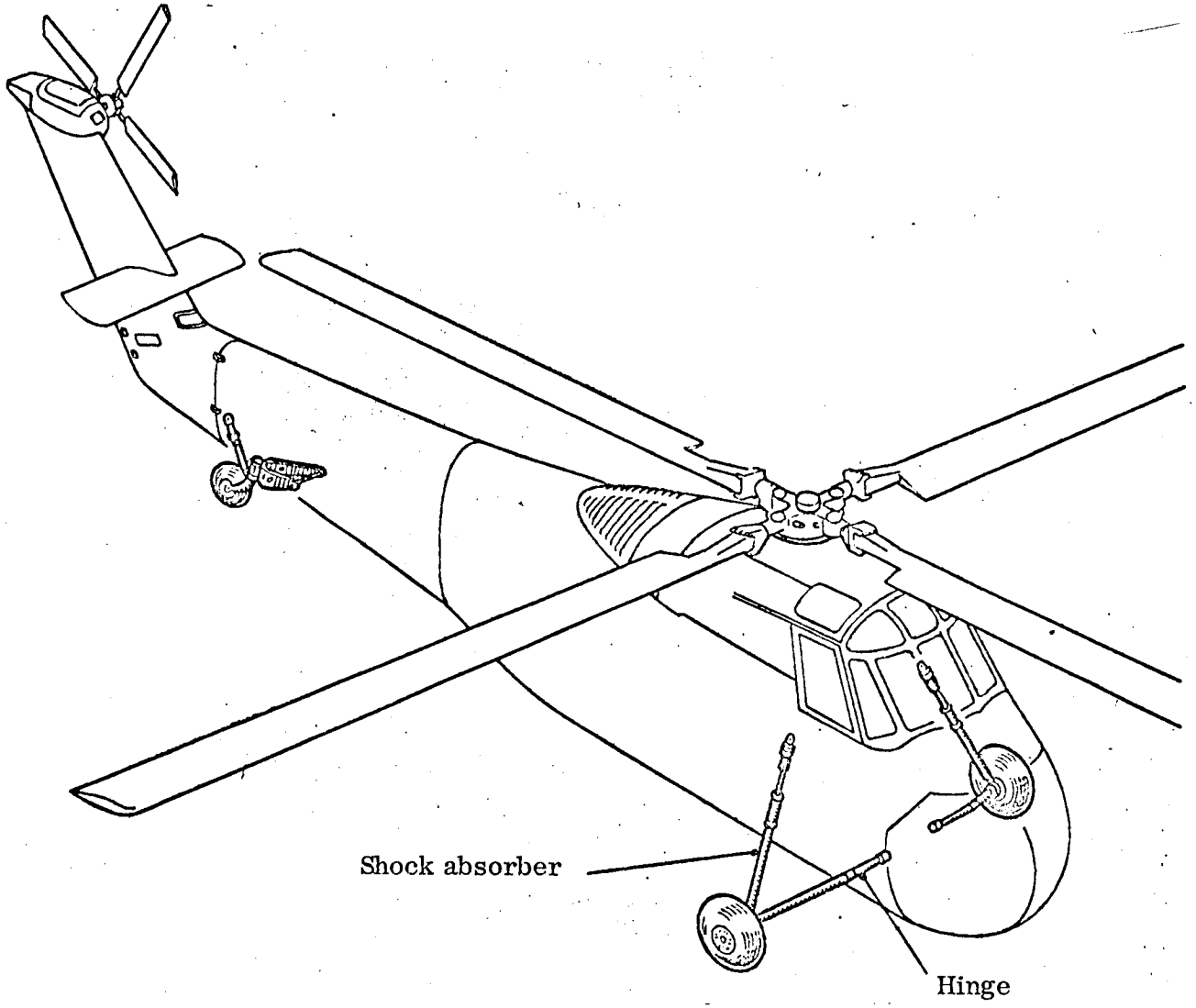

b) Conventional landing gear

Fig. 9-1. Landing Gears.

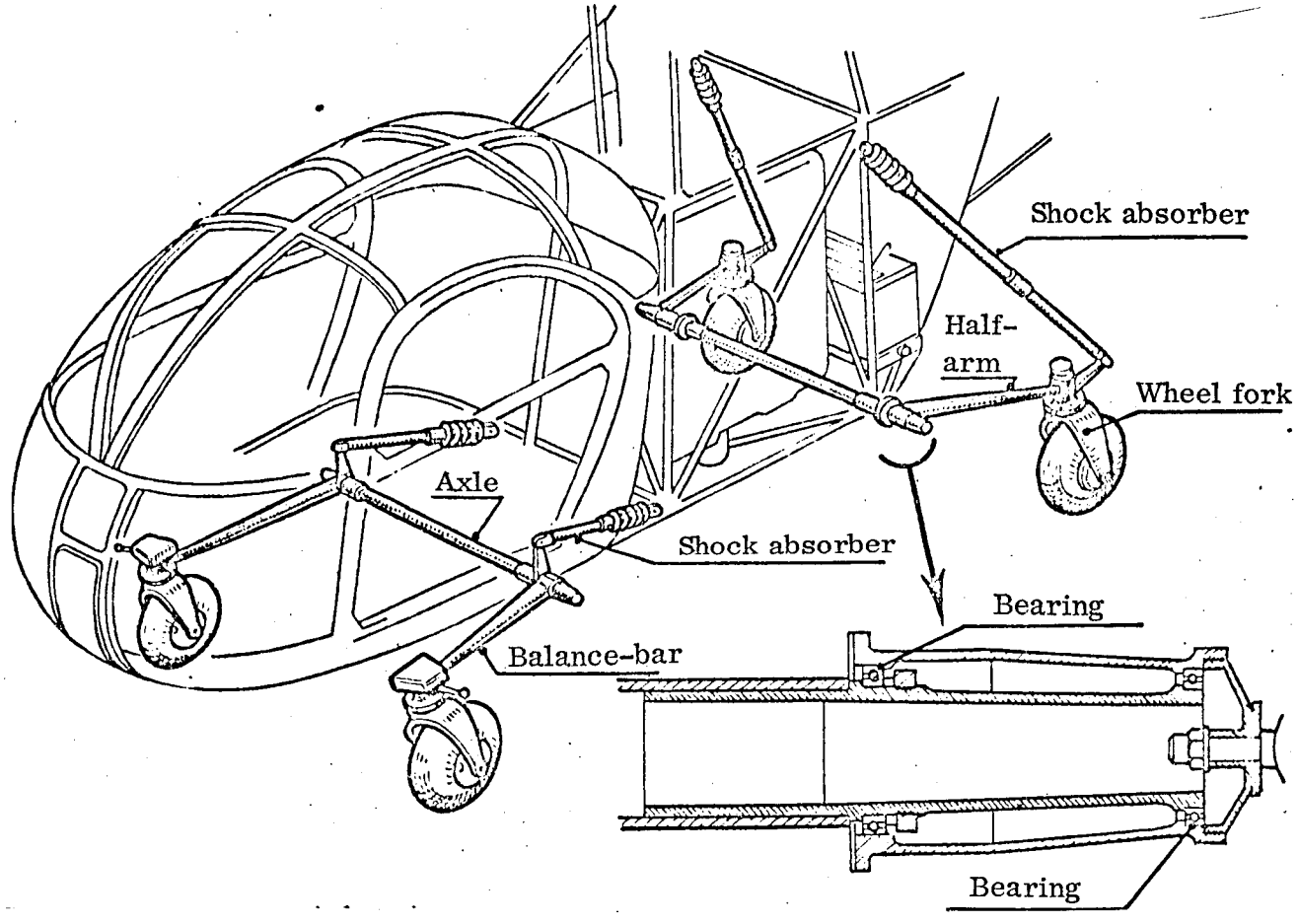

c) Quadricycle landing gear

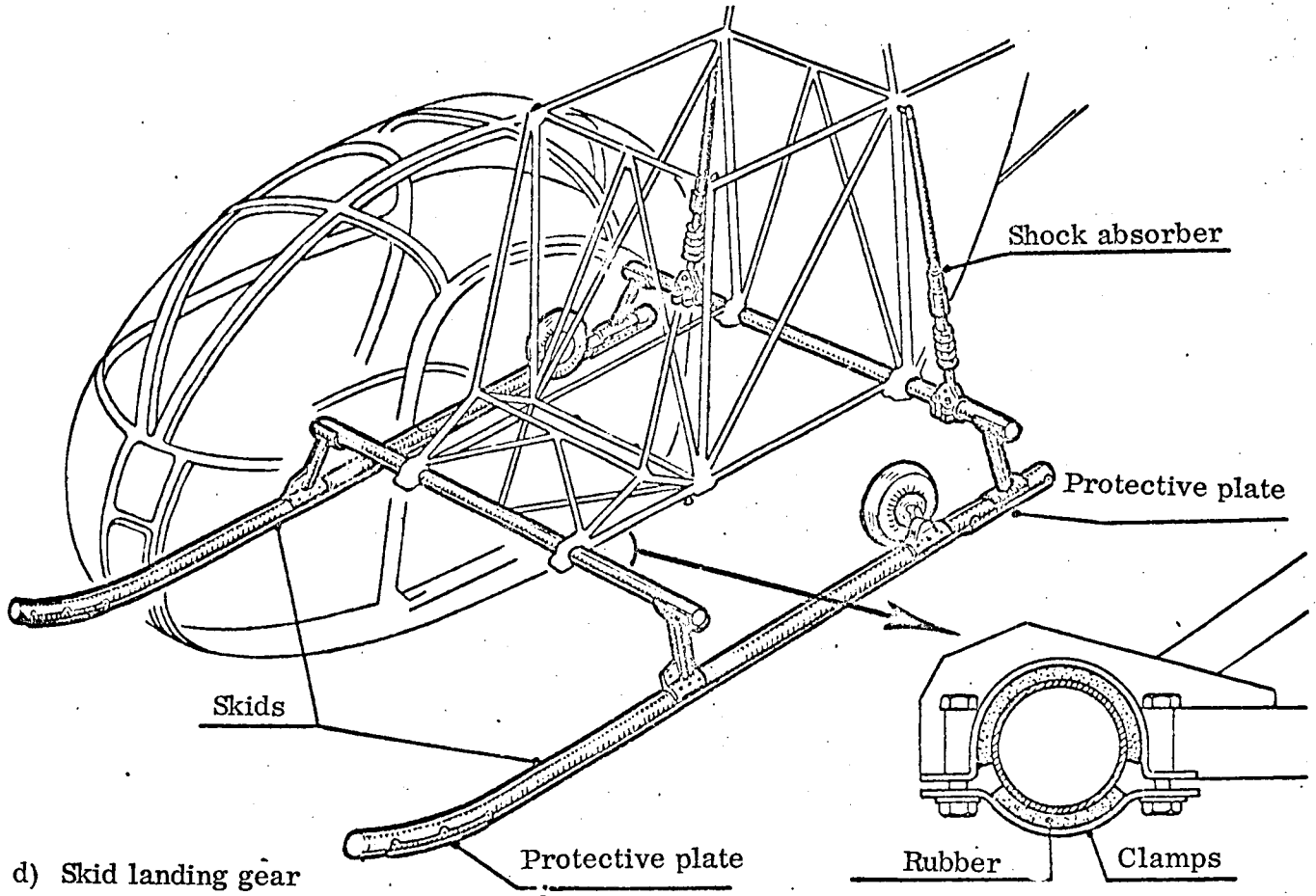

d) Skid landing gear

Figure 9-1. Landing Gears (continued).

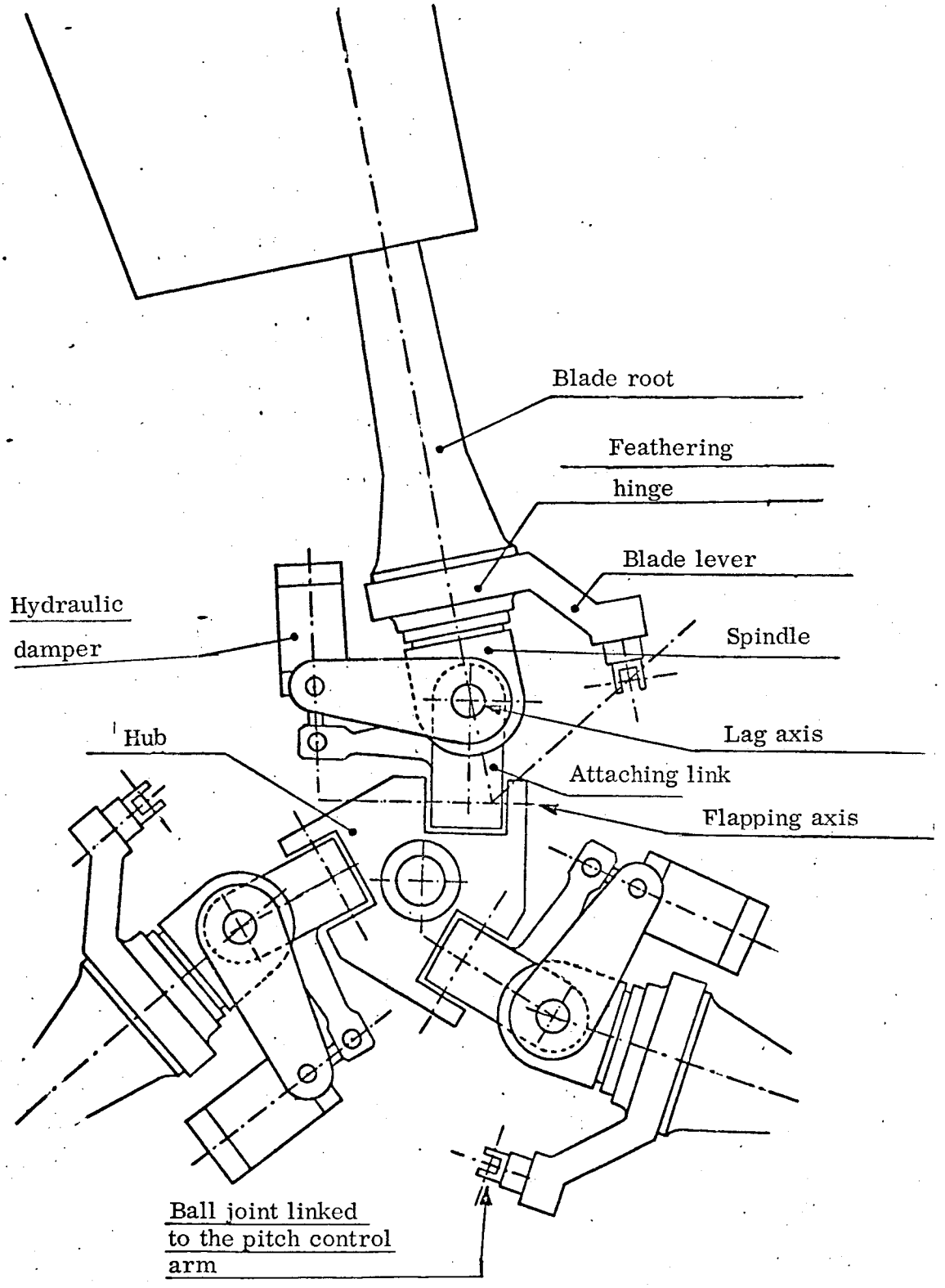

Figure 9-2. Articulated-Blade Hub (diagram).

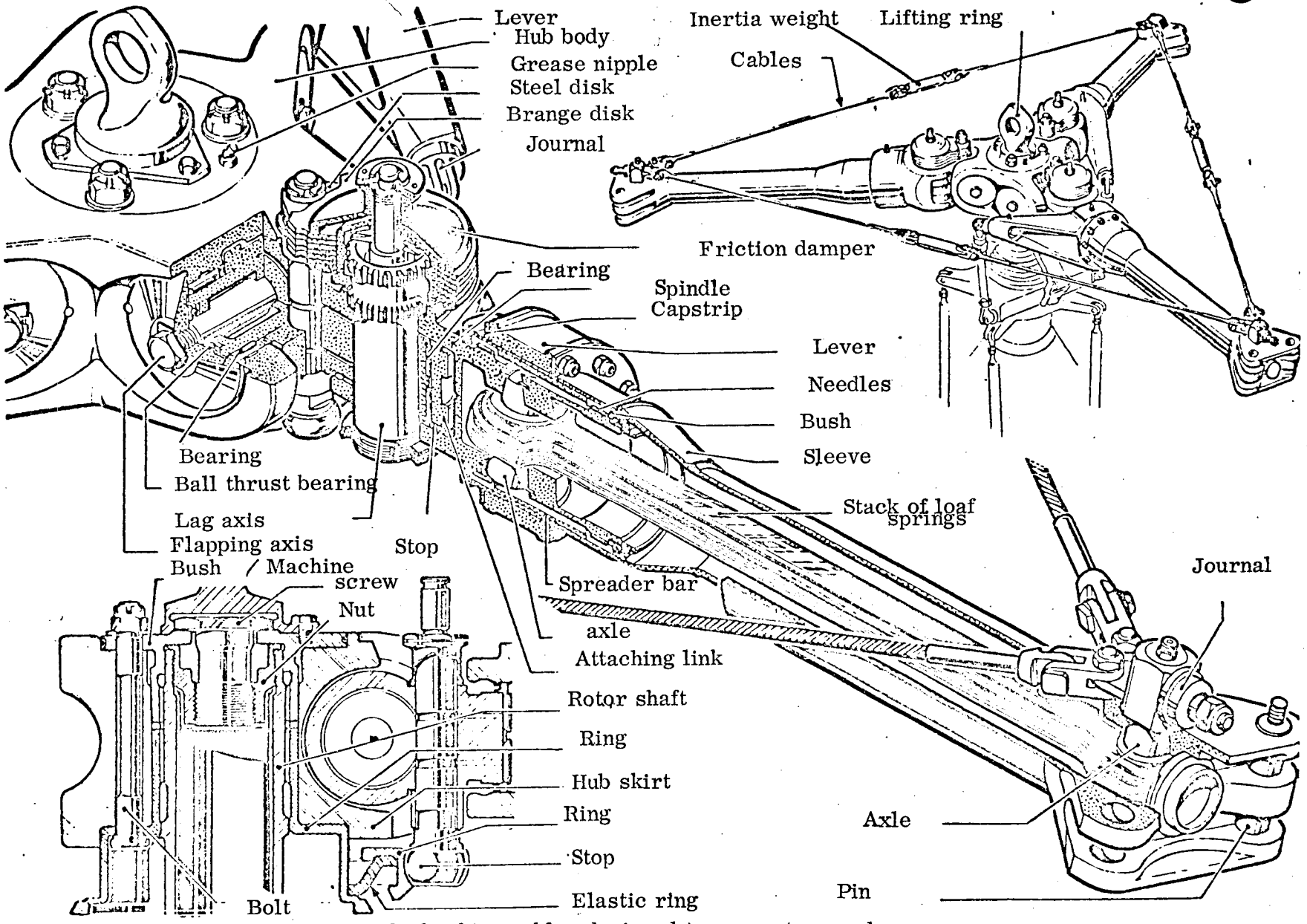

Note the braking cables designed to prevent ground resonance.

Figure 9-3, a. Three-Blade Hub (SE 3130).

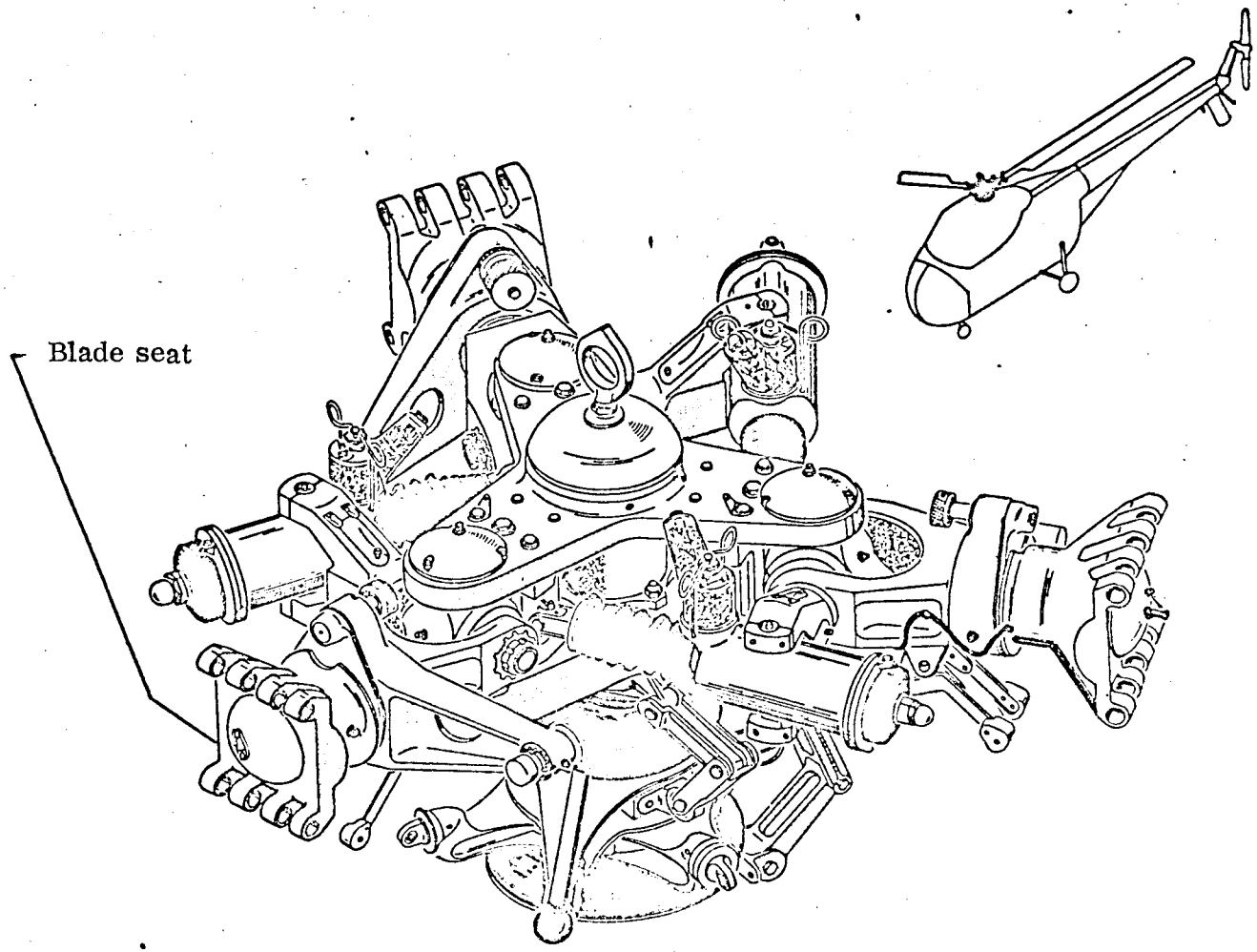

Figure 9-3,b. Hub of the Skorsky S55.

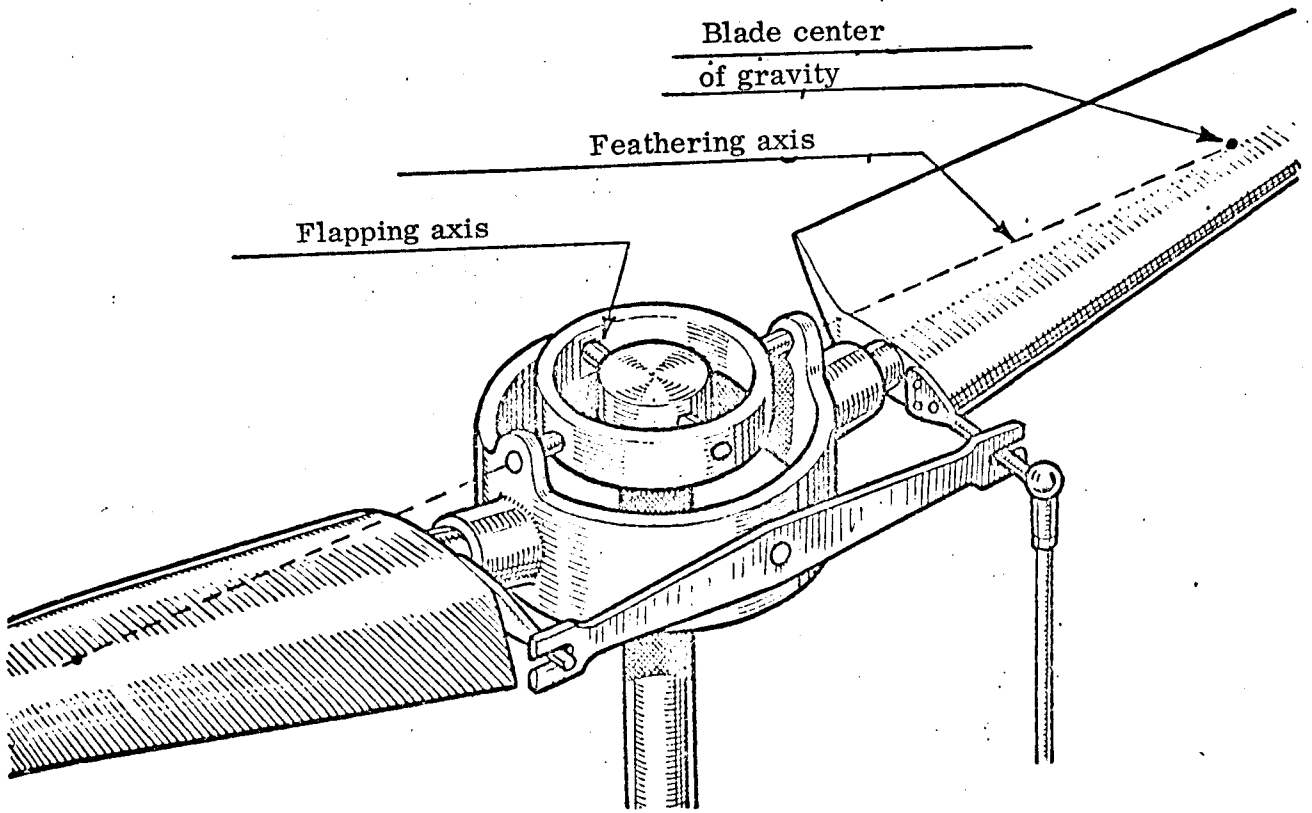

Figure 9-4, a. See-Saw Rotor. Diagram.

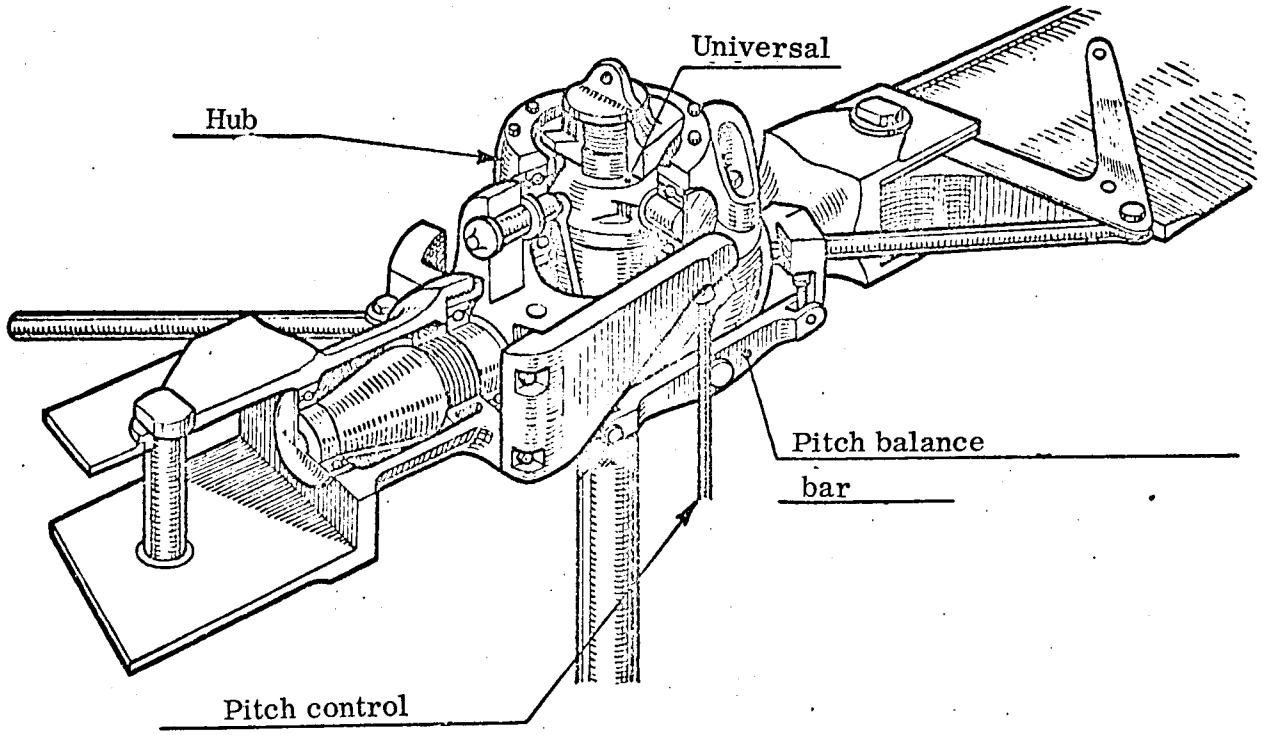

Figure 9-4,b. See-Saw Rotor. Bell 47D.

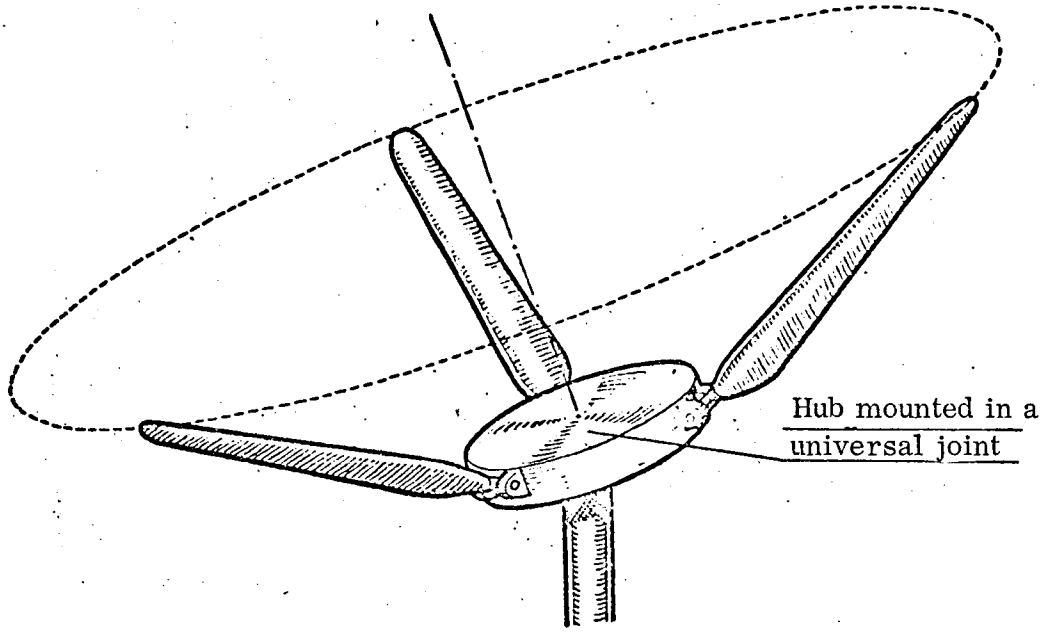

Figure 9-5. Floating Hub. Diagram.

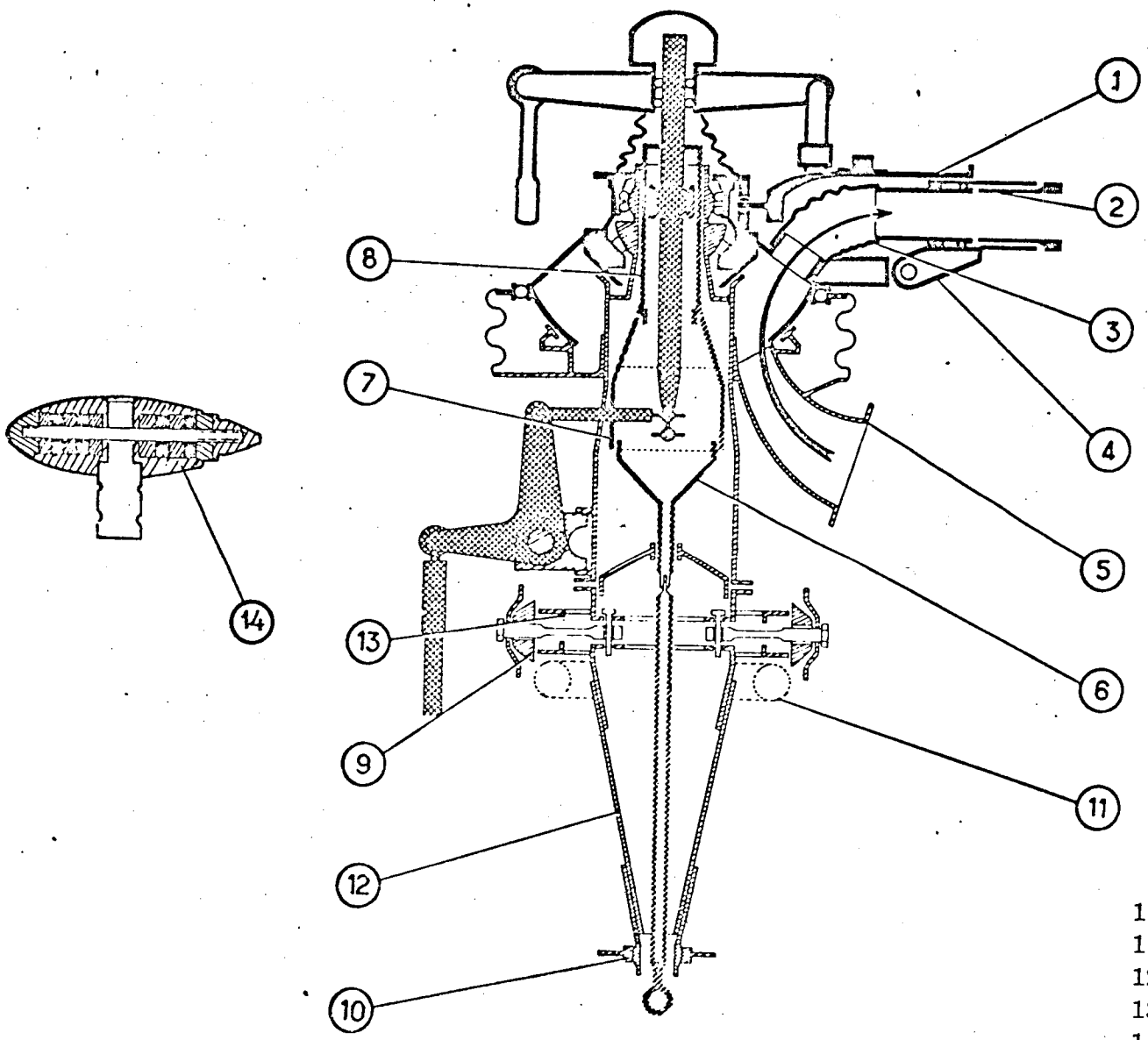

1 blade root
2 bushing
3 elbow joint
4 blade root stop
5 duct
6 control lug
7 trundle
8 slideway
9 "Pedistra" damper
10 taggle joint
11 upper pylan ring
12 cane
13 ring
14 anti-weaving weight

Figure 9-6, a. Floating Hub (Djinn). Cross Section.

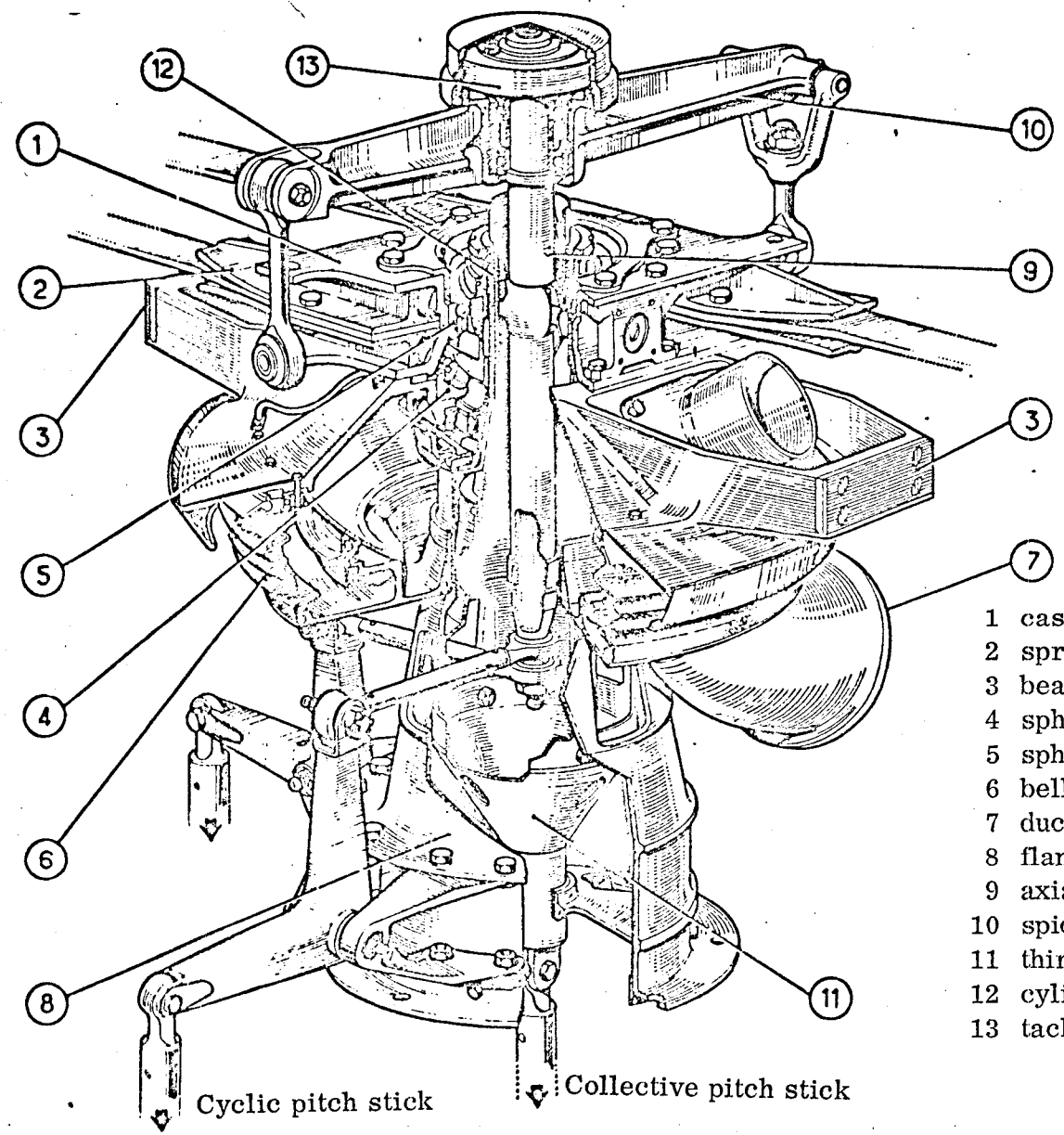

1 case
2 spring attachment
3 bearing crankcase
4 spherical thrust bearing
5 spherical center bearing
6 bellows
7 duct
8 flange
9 axial pitch lever
10 spider arm
11 thimble
12 cylinder
13 tachometer generator

Figure 9-6,b. Floating Hub (Djinn). Perspective View.

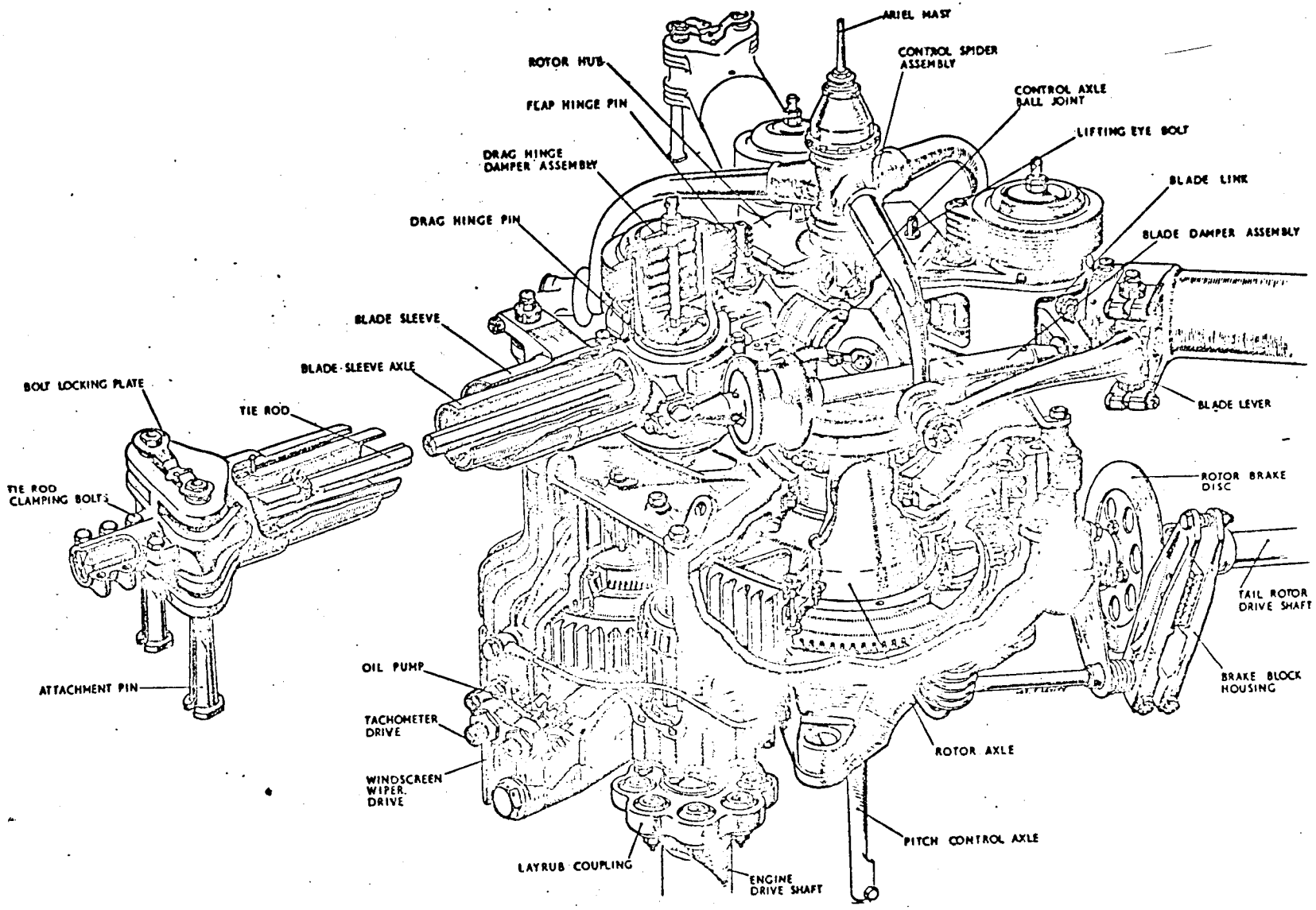

Note the elastic inter-blade couplings designed to protect against ground resonance

Figure 9-7. Transmission Box and Rotor Hub (Bristol 171).

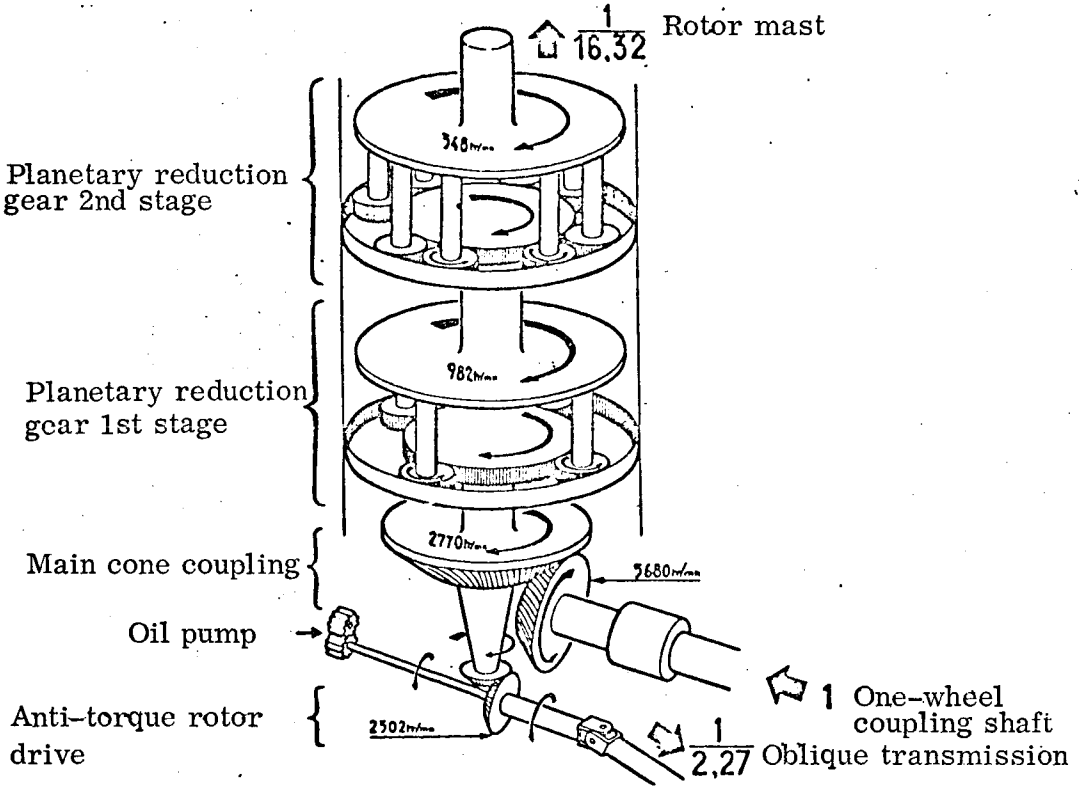

a) Operational diagram

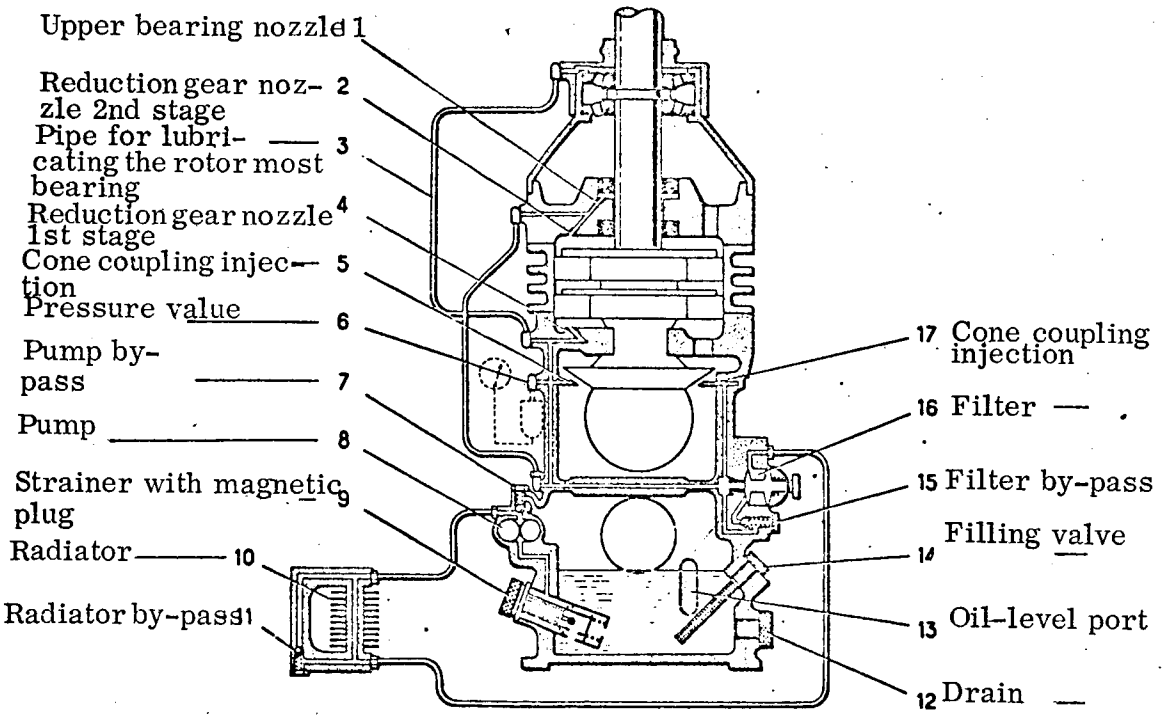

b) Lubrication diagram

Figure 9-8. Main Reduction Gear for a Turbine-Engine Helicopter (SE 3130).

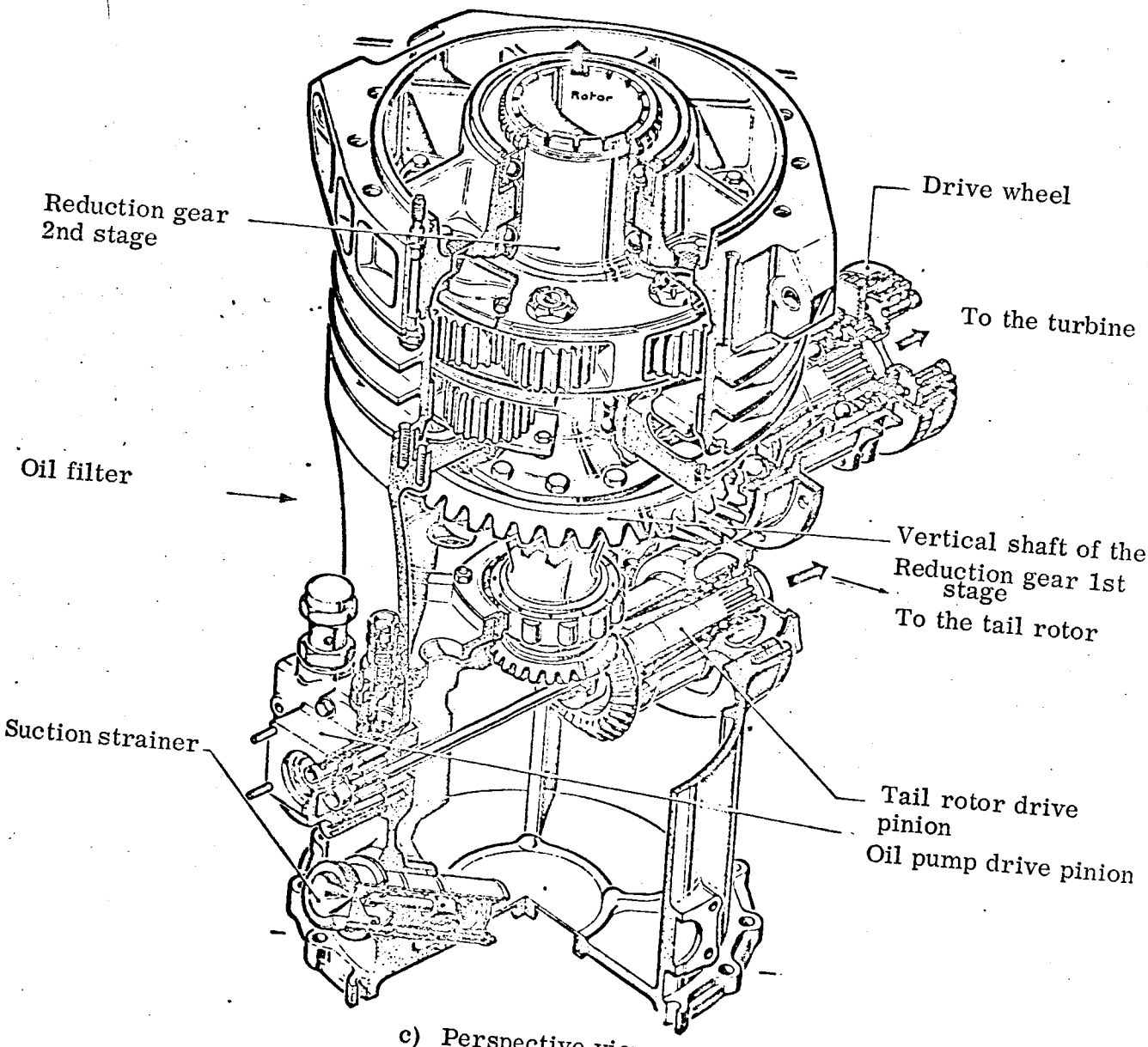

c) Perspective view

Figure 9-8. Main Reduction Gear for a Turbine Helicopter (SE 3130).

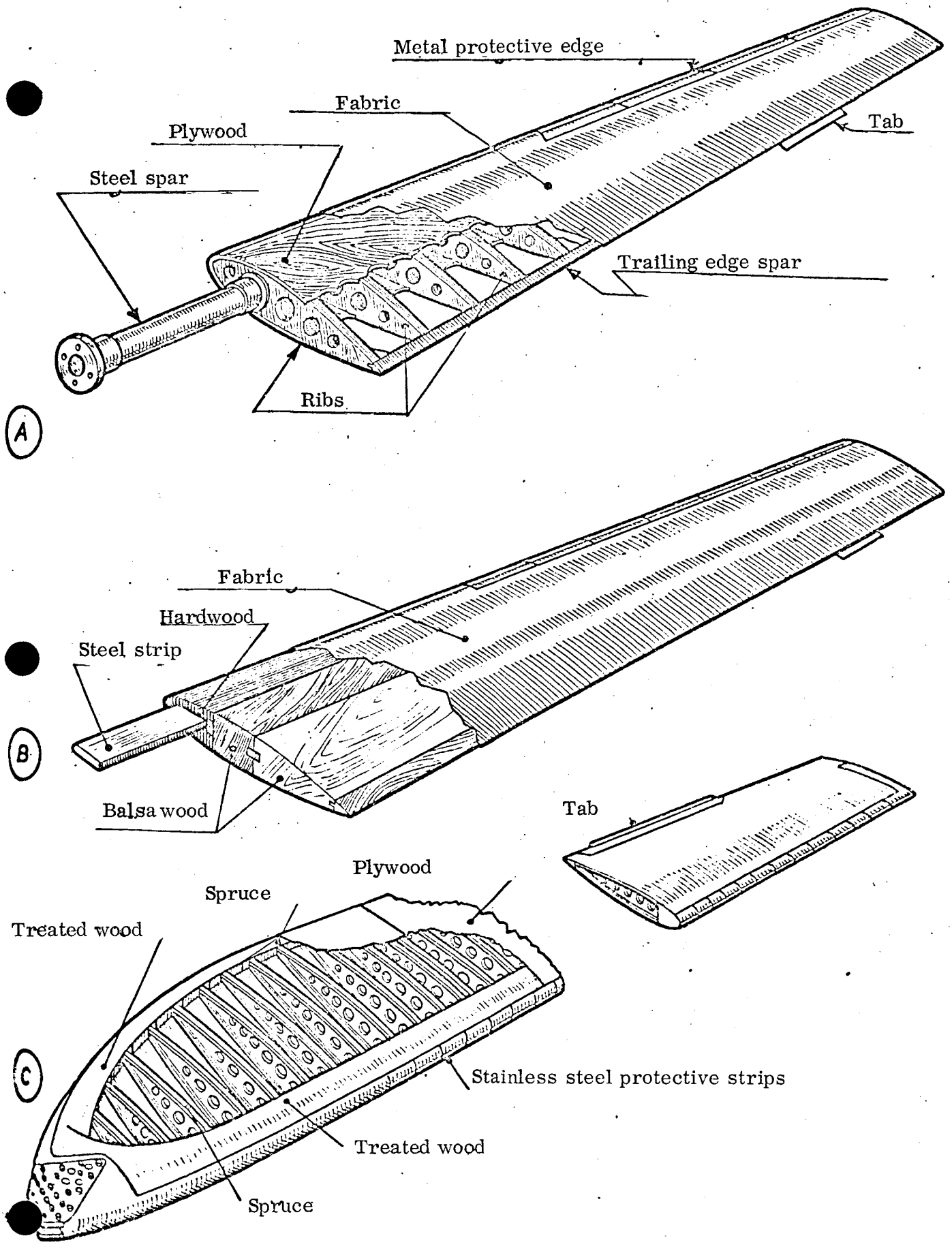

Figure 9-9. Several Types of Blades.

1 spar
2 trailing edge
3 counterweight
4 nozzle
5 nozzle fairing
6 stretches
7 tab
8 tie rods
9 spar
10 filler
11 springs
12 strut
13 spring carrier arm
14 blade root
15 pitch control lever
16 blade bearing stop

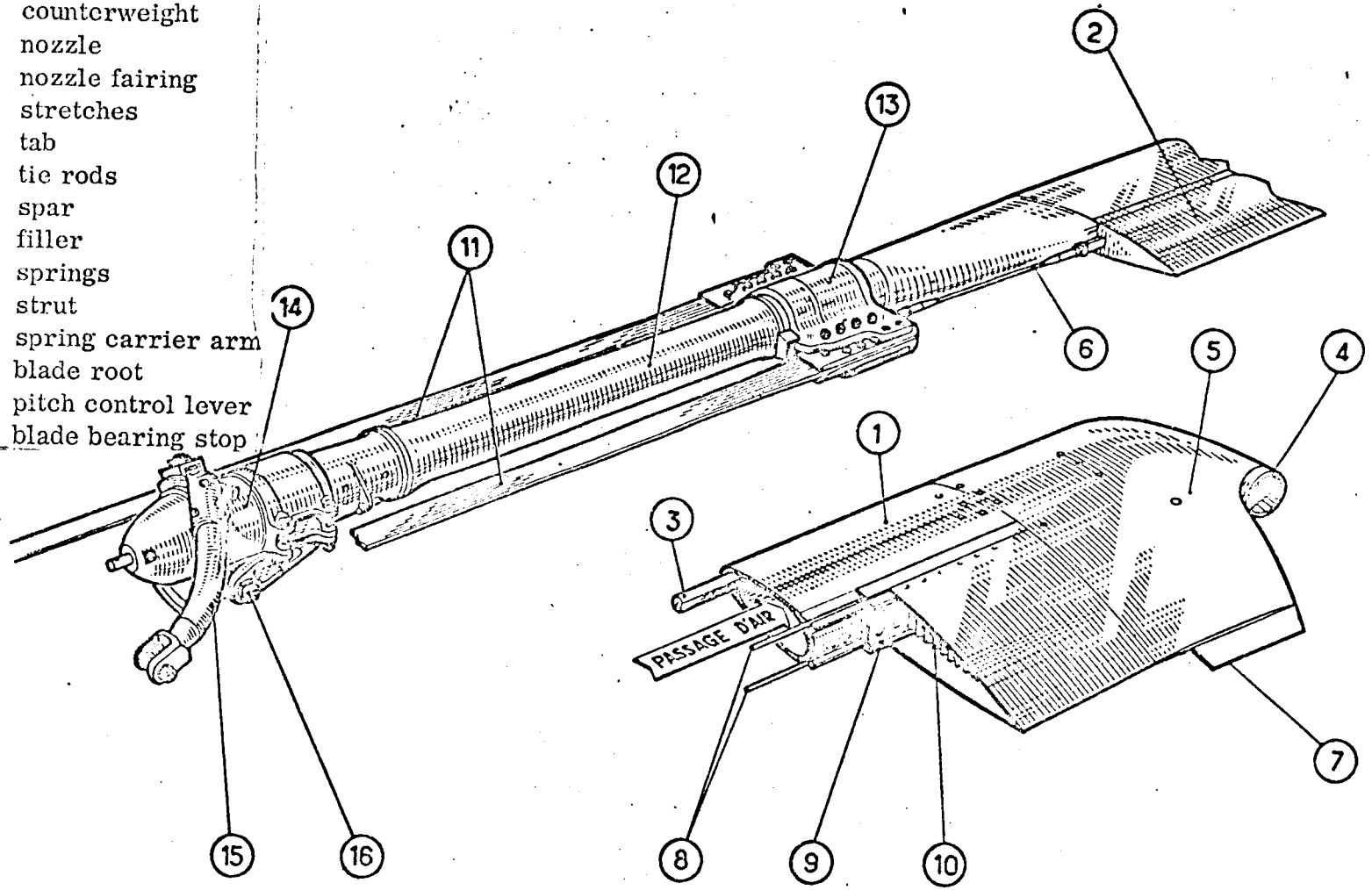

(D) Blade for SO 1221 Djinn

Figure 9-9. (Cont'd). Several Types of Blades.

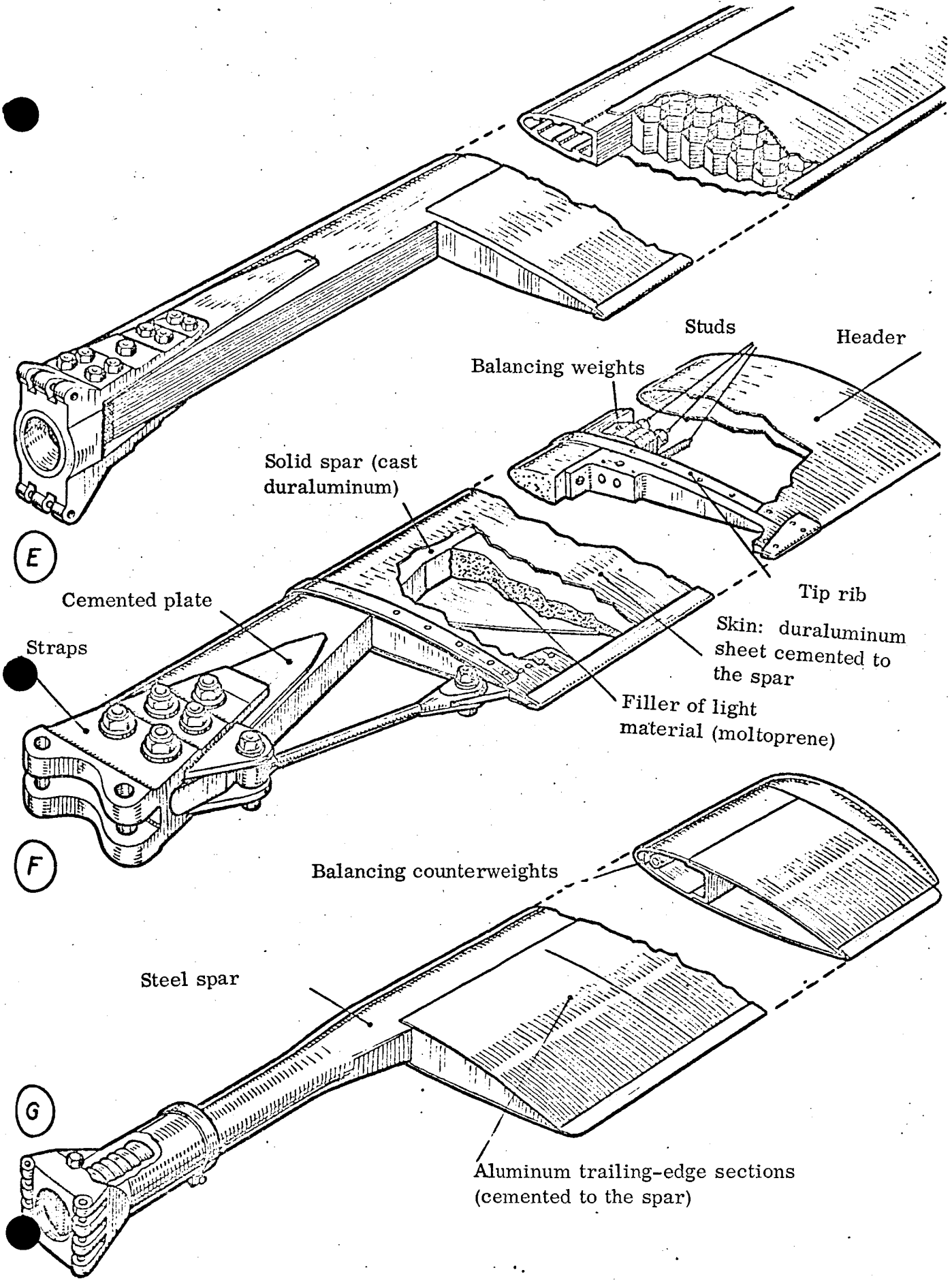

Figure 9-9. (Cont'd). Several Types of Blades.

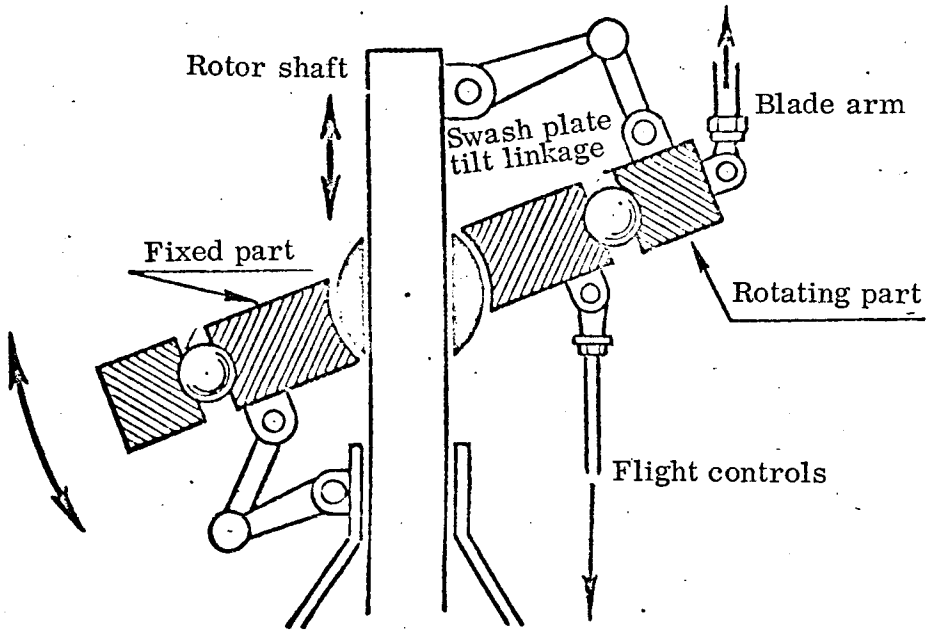

a) Diagram

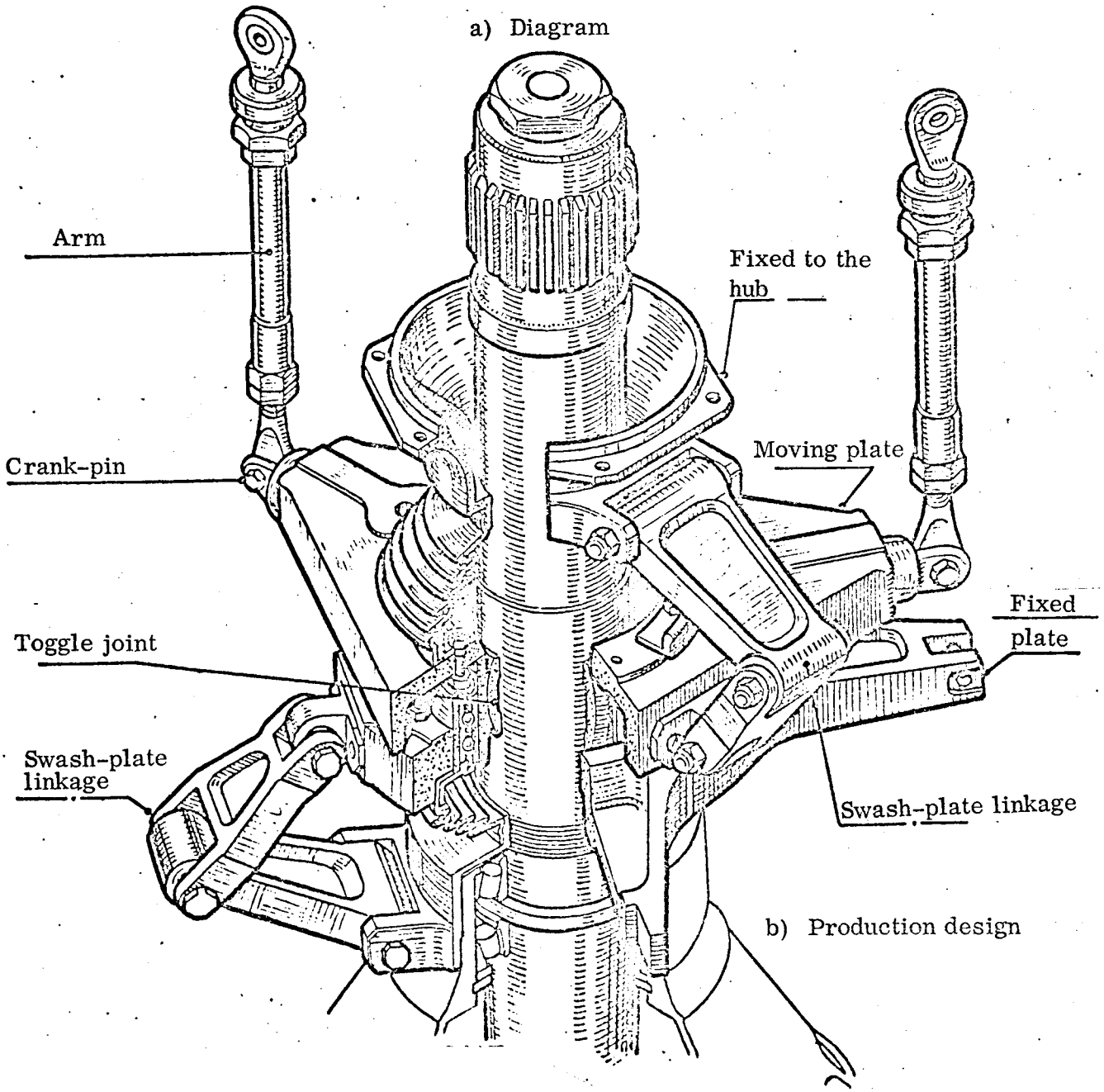

b) Production design

Figure 9-10. Swashplate

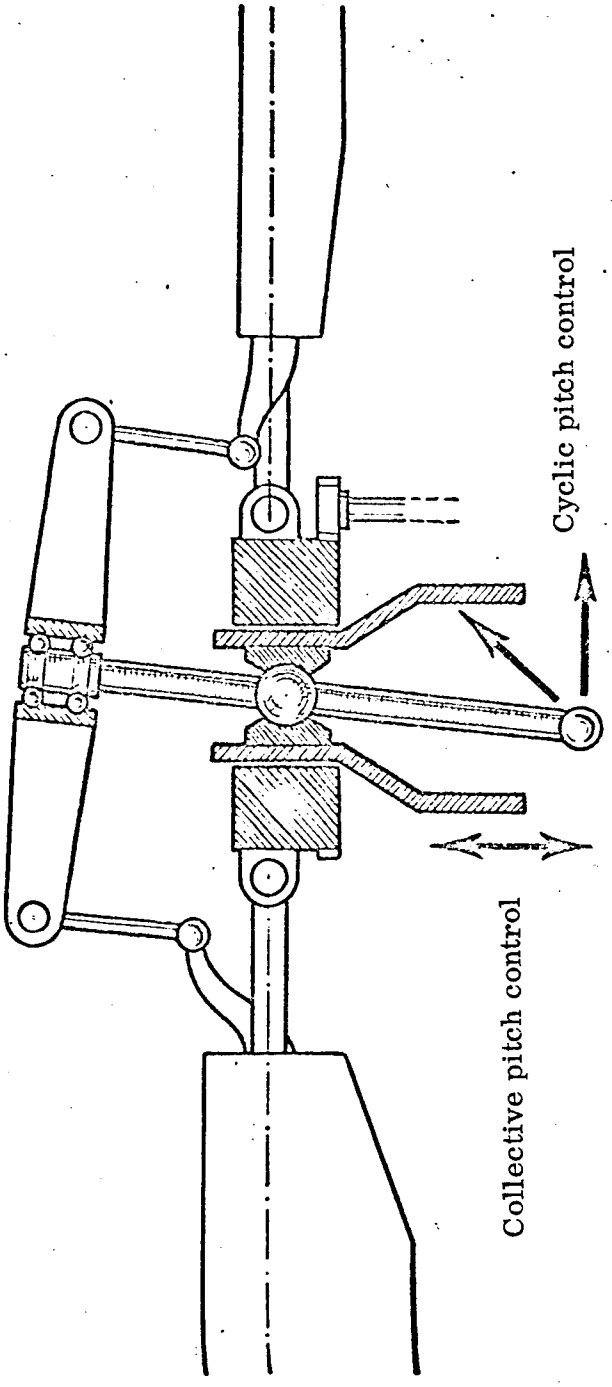

Figure 9-11. Spider (diagram).

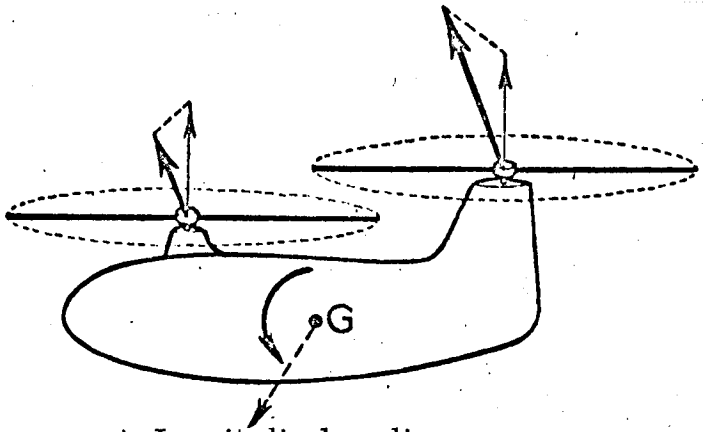

a) Longitudinal cyclic

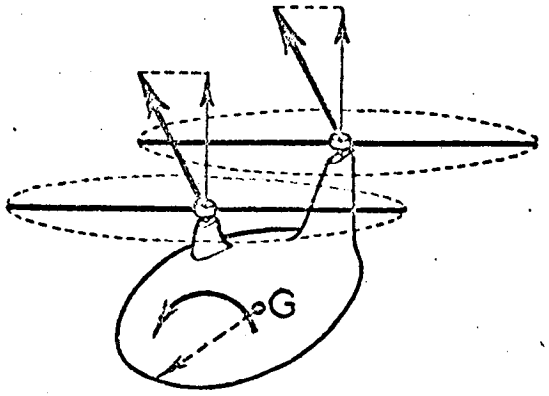

b) Lateral cyclic

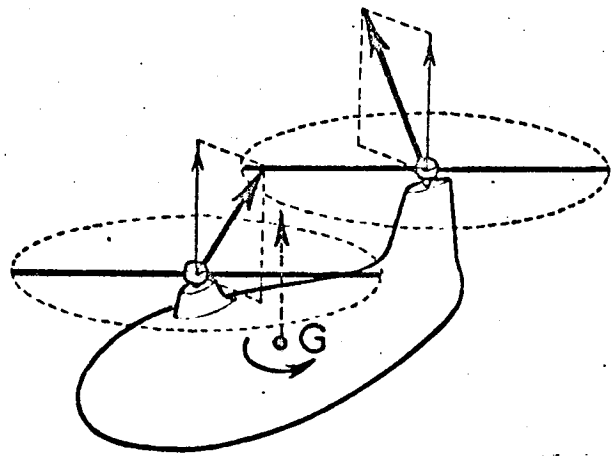

c) Rudder bar. (Yaw control)

Figure 9-12. Control Principles for a Tandem Two-Rotor Helicopter.

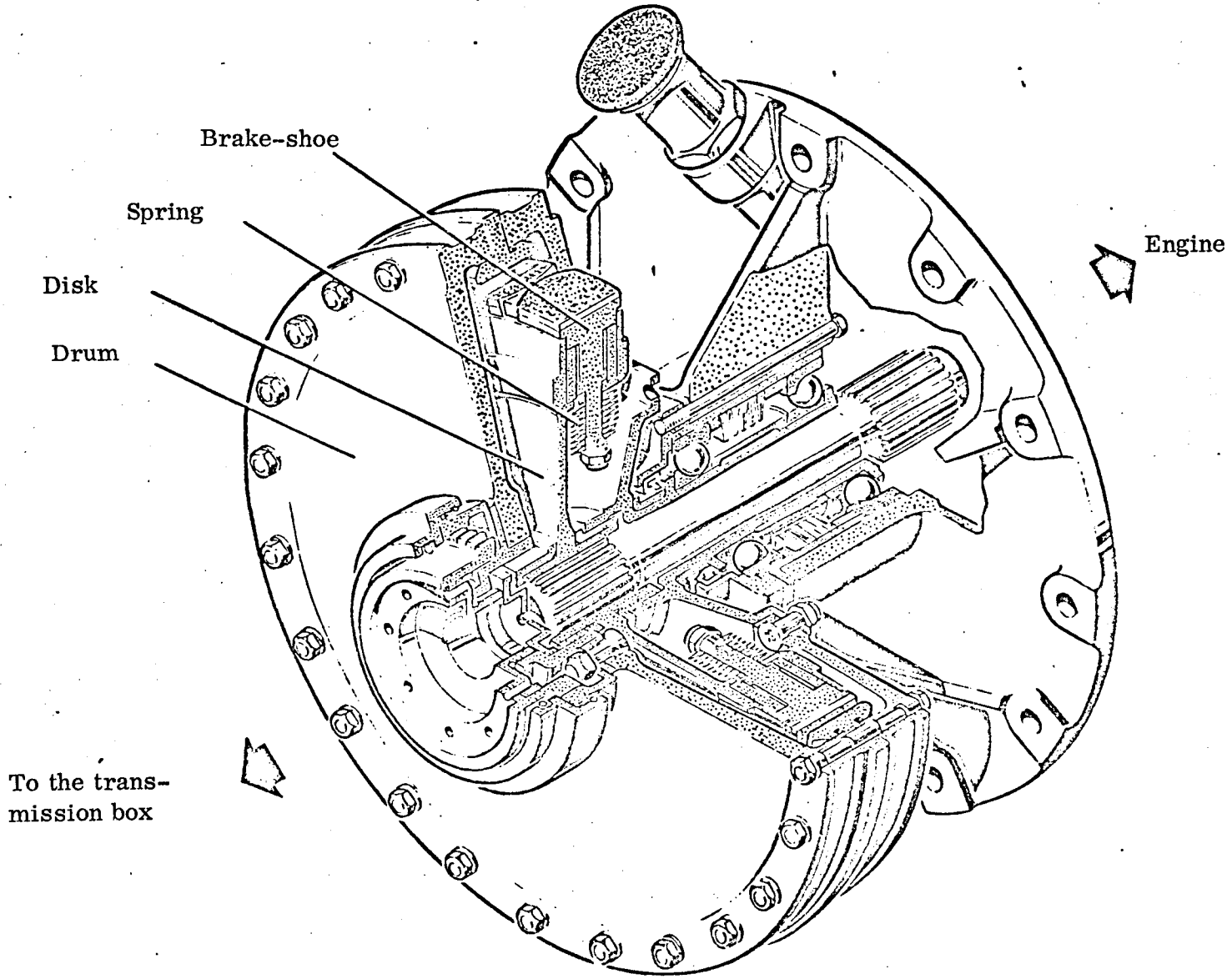

Figure 9-13. Clutch.

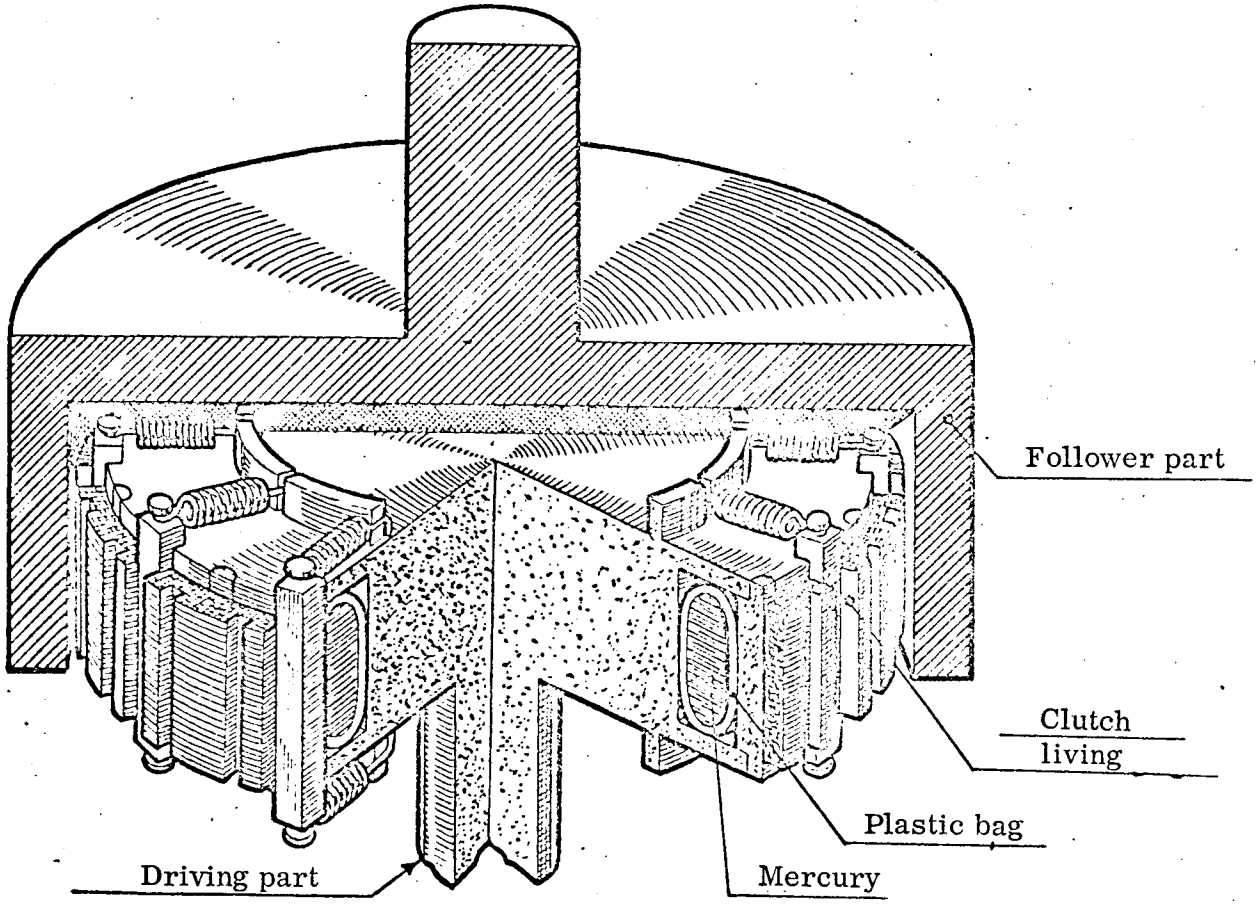

Figure 9-14. Diagram of a Mercury Clutch.

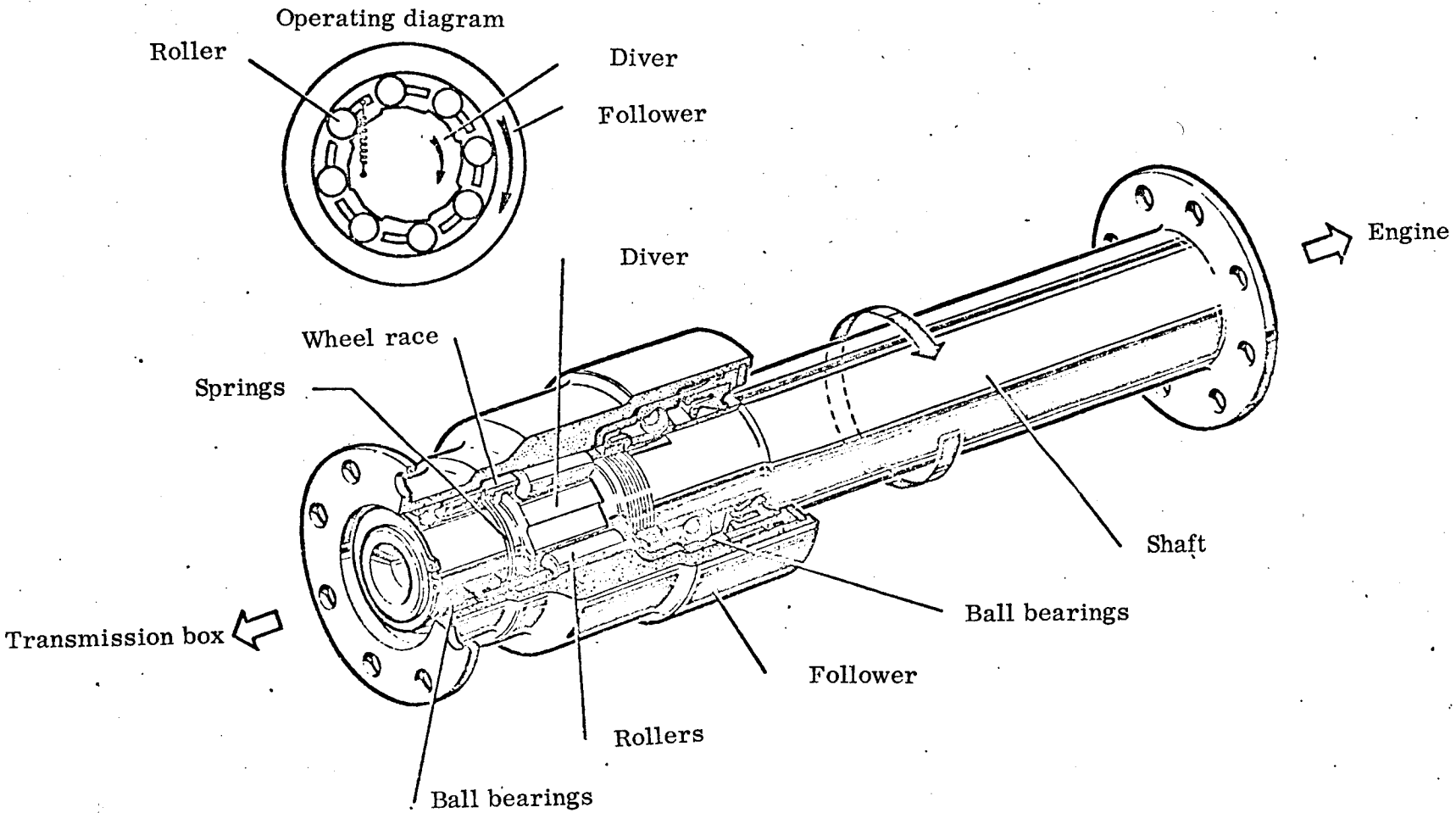

Figure 9-15. Free Wheel.

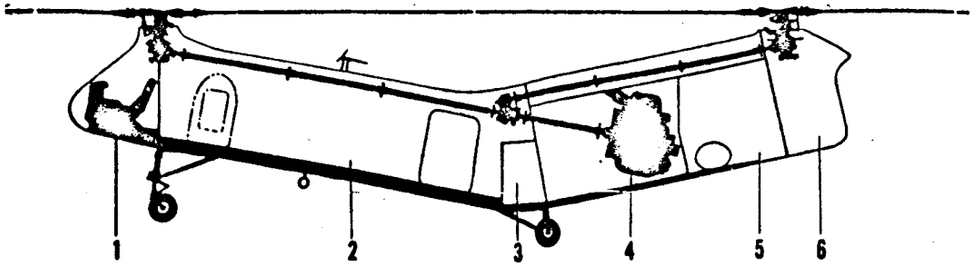

1 Pilot's compartment
2 Passenger compartment
3 Fuel compartment
4 Engine
5 Accessary compartment
6 Tail

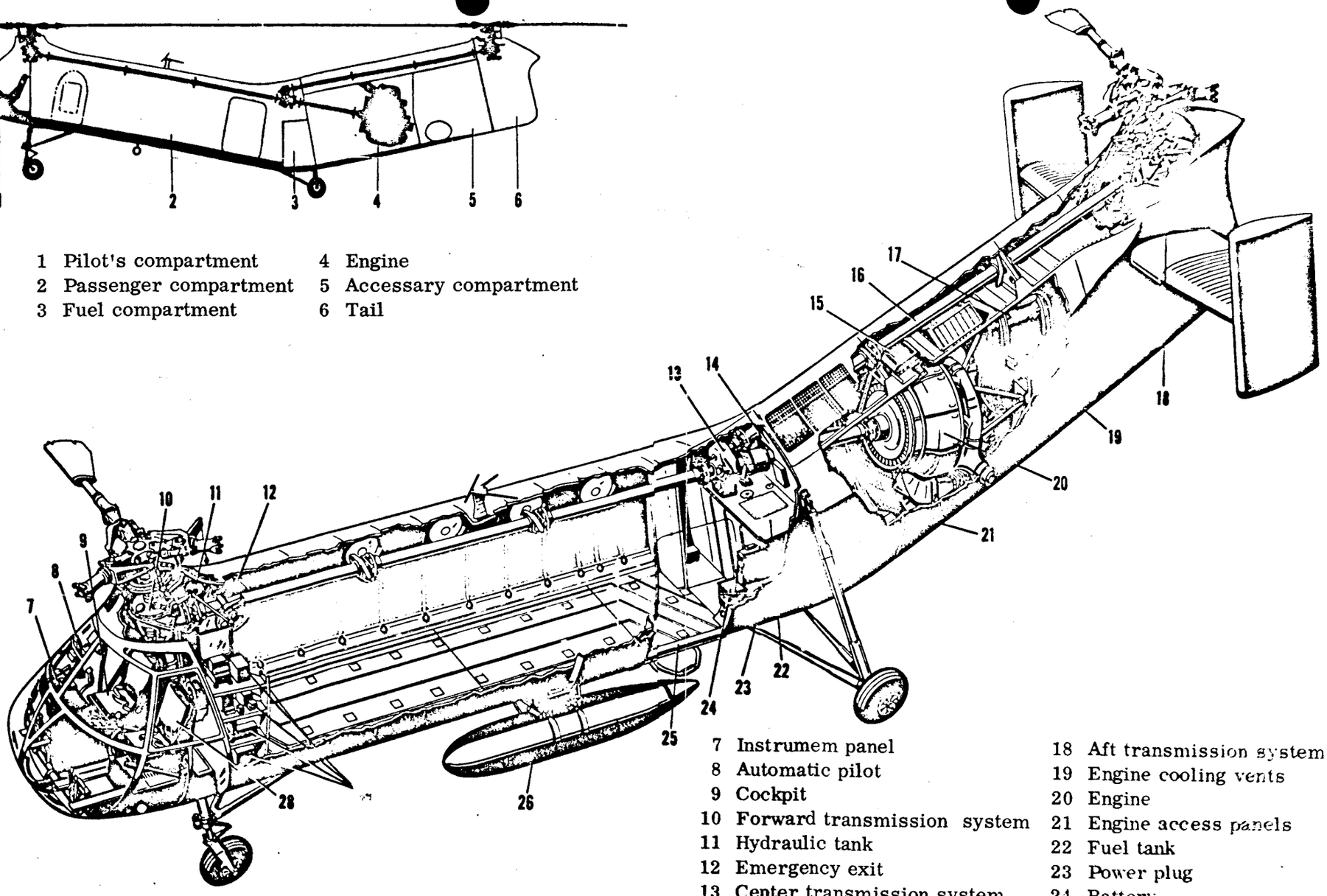

7 Instrumem panel
8 Automatic pilot
9 Cockpit
10 Forward transmission system
11 Hydraulic tank
12 Emergency exit
13 Center transmission system
14 Fireproof bulkhead
15 Engine-oil radiator
16 Transmission shaft
17 Engine oil tank
18 Aft transmission system
19 Engine cooling vents
20 Engine
21 Engine access panels
22 Fuel tank
23 Power plug
24 Battery
25 Main exit
26 External tank
27 Radio equipment
28 Copilot's cockpit

Figure 9-17. Vertal H-21. Overall Arrangement.

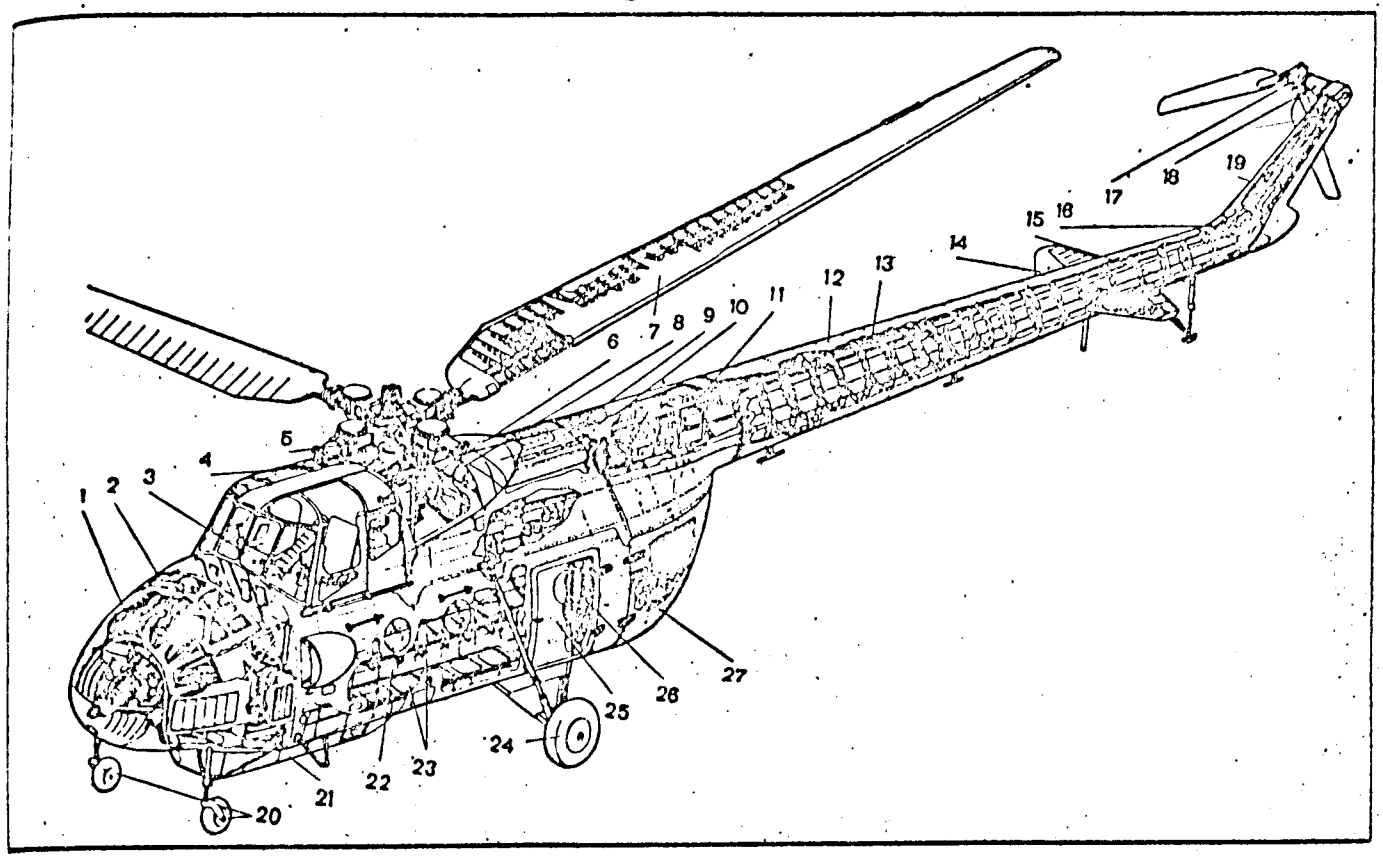

LEGEND

1 Engine
2 Oil tank
3 Cockpit
4 Swashplate
5 Main rotor hub
6 Main reduction gear
7 Main rotor blade
8 Hydraulic fluid tank
9 Fuel tank
10 Tank for rotor de-icing fluid
11 Radio
12 Tail cone
13 Transmission
14 Stabilizer
15 Tail skid
16 Intermediate reduction gas
17 Tail rotor
18 Tail reduction gear
19 Tail-tip cone
20 Front wheels
21 Navigator's cockpit
22 Cargo compartment
23 Passenger seats
24 Main landing gear
25 Side door
26 Wench
27 Doors for bulky loads

Figure 9-18. Over-All View of the MIL-4.

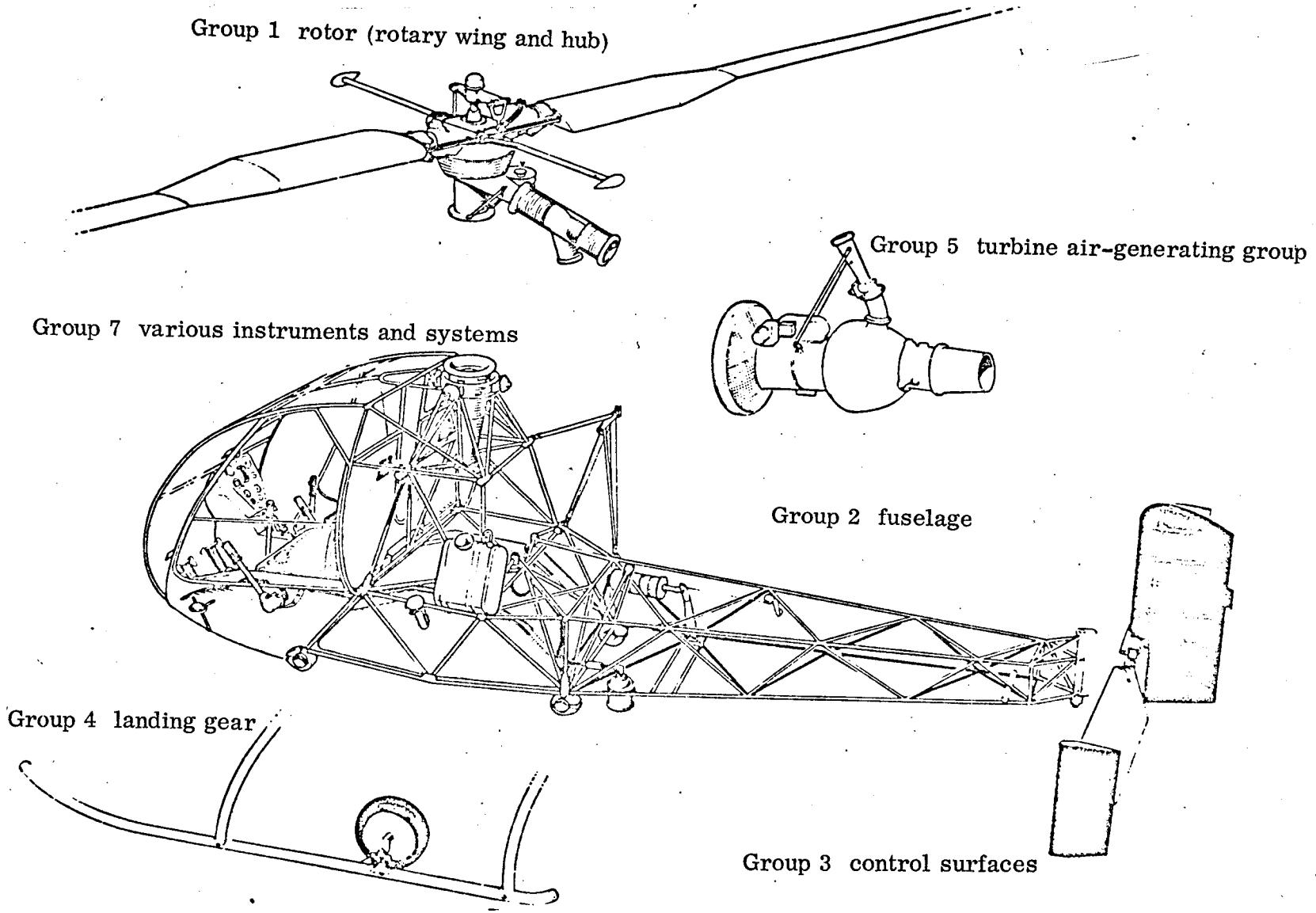

Figure 9-19. Breakdown of the SO 1221 Djinn.

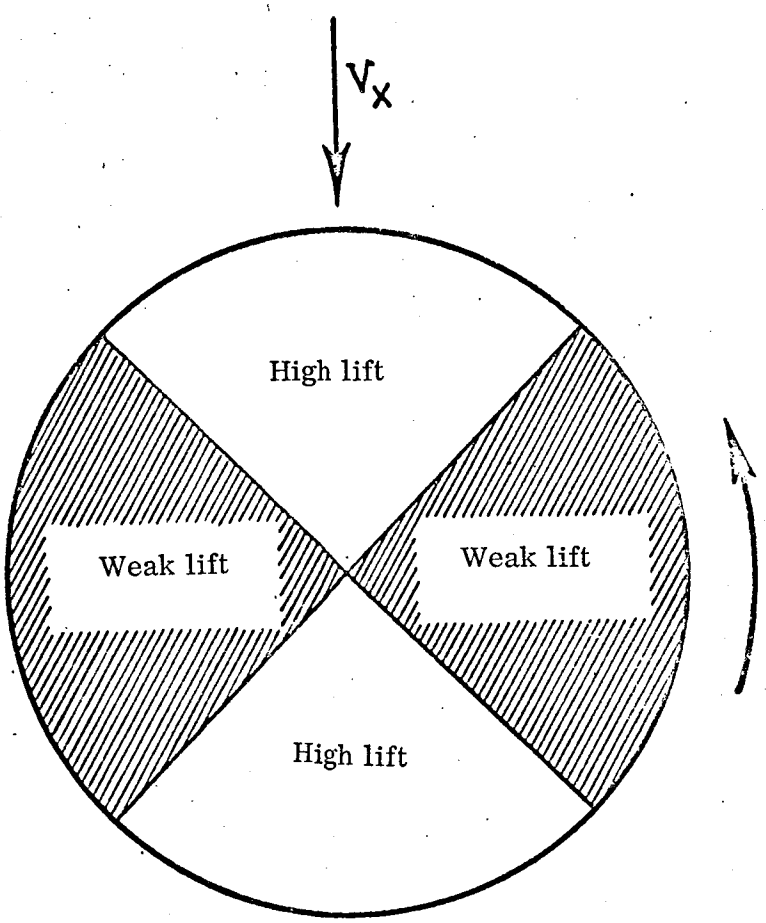

Figure 10-1. Principle of Two-Cycle Pilotage.

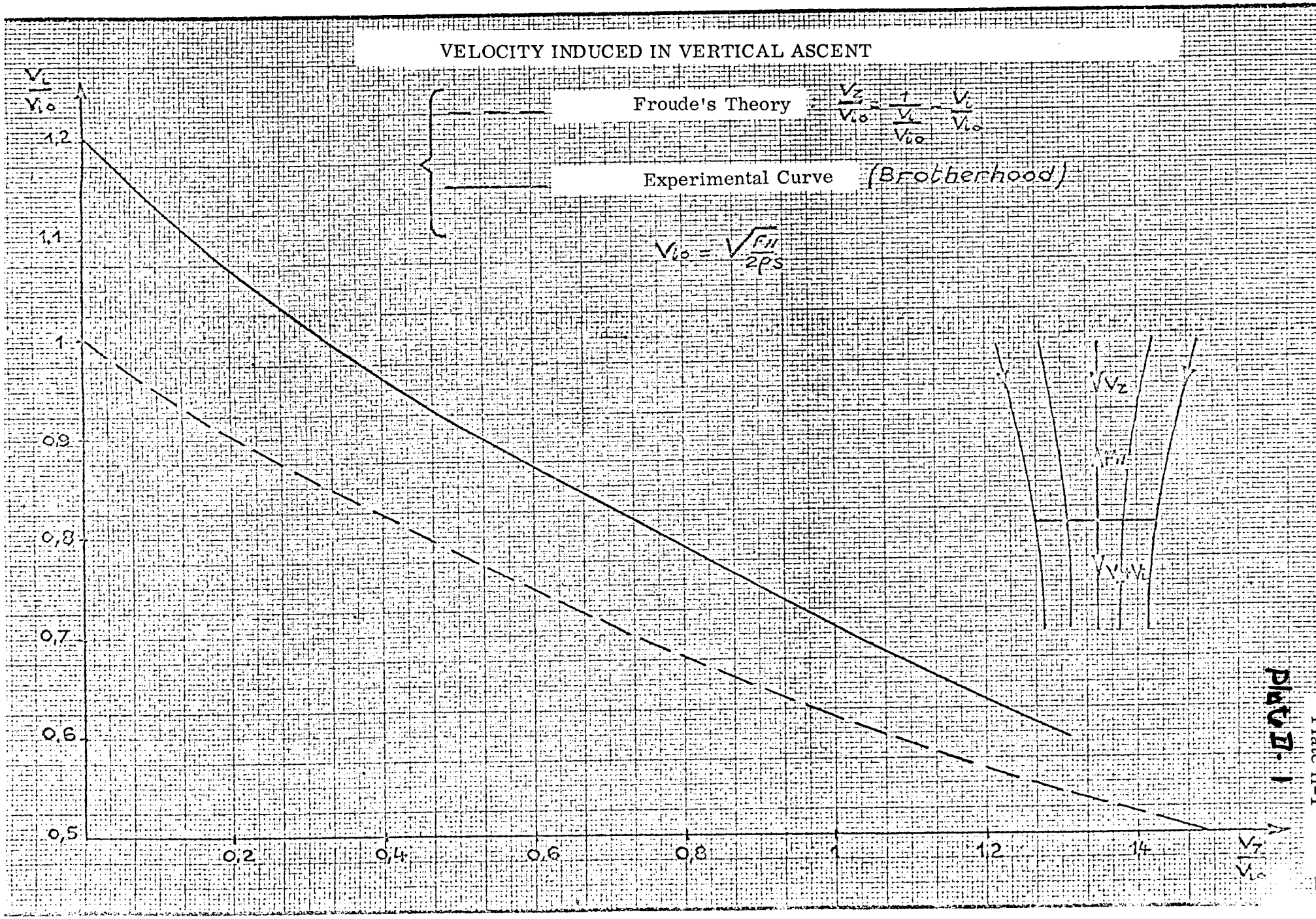
VELOCITY INDUCED IN VERTICAL ASCENT
Froude's Theory
Experimental Curve (Brotherhood)
$\frac{V_z}{V_{i0}} = \frac{1}{\frac{V_i}{V_{i0}}} - \frac{V_i}{V_{i0}}$
$V_{i0} = \sqrt{\frac{F_H}{2\rho S}}$
$\frac{V_i}{V_{i0}}$
1,2
1,1
1
0,9
0,8
0,7
0,6
0,5
0,2
0,4
0,6
0,8
1
1,2
1,4
$\frac{V_z}{V_{i0}}$
V_z
F_H
V_i
PLATE I

VELOCITY INDUCED IN VERTICAL FLIGHT

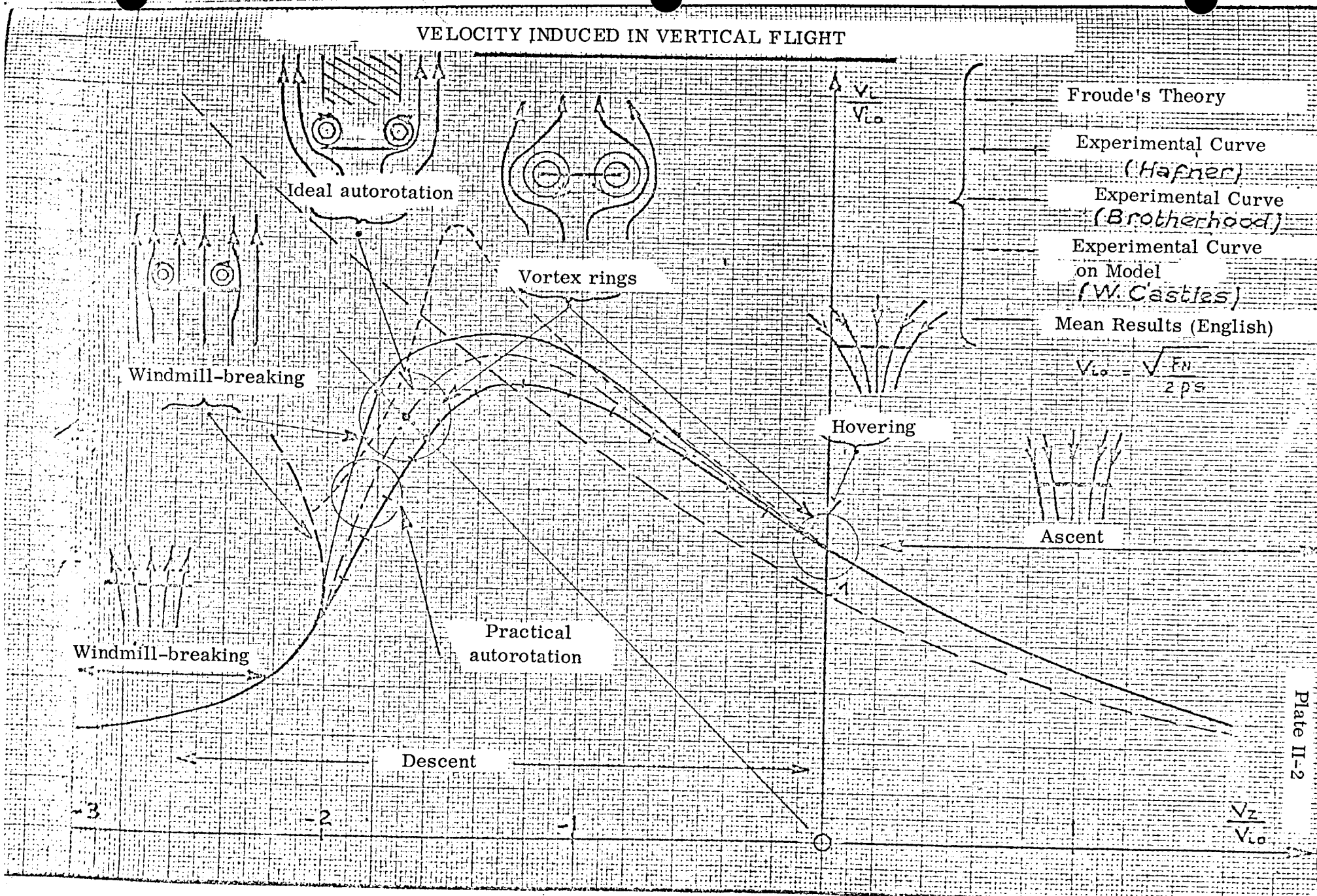

Plate II-2

THE OPTIMUM ROTOR CONSIDERING INDUCED TANGENTIAL VELOCITIES

(From J. Shapiro, [1]

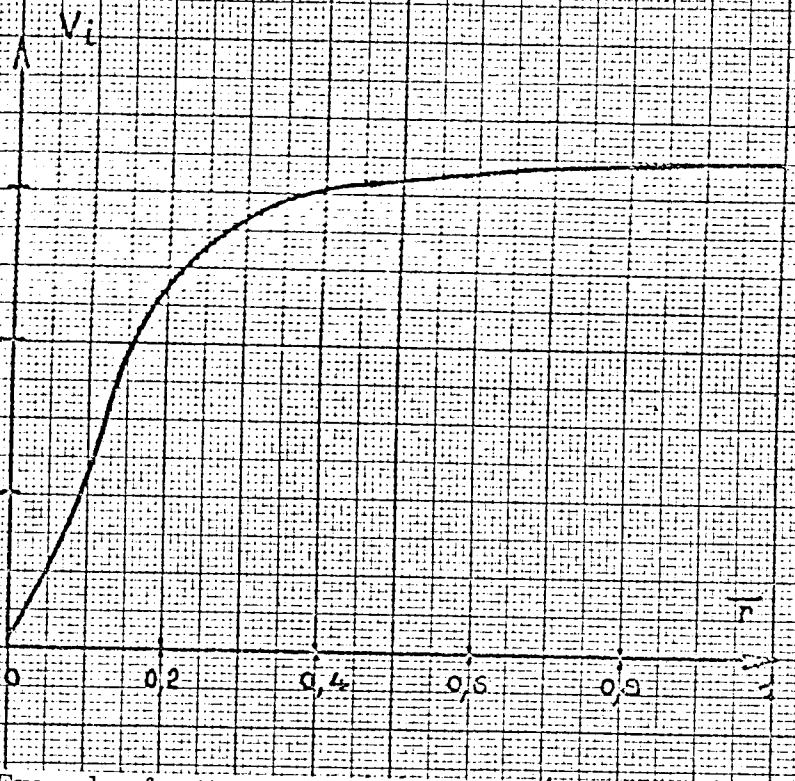

a) Example of optimum distribution of induced velocity

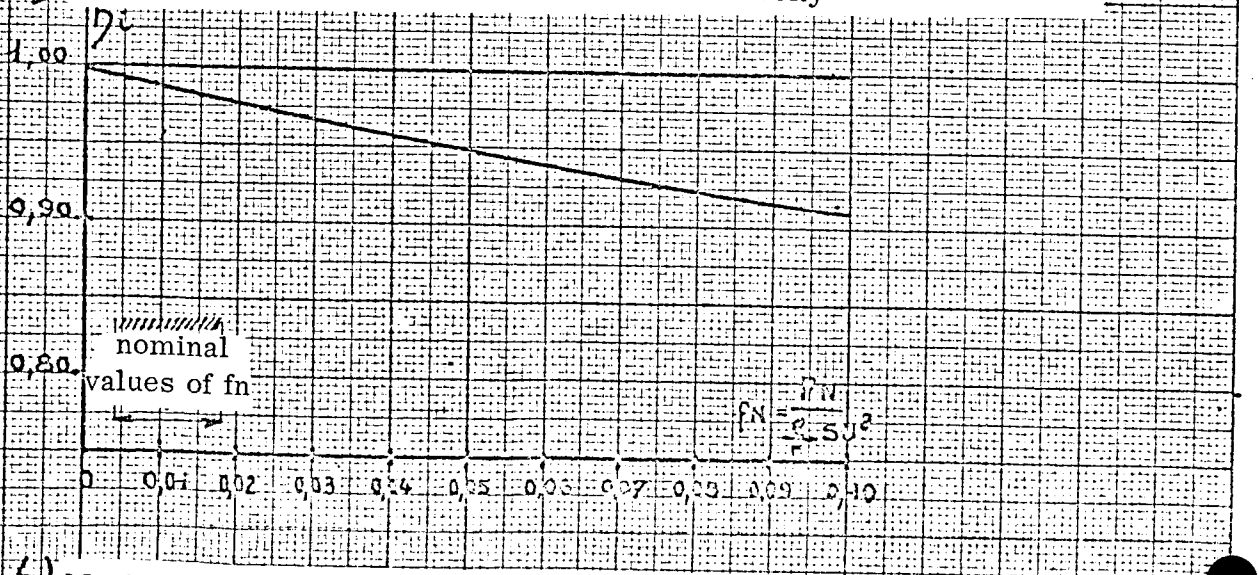

b) Maximum induced efficiency of a rotor

VELOCITIES INDUCED IN HOVERING

Plate II-4

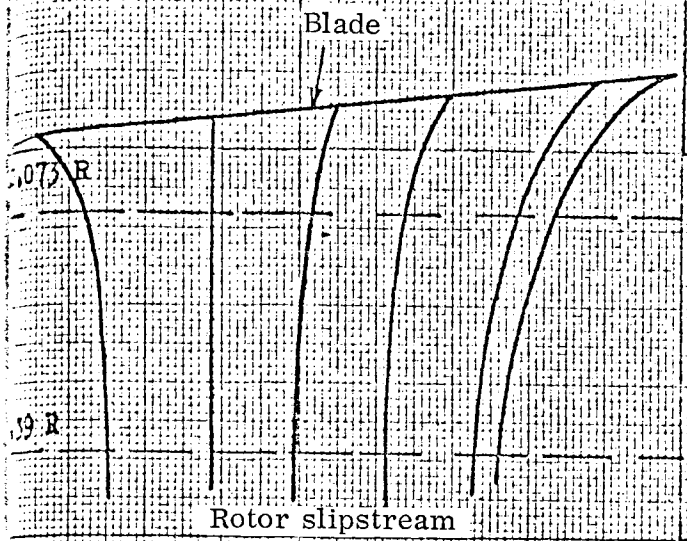

Experimental curves (Brotherhood (R and M n° 2521)

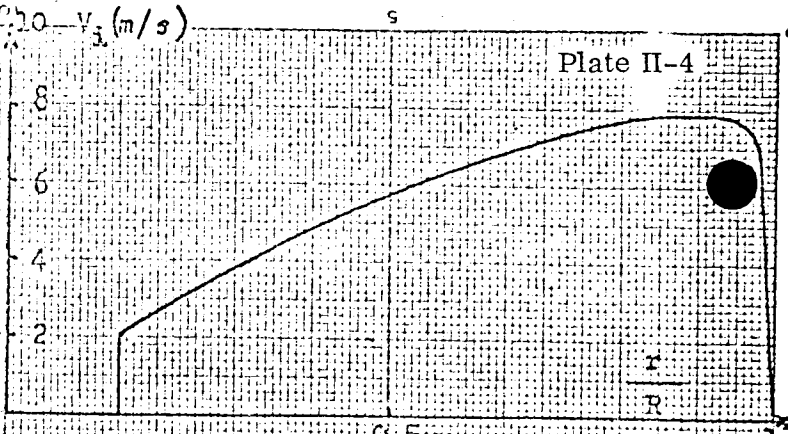

Induced velocities in the rotor plane

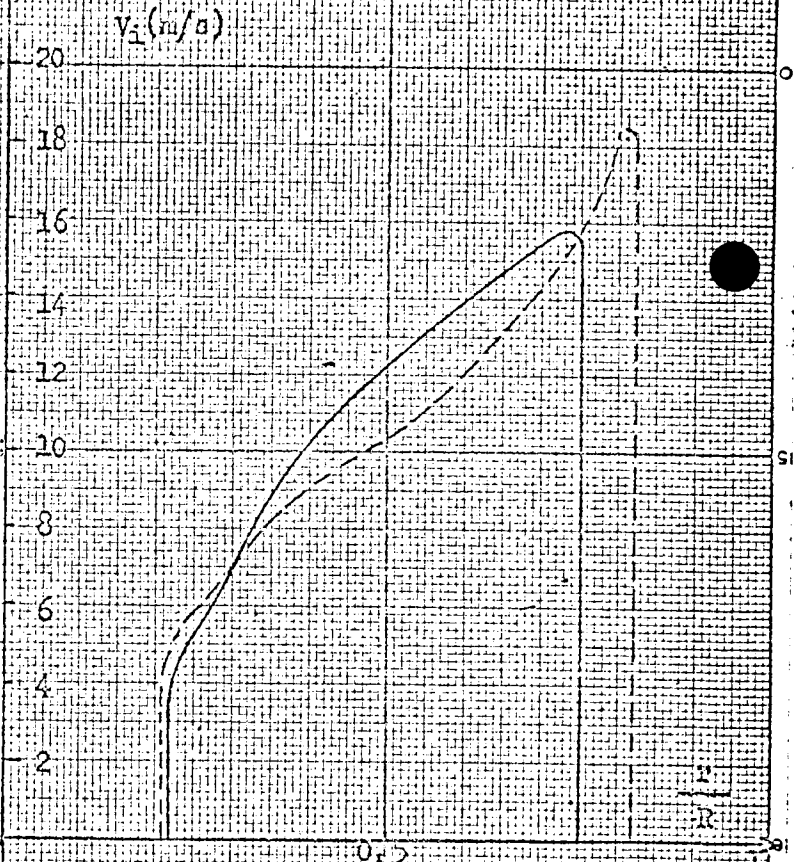

Velocities induced below the rotor

in a plane at 0.073 R from the rotor

in a plane at 0.39 R from the rotor

Remarks:

at 0.39 R the flow is steady (virtually infinity); note supervelocities under blade disk (not foreseen by Fronde's theory)

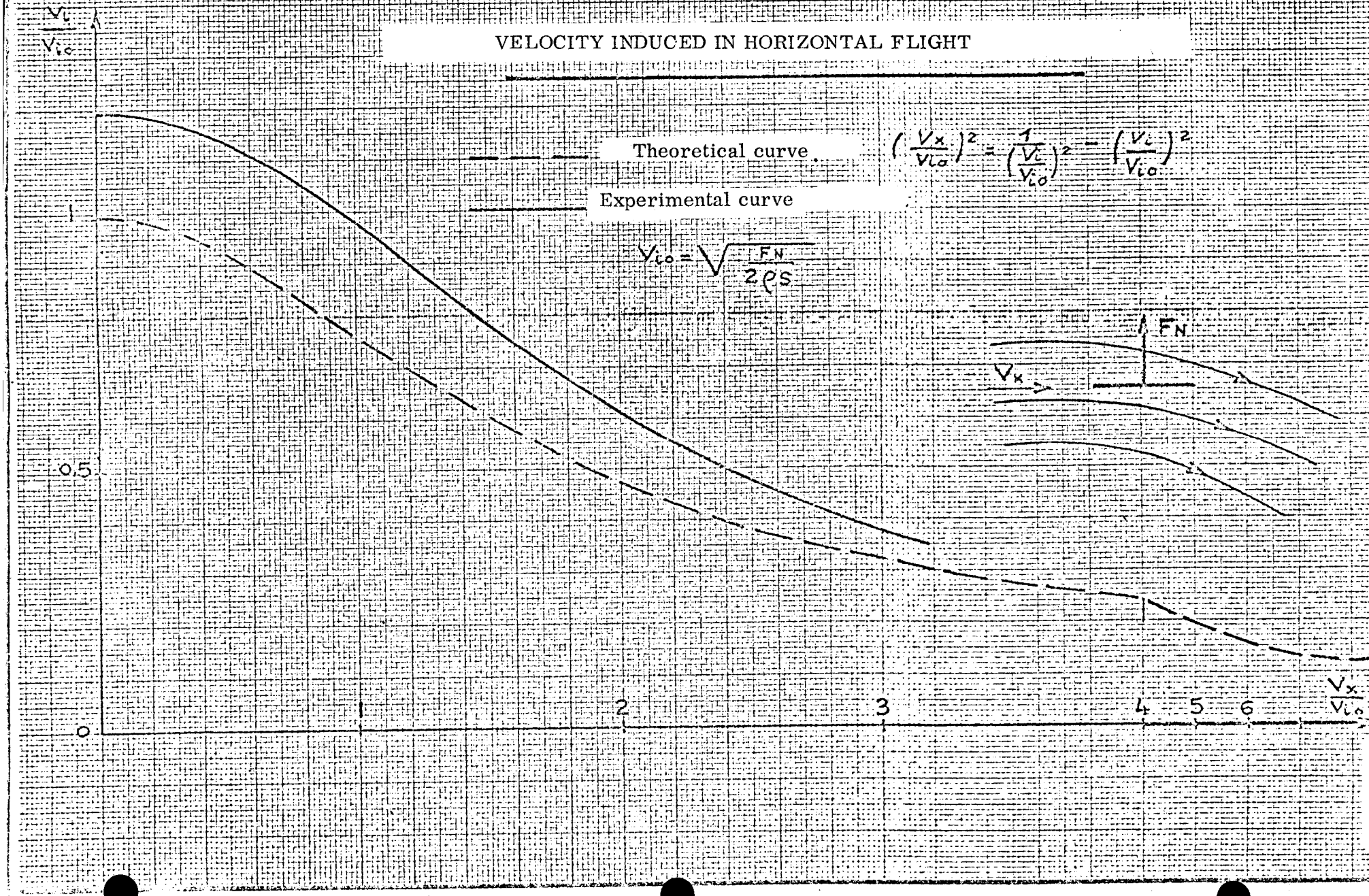
VELOCITY INDUCED IN HORIZONTAL FLIGHT
Vi / Vio
Theoretical curve
Experimental curve
$\left(\frac{V_x}{V_{io}}\right)^2 = \left(\frac{1}{\frac{V_i}{V_{io}}}\right)^2 - \left(\frac{V_i}{V_{io}}\right)^2$
$V_{io} = \sqrt{\frac{F_N}{2\rho S}}$
F_N
V_K
1
0,5
0
1
2
3
4
5
6
$\frac{V_x}{V_{io}}$

Plate II - 6 - A

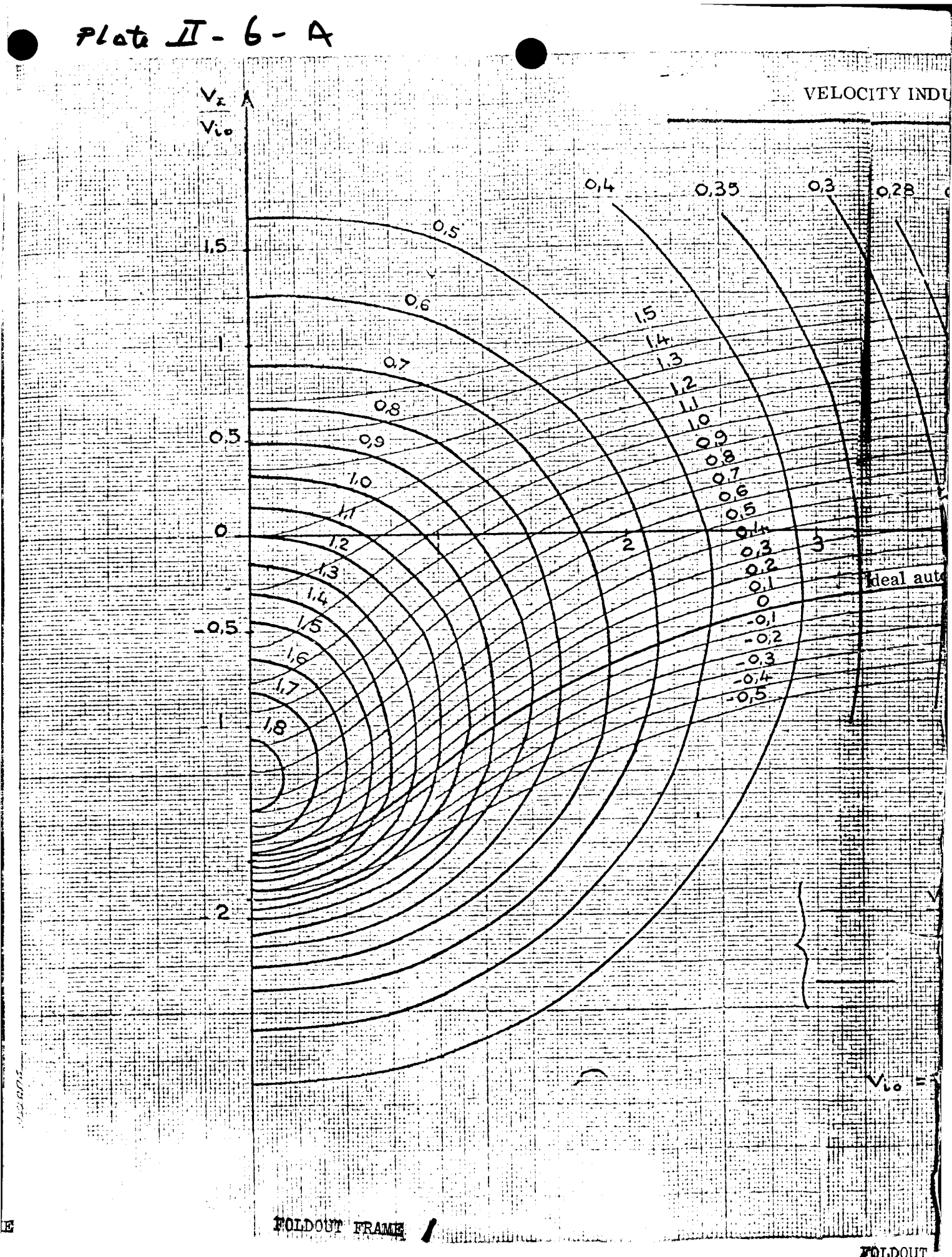
VELOCITY INDU
$\frac{V_x}{V_{i0}}$
1,5
1
0,5
0
-0,5
-1
-2
0,5
0,6
0,7
0,8
0,9
1,0
1,1
1,2
1,3
1,4
1,5
1,6
1,7
1,8
0,4
0,35
0,3
0,28
1,5
1,4
1,3
1,2
1,1
1,0
0,9
0,8
0,7
0,6
0,5
0,4
0,3
0,2
0,1
0
-0,1
-0,2
-0,3
-0,4
-0,5
2
3
Ideal aut
V_{i0} =

CED ACROSS THE ROTOR

(After A. Oliver)
(Report N°. AAEE/Res/264)

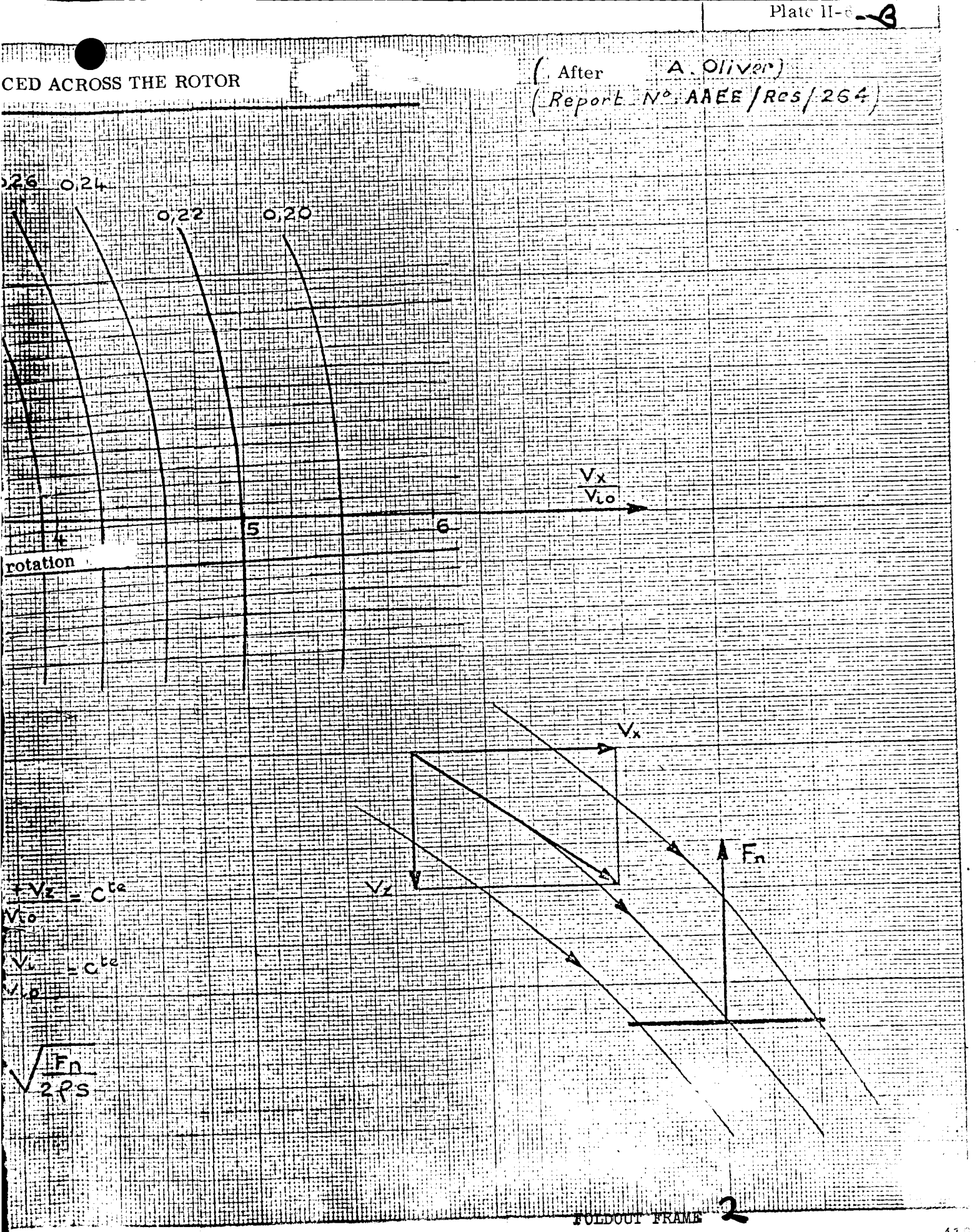

FOLDOUT FRAME 2

FRAME

DISTRIBUTION OF INDUCED VELOCITY AS A FUNCTION OF SPEED IN FORWARD FLIGHT

(After R. Colaroon, NACA, AAR N° L5F25b)

$$\frac{V_i}{V_{io}} = \frac{V_{im}}{V_{io}} + \frac{V_{ic}}{V_{io}} \frac{r}{R} \cos\psi$$

$$\left\{ \frac{V_{im}}{V_{io}}, \frac{V_{ic}}{V_{io}} \right.$$

$$V_{io} = \sqrt{\frac{F_N}{2\rho S}}$$

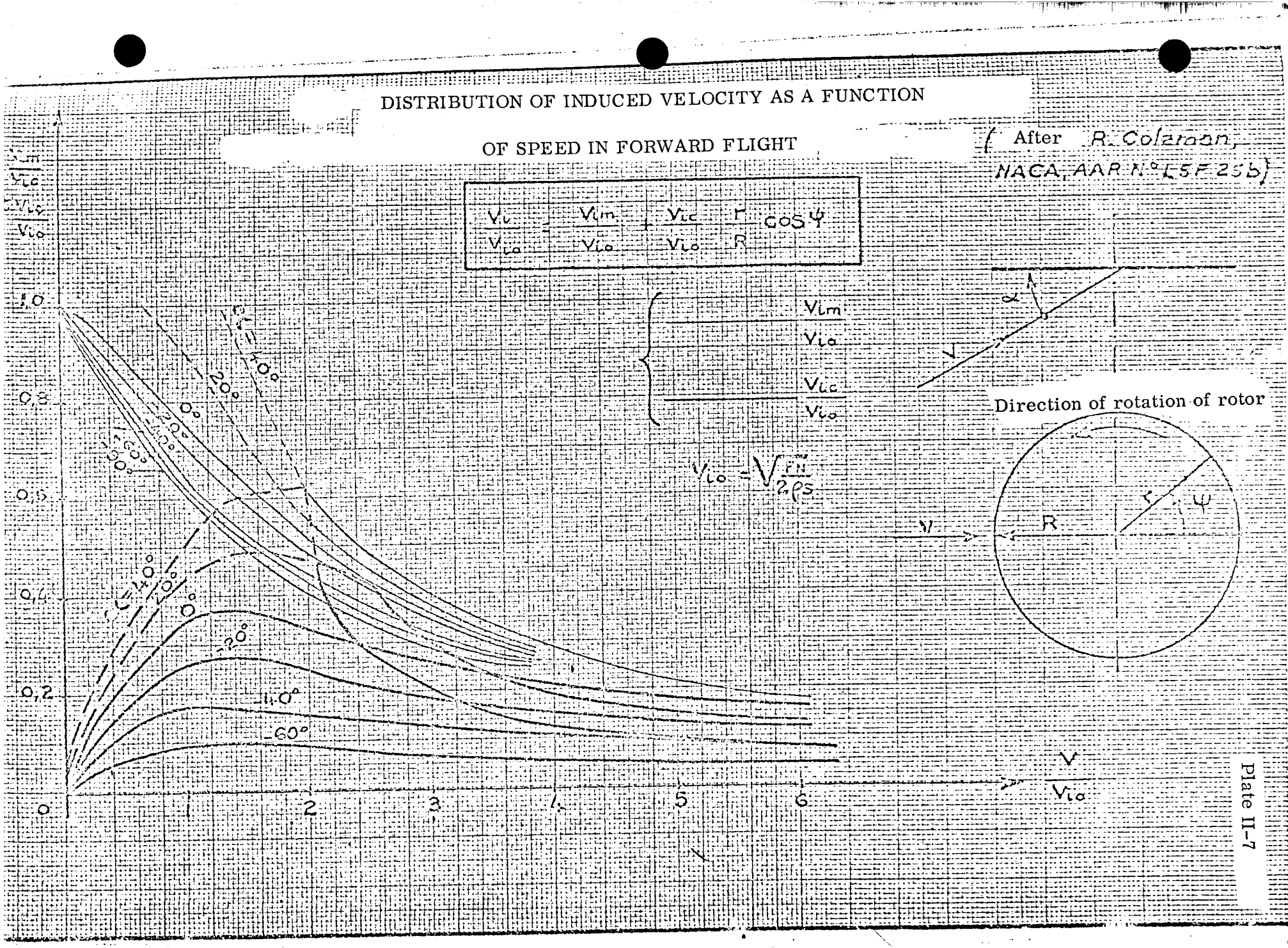

Plate II-7

DISTRIBUTION OF VELOCITIES INDUCED IN FORWARD FLIGHT ALONG THE OX-AXIS

(NACA TN 2912)

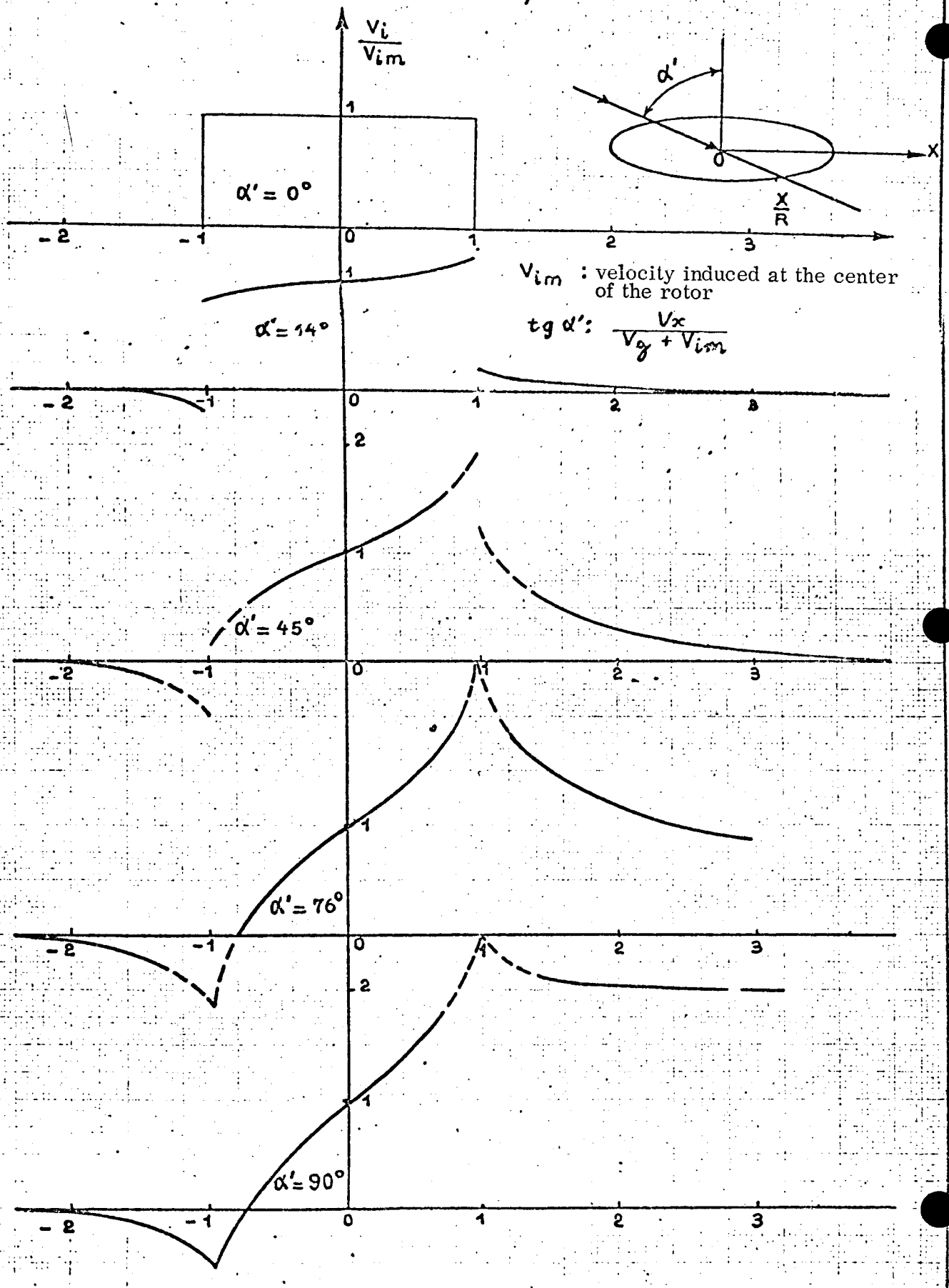

V_{im} : velocity induced at the center of the rotor

$tg\ \alpha' : \frac{V_x}{V_g + V_{im}}$

DISTRIBUTION OF INDUCED VELOCITIES IN TRANSLATION ALONG THE OY-AXIS

(NACA TN 2912)

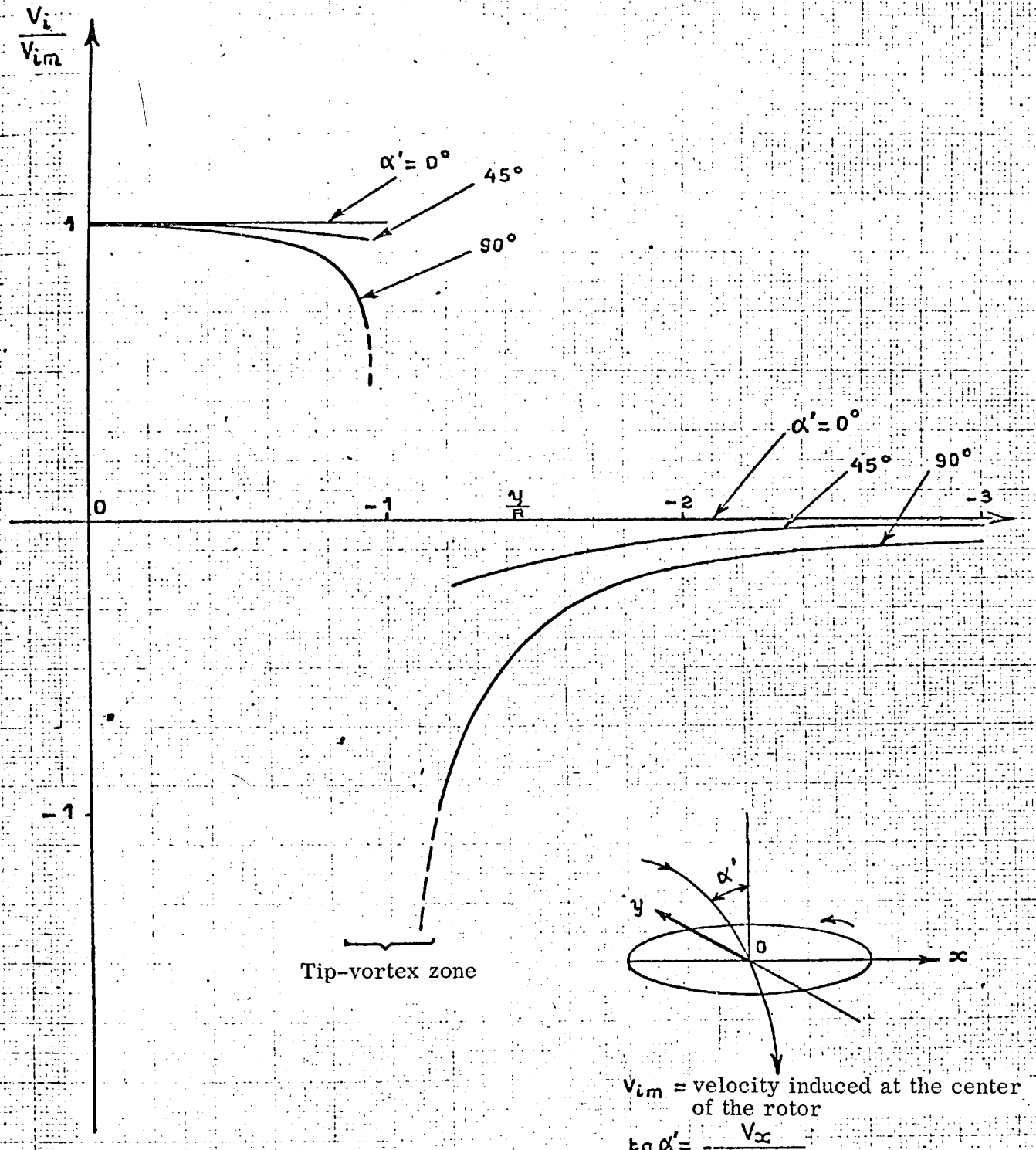

V_{im} = velocity induced at the center of the rotor

$$\operatorname{tg} \alpha' = \frac{V_x}{V_z + V_{im}}$$

POLAR DIAGRAM OF AUTOROTATION

(Lapresle)

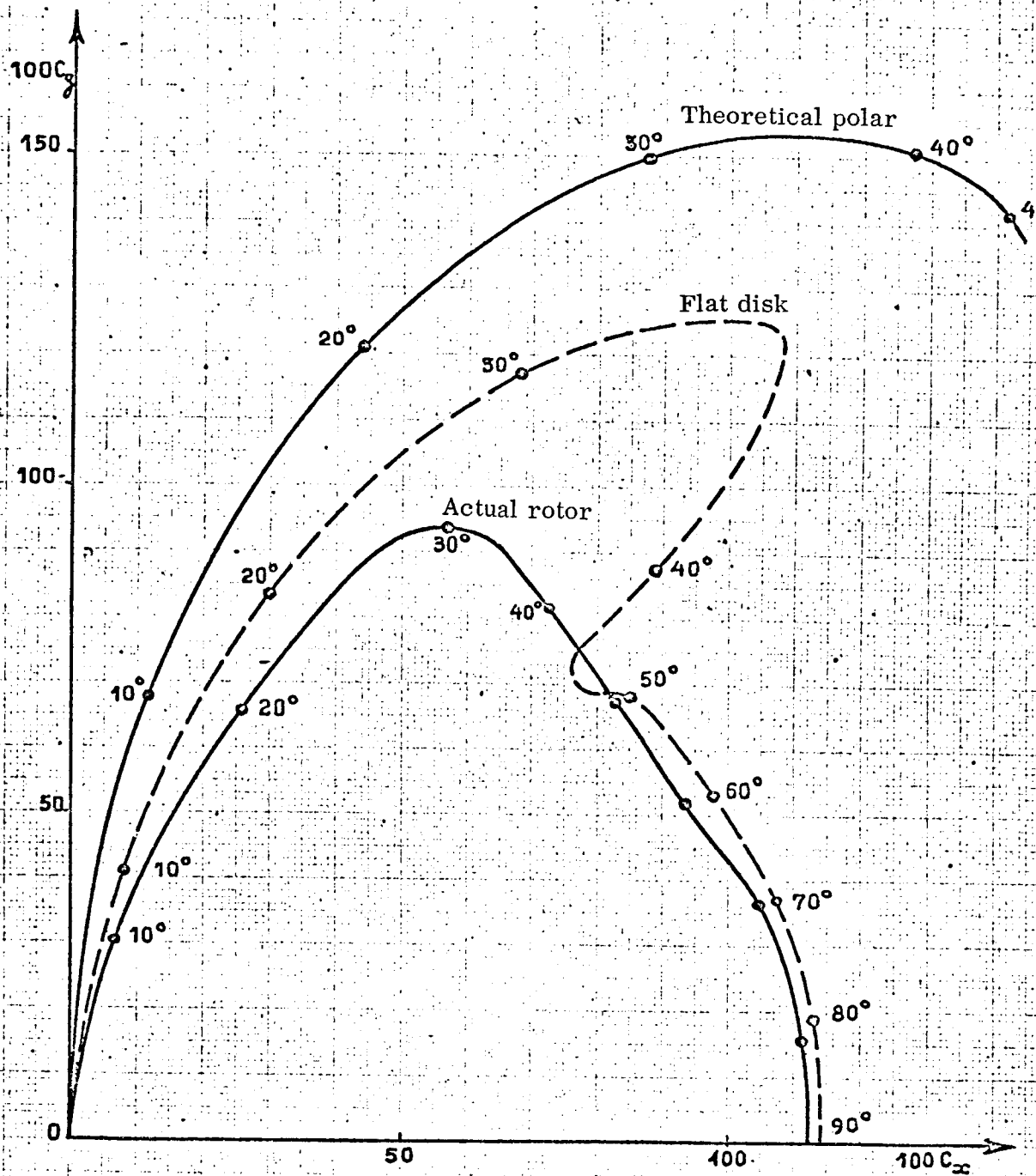

The curves are graduated in terms of angle of attack α of the disk

Note that Fx/Fg is always very close to tan α:
The resultant Fn is essentially normal to the rotor disk

POLAR DIAGRAM OF AUTOROTATION

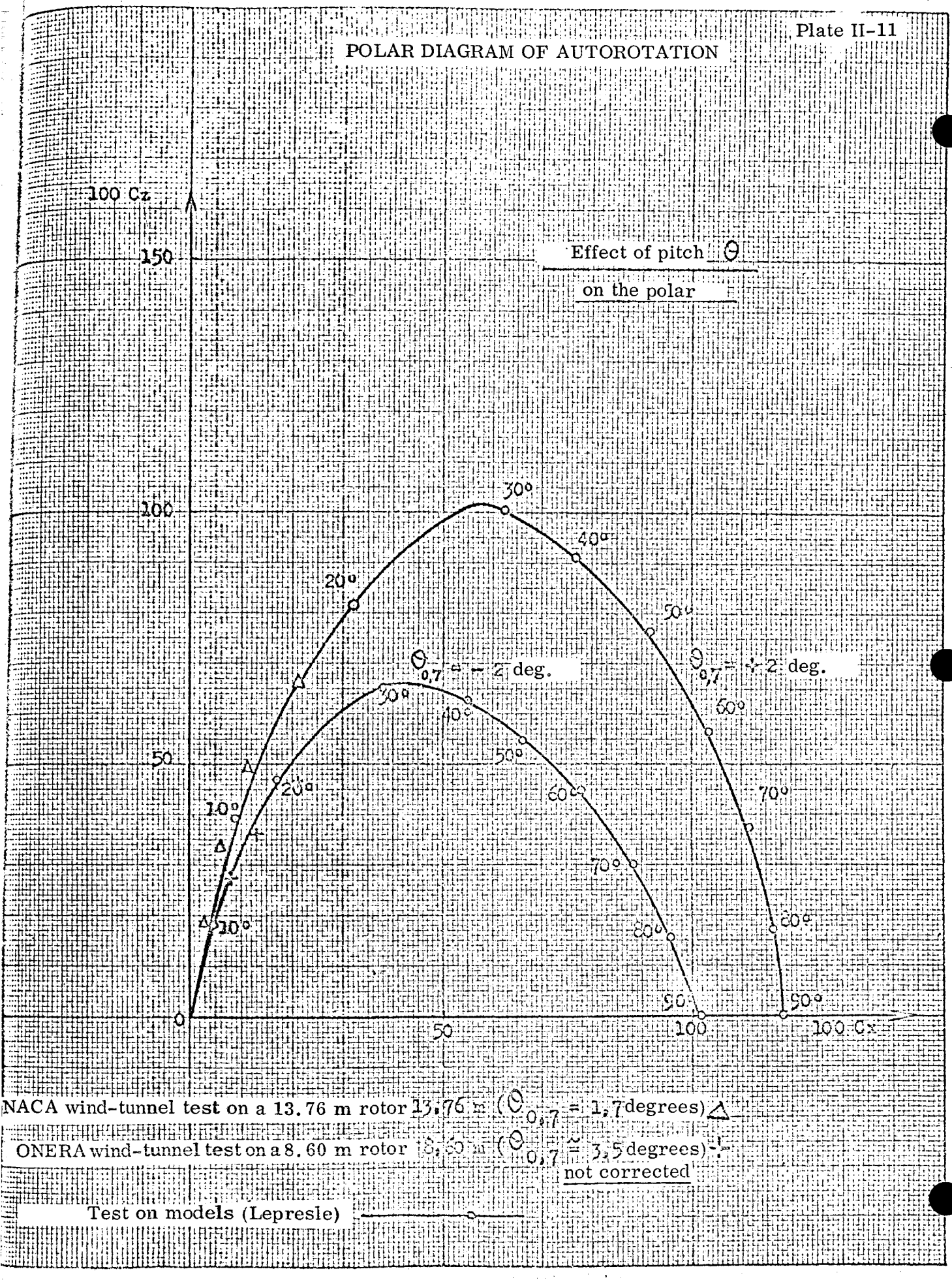

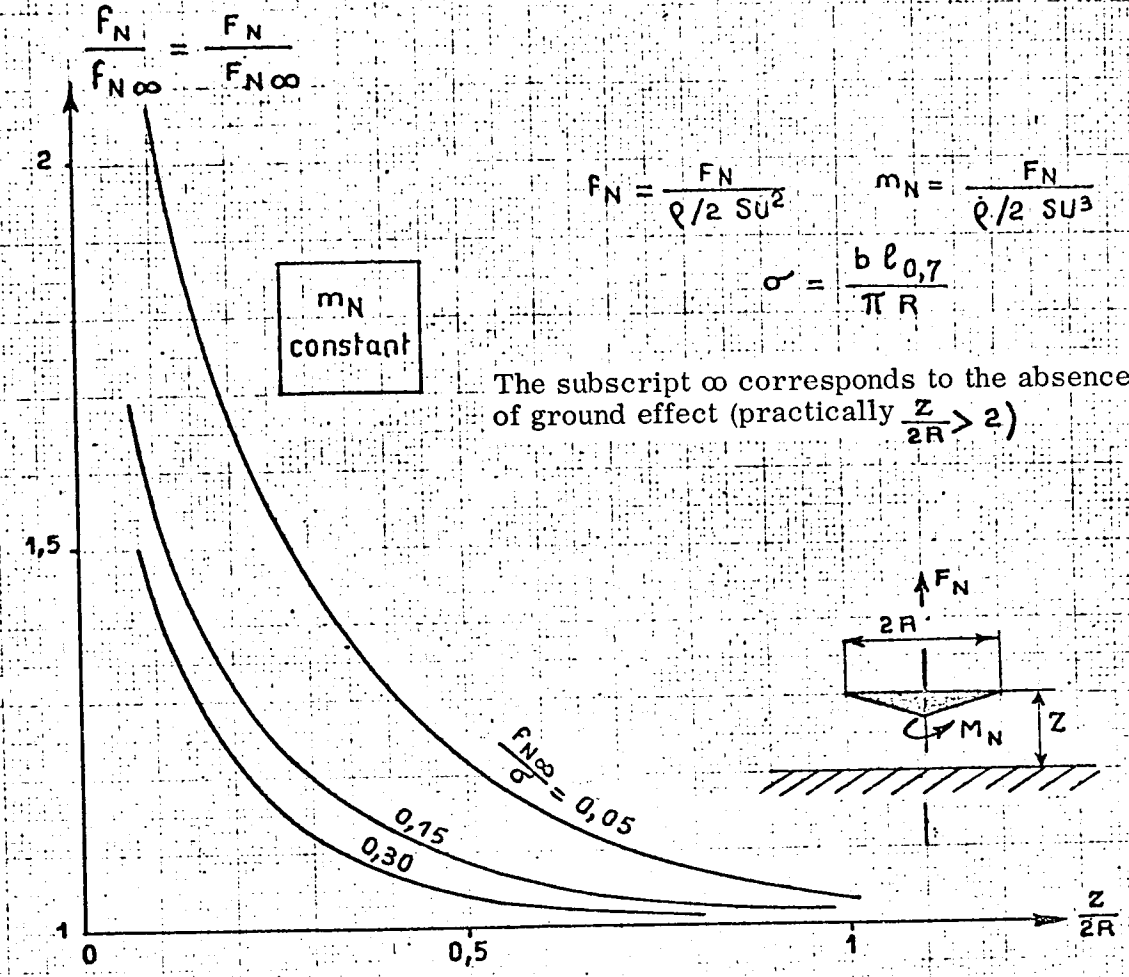

EFFECT OF THE GROUND ON THE PERFORMANCE
OF A ROTOR AT CONSTANT POWER
(After Zbrozek)

Coaxial rotors

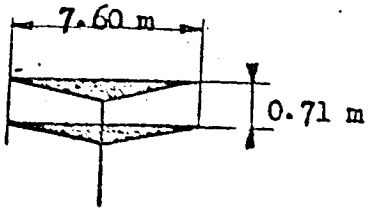

Rotor in tandem

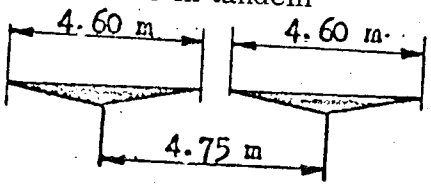

HOVERING

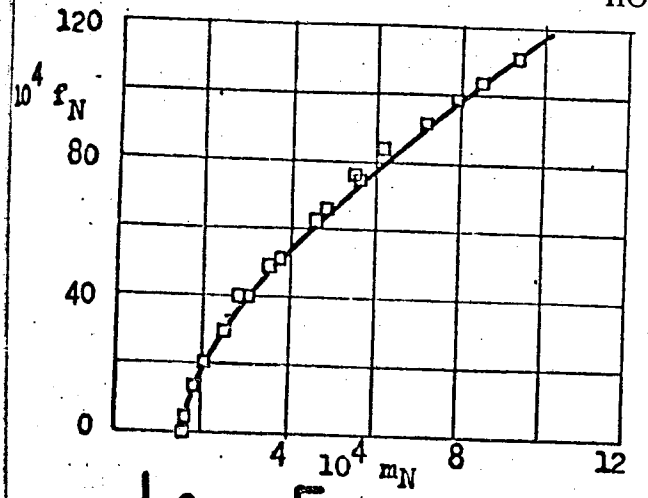

$$f_N = \frac{F_N}{\frac{\rho}{2} S \Omega^2 R^2}$$

$$m_N = \frac{P}{\frac{\rho}{2} S \Omega^3 R^3}$$

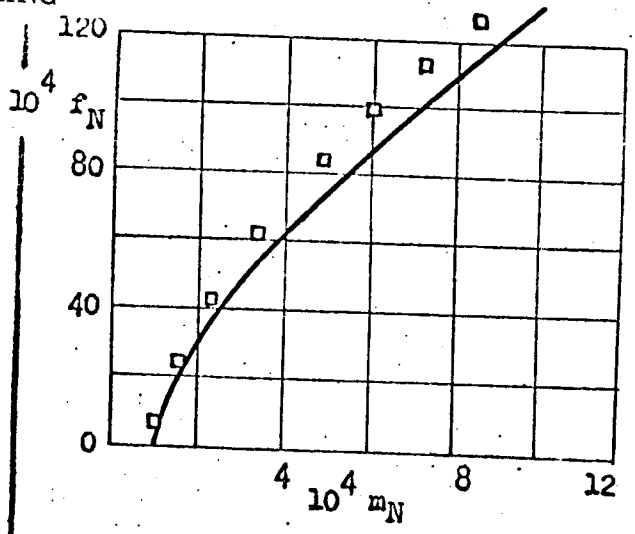

HORIZONTAL FLIGHT

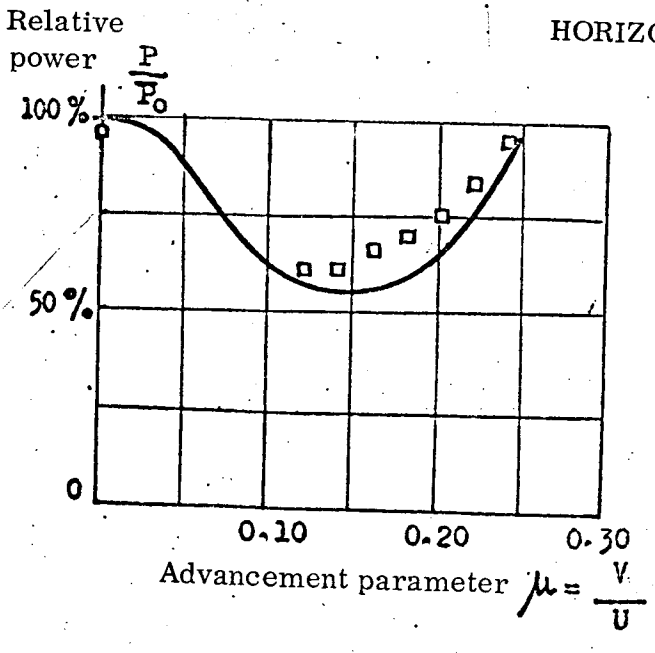

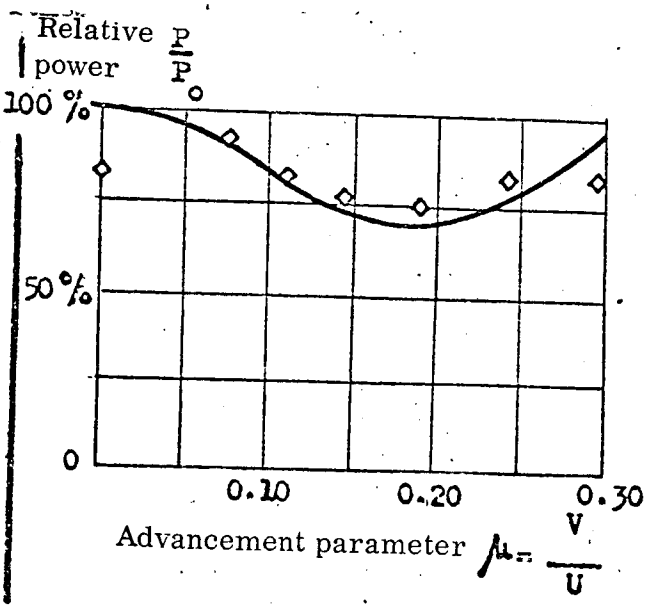

For the 4 diagrams, the solid lines relate to a single rotor of the same solidity σ.

Plate III-1

FLAPPING OF AN ARTICULATED-BLADE ROTOR

MOCKUP ROTOR

R = 0,933 m
σ = 0,057
ρ_z = 0,176

Flapping calculated by approximate formulas of Appendix III-2

The preceding flapping calculated for the effect of unequal induced velocities (Formulas 2-27)

Curve and experimental plots

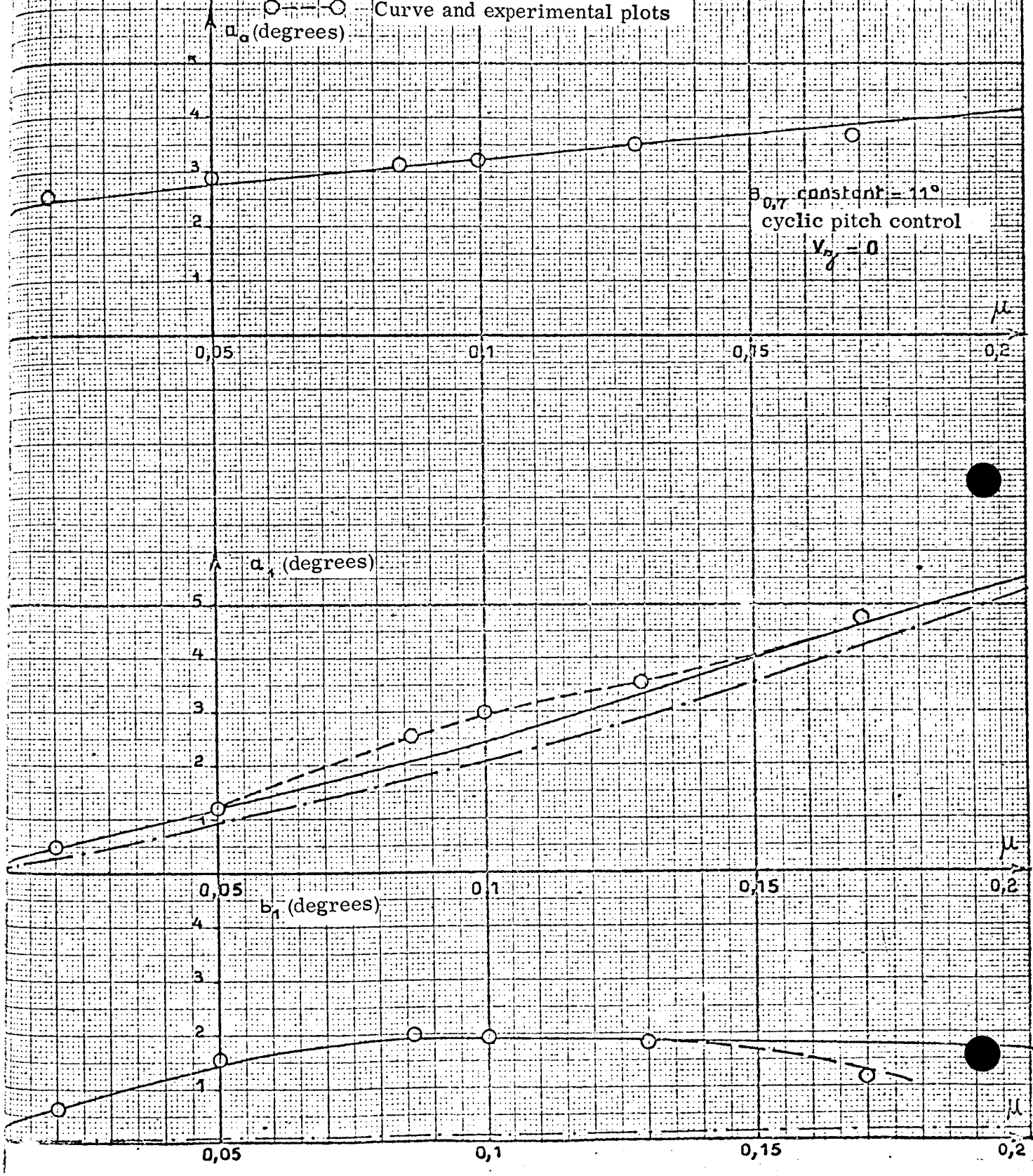

OPERATIONAL LIMIT OF AN ARTICULATED-BLADE ROTOR DUE TO TIP STALL OF A RETREATING BLADE

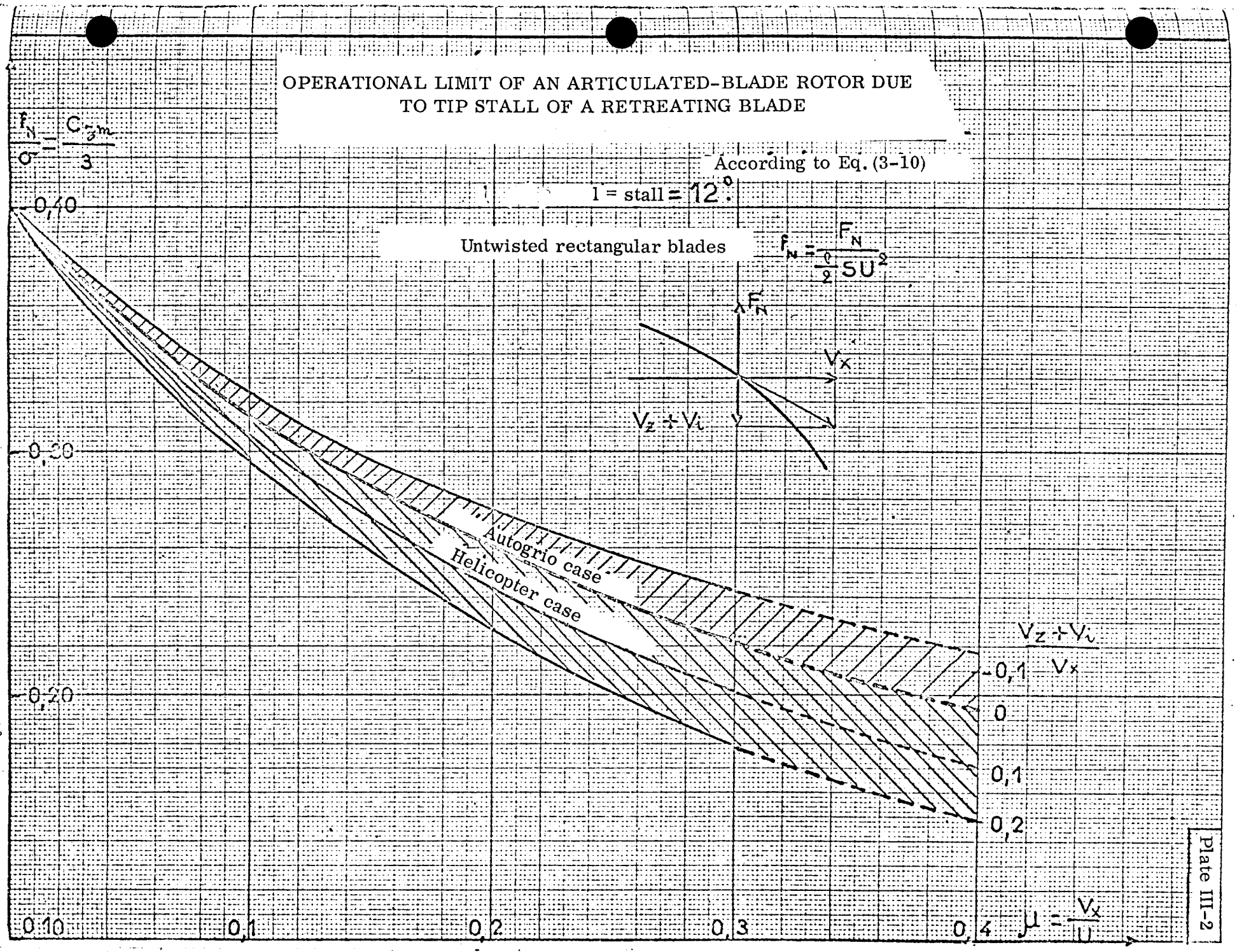

Plate III-2

SPEED LIMITATIONS OF AN ARTICULATED-BLADE ROTOR DUE TO TIP STALL OF THE RETREATING BLADE (HELICOPTER FLIGHT); according to [2].

Experimental statistical curve valid

for $C_{z\,max} = 1{,}2$ — moderate twist

$$(U - V_x)\sqrt{\frac{\rho}{\rho_0}} \simeq 6{,}95\sqrt{\frac{F_N}{S\sigma C_{z\,max}}} \qquad C_{z\,max} = 1{,}2$$

Example: $\frac{F}{S\sigma} = 400\ kg/m^2$ — $U = 200$ m/sec — $\frac{\rho}{\rho_0} = 0{,}9$

Read on the curve are:

$$(U - V_x)\sqrt{\frac{\rho}{\rho_0}} = 126{,}5 \text{ m/sec}$$

$$U - V_x = \frac{126{,}5}{\sqrt{0{,}9}} = 134 \text{ m/sec}$$

$V_x = 200 - 134 = 66$ m/sec = 238 km/hr

If $C_{z\,max} \neq 1{,}2$, correct $(U - V_x)\sqrt{\frac{\rho}{\rho_0}}$ by the factor $\sqrt{\frac{1{,}2}{C_{z\,max}}}$

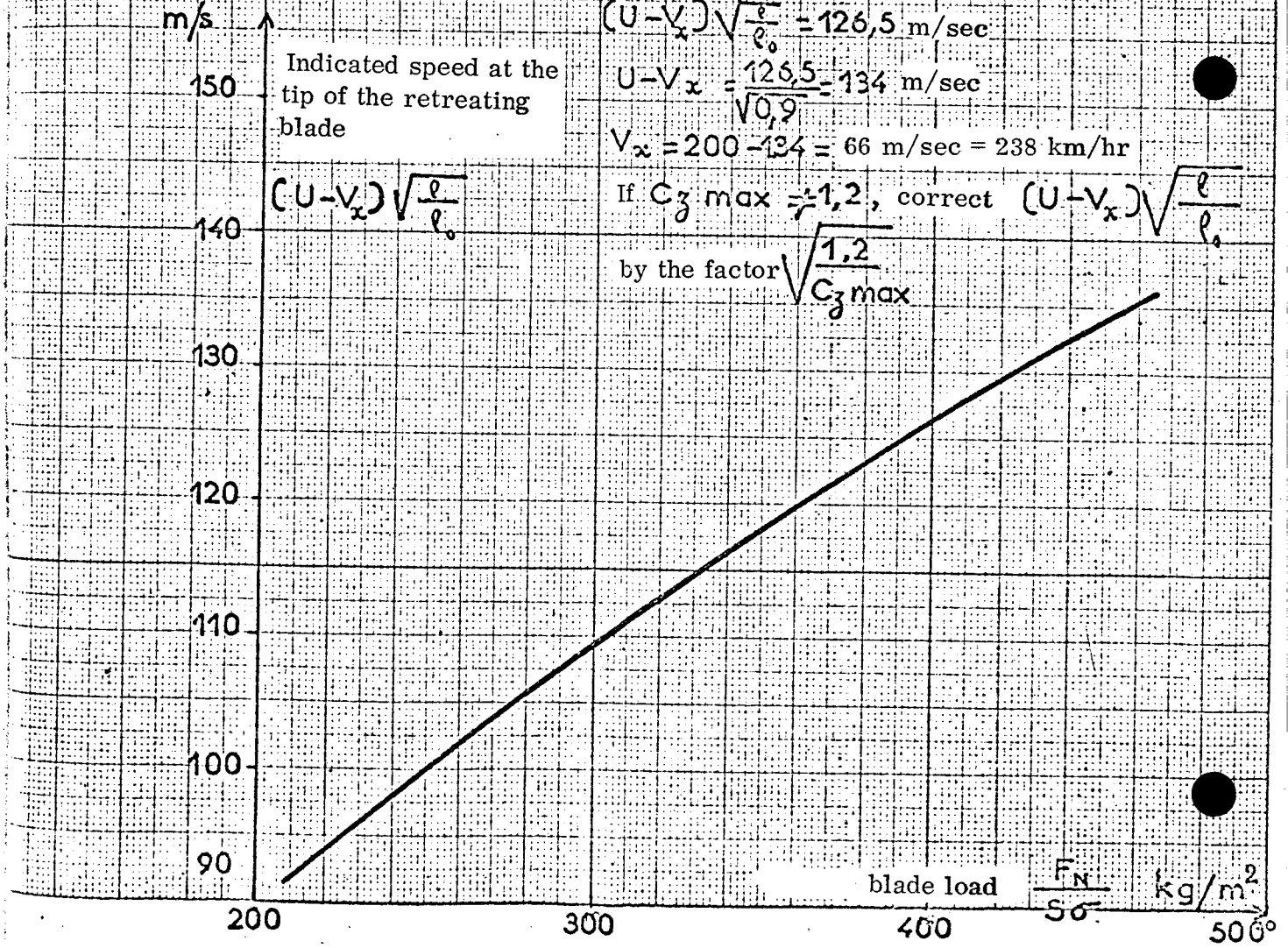

CORRECTION FOR THE RESPONSE TIME OF THE ROTOR (Sissingh); according to [1].

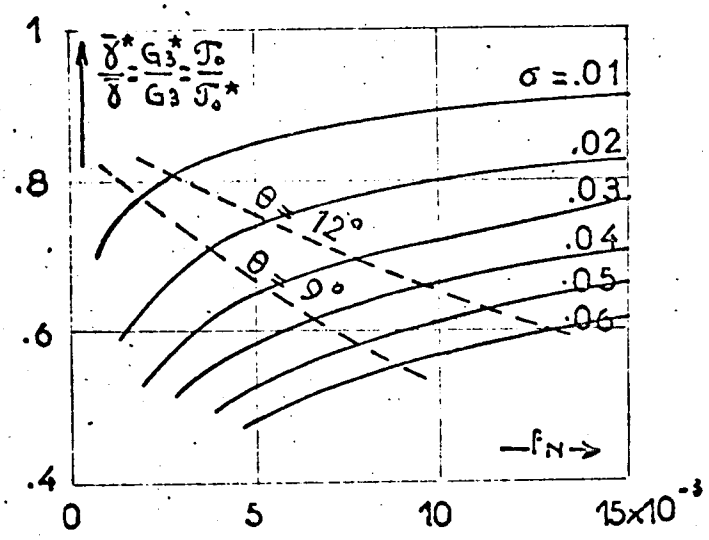

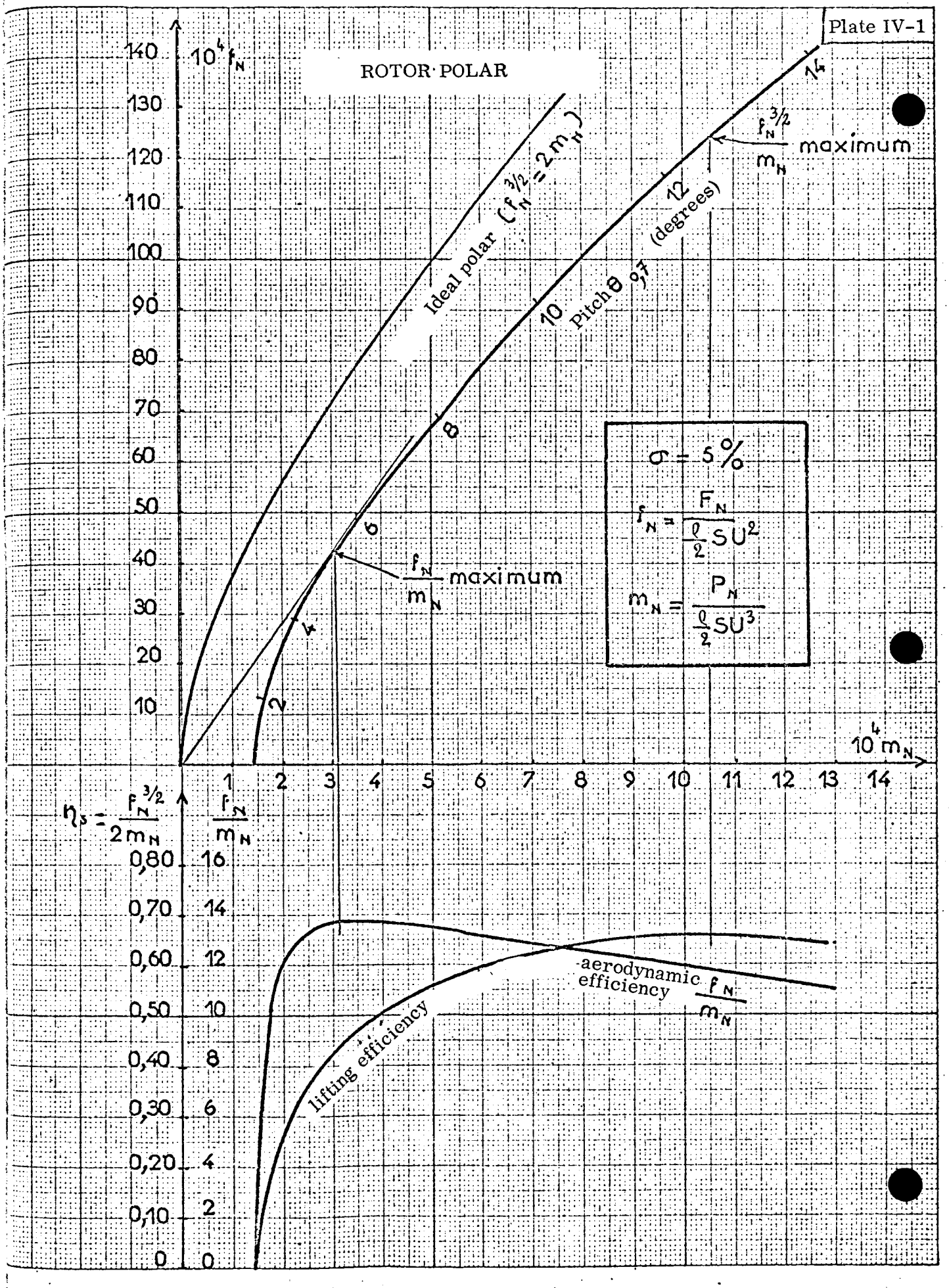
ROTOR POLAR
$10^4 f_N$
140
130
120
110
100
90
80
70
60
50
40
30
20
10
Ideal polar ($f_N^{3/2} = 2 m_N$)
Pitch θ 0,7
(degrees)
14
12
10
8
6
4
2
$\frac{f_N^{3/2}}{m_N}$ maximum
$\frac{f_N}{m_N}$ maximum
$\sigma = 5\%$
$f_N = \frac{F_N}{\frac{\rho}{2} S U^2}$
$m_N = \frac{P_N}{\frac{\rho}{2} S U^3}$
$10^4 m_N$
1 2 3 4 5 6 7 8 9 10 11 12 13 14
$\eta_s = \frac{f_N^{3/2}}{2 m_N}$
$\frac{f_N}{m_N}$
0,80
0,70
0,60
0,50
0,40
0,30
0,20
0,10
0
16
14
12
10
8
6
4
2
0
aerodynamic efficiency $\frac{f_N}{m_N}$
lifting efficiency

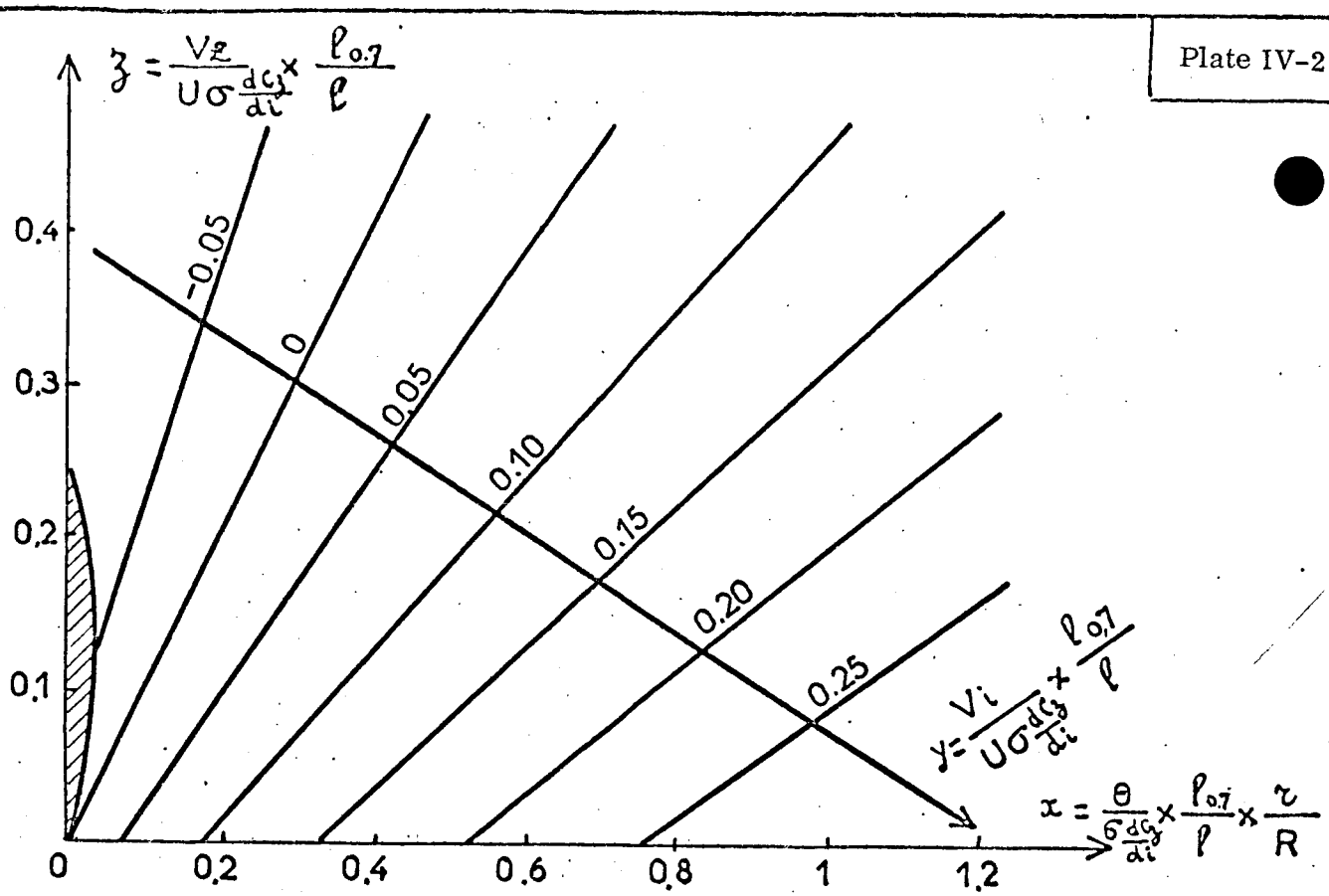

Distribution of induced velocity in vertical flight

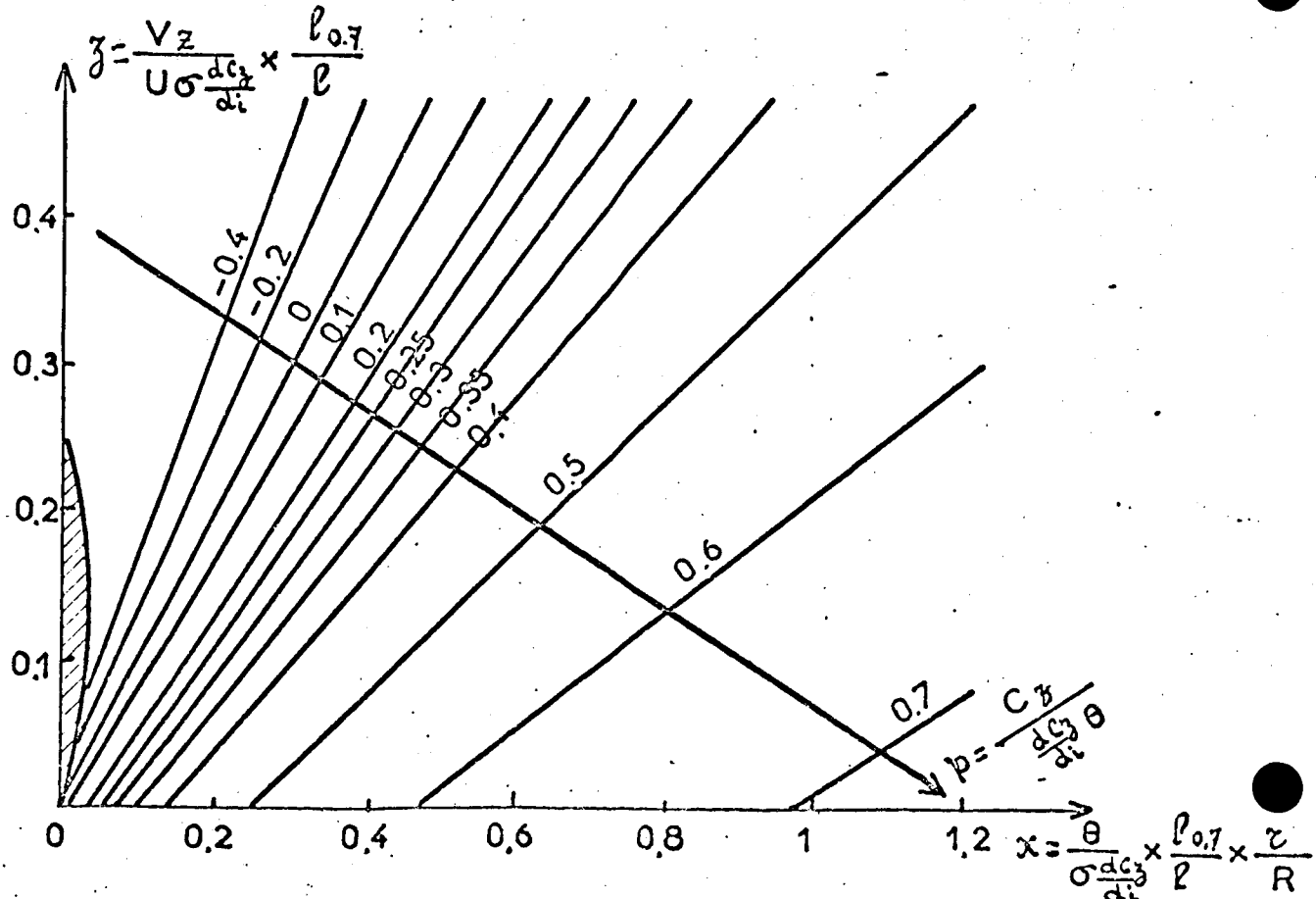

Distribution of C_z in vertical flight

GRAPH FOR CALCULATING THE INDUCED PITCH ANGLE IN HOVERING

$$\frac{1}{\frac{b\bar{l}}{2\pi\bar{r}}\left(\frac{dc_z}{di}\right)_\infty}$$

$\left[\left(\frac{dc_z}{di}\right)_\infty$ in C_z per degree$\right]$

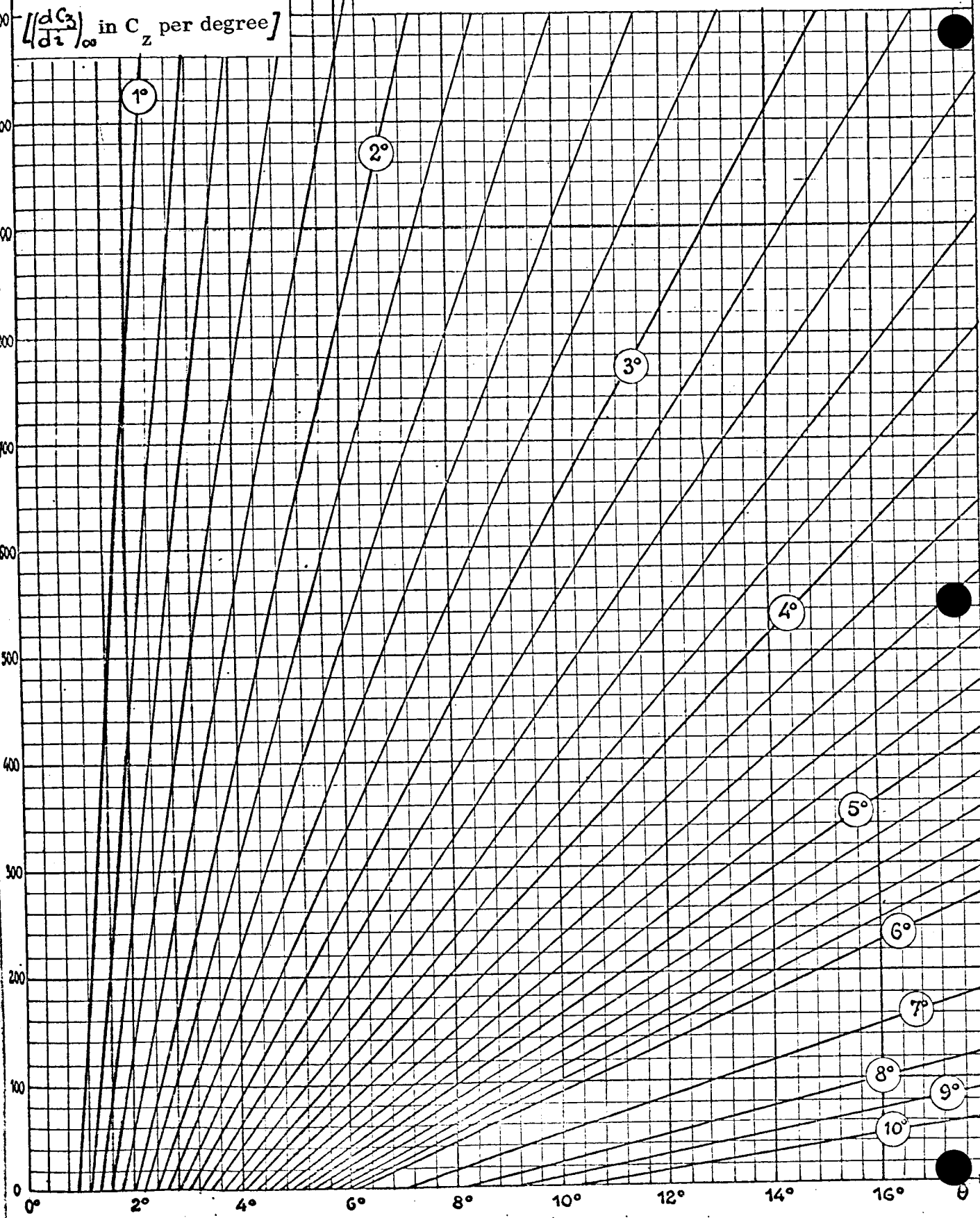

GRAPH FOR CALCULATING THE THRUST IN HOVERING

$F_N = \frac{\rho}{2} \pi R^2 \omega^2 R^2 . \mathcal{E} . 10^{-4}$ ($\mathcal{E}$ = integrated area in cm^2) Scale: 1 cm^2 = 0.002 x 0.05 = 0.0001

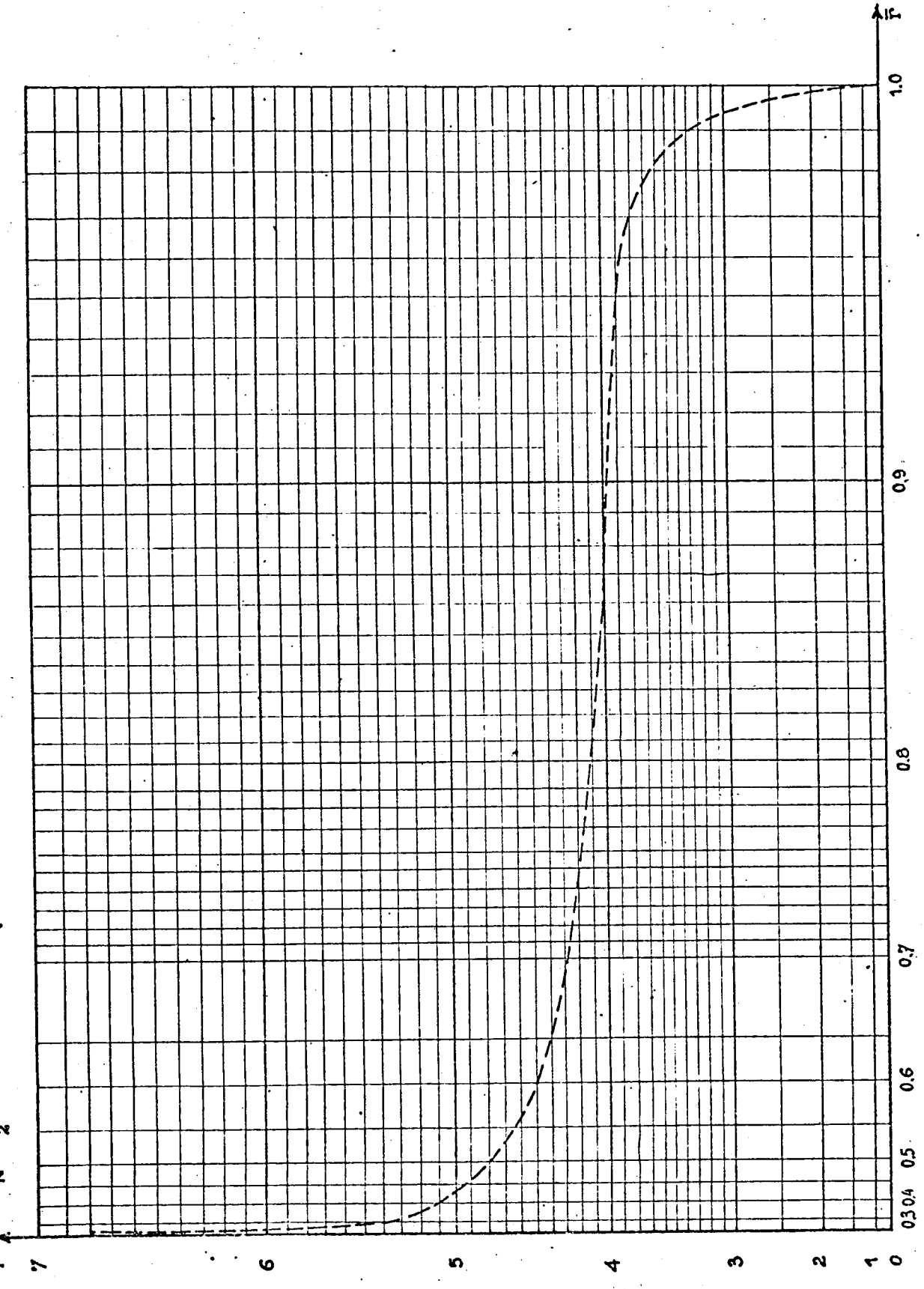

PRECEDING PAGE BLANK NOT FILMED.

CORRECTIONS FOR BLADE TIP LOSSES (After P. R. Payne)

(Based on R&M - 1674 by Lock and Yeatman)

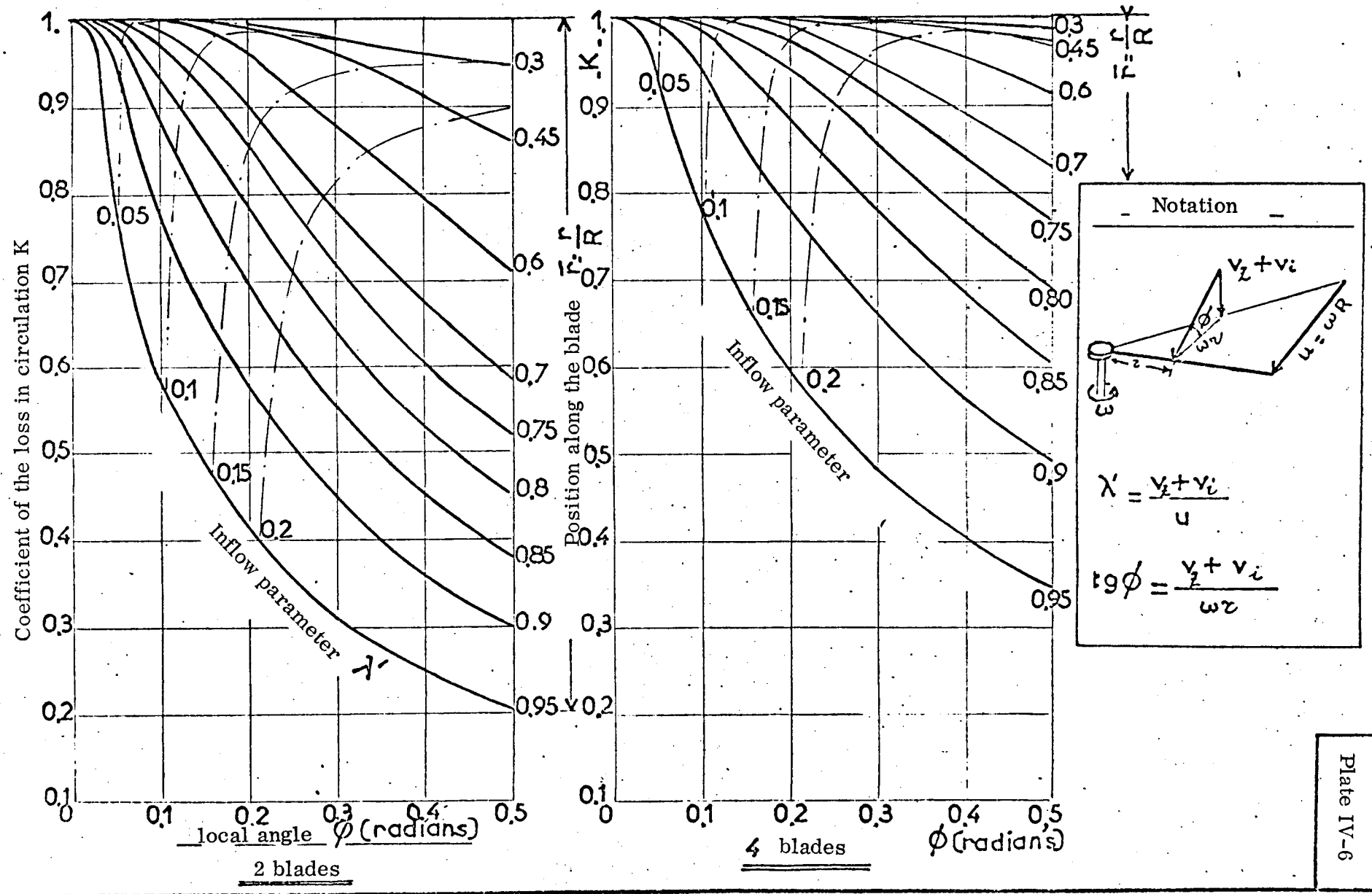

Plate IV-6

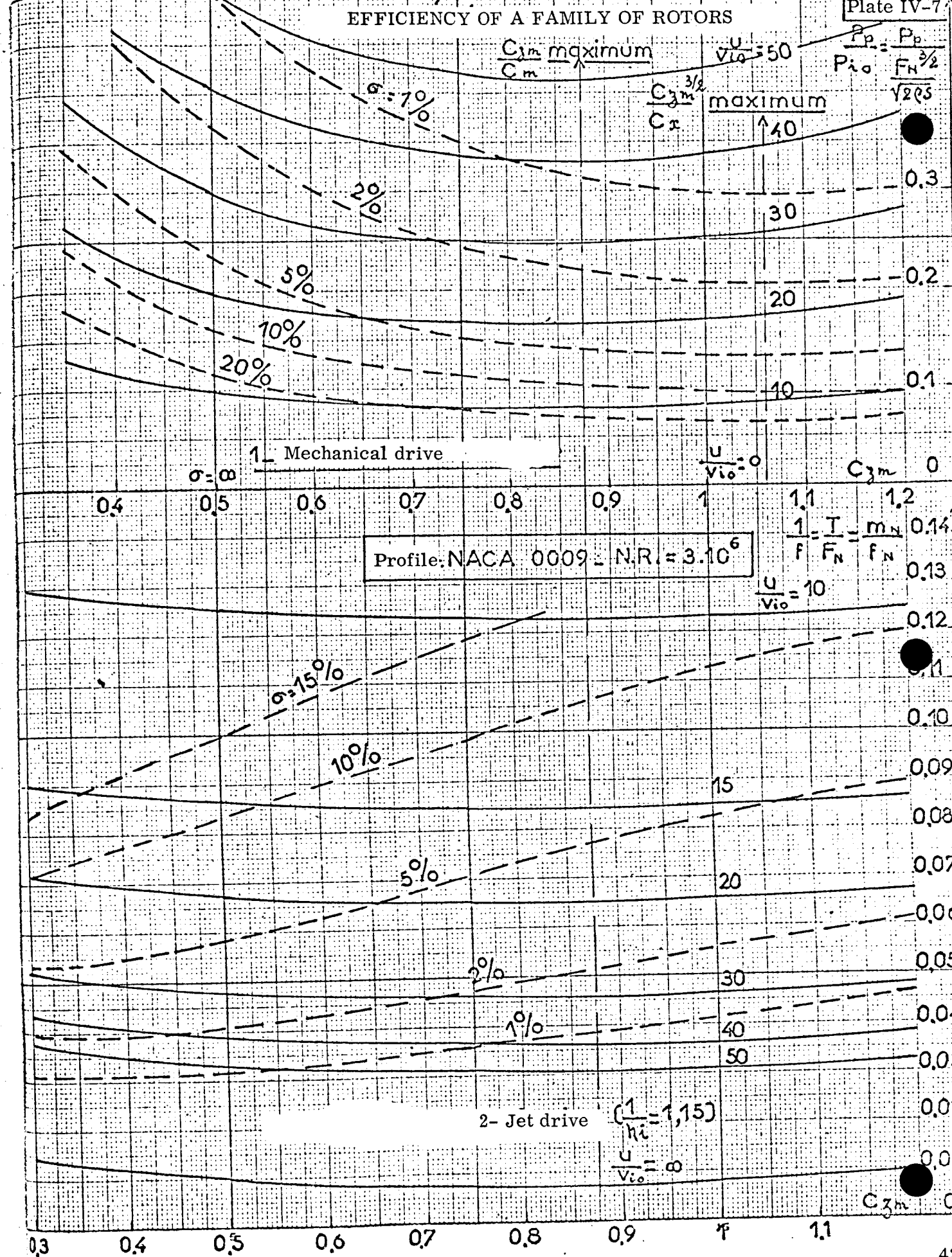
EFFICIENCY OF A FAMILY OF ROTORS
$\frac{C_{3m}}{C_m}$ maximum
$\frac{C_{3m}^{3/2}}{C_x}$ maximum
$\frac{P_p}{P_{i_0}} = \frac{P_p}{\frac{F_N^{3/2}}{\sqrt{2\rho S}}}$
$\frac{u}{v_{i_0}} = 50$
40
30
20
10
$\sigma = 7\%$
2%
5%
10%
20%
0.3
0.2
0.1
1- Mechanical drive
$\sigma = \infty$
$\frac{u}{v_{i_0}} = 0$
C_{3m} 0
0.4 0.5 0.6 0.7 0.8 0.9 1 1.1 1.2
$\frac{1}{f} = \frac{T}{F_N} = \frac{m_N}{f_N}$
0.14
0.13
Profile: NACA 0009 - N.R. = 3.10^6
$\frac{u}{v_{i_0}} = 10$
0.12
0.11
0.10
$\sigma = 15\%$
10%
15
0.09
0.08
5%
20
0.07
0.06
2%
30
0.05
1%
40
0.04
50
0.03
2- Jet drive ($\frac{1}{hi} = 1,15$)
$\frac{u}{v_{i_0}} = \infty$
0.02
0.01
C_{3m} 0
0.3 0.4 0.5 0.6 0.7 0.8 0.9 1 1.1

EFFICENCY OF A ROTOR IN HOVERING (After A. Stepan)

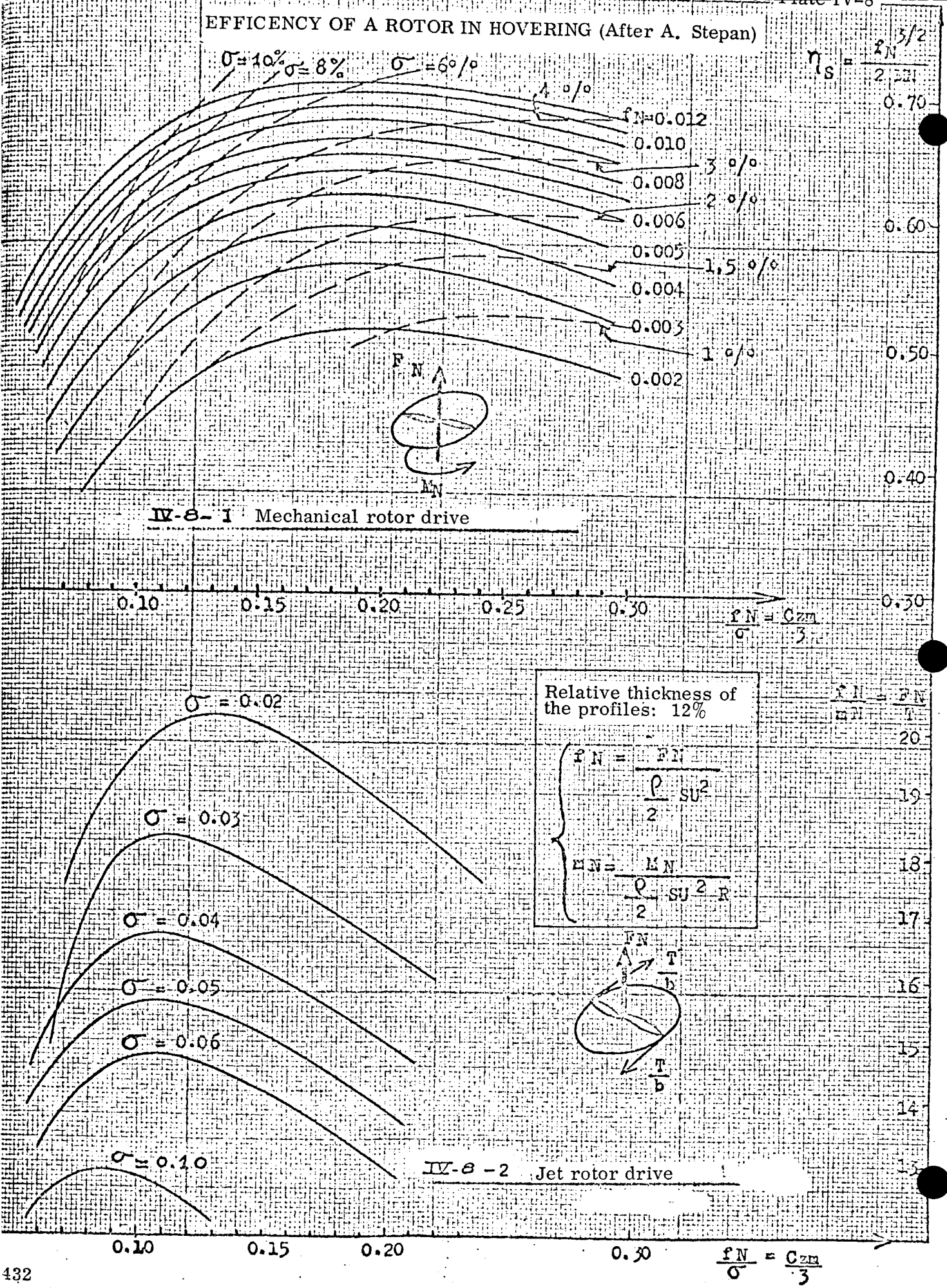

IV-8-1 Mechanical rotor drive

Relative thickness of the profiles: 12%

$$f_N = \frac{F_N}{\frac{\rho}{2} S u^2}$$

$$m_N = \frac{M_N}{\frac{\rho}{2} S u^2 R}$$

IV-8-2 Jet rotor drive

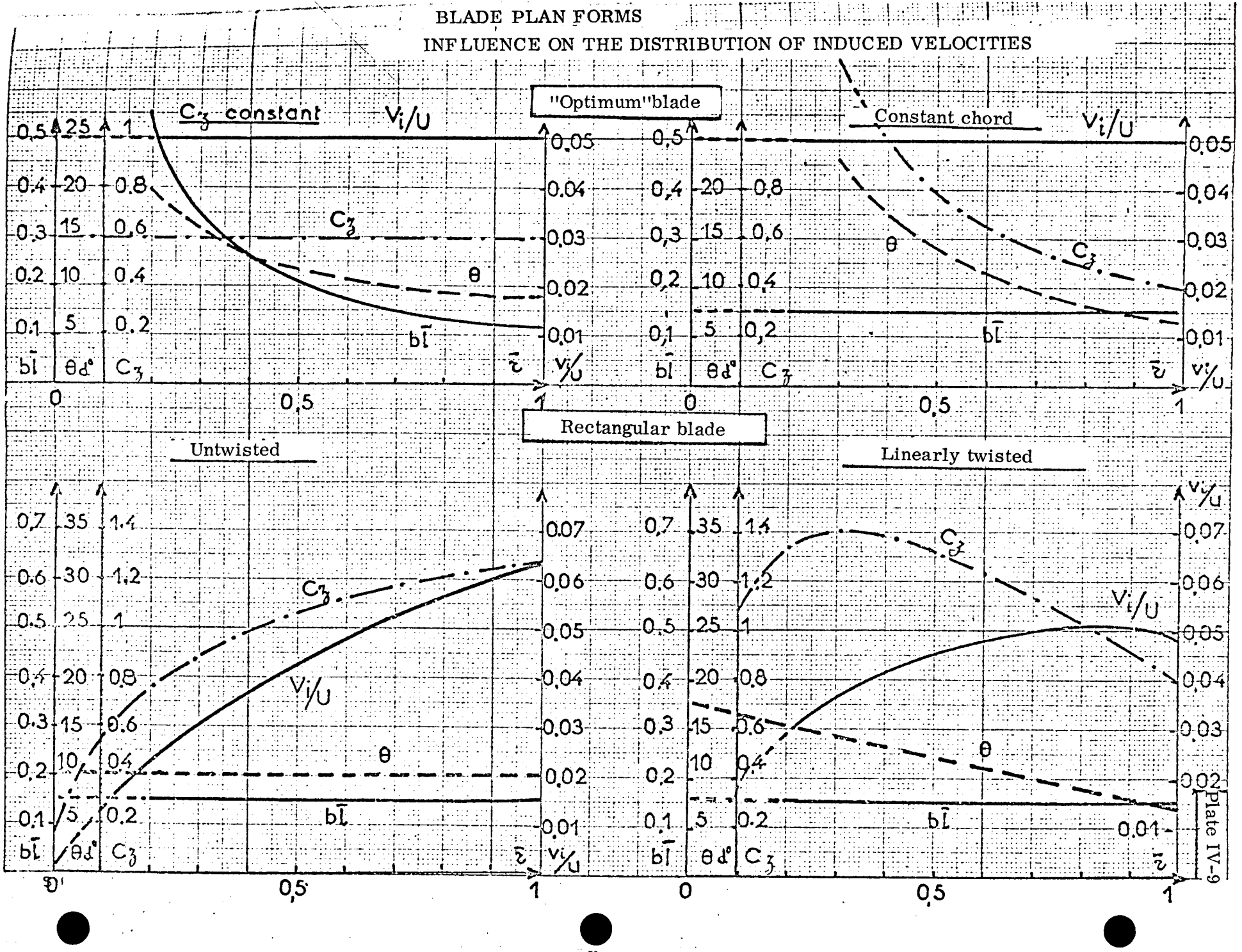
BLADE PLAN FORMS
INFLUENCE ON THE DISTRIBUTION OF INDUCED VELOCITIES
"Optimum" blade
Cz constant
Vi/U
Cz
θ
b̄l̄
r̄
Constant chord
Rectangular blade
Untwisted
Linearly twisted
Plate IV-9

POWER AS A FUNCTION OF VELOCITY

Helicopter A

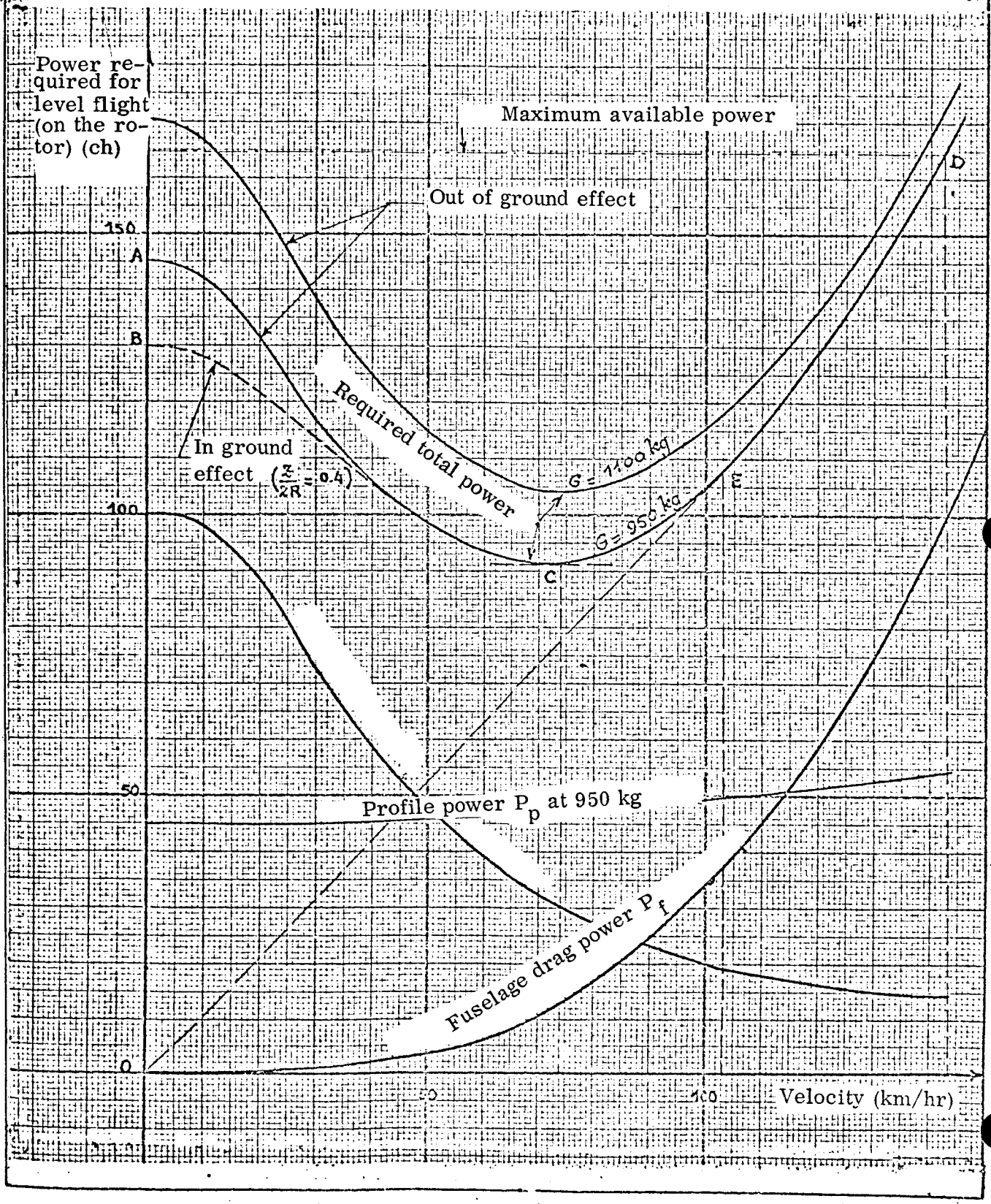

AUTOROTATION PERFORMANCE (.E.V. Tests)

Helicopter A-

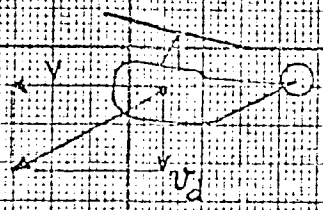

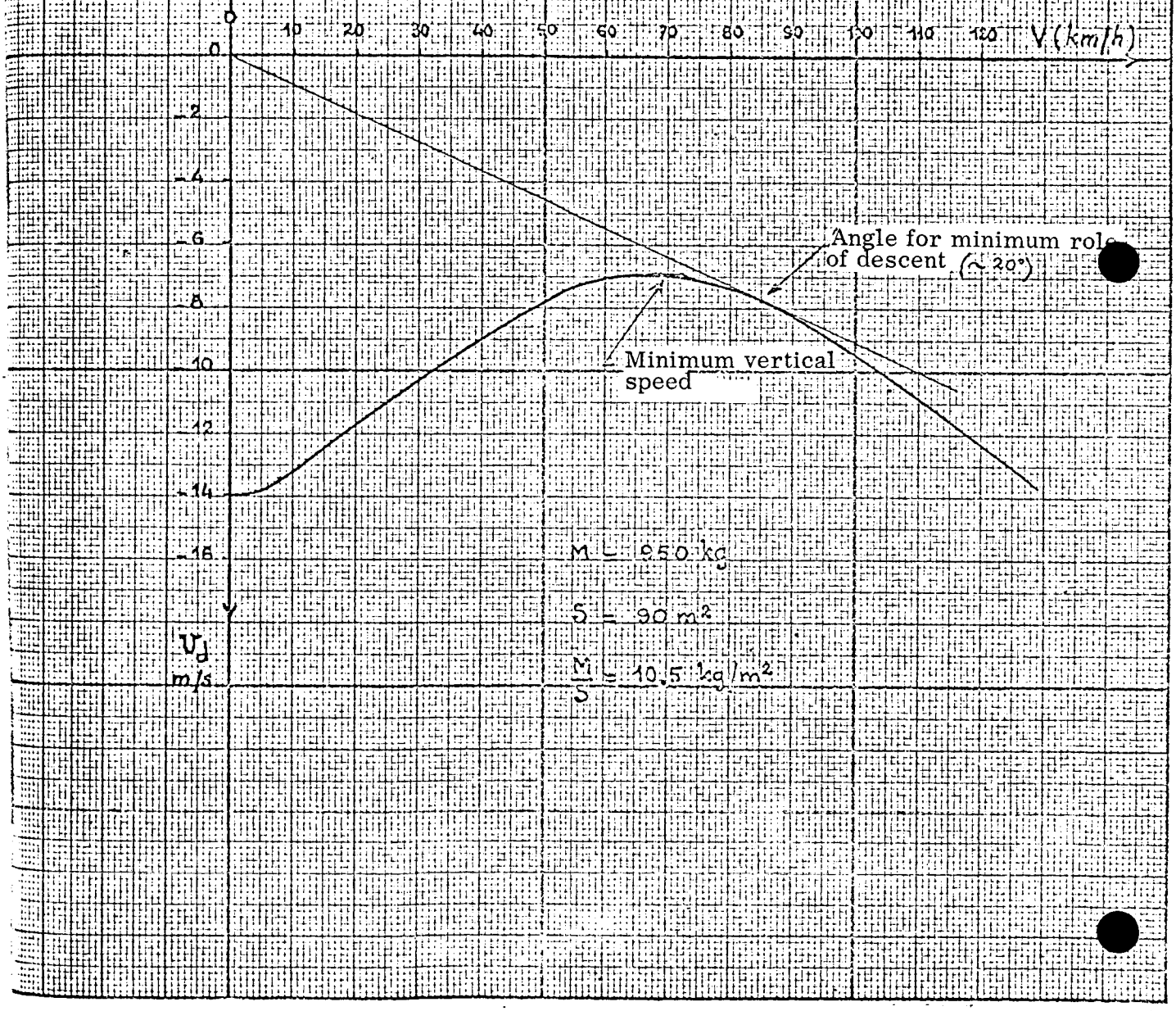

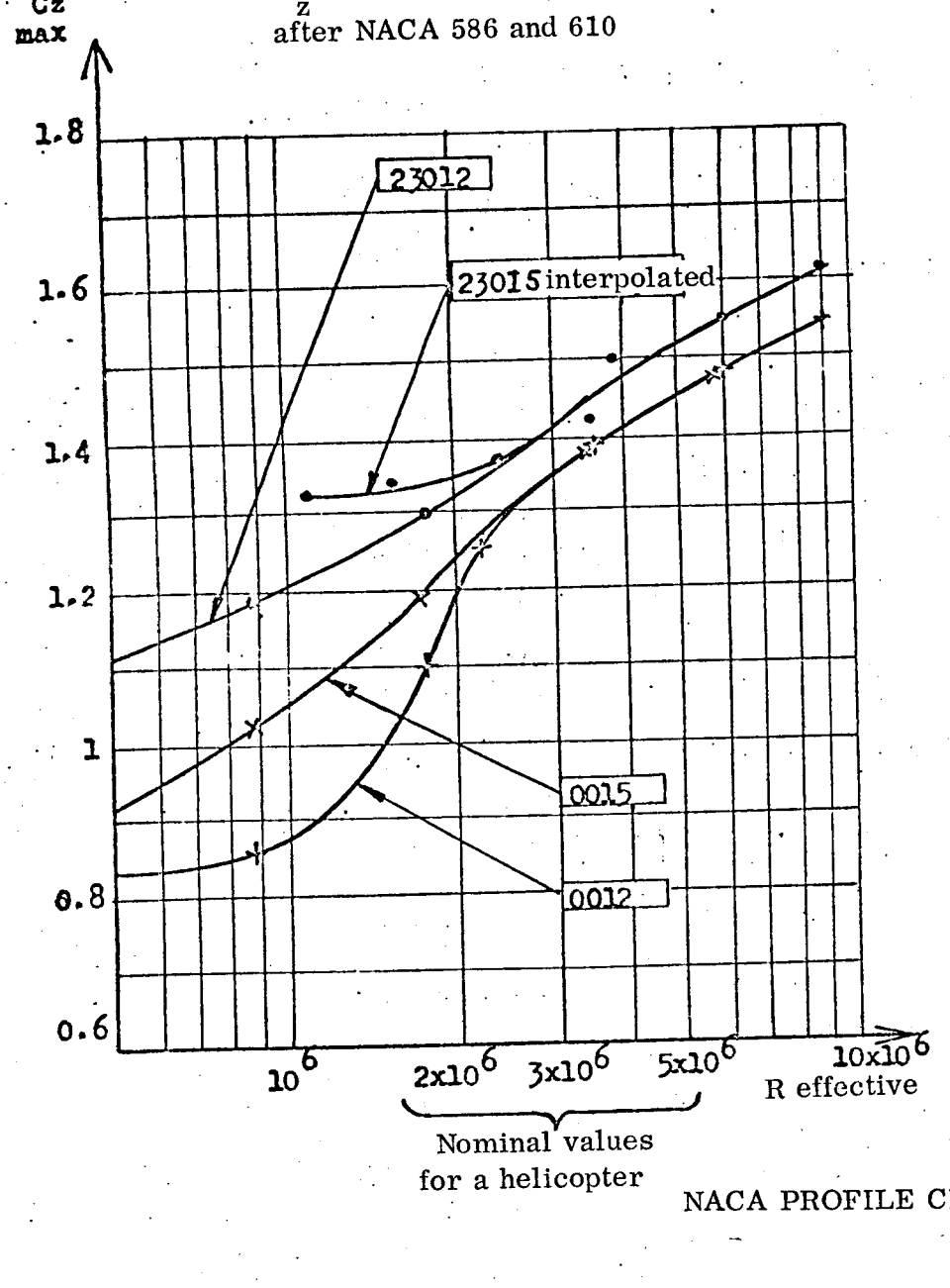

C_z max of various profiles after NACA 586 and 610

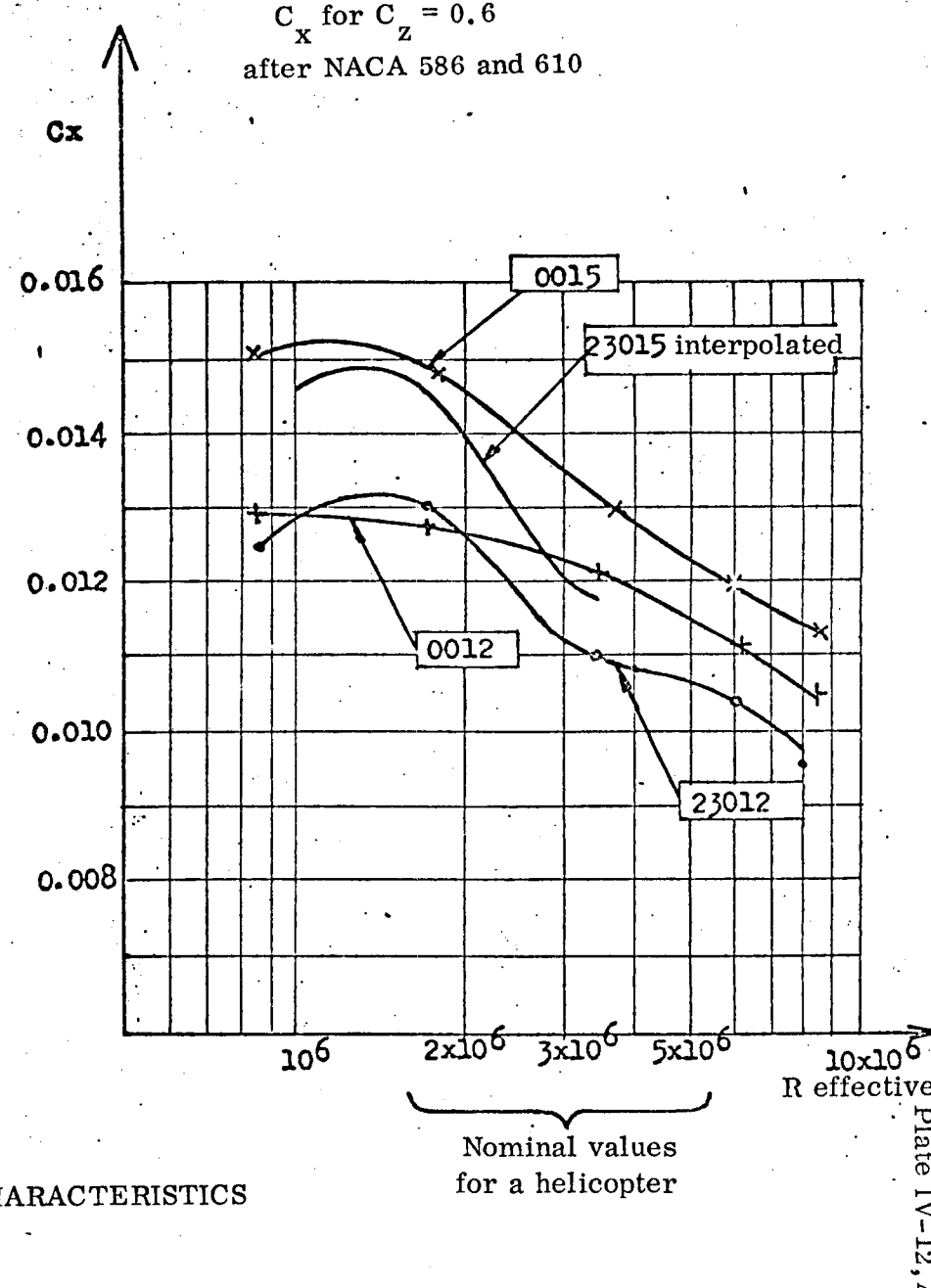

C_x for $C_z = 0.6$ after NACA 586 and 610

NACA PROFILE CHARACTERISTICS

CHARACTERISTICS OF A NACA 0012 PROFILE

(After TN 3361)

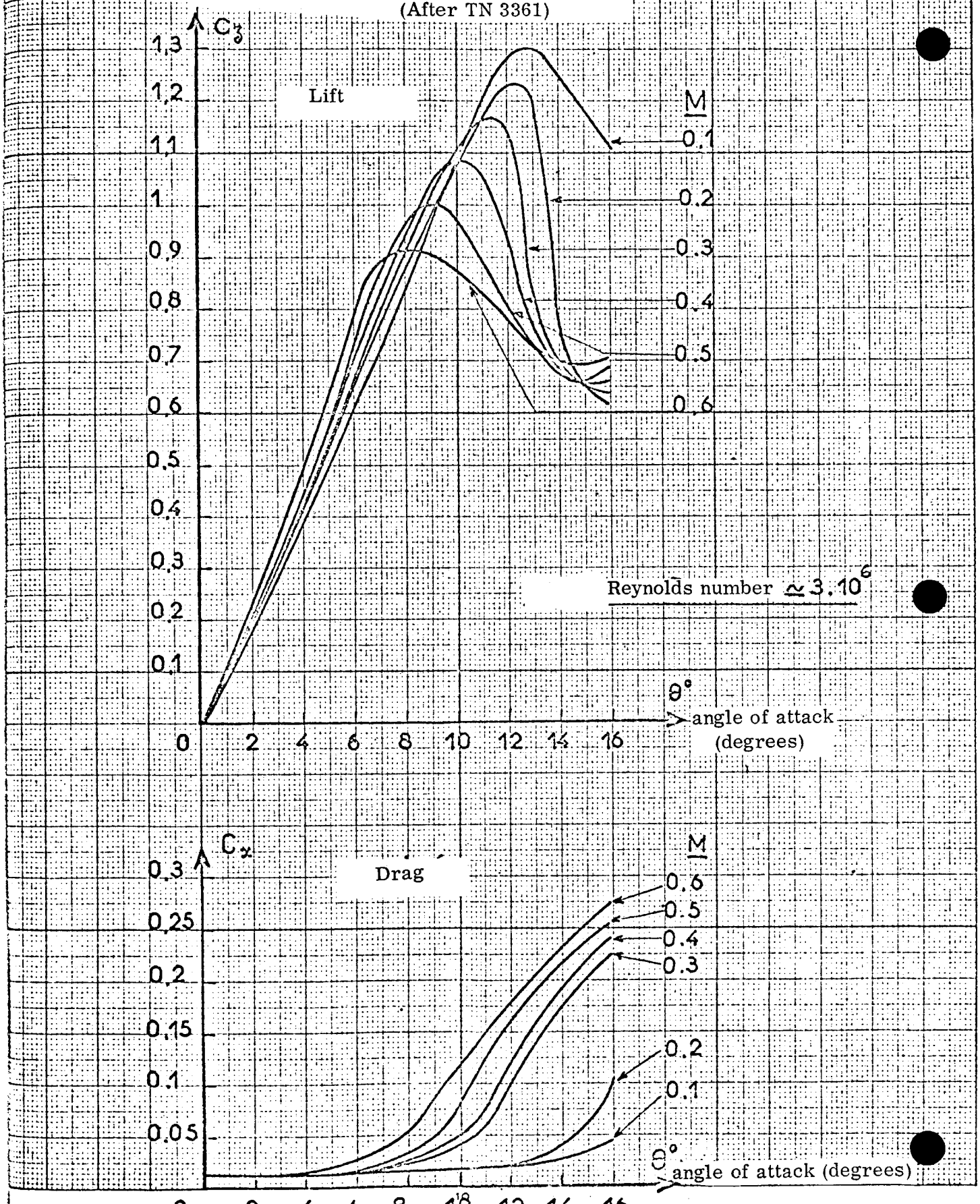

COMPARATIVE CHARACTERISTICS OF NACA 8H12 AND 0012 PROFILES

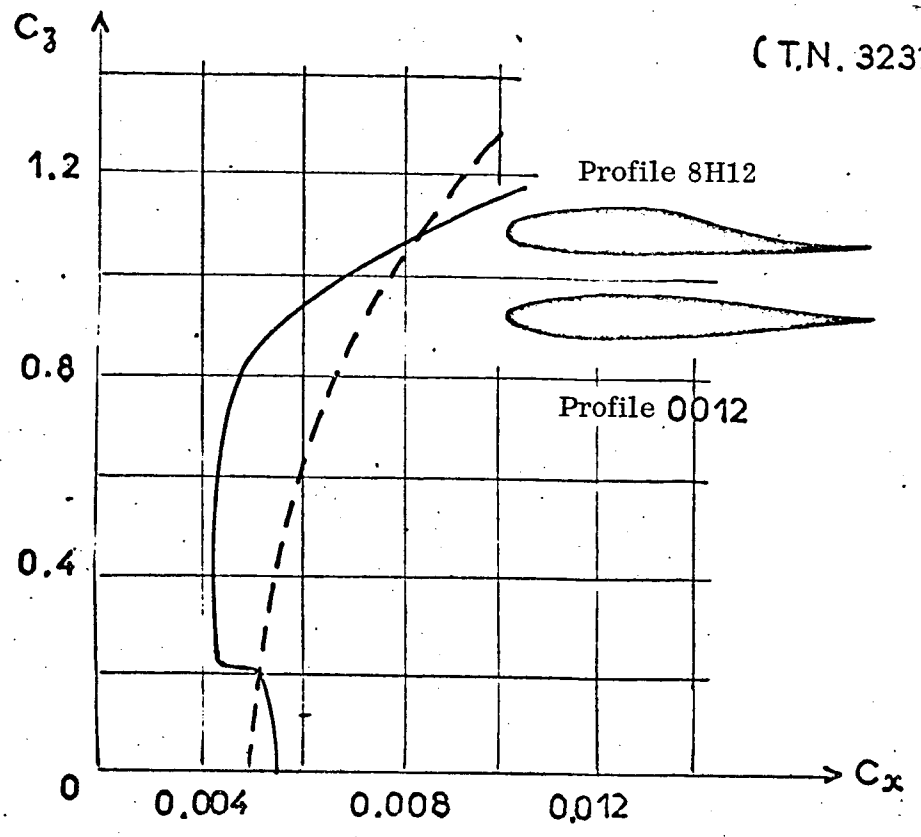

INFLUENCE OF THE PRECISINESS OF THE 8H12 PROFILE ON PERFORMANCE

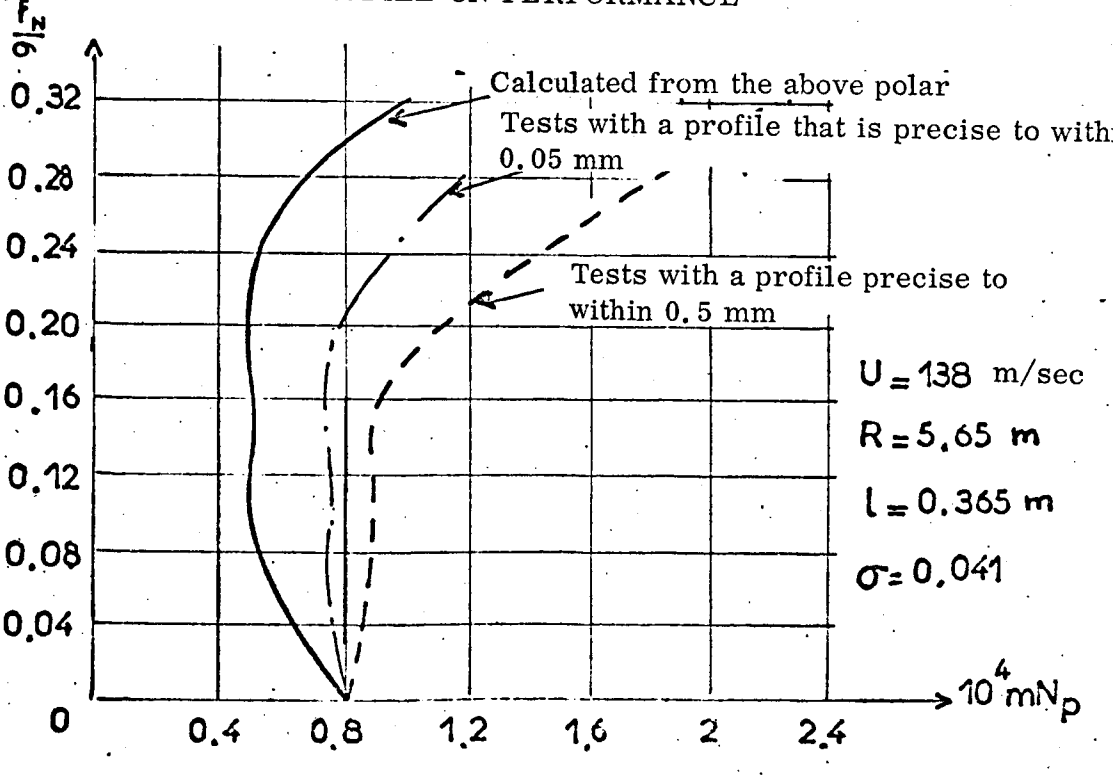

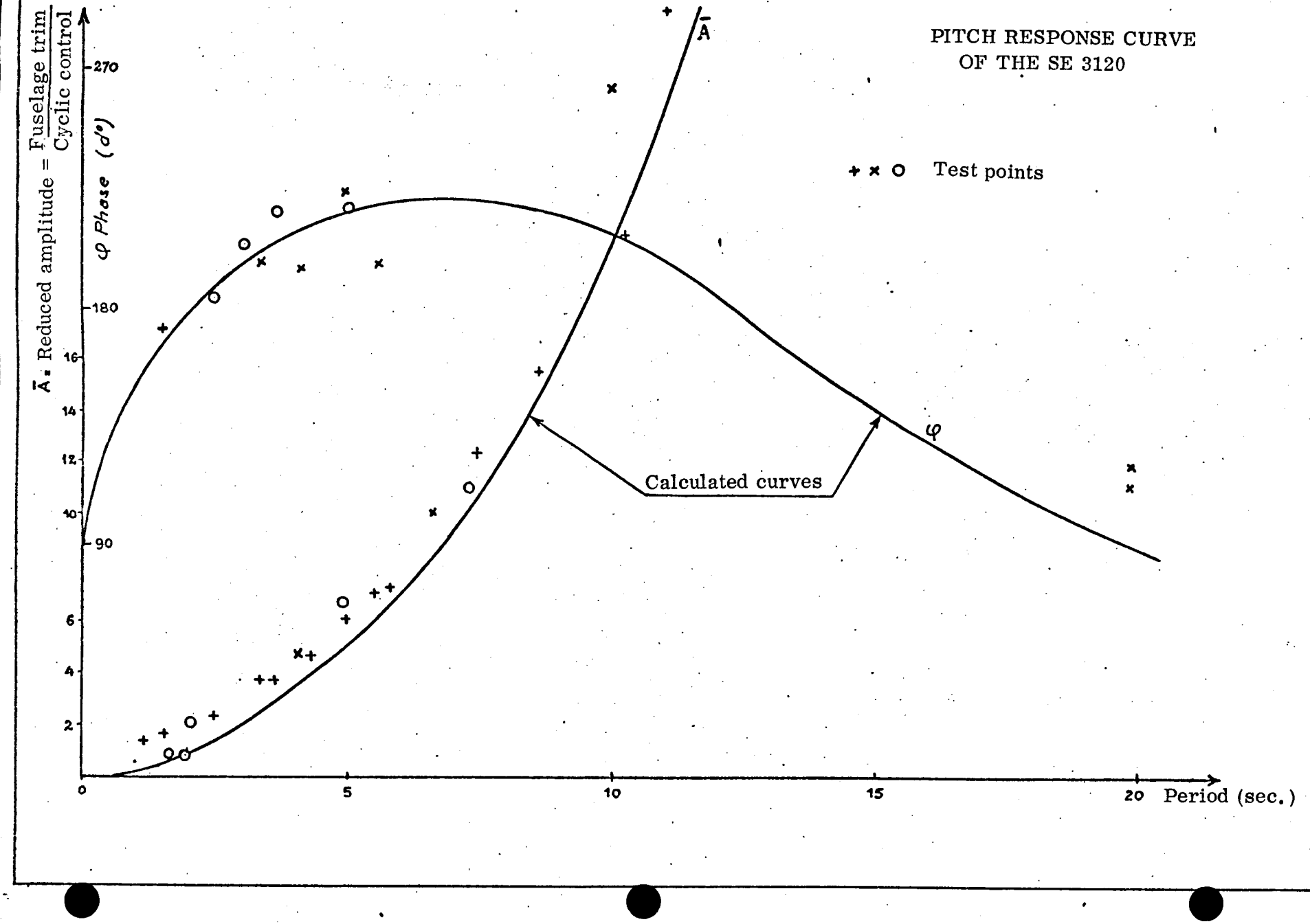
PITCH RESPONSE CURVE
OF THE SE 3120
Test points
Calculated curves
Ā = Reduced amplitude = Fuselage trim / Cyclic control
φ Phase (d°)
Ā
φ
270
180
90
16
14
12
10
6
4
2
0
5
10
15
20
Period (sec.)

Plate V-1

Plate V-3-1

HELICOPTER B: roll response (trim)
Natural motion-Period 1_r=0.95 sec.
Doubling time =4.65 sec

PRECEDING PAGE BLANK NOT FILMED.

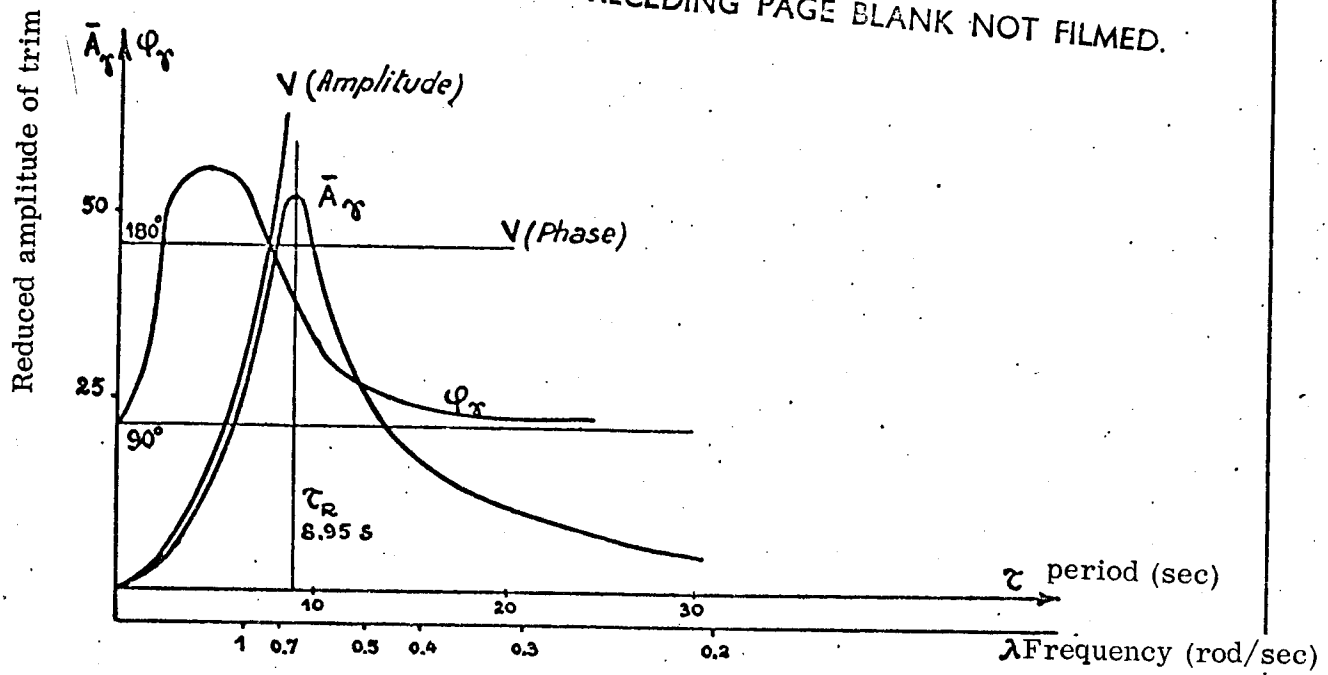

Plate V-3-2

HELICOPTER B: roll response
(displacement velocity)

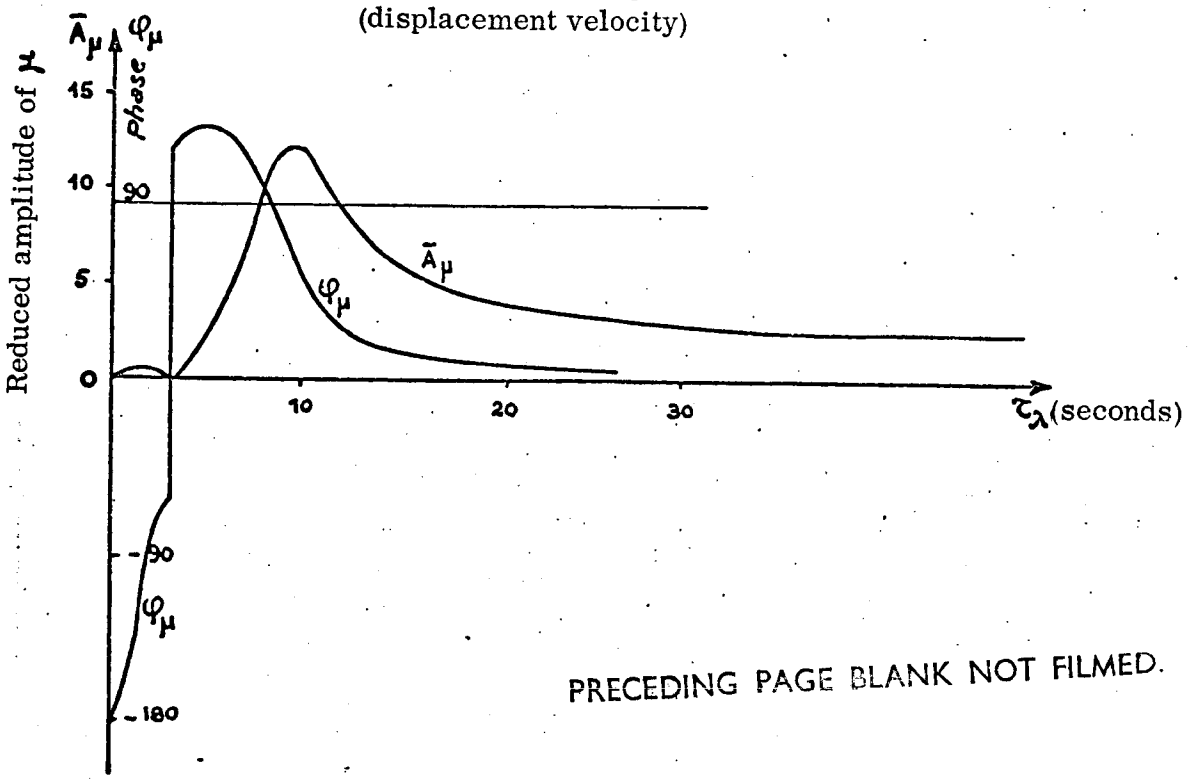

PRECEDING PAGE BLANK NOT FILMED.

PRECEDING PAGE BLANK NOT FILMED.

Plate V-4-1

HELICOPTER SO 1120-roll response

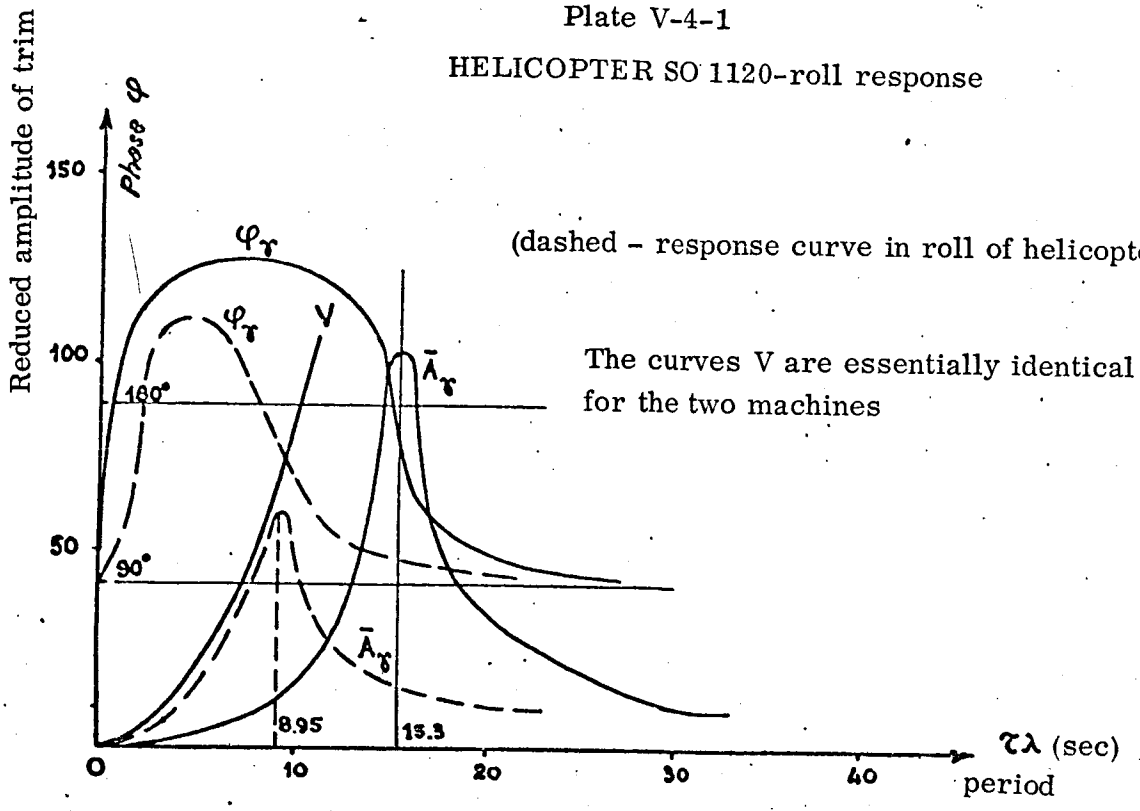

(dashed – response curve in roll of helicopter A)

The curves V are essentially identical for the two machines

Plate V-4-2

HELICOPTER SO 1120-pitch response

(Dashed – response curves in roll of the same machine)

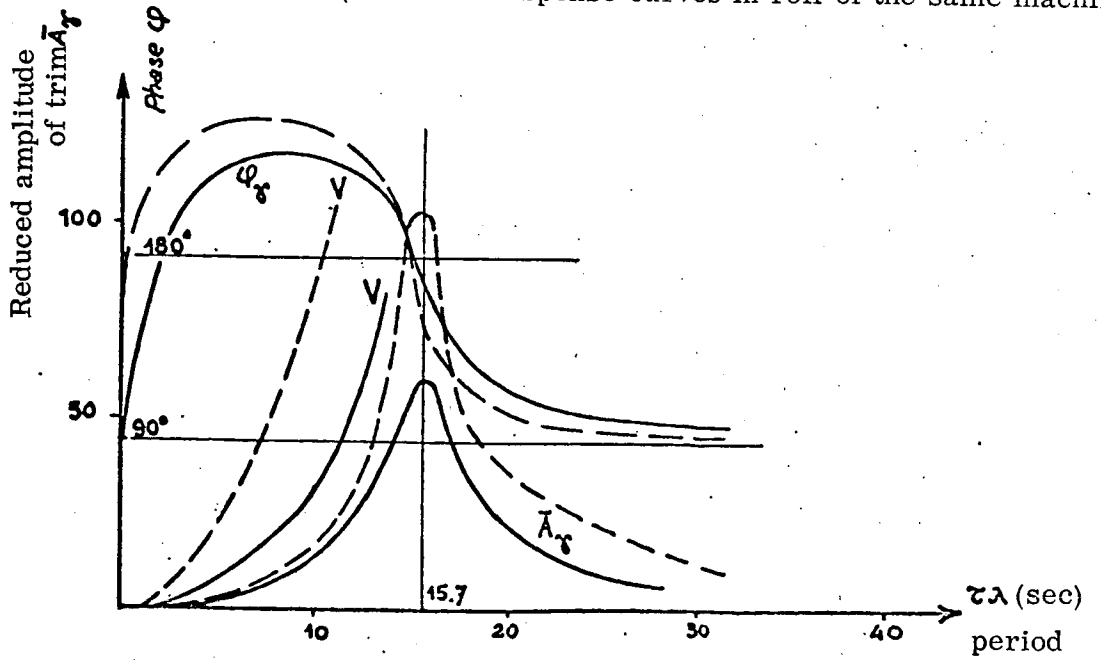

Plate V-5-1

Nyquist curve (R_p, F_p, F_γ) for helicopter B in roll.

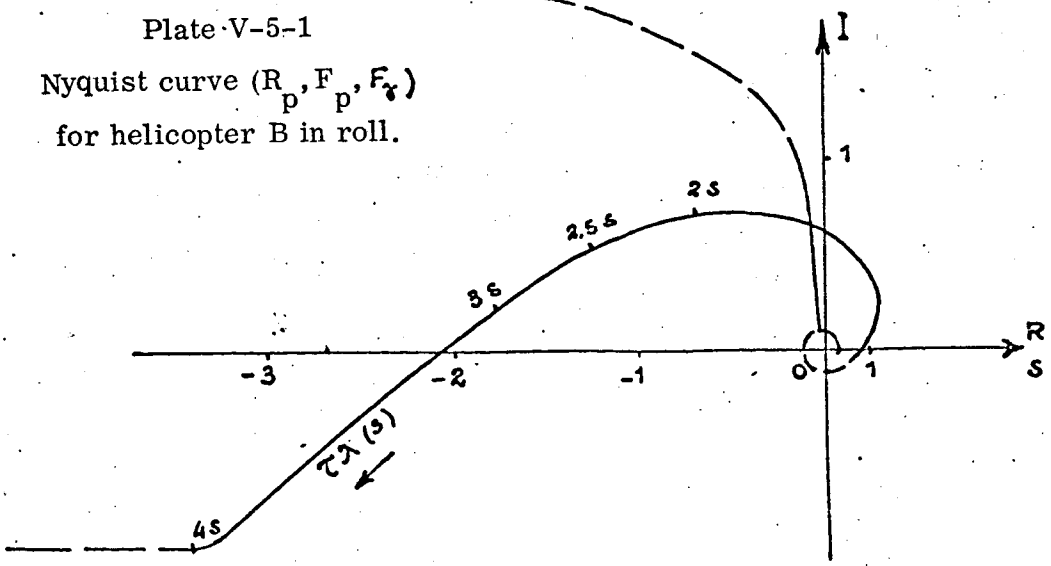

Plate V-5-2

Nyquist curve for a pursuit aircraft - roll

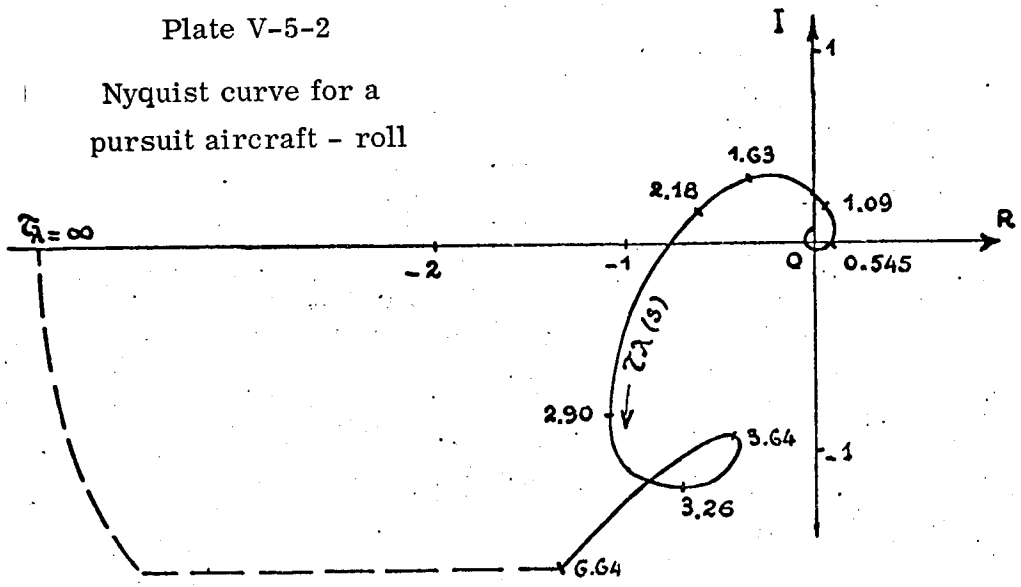

Plate V-5-3

Nyquist curve for helicopter SO 1120 (roll)

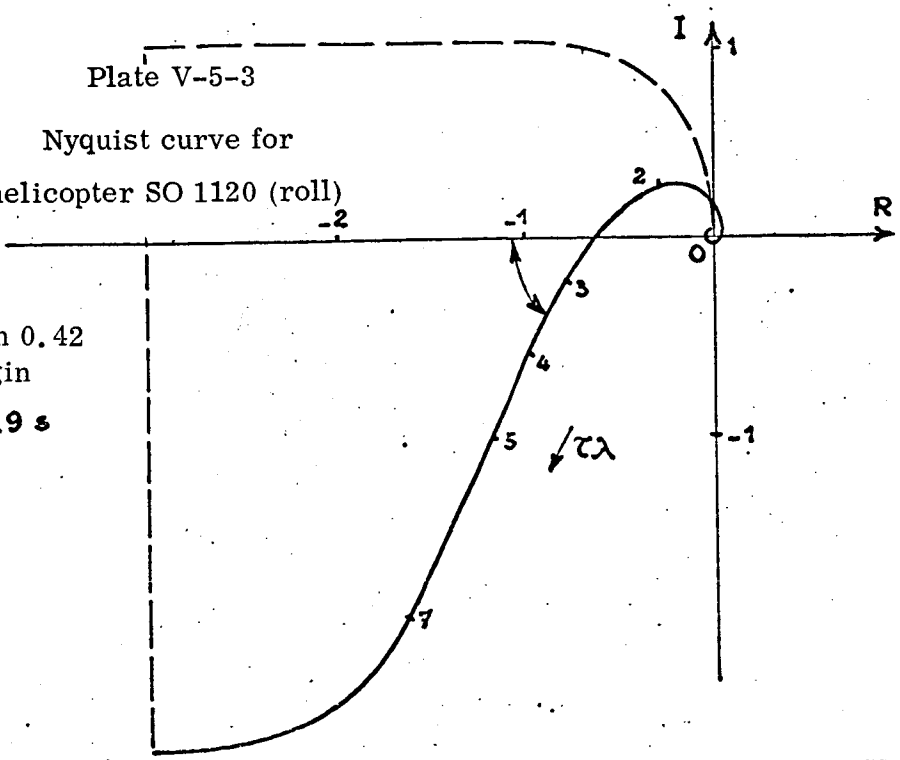

Gain margin 0.42
Phase margin
$\tau_{\alpha p} = 2.9$ s

EFFECT OF A STABILIZER ON THE CRITICAL CURVES

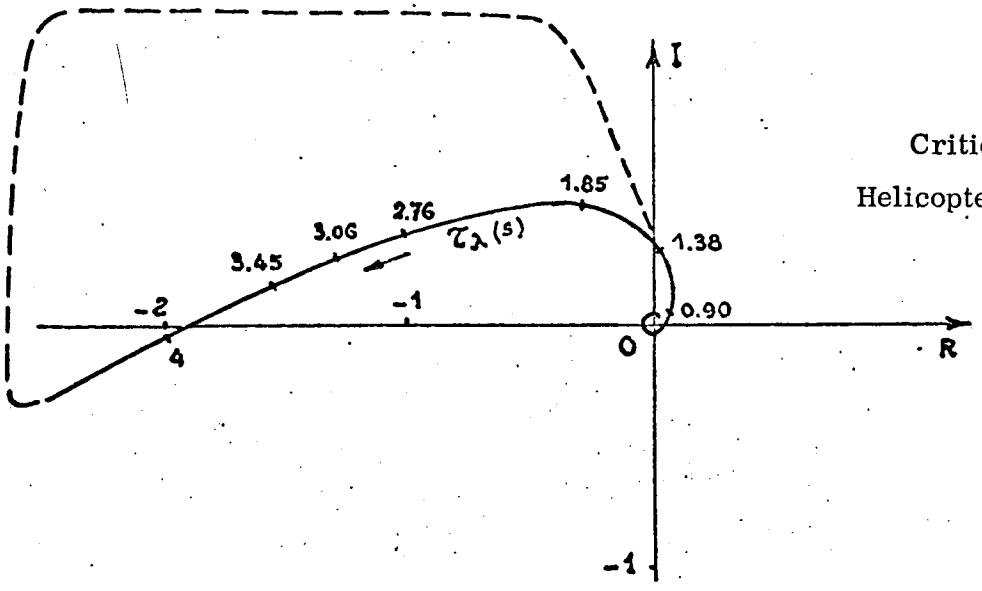

Plate V-6-1

Critical curve $R_p F_p F_l$

Helicopter C without stabilizer

- Roll -

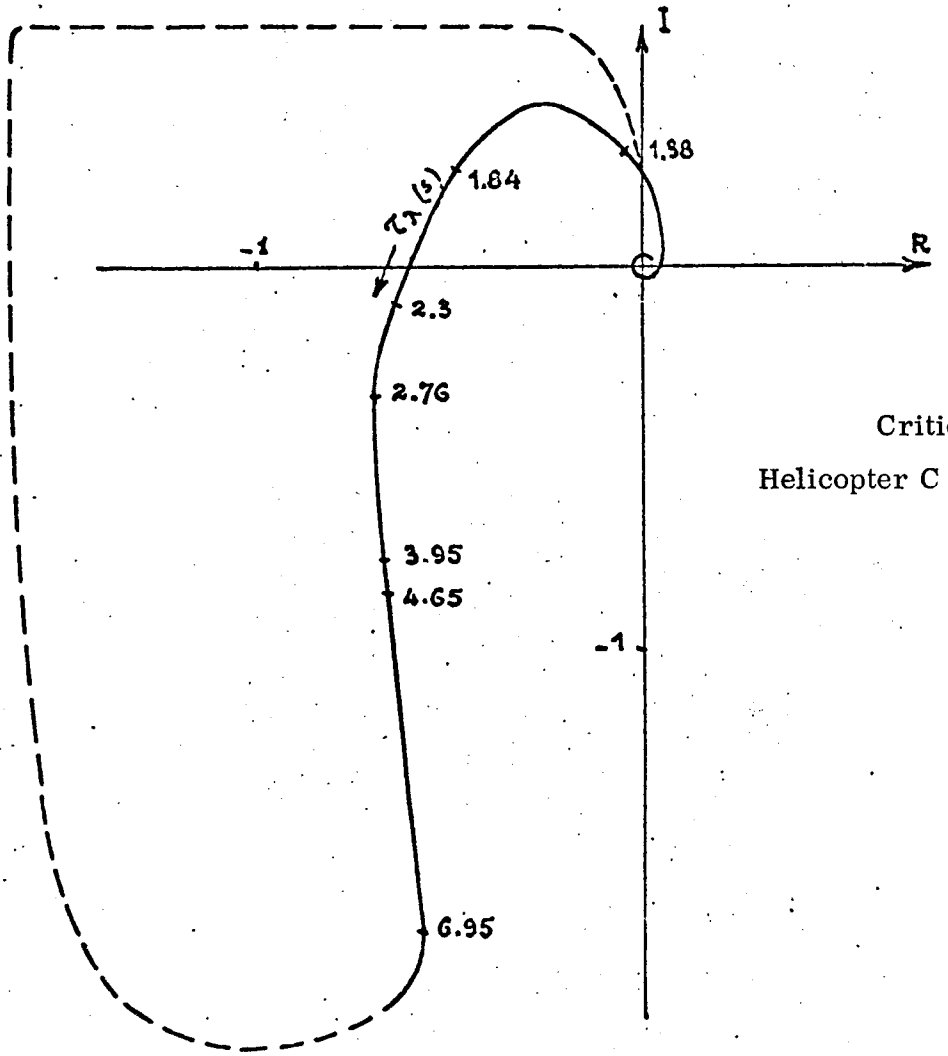

Plate V-6-2

Critical curve $R_p F_p F_l$

Helicopter C with gyroscopic stabilizer

- Roll -

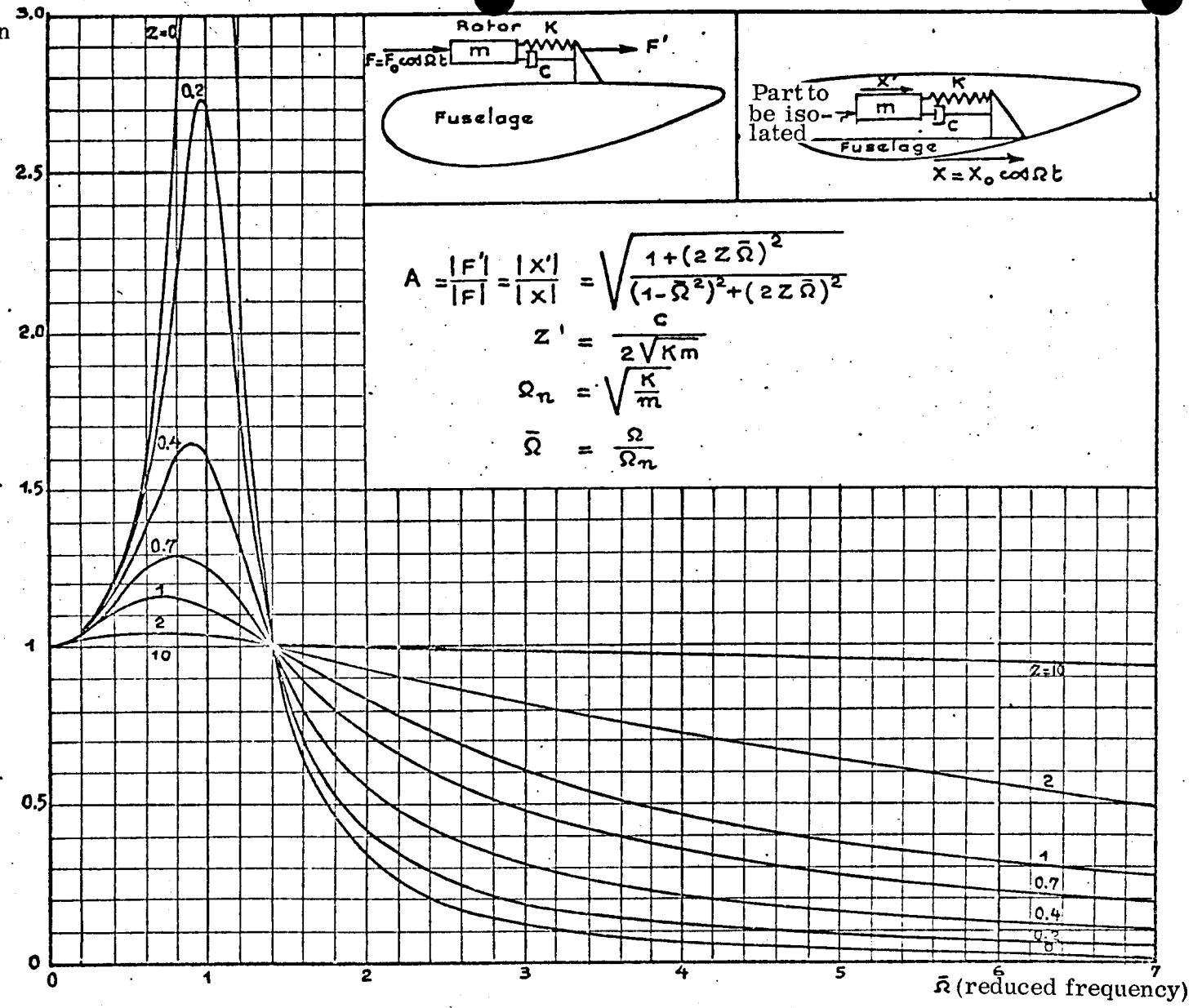

Plate VI-1. TRANSMISSION COEFFICIENT OF A SECOND-ORDER LINEAR SYSTEM

AMPLIFICATION CURVES OF A PENDULUM DAMPER

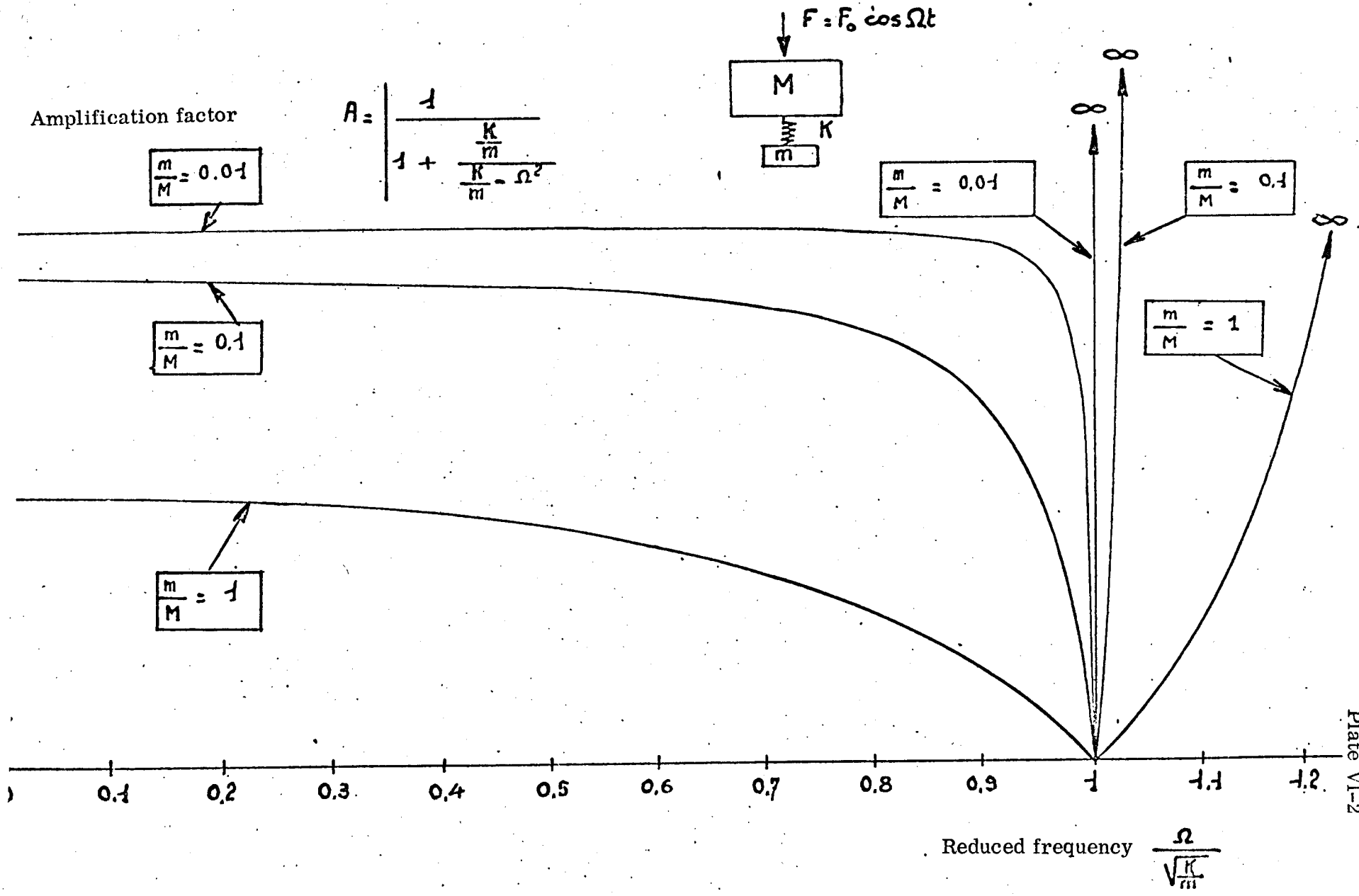

Plate VI-2

EXAMPLE OF AIRFRAME RESONANCES

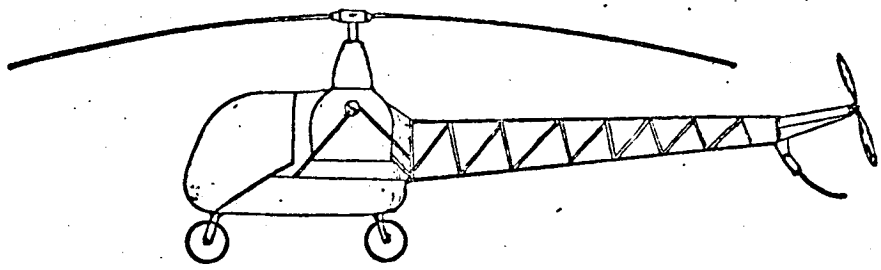

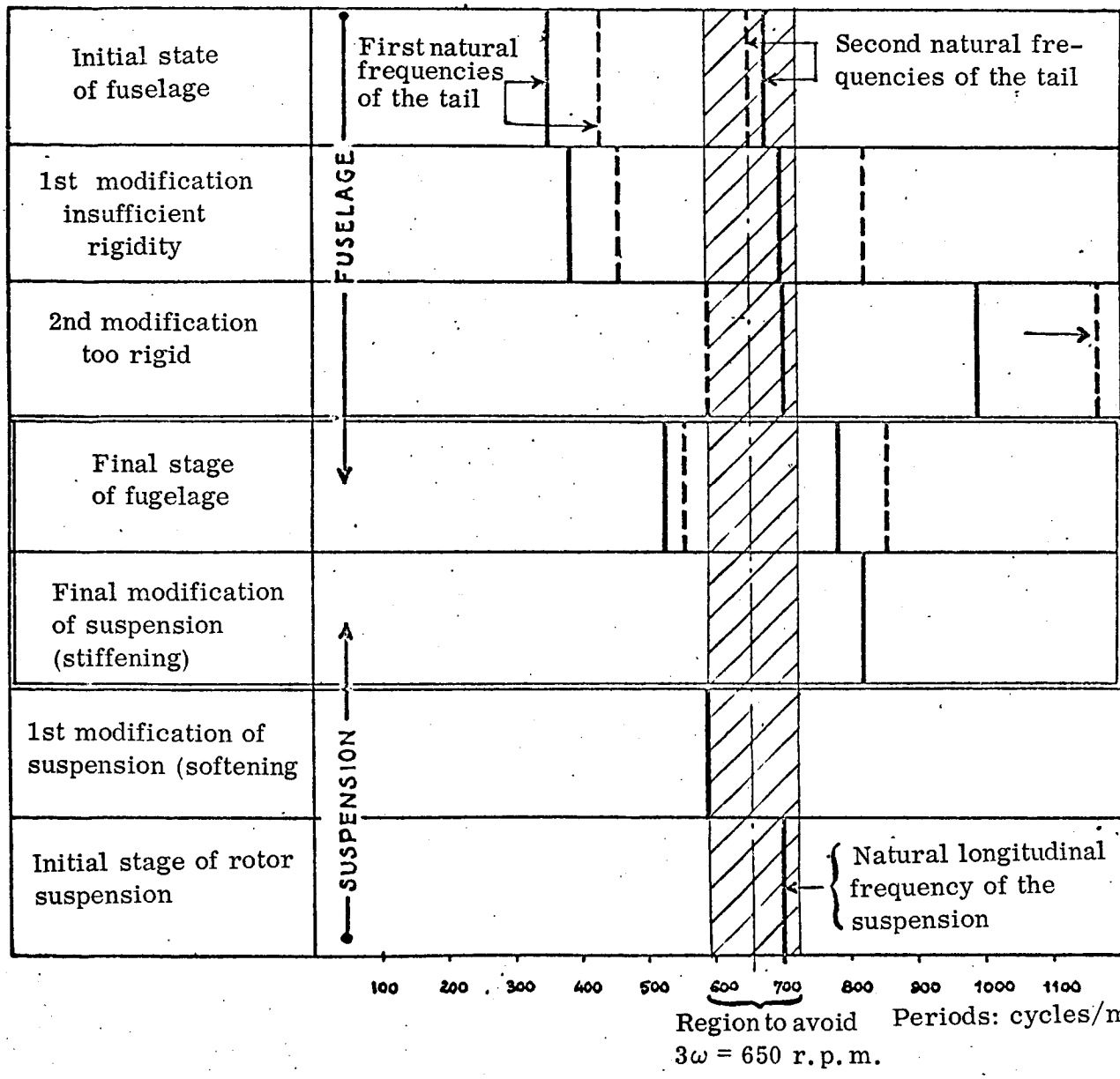

— — — horizontal resonances

——— vertical resonances

Note: For a three-blade: the dangerous excitation is at 3ω

GROUND RESONANCE

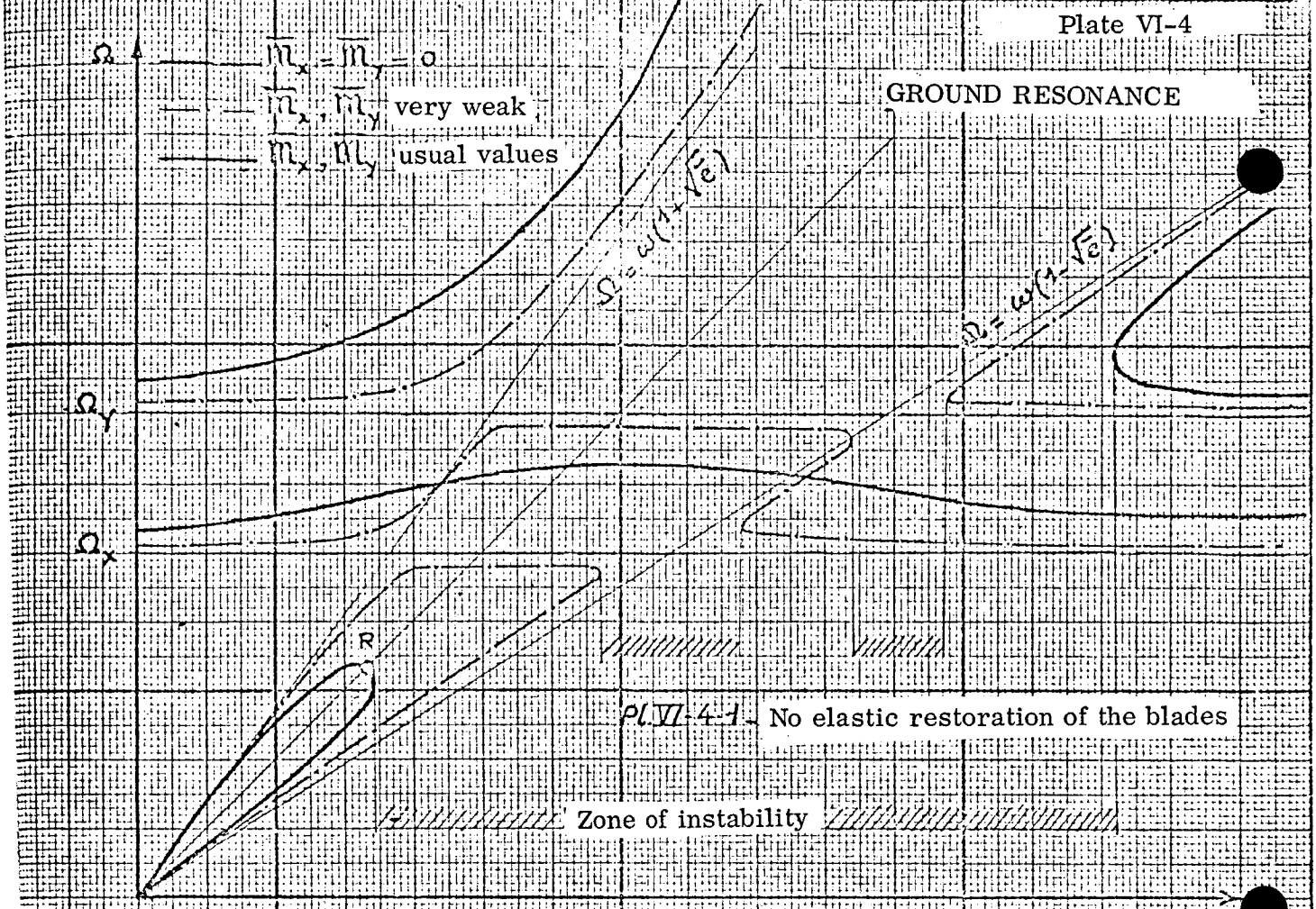

Pl. VI-4-1. No elastic restoration of the blades

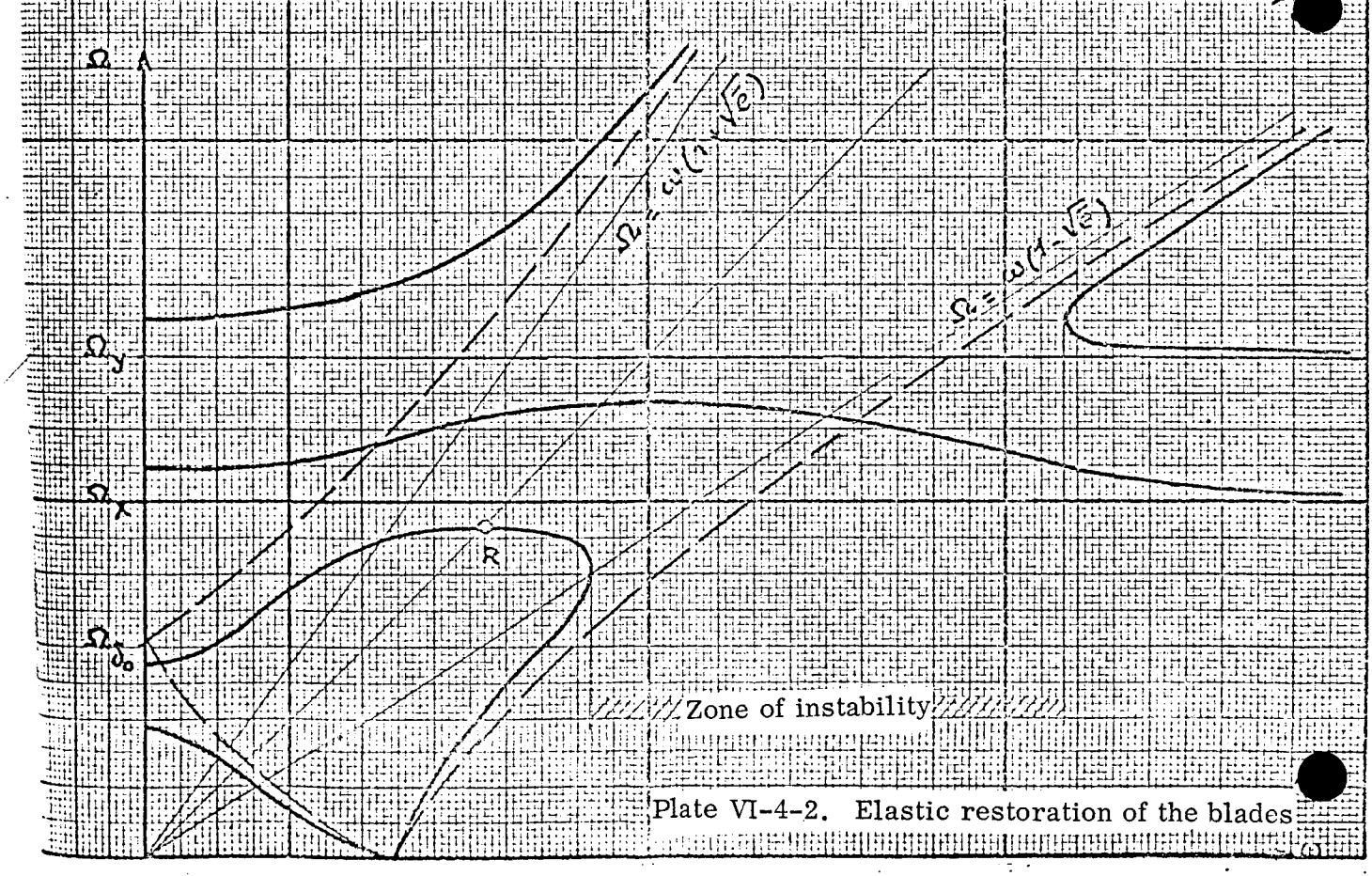

Plate VI-4-2. Elastic restoration of the blades

FORCES ON A HELICOPTER BLADE

Examples of Distribution of Vertical Flexure Moments

(SE 3 120 - ALOUETTE I)

Average moments

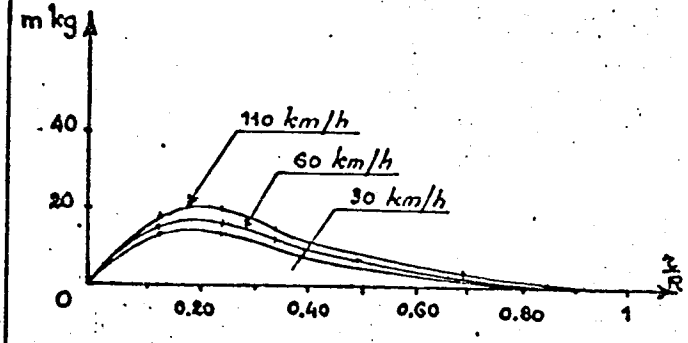

Alternating moments

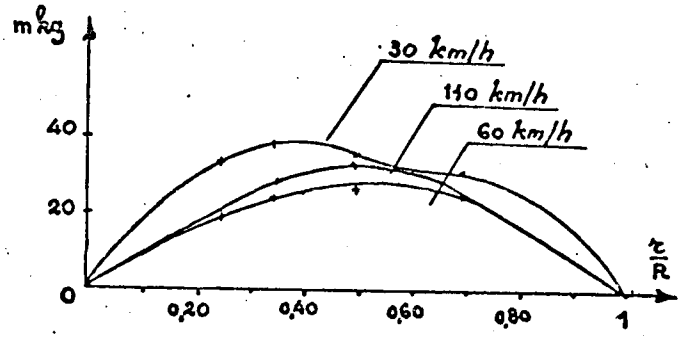

Level Flight

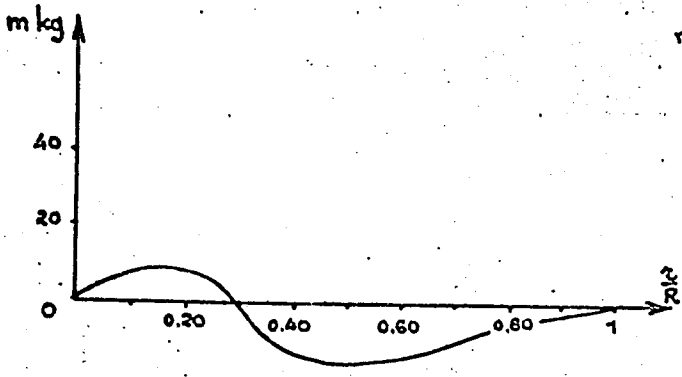

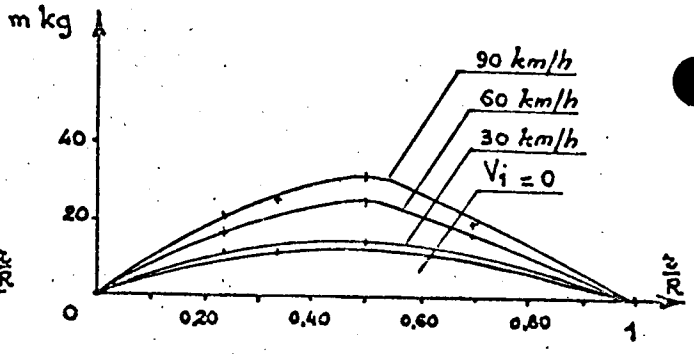

Autorotation

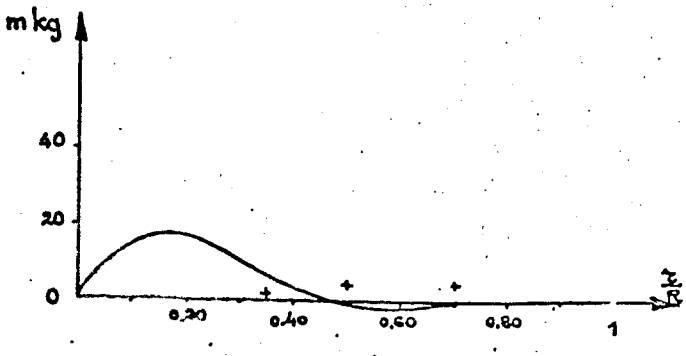

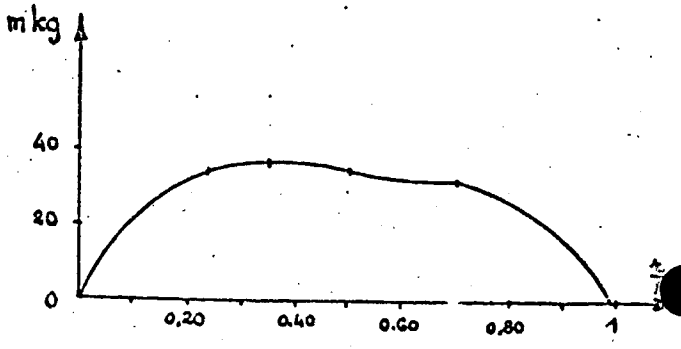

Landing in Autorotation

FORCES ON A HELICOPTER BLADE

Development of the Maximum Alternating Stress as a Function of Velocity

(SE 3120 n° 01 - ALOUETTE I .)

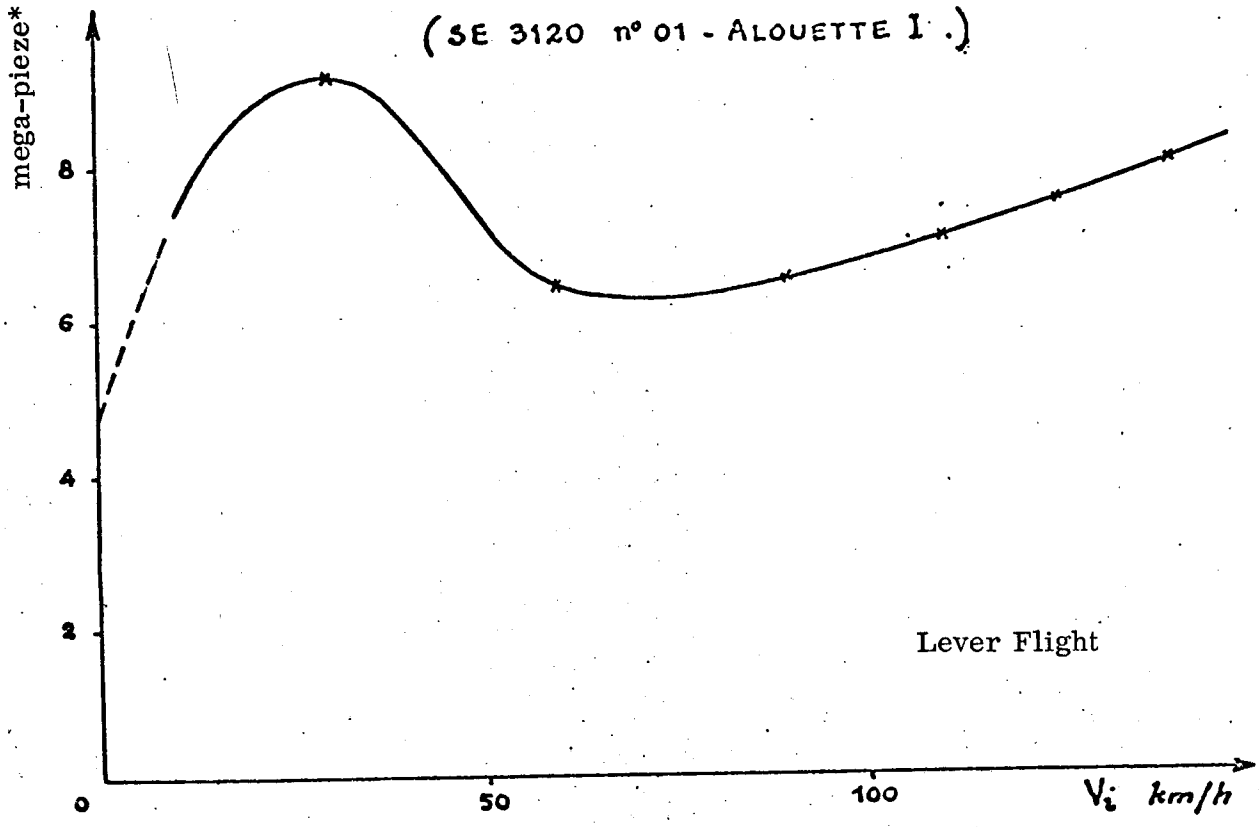

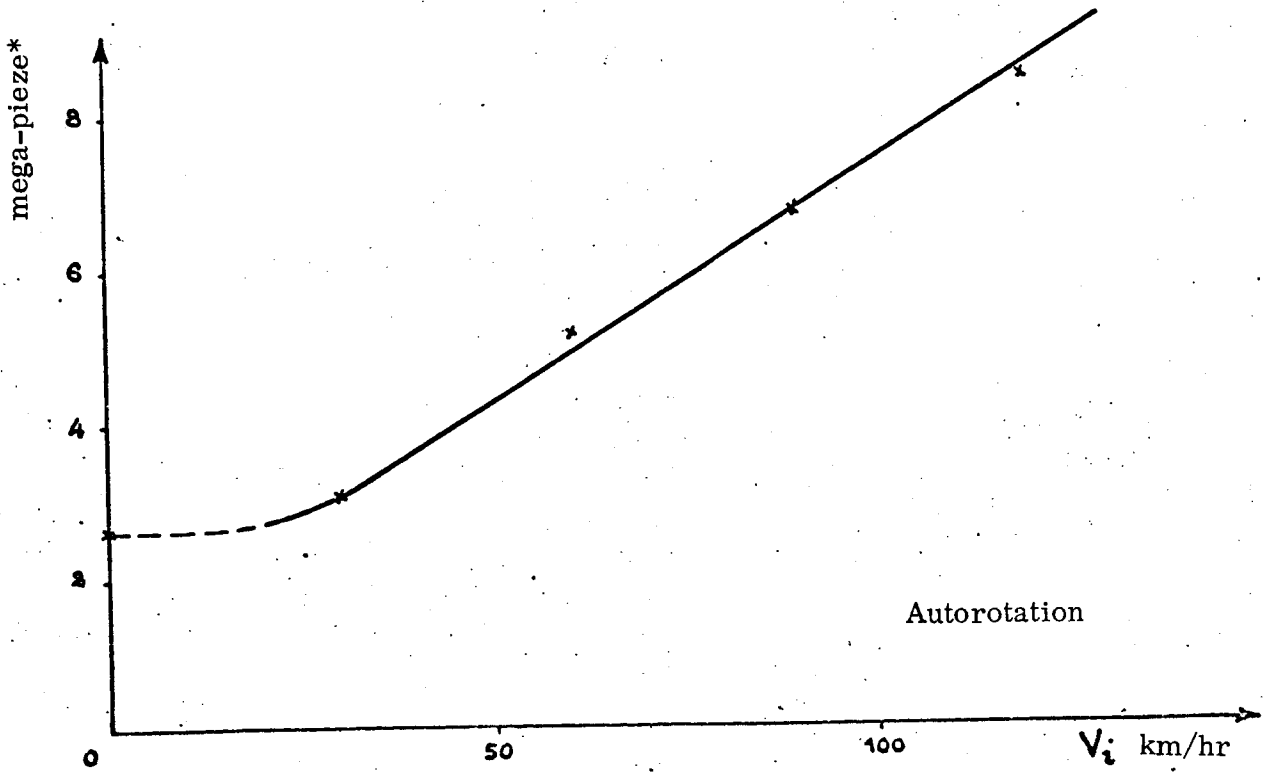

*Tr. Note: 1 pieze = 10^{-2} bars

FORCES ON A HELICOPTER BLADE

Diagram of blade resonance

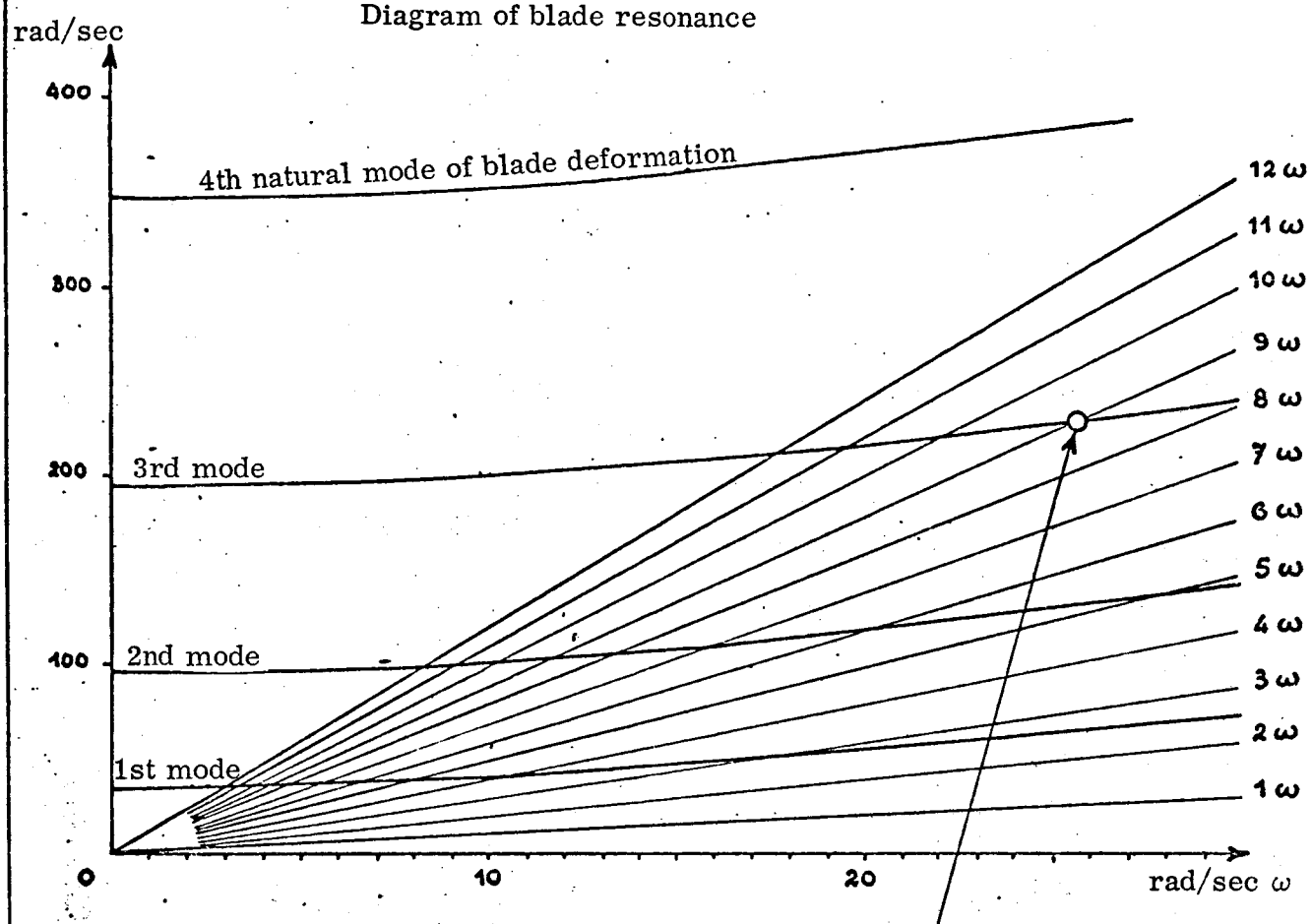

Harmonic analysis of flight case V_i = 120 km/hr, N_{rotor} = 25.8 rod/sec (0.5 R)

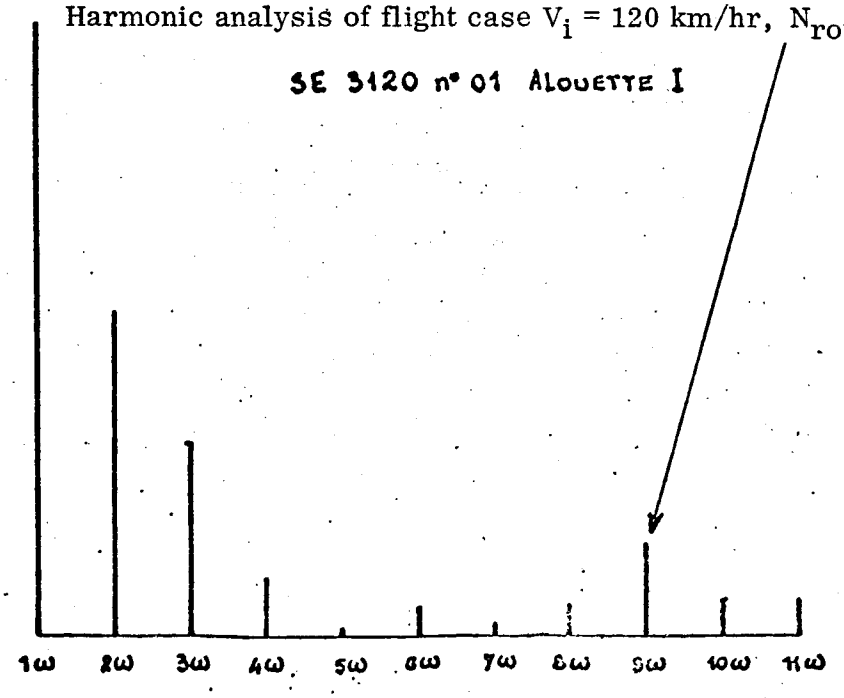

COMPARISON OF DIFFERENT ROTOR DRIVE MODES

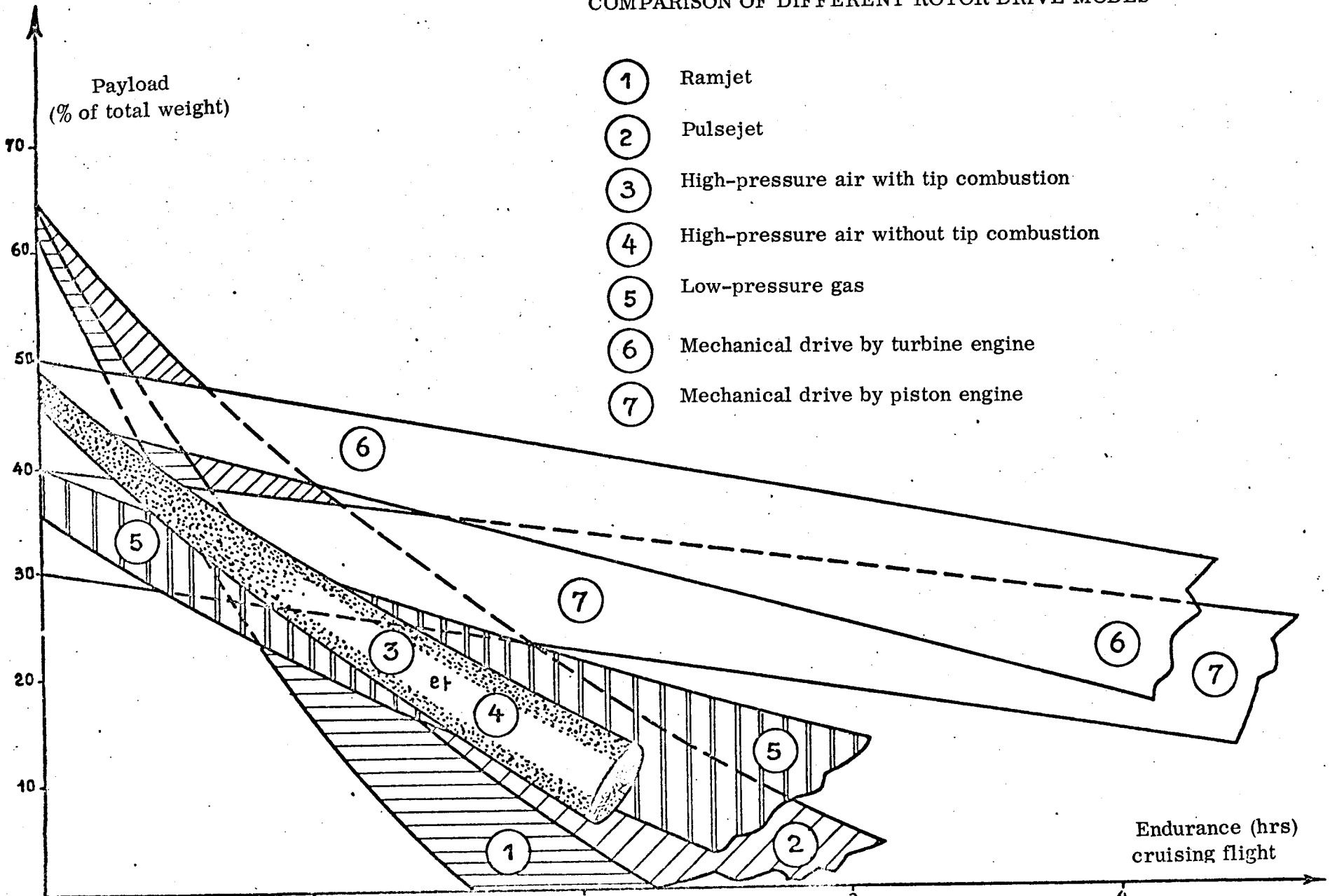

Plate VIII-1

INFLUENCE OF TIP SPEED ON THE CHARACTERISTICS OF VARIOUS THERMAL PROPULSION SYSTEMS

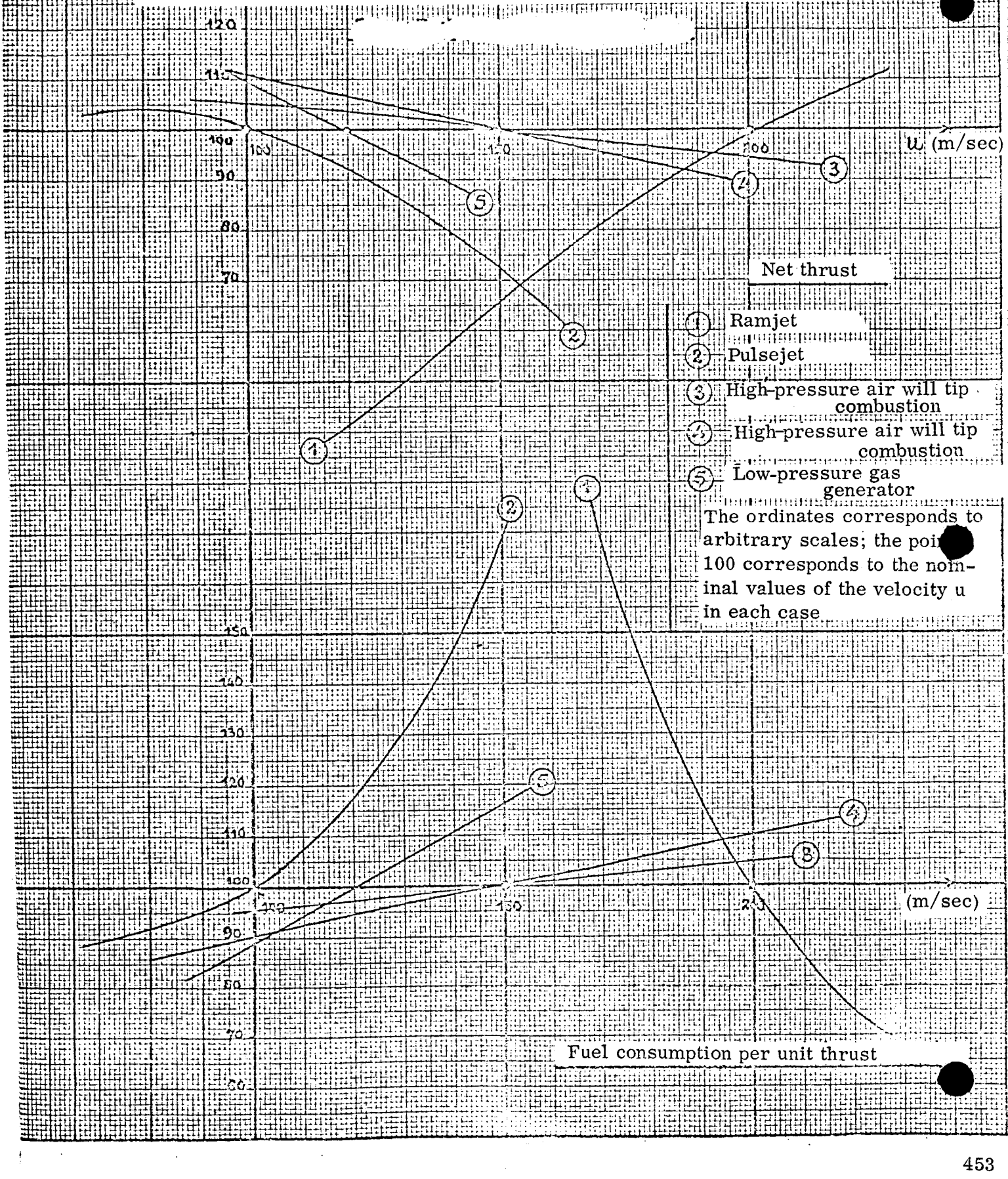

PRECEDING PAGE BLANK NOT FILMED.

Plate VIII-5

STUDY OF "OVERCOUPLING"

PRECEDING PAGE BLANK NOT FILMED.

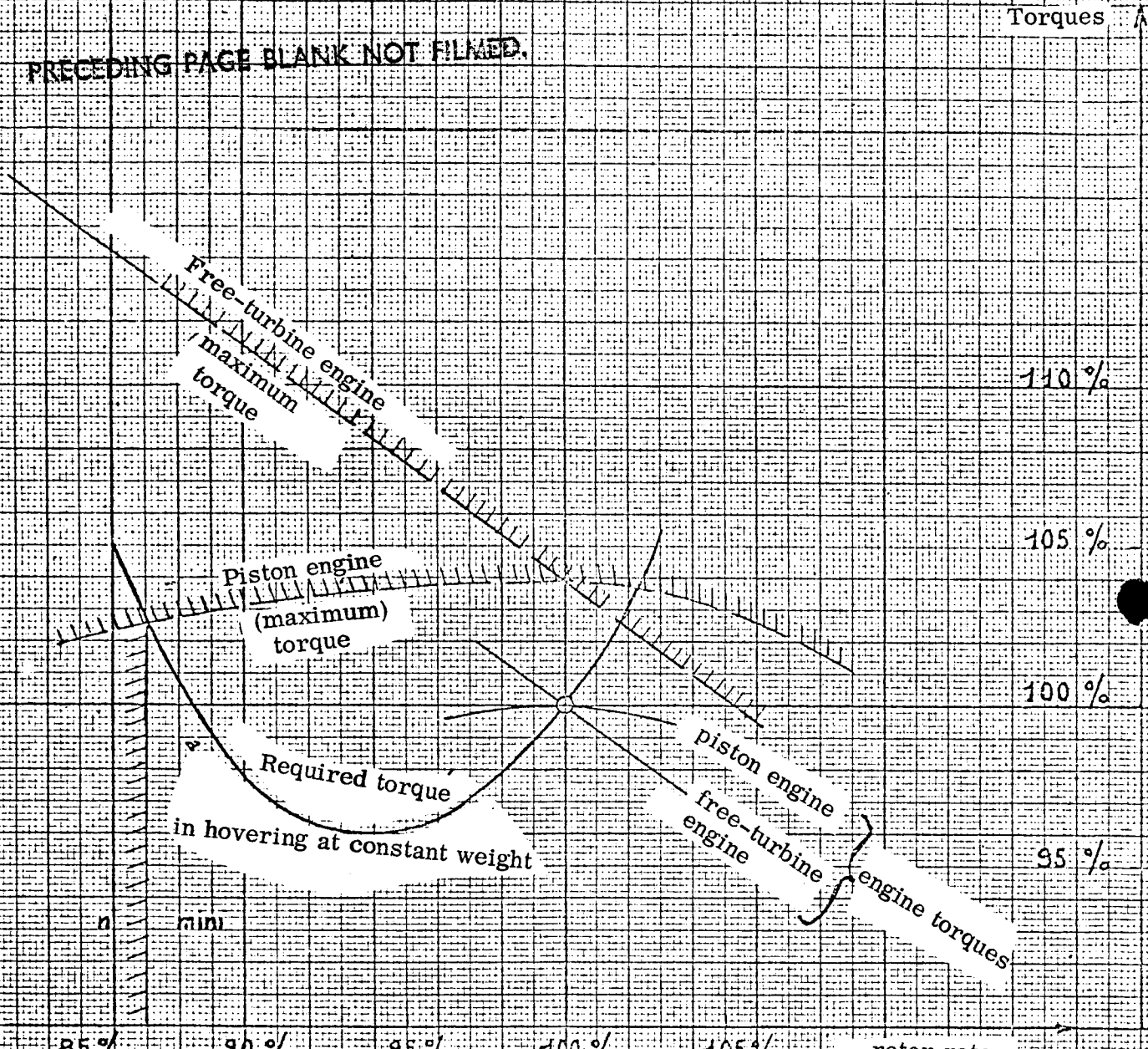

PRECEDING PAGE BLANK NOT FILMED.

FREE-TURBINE ENGINE

Drive Torques

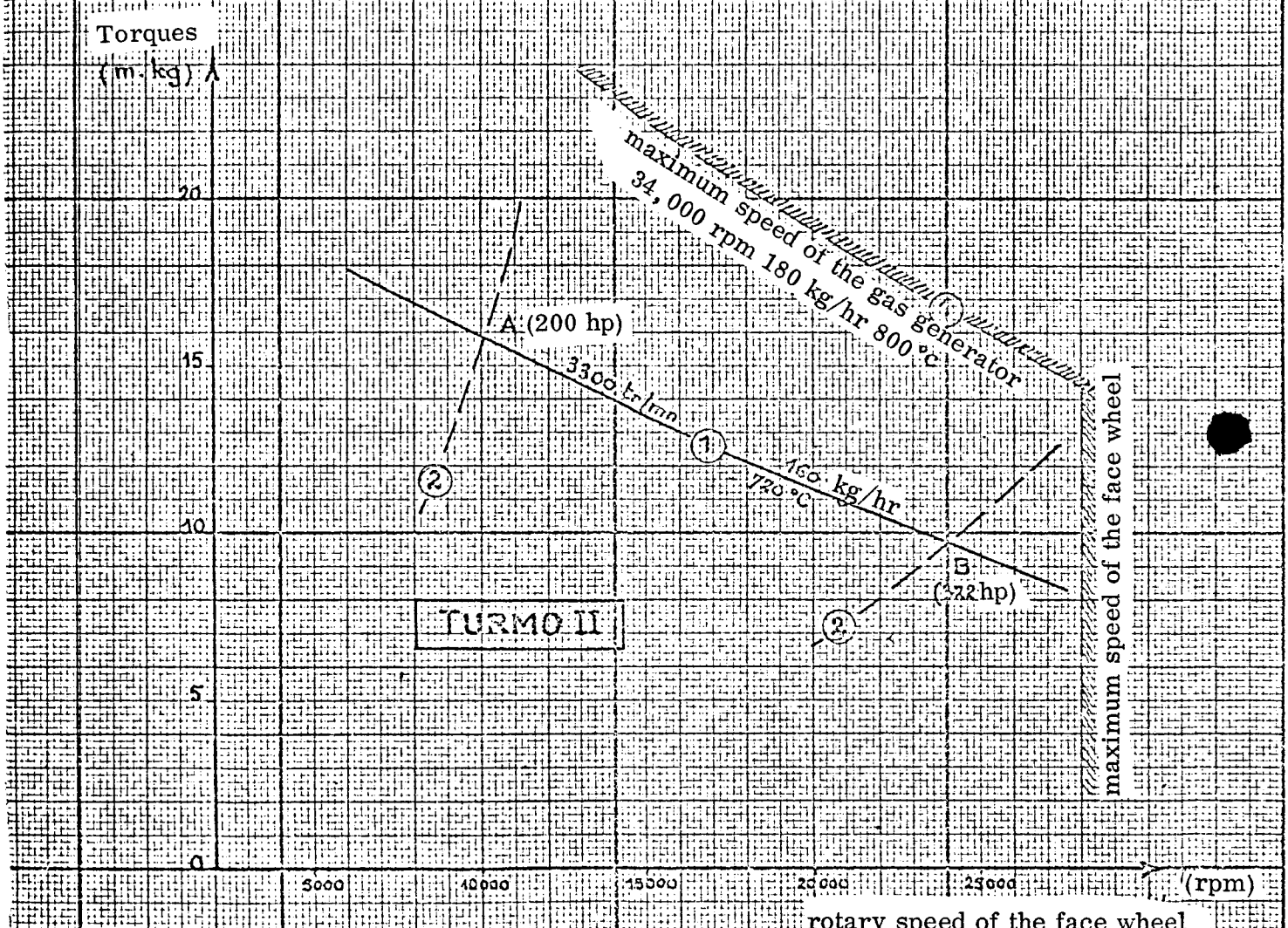

(1) Drive torque, fixed generator control (i.e., temperature, fuel flow rate, and generator speed constant).

(2) Typical opposing torque (proportional to the square of the velocities)

DEVELOPMENT OF WEIGHT ESTIMATE FOR A HELICOPTER

AS A FUNCTION OF THE ROTOR DISK LOADING

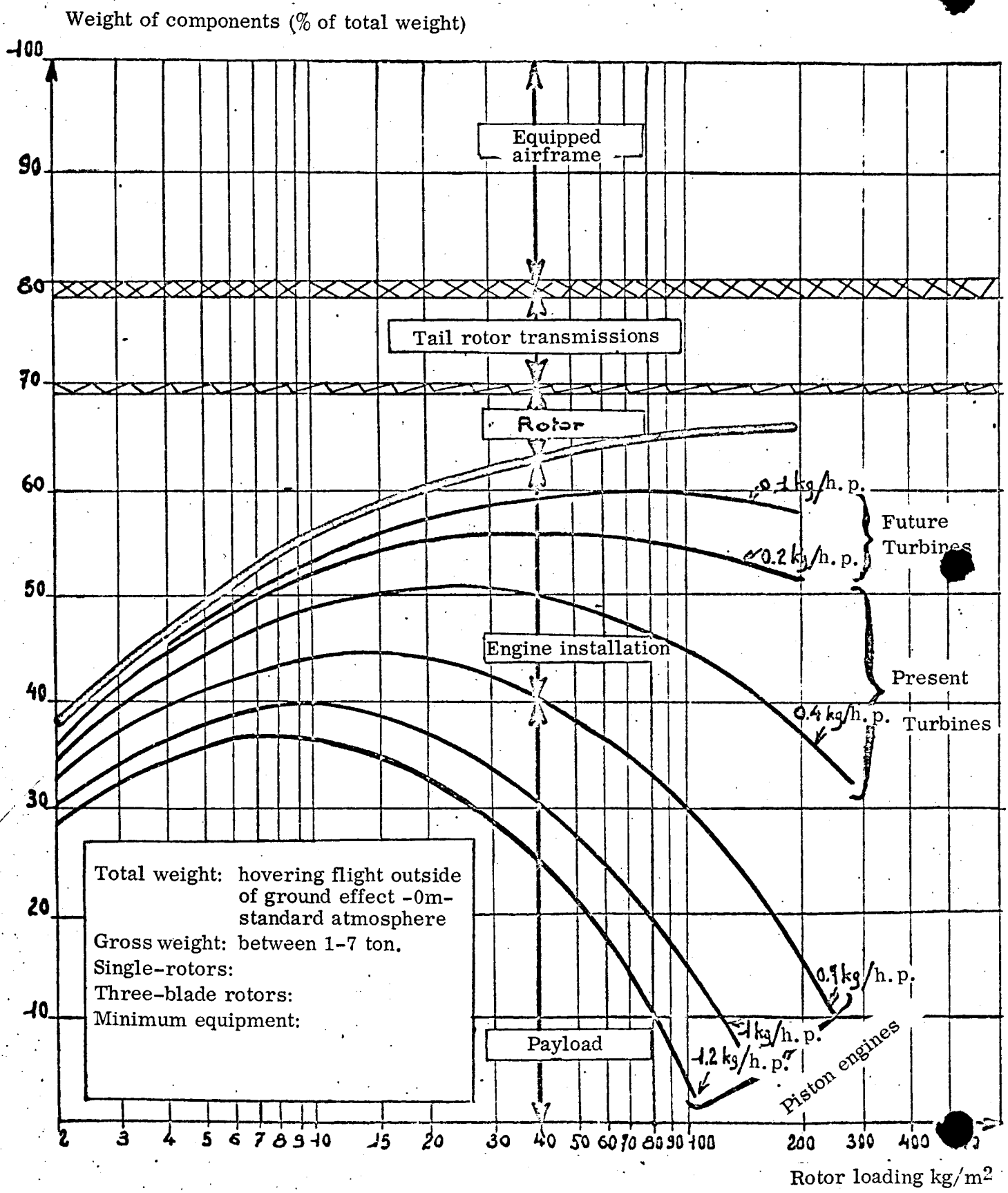

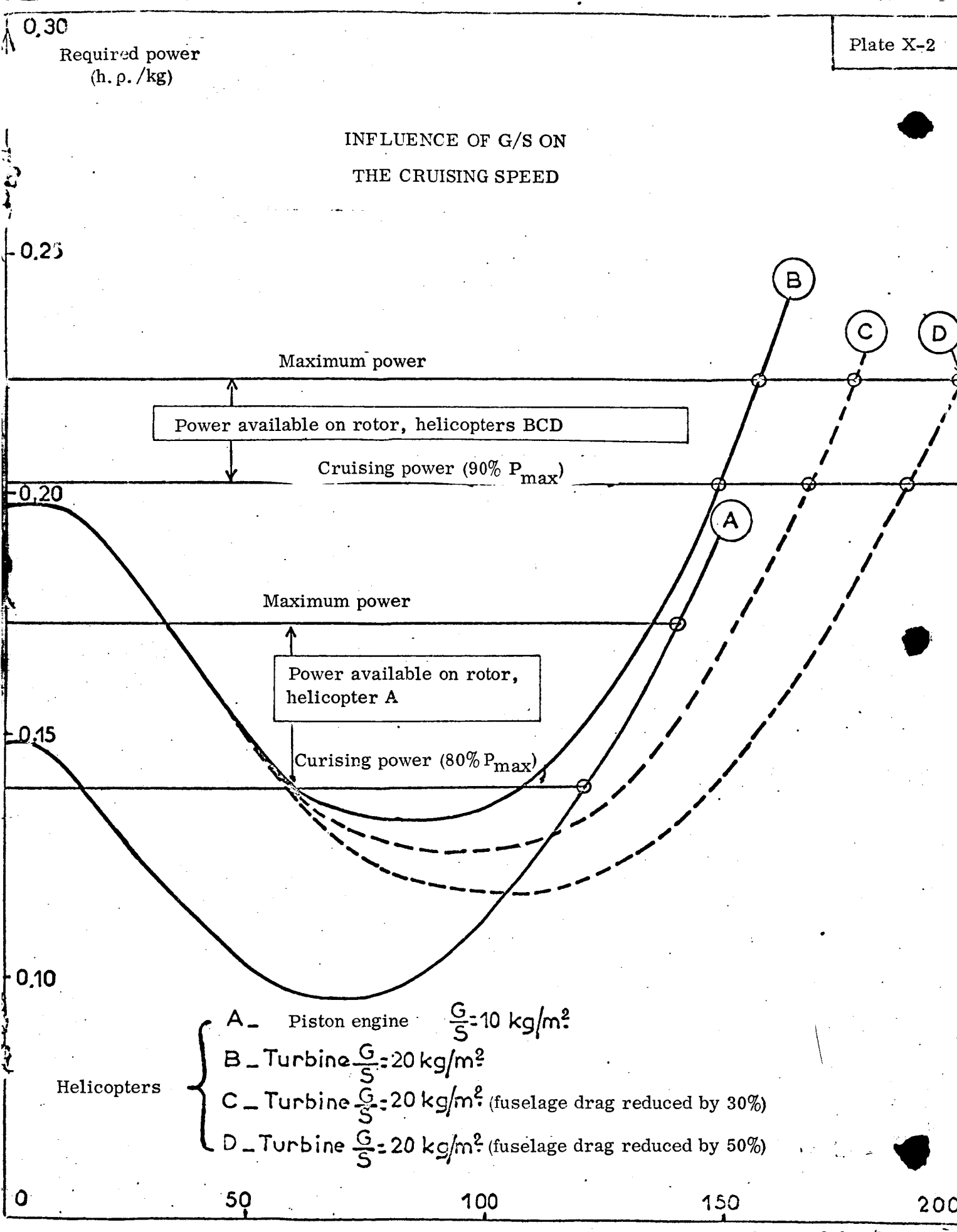
INFLUENCE OF G/S ON
THE CRUISING SPEED
0.30
Required power
(h. p./kg)
0.25
0.20
0.15
0.10
Maximum power
Power available on rotor, helicopters BCD
Cruising power (90% P_{max})
Maximum power
Power available on rotor, helicopter A
Curising power (80% P_{max})
A
B
C
D
Helicopters
A_ Piston engine $\frac{G}{S}$=10 kg/m²
B_Turbine $\frac{G}{S}$=20 kg/m²
C_Turbine $\frac{G}{S}$=20 kg/m² (fuselage drag reduced by 30%)
D_Turbine $\frac{G}{S}$=20 kg/m² (fuselage drag reduced by 50%)
0
50
100
150
200
Flight speed (km/hr)